



HAL
open science

La matière organique sédimentaire marqueurs d'environnement. Des roches mères pétrolières aux sédiments organiques actuels.

Mohammed Boussafir

► **To cite this version:**

Mohammed Boussafir. La matière organique sédimentaire marqueurs d'environnement. Des roches mères pétrolières aux sédiments organiques actuels.. Géochimie. Université d'Orléans, 2008. tel-00356954

HAL Id: tel-00356954

<https://theses.hal.science/tel-00356954>

Submitted on 29 Jan 2009

HAL is a multi-disciplinary open access archive for the deposit and dissemination of scientific research documents, whether they are published or not. The documents may come from teaching and research institutions in France or abroad, or from public or private research centers.

L'archive ouverte pluridisciplinaire **HAL**, est destinée au dépôt et à la diffusion de documents scientifiques de niveau recherche, publiés ou non, émanant des établissements d'enseignement et de recherche français ou étrangers, des laboratoires publics ou privés.

HABILITATION À DIRIGER DES RECHERCHES

PRESENTÉE À

L'UNIVERSITÉ D'ORLÉANS

PAR

MOHAMMED BOUSSAFIR

Maître de Conférences, UFR Sciences, Université d'Orléans
Enseignant Chercheur UMR 6113, ISTO

LA MATIÈRE ORGANIQUE SEDIMENTAIRE MARQUEUR D'ENVIRONNEMENT DES ROCHES MÈRES PETROLIGÈNES AUX SEDIMENTS ORGANIQUES ACTUELS



Le Lac Pavin, véritable aquarium scientifique : l'anoxie y est permanente en profondeur

Soutenue publiquement le 27 Juin 2008

Devant le Jury composé de :

M. François BAUDIN,	Professeur à l'Université de Paris VI (Rapporteur)
M. Raymond MICHELS ,	Chargé de Recherche (HdR) à l'Université de Nancy I (Rapporteur)
M. Luc ORTLIEB ,	Directeur de Recherche à l'IRD (Rapporteur)
Mme Sylvie DERENNE	Directeur de Recherche à BIOEMCO Paris (Examinateur)
Mme Elisabeth VERGES	Directeur de Recherche à l'ISTO (Examinateur)
M. Ary BRUAND	Professeur à l'Université d'Orléans (Examinateur)
M. Abdelfettah SIFEDDINE	Directeur de Recherche à l'IRD (Examinateur)

Sommaire

Préambule	3
INTRODUCTION ET PARCOURS DE RECHERCHE	6
PARTIE I - PRATIQUE METHODOLOGIQUE EN GEOLOGIE DE LA MO	
<hr/>	
I- INTRODUCTION.....	12
II- LA PETROGRAPHIE ORGANIQUE	14
III- L'AVENEMENT D'UNE SCIENCE : LA GEOCHIMIE ORGANIQUE	15
III-1 La géochimie globale	
III-2 La géochimie moléculaire ou Biogéochimie	
Références citées dans la partie I.....	22
PARTIE II - MODES DE FOSSILISATION DE LA MATIERE ORGANIQUE SEDIMENTAIRE	
<hr/>	
I – INTRODUCTION	27
II- LES MECANISMES DE « PRESERVATION » DE LA MO PETROLIGENE	28
II-1- La diagenèse précoce et le recyclage de la MO	
II-2- La préservation de la MO pétrolière	
III- COUPLAGE DE LA GEOCHIMIE MOLECULAIRE ET DE LA MICROSCOPIE ELECTRONIQUE A TRANSMISSION DANS L'ETUDE DES MOS.....	40
III-1 La préservation des MO des argiles du Kimméridgien (la thèse et l'après thèse)	
III-2 Relation MO et cyclicités sédimentaires des argiles du Kimméridgien	
III-3 Productivité organique et diagenèse précoce	
III-4 L'accumulation de matières organiques en domaine de pente continentale	
III-5 Rôle de la fraction argileuse dans le transfert et la préservation de la MO en environnement sédimentaire	
IV- CONCLUSIONS ET PERSPECTIVES	52
Références citées dans la partie II	55
PARTIE III - BIOGEOCHIMIE DE LA MO SEDIMENTAIRE APPLIQUEE AUX RECONSTITUTIONS DES PALEOENVIRONNEMENTS ET DES PALEOCLIMATS	
<hr/>	
I- INTRODUCTION	63
I-1 La variabilité climatique et les climats passés	
I-2 La MO outils de reconstitutions climatiques et environnementales	
II- LA CALIBRATION EN ENVIRONNEMENT ACTUEL	66
II-1 Distribution et état de préservation de la matière organique sédimentaire des sédiments superficiels du Lac Caço (Maranhão, Brésil)	
II-2 Suivi de la composition moléculaire des producteurs actuels, de la MO dissoute de la colonne d'eau et de la MO sédimentaire de surface du Lac Pavin (Massif Central Français)	
III- ARCHIVES SEDIMENTAIRES, PALEOENVIRONNEMENT ET PALEOCLIMATS	72
III-1 Les études réalisées en domaine lacustre	
III-2- Les études réalisées en domaines marins d'upwelling	
IV- CONCLUSIONS ET PERSPECTIVES	89
Références citées dans la partie III	93

PARTIE IV - AUTRES ACTIONS DE RECHERCHES

I- UNE ROCHE MERE	98
II- UN CHARBON	100
III- UNE ROCHE RESERVOIR	103
IV- UN SOL	106
Références citées dans la partie IV	107

PARTIE V - PROGRAMME DE RECHERCHE

ARCHIVES SEDIMENTAIRES DES ZONES D'UPWELLING DU PACIFIQUE EST: BIOGEOCHIMIE ET CALIBRATION DES BIOMARQUEURS PALEOCEANOGRAPHIQUES ET PALEOCLIMATIQUES

I- SITUATION DU PROJET	109
II- ARGUMENTATION SUR LE CHOIX DU SITE ET DES METHODES	111
II-1 Choix de la zone d'études	
II-2 Importance du marqueur biogéochimique :	
II-3 Résumé du projet et de ses objectifs	
II-4 Zones d'étude et collaborations	
III- METHODOLOGIE & ADEQUATION DU PROJET	119
III-1 Méthodologie :	
III-2 Adéquation du projet au programme de l'ISTO et à ses moyens analytiques	
III-4 Apport de ce projet à la communauté nationale et Internationale	
Références citées dans la partie V	122

PARTIE VI - NOTICE INDIVIDUELLE ET LISTES DES PUBLICATIONS

I- NOTICE INDIVIDUELLE	127
I-1 Encadrements de la recherche :	
I-2 Résumé des activités d'enseignements	
I-3 Participations aux programmes nationaux et internationaux	
I-4 Activité d'animation scientifique et d'administration de la recherche	
I-5 Développement de technique de laboratoire	
I- 6 Coopération industrielles et valorisation	
II- LISTE DES PUBLICATIONS	133
I-1 Publication de RANG A avec comité de lecture	
I-2 Publications de Rang B : revues scientifiques à faible <i>citation-index</i> et résumés étendus	
I-3 Participations à des congrès	

PARTIE VII - ANNEXES : EXEMPLAIRES DE QUELQUES PUBLICATIONS

(ANNEXES IMPRIMEES A PART, DOCUMENT JOINT, PAGES 145-391)

Préambule

Avant de commencer le bilan de mes travaux et les principaux résultats obtenus j'aimerais faire une introduction, un peu à la marge des préoccupations scientifiques ou presque, mais qui permet de positionner cette HdR.

« Rappeler l'histoire c'est gérer efficacement le présent et mieux s'armer pour réussir le futur » : C'est avec cette phrase que j'ai envie de situer ce mémoire. Tracer le cheminement de mes connaissances aura un double écho. Le premier, important, c'est de mieux placer mon expérience de recherche dans le contexte de cette vaste discipline qui est la géologie de la MO. Le deuxième impact, peut être subsidiaire, c'est de confronter mes acquis dans ce domaine et peut être rejoindre mes collègues habilités à diriger des recherches, étape considérée comme importante aux yeux de la plupart des collègues étape qui reste plus administrative que scientifique pour d'autres. Pour ma part j'ai tranché, il faut concilier ces deux mondes : je le fais. Il est vrai que l'exercice ne doit pas être uniquement considéré comme une obligation académique mais également comme une nécessité scientifique qui permet de présenter l'état des lieux des recherches dans mon domaine. Généralement cet exercice est profitable pour le futur habilité, mais doit également l'être par un nécessaire recul scientifique en présentant une vision la plus globale possible au service de notre communauté scientifique. Pour cela, je vais essayer de faire passer comme même un message, ne serait ce que pour les idées que je défends les leçons tirées de notre manière de faire la SCIENCE et les orientations que je souhaite voir émerger pour le futur de notre discipline puis à une échelle plus modeste les projets que je désire développer.

Le baromètre d'un chercheur scientifique comme chacun le sait se mesure essentiellement par le nombre de publications. Qu'en est-t-il d'un l'habilité à diriger des recherches. Pour moi, en plus de ces considérations comptables pour tout chercheur, un habilité à diriger des recherches doit l'être par ses compétences à la fois techniques et scientifiques, c'est quelqu'un qui s'investit énormément dans la formation par la recherche des masters et de thésard, c'est un entraîneur, un meneur de troupes. Ce n'est pas un acteur de la recherche, c'est plutôt l'auteur et le metteur en scène. En posant cette définition je place la barre très haute et rends difficile ma tâche dans le sujet qui nous concerne notamment dans l'élaboration de ce mémoire.

À présent regardant un peu ce que je propose comme titre : **LA MATIERE ORGANIQUE SEDIMENTAIRE MARQUEURS D'ENVIRONNEMENT : Des roches mères pétrologènes aux sédiments organiques actuels**

Ce titre est très vaste et peut paraître présomptueux. Quand on travaille sur la MO pour ses processus et qu'en même temps on utilise cette MO comme outils d'étude des archives sédimentaire et des environnements de surface en général , sur différents substrat et quelque soit les âges de ces substrats porteurs on est sollicité de toutes parts. Ce qui inévitablement fait de nous en reprenant une expression populaire des « touche à tout ». Telle était ma difficulté de trouver les mots justes pour exprimer toutes ces dernières années de labeur scientifique. Tout d'abord il est honnête de préciser (à ceux qui ne connaissent pas mon travail et qui seraient amenés à lire ces quelques lignes) que je ne me considère pas comme l'inventeur du principe de « préservation » de la MO ni celui qui peut se prévaloir de l'aspect matières organiques : outils de dépouillements des archives du climat et de l'environnement en milieu sédimentaire. Même si, j'ai à un moment ou un autre modestement participé au sein d'un groupe à l'évolution des idées et débats en pétrologie organique.

Une deuxième difficulté qui se rajoute à cette dernière est la présentation de ces années d'expérience. La question est comment peut se présenter un mémoire d'habilitation ? Comme une synthèse des travaux qui finit par des perspectives présentant une large vision des orientations scientifiques de la discipline concernée ? Ou, comme un catalogue des résultats et articles avec une partie introductive et une partie conclusion et perspective. Voilà les deux extrêmes. Dans ce domaine, les structures des rapports HDR sont aussi nombreuses que les carrières des scientifiques qui les présentent. L'HDR est pratiquement le reflet de la personnalité et de l'expérience de chacun. Elle dépend également de la durée de cette expérience, c'est-à-dire le temps qui sépare la thèse de l'HdR. Plus on attend, plus la difficulté de synthèse devient importante obligeant de passer sous silence quelques actions scientifiques qui deviennent de ce fait à la marge. Ce mémoire peut être considéré comme intermédiaire des deux visions extrêmes que je viens de présenter. Il peut être vu comme un catalogue de mes travaux de recherche regroupés sur deux chapitres : l'un sur la préservation de la MO et l'autre sur son utilisation comme marqueur de paléoenvironnement et de paléoclimat. Mais avec un certain effort de synthèse présenté au début de chacun de ces chapitres et une conclusion et des orientations scientifiques les plus larges possibles présentées en fin de chapitre. Un autre chapitre qui ouvre le mémoire et définit les termes utilisés est une synthèse, des réflexions, critiques et autocritiques (mais qui se veulent constructives) sur l'évolution de la méthodologie et les

dérives de celle-ci dans le domaine de la pétrologie organique. Je finis par un projet personnel de portée assez large : le projet de toute une vie scientifique suivis par un chapitre relatant mon expérience d'enseignant chercheur.

L'état d'élaboration de chacun des travaux présentés est variable, et dépend entre autres de l'investissement en terme de temps donné aux projets mais également des priorités, du nombre de personnes impliquées, de l'octroi d'une thèse mais également de mes disponibilités qui sont, eu égard à mon statut d'enseignant chercheur, très variables au cours de l'année. Il reste cependant que, quelle que soit la quantité ou la qualité des résultats obtenus, ce serait une erreur de considérer les problèmes abordés comme résolus et les thématiques épuisées. Au contraire, dans nos thématiques actuelles la résolution d'une question n'est que partielle et fait souvent appel à une autre : ce qu'on appelle des perspectives dans notre jargon scientifique. Le changement de thématique est souvent lié à l'effet de mode mais surtout aux opportunités de financement qui s'offrent à nous.

La vitesse à laquelle on obtient des résultats est plus ou moins lente en fonction d'une part des outils mis en œuvre (l'outil moléculaire demande plus de temps en terme de dépouillement d'analyses) mais également à ma vitesse personnelle de travail. On peut certainement faire mieux dans un temps plus court mais également beaucoup moins bien et plus lentement.

Je dois finir ce préambule avec une pensée pleine d'amitié, de fraternité et surtout de remerciements à tous mes collègues et amis(es) de l'ISTO, à tous mes thésards, stagiaires et étudiants et à tous mes collaborateurs extérieurs à l'ISTO. Sans tout ce beau monde ma recherche n'aurait pas progressée, mon expérience ne se serait pas forgée... tout simplement cette HDR n'existerait pas.

Par crainte d'oublier quelqu'un je ne ferais pas la liste, qui risque de toute manière d'être interminable et probablement incomplète, de tous mes amis et collègues qui m'ont accompagnés dans mon parcours. Ils se reconnaîtront.

Pour finir je dédie ce mémoire à ma Femme Yasmina, à mes deux filles Wissam et Samia et à mon fils Yassine.

INTRODUCTION ET PARCOURS DE RECHERCHE

INTRODUCTION ET PARCOURS DE RECHERCHE

1- introduction:

La rédaction de ce mémoire est l'occasion de présenter ici une synthèse sur les connaissances acquises ces dernières années dans le domaine de l'étude de la MO, sa sédimentation et sa fossilisation ainsi que son utilisation comme outil de reconstitution paléoenvironnementale et paléoclimatique . Tous ces travaux ont été développés dans le cadre des thématiques de l'équipe Matière Organique de l'ISTO, et en étroite collaboration avec l'unité de recherche PALEOTROPIQUE de l'IRD (Bondy) en ce qui concerne plus particulièrement les travaux réalisés en Amérique du sud. Ceci entre dans le cadre des collaborations habituelles de l'équipe MO basé sur la mise en commun avec d'autres laboratoires de ses problématiques scientifiques et de ses approches analytiques.

Avant de commencer le bilan de mes travaux et les principaux résultats obtenus j'aimerais situer ces derniers dans cette discipline de pétrologie organique, Une phrase empruntée de Georges Dumesnil éminent archéologue, ouvrirait le premier chapitre de ma thèse (Boussafir, 1994a) et résume bien ma participation à ce champ disciplinaire. « *Dans les arts, dans les lettres, un homme peut présenter une œuvre en disant vraiment qu'elle est sienne. Il n'en est pas de même dans nos fouilles, où chacun à son heure prolonge de quelques mètres la tranchée ouverte par d'autres, avec des outils que d'autres ont apprivoisés, et puis s'en va, transmettant la consigne.* »

Voici résumés ci-dessous les principaux thèmes de recherche que j'ai développés au cours de ces dernières années depuis mon arrivée dans le laboratoire orléanais en septembre 1997 en tant que maître de conférence ainsi que les points forts de mon activité.

Les objectifs et les thèmes abordés au cours de mes travaux de recherche se focalisent sur l'étude de la Matière Organique (MO) sédimentaire dans différents environnements naturels, lacustres et marins, actuels et anciens. Il s'agit plus particulièrement de :

- l'étude de l'origine et du mode de fossilisation de la MO dans différents environnements sédimentaires.
- l'identification de la nature et de l'état de préservation de cette MO dans les archives sédimentaires marines et lacustres.
- l'étude de la MO aux fins de reconstitutions paléoenvironnementales et paléoclimatiques au cours du Quaternaire récent.
- le rôle des phyllosilicates dans le transfert et la fossilisation de la MO ainsi que les processus biogéochimiques qui accompagnent sa sédimentation.

Spécialiste de la sédimentation et de la diagenèse de la MO lacustre et marine, ancienne et récente, j'ai mis en œuvre une méthodologie basée sur une double approche pétrographique et géochimique. Les observations pétrographiques sont réalisées à différentes échelles allant de l'apparence morphologique des sédiments riches en matières organiques jusqu'à la texture ultrafine de cette dernière observée au MET; en passant par toutes les méthodes usuelles de la microscopie photonique. La partie géochimique concerne à la fois les analyses élémentaires globales et la composition moléculaire des fractions d'hydrocarbures solubles (extraites aux solvants organiques) et insolubles (fournies par la pyrolyse *off-line* et *on-line*). Dans la pratique, ces investigations recherchent pour chaque fraction organo-sédimentaire une composition moléculaire spécifique et donc une origine et un mécanisme de fossilisation caractéristique. Ceci permet de suivre la fraction organique depuis sa production, son transfert dans la colonne d'eau jusqu'à son accumulation dans les sédiments. Mes compétences de pétrographe se trouvent doublées avec celles d'un chimiste organicien qui dépouille les informations portées par les fractions organiques des sols, sédiments et roches. La deuxième spécificité de mon travail est liée à mes activités dans le domaine des reconstitutions paléoclimatiques et paléoenvironnementales focalisées sur le domaine tropical. Ces travaux menés depuis mes recherches post-doctorales m'ont permis de suivre l'évolution des marqueurs organiques dans les enregistrements sédimentaires mais aussi dans les milieux naturels actuels en vue de calibrer le signal organique.

2- Mon parcours scientifique :

Ma formation de base m'a permis d'acquérir des connaissances solides en géologie. Le travail d'initiation à la recherche (DEA) réalisé à Strasbourg m'a permis de (1) caractériser la pétrographie des différents faciès basaltiques de la plus vieille croûte océanique forée dans le bassin de Pigafetta (Pacifique West, LEG 129 d'ODP). (2) d'analyser la signature isotopique des magmas à l'origine de ces basaltes montrant ainsi qu'ils proviennent d'un mélange de sources magmatiques diverses. (3) de dater par des méthodes K/Ar et Ar/Ar les basaltes de cette plus vieille croûte océanique située sous le Pacifique Ouest. Après ce DEA, j'ai intégré l'UMR Sédimentation et Diagenèse de la Matière Organique à Orléans (dir. JR Disnar) et plus particulièrement dans le groupe de pétrographie organique (URPO) pour une thèse sur l'origine et le mode de fossilisation de la MO des argiles du Kimméridgien du Yorkshire. Ces travaux de thèse, réalisés sous la direction de Elisabeth Lallier-Vergès, ont été menés dans le cadre du GdR « Relations et processus organo-minéraux en environnements sédimentaires » du CNRS dirigé par Philippe Bertrand, et m'ont permis de travailler au sein d'un ensemble de collaborations très construit. Mes travaux ont ainsi pu être confrontés aux travaux de E. Lallier-Vergès sur la sulfato-réduction et de P. Bertrand sur

les flux de carbone. L'ensemble de ces travaux ont permis une avancée majeure dans la compréhension des mécanismes de transfert de la MO et de sa fossilisation dans les sédiments. Le couplage méthodologique pétrographie fine et biogéochimie moléculaire que j'ai plus particulièrement réalisé dans ma thèse, a été basé sur des développements méthodologiques que j'ai mis au point : microprélèvements et préparation des MO et des roches organiques pour les études ultrastructurales au MET.

À l'issue de ma thèse, ce couplage pétrographie et géochimie moléculaire, ainsi que la collaboration étroite entre Orléans (E. Lallier-Vergès, P. Bertrand) et l'Ecole de Chimie de Paris (Claude Largeau, Sylvie Derenne), m'ont notamment permis de publier un article de synthèse dans *Geochimica et Cosmochimica Acta* 1995, puis un modèle conceptuel de fossilisation de la MO qui prend en compte les différents mécanismes intervenant dans l'accumulation organo-sédimentaire en environnement marin (*Marine and Petroleum Geology*, 1997).

Mon activité de recherche post-doctorale s'est poursuivie au sein de l'unité « sédimentation et diagenèse de la MO » ; en tant que chercheur contractuel sur des problématiques ayant pour principal outil, l'analyse moléculaire de la MO, appliquée à la reconstitution paléoenvironnementale et paléoclimatique. Puis, j'ai effectué un stage post-doctoral au sein de l'équipe de Claude Largeau et Sylvie Derenne. Il s'agissait d'étudier par pyrolyse *off-line* des MO insolubles provenant de stades climatiques distincts enregistrés dans des archives sédimentaires lacustres en milieu intertropical (Lac Tritrivakely à Madagascar). Les résultats de cette étude ont permis de montrer que la composition biogéochimique de sédiments représente un outil sensible et puissant, recelant des potentialités énormes, et dont le développement est devenu dès lors indispensable dans les reconstitutions climatiques (Boussafir et al. 2000).

J'ai alors présenté un projet, ciblé sur les études biogéochimiques des archives sédimentaires lacustres, qui m'a permis d'intégrer le corps des enseignants chercheurs de l'Université d'Orléans en septembre 1997. Cette nomination était l'occasion pour moi de poursuivre des études paléoclimatiques et paléoenvironnementales notamment dans les milieux tropicaux d'Amérique du Sud. En effet, dans ce cadre, une thèse en biogéochimie moléculaire codirigée par Jean-Robert Disnar et moi-même a été effectuée par J. Jacob (2003). Elle a concerné l'étude de la MO en tant que marqueur des changements climatiques depuis le dernier maximum glaciaire (20 000 ans) du lac Caço situé au Nord Est du Brésil.

Ce sujet a été mené en étroite collaboration avec l'UR Paléotropique de l'IRD et avec les chercheurs brésiliens de l'Université Fédérale Fluminense de l'état de Rio De Janeiro. Une autre étude, dans le cadre de mon encadrement par la recherche de différents masters, a été menée en parallèle et a concerné la calibration des paramètres pétrographiques et géochimiques globaux sur le même site. La suite de ma carrière scientifique a été marquée par une collaboration étroite, toujours en géochimie moléculaire, aux différents programmes développés par l'IRD en Amérique du sud. Ces collaborations m'ont notamment permis, d'effectuer deux missions d'échantillonnages : l'une sur le lac Caço au Brésil, l'autre sur la baie de Mejillones au Nord du Chili, et de former par la même occasion des étudiants et chercheurs en Amérique du Sud. Une thèse actuellement en cours (M. Gurgel) concerne les sédiments d'upwellings sur les côtes Est et Ouest de l'Amérique du Sud et est menée sous la codirection de E. Lallier-Vergès de l'ISTO, A. Sifeddine de l'IRD et moi même.

J'ai également participé à l'encadrement scientifique de la thèse de Laetitia Pichevin (2004) du laboratoire EPOC de Bordeaux. Ma contribution concernait les aspects pétrographiques et moléculaires du contenu organique des archives sédimentaires de l'upwelling du Benguela (Pichevin et *al.* 2004). Parallèlement à tous ces travaux, j'ai pu ouvrir un nouveau chantier à l'ISTO sur l'étude des interactions argiles/MO en milieux lacustres et marins. Des pièges, permettant ces interactions, ont été mis au point, et des expérimentations, *in vitro* et *in vivo* sur différents substrats argileux (de synthèse et naturels), ont été réalisés avec succès. Ces expérimentations ont concerné la zone photique oxygénée et la zone anoxique du Lac Pavin et de la Baie de Mejillones au Chili. Ce travail a fait l'objet d'une thèse sous la co-direction scientifique de J.L. Robert et moi-même (Sylvain Drouin, 2007).

Bien entendu, une part très importante de mes activités a été consacrée à l'enseignement (préparations, interventions, organisation des filières, administration pédagogique, encadrement de DEA et Master1 & 2 , participation comme membre titulaire aux commissions de spécialistes 35 & 36 universitaire et comme trésorier du département géosciences et environnements). Depuis ma nomination, mon service pédagogique a été en moyenne 1,5 fois le service statutaire annuel d'un enseignant chercheur.

PARTIE I

PRATIQUE METHODOLOGIQUE EN GEOLOGIE DE LA MO.

I- INTRODUCTION

Constituant ubiquiste de notre environnement, la matière organique (MO) est présente dans les eaux, les sols, les sédiments et les roches qu'ils soient récents ou anciens. C'est pour cette raison qu'elle fait l'objet de multiples recherches effectuées dans des disciplines différentes et pour des problématiques touchant tous les domaines des sciences de la vie et de la terre. Cette diversité a permis un développement accru des méthodes d'analyses de la MO et la mise au point de méthodologies nouvelles créant ainsi de véritables passerelles disciplinaires. Je citerai comme exemple l'utilisation des méthodes de la microscopie électronique développée par les biologistes pour l'étude de la structure et de la physiologie cellulaire ou encore les méthodes analytiques classiques de chromatographie, spectroscopie IR et RX, spectrophotométrie, RMN, et spectrométrie de masse propre à la chimie organique. Ces deux mondes pétrographique et géochimique ont été associés dans le domaine de la pétrologie organique permettant une avancée scientifique considérable au cours des vingt dernières années. La multidisciplinarité n'est pas une exclusivité du domaine de la pétrologie organique. C'est une particularité propre aux géosciences en général par leur position à la frontière des sciences du vivant, de la physique et de la chimie voire des mathématiques pour tous les aspects modélisation des phénomènes géologiques passés et futurs.

Les investigations analytiques sont basées sur une bonne logique scientifique, propre aux sciences expérimentales. Cela commence par une problématique de recherche où la question scientifique est centrale et les objectifs précis ensuite les moyens nécessaires à l'étude sont choisis en respectant un ordre et une progression dans la finesse analytique (du global généralement moins coûteux vers le moléculaire ou l'isotopique, plus coûteux en temps et en moyens). Malheureusement cette règle n'est pas toujours respectée. Les exemples sont nombreux où l'étude fine devance la caractérisation globale.

La plupart des travaux réalisés sur notre outil à tous la MO, notamment à l'ISTO, obéissent pour une grande part à une logique de progression analytique. Un examen pétrographique des carottes ou des sédiments, parfois leur cartographie RX, permet une vue globale sur le faciès et sa distribution, et par la suite un choix d'échantillonnage précis avec une résolution la plus adaptée et la plus haute possible. Ces échantillons choisis sont analysés par Rock-Eval et les teneurs quantitative et qualitative de la MO sont évaluées de façon globale permettant ainsi de cibler l'étude pétrographique du palynofaciès puis du microscope électronique à transmission si nécessaire. Le Rock-Eval est de ce fait indispensable avant toute investigation ultérieure. Ce dernier nous permet d'avoir une idée primordiale sur la quantité de MO fossilisée (le carbone organique total, COT%). Ce paramètre indispensable couplé aux indices d'hydrogénation et d'oxygénation de la MO

calculés à partir des spectres obtenus par la pyrolyse sous condition inerte nous permet d'avancer des hypothèses et des pistes d'interprétation en termes de sources possibles combinées ou non à de la diagenèse. Ceci amène des interrogations auxquelles le palynofaciès nous fournit assez souvent des éléments de réponse. Le moléculaire vient ensuite dans des cas précis de recherche de marqueurs spécifiques de sources de Matières Organiques Sédimentaires (MOS) amorphes, pour la caractérisation d'un environnement diagénétique précis ou pour rechercher des marqueurs environnementaux ou climatiques.

En fonction des substrats porteurs les objectifs et les méthodes d'études de la MO sont adaptés. La MO des sols est largement étudiée par les pédologues pour son importante réactivité (complexation, piègeage et relargage) en particulier envers les éléments véhiculés dans les couvertures pédologiques et les cours d'eau comme les métaux et les polluants. La MO des eaux quant à elle intéresse les biologistes et les géochimistes pour son rôle dans l'équilibre ou le déséquilibre trophique du milieu aquatique. Enfin, la MO des sédiments anciens intéressait à juste titre les industries du charbon d'abord puis pétrolières ensuite pour son utilité énergétique. Ces industries ont permis, depuis un demi-siècle, et grâce aux moyens matériels et financiers investis, le développement rapide de la pétrographie et de la géochimie organique. J'évoque dans deux parties de ce mémoire notre mutation scientifique et la migration des géologues, climatologues et bien d'autres vers des séries plus récentes en vue de reconstitution des climats et environnements passés. En utilisant au départ des moyens globaux pétrographiques mais aussi géochimiques globaux (Lallier vergès et *al.*, 1993 ; Di-giovanni et *al.*, 1998, Sifeddine et *al.*, 1994, 1996, 1998, 2001 et 2003 ; Mayers et lallier-Vergès 1999 ; Noël et *al.*, 2001). Par la suite l'utilisation de moyen de biogéochimie moléculaire (Rosell-Mele et *al.*, 1997 ; Pailler et *al.* 2002 ; Boussafir et *al.* 2000 ; Jacob 2003 ; Jacob et *al.* 2004 et 2005) ou d'isotopie moléculaire (Huang et *al.*, 1999 et 2000).

Il faut admettre cependant certaines dérives dans la pratique de notre discipline. Notre richesse analytique n'a malheureusement pas toujours été utilisée à bon escient et avec parcimonie. Au contraire certains travaux fustigeaient la multidisciplinarité analytiques comme si la multiplication analytique était un passage obligatoire et que la qualité du travail scientifique passait par là. Ce qui a eu un effet boule-de-neige aboutissant à une surenchère méthodologique entre les laboratoires où l'analyse elle même, par le nombre des méthodes d'études utilisées, prenait le pas sur l'information scientifique recherchée. Le « screening » systématique est devenu la règle incontournable pour toute bonne étude. Cette multi-analyse, n'était pas toujours justifiée, pour preuve, l'exemple de certains travaux partant d'un charbon humique bien caractérisé, pétrographiquement chimiquement (RE, IR, RX, RMN) et parfois moléculairement, arrivant à conclure qu'il s'agit de MO de type III. Les exemples sont malheureusement nombreux dans d'autres types d'environnements. La règle des sciences expérimentales est oubliée l'espace d'une étude dite approfondie.

II- LA PETROGRAPHIE ORGANIQUE

Les études en pétrographie organique au sens strict, sont bien adaptées aux échantillons bruts consolidés. Ce type d'observation héritée de la pétrographie des charbons permet l'analyse macérale et du microlithotype, ainsi que la mesure du paramètre de maturité thermique comme le pouvoir réflecteur de la vitrinite ou l'analyse spectrale de la fluorescence. Les sédiments récents et notamment quaternaires ne sont pas adaptés à ce genre d'observation et d'analyse. Ces sédiments subissent un protocole chimique permettant de dissoudre la fraction minérale et d'isoler et concentrer le contenu organique particulaire. L'observation au microscope photonique permet de caractériser l'ensemble des constituants organiques particuliers figuré et amorphe : c'est le palynofaciès (Durand et Nicaise 1980, Combaz 1980, Robert, 1985). C'est le palynofaciès qui a été utilisé en premier lieu et permis à de nombreuses études appliquées au paléoenvironnement et au paléoclimat d'aboutir à des conclusions intéressantes. Ceci grâce au calcul de rapport qui permet de quantifier la balance entre les apports allochtone et autochtone. Dans le cas des sédiments lacustres le rapport entre les apports du bassin versant comparés à la production dans le lac s'est révélé sensible et fidèle aux fluctuations climatiques et environnementales. Certaines Matières Organiques Amorphes (MOA) dite rougeâtre permet d'apprécier les apports provenant de l'érosion des sols.

La plus grande évolution méthodologique qu'a connu le palynofaciès réside dans le désir des pétrographes organiciens d'améliorer la quantification des particules organiques observées entre lame et lamelle. Pendant longtemps nous avons utilisé un compteur de points. Cette méthode a été remise en cause par une analyse d'image (Sifeddine non publié) qui a révélé que le compteur de points sous-estime l'abondance des grandes particules et surestime logiquement l'importance des petites particules car pour chacune de ces particules une unité de valeur a été comptée quelle qu'en soit la surface. Après ce constat, nous sommes passés à une évaluation surfacique grâce à un abaque micrométrique intégré aux oculaires. Ce qui a largement corrigé la distorsion quantitative obtenue par le comptage des points. La représentation en valeurs relatives des différentes fractions pose encore un problème car elle ne prend pas en considération la richesse en carbone organique d'un échantillon à l'autre puisque pour chacun d'eux la somme des fractions quantifiées est normalisée à 100%. Une autre évolution dans ce domaine est l'utilisation d'un standard interne permettant une quantification absolue de chaque type de particules exprimé sous forme d'une concentration. J'ai réalisé à Orléans une première étude basée sur cette méthode de quantification absolue, appliquée aux sédiments d'upwelling du Pérou dans le cadre d'un stage de recherche en Master II (Belhassine, 2006).

Le travail de comptage reste malgré tout un travail long et fastidieux qui demande de la minutie et de la patience. Une prochaine étape serait d'automatiser ce procédé par un analyseur d'image et une platine automatisée. Les idées ne manquent pas à cet égard et des appareils similaires existent déjà pour l'étude palynologique.

Une autre innovation pétrographique de ces dernières années est l'utilisation de la Microscopie Electronique à Transmission dans l'étude de la texture ultrafine des MOA du palynofaciès. Des méthodes de préparation ont été mises au point à ce sujet dans le cadre de mon doctorat qui ont permis plusieurs collaborations scientifiques. Ces observations couplées aux analyses EDS ponctuelles se pratiquent sur des coupes ultraminces d'environ 500Å d'épaisseur. Le protocole, permettant l'obtention de ces coupes et leurs observations, est présenté par *Boussafir, 1994 et Boussafir et al 1995*. L'observation des différents types de MOA isolées nécessite la réalisation de concentrés de chacun de ces types. Ces concentrés de matière organique amorphe sont devenus possibles grâce à mon adaptation d'un micromanipulateur associé à un stéréomicroscope. Ce micromanipulateur, analogue à celui utilisé en biologie cellulaire permet d'isoler et de stocker des particules d'une taille moyenne de 30 à 40 µm. Le seul souci possible avec cette méthode de microprélèvement est de repérer les MOA observées entre lame et lamelle (palynofaciès) à partir d'une suspension dans l'eau de ces mêmes particules. Cette méthode pétrographique mise au point dans le cadre de mon doctorat en 1992 n'a malheureusement pas été exploitée au maximum de ses possibilités. Le travail à réaliser est encore plus minutieux que le comptage palynofaciès.

Les études pétrographiques sont indispensables et restent complémentaires à la géochimie organique.

III- L'avènement d'une science : La géochimie organique

La géochimie organique a permis de répondre aux interrogations que se posaient les scientifiques à la fin du XIX^{ème} siècle sur l'origine du pétrole. Son développement au milieu du XX^{ème} siècle a de ce fait été lié à celui de l'exploration pétrolière. La géochimie organique n'a atteint le statut de discipline propre, ou de science autonome que peu après 1960 (Durand, 2003). Les années 1965-1985 sont considérées comme les années glorieuses pour cette discipline : pendant cette période les mécanismes de la formation des gisements de pétrole et de gaz naturel ont été compris et expliqués. De nombreux biomarqueurs, témoins de l'origine organique du pétrole ont été identifiés (Durand, 2003).

La suite est marquée par le rapprochement de la géochimie organique avec la science des charbons et notamment la pétrographie des macéraux, l'analyse des microlithotypes, la réflectance de la vitrinite et la fluorescence spectrale des mégaspores. L'association

d'études pétrographique et géochimique a été dès lors regroupée dans le terme pétrologie organique. Au même moment, la géochimie organique s'est intéressée à des domaines variés, tels que la sédimentologie organique, la diagenèse des sédiments riches en MO ou la formation des gîtes minéraux.

La géochimie organique appliquée à l'exploration et à la production de pétrole et plus généralement des combustibles fossiles, est actuellement en phase de veille scientifique à l'ISTO. L'avenir de cette discipline à plus long terme sera dans l'étude des interactions des produits de l'activité humaine, en particulier les polluants organiques et les gaz à effet de serre, avec la géosphère, la recherche d'un développement durable et des énergies renouvelables.

Actuellement, on assiste à une application croissante des connaissances acquises en géochimie organique à des domaines autres que l'exploration pétrolière. En effet, la géochimie organique s'intéresse de plus en plus à des problématiques orientées vers la géodynamique externe et la sédimentologie récente appliquée à la reconstitution des paléoenvironnements et paléoclimats, à la compréhension des processus diagénétiques dans les environnements actuels (comme les tourbières), à l'archéologie et la sédimentation historique ou à la participation de la MO fossile dans le cycle global du carbone. Ces différents aspects sont actuellement couverts (dans l'ensemble) par les programmes de recherche développés par l'équipe « MO » de l'ISTO.

Comme cité plus haut, la géochimie organique était réservée initialement au domaine de l'industrie des combustibles fossiles et notamment du pétrole. J'ai moi-même participé à certains travaux dans ce domaine (Partie III de ce mémoire : Nzoussi et *al.* 2005 ; Copard et *al.* 2000, Huc et *al.*, 2000). Les applications de la sédimentologie et géochimie organique aux reconstitutions paléoenvironnementales et paléoclimatiques sont plus récentes (Sifeddine et *al.*, 1994 ; Meyers et Lallier-Vergès, 1999 ; Meyers, 2003). Pourtant, les matières organiques, omniprésentes dans les systèmes naturels, avec des teneurs pouvant aller de moins de 1 % (roches anciennes, sédiments des fonds océaniques) jusqu'à plus de 50 % (charbons, tourbes, schistes bitumineux) sont des composants extrêmement sensibles, affectés par les changements de leurs sources (communautés végétales et microbiennes) ou par différents facteurs abiotiques, comme le climat ou l'environnement, contrôlant leur production. Elles constituent de puissants traceurs des milieux naturels et du climat. Une partie des informations qu'elles recèlent est ensuite préservée lors de l'archivage dans les sols, sédiments et roches.

Les études géochimiques sont variées et passent de la caractérisation élémentaire globale à de la biogéochimie moléculaire voire isotopique.

III-1 - La géochimie globale

Il s'agit de l'étude de la MO par pyrolyse Rock-Eval ou par un CNS (LECO et autre système équivalent). Le Rock-Eval, l'appareil le plus fréquemment utilisé a été inventé par et pour les pétroliers. Il a été conçu pour fournir des informations sur la quantité d'hydrocarbures libres, le type et l'état d'évolution de la MO qu'elles contiennent (*Espitalié et al., 1977, 1985a, 1985b*). Il commence à être démocratisé pour l'étude des sédiments récents (*Di-Giovanni et al., 1998 ; Lafargue et al., 1998 ; Disnar et al., 2000, 2003*). Cette méthode permet de mesurer les teneurs en carbone organique total (COT en %), et de calculer des indices comme celui d'hydrogène (IH, en mg HC.g⁻¹ de COT) représentant la quantité des composés hydrocarbonés libérés au cours de la pyrolyse rapportée au COT, ou d'oxygène (IO, en mg CO₂ g⁻¹ COT) représentant le quantité de gaz carbonique libérées au cours de la phase de pyrolyse également rapportée au COT « Il quantifie le caractère oxygéné ou oxydé de la MO ».

Un dernier paramètre le TpS₂ (°C) représentant la température de craquage à laquelle la production de composés hydrocarbonés est maximale : c'est la température correspondant au sommet du pic S₂. Ce paramètre peut être utilisé dans la discrimination des horizons pédologiques et du caractère plus labile ou plus réfractaire des composés bio-géo-macromoléculaires.

L'une de l'évolution méthodologique découlant des analyses Rock-Eval est la possibilité de décortiquer le signal de pyrolyse sous azote : c'est la déconvolution du signal S₂. Cette nouvelle application a déjà montré ses possibilités, que ce soit dans l'étude des sols (*Disnar et al., 2003; Sebag et al., 2006*) ou dans celle des variations de Tmax liées à une altération supergène de charbons (*Copard, 2002*). Toutefois des précautions doivent être de rigueur lors de ces déconvolutions, car elles peuvent apporter des solutions multiples et deviennent de ce fait aléatoires sans signification compositionnelle. En ce qui concerne les signaux S₃CO et S₃CO₂ du Rock-Eval, le nombre de courbes élémentaires rend difficile voire illusoire l'application d'une telle méthode. Dans tous les cas, la compréhension des signaux primaires du Rock-Eval, préalable essentiel à la compréhension des indices usuels, doit être validée par une approche moléculaire. La spectrométrie infra-rouge et l'analyse de la lignine seront les premières méthodes à mettre en oeuvre, notamment pour comprendre les variations de TpS₂. D'autres méthodes, couplant par exemple une pyrolyse du même type que celle du Rock-Eval directement à un spectromètre de masse, sont également le complément nécessaire pour mieux comprendre les paramètres du Rock-Eval. La comparaison des signaux obtenus par ces méthodes avec ceux du Rock-Eval sera sans doute d'un grand intérêt dans toutes les problématiques abordées avec ce type d'appareil.

III-2 La géochimie moléculaire ou Biogéochimie

III-2-1 la **Biogéochimie en environnement sédimentaire**

La notion de biogéochimie a été « inventée » par le savant russe Vladimir I. Vernadsky (1863-1945). En 1971, l'écologiste Eugene P. Odum définit la biogéochimie comme étant « l'étude du processus cyclique de transfert des éléments chimiques de l'environnement à partir des milieux abiotiques vers les organismes qui à leur tour retransmettent ces constituants à l'environnement ». Cette notion a permis à de nombreux laboratoires de disciplines scientifiques diverses (situées à l'interface Biologie et Géochimie) d'utiliser de façon très large la notion de Biogéochimie. Toutes ces disciplines ont pour point commun le comportement, actuel ou passé, dans les milieux naturels (la colonne d'eau, les sols ou les sédiments), des molécules héritées du vivant ou des éléments chimique recyclé par ceux-ci.

La notion de biogéochimie des environnements sédimentaires, telle que je l'utilise dans ce projet, s'intéresse aux processus que subissent les MO produites par la biomasse pendant leur transfert jusqu'à leur fossilisation. Cette notion intègre d'une part, les études de biomarqueurs moléculaires dans les environnements actuels et passés et d'autre part les processus de dégradation et de recyclage de la MO dans la colonne d'eau en milieu oxygéné ou anoxique. Des processus organo-sédimentaires liés au processus de sulfato-réduction et de dénitrification en milieu anoxique, les processus et les mécanismes de préservation de la MO et des biomarqueurs associés à cette dernière dans les sédiments font partie intégrante de cette discipline qu'est la biogéochimie sédimentaire.

III-2-1 Le biomarqueur en général

Au cours des trois dernières décennies, et sous l'impulsion majeure de l'exploration pétrolière puis des études environnementales, la géochimie organique moléculaire a connu un développement méthodologique considérable. Grâce aux méthodes couplées de séparation chromatographique et d'analyse en spectrométrie de masse nous sommes aujourd'hui capables de lire l'information moléculaire jusque dans ses plus petits détails (Stoechiométriques, structuraux, stéréochimiques, isotopique)

Les matières organiques sont constituées de diverses familles de composés comme les acides aminés, les sucres, la lignine ou les lipides. La fraction la plus exploitée en géochimie organique comprenant la plupart des biomarqueurs connus de nos jours, est celle des lipides d'une part pour la diversité des molécules qui la composent et d'autre part parce qu'il s'agit

d'une famille de composés plus ou moins résistants, caractéristique liée à leurs fonctions souvent de rigidifiant du squelette organique dans les cellules vivantes.

Ainsi, on peut détecter plusieurs centaines de molécules distinctes au sein d'un même échantillon sédimentaire. Certaines molécules sont spécifiques d'organisme(s) dont elles sont issues puisqu'elles dérivent de voies biosynthétiques typique et particulière (Botryococcènes pour l'algue botryococcus, Hopanes pour les bactéries, Stéroïdes pour certaines algues, ou les triterpènes pentacycliques pour les végétaux supérieurs...). Certains de ces biomarqueurs spécifiques, comme les alcénones et les tétraéthers lipidiques sont utilisés pour des *proxies* climatiques. Il s'agit de véritables paléothermomètres des eaux de surface dans lesquels les organismes sources ce sont développés (voire III-2-2).

L'analyse de ces molécules demande des compétences techniques qui peuvent paraître complexes pour des sédimentologues mais qui sont le quotidien d'un chimiste. L'identification et la quantification des différentes molécules sont réalisées par couplage d'un chromatographe en phase gazeuse (CPG) et d'un spectromètre de masse (SM). L'analyse se fait (1) sur les fractions lipidiques libres dont les différentes familles (acide gras, alcool, HC alyphatiques, cyclique et aromatique) sont préalablement séparées au laboratoire en chromatographie liquide ou (2) sur les pyrolysats de la fraction insoluble particulaire. Ces aspects de la géochimie organique associée aux études classiques de sédimentologie ont rendu possible l'établissement d'une véritable stratigraphie moléculaire.

III-2-2 Les biomarqueurs paléothermomètres :

La puissance analytique qu'offre la géochimie organique, appliquée aux archives sédimentaire, porte en germe la capacité de proposer des méthodes quantitatives de reconstitution de certaines conditions climatiques locales (températures des eaux, salinité, pression du CO₂, paléoproduktivité, conditions redox...) contribuant ainsi à la compréhension des systèmes régionaux où interagissent le climats et les cycles biogéochimiques et par la même occasion l'amélioration des modèles paléoclimatiques globaux. La prise de conscience des potentialités qu'offre cette discipline s'exprime par la présence de sessions spécialisés en paléoclimatologie et en paléoocéanographie des congrès internationaux en géochimie organique mais surtout d'une augmentation exponentiel des participants à ces sessions au fil des éditions.

La biogéochimie a déjà fourni deux paléothermomètres moléculaires des eaux de surface qui sont désormais utilisés en routine en domaine marin : les alcénones et le TEX₈₆. En domaine continental, ces outils sont en cours de calibration pour estimer les températures des eaux lacustres. Les alcénones sont des cétones à longue chaîne dont le degré d'insaturation varie en fonction de la température des eaux de croissance des organismes sources (principalement le coccolithophoridé *Emiliana huxleyi*). Différentes études de calibration ont permis de démontrer des relations linéaires entre le degré d'insaturation des alcénones (U_{37}^k) et la température des eaux de surface marines (Prahl et Wakeham, 1987). On ne compte plus les références bibliographiques traitant des alcénones et de leurs applications comme proxy de paléotempérature de surface de toutes les régions du monde. Parmi les laboratoires français qui ont excellé dans ce domaine, on citera le laboratoire de Géochimie et Paléocéanographie de E. Bard au CEREGE à Marseille, ou l'équipe *évolution du climat* du LSCE à Gif-sur-Yvette.

L'indice TEX₈₆ (Schouten, 2002) est fondé sur des molécules de types tétraéthers lipidiques : rigidifiant des membranes de Crénarchéotes (bactéries du picoplancton) dont les proportions varient en fonction de la température des eaux dans lesquelles ces organismes se sont développés.

Je co-dirige actuellement une thèse (Marcio Gurgel) s'intéressant de près à la mise en évidence de proxies de paléotempérature de surface sur des sédiments provenant de deux zones d'upwelling (Cabo Frio au Brésil et Callao pour le Pérou) et enregistrant l'évolution du climat depuis 12000 ans. Les résultats obtenus sur ces 12000 ans de sédiments provenant de part et d'autre de l'Amérique du Sud Tropicale ont déjà fait l'objet de plusieurs participations à des congrès nationaux et internationaux et des publications sont en cours de rédaction dans le cadre de la rédaction de cette thèse.

III-2-3- Les biomarqueurs et l'isotopie moléculaire: le D/H

La puissance analytique en géochimie organique a fait dernièrement un grand pas en avant grâce aux récents développements qui permettent la mesure des isotopes stables (du carbone ($d^{13}C$), voire de l'hydrogène (D/H)) spécifiquement sur chaque molécule. Ceci a été rendu possible grâce au couplage de la chromatographie suivie d'une interface de combustion-pyrolyse puis d'une spectrométrie isotopique (CPG-C-IRMS).

Le message isotopique du D/H enregistré par ces molécules témoigne de la quantité et de la charge isotopique de l'eau utilisée par l'organisme ainsi que des processus

métaboliques qui contrôlent leur synthèse. L'intérêt de cette méthode analytique, qui n'est qu'au début de son développement, est de pouvoir mesurer dans le même échantillon le D/H de marqueurs moléculaires spécifiques d'organismes qui se sont développés dans différents compartiments (eau lacustre ou marine, sol, bassin versant...) utilisant donc des sources différentes d'eau.

La calibration et les applications du D/H moléculaire pour reconstituer les variations du cycle hydrologique est l'une des préoccupations majeurs des isotopistes organiciens. Les premiers travaux sont assez récents (Sessions et *al.* ; 1999, Sauer et *al.* 2001 ; Zhang et Sachs ;2007) et montrent que le D/H de molécules organiques est l'expression exacte de celui des eaux dans lesquelles la biosynthèse organique est réalisée. Lors d'études de calibration sur des lacs nord-américains et européens, Huang et *al.* (2002) et Sachs et *al.* (2004) ont pu montrer que le D/H de différentes molécules capture celui des eaux météoriques et des eaux lacustres, en relation directe avec la température moyenne annuelle enregistré et l'évaporation.

Les travaux de Shuman et *al.* (2006) indiquent que cette approche permet également de reconstituer à la fois les précipitations hivernales et estivales en zone tempérée. En zone tropicale, le D/H de molécules produites par des végétaux supérieurs a été utilisé pour reconstituer les variations d'humidité en Amérique du Sud (Jacob et *al.*, 2007) et en Afrique (Schefuß et *al.*, 2005) durant le Quaternaire récent. Il faut noter que la mesure du D/H n'a été réalisée jusqu'à présent, que sur des molécules relativement communes (alcanes et acides gras). Deux exceptions notables sont apportées par les travaux de Andersen et *al.* (2001) et de Zhang et Sachs (2007) qui ont réalisé ces mesures sur des molécules spécifiques du phytoplancton marin et lacustre (alcénones et botryococcènes).

Avec ces deux derniers aspects pointus de la biogéochimie moléculaire (les paléothermomètres et l'isotopie moléculaires et ses applications diverses) des nouvelles perspectives de recherche s'ouvrent pour nous. La proposition de Projets de recherche utilisant la MO et ses *proxies* quantitatifs dans des problématiques de reconstitution des environnements et climats passés notamment à haute résolution est une évidence d'où découle le projet que je propose cinquième partie de ce mémoire.

Références citées dans la partie I :

- Andersen, N., Paul, H., Bernasconi, S.M., McKenzie, J.A., Behrens, A., Schaeffer, P. et Albrecht, P., (2001) Climate variability during Messinian salinity crisis: evidence from deuterium concentrations in individual biomarkers. *Geology*, 29, 799-802.
- Belhassine K., (2006) - Sédimentation organique subactuelle du système d'upwelling de la plateforme centrale du Pérou. Géochimie globale et pétrographie organique. Rapport de Master recherche, FluxEnv. Université d'Orléans, 40p.
- Boussafir M., Gelin F., Lallier-Vergès E., Derenne S., Bertrand P. & Largeau C. (1995b) - Electron microscopy and pyrolysis of kerogens from the Kimmeridge Clay Formation, UK : source organisms, preservation process and origin of microcycles. *Geochimica Cosmochimica Acta* 59, 3731-3747.
- Boussafir M., Laggoun-Défarge F., Derenne S. & Largeau C. (2000) - Bulk and pyrolytic studies of insoluble organic matter from Trittivakely lake sediments (Interglacial-like and last maximum glacial stages). *Applied Pyrolysis*, 2000, Sevilla, p. 107
- Boussafir M., Lallier-Vergès E., Bertrand P. & Badaut-Trauth D.(1994) - Structure ultrafine de la matière organique des roches mères du Kimméridgien du Yorkshire. *Bulletin de la Société Géologique de France*, t. 165, n°4, 355-363.
- Combaz A., 1980. *Les kérogènes vus au microscope*. In Kérogène – Insoluble Organic Matter from Sedimentary Rocks. B. Durand, édition Technips, Paris, 55-87.
- Copard Y. (2002) - Altération diagénétique et post-diagénétique (thermicité, oxydation) des charbons carbonifères du Massif Central français (Saint-Etienne, Graissessac et autres lieux). Thèse de l'Université d'Orléans 247p.
- Copard Y., Disnar J.-R., Becq-Giraudon J.-F., Boussafir M. (2000) - Evidence and effects of fluid circulation on organic matter in intramontane coalfields (Massif central, France). *International Journal Coal Geology*, 44, 49-68.
- Di-Giovanni Ch., Disnar J.R., Bichet V., Campy M. & Guillet B., 1998. *Geochemical characterization of soil organic matter and variability of a post detritical organic supply (Chaillexon lake, France)*. *Earth Surface Processes and Landforms*, 23, 1057-1069.
- Disnar, J. R., Guillet, B., Kérais, D., Di-Giovanni, C., (2003) - Soil organic matter (SOM) characterization by Rock-Eval pyrolysis: scope and limitations. *Organic Geochemistry*, Vol. 34, 327-343.
- Disnar, J. R., Guillet, B., Kérais, D., Massif, R. et Di-Giovanni, C., (2000) - Soil organic matter (SOM) characterization by Rock-Eval pyrolysis : main classical parameters. In "Entering the Third Millenium with a common approach to humic substances and organic matter in water, soil and sediments". Proc. IHSS 10. 2, 1211-1214. Progep, Toulouse.
- Durand B. et Nicaise G., (1980) – Procedures for kerogen isolation. In « Kerogen », B. Durand ed., Edition Technip, Paris, 35-52.
- Durand B., (2003) - A History of Organic Geochemistry *Oil & Gas Science and Technology Technip*, – Rev. *IFP*, Vol. 58 (2003), No. 2, 203-231.
- Espitalié, J., Deroo, G. et Marquis, F., (1985) - La pyrolyse Rock-Eval et ses applications; première partie. *Revue de l'Institut Français du Pétrole* 40, 563-579. Espitalié, J., Deroo, G. et Marquis, F., 1985b. La pyrolyse Rock-Eval et ses applications; deuxième partie. *Revue de l'Institut Français du Pétrole* 40, 755-784.
- Espitalié, J., Laporte, J.L., Madec, M., Marquis, F., Leplat, P., Paulet, J. et Boutefeu, A., (1977) - Méthode rapide de caractérisation des roches mères, de leur potentiel pétrolier et de leur degré d'évolution. *Revue de l'Institut Français du Pétrole* 32/1, 23-42.

- Huang, Y., Shuman, B., Wang, Y., Webb III, T., (2002) - Hydrogen isotope ratios of palmitic acid in lacustrine sediments record late Quaternary climate variations. *Geology* 30, 1103–1106.
- Huang, Y., Shuman, B., Wang, Y., Webb III, T., (2004) - Hydrogen isotope ratios of individual lipids in lake sediments as novel tracers of climatic and environmental change: a surface sediment test. *J. Paleolimnol.* 31, 363-375.
- Huang, Y., Street-Perrott, F.A., Perrott, F.A., Metzger, P., Eglinton, G., (1999) - Glacial-interglacial environmental changes inferred from the molecular and compound-specific $\delta^{13}\text{C}$ analyses of sediments from Sacred Lake, Mt. Kenya. *Geochim. Cosmochim. Ac.* 63, 1383–1404.
- Huc A.Y., Nederlof P., Debarre R., Carpentier B., Boussafir M., Laggoun-Défarge F. (2000) - Pyrobitumen occurrence and formation in a Cambro-Ordovician sandstone reservoir, Fahud Salt Basin, North Oman *Chemical Geology*, 168, 99-112.
- Jacob, J., (2003) - Enregistrement des variations paléoenvironnementales depuis 20000 ans dans le Nord Est du Brésil (Lac Caço) par les triterpènes et autres marqueurs organiques. Thèse de l'Université d'Orléans, 296p.
- Jacob, J., Disnar, J.R., Boussafir, M., Sifeddine, A., Albuquerque, A.L.S., Turcq, B., (2004) - Major environmental changes recorded by lacustrine sedimentary organic matter since the Last Glacial Maximum under the tropics (Lagoa do Caço, NE Brazil). *Palaeogeogr., Palaeoclim., Palaeoeco.* 205, 183-197.
- Jacob, J., Disnar, J.R., Boussafir, M., Sifeddine, A., Albuquerque, A.L.S., Turcq, B., (2005) - Pentacyclic triterpene methyl ethers in recent lacustrine sediments (Lagoa do Caço, Brazil). *Org. Geochem.* 36, 449-461.
- Jacob, J., Huang, Y., Disnar, J.R., Sifeddine, Boussafir, M., A., Albuquerque, A.L.S., Turcq, B., (2007) - Paleohydrological changes during the last deglaciation in Northern Brazil. *Quaternary Science Reviews* 26, 1004-1015.
- Lafargue, E., Marquis, F. et Pillot, D., (1998) - Rock- Eval 6 applications in hydrocarbon exploration, production, and soil contamination studies. *Revue de l'Institut Français du Pétrole* 53/4, 421– 437.
- Lallier-Vergès E., Sifeddine A., De Beaulieu J. L., Reille M., Tribouvillard N., Bertrand P., Mongenot T., Thouveny N., Disnar J.-R., Guillet B. (1993) - Sensibilité de la sédimentation organique aux variations climatiques du Tardi-Würm et de l'Holocène; le lac du Bouchet (Haute-Loire, France). *Bulletin de la Société Géologique de France* 164, 5, 661-673
- Meyers, P.A. et Lallier-Vergès, E., (1999) - Lacustrine sedimentary organic matter records of late quaternary paleoclimates. *Journal of Paleolimnology* 21, 345–372.
- Meyers, P.A., (2003) - Applications of organic geochemistry to paleolimnological reconstructions: a summary of examples from the Laurentian Great Lakes. *Organic Geochemistry* 34, 261-289.
- Noël, H., Brauer, A., Garbolino, E., Lallier-Vergès, E., de Beaulieu, J.L, Disnar, J.R., 2001. Sedimentary organic matter as a marker of soil erosion during the last millenia (Annecy Lake). *Journal of Paleolimnology*, 25, 229-244.
- Nzoussi P., Khamli N., Disnard J.-R., Laggoun-Défarge F., Boussafir M. (2005) - Cenomanian-Turonian organic sedimentation in North-Western Africa : a comparison between Tarfaya (Morocco) and Senegalo-Mauritanian (Senegal) Basins. *Sedimentary Geology*, 177, 3-4, 271-295.
- Odum E.P. (1971) - *Fundamentals of Ecology*, Philadelphia, W.B. Saunders Company, 3rd ed.
- Pailler D., Bard E., (2002) - High-frequency paleoceanographic changes during the past 140 000 years recorded by the organic matter in sediments off the Iberian Margin,

- Palaeogeogr. Palaeoclimatol. Palaeoecol. 181, 431–452.
- Prahl, F. G. et Wakeham, S. G., (1987) - Calibration of unsaturation patterns in long-chain ketone compositions for paleotemperature assessment. *Nature* 330, 367-369.
- Robert P., (1985) – Histoire géothermique et diagenèse organique. *Bulletin des centres de recherches exploration production- Elf-aquitaine*, 8, 345p
- Rosell-Mele A., Maslin M.A., Maxwell J.R., Schaeffer P., (1997) - Biomarker evidence for Heinrich events, *Geochim. Cosmochim. Acta* 61, 1671–1678.
- Sachse, D., Radtke J. et Gleixner, G., (2004) - Hydrogen isotope ratios of recent lacustrine sedimentary n-alkanes record modern climate variability. *Geochimica et Cosmochimica Acta* 68, 4877-4889.
- Sauer, P.E., Eglinton, T.I., Hayes, J.M., Schimmelmann, A. et Sessions, A.L., (2001) - Compound-specific D/H ratios of lipid biomarkers from sediments as a proxy for environmental and climatic conditions. *Geochimica et Cosmochimica Acta*, 65, 213-222.
- Schefuß, E., Schouten, S. et Schneider, R.R., (2005) - Climatic controls on central African hydrology during the past 20,000 years. *Nature* 437, 1003-1006.
- Schouten, S., Hopmans, E.C., Schefuß, E. et Sinninghe Damste, J.S., (2002) - Distributional variations in marine crenarchaeotal membrane lipids: a new tool for reconstructing ancient sea water temperatures? *EPSL* 204, 265-274.
- Sebag D., Disnar J.-R., Guillet B., Di Giovanni C., P. Verrecchia E., Durand A., (2006) - Monitoring organic matter dynamics in soil profiles by 'Rock-Eval pyrolysis' : bulk characterization and quantification of degradation. *European Journal of Soil Science* 57, 344
- Sessions, A.L., Burgoyne, T.W., Schimmelmann, A. et Hayes, J., (1999) - Fractionation of hydrogen isotopes in lipid biosynthesis. *Organic Geochemistry* 30, 119.
- Shuman, B., Huang, Y., Newby, P., Wang, Y., (2006) - Compound-specific isotopic analyses track changes in seasonal precipitation regimes in the Northeastern United States at ca 8200 cal yr BP. *Quat. Sci. Rev.* 25, 2992-3002.
- Sifeddine A., Bertrand P., Fournier M. B. P., Martin L., Servant M., Soubiès F., Suguio, K., Turcq, B. (1994) - La Sédimentation Organique Lacustre En Milieu Tropical Humide (Caraja, Amazonie Orientale, Bresil): Relation Avec Les Changements Climatiques Au Cours Des 60 000 Dernieres Annees.. *Bulletin de la Societe Geologique de France. Paris (Franca):* , 165, 6, 613 - 621,
- Sifeddine, A., Albuquerque, A.L.S., Ledru, M-P., Turcq, B., Knoppers, B., Martin, L., Zamboni de Mello, W., Passenau, H., Landim Dominguez, J.M., Campello Cordeiro, R., Abrao, J.J., Bittencourt, A.C., (2003) - A 21000 cal years paleoclimatic record from Caçó Lake, northern Brazil: evidence from sedimentary and pollen analyses. *Palaeogeogr., Palaeoclim., Palaeoeco.* 189, 25-34.
- Sifeddine, A., Bertaux, J., Mourguiart, Ph., Disnar, J.R., Laggoun-Défarge, F., (1998) - Etude de la sédimentation lacustre d'un site de forêt d'altitude des Andes centrales (Bolivie). *Implications Paléoclimatiques. B. Soc. Geol. Fr.* 169, 395-402.
- Sifeddine, A., Bertrand, Ph., Lallier-Vergès, E. et Patience, A., (1996) - The relationships between lacustrine organic sedimentation and palaeoclimatic variations. *Lac du Bouchet, Massif Central, France. Quaternary Science Reviews* 15, 203-211.
- Sifeddine, A., Martin, L., Turcq, B., Volkmer-Ribeiro, C., Soubiès, F., Campello Cordeiro, R., Suguio, K., (2001) - Variations of the Amazonian rainforest environment: a sedimentological record covering 30,000 years. *Palaeogeogr., Palaeoclim., Palaeoeco.* 168, 221-235.
- Zhang Z., Sachs J. P., (2007) - Hydrogen isotope fractionation in freshwater algae: I. Variations among lipids and species. *Organic Geochemistry*, 38, 4, 582-608

PARTIE II
MODES DE FOSSILISATION
DE LA MATIERE ORGANIQUE SEDIMENTAIRE

I – INTRODUCTION

Le devenir des Matières Organiques (MO) dans les environnements sédimentaires a depuis quelques dizaines d'années occupé une part importante de la communauté des organiciens. Les diverses études effectuées ont concerné des sédiments provenant de différents environnements naturels, aussi bien des séries anciennes (notamment pétrolières) que des séries plus récentes, d'âge quaternaire, lacustres et/ou marines. L'intérêt suscité par ces dernières est justifié par la nature et l'importance de la sédimentation organique de ces milieux tant pour leur intérêt économique (environnement favorable aux dépôts des MO pétrolières) que pour leur intérêt scientifique (diagenèse, environnements et climats passés). En effet, les milieux lacustres et les milieux marins d'upwelling présentent des conditions physico-chimiques favorables qui permettent une haute productivité organique et un enregistrement organo-sédimentaire d'une très bonne résolution temporelle. Cette partie du mémoire, s'intéressera au devenir de la MO après son dépôt et aux processus qui permettent sa fossilisation.

La plupart des environnements qui enregistrent une haute productivité organique sont propices au dépôt de sédiments organiques dès lors qu'une part de MO produite échappe à l'oxydation et à l'activité bactérienne, synonymes de dégradation. Les trois mécanismes, dégradation-recondensation, préservation sélective et sulfuration naturelle, sont aujourd'hui reconnus comme permettant une protection effective et durable des MO dans les environnements sédimentaires naturels. Leurs modes d'action, les facteurs contrôlant leur mise en place et leur stabilité au cours du temps, ont été plusieurs fois discutés et semblent à présent bien établis. Les premiers paragraphes de cette partie permettront de dresser un résumé des avancées scientifiques enregistrées dans ce domaine, dans ce champ disciplinaire que représentent l'origine et le mode de fossilisation « ou de préservation » de la MO sédimentaire. Les années 90 ont vu l'avènement d'une nouvelle hypothèse que représente le piégeage par les fractions minérales, et plus spécifiquement les argiles. L'intégration des interactions organo-minérales comme mécanisme de préservation effectif, reste encore discutée. Les premiers résultats, preuves de l'efficacité de l'adsorption minérale, sont résumés plus loin. Je finirai, ce premier chapitre par les résultats obtenus sur le rôle des fractions minérales et notamment argileuses dans la préservation de la MOS (thèse de Sylvain Drouin soutenue en Juin 2007).

II- LES MECANISMES DE « PRESERVATION » DE LA MO PETROLIGENE

Plusieurs travaux dont de nombreuses thèses ont été menés au cours des 20 dernières années sur le devenir de la matière organique (MO) dans les environnements sédimentaires. Le premier objectif était de comprendre par quels mécanismes, la MO produite dans les différents écosystèmes de la surface de la Terre, pouvait partiellement échapper à son destin biologique : la biodégradation et au-delà, la minéralisation en CO₂ et H₂O. Le deuxième était de comprendre comment certaines de ces MO, particulièrement les MO aquatiques, pouvaient par la même occasion, conserver ou acquérir une certaine qualité pétroligène, et former *in fine* des kérogènes riches en composés hydrocarbonés. Les développements dans ce domaine étaient liés aux questionnements de l'exploration pétrolière. En effet, l'une des préoccupations des pétroliers était de comprendre le mode de formation des roches mères pétroligènes et de relier leurs textures et leur composition à leur qualité hydrocarbonée et donc leurs potentiels en hydrocarbures.

Dans ce domaine, les équipes américaines, contrairement aux équipes européennes, ont essentiellement abordé les aspects dégradation et recyclage et beaucoup moins le point de vue préservation. Ces deux approches sont complémentaires dans le traitement du sujet « transfert et fossilisation du matériel organique vers les sédiments ». Ci-dessous, est présenté un résumé exhaustif des connaissances sur les deux aspects : aspect diagenèse et recyclage puis les aspects de préservation pour lesquels la contribution vient essentiellement de la communauté scientifique européenne.

II-1 La diagenèse précoce et le recyclage de la MO

L'ensemble des études montre que plus de 90% de la MO primaire qui se développe dans la zone photique est consommée par les organismes brouteurs et les bactéries avant d'atteindre le sédiment (Menzel, 1974). Elle est dégradée au cours de son transfert dans la colonne d'eau principalement par oxydation dans la zone oxiqne et sulfato-réduction dans la zone anoxique (Jørgensen, 1982). Dans une moindre mesure, elle peut-être détruite par dénitrification, méthanogenèse ou lors de la réduction des oxydes de fer et de manganèse.

L'oxydation conduit à la minéralisation de tout ou partie de la MO et permet la libération de MO particulières et dissoutes. L'oxydation est contrôlée en tout premier lieu par la teneur en oxygène dissous des eaux mais également par l'intensité de l'activité biologique bactérienne et zooplanctonique. Ainsi lors du broutage, la destruction de la MO primaire à la fois par l'action enzymatique et mécanique, aide à la décomposition aérobie (Huc, 1988a).

Les processus de sulfato-réduction agissent dès épuisement de l'oxygène dissous du milieu. Ils sont contrôlés par l'activité anaérobie des bactéries qui tirent leur énergie de ce processus chimique. L'eau de mer fournit les sulfates nécessaires à la sulfato-réduction. Les sulfures libérés dans la colonne d'eau vont s'associer aux métaux réactifs pour former des sulfures métalliques (Berner, 1964a et b) ou être incorporés dans la MO (Westrich et Berner, 1984). Ils peuvent également se dissocier en H^+ et HS^- au contact de la zone oxygène, et participer ainsi à l'abaissement du pH qui favorise la dissolution des carbonates.

Des études *in situ* ont démontré que sulfato-réduction et oxydation avaient le même potentiel de dégradation de MO (Jørgensen, 1982), dès lors que les flux organiques étaient importants (Dauwe et al., 2001).

Les cinétiques de dégradation dans les colonnes d'eau lacustres et marines sont contrôlées par de nombreux facteurs touchant à la fois aux propriétés intrinsèques des MO et aux caractéristiques du milieu.

Ainsi, parmi les propriétés intrinsèques, la composition chimique des MO joue un rôle prépondérant. Certaines MO, biorésistantes, présentent un caractère réfractaire aux agents agresseurs. A l'opposé, des MO labiles seront métabolisées au cours du recyclage zooplanctonique et bactérien (Cauwet, 1981). De même, plus le matériel organique est jeune, plus celui-ci est rapidement et efficacement dégradé (Keil et al., 1994). La dégradation moindre de la MO plus ancienne s'explique par une probable concentration des composés réfractaires. La densité (Sturm and Matter, 1978) et dans une moindre mesure, la forme des MO particulières influencent également leur devenir dans les colonnes d'eau. Une MO de faible densité et/ou présentant une forme plate sédimentant plus lentement, restera plus longtemps en suspension et sera donc plus rapidement dégradée qu'une grosse particule plus dense et/ou sphérique. La formation d'agrégats par fixation sur des surfaces minérales ou incorporation dans des pelotes fécales sont autant de processus à même d'augmenter les vitesses de décantation des MO et donc de réduire leur temps de transfert dans les colonnes d'eau (Wackeham et al., 1984a et b). De même les mucilages organiques jouent un rôle prépondérant dans les vitesses d'exportation des MO vers les sédiments (Alldredge et Gotschalk, 1989). En ce sens, ces processus participent également à une meilleure préservation des MO. La formation des floccs organiques des agrégats organo-minéraux est conditionnée par le taux de production phytoplanctonique, la taille des organismes et les conditions physico-chimiques du milieu (Jackson, 1990).

Parmi les caractéristiques du milieu influençant l'intensité de la dégradation des MO, on compte la morphologie du bassin et le degré d'oxygénation de la colonne d'eau. Plus le bassin est profond, plus les temps de transfert depuis la zone de production primaire

jusqu'au sédiment sont longs, et les risques de recyclage importants (Degens et Mopper, 1975). Le degré d'oxygénation est également un paramètre essentiel. Il contraint la zone d'action des processus physico-chimiques de dégradation par oxydation. L'hydrodynamisme et le degré de stratification de la colonne d'eau sont deux autres paramètres susceptibles d'influer sur le taux de dégradation de la matière organique. Ces facteurs affectent principalement le devenir des MOS dissoutes et particulaires de petite taille. Ils s'opposent l'un l'autre si bien que la naissance d'un courant dans un milieu stratifié, crée un gradient horizontal de pression mettant en mouvement le fluide et les éléments fins qu'il porte (Bournet, 1996). On distingue différents types de mouvements convectifs selon leur origine. On différencie les courants de densité, liés soit au réchauffement différentiel des eaux soit à l'impact d'un affluent, des courants liés aux vents et aux ondes internes. Si leur zone d'action ne sont pas les mêmes, leurs effets sur les MO sont identiques. Ils conduisent généralement à une augmentation des temps de rétention des MO et à la réoxygénation des couches profondes de la colonne d'eau. Les stratifications des colonnes d'eau ont différentes origines et diffèrent en fonction du milieu, marin ou lacustre. En milieu lacustre, la principale stratification est d'origine thermique. Elle résulte d'un contraste de densité des eaux, fonction de leur température (Hutchinson, 1957). En milieu marin se créent essentiellement des stratifications chimiques, dues à des contrastes de compositions découlant parfois de l'activité biologique. Les stratifications agissent telles des trappes à sédiments en maintenant en suspension les MO dissoutes et les particules organiques les plus fines (Sturm and Matter, 1972, 1978). Tous ces paramètres biologiques, physicochimique et hydrodynamique agissent de concert et influencent directement les flux de MO exporté ainsi que les processus expliquant sa non dégradation et donc au final sa préservation.

Ce terme « préservation » de la MO n'a pas toujours fait l'unanimité quant à son exacte signification. Il peut en effet être ambigu, car quand les géochimistes organiciens raisonnent en terme de préservation à l'échelle moléculaire, les pétrographes se fondent sur les observations des structures biologiques apparentes. De leur côté, les sédimentologues parlent du carbone organique préservé par comparaison au carbone organique recyclé. Ce carbone correspond alors à la totalité de la MO accumulée quelle que soit sa qualité de préservation. Par exemple, l'inertinite, un macéral ligno-cellulosique complètement oxydé, composant des charbons humiques, est pour le pétrographe un type de MO dont les structures biologiques sont bien préservées même si son potentiel pétrologène est quasi négligeable et donc inerte. Pour le géochimiste notamment dans la recherche pétrolière, une matière organique est bien préservée lorsqu'elle possède un potentiel élevé en hydrocarbures.

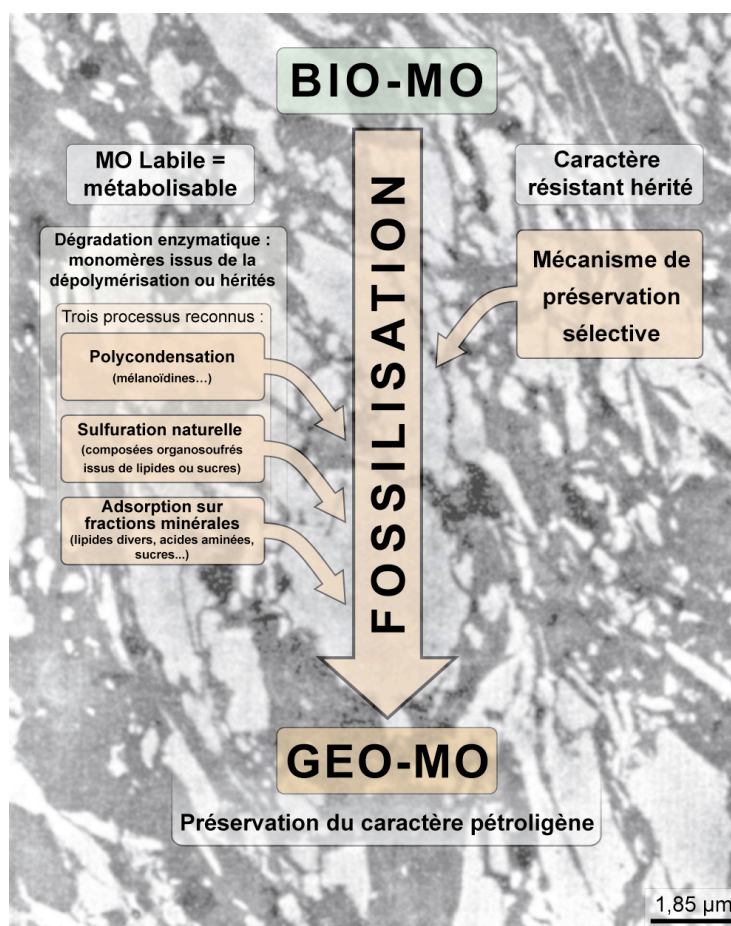
II-2 La préservation de la MO pétrologène

Le terme de « préservation » pour la plupart des organiciens peut être assimilé à celui de « fossilisation » de la MO. Il concerne tout composant organique échappant au recyclage et à l'action des processus qui interviennent pendant toutes les étapes de la diagenèse organique depuis la mort de l'organisme jusqu'à la fossilisation sous forme de kérogène.

Les connaissances dans le domaine de la préservation de la MO se sont accrues pendant les deux dernières décennies, grâce notamment aux approches multidisciplinaires et à l'utilisation de méthodes d'analyses pointues, comme la microscopie électronique à transmission et son association systématique avec les techniques de la biogéochimie moléculaire. Ce couplage a permis l'analyse directe des fractions organiques sédimentaires observées classiquement en pétrographie photonique et de relier à une texture ultrafine caractérisée au MET, une composition moléculaire spécifique. On associa ainsi à chacune de ces fractions l'un des mécanismes de préservation reconnue.

Pour s'accumuler, les constituants de la matière organique sédimentaire doivent être préservés de la biodégradation, c'est-à-dire échapper à l'action enzymatique et oxydante combinée des organismes brouteurs et des microorganismes bactériens. Différents mécanismes peuvent intervenir et n'agissent pas de façon identique sur tous les constituants en raison de la variété de leurs compositions moléculaires originelles. Il est donc facile de comprendre que de la structure chimique des constituants d'une biomasse donnée va dépendre son potentiel de préservation (Figure II-1). Cette nature et composition des producteurs vont de pair avec les conditions du milieu de dépôts et influencent directement la qualité et la quantité de MO incorporée dans le sédiment. Les différentes études menées montrent que toutes les MO ne sont pas égalitaires devant la dégradation. Si certaines MO possèdent des propriétés intrinsèques qui leur confèrent une résistance naturelle à la dégradation (processus de préservation sélective), d'autres MO potentiellement métabolisable, vont acquérir cette biorésistance après des processus diagénétiques physico-chimiques modifiant leur texture et leur composition comme le mécanisme de dégradation suivie de la polycondensation ou de sulfuration naturelle.

Ci-dessous une synthèse bibliographique, comprenant les travaux que j'ai effectué au sein de l'équipe MO à Orléans, sur les mécanismes impliqués dans la préservation de la MO sédimentaire.



MO nanoscopiquement amorphe observée au MET, argiles du Kimméridgien du Yorkshire (GB). M. Boussafir

Figure II-1 : De la nature des biomasses (BIO-MO) et des conditions du milieu de dépôt dépendent la qualité et la quantité de MO incorporée dans le sédiment (GEO-MO). Toutes les MO n'ont pas la même réactivité à la dégradation. Si certaines MO possèdent des propriétés intrinsèques qui leur confèrent une résistance naturelle (processus de préservation sélective), d'autres MO vont acquérir cette biorésistance après des processus chimiques de modification de leur composition (mécanisme de dégradation – recondensation ; sulfuration naturelle).

II-2-1 Les différents mécanismes de fossilisation

II-2-1-1 Le mécanisme de dégradation-recondensation

Il a été reconnu dans les études pionnières et a longtemps été considéré comme étant le seul processus majeur impliqué dans la formation du kérogène. Ce processus de préservation de la MO s'intègre dans le modèle de Tissot et Welte (1984) qui conduit à la formation du kérogène. Selon ce modèle, le kérogène est défini comme le résultat de

réactions de polymérisation et recondensation des produits de dégradation de biopolymères métabolisables. L'action enzymatique des bactéries sur les protéines et les polysaccharides conduit à leur fragmentation en monomères (acides aminés et sucres). Pour partie, les monomères sont détruits, mais par des processus de recombinaison aléatoire selon des réactions de polycondensation de type Maillard (Maillard, 1913) certains forment des géopolymères, appelés mélanoïdines. Les recombinaisons multiples contribuent à la formation de mélanoïdes à l'insolubilité et l'inertie croissantes conduisant à la formation du géopolymères, briques élémentaires du kérogène. Les produits organiques labiles préservés par dégradation-recondensation se caractérisent donc par un aspect amorphe et par l'absence de structures biologiques en microscopie électronique à transmission. Les spectres de pyrolyse de ces géopolymères sont pauvres, et dominés par des produits phénoliques et furanniques (Boon et *al.*, 1984).

Les lipides sont pour l'essentiel exclus de ces processus de préservation même si des travaux ont démontré qu'ils peuvent s'incorporer aux mélanoïdes (Larter et Douglas, 1980; Rubinsztain et *al.*, 1986a, b).

Initialement définis dans des roches mères anciennes, des produits organiques particuliers et dissous issus de processus de dégradation-recondensation ont été décrits dans des sédiments récents d'upwelling (Zegouagh et *al.*, 1999) et dans des colonnes d'eau, (van Heemst et *al.*, 1993; Peulvé et *al.*, 1996). Ce processus ayant un très faible rendement ne peut expliquer, à lui seul, la formation et l'existence de roches sédimentaires très riches en MO.

II-2-1-2 Le mécanisme de préservation sélective :

La découverte de roches constituées d'accumulation de microfossiles organiques, comme les torbanites où la MO est principalement composée de restes fossiles de la microalgue coloniale *Botryococcus braunii*, a conduit à envisager un second mécanisme de préservation (Largeau et *al.*, 1984, 1986) : la préservation sélective. Ce mécanisme est basé sur la présence dans certains organismes de biomacromolécules (non-hydrolysable) présentant une résistance extrêmement forte aux dégradations chimiques et microbiennes (Tegelaar et *al.*, 1989). Au même moment l'observation au microscope électronique à transmission de restes de structures membranaires algaires, appelé dès lors « ultralaminae », ont été mises en évidence dans des roches mères (Raynaud et *al.*, 1989). L'étude de ces membranes a montré leur résistance à l'hydrolyse, et aux attaques bactériennes, suggérant qu'il s'agit d'un héritage direct de membranes cellulaires (Raynaud et *al.*, 1989). En effet, l'étude de diverses microalgues actuelles (*Botryococcus braunii*, *Scenedesmus quadricauda*, *Scenedesmus communis*, *Chlorella fusca*...) par des méthodes

spectroscopiques (RMN¹³C à l'état solide, IRTF), pyrolytiques et microscopiques (microscopie électronique à balayage et à transmission) a montré que les parois externes de ces organismes sont constituées de biopolymères résistants, non hydrolysables, appelés algaenanes (Berkaloff et *al.*, 1984 ; Kadouri et *al.*, 1988 ; Derenne et *al.*, 1989, 1991, 1992a). Ces biopolymères, intrinsèquement résistants aux dégradations bactériennes et physico-chimiques sont sélectivement préservés dans le sédiment, contrairement aux contenus cellulaires correspondant à du matériel organique labile et donc facilement dégradé (Largeau et *al.*, 1986 ; Derenne et *al.*, 1991).

Certaines caractéristiques morphologiques de ces microalgues vont se retrouver dans la MO sédimentaire (Largeau et *al.* 1990a), elles sont fonction de l'épaisseur de la paroi. Les parois épaisses (environ 200 nm) de *Botryococcus braunii* conservent la morphologie des colonies, expliquant l'observation de microfossiles dans les torbanites. Dans le cas d'algues à parois fines (de 10 à 30 nm), la forme des cellules n'est plus reconnaissable, les parois s'accolent en faisceaux appelés ultralaminae. Ces structures ont été par la suite observées en MET dans un grand nombre de kérogènes qui étaient jusqu'alors considérés comme amorphes en microscopie photonique (Largeau et *al.*, 1990b ; Boussafir et *al.*, 1995, 1997)

Les algaenanes sont caractérisées par une structure chimique hautement aliphatique. Ces biopolymères (Tegelaar et *al.*, 1989), possédant un caractère biorésistant, préservent leur propriétés chimiques et morphologiques lors des processus de diagenèse (Largeau et *al.*, 1986). L'analyse moléculaire combinée d'ultralaminae fossiles, provenant des gisements lacustres de Rundle Oil Shale et Green River Shale, et de phytoplanctons actuels à parois externes (Derenne et *al.*, 1991) a souligné, outre une distribution bimodale des n-alkylnitriles similaire, prouvant leur lien de parenté, la présence de biopolymères aliphatiques. La distribution de cette série reflète l'origine lacustre ou marine des organismes sources (Derenne et *al.*, 1992b). Leur pyrolyse libère des groupements de type n-alkylnitriles dérivant du clivage thermique et de la déshydratation des fonctions azotées pré-existantes dans les parois des algues chlorophycées (Derenne et *al.*, 1991), ainsi que n-alkanones, par clivage thermique des ponts alkyl-O-C entre chaînes (CH₂)_n avec des distributions variant en fonction des espèces d'algues chlorophycées analysées (Derenne et *al.*, 1992). Il est donc possible de retrouver la nature de la MO résistante, à l'origine de la genèse du kérogène, par l'étude des produits de pyrolyse (Derenne et *al.*, 1992). Les kérogènes issus de ce mécanisme par préservation sélective des macromolécules résistantes se caractérisent donc par un certain nombre de traits morphologiques parfois associés à une signature chimique particulière. Selon le genre et l'espèce de l'algue considérée, les polymères résistants localisés dans les parois peuvent représenter jusqu'à 33% de la biomasse totale. Ce processus se caractérise par un meilleur rendement que le processus de dégradation-

recondensation puisqu'une part importante de la biomasse de départ est préservée (Largeau et Derenne, 1993).

Outre les ultralaminae dont la structure est microscopiquement conservée mais non discernable en microscopie optique, on trouve également d'autres types de MO sélectivement préservés. Les cuticules, spores, pollens et tissus subérisés de certaines plantes supérieures terrestres sont également préservés de manière sélective lors des processus de dégradation organique (Tegelaar et al., 1989, Boussafir 1994, Boussafir et al. 1995, 1997). Ces composés organiques sont intégralement fossilisés. Les structures biologiques et chimiques sont préservées et s'observent en microscopie optique. Ces MO sélectivement préservées s'observent dans les sédiments marins prioritairement lorsque la production organique du milieu est faible, et fortement dégradée (Boussafir et al., 1997).

Enfin il existe un dernier type de MO sélectivement préservée lors des processus de dégradation organique. Ces MO sont le fruit de réorganisations de macromolécules biorésistantes. Aucune structure biologique n'est conservée si bien que la MO est nanoscopiquement amorphe. On parle alors de MO diffuse amorphe (Boussafir et al., 1997).

II-2-1-3 Le mécanisme de sulfuration naturelle

Les deux mécanismes décrits précédemment ne permettent pas d'expliquer la présence d'unités organo-soufrées, contenant par exemple des thiophènes, dans de nombreux kérogènes (par exemple, Sinninghe Damsté et al., 1989 ; Schaeffer et al., 1995). Les teneurs en soufre organique de certains sédiments, remarquables au regard des concentrations présentes dans la biomasse (rapport S_{org}/C jusqu'à 0,1 dans les sédiments contre moins de 0,03 dans la biomasse), ont mis en évidence le rôle majeur du soufre dans la préservation des MO sédimentaires (Francois, 1987).

Une réaction entre le soufre inorganique et la MO a été mise en évidence par de nombreux auteurs (par exemple Nissenbaum et Kaplan, 1972), bien que le mécanisme d'incorporation du soufre dans des lipides soit encore mal connu. Il apparaît toutefois que seules certaines classes de lipides fonctionnalisés comme les hydrocarbures insaturés, les cétones et les aldéhydes, ainsi que les sucres, réagissent avec le soufre élémentaire et/ou H_2S pour former des composés organo-soufrés (COS) (Schouten et al., 1994). Basé sur la nature des COS obtenus dans des simulations ou observés dans la nature, deux modes d'incorporation du soufre dans les lipides ont été proposés : intermoléculaire et intramoléculaire (Sinninghe Damsté et al., 1989). La sulfuration naturelle consiste donc en l'incorporation de soufre dans la structure interne de la molécule ou entre les molécules organiques lipidiques. Dans les deux cas, le soufre est assimilé au niveau des insaturations. Dans le cas d'une incorporation intramoléculaire, il permet la formation de molécules

cycliques soufrées du type thiophènes ou thiolanes (Sinninghe Damsté et de Leeuw, 1990). Dans le cas d'une incorporation intermoléculaire, le soufre permet d'augmenter le poids moléculaire des lipides par la formation de macromolécules. Il a été montré que cette incorporation du soufre a lieu à un stade précoce de la diagenèse organique (par exemple Aizenshtat et Stoler, 1983 ; Lallier-Vergès et *al.*, 1997, Boussafir et *al.*, 1994, 1995, 1997). Différents auteurs ont ainsi détecté de nombreux produits soufrés dérivés de ce processus dans des sédiments récents (par exemple Aizenshtat et Stoler, 1983).

La sulfuration naturelle est contrôlée par l'activité des bactéries sulfato-réductrices en milieu anoxique (Boussafir et *al.* 1995, 1997 ; Mongenot et *al.*, 1997, Ribouleau et *al.* 2000). Elle nécessite donc l'apport massif de MO métabolisable (Boussafir 1994 ; Tribovillard et *al.*, 1994). En contrepartie de cette dégradation le métabolisme des bactéries réduit les sulfates de l'eau et produit des sulfures. Ces derniers sous forme de HS^- et H_2S sont massivement libérés, et sont consommés soit par la précipitation de sulfure de fer (processus de pyritisation, Sinninghe Damsté et de Leeuw, 1990), soit par sa dissémination dans la masse d'eau, soit lors des réactions de sulfuration des MO en réagissant avec les lipides fonctionnalisés présents dans le milieu. Les résultats obtenus sur les formations du Kimméridgien ont montré que la limitation en fer favorise et accentue l'incorporation du soufre dans la MO métabolisable (Boussafir et *al.*, 1995). En effet, en présence de fer, H_2S formera préférentiellement des sulfures de fer en raison de la grande affinité de cet élément pour le soufre. Les environnements dans lesquels le mécanisme de sulfuration se met en place sont caractérisés par des degrés de pyritisation ($\text{S pyritique} / \text{S total}$) proches de 1, signe que la teneur en fer est le facteur limitant la synthèse de la pyrite (Lallier-Vergès et *al.* 1993 ; Tribovillard et *al.*, 1994; Mongenot et *al.*, 1997). Ce processus de préservation est accéléré dans les milieux aquatiques euxiniques, milieux dans lesquels l'absence de circulation verticale d'eau interdit le renouvellement des eaux profondes, et donc leur oxygénation.

Alors que le processus de préservation sélective permet à la MO d'échapper à la minéralisation, même dans des conditions oxiques et avec ou sans productivité primaire importante, ce processus ne peut se développer que si l'environnement est anoxique et si des bactéries sulfato-réductrices prolifèrent en raison d'un apport accru de MO labile, donc facilement métabolisable (Boussafir et *al.*, 1994, 1995, 1997). Ce processus est d'autant plus important que la productivité primaire est importante.

D'un point de vue pétrologène, les MO préservées par sulfuration se caractérisent par des valeurs d'indice d'hydrogène (IH) élevées, autour de 800-900 mg d'hydrocarbure par gramme de carbone organique total (mg HC/g COT) et par la présence de composés organo-soufrés dans les produits de pyrolyse. Elles apparaissent amorphes gélifiées

oranges en microscopie optique et amorphe en microscopie électronique à transmission (Boussafir et *al.*, 1995; Mongenot et *al.*, 1999).

II-2-2 Le mécanisme de "protection par adsorption"

Plusieurs études concevaient déjà que le gain de masse généré par la formation de complexes organo-minéraux, participait indirectement à la préservation des MO, en permettant de réduire leur temps de transfert dans les colonnes d'eau (Wackeham, 1984a et b; Jackson et *al.*, 1990). Au-delà de ce rôle secondaire, des indices plus ou moins directs soulignant la corrélation qui lie les fractions organiques et minérales dans des sédiments, ont conduit à conclure que les interactions argilo-organiques pourraient offrir aux MO labiles une protection active face aux agents de dégradation (Mayer, 1994; Keil et *al.*, 1994). Quelques travaux ont par la suite cherché à caractériser plus en détail les relations argilo-organiques dans des sédiments naturels ou à modéliser les processus d'interaction par des études en laboratoire, afin d'en comprendre leurs principes et d'appréhender leur rôle dans le cycle du carbone organique. Cependant ces travaux ont trop souvent fondé leurs conclusions sur l'étude des seuls sédiments, en délaissant une analyse complète des processus d'interaction depuis les zones de production des MO où elles sont susceptibles d'être piégées jusqu'à leur préservation. De même, l'implication de la phase minérale dans la protection des MO reste encore aujourd'hui relativement mal comprise. Tout juste est-il supposé que le piégeage des molécules organiques permet de réduire leur disponibilité à la dégradation bactérienne (Sugai et Henrichs, 1992; Mayer, 1994; Hedges and Keil, 1995).

Bien que permettant d'expliquer la formation de nombreuses roches-mères, les mécanismes décrits ci-dessus ne rendent pas compte de l'association préférentielle de la MO sédimentaire avec des sédiments de faible granulométrie observée depuis de nombreuses années (par exemple Premuzic et *al.*, 1982 et Romankevich, 1984). Des mécanismes de préservation de la MO par les minéraux sont cependant envisagés depuis une cinquantaine d'années, puisque dès 1942, Ensminger et Gieseking ont proposé une adsorption interfoliaire dans les argiles gonflantes. En 1990, van Veen et Kuikman ont proposé une protection dans des pores interparticulaires, suffisamment petits pour exclure les cellules bactériennes. Ces hypothèses n'ont cependant pas pu être démontrés.

La teneur en carbone organique dans les sédiments montre en général une baisse de la concentration en Corg à partir de l'interface eau-sédiment jusqu'à un niveau dit "réfractaire" (Bernier, 1982, Henrichs et Reeburgh, 1987 ; Mayer, 1994a). L'existence d'une relation entre la surface spécifique des minéraux et la concentration en Corg a montré que ce niveau dit "réfractaire" correspond à l'équivalent d'une couverture monomoléculaire (monolayer équivalent, ME) (Weiler et Mills, 1965, Suess, 1973 ; Tanoue et Handa, 1979 ; Mayer 1994a, b). Dans une étude portant sur un grand nombre d'échantillons issus

d'environnements et de lieux géographiques divers, Mayer (1994b), étend ce résultat à tous les sédiments aluminosilicatés des plateformes continentales recevant un apport modéré en MO (donc en dehors des embouchures de rivière et des upwellings) et non surmontés par une colonne d'eau appauvrie en oxygène. Ces derniers présentent des couvertures supérieures à la monocouche, soit du fait de l'établissement d'un équilibre avec les eaux interstitielles riches en MO dissoute, soit grâce au temps d'exposition très bref à l'oxygène, permettant la préservation de composés organiques sensibles à l'oxygène tels que les pigments et les lipides insaturés. Par contre, les sédiments déposés dans des environnements à faible apport et/ou à fort taux de pénétration de l'oxygène, telles que les eaux profondes ou les talus continentaux et les sommets des turbidites, présentent un taux de couverture inférieur à la monocouche.

Diverses études ont montré que la surface des minéraux était très supérieure à celle attendue par la taille des grains, du fait de leur rugosité. Cette surface serait constituée en majeure partie de pores, de diamètre moyen inférieur à 8 nm (Weiler et Mills 1965 ; Groenland et Mott, 1978 ; Titley, 1987, Murray et Quirk, 1990a, b ; Mayer, 1994a).

La confrontation de la relation surface des minéraux-concentration en Corg avec la nature des surfaces minérales, ajoutée au fait que 90% de la MO ne peut pas être séparée physiquement de sa matrice minérale (Mayer, 1993 ; Keil et *al.*, 1994a, b), a amené Mayer (1994a, b) à proposer que les composés organiques étaient adsorbés dans les mésopores suffisamment petits pour exclure les enzymes hydrolytiques, et donc protéger la MO des attaques biologiques.

De plus, l'adsorption dans de petits pores favorise la condensation. En effet, tout d'abord, Wächtershäuser (1988) a montré que certaines réactions de condensation sont favorisées à la fois cinétiquement et thermodynamiquement lorsque les réactifs sont adsorbés. Les réactions de condensation ont le temps de se produire, puisque la compétition des réactions biologiques (plus rapides) est écartée (Collins et *al.*, 1995).

Alors qu'il était généralement admis que la ME était composée de MO réfractaire, Keil et *al.* (1994) ont montré que lorsque l'on désorbe de la MO et qu'on la met en présence de la faune bactérienne présente dans la colonne d'eau au-dessus du prélèvement, 70% de la MO désorbée, soit 17% à 45% de la MO totale est reminéralisée en 6 jours, les sédiments ayant jusqu'à 500 ans. Une grande partie de la MO sédimentaire est donc hautement réactive et uniquement préservée par son environnement. Des résultats similaires avaient été obtenus sur des composés monomériques tels que les acides aminés (Henrichs et Sugai, 1993 ; Wang et Lee, 1993). Par contre, des polymères adsorbés tels que les protéines sont soit préservés, soit dégradés plus rapidement (Marshman et Marshall, 1981). En fait, l'effet des associations MO-minéraux sur la réactivité de la MO face aux agresseurs chimiques et

biologiques, tels que lors des processus de dégradation oxygénée lente des sédiments profonds et des turbidites est encore à élucider (Hedges et Keil, 1995).

L'adsorption est généralement réversible, mais des travaux de Mayer (1993) et de Keil et *al.* (1994) ont montré que, dans des sédiments récents, plus de 90% de la MO ne peut pas être physiquement séparée de sa matrice minérale. Cette adsorption est à la fois influencée par la nature de la MO (Zullig et Morse, 1988) et les minéraux (Pinck et *al.*, 1954 ; Kobayashi et Aomine, 1967 ; Greaves et Wilson, 1973 ; Lorenz et Wackemagel, 1987). Il a été de plus montré que l'adsorption pouvait se produire à la surface de composés organiques. En effet, les substances humiques sont riches en sites chargés négativement (Parks, 1975 ; Schnitzer et Khan, 1972) avec lesquels peuvent réagir les composés chargés positivement. Rosenfeld (1979) a montré sur un sédiment argileux que l'adsorption cessait après traitement au peroxyde, suggérant que la MO servait de support à l'adsorption.

Des études en microscopie électronique de sédiments actuels de plateformes ont été effectuées (Ransom et *al.*, 1998) afin de tester la validité de ce mécanisme. Des observations *in situ* en MET de la MO de marges continentales (Ransom et *al.*, 1997,1998) ont montré que dans ces sédiments récents, la MO apparaît exclusivement associée aux domaines riches en argiles, mais il n'a pas été observé d'enrobage organique des grains minéraux, infirmant ainsi l'hypothèse de l'adsorption en monocouches, même si le principe de protection et de préservation des MO par les minéraux n'est pas remis en question

Cependant il reste de nombreuses inconnues comme la quantité de produits effectivement adsorbés, leur nature, la nature des liaisons chimiques, la dynamique des échanges entre la MO dissoute des eaux interstitielles et la phase solide...etc. Les travaux réalisés dans ce domaine sont fragmentaires et montrent que le champ d'investigation reste assez large. Pour cette problématique l'association des compétences dans le domaine de la géochimie et de la pétrographie organique et des compétences en minéralogie et cristallographie des fractions phyllosilicatées, devient indispensable. J'ai effectué des travaux plus récents dans ce domaine, à l'Institut des Sciences de la Terre d'Orléans. Ces travaux réalisés en grande partie dans le cadre de la thèse de Sylvain Drouin, associent ces compétences et expérimentent ce phénomène au laboratoire et en milieux naturels lacustres et marins. Les premiers résultats (Drouin 2006) minimisent le rôle de la capacité d'échange cationique des argiles, excluent toute intercalation de MO dans l'espace interfoliaire et proposent des liaisons chimiques possibles entre les deux phases minérales et organiques. Une sélectivité organique de l'adsorption a été également mise en évidence en fonction du type d'argiles. Des saponites de synthèse montre que quand la charge de surface de l'argile est faible l'adsorption est plus efficace en termes de carbone organique et favorise les molécules de grande taille notamment aliphatiques contrairement à la même saponite de plus haute charge.

III- COUPLAGE DE LA GEOCHIMIE MOLECULAIRE ET DE LA MICROSCOPIE ELECTRONIQUE A TRANSMISSION DANS L'ETUDE DES MOS

Les travaux que j'ai pu réaliser au cours de ces dernières années de recherche, notamment par la participation à l'encadrement d'étudiants orléanais et non-orléanais, ont permis de proposer des modèles de formation des MO dans ce débat animé que représentaient les mécanismes de préservation de la MO pétrologène. Ces travaux ont pour une grande part associé les études pétrographiques à différentes échelles d'observations et notamment ultrastructurales à l'analyse moléculaire du kérogène. Les résultats par thèmes abordés sont résumés ici. Les publications que j'ai choisi pour illustrer ce thème sont regroupées par ordre chronologique en annexes (ANNEXES 1, 2, 3, 4, 5, 6, 7 et 10).

III-1 La préservation des MO des argiles du Kimméridgien (la thèse et l'après thèse)

Les travaux que j'ai réalisés sur la formation des argiles kimméridgiennes (KCF) ont montré qu'elles présentent en grande majorité une fraction organique totalement amorphe même à l'échelle nanoscopique (Boussafir et al., 1994). La géochimie moléculaire a révélé des proportions relativement importantes de composés organo-soufrés de type n-alkyl-5Me-thiophène dans cette MO nanoscopiquement amorphe, témoignant ainsi d'une préservation par incorporation du soufre (sulfuration) dans les molécules lipidiques (Boussafir et al., 1995a, 1995b). Ce mécanisme s'accompagne d'une condensation de macromolécules dont le caractère réfractaire à la dégradation a été probablement acquis. Son association systématique à la fraction argileuse a prouvé le caractère synsédimentaire de l'amorphisation de ce type de MO et nous a révélé les liens possibles avec la fraction argileuse considérée à l'époque comme acteur d'une accélération de la sédimentation par floculation argilo-organique. La distribution de ce type de MO, dans le sédiment, observée au MEB rappelle celui des voiles bactériens et/ou algaires qui se forment à l'interface eau/sédiment. Mes résultats sur l'étude détaillée du contenu organique global des sédiments ont également montré que le processus de préservation sélective (minoritaire) concernait les débris de végétaux terrestres et les restes algaires. Ces fractions organiques n'ont pas joué un rôle quantitativement déterminant dans la cyclicité organique d'origine climatique étudiée.

Les différents mécanismes conduisant à la formation d'une matière organique pétrologène ont été intégrés dans un schéma plus général nous permettant de proposer (Boussafir & Lallier-Verges, 1997) un modèle interprétatif de fossilisation des MO sédimentaires marines riches en hydrocarbures (Figure II-2). Ce modèle met, pour la première fois, en évidence les liens entre les organismes initiaux, leur contribution en

produits organiques dans le milieu et les mécanismes de leur préservation respectifs, expliquant les structures observées dans la MO totale.

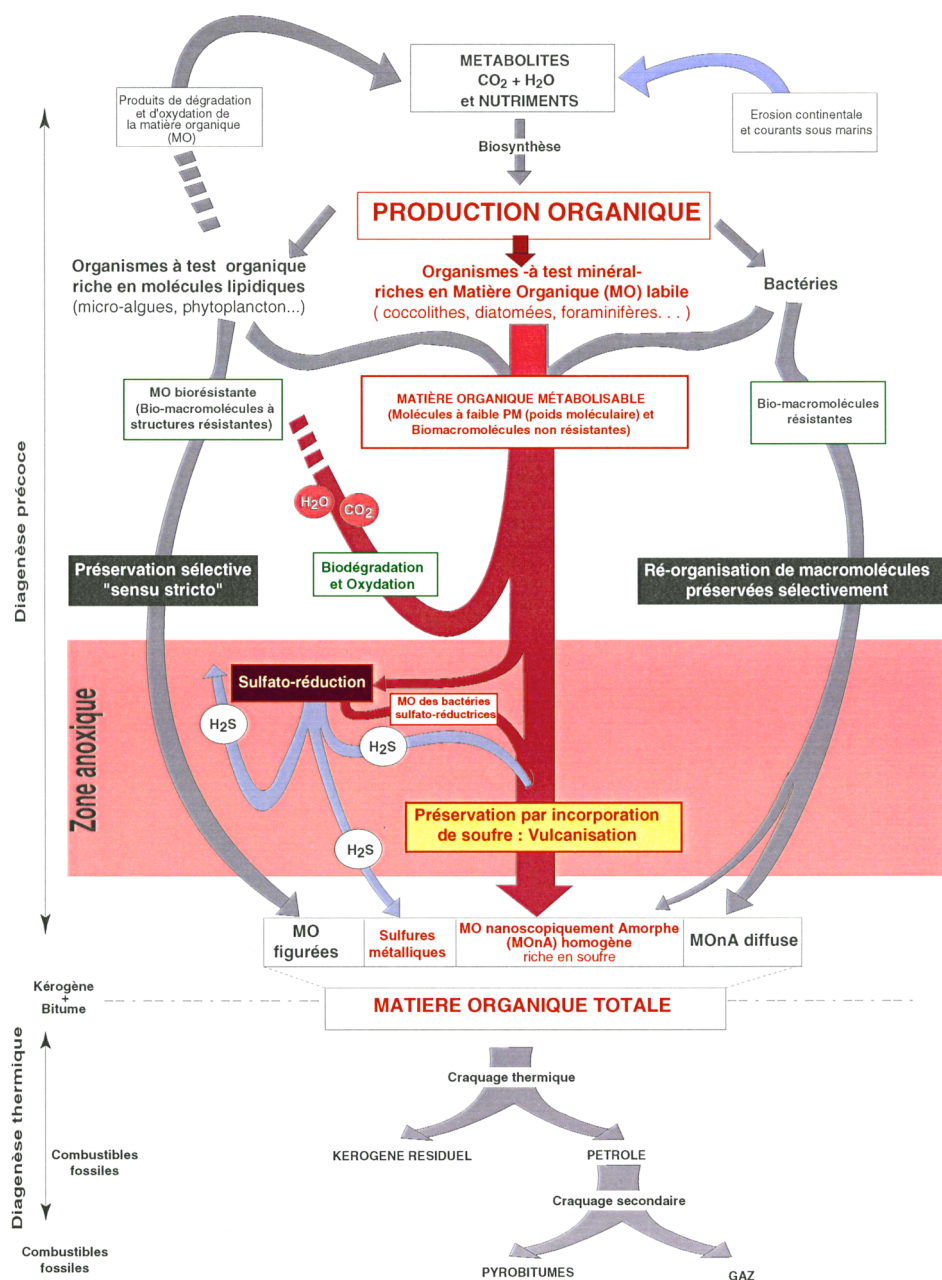


Figure II-2 - Modèle global de fossilisation des MO (Boussafir et Lallier-Vergès, 1997)

III-2- Relation MO et cyclicités sédimentaires des argiles du Kimméridgien.

L'une des avancées considérables dans ce thème concernait les relations qui pouvaient exister entre la fossilisation et la cyclicité sédimentaire observée dans les *Kimmeridge Clay Formation* (KCF). Les observations pétrographiques, effectuée à différentes échelles (microscopie optique, MEB/ER et MET), ont démontré que la cyclicité correspond à des accumulations variables de MO d'origine phytoplanctonique liées à **une variation de**

productivité primaire. La variation qualitative et quantitative du contenu organique est directement liée à la cyclicité des flux organiques exportés vers le fond du bassin, formés essentiellement d'organismes phytoplanctoniques sans test minéral. Cette matière organique se matérialise dans les sédiments sous une forme nanoscopiquement amorphe qui dilue plus ou moins les autres flux organiques sédimentaires.

La texture ultrafine des différentes fractions reste inchangée malgré les variations des teneurs en carbone organique total (COT) et des index d'hydrogène (IH). Aucun changement n'a été mis en évidence le long des cycles, mis à part les variations de proportions. (Boussafir et *al.*, 1995a et b, Boussafir et Lallier- Vergès 1997, Lallier-Vergès et *al.*, 1997)

Les bons résultats obtenus sur les KCF nous ont encouragé à travailler sur des séries plus récentes notamment dans l'environnement marin actuel particulièrement dans les zones d'upwellings. Ce travail a été réalisé dans le cadre de ma participation à l'encadrement d'un thésard allemand Andreas Lükge sur la partie biogéochimie et pétrographie ultrastructurale. Cette étude nous a montré que les sédiments néogènes, marins des upwellings du Pérou et de l'Oman, présentent une forte variabilité quantitative et qualitative de leur contenu organique. L'objectif majeur était de caractériser la fraction organique de ces sédiments par l'analyse moléculaire et ultrastructurale, pour déterminer si cette variabilité est induite par des variations de productivité primaire (liées au système de mousson), et / ou par le déplacement de la zone à minimum d'oxygène. Les sédiments de ces upwellings riches de 86 à 98% de MOA dérivée directement de la production phytoplanctonique le long de la colonne d'eau ou à l'interface eau sédiments. Le taux de dégradation a été estimé en comparant le COT fourni par la production récente et les flux de MO accumulés dans les sédiments (Figure II-3). Cette comparaison montre une minéralisation variable entre 90 à 99 % du carbone organique initialement produit. Tout le sédiment a subi une sulfato-réduction bactérienne avec 1 à 3% du carbone organique primaire recyclé en zone anoxique. Comme dans les KCF une partie de la MO est préservée par sulfuration naturelle ce qui explique les hautes valeurs de l'IH dans certains niveaux des sédiments. Pour la première fois on a montré que dans l'un des sites profonds étudiés, situé en dehors de la cellule d'upwelling, la quantité de MO accumulées est significativement élevée. Ce résultat a permis de montrer que les processus de transport sédimentaire, comme les courants de turbidité, sont aussi importants que la productivité organique dans l'apport et l'enrichissement des sédiments en MO. Ces résultats ont fait l'objet d'une participation à congrès et d'une publication dans la revue *Organic Geochemistry* (Lükge et *al.*, 1996).

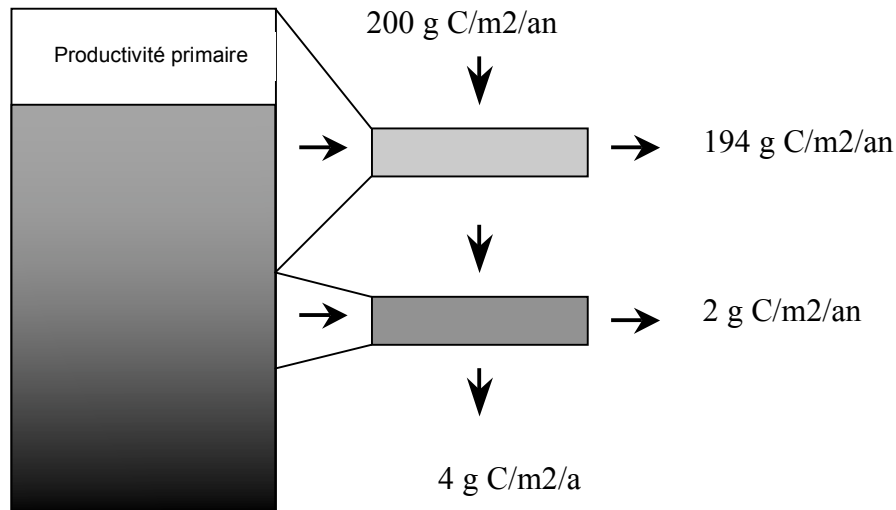


Figure II-3 : Taux de production et de minéralisation du C organique en zone oxiq. puis par processus de sulfato-réduction pour le site 723. Ce site est situé dans un petit bassin moins affecté par l'érosion que les autres sites étudiés sur cette zone de la marge continentale péruvienne (Lükge et *al.*, 1996).

III-3 Productivité organique et diagenèse précoce

III-3-1 Argiles du Kimméridgien d'Angleterre:

Ce travail a permis de montrer que les effets de la sulfato-réduction, tels qu'ils sont enregistrés dans les sédiments, peuvent rendre compte des variations de productivité primaire. Si on suppose que l'apport en sulfate n'est pas limité, la sulfato-réduction produit d'autant plus de H₂S que la quantité de matière organique métabolisable qui arrive en domaine anoxique est importante. Compte tenu de la grande quantité de MO métabolisable qui arrive pendant les périodes de forte productivité phytoplanctonique, la sulfato-réduction atteint des taux très forts et la libération d'H₂S en quantité importante participe à l'élaboration du milieu anoxique. Il est donc fort probable dans le cas des argiles du Kimméridgien que l'anoxie soit une conséquence du flux organique métabolisable qui arrive au sédiment et donc de la productivité organique initiale.

Ces résultats ont ainsi contribué à montrer que dans les processus de sulfato-réduction, lorsque le fer est limitant à la pyritisation, l'H₂S en excès s'incorpore dans la MO, essentiellement lipidique, en formant des composés organosoufrés (Figure II-4) et conférant

probablement à la MO une certaine résistance à la dégradation (Boussafir et *al.*, 1995b, Bertrand et *al.*, 1994, Gelin et *al.*, 1995).

Cette étude a permis de mettre en exergue ce **double rôle de la sulfato-réduction**. Ce processus bactérien dégrade à la fois de grande quantité de carbone organique, mais préserve d'autant mieux la matière organique non dégradée en libérant une grande quantité de soufre nécessaire pour fixer les molécules qui deviennent de ce fait biorésistantes.

L'activité sulfato-réductrice est donc induite par la production primaire qui reste le paramètre précurseur dans l'accumulation de la matière organique des argiles du Kimméridgien.

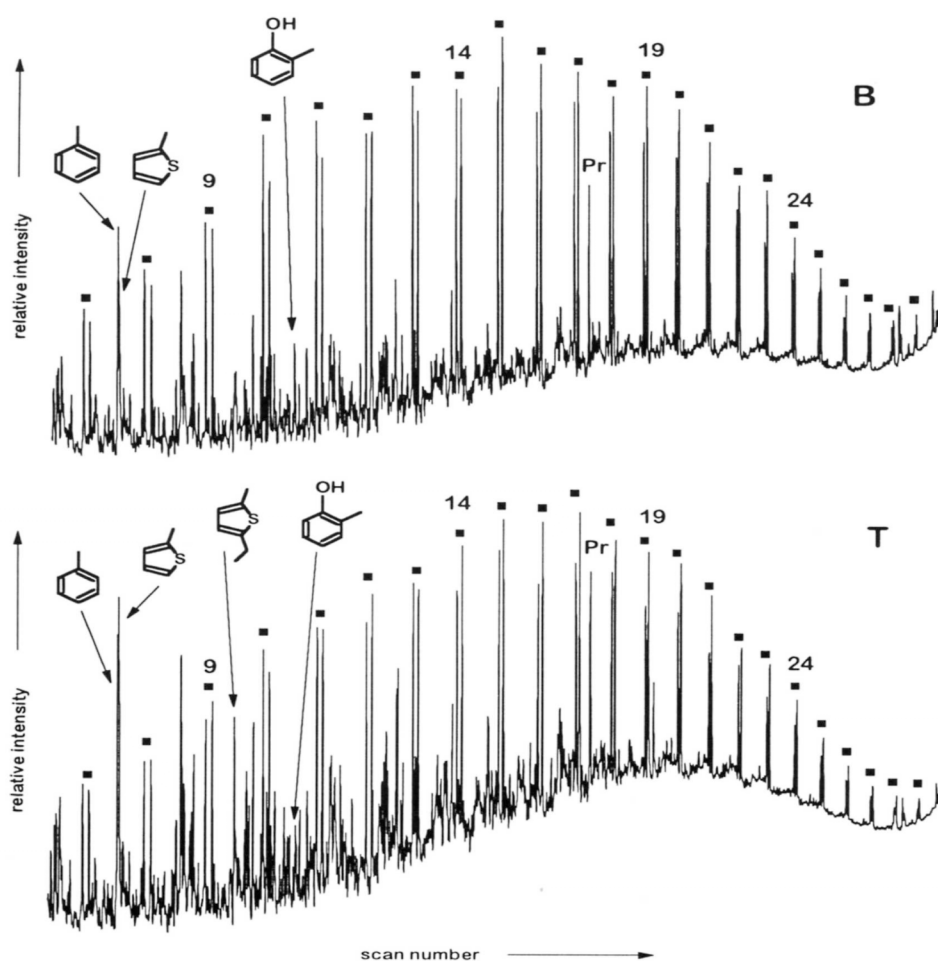


Figure I-4 : Chromatogramme obtenu sur la flash-pyrolyse de la MO insoluble d'échantillons représentatifs de phases de production, faible (B) et forte (T). Cette analyse montre que les composés organosoufrés sont en plus grande concentration dans l'échantillon représentatif de la phase la plus productive. Ceci nous a permis de montrer qu'au cours des périodes de haute productivité organique, le mécanisme de sulfato-réduction en milieu anoxique était plus actif

III-3-2 Environnement lagunaire kimméridgien - Jura Français (contribution à la thèse de Thierry Mongenot, Paris VI)

Le modèle d'accumulation organique élaboré dans le Kimméridgien du Yorkshire a été recherché dans d'autres formations sédimentaires riches en hydrocarbures que sont les laminites bitumineuses d'Orbagnoux (contexte de lagon kimméridgien du Jura Français). Ce travail a été réalisé dans le cadre d'une thèse soutenue par Thierry Mongenot que j'ai encadrée sur les aspects concernant la texture ultrafine de la MO au MET. L'extraordinaire enrichissement en soufre de ces sédiments associé à une préservation massive des produits lipidiques s'est révélé issu d'une sulfuration précoce et intense d'une MO d'origine cyanobactérienne & algaire. Ces études ont permis de montrer que cette sulfuration avait pour conséquence l'amorphisation quasi-totale de la MO originelle, dominante dans le faciès le mieux préservé que représentent les « laminites noires ». Les cinq faciès carbonatés qui composent la formation des laminites bitumineuses d'Orbagnoux résultent de l'interaction entre l'installation de tapis cyanobactériens et la décantation de coccolithes. Ce matériel sédimentaire s'est déposé dans un lagon où des épisodes d'oxygénation généralisée de la colonne d'eau alternaient avec des périodes où la base de la zone photique était anoxique. Le sédiment était habituellement réducteur bien que des épisodes très oxydants, associés à l'assèchement du milieu, aient été mis en évidence. Ce travail a donné lieu à une publication (Mongenot et *al.*, 1997)

III-4- L'accumulation de matières organiques en domaine de pente continentale

Cette étude correspond à ma contribution dans la thèse de Laetitia Pichevin, thèse de l'Université de Bordeaux I, sous la direction conjointe de Philippe Bertrand et de Jean Robert Disnar, et soutenue le 19 février 2004. L'étude présentée a été réalisée dans le cadre du GDR marges dans l'atelier « sédimentation organique profonde » dirigé par François Baudin, cet atelier a rassemblé plusieurs partenaires (le laboratoire EPOC de Bordeaux 1, l'ISTO, et le Muséum d'Histoire Naturelle de Paris).

La partie de la thèse que j'ai co-encadrée, s'est attachée à comprendre les mécanismes et facteurs qui, à travers les deux derniers cycles climatiques, ont présidé à une accumulation importante de matière organique sur la pente continentale. Ceci nous est apparu primordial à plusieurs égards. D'une part, le développement de la prospection pétrolière off-shore poussait les scientifiques de ce domaine à l'élargissement des champs d'investigation : en travaillant davantage sur les conditions de formation de roches-mères encore peu connues, l'étude du cas du Benguela peut participer à l'identification de

nouvelles régions pétrolifères. D'autre part, ce type d'investigation est très important dans le débat climatique actuel, notamment sur le rôle central accordé au cycle du carbone dans la régulation du climat mondial. Ce qui fait des systèmes d'upwellings l'un des moteurs supposés des variations climatiques quaternaires (Voir Partie III de ce rapport d'HdR).

À travers ces études détaillées en pétrographie et géochimie moléculaire de la matière organique sédimentaire prélevée sur deux carottes, nous nous sommes attaché à dégager les mécanismes qui induisent la préservation d'une quantité importante de carbones organiques à des profondeurs supérieures à 1000 m, ainsi que les facteurs qui contrôlent la distribution dans le temps et dans l'espace de la quantité et de la qualité de la matière organique sur cette pente continentale. Le système d'upwelling sud-africain est le système le plus productif actuellement, notamment au large de la cellule centrale de Lüderitz. Par ailleurs, la sédimentation à l'échelle de la marge est principalement de type hémipélagique, aucun processus gravitaire n'est enregistré dans les carottes prélevées depuis le bassin du Cap jusqu'en Angola. La fraction exportée à 1000 m représente environ 2% de la production primaire à proximité de cette même cellule (Fisher et al., 2000). L'intensité de la diagenèse étant directement proportionnelle au flux de particules organiques labiles gagnant l'interface eau-sédiment, l'oxygène est rapidement consommé dans les 15 premiers mm du sédiment (Hensen et al., 2000).

Nous avons pu montrer que la MO accumulée sur la pente continentale namibienne apparaît principalement sous deux formes, procédant chacune de mécanismes biogéochimiques particuliers intervenant à différentes étapes de la sédimentation. Des associations entre particules organiques et minérales dans la colonne d'eau sont à l'origine de la formation d'agrégats au sein desquels la MO est protégée de la dégradation pendant le transport et dans le sédiment.

Les teneurs en carbone organique (COT) lié aux agrégats sont similaires pour les deux sites et oscillent entre 1 et 4% du sédiment total (figure II-5), ce qui représente une part non négligeable du COT accumulé en bas de pente mais ne constitue qu'une faible proportion du COT enregistré à 1000m.

Il semble, par ailleurs, que la formation des agrégats soit quantitativement limitée, en premier lieu, par les apports organiques, mais également par la « non-disponibilité » en minéraux (quantité, type de minéraux, adhérence du matériel, probabilité de rencontre) lorsque les flux organiques exportés ne sont plus limitants. Sur la pente supérieure, la majeure partie de la MO sédimentaire n'est pas liée à la fraction minérale et apparaît parfaitement amorphe même à très fort grossissement. Les analyses EDS révèlent l'existence de soufre lié à cette MO, ce qui montre que celle-ci est partiellement formée de

composés organo-soufrés. L'incorporation de soufre dans les molécules organiques a lieu dans le sédiment en conditions anoxiques dès la diagenèse précoce (Sinninghe-Damsté et al., 1989).

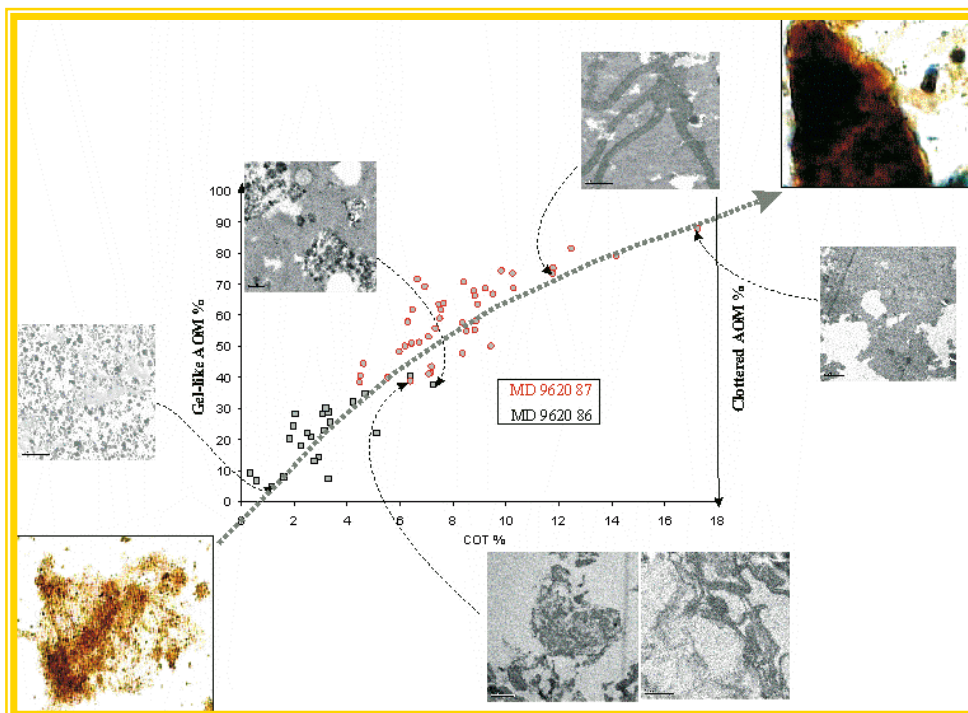


Figure II-5 : Évolution de la fréquence des deux types de MOA du palynofaciès et de la texture ultrafine du contenu organique en fonction des teneurs en carbone organique des deux carottes situées en haut (en rouge) et en bas (en noir) de pentes (Pichevin 2004)

Pour la première fois avec un détail aussi précis nous avons mis en évidence une relation entre des argiles nanoscopiques de types smectites (figure II-6) probablement en cours d'aggradation et de la MOA diffuse. Ce type de MOA présente une texture radicalement différente de celles des MOA préservée par sulfuration naturelle.

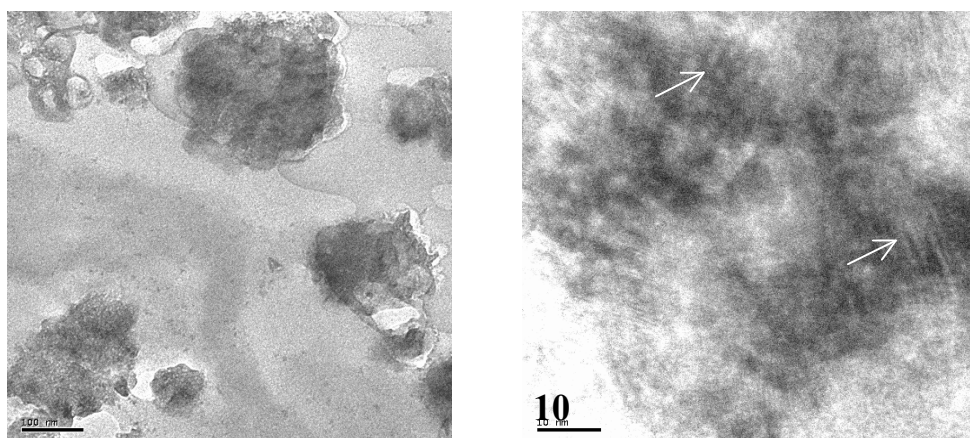


Figure II-6 : Exemple d'ultrastructures observées sur la MOA granulaire du palynofaciès. Faible grandissement MET et détail à droite montrant une association intime entre les argiles (flèche blanche) en cours d'aggradation et la MOA. (Pichevin et al., 2004)

L'abondance de MO sulfurée à 1000 m témoigne qu'une quantité importante de MO a pu gagner le sédiment sans subir d'altération importante dans la colonne d'eau, suggérant une exportation efficace depuis la zone productive jusqu'au site de dépôt. Ainsi, l'abondance de MO en haut comme en bas de pente semble principalement contrôlée par les flux organiques : ceux-ci doivent être suffisamment importants pour, d'une part, s'associer à une grande partie de la fraction minérale disponible pour l'agrégation et d'autre part, favoriser la mise en place de conditions anoxiques sous la surface du sédiment et permettre la préservation de MO sous forme amorphe sulfurée.

III-5- Rôle de la fraction argileuse dans le transfert et la préservation de la MO en environnement sédimentaire

Il s'agit d'une étude sur les interactions argiles/MO et sur les processus biogéochimiques que la MO subit à cette occasion dans une colonne d'eau lacustre stratifiée (oxygéné et anoxique). C'est un projet que j'ai initié à l'ISTO et qui a profité d'une bourse de thèse ministérielle. Cette thèse co-dirigée par J.L. Robert pour la partie minéralogie des argiles, a été réalisée par Sylvain Drouin et soutenue en juin 2007. Nous avons dans un premier temps testé la possible fixation de molécules lipidiques, génératrices d'hydrocarbures, sur des phyllosilicates en contexte de colonne d'eau lacustre et marine. Dans un deuxième temps, le rôle joué par la phase minérale dans les mécanismes de piégeage depuis les zones de production organique jusqu'au sédiment a été évalué. Pour cela, des expériences de simulation d'interactions entre des lipides simples et des substrats argileux de synthèse ont été réalisées au laboratoire (*in-vitro*), ainsi que des expériences d'interaction sur site dans la colonne d'eau entre des argiles de synthèse, des argiles naturelles et des bio-polymères produits *in situ*.

Pour réaliser ces expérimentations, j'ai mis au point de nouveaux pièges à particules sédimentaires permettant de garder les argiles introduites dans le milieu au cours des interactions argiles / MO dissoutes du lac.

A la suite de ces expérimentations, la pérennité des complexes argilo-organiques a été éprouvée chimiquement. Ceci afin de discuter la part réelle que les processus d'adsorption sont susceptibles de jouer dans la préservation des composés organiques labiles dans la colonne d'eau. Un nouveau modèle de fossilisation de la MO pétrologène, intégrant les processus d'interaction argilo-organique a été proposé à l'issue de ce travail.

Cette étude faisant appel à la double compétence « argiles » et « MO » s'est intégrée dans une action transversale regroupant deux équipes de l'ISTO. L'approche s'est résolument voulue à la fois minéralogique et géochimique et a fait appel aux méthodes analytiques propres à chacun de ces domaines. Ainsi les interactions organo-minérales ont-

elles été caractérisées aussi bien au moyen d'analyses globales et moléculaires de la MO, que d'analyses physiques par diffraction des rayons X et par XPS des assemblages argilo-organiques.

Les résultats les plus marquants ont montré que le piégeage est restreint strictement à de l'adsorption en surface et en bordure des phases minérales. Aucune intercalation de composé organique dans l'espace interfoliaire des argiles n'a été mise en évidence. Il se dégage des expérimentations en laboratoire, que le facteur prépondérant à l'adsorption est la nature des composés organiques et plus spécifiquement la nature des groupements fonctionnels.

Ci-dessous deux figures (figure II-7 et II-8) illustrent les phénomènes d'interactions entre les produits hydrocarbonés et des argiles de basse charge et de hautes charges, le type de liaison qui entre en compte dans le phénomènes d'adsorptions, le type de molécules et leurs site de préférence.

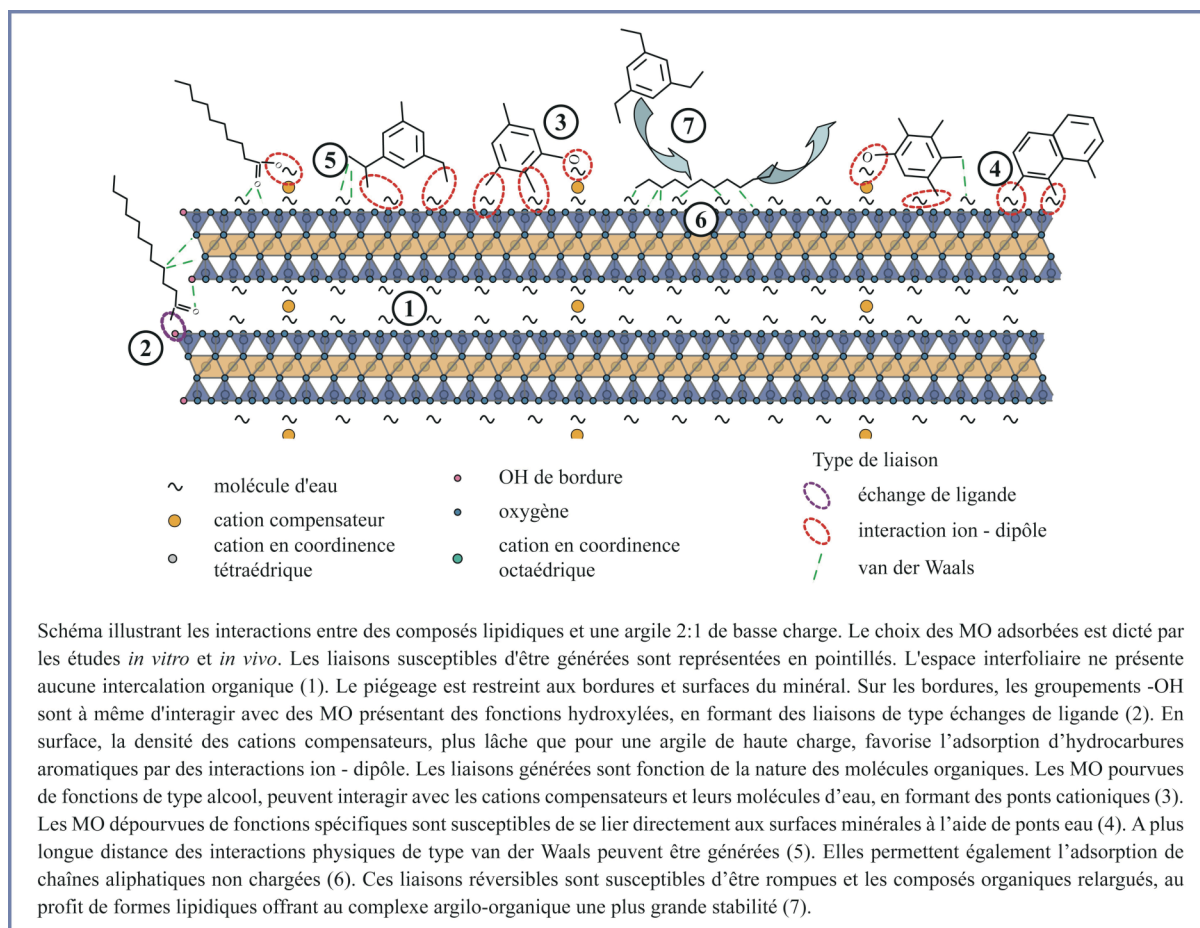


Figure II-7 : Modèle d'adsorption organique sur les argiles de basse charge.

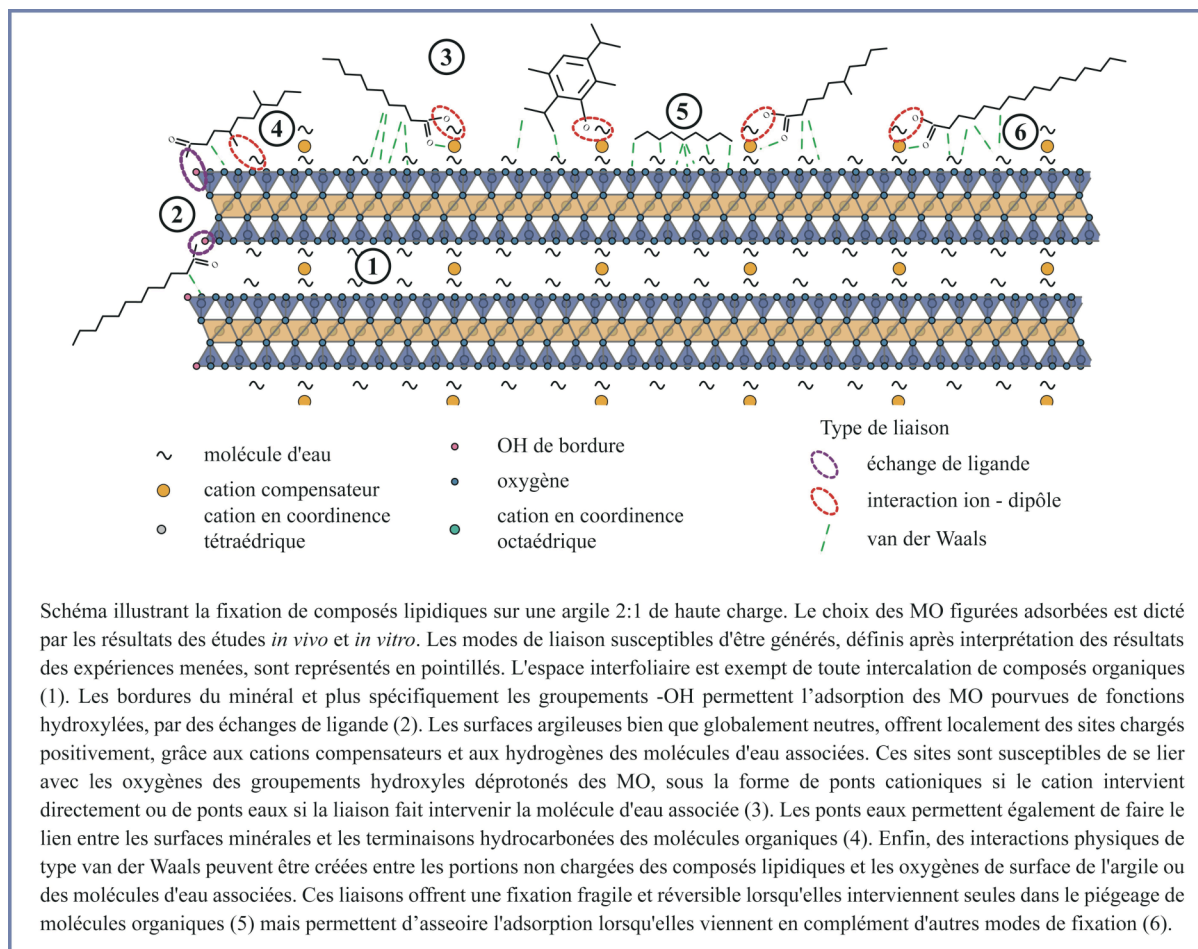


Figure II-8 : Modèle d'adsorption organique sur les argiles de haute charge.

Au terme des interactions *in situ*, il apparaît que le piégeage se fait en faveur des MO "fraîches". Les charges de surface des minéraux argileux contrôlent également la nature et les proportions de composés adsorbés. La grande stabilité des assemblages argilo-organiques formés lors des expériences *in vitro* et *in vivo*, éprouvée par des attaques alcalines, met en lumière l'existence de liaisons fortes et probablement multiples entre les phases minérales et organiques. Cette stabilité démontre le caractère pérenne des assemblages, en environnement naturel. En adsorbant durablement les composés organiques, les argiles participent à réduire leur disponibilité aux agents agressifs durant leur transfert dans les colonnes d'eau. Ce constat associé à la forte stabilité des complexes vis-à-vis des agressions alcalines, on peut dire que les interactions argilo-organiques sont un mode de préservation à part entière, au même titre que les processus de dégradation-recondensation, de sulfuration naturelle ou de préservation sélective, permettant l'incorporation de MO métabolisable dans les sédiments (Drouin 2007, Drouin et al., Soumis)

IV- CONCLUSIONS ET PERSPECTIVES

L'étude de l'origine et des modes de fossilisation de la MO a permis d'une part de comprendre les mécanismes qui favorisent l'augmentation des flux de carbone stockés de façon pérenne dans les sédiments. D'autre part, ces mécanismes permettent de comprendre pourquoi, dans certains sites, la quantité de MO accumulée est supérieure à celle attendue dans des conditions environnementales classiques où le recyclage biologique et la minéralisation du carbone organique sont naturellement importantes. L'étude de ces mécanismes a permis par la vivacité et la densité des travaux réalisés de déplacer le débat productivité/anoxie qui animait depuis des décennies les sédimentologues organiciens (issue pour la plus grande part du milieu pétrolier) vers un débat sur le couple productivité/préservation. Nous avons pu montrer grâce aux travaux réalisés sur divers sites marins et lacustres que l'accumulation de la MO était le fruit de la productivité qui est le moteur initial d'enrichissement organosédimentaire et que la fossilisation finale peut être accentuée grâce aux mécanismes de préservation comme la sulfuration naturelle. En effet, l'apport massif de MO métabolisable (sans doute avec le concours de la fraction argileuse, malheureusement moins bien mis en lumière dans les études réalisées) provoque un grand développement bactérien au point que la pyritisation, frein à la sulfuration organique, se retrouve plafonnée et limitée par une consommation totale du Fer disponible, ce qui provoque une augmentation exponentielle de la préservation de la MO par ce mécanisme. Malheureusement, à ce jour, aucune démonstration expérimentale, sur la résistance des MO sulfurée à l'oxydation et à la biodégradation pour prouver qu'il s'agit bien d'un mécanisme de fossilisation, n'ont été entreprises.

Le travail réalisé sur la réactivité argiles/MO le long de la colonne d'eau du Lac Pavin montre que cette sulfuration s'initie sur la MO alors qu'elle est déjà associée et portée par les argiles. Notre étude a montré pour la première fois, que la sulfuration agit déjà dans la colonne d'eau anoxique, avant même l'arrivée de la MO métabolisable aux sédiments. *Cette étude est la preuve que les différents mécanismes évoqués, souvent étudiés séparément, agissent de concert : les argiles pouvant être, par exemple, le support aux phénomènes de dégradation-recondensation ou à la sulfuration naturelle. Dans les sédiments ces mêmes argiles peuvent protéger physiquement des enzymes bactériennes des particules organiques préservées sélectivement.* La productivité à elle seule ne peut pas expliquer les flux accrus de MO vers les sédiments. Plusieurs environnements carbonatés, comme les milieux récifaux ou les craies coccolithiques du bassin de Paris, réputés comme les plus productifs au monde ne fossilisent pas des quantités appréciables de MO. La MO produite, dissoute pour l'essentiel, se dégrade par recyclage biologique. Nous savons maintenant grâce au travail réalisé sur la réactivité argiles/MO que le rôle des argiles est primordial, la floculation et la formation de pelotes fécales sont les premiers complices permettant à la MO

d'échapper à ses agresseurs physicochimiques et biologiques combinés. Sans ces deux transporteurs de qualité : argiles et pelotes fécales , le temps de transit de la MO facilement métabolisable serait supérieur à la cinétique de la dégradation. Le transfert vers les sédiments s'en retrouve affaibli. Ceci est beaucoup moins évident en domaine lacustre où la part de la MO particulaire provenant du bassin versant et des alentours du lac est importante. La préservation sélective joue un rôle primordial dans ces types d'environnements. Cette différence entre les flux de MO sélectivement préservée (allochtone pour l'essentiel) et MO produite dans le milieu et fossilisée après de légères transformations diagénétiques (MO autochtone pour l'essentiel) enregistre un balancement au cours du temps qui est sensible aux variations que peut subir l'environnement et notamment sous l'influence du climat (Voir Partie III de ce rapport d'HdR). En milieu marin, la fraction héritée des producteurs et préservée sélectivement sous forme particulaire est moins représentative et joue un rôle annexe dans le transfert du carbone vers le sédiment.

Les travaux réalisés dans le domaine des caractérisations des molécules biorésistantes et la connaissance moléculaire du matériel organique fossilisé reste une voie de recherche importante à l'amont de la calibration. En effet nombreux produits restent non résolus sur la plupart des chromatogrammes étudiés en environnement marin ou lacustre. La connaissance accrue de ces produits est indispensable pour la calibration de l'utilité du biomarqueur lui-même et la calibration et la découverte de nouveaux marqueurs environnementaux ou climatiques. Ces études continueront d'enrichir notre connaissance des biomarqueurs de source directement hérités des biomarqueurs d'environnement diagénétique légèrement transformés. Ces travaux sont indispensables dans le développement de cet outil puissant que représente la MO sédimentaire.

La deuxième voie qui reste à explorer dans le domaine de la préservation de la MO sédimentaire est celle des interactions MO/argiles. Nous avons fait des progrès dans ce domaine grâce aux travaux réalisés au cours de la thèse de Sylvain Drouin. Le rôle primordial de l'argile est bien compris, les processus le sont moins. Je souhaiterais continuer ce travail notamment en m'intéressant de façon globale au phénomène de floculation en environnements aquatiques, et à l'étude de la stabilité et la dégradabilité des complexes organominéraux en environnement sédimentaire.

L'intérêt manifesté par le comité d'évaluation de l'ISTO et par notre communauté scientifique des organiciens en général pour la problématique réactivité argile MO nous encourage à poursuivre nos efforts dans ce domaine et proposer une suite aux travaux actuels en élargissant (par exemple) cette problématique à d'autres espèces minérales que l'argile. Les travaux réalisés nous ont permis d'étudier le phénomène d'adsorption en milieu

naturel lacustre, aborder de façon superficielle ces relations en milieu productif marin et réaliser avec succès des expérimentations in vitro au laboratoire. Les expérimentations sur une éventuelle résistance à la dégradation de ces complexes, prévues au départ dans ce sujet, et non abordées par manque de temps, constituent une évolution naturelle de ce travail. Cette partie du sujet reste à ce jour inexplorée par les communautés scientifiques nationale et internationale s'intéressant à ce type d'interactions. L'un des objectifs sera par exemple d'étudier l'adsorption et la formation d'agrégats en s'intéressant cette fois-ci aux fractions organiques dans leur totalité (particulaire et dissoute) notamment en environnement productif marin. Le phénomène de floculation organo-argileuse mais aussi organominérale en général est assez mal connu, il s'agira donc de comprendre comment cette floculation est-elle possible et quels sont les paramètres favorables en milieu sédimentaire. Cet aspect peut être approché grâce à des expérimentations au laboratoire en variant à souhait les paramètres physicochimiques du milieu, les compositions minéralogiques et organiques. L'accent doit être mis sur les aspects texturaux et micro-texturaux de ces assemblages et sur le comportement cristallographique de la fraction argileuse au cours de la floculation. Le degré de stabilité des complexes organo-argileux ainsi formés doit être mis à l'épreuve en fonction, d'une part des fractions minérales utilisées et d'autre part, en fonction des polymères organiques naturels qui rentrent en jeu. Cet aspect, preuve directe du caractère préservateur de ces associations, doit être étudié grâce à des expérimentations de dégradation oxydative en milieu sec et de biodégradation en milieu aqueux.

Références citées dans la partie II

- Aizenshtat et Stoler (1983) - The geochemical sulphur enrichment of recent organic matter by polysulfides in the Solar Lake. *Advances in Organic Geochemistry*, 1981, 279-288.
- Allard B., Templier J. et Largeau C (1997) - Artfactual origin of mycobacterial bacteran. Formation of melanoidin-like artefact macromolecular material during the usual isolation process. *Organic Geochemistry*, 11-12, 691-703.
- Allredge A. L., Gotschalk C. C. (1989) - Direct observations of the mass flocculation of diatom blooms: characteristics, settling velocities and formation of diatom aggregates. *Deep Sea Research* 36 (2), 159-171. Berkaloff et al., 1984 ;
- Berkaloff C., Rousseau B., Coûte A., Casadevall E., Metzger P., et Chirac C. (1984) - Variability of cell wall structure and hydrocarbon type in different strains of *Botryococcus braunii*. *Journal of Phycology*, 20, 377-389.
- Berner R. A. (1964a) - Distribution and diagenesis of sulfur in some sediments from the Gulf of California. *Marine Geology* 1, 117-140.
- Berner R. A. (1964b) - An idealized model of dissolved sulfate distribution in recent sediments. *Geochimica et Cosmochimica Acta* 28 (9), 1497-1503.
- Berner R. A. (1982) - Burial of organic carbon and pyrite sulphur in modern ocean : its geochemical and environmental significance. *American Journal of Science*, 282, 451-473.
- Bertrand, P. and Lallier-Vergès, E. (1993) - Past sedimentary organic matter accumulation and degradation controlled by productivity. *Nature*, 364, 786-788.
- Bertrand P., Lallier-Vergès E. & Boussafir M. (1994) - Enhancement of both accumulation and anoxic degradation of organic carbon controlled by cyclic productivity: a model. *Organic Geochemistry*, 22, pp. 511-520.
- Boon J. J. et de Leeuw J. W. (1987) - Amino acid sequence information in proteins and complex proteinaceous material revealed by pyrolysis-capillary gas chromatography-low and high resolution mass spectrometry. *Journal of Analytical and Applied Pyrolysis* 11, 313-725
- Boon J. J., de Leeuw J. W., Rubinztain Y., Aizenshtat Z., Ioselis P., Ikan R. (1984) - Thermal evolution of some model melanoidins by Curie Point pyrolysis-mass spectrometry and chromatography-mass spectrometry. *Organic Geochemistry* 6, 805-811.
- Bournet P. E. (1996) - Contribution à l'étude hydrodynamique et thermique du lac du Bourget, courants de densité et ondes internes. Thèse de Doctorat, Ecole Nationale des Ponts et Chaussées, 269pp.
- Boussafir M., Gelin F., Lallier-Vergès E., Derenne S., Bertrand P. & Largeau C. (1995b) - Electron microscopy and pyrolysis of kerogens from the Kimmeridge Clay Formation, UK : source organisms, preservation process and origin of microcycles. *Geochimica Cosmochimica Acta* 59, pp. 3731-3747.
- Boussafir M., Lallier-Vergès E. (1997) - Accumulation of organic matter in the Kimmeridge Clay formation (KCF): an update fossilisation model for marine petroleum source-rocks. *Marine and Petroleum Geology*, 14, 1, 75-83.
- Boussafir M., Lallier-Vergès E., Bertrand P. & Badaut-Trauth D. (1995a) - SEM and TEM studies of organic matter and source rock microfacies from a short-term organic cycle of kimmeridgian source-rocks. In: "Organic matter accumulation: The Organic Cyclicities of the Kimmeridge Clay Formation (Yorkshire , G.B.) and the Recent Maar Sediments (Lac du Bouchet)". E. Lallier-Vergès, N. Tribovillard & P. Bertrand (eds.). Springer-Verlag, Heidelberg. *Lecture Notes in Earth Sciences* 57, pp. 15-30.

- Boussafir M., Lallier-Vergès E., Bertrand P. & Badaut-Trauth D. (1994) - Structure ultrafine de la matière organique des roches mères du Kimméridgien du Yorkshire. Bulletin de la Société Géologique de France, t. 165, n°4, pp.355-363.
- Boussafir M., Laggoun-Défarge F., Derenne S. & Largeau C. (2000) - Bulk and pyrolytic studies of insoluble organic matter from Tririvakely lake sediments (Interglacial-like and last maximum glacial stages). Applied Pyrolysis, 2000, Sevilla, p. 107.
- Cauwet G. (1981) - Non living particulate matter. In : Marine organic chemistry, Dursma E. K. and Dawson R. eds 31, 71-89.
- Collins M. J., Bishop A. N. et Farimond P. (1995) - Sorption by mineral surfaces : Rebirth of the classical condensation pathway for kerogen formation ? Geochimica et Cosmochimica Acta, 59 , 2387-2391.
- Collins M. J., Bishop A. N., Farrimond P. (1995) - Sorption by mineral surfaces: Rebirth of the classical condensation pathway for kerogen formation? Geochimica et Cosmochimica Acta 59(11), 2387-2391.
- Dauwe B., Middelburg J. J., Herman P. M. J. (2001) - Effect of oxygen on the degradability of organic matter in subtidal and intertidal sediments of the North Sea area. Marine Ecology-Progress Series 215, 13-22.
- Degens E. T., Mopper K. (1975) - Early diagenesis of organic matter in marine soils. SCI. 119, 65-72.
- Derenne S., Largeau C., Casadevall E. et Berkaloff C. (1989) - Occurrence of a resistant Biopolymer in the L race. Botryococcus braunii. Phytochemistry, 28, 1137-1142.
- Derenne S., Largeau C., Casadevall E., Berkaloff C., Rousseau B. (1991) - Chemical evidence of kerogen formation in source rocks and oil shales via selective preservation of thin resistant outer walls of microalgae : Origin of ultralaminae. Geochimica et Cosmochimica Acta 55, 1041-1050.
- Derenne S Largeau C., Berkaloff C., Rousseau B., Wilhelm C. et Hatcher P (1992a) - Non-hydrolysable macromolecular constituents from outer walls. Chlorella fusca and Nanochlorum eucaryotum. Phytochemistry, 31, 1923-1929.
- Derenne S., Le Berre F., Largeau C., Hatcher P., Connan J. et Raynaud J. F. (1992b) - Formation of ultralaminae m marine kerogens via selective preservation of thin resistant outer walls of microalgae. Organic Geochemistry. 19 345-350
- Drouin S. (2007) - Rôle des phyllosilicates dans la préservation et la fossilisation de la Matière Organique pétrologène. Thèse de l'Université de Orléans
- Fisher G., Ratmeyer V., and Wefer G. (2000) - Organic carbon fluxes in the Southern Ocean: relationship to primary production compiled from satellit radiometer data. Deep-sea Research II 47, 1961-1997.
- Francois R. (1987) - A study of sulphure enrichment in the humic fraction of marine sediments during early diagenesis. Geochimica et Cosmochimica Acta 51, 17-27.
- Gelin F., Boussafir M., Derenne S., Largeau C. & Bertrand P. (1995) - Study of qualitative and quantitative variations in kerogen chemical structure along a microcycle: correlation with ultrastructural features In: "Organic matter accumulation: The Organic Cyclicities of the Kimmeridge Clay Formation (Yorkshire , G.B.) and the Recent Maar Sediments (Lac du Bouchet)". E. Lallier-Vergès, N. Tribovillard & P. Bertrand (eds.). Springer-Verlag, Heidelberg. Lecture Notes in Earth Sciences 57, pp. 31-47.
- Greaves M. P. et Wilson M. J. (1973) - Effects of soil microorganisms on montmorillonite-adenine complexes. Soil Biology and Biochemistry, 5, 275-276.

- Greenland D. J. et Mott C. J. B. (1978) - Surfaces of soil particles. In *The Chemistry of Soil Constituents*, eds. D. J. Greenland et M. H. B. Hayes, Wiley, New York, p 321-353.
- Hedges J. I. et Keil R. G. (1995) - Sedimentary organic matter preservation: an assessment and speculative synthesis. *Marine Chemistry*, 49, 81-115.
- Hedges J. I., Keil R. G. (1995) - Sedimentary organic matter preservation: an assessment and speculative synthesis. *Marine Chemistry* 49(2-3), 81-115.
- Hedges J. I., Keil R. G. et Benner R. (1997) - What happens to terrestrial matter in the ocean ? *Organic Geochemistry*, 27,195-212.
- Henrichs S.M., and Reeburg W.S. (1987) - Anaerobic mineralization of marine sediment organic matter: rates and the role of anaerobic processes in the oceanic carbon economy. *Geomicrobiology* 5, 191-237.
- Henrichs S. M. (1993) - Early diagenesis of organic matter: the dynamics (rates) of cycling of organic compounds. In *Organic Geochemistry. Principles and applications*, eds. M. H. Hengel et S. A. Macko, Plenum Press, New York, London.
- Hensen C., Zabel M., and Schulz H. D. (2000) - A comparison of benthic nutrient fluxes from deep-sea sediments off Namibia and Argentina. *Deep-Sea Research Part II-Topical Studies in Oceanography* 47, 2029-2050.
- Huc A. Y. (1988a) - Sedimentology of organic matter. In : *Humic substances and their role in the environment*, Dahlen Konferenzen, Frimmel F. H. and Christman R. F. eds, Wiley, Chichester, 215-243.
- Hutchinson G. E. (1957) - *A Treatise on Limnology. I, Geography, Physics and chemistry*, John Wiley and Sons, NY 1.
- Jackson G. A. (1990) - A model of the formation of marine algal flocs by physical coagulation processes. *Deep Sea Research Part A. Oceanographic Research Papers* 37 (8), 1197-1211.
- Jørgensen B. B. (1982) - Mineralization of organic matter in the sea bed. The role of sulphate reduction. *Nature* 296, 643-645.
- Kadouri A., Derenne S., Largeau C., Casadevall E. et Berkaloff C. (1988) - Resistant biopolymer in the outer walls. *Botryococcus braunii*, B Race, *Phytochemistry*, 27, 551-
- Keil R. G., Tsamakis E., Futh C. B., Giddings C., Hedges J. I. (1994a) - Mineralogical and textural controls on the organic composition of coastal marine sediments: Hydrodynamic separation using SPLITT-fractionation. *Geochimica et Cosmochimica Acta* 58, 879-893.
- Keil R. G., Montlucon D. B. Prah F. G. Hedges J. I. (1994b) - Sorptive preservation of labile organic matter in marine sediments. *Nature* 370 (6490), 549-552.
- Kobayashi Y. et Aomine S. (1967). - Mechanism of inhibitory effect of allophane and montmorillonite on some enzymes. *Soil Science and Plant Nutrition*, Tokyo, 13, 189-194.
- Lallier-Vergès E., Hayes J., Boussafir M., Zaback D., Tribovillard N., Connan J. & Bertrand P. (1997) - Productivity-induced sulfur enrichment of organic-rich sediments. *Chem. Geol.* 34: 277-288.
- Lallier-Vergès, E., Bertrand, P., Huc, A.Y., Bückel, D. and Tremblay, P. (1993) - Control of the preservation of organic matter by productivity and sulphate reduction in Kimmeridgian shales from Dorset (UK). *Mar. and Petrol. Geol.*, 10, 600-605.
- Lallier-Vergès E., Hayes J., Boussafir M., Zaback D., Tribovillard N., Connan J., Bertrand P. (1997) - Productivity-induced sulphur enrichment of hydrocarbon-rich sediments from the Kimmeridge Clay Formation. *Chemical Geology*, 134, 4, 277-288.

- Largeau C. et Derenne S. (1993) - Relative efficiency of the Selective Preservation and Degradation. Recondensation pathways in kerogen formation. Source and environment influence on their contributions to type I and II kerogens. *Organic Geochemistry*, 20, 611- 615.
- Largeau C., Casadevall E., Kadouri A., Metzger P. (1984) - Formation of botryococcus-derived kerogens. Comparative study of immature torbanites and of the extant alga *Botryococcus braunii*. *Organic Geochemistry* 6, 327-332.
- Largeau C., Derenne S., Casadevall E., Kadouri A., Sellire N. (1986) - Pyrolysis of immature Torbanite and the resistant biopolymer (PRB A) isolated from extant alga *Botryococcus braunii*. Mechanism of the formation and structure of torbanite. In: D. Leythäuser and J. Rullkötter eds, *Advances in Organic Geochemistry 1985*, Pergamon Press, Oxford, *Organic Geochemistry* 10, 1023-1032.
- Largeau C., Derenne S., Casadevall E., Berkaloff C., Corolleur M., Lugardon B., Raynaud J.F. et Connan J. (1990a) - Occurrence and origin of "ultralaminar" structures in "amorphous" kerogens of various source rocks and oil shales. *Organic Geochemistry*, 16, 889-895.
- Largeau C., Derenne S., Clairay C., Casadevall E., Raynaud J.F., Lugardon B., Berkaloff C., Corolleur M. et Rousseau B. (1990b) - Characterisation of various kerogens by Scanning Electron Microscopy (SEM) and Transmission Electron Microscopy (TEM) - Morphological relationships with resistant outer walls in extant microorganisms. *Mededelingen Rijks Geologische Dienst*, 45, 91-101.
- Larter S. R., Douglas A. G. (1980) - Melanoidins-kerogen precursors and geochemical lipid sinks: a study using pyrolysis gas chromatography (PGC). *Geochimica et Cosmochimica Acta* 44, 2087-2095.
- Lorenz M. G. et Wackemagel W. (1987) - Adsorption of DNA to sand and variable degradation rates of adsorbed DNA. *Applied and Environmental Microbiology*, 53, 2948- 2952.
- Lückge A., Boussafir M., Lallier-Vergès E. & Littke. R. (1996) - Comparative study of organic matter preservation in immature sediments along the continental margins of Peru and Oman. Part I : Results of petrographical and bulk geochemical data. *Organic Geochemistry*. 24, pp.437-451.
- Maillard L. C. (1913) - Action des acides aminés sur les sucres: formation des mélanoidines par voie méthodique. *Compte-rendu de l'Académie des sciences* 154, 66-68.
- Marshman N. A. et Marshall K. C. (1981) - *Soil Biology and Biochemistry*, 13, 127-134.
- Mayer L. M. (1993) - Organic matter at the sediment-water interface. In *Organic Geochemistry Principles and Applications*, Vol. 12 (Engel M. H., and Macko S. A., Eds.), pp. 171-184. Plenum Press.
- Mayer L. M. (1994a) - Surface area control on organic carbon accumulation in continental shelf sediments. *Geochimica et Cosmochimica Acta*, 58,1271-1284.
- Mayer L. M. (1994b) - Relationships between mineral surfaces and organic carbon concentrations in soils and sediments. *Chemical Geology*, 114, 347-363.
- Menzel D. W. (1974) - Primary productivity, dissolved and particulate organic matter, and the sites of oxidation of organic matter. In : *The Sea. Marine Chemistry*, Goldberg D. (eds), New York-London-Toronto : Wiley 5, 659-678.
- Mongenot T. (1998)- Études pétrographiques et géochimiques d'un dépôt sédimentaire très riche en soufre organique (Orbagnoux, Kimméridgien supérieur) - reconstitution paléoenvironnementale - mécanisme de préservation de la matière organique - Thèse de l'Université d'Orléans

- Mongenot T., Boussafir M., Derenne S., Lallier-Vergès E., Largeau C., Tribovillard N. (1997) - Sulphur-rich organic matter from bituminous laminites of Orbagnoux (France, upper Kimmeridgian); the role of early vulcanization. *Bulletin de la Société Géologique de France*, 168, 3, 331-341.
- Mongenot T., Derenne S., Largeau C., Tribovillard N. P., Lallier-Vergès E., Dessort D., Connan J. (1999) - Spectroscopic, kinetic and pyrolytic studies of the sulfur-rich Orbagnoux deposit (Upper Kimmeridgien, Jura). *Organic Geochemistry* 30, 39-56.
- Murray R. S. et Quirk J. P. (1990a) - Surface area of clays. *Langmuir*, 6,122-124.
- Murray R. S. et Quirk J. P. (1990b) - Intrinsic failure and cracking of clay. *Soil Science Society of America Journal*, 54,1179-1184.
- Nissenbaum A. et Kaplan I. R. (1972) - Chemical and isotopic evidence for the in-situ origin of marine humic substances. *Limnological Oceanography*, 17, 570-582.
- Parks G. A. (1975) - Adsorption in the marine environment. In *Chemical Oceanography*, eds. J. P. Riley et G. Skirrow, Academic Press, New York, 1, 241-308.
- Peulvé S., de Leeuw J. W., Sicre M. A., Baas M., Saliot A. (1996) Characterization of macromolecular organic matter in sediment traps from the northwestern Mediterranean Sea. *Geochimica et Cosmochimica Acta* 60, 1239-1259.
- Pichevin L. (2004) - Sédimentation organique profonde sur la marge continentale namibienne (Lüderitz, Atlantique Sud-Est) : impacts des variations climatiques sur la paléoprodutivité, Thèse de l'Université Bordeaux.
- Pichevin L., Bertrand P., Boussafir M., Disnar J.-R. (2004) - Organic matter accumulation and preservation controls in a deep sea modern environment: an example from Namibian slope sediments. *Organic Geochemistry*, 35, 5, 543-559.
- Pinck L. A., Dyal R. S. et Allison F. (1954) - Protein-montmorillonite complexes, their preparation and the effects of soil microorganisms on their decomposition. *Soil Science*, 78,109-118.
- Premuzic E. T., Benkovitz C. M., Gaffney J. S. et Walsh J. J. (1982) - The nature and distribution of organic matter in the surface sediments of world oceans and seas. *Organic Geochemistry*, 4, 63-77.
- Ransom B., Bennett R. H., Baerwald R., Shea K. (1997) TEM study of in situ organic matter on continental margins: occurrence and the 'monolayer' hypothesis. *Marine Geology* 138, 1-9.
- Ransom B., Kim D., Kastner M. et Wainwright S. (1998) - Organic matter preservation on continental slopes : Importance of mineralogy and surface area. *Geochimica et Cosmochimica Acta*, 62, 1329-1345.
- Raynaud J. F., Lugardon B., Lacrampe-Couloume G. (1989) Structures lamellaires et bactéries, composants essentiels de la matière organique amorphe des roches mères. *Bulletin des Centres de Recherches Exploration-Production Elf-Aquitaine* 13, 1-21.
- Riboulleau A., Derenne S., Sarret G., Largeau C., Baudin F., and Connan J. (2000) Pyrolytic and spectroscopic study of a sulphur-rich kerogen from the "Kashpir oil shales" (Upper Jurassic, Russian platform). *Organic Geochemistry* 31, 1641-1661.
- Romankevich E. A. (1984) - Sources of organic matter in the ocean. In *Geochemistry of Organic Matter in the Ocean*, Springer Verlag, Berlin, 4-26.
- Rosenfeld J. K. (1979) - Amino acid diagenesis and adsorption in near shore anoxic sediments. *Limnological Oceanography*, 24,1014-1021.

- Rubinsztain Y., Yariz S., Ioselis P., Aizenshtat Z., Ikan R. (1986a) Characterization of melanoidins by IR spectroscopy-I. Galactose-glycine melanoidins. *Organic Geochemistry* 9, 117-125.
- Rubinsztain Y., Yariz S., Ioselis P., Aizenshtat Z., Ikan R. (1986b) Characterization of melanoidins by IR spectroscopy-II. Melanoidins of Galactose with arginine, isoleucine, lysine and valine. *Organic Geochemistry* 9, 371-374.
- Schaeffer Ph., Reiss C. et Albrecht P. (1995) - Geochemical study of macro molecular organic matter from sulphur-rich sediments of evaporitic origin (Messinian of Sicily) by chemical degradations. *Organic Geochemistry*, 23, 567-581.
- Schnitzer M. et Khan S. U. (1972) - *Humic Substances in the environment*. Marcel Dekker. 327p.
- Schouten S., De Graaf W., Sinninghe Damste J.S., van Driel G. B. et de Leeuw, J. W. (1994) - Laboratory simulation of natural sulphurisation : II Reaction of multi-functionalised lipids with inorganic polysulphides at low temperatures. *Organic Geochemistry*, 22, 825- 834.
- Sinninghe Damste J. S., Eglinton T. I., de Leeuw J. W. et Schenck P. A. (1989) - Organic sulphur in macromolecular organic matter. I. Structure and origin of sulphur-containing moieties in kerogen, asphaltenes and coals as revealed by flash pyrolysis. *Geochimica et Cosmochimica Acta*, 53, 873-889.
- Sinninghe Damsté J. S., de Leeuw J. W. (1990) - Analysis, structure and geochemical significance of organical-bound sulphur in the geosphere: state of the art and future research. *Organic Geochemistry* 16, 1077-1101.
- Sturm M., Matter A. (1972) - Sedimente und Sedimentationsvorgänge im Thunersees. *Eclogae geol. Helv.* 65 (3), 563-590.
- Sturm M., Matter A. (1978) - Turbidites and varves in Lake Brienz (Switzerland): deposition of clastic detritus by density currents. *Special Publication of the International Association of Sedimentologists* 2, 147-168.
- Suess E. (1973) - Interaction of organic compounds with calcium carbonate-II. Organo-carbonate association in recent sediments. *Geochimica et Cosmochimica Acta* 37, 2435-2447.
- Sugai S. F., Henrichs S. M. (1992) - Rates of amino acid uptake and mineralization in Resurrection Bay (Alaska) sediments. *Marine Ecology, Progress Series* 88, 129-141.
- Tanoue E. et Handa N. (1979) - Differential sorption of organic matter by various sized sediments particles in recent sediment from the Bering Sea. *Journal of the Oceanography Society of Japon*, 35,199-208.
- Tegelaar E. W., de Leeuw J. W., Derenne S., Largeau C. (1989) - A reappraisal of kerogen formation. *Geochimica et Cosmochimica Acta* 53, 3103-3106.
- Tissot B. P., Welte D. H. (1984) - *Petroleum formation and occurrence*. 2nd edition. Springer-Verlag, New York, 699 p.
- Titley J. G., Clegg G. A., Glasson D. R. et Miliward G. E. (1987) - Surface areas and porosities of particulate organic matter in turbid estuaries. *Conference Shelf Res.* 7, 1363- 1366.
- Tribovillard N. P., Desprairies A., Lallier-Vergès E., Bertrand P. (1994) - Vulcanization of lipidic organic matter in reactive-iron deficient environments : a possible enhancement for the storage of hydrogen-rich organic matter. *C.R. Acad. Sci. Paris* 319 (2), 1199-1206.

- Van Heemst J. D. H., Baas M., de Leeuw J. W., Renner R. (1993) - Molecular characterization of marine dissolved organic matter. In: O.K. Øygard eds, Organic Geochemistry, Folch Hurtigtryhk, 694-698.
- Van Veen J. A. V., Kuikman P. J. (1990) - Soil structural aspects of decomposition of organic matter by micro-organisms. *Biogeochemistry* 11 (3), 213-233.
- Wächtershäuser G. (1988) - Before enzymes and templates: Theory of surface metabolism. *Microb. Revue*, 52,452-484.
- Wakeham S. G., Farrington J. W., Gagosian R. B. (1984a) - Variability in lipid flux and composition of particulate organic matter in the Peru upwelling region. *Organic Geochemistry* 6, 204-215.
- Wakeham S. G., Farrington J. W., Gagosian R. B. (1984b) - Biogeochemistry of particulate organic matter in the oceans : results from sediment trap experiments. *Deep Sea Research* 31, 509-528.
- Wang X.-C., Lee C. (1993) - Adsorption and desorption of aliphatic amines, amino acids and acetate by clay minerals and marine sediments. *Marine Chemistry* 44, 1-23.
- Weiler R. R. et Mills A. A. (1965) - Surface properties and pore structure of marine sediments. *Deep-Sea Research*, 12, 51-529.
- Westrich, J. T., Berner R. A. (1984) - The role of sedimentary organic matter in bacterial sulfate reduction: the G model tested. *Limnology and Oceanography* 29 (2), 236-249.
- Zegouagh Y., Derenne S., Largeau C., Bertrand P., Sicre M. A., Rousseau B. (1999) - Refractory organic matter in sediments from the North-West African upwelling system: abundance, chemical structure and origin. *Organic Geochemistry* 30, 101-118.
- Zullig J. J. et Morse J. W. (1988) - Interaction of organic acids with carbonate mineral surfaces in sea water and related solutions : I. Fatty acid adsorption. *Geochimica et Cosmochimica Acta*, 52,1667-1678.

PARTIE III

BIOGEOCHIMIE DE LA MO SEDIMENTAIRE APPLIQUEE AUX RECONSTITUTIONS
DES PALEOENVIRONNEMENTS ET DES PALEOCLIMATS

I- INTRODUCTION

I-1 La variabilité climatique et les climats passés :

Les travaux de recherche en paléoclimatologie concernent essentiellement la période quaternaire et ont pour but de comprendre et de décrire par modélisation les modalités selon lesquelles le climat se modifie avec des échelles de temps allant de quelques dizaines d'années jusqu'à des centaines de milliers d'années. Ces modifications se produisent sous l'influence externe de facteurs astronomiques susceptibles de modifier la quantité d'énergie reçue par la surface de la terre ou sa répartition temporelle ou géographique. Mais des facteurs internes plus ou moins liés au climat global, peuvent venir moduler cette influence car le système climatique de notre planète dépend de l'action parallèle de l'atmosphère, des océans et des calottes de glace avec un rôle et une dynamique spécifique pour chacun de ces réservoirs. Non seulement ces différents compartiments interagissent entre eux de façon non linéaire, mais ils sont aussi en relation avec d'autres systèmes complexes, tel le cycle du carbone. Leur interaction peut être à l'origine de rétroactions dites positives quand elle accentue le processus induit par la contrainte externe, ou négatives quand elle atténue l'effet de ce processus. La variabilité naturelle du climat est forte, mais reste mal connue.

Depuis plus de vingt ans, modélisateurs, paléoclimatologues et océanographes explorent parallèlement les oscillations climatiques les plus rapides, les phénomènes de seuil qui déclenchent les transitions brutales, pour caractériser les changements de climat et le moyen annonciateur de ces transitions. La plupart de ces travaux ont pour but principal la documentation et la compréhension des variabilités naturelles de notre système climatique : océans – atmosphère - calottes de glaces.

Une partie de ces études parmi les plus récentes, se concentre sur les derniers millénaires en le replaçant dans le débat climatique actuel, ceci afin d'étudier l'influence de l'activité anthropique sur ce système. La justification principale de toutes ces études était motivée par les prévisions et les inquiétudes concernant l'augmentation de *la température* puis la hausse du *niveau marin* que risque de subir notre planète au cours du siècle prochain. Les fluctuations passées de ces deux paramètres peuvent être caractérisées à différentes échelles de temps et d'espace grâce aux marqueurs paléoclimatiques.

La mise au point de nouvelles méthodes quantitatives et la modernisation des moyens analytiques usuels (basés sur les géochimies organique, isotopique et minérale) et sur une chronostratigraphie de haute résolution, permettent maintenant de reconstituer avec une grande finesse les variabilités climatiques passées. Plusieurs publications traitent la chronologie des événements climatiques et leurs calibrations (Austin et al., 1995 ; Goslar et al., 1995 ; Bard 1988, Bard et al., 1998, Bard et al., 2004a, b et c ; Bard et al., 2006). De

nombreuses archives sédimentaires enregistrent les marqueurs climatiques, et leur confrontation a été fructueuse dans de nombreux cas. Il faut noter que la comparaison des résultats provenant de sites « marins, lacustres, glaciers, polaires... » et d'échantillonnages « sédiments, spéléothème, coraux, glaces... » variés, n'est possible qu'avec une chronostratigraphie et des datations précises des événements observés. Ces données chronologiques sont évidemment indispensables pour tenter de comprendre l'enchaînement des causes des variabilités passées et relier les résultats provenant des différentes régions et environnements de notre planète (Genty et al., 2003). Les nombreuses études dans ce domaine ont montré par exemple que le climat du dernier millénaire a connu des changements relativement importants « Petit Âge Glaciaire, Optimum Médiéval » du même ordre de grandeur que le réchauffement climatique actuel.

Les études réalisées à une échelle chronologique plus grande, dans un but d'affiner les modèles (comme par exemple les modèles de simulation des changements rapides des climats glaciaires proposé par Ganopolski & Rahmstorf 2001), montrent que l'histoire du climat se caractérise par des événements brusques. Parmi les événements récents les plus étudiés, on retrouve : les événements de Dansgaard–Oeschger « phase de refroidissement » (Dansgaard et al. 1989, Dansgaard et al. 1993) et les événements de Heinrich « phase de réchauffement » (Heinrich H., 1988, Bard et al., 2000), caractérisés par des transitions abruptes s'effectuant en moins d'un siècle et intercalés dans des variabilités de grandes amplitudes. La dernière période glaciaire est marquée par l'occurrence de ces événements climatiques de grande ampleur.

Leurs fréquences est de l'ordre du millier d'années, mais les transitions sont extrêmement brèves, à peine quelques décennies et donc à l'échelle d'une vie humaine. Ces événements ont été soulignés aussi bien au cours des périodes glaciaires qu'au cours des périodes interglaciaires mais rarement par des études sur la MO et sur leurs biomarqueurs (Rosell-Mele et al., 1997, Paillet et al. 2002). La signature sédimentaire de ces événements se retrouve dans l'ensemble de la zone Nord-Atlantique, mais également sur les continents adjacents (Bond et al., 1993 ; Dowdeswell et al., 1995 ; Bard et al., 2006). Les travaux sur l'enregistrement de ces événements sont rarement étudiés en milieu continental et leur mise en évidence dans les archives continentales est moins facile et moins fréquente qu'en milieu marin (Allen et al. 1999).

⇒ Des perspectives de recherche en milieu continental sont de ce point de vue là importantes, notamment sur les environnements tropicaux.

En effet, le peu de travaux réalisés sur les basses latitudes, zones qui constituent mon terrain d'étude dans cette problématique scientifique, montrent que ces fluctuations se manifestent principalement par des variabilités hydrologiques. Des travaux récents (Peterson

et *al.*, 2000; Wang et *al.*, 2004; Cruz et *al.*, 2005) montrent que les variations du cycle de vapeur d'eau au dessus de l'Amérique du sud tropicale influencent directement la circulation atmosphérique et océanique à l'échelle globale. Les températures, quant à elles, présentent localement de faibles fluctuations. Malgré tout, aucun consensus ne ressort sur l'influence des zones tropicales dans la variabilité climatique de notre planète (Stoeker et *al.*, 2003). Cette zone est ma cible d'étude pour mes projets futurs présentés en Partie V de ce mémoire.

I-2 La MO outil de reconstitutions climatiques et environnementales

Des études parallèles, dédiées à l'impact des variations climatiques passées sur les paléocosystèmes se sont développées grâce à l'établissement par les climatologues (sur les carottes de glaces et de sédiments provenant des nombreux Leg ODP) d'une très bonne stratigraphie climatique au Quaternaire. Ces études sont essentielles pour la caractérisation des paléoenvironnements.

Pour alimenter les modèles théoriques, les différentes études s'efforcent de caractériser site par site l'influence des variations climatiques déjà bien établies, en relation avec l'évolution des environnements passés tels que :

- (1) les variations du couvert végétal, les fluctuations de l'hydrologie et des températures en milieux continentaux
- (2) les variations des paléocirculations et des paléoproduktivités en milieux océaniques.

Un autre aspect particulièrement important dans le débat qui nous anime actuellement, concerne le cycle du carbone et l'effet de serre associé ; avec notamment l'influence que peuvent avoir les fluctuations climatiques à l'échelle globale, sur les évolutions des éventuels puits de carbone. Il s'agit notamment de l'importance de la séquestration du carbone par la fossilisation des MO dans les tourbières, les sédiments marins et lacustres .

Mes travaux dans ce domaine s'inscrivent tous dans ces deux aspects (paléoenvironnement et séquestration du carbone) en apportant des données sur les taux de séquestration du carbone en milieu producteur, avec en arrière plan, une participation implicite à la caractérisation du cycle du carbone.

L'utilisation de l'outil organique est récente comparée aux différentes méthodes classiquement utilisées en climatologie tel que la géochimie minérale ou la géochimie des isotopes stables : mes études se basent sur l'utilisation du matériel organique séquestré dans des séries lacustres et marines afin de caractériser la variabilité organosédimentaire. J'ai travaillé sur des sédiments actuels ou passés d'âges variés :

- une série marine d'upwelling, sur un cycle de dépôt court d'environ 500 ans,
- des séries lacustres et marines d'environ 20 Kans

- et une étude qui intègre la totalité du dernier cycle climatique réalisée sur l'upwelling marin du Benguela.

Mes travaux avaient un objectif double. (1) Utiliser les biomarqueurs de sources et d'environnement déjà reconnus pour suivre l'origine et l'état de préservation des MO. Ceci permet grâce à une chronostratigraphie bien établie, de comprendre les fluctuations des apports organiques, l'évolution du paysage végétal et de la paléoproduktivité en fonction des données climatiques connues dans la région d'étude. (2) Rechercher en biogéochimie moléculaire de nouveaux marqueurs de sources mais également de nouveaux marqueurs climatiques permettant de quantifier les paléotempératures, la paléosalinité ou la paléohumidité. Ceci a notamment été rendu possible grâce à l'application des méthodes isotopiques, dont la mesure de l'hydrogène sur des marqueurs organiques moléculaires spécifiques.

Ci-dessous les résumés de mes résultats avec tout d'abord deux essais de calibration organique actuelle dans deux systèmes lacustres. Le premier concerne le milieu tropical en étudiant la distribution spatiale de la MO des sédiments de surface et des producteurs du Lac Caço situé dans le Nord-Est brésilien. L'autre étude, en milieu tempéré (Lac Pavin, France) tente de suivre la composition moléculaire des producteurs organiques actuels, celle de la MO dissoute produite par dégradation dans le Lac et celle de la MO fossilisée dans les sédiments de surface. Sont également présentés ci-dessous les résumés des objectifs et des résultats obtenus sur les archives sédimentaires lacustres et marins d'upwelling, en milieux tropical et intertropical. Les publications illustrant ce thème sont en annexes ([Annexes 10 à 14](#), [et 16 à 18](#))

II- LA CALIBRATION EN ENVIRONNEMENT ACTUEL

Les études paléoenvironnementales entreprises depuis plus d'une dizaine d'années sur les sédiments lacustres par l'équipe MO à Orléans ont montré que le signal organique reste assez complexe. En effet, en plus des sources organiques qui peuvent être diverses, les transformations diagénétiques précoces diversifient davantage le signal moléculaire. Ce filtre diagénétique peut à certains égards masquer l'information paléoenvironnementale ou paléoclimatique (marqueurs de source organique altérés) comme il peut parfois la révéler en la purifiant (information sur les conditions d'incorporation de la matière organique dans les sédiments). Pour toutes ces raisons la calibration préalable entre ce qui est produit dans la colonne d'eau, les transformations lors du transfert et la MO incorporée dans les sédiments devient nécessaire. Malheureusement ces travaux par manque de temps et de personnes impliquées n'ont pas dépassé l'état embryonnaire. J'ai pu malgré tout réaliser quelques études préliminaires. Voici le résumé des résultats obtenus et les idées que j'aimerais

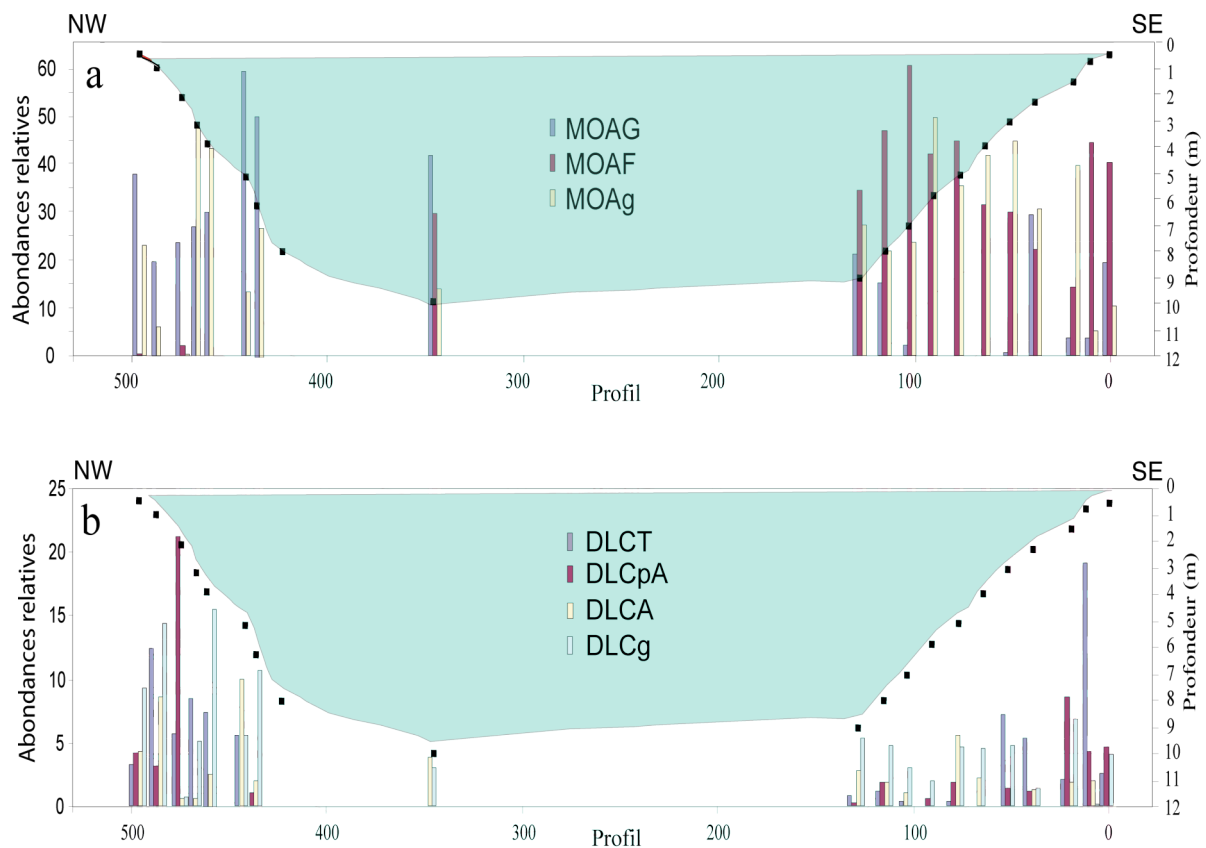
développer davantage dans mes travaux et projet futurs à propos du sujet calibration (Cf. Partie V projets).

II-1 Distribution et état de préservation de la matière organique sédimentaire des sédiments superficiels du Lac Caço (Maranhão, Brésil).

Cette étude s'est focalisée sur le couple production/diagenèse organique précoce et leur rôle respectif dans le remplissage sédimentaire lacustre. Elle nous a révélé que les principaux fournisseurs de la MO dans le lac étaient les joncs et les épiphytes avec une grande hétérogénéité dans la distribution et l'état de dégradation de la MO sur ces sédiments de surface.

Les résultats acquis en géochimie globale et pétrographie ont permis de comprendre comment un lac oligotrophe, comme le Lac Caço a pu accumuler 4 à 6 m de sédiments organiques. Ils ont également permis d'identifier les sources d'un tel remplissage organique.

Les études paléoenvironnementales antérieures ont montré que le niveau du lac avait fluctué depuis 20 000 ans (Sifeddine et al. 2003). Cette variation bathymétrique se traduisait parfaitement dans les archives sédimentaires en terme de variabilité de la diagenèse précoce de la MO (Boussafir et al., 2003).



Le transfert des débris végétaux de la bordure du Lac vers l'intérieur s'accompagne de sa gélification progressive (Figure III-1). De ce fait, l'essentiel de la gélification, s'observe dans les zones les plus profondes. L'évolution de l'amorphisation des débris ligneux reflète ici parfaitement, le rôle de la diagenèse précoce dans les environnements aquatiques. La matière organique amorphe quant à elle montre une tendance générale à l'augmentation de fréquence depuis les berges vers le centre du lac. Cette observation nous a permis de mettre en relation un indice de gélification organique avec l'épaisseur de la colonne d'eau ; et de calibrer ce paramètre pour la MO archivée dans les sédiments (figure III-2).

L'étude moléculaire reste encore à réaliser. Cette étude proposée plusieurs fois en stage de recherche n'a pas rencontré le succès escompté. Les perspectives de recherche sont de pouvoir suivre l'évolution moléculaire des producteurs et la distribution spatiale de biomarqueurs spécifiques avec les produits de dégradation diagénétique de ces derniers dans les sédiments de surface du lac. Ceci permettra de suivre les marqueurs moléculaires de source et de diagenèse et de tester leur évolution le long de la série sédimentaire ayant servi à l'étude paléoenvironnementale et paléoclimatique (Jacob et *al.*, 2004 a et 2004b et 2005)

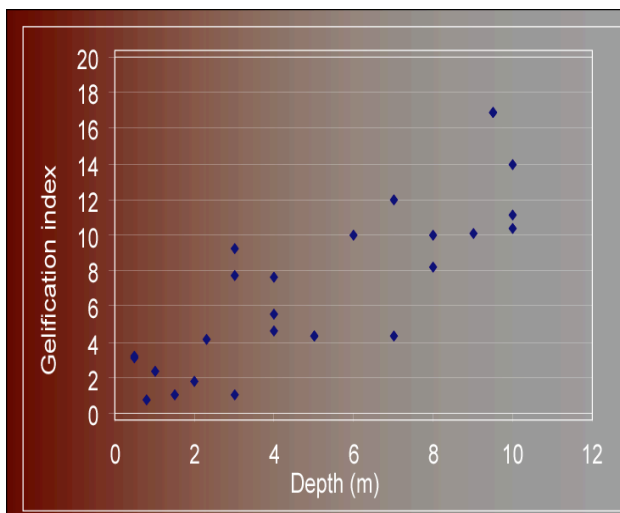


Figure III-2: Relation entre l'indice de gélification déduit du palynofaciès et l'épaisseur de la tranche d'eau du lac Caço. L'utilisation de cet indice pourra permettre de suivre l'évolution bathymétrique du lac au cours du temps. La variation de ce paramètre de paléo-niveau sera l'expression directe de la variation de l'humidité et de la pluviosité sur le bassin versant du Lac Caço.

II-2- Suivi de la composition moléculaire des producteurs actuels, de la MO dissoute de la colonne d'eau et de la MO sédimentaire de surface du Lac Pavin (Massif Central Français)

L'objectif principal de ce travail était d'étudier et de comparer la composition moléculaire de la fraction lipidique contenue : dans les organismes producteurs récoltés sur place dans le Lac ; dans la MO dissoute de l'eau prélevée à différentes profondeurs de la

colonne d'eau oxic et anoxique ; puis dans la MO des 30 premiers cm de sédiments de surface. Ces derniers représentent deux stades diagénétiques différents séparés par leurs textures sédimentaires et leurs couleurs en deux parties égales de 15 cm chacune (Figure III-3).

Ce travail fait partie d'un projet que j'ai initié à l'ISTO et qui cherche à comprendre le rôle de la fraction minérale (notamment argileuse) dans le transfert le long de la colonne d'eau des MO sédimentaires et de leur préservation. La connaissance des différentes fractions moléculaires (de la biomasse produite, de la MO dissoute dans l'eau à différentes profondeurs réparties sur la zone oxygénée et la zone anoxique puis des sédiments) susceptible de réagir avec nos argiles était primordiale pour les travaux de thèse réalisés par Sylvain Drouin soutenue en juin 2007 (cf. Partie II de ce mémoire).

Cette étude nous a montré que les lipides extractibles de ces différentes fractions sont dominés par la famille des alcools, et notamment les polycycliques, avec une diversité remarquable (Boussafir et *al.*, 2005). Les algues macrophytes et les algues phytoplanctoniques présentent les mêmes familles moléculaires avec des proportions relatives différentes. Certaines de ces fractions lipidiques se retrouvent dans la matière organique dissoute de l'eau et dans les sédiments de surface avec quelques altérations notables liées à leur transfert à travers la colonne d'eau.

La composition des lipides extractibles de la colonne d'eau de la zone anoxique est plus riche et mieux préservée que dans la zone oxygénée. Ceci s'explique par un relargage de MO dissoute à partir du sédiment et provenant de la transformation des MO métabolisables déposées sous formes particulières, expliquant ainsi leur absence dans le contenu organique dissous de la colonne d'eau oxic.

La comparaison moléculaire des sédiments représentant deux stades diagénétiques différents, met en évidence des transformations moléculaires importantes au cours de la diagenèse. Par exemple : les défonctionnalisations précoces de certaines molécules, la concentration de plus en plus importante de certains composés aliphatiques et la disparition d'une partie de certaines familles moléculaires, parfois de façon remarquable, à l'exemple des alcools polycycliques.

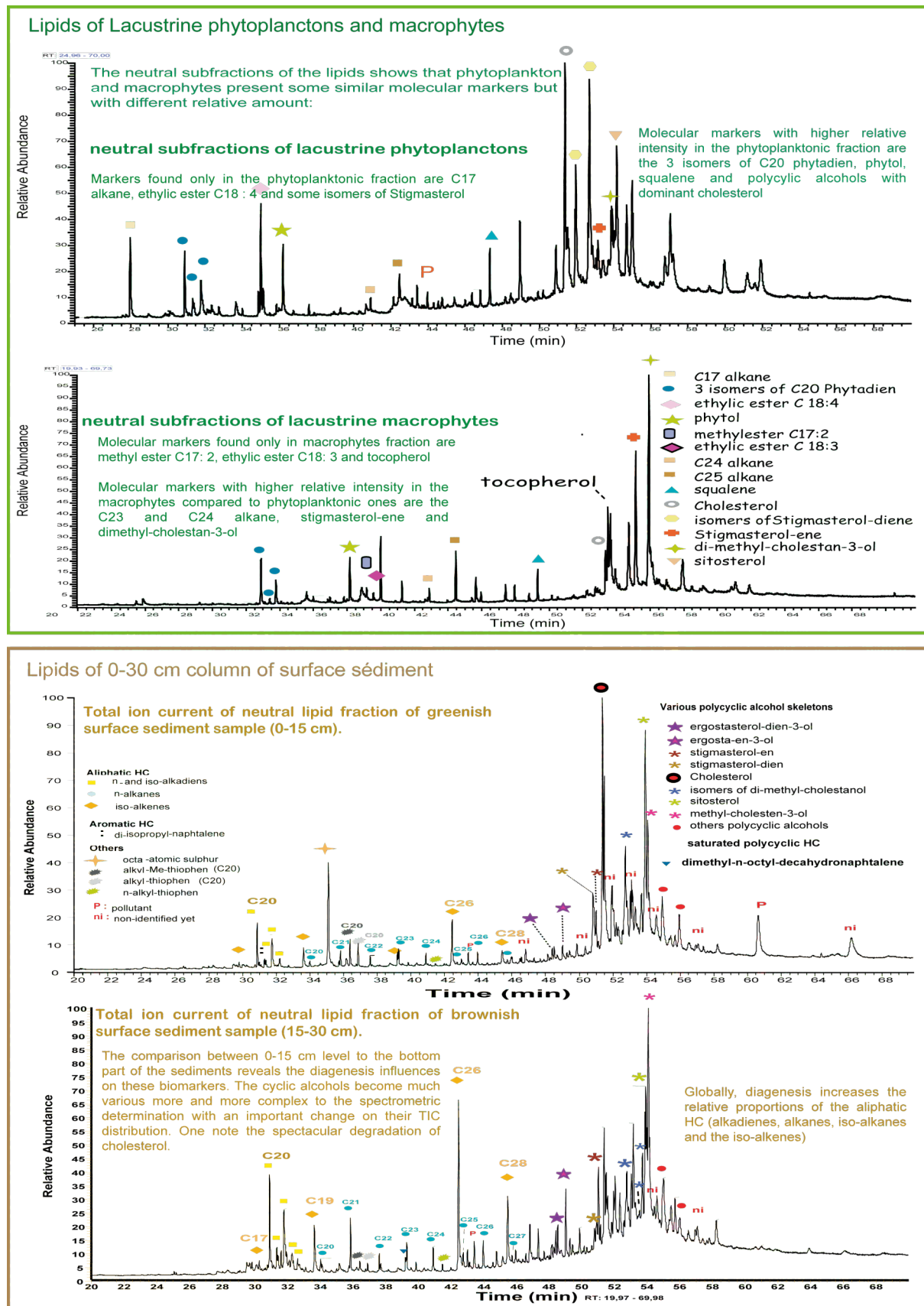


Figure III-3 : Comparaisons des chromatogrammes de la fraction neutre totale obtenue sur les sources organiques produites dans le lac et sur les sédiments de surfaces (Boussafir et al., 2005).

III- ARCHIVES SEDIMENTAIRES, PALEOENVIRONNEMENT ET PALEOCLIMATS

Comme il est évoqué en introduction de cette partie, les archives géologiques (glaces, sédiments) constituent le seul accès, indirect, à l'histoire climatique de la Terre et de son évolution. Il est vrai que dans le domaine océanique, l'utilisation d'outils comme le $\delta^{18}\text{O}$ des carbonates biogéniques ou des alcénones de la MO des sédiments permettent, par exemple, de retrouver les températures des eaux marines et les modalités de la circulation thermohaline. De la même manière en contexte glaciaire, le $\delta^{18}\text{O}$ des cristaux de glace ainsi que les taux de cendres ou de nitrates mesurés à haute résolution sur des carottes de glace se sont avérés d'excellents transcrits des paléoclimats et de la circulation atmosphérique. La combinaison de ces données a permis de construire des modèles climatiques globaux. Le manque de paramètres aussi puissants dans le domaine continental, a longtemps laissé subsister des inconnues sur le comportement de ces modèles et leur influence sur l'environnement continental.

III-1 Les études réalisées en domaine lacustre :

Parmi les archives continentales, les sédiments lacustres se caractérisent souvent par des taux de sédimentation élevés, ce qui restitue un enregistrement sédimentaire à haute résolution. En outre, à l'exception des apports éoliens, les sources minérales et organiques qui contribuent à ces sédiments sont restreintes au bassin versant du lac et témoignent donc des conditions environnementales locales. Cette valeur locale des archives lacustres peut réciproquement être considérée comme un atout pour décrire, dans le détail, les mécanismes complexes et couplés du climat. La complexité du monde vivant s'exprime notamment au niveau de la composition chimique des organismes, à travers la diversité et l'agencement de leurs constituants moléculaires fondamentaux (monomères) lorsqu'une part de ce matériel organique est fossilisée. Mes travaux dans ce thème concernent les études moléculaires de la MO et de leurs variations qualitatives et quantitatives dans les archives sédimentaires lacustres au cours du Quaternaire récent afin de suivre l'influence des variabilités climatiques sur l'environnement. Voici en résumé, quelques résultats majeurs.

III-1-1 Composition moléculaire des MO de deux stades climatiques distincts enregistrés en contexte intertropical (Lac Tritrivakely, Madagascar)

Cette étude a été réalisée par pyrolyse off-line de la MO insoluble de deux niveaux lacustres climatiquement distincts dans le laboratoire de Biogéochimie à l'école de chimie de Paris dirigé à l'époque par Claude Largeau. A cette occasion les analyses effectuées en

collaboration avec Sylvie Derenne (l'actuelle responsable de ce même laboratoire) m'ont permis de caractériser la composition moléculaire de MO provenant de sédiments lacustres récents (Holocène, Lac Tritrivakely à Madagascar) représentant un stade climatique glaciaire et un stade interglaciaire (Boussafir et al., 2000).

Les résultats ont permis de souligner qu'en période glaciaire la sédimentation organique est dominée par les apports détritiques et/ou par l'installation des végétaux supérieurs, ce qui caractérise une sédimentation de climat relativement plus sec.

En période interglaciaire, la sédimentation organique est dominée par la MO phytoplanctonique (preuve d'une installation d'une colonne d'eau), ce qui caractérisera un climat plus humide. Lors des transitions phase humide, phase sèche, la biomasse végétale migrait du bassin versant vers le bassin de sédimentation et inversement. La sédimentation organique alterne ainsi entre une sédimentation lacustre autochtone à laquelle s'associent des apports en provenance du bassin versant (phase humide) et une sédimentation palustre voire tourbeuse (phase sèche).

Ces résultats montraient pour la première fois que l'enregistrement organique, en milieu lacustre, pendant les alternances climatiques s'enregistre de façon inverse en haute latitude qu'en basse latitude. En effet, les résultats obtenus sur des lacs français montrent que les apports allochtones sont quantitativement plus importants que la production autochtone pendant les phases glaciaires. La sédimentation organique est très faible voire inexistante pendant ces phases de climats froids et plus secs qu'en basse latitude où l'inverse se produit.

III-1-2- Variations paléoenvironnementales et paléoclimatiques depuis 20 kans en contexte tropical

Ces travaux ont été réalisés dans le cadre de la thèse de Jérémy Jacob à l'Institut des Sciences de la Terre d'Orléans sous la co-direction de Jean-Robert Disnar et moi-même. Le sujet de cette thèse est le fruit d'une première collaboration avec l'IRD sur l'Amérique du Sud. Il s'agit d'une collaboration tripartite reliant l'Université Fédérale de Fluminense (UFF, Niteroi, Etat de Rio de Janeiro), l'IRD (Unité PaléoTropicale) et l'ISTO. Ce projet avait pour ambition, la reconstitution des environnements qui se sont succédés en Amérique du Sud depuis 20 000 ans. Et par la même occasion, la mise en évidence de nouveaux marqueurs organiques, en domaine lacustre, pour contraindre les variations environnementales et climatiques depuis la fin du Dernier Maximum Glaciaire (DMG), dans le Nord Est du Brésil (Lac Caço, Etat de Maranhão).

Entre la forêt amazonienne humide à l'Ouest et la savane sèche à l'Est, le Lac Caço est remarquablement positionné pour enregistrer finement les changements de la végétation. Par ailleurs, ce lac est situé dans la zone de balancement entre les positions estivale et hivernale de la Zone de Convergence InterTropicale (Figure III-4), ce qui lui confère un intérêt évident pour retracer les changements climatiques.

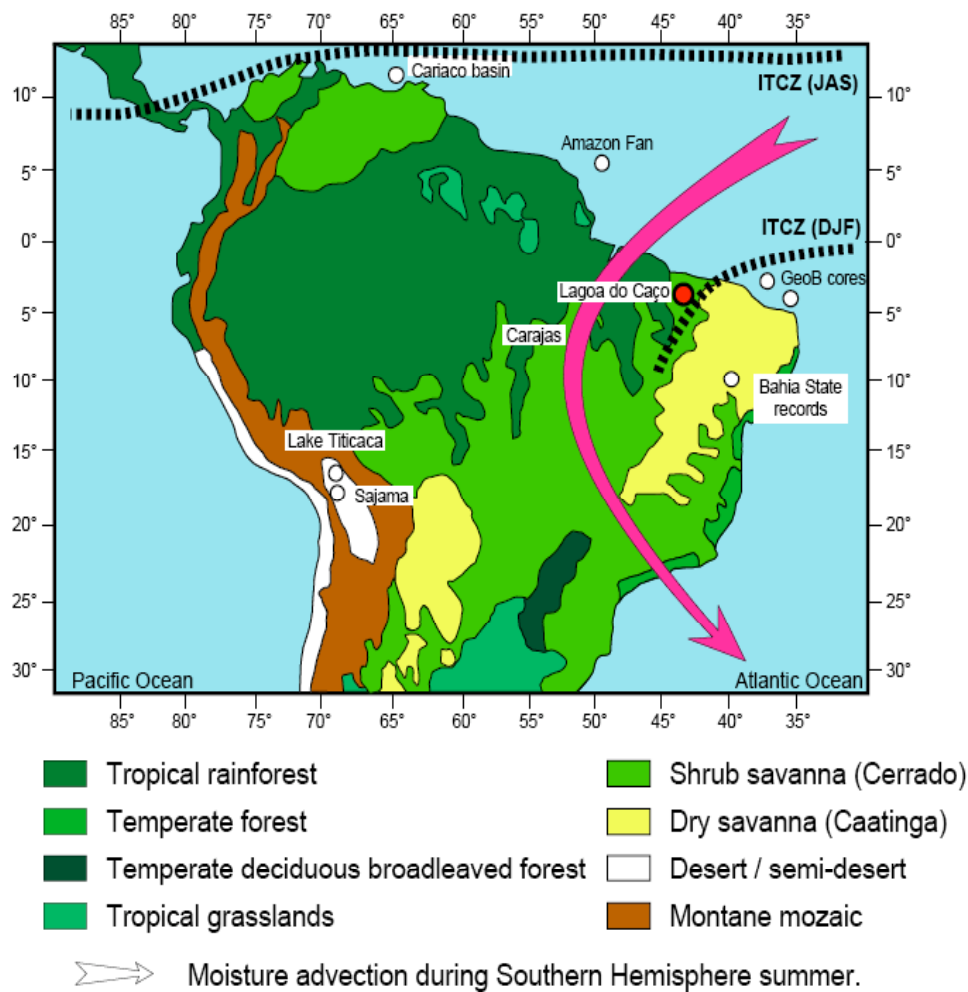


Figure III-4 : Localisation du site d'étude, positions estivale et hivernale de la ZCIT et distribution actuelle des écosystèmes (Image , IRD Paléotropique).

Les finalités de ce travail étaient de comprendre comment s'expriment les variations climatiques connues aux hautes latitudes sur les environnements tropicaux, en contexte continental ; de savoir quelles étaient les conditions qui régnaient en Amérique du Sud pendant le Dernier Maximum Glaciaire (DMG) ; et de montrer comment le Dryas Récent était enregistré dans les Tropiques.

Ce travail avait deux finalités : (1) l'étude de la variation quantitative et qualitative du contenu organique le long de ces 20 kans d'archives lacustres, et (2) la recherche de nouveaux biomarqueurs et d'autres indices biogéochimiques extraits de la matière organique sédimentaire lacustre.

Les sédiments prélevés sur une carotte ont fait l'objet d'une étude de la matière organique (MO) qu'ils renferment afin d'en déterminer les sources et conditions de préservation. Combinées à diverses autres données géologiques et géochimiques, ces informations ont été exploitées pour reconstituer l'évolution du lac et de son environnement (Jacob 2003, Jacob et *al.*, 2004).

Ainsi, la combinaison d'analyses par pyrolyse Rock Eval et d'observations pétrographiques, appuyées par des datations ^{14}C et des observations sédimentologiques, nous a permis de distinguer quatre phases majeures dans les derniers 20000 ans d'histoire que le lac a enregistré.

La première phase, datée de la fin du Dernier Maximum Glaciaire (DMG), se marque notamment par une MO issue de végétaux supérieurs, remarquablement bien préservée au sein d'un sédiment de granulométrie pourtant assez grossière. Selon toute vraisemblance, cette MO a été produite dans un système palustre éphémère, puis rapidement enfouie. Cet épisode sédimentaire s'est probablement déroulé sous un climat relativement aride marqué par des précipitations peu fréquentes, mais fortes.

Entre 19240 et 17250 ans cal B.P., des évidences telles qu'une MO bien hydrogénée, attestent désormais de l'existence d'un vrai lac, ainsi que d'un climat relativement plus humide et d'une saisonnalité assez prononcée.

Après un changement environnemental drastique daté de 17250ans cal B.P., les conditions de sédimentation semblent s'approcher de celles qui subsistent encore actuellement, avec des apports minéraux réduits et une MO très dégradée, issue de végétaux supérieurs. Cependant, l'évolution de la température maximum de pyrolyse TpS2 marque ensuite une amélioration globale de la qualité de la MO. Les variations abruptes qu'enregistre aussi ce paramètre dans l'intervalle considéré pourraient alors témoigner de changements rapides de l'environnement, sous le contrôle de variations climatiques abruptes.

Enfin, les conditions voisines de l'Actuel semblent établies il y a au moins 5600 ans. Depuis cette époque, l'enregistrement d'éventuels changements environnementaux a probablement été tamponné par l'importance relative de la tranche d'eau à l'aplomb du site foré, ainsi que par l'éloignement relatif de ce site, du lieu de production essentiel de la MO actuel : la ceinture de joncs proche de la rive du lac.

Les extraits lipidiques des sédiments du Lac Caço ont été étudiés par chromatographie en phase gazeuse - spectrométrie de masse (CG-SM). La fraction neutre de ces extraits contient une famille d'éthers méthyliques de triterpanes pentacycliques qui n'ont, à notre connaissance, jamais été décrits jusqu'à maintenant dans des sédiments. Plusieurs de ces composés avec des structures de type oléanane, taraxerane, ursane, bauerane, ainsi que des hopanes réarrangés (fernane et arborane), ont été identifiés par comparaison avec des composés standards disponibles. D'après la bibliographie traitant de ces molécules, les éthers méthyliques de triterpanes pentacycliques seraient essentiellement produits par des graminées telles que celles qui peuplent actuellement les savanes sous des basses latitudes. Les implications géochimiques, paléoenvironnementales et phytochimiques de la découverte de ces molécules dans des sédiments a été discutée (Jacob et *al.*, 2005).

Outre les éthers méthyliques décrits dans le paragraphe précédent, les sédiments du Lac Caço contiennent également de l'onocérane I, une molécule peu commune dans les sédiments et pétroles, et qui est ici identifiée pour la première fois dans une série d'âge Quaternaire. Dans des sédiments plus anciens où elle a été trouvée, cette molécule était supposée provenir de fougères ou de mousses. L'inventaire des sources possibles de ce composé à travers une revue de la littérature spécialisée et la confrontation du résultat de cette recherche avec des données palynologiques et paléoclimatiques, nous permet d'exclure les fougères et mousses comme précurseurs végétaux de cette molécule dans les contextes écologique et environnemental du Lac Caço. En fait, si l'on considère que l'onocérane I est abondant dans la fraction lipidique des sédiments datés du Dernier Maximum Glaciaire et du Dryas Récent, les deux périodes les plus sèches qu'a connues le nord-est du Brésil, ce composé peut être considéré comme un indicateur du développement de plantes adaptées à des conditions sèches ou semi-arides (Jacob et *al.*, 2004b).

Des dérivés diagénétiques de triterpènes pentacycliques ont aussi été mis en évidence dans les sédiments. Ils ont permis de retracer la dynamique du peuplement végétal du bassin versant et des bords du lac, ainsi que les conditions de dépôt des sédiments en fonction des changements climatiques (Jacob et *al.*, 2007-a).

Au total, ce travail a d'abord permis l'identification d'une cinquantaine de marqueurs moléculaires, dont certains n'avaient pas encore été décrits antérieurement. La présence de ces composés a été mise à profit pour une reconstitution des environnements passés dans la zone d'étude. Cette approche moléculaire apparaît comme un complément voire un

supplément utile de la palynologie. Par exemple, la plupart de ces molécules sont potentiellement indicatrices d'un seul genre ou d'une seule espèce, ce que la palynologie ne permet pas pour le moment en Amérique du Sud en ce qui concerne les pollens de graminées et de légumineuses (Salgado- Labouriau, 1997). Par ailleurs, les pollens de ces plantes sont aisément dégradés alors que les PTME, et peut-être l'onocérane, apparaissent assez résistants à une diagenèse précoce.

L'intérêt de ces molécules réside dans leur origine très locale, leurs sources végétales étant nécessairement restreintes au bassin versant alors que les pollens des plantes anémophiles ou entomophiles peuvent être disséminés à l'échelle régionale. Les biomarqueurs ont une portée locale, donc précise, en domaine lacustre. Selon Colinvaux *et al.* (2000), les seules évidences directes des successions végétales dans le bassin de l'Amazone sont les pollens enregistrés soit dans les sédiments des lacs, soit dans ceux du delta de l'Amazone. Souhaitons que dans un futur proche, par l'identification d'autres marqueurs très spécifiques et leur utilisation plus large, la géochimie moléculaire pourra compléter, dans la mesure de ses limites, les résultats des études palynologiques.

Dans la continuité de ces travaux de thèse, l'analyse isotopique du D/H moléculaire a permis de suivre les variations d'humidité dans la région depuis 20 000 ans. Il s'agit du premier essai de quantification des variations hydrologiques en contexte tropical, à partir d'une série sédimentaire lacustre. Huang *et al.* (2002) ont montré que le rapport D/H de molécules produites par le phytoplancton, tel que l'acide gras à 16 atomes de carbone (nC_{16} AG), capture le D/H des eaux lacustres (δD_{wat}) (Jacob *et al.*, 2007b). En contexte tropical, le δD_{wat} dépend essentiellement de l'abondance des précipitations. Le D/H de molécules produites par les végétaux terrestres (δD_{hp}), tel l'acide gras à 30 atomes de carbones (nC_{30} AG), lui aussi conditionné par la quantité de précipitations, est affecté par les fractionnements isotopiques survenant lors de l'évaporation de l'eau du sol ou la transpiration au niveau des feuilles. Il constitue donc un indice de la quantité d'eau disponible pour la plante, soit de l'humidité relative. La combinaison de ces deux indices permet d'accéder à l'humidité relative, à la quantité de précipitations, et à l'intensité de l'évapo-transpiration. Les variations de ces trois paramètres durant les 20 000 dernières années sont illustrées en Figure III-5. Elles sont comparées aux variations d'abondance d'onocérane I et du rapport entre pollens d'arbres (AP) et pollens d'espèces herbacées (NAP).

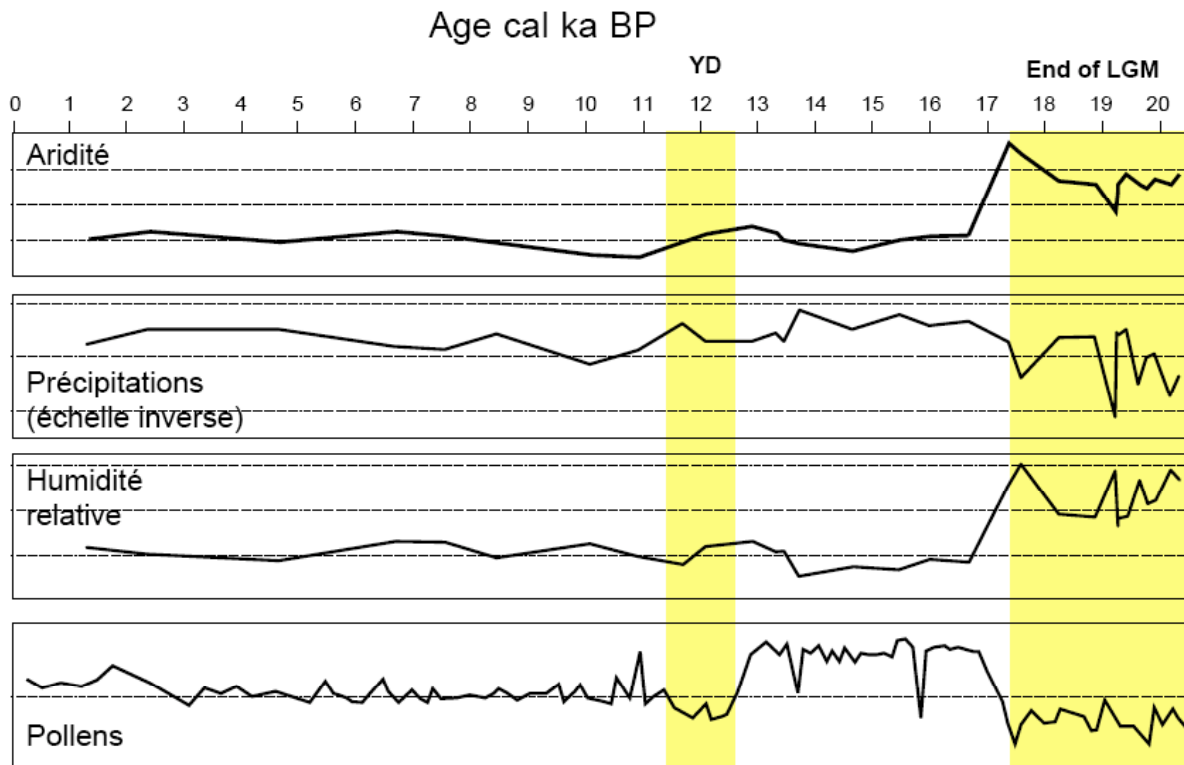


Figure III-5 : Evolution climatique dans la région du Lac Çaço depuis 20 000 ans (Jacob et al., 2007b).

Le δD_{hp} indique deux périodes caractérisées par un climat plus sec : la fin du DMG (entre 20 et 17 000 ans) et, dans une moindre mesure, le Dryas Récent (entre c.a. 13 500 et 11 500 ans), en accord avec les résultats moléculaires et palynologiques. Le $\epsilon_{hp/wat}$ indique que ces périodes sèches correspondent à des périodes de plus forte évapo-transpiration mais également à davantage de précipitations comme l'attestent les faibles valeurs de δD_{wat} . En fait, nous attribuons ces faibles valeurs à des précipitations rares mais brutales qui permettent le développement de populations algaires opportunistes pendant une courte saison humide alors que le δD_{hp} témoigne d'une longue saison sèche qui affecte les végétaux terrestres. Ces résultats ont fait l'objet d'une publication dans QSR (Jacob et al., 2007-b).

III-2- Les études réalisées en domaines marins d'upwelling

III-2-1- Enregistrements moléculaires de la matière organique sédimentaire en zones d'upwellings des marges de l'Amérique du Sud

III-2-1-1 Archives sédimentaires des 12 000 derniers ans :

Ces travaux en cours de finalisation, sont réalisés dans le cadre de la co-direction de la thèse de Marcio Gurgel au sein de l'Institut des Sciences de la Terre d'Orléans (ISTO) avec Elisabeth Vergès de l'ISTO et Abdelfettah Sifeddine de l'IRD. Le sujet de cette thèse fait suite aux collaborations de l'ISTO avec l'IRD sur l'Amérique du Sud. Il s'agit plus particulièrement de l'étude détaillée de la matière organique des archives sédimentaires marines et de l'évolution des marqueurs paléoenvironnementaux et paléoclimatiques *au cours de l'Holocène* de part et d'autre de l'Amérique du Sud (Figure III-6). Les sédiments étudiés proviennent de l'upwelling saisonnier de *Cabo Frio (SE Brésil) pour la côte Est* et de l'upwelling du *Pérou/Chili pour la côte Ouest* (figure II-6).

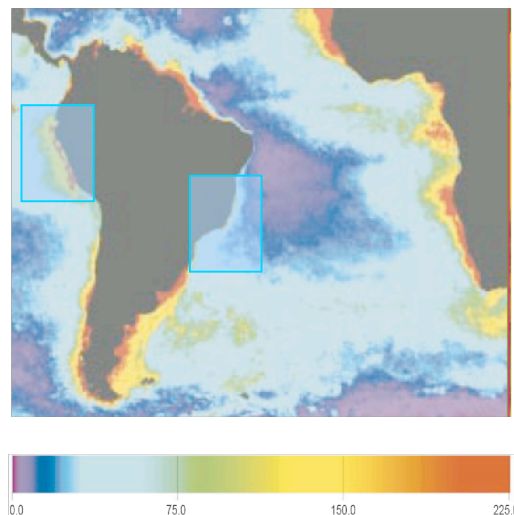


Figure III- 6 : Apports annuels moyen en carbone photosynthétique (g C/m²). (d'après Falkowski et al, 1998). Les valeurs les plus hautes sont situées en zone d'upwelling. Position des zones d'études

Ces travaux ont pour ambition de caractériser les processus de sédimentation de la matière organique dans deux environnements d'upwelling de part et d'autre de l'Amérique du Sud. Le deuxième objectif est de déterminer les variations climatiques enregistrées, leurs variabilités ainsi que leurs interconnexions (Gurgel et *al.*, 2005 ; 2007).

Voici en résumé quelques résultats obtenus sur les carottes de Cabo Frio, Brésil. Les résultats sur l'upwelling du Pérou sont en cours de dépouillement et ne seront pas résumés dans ce rapport.

Les résultats obtenus montrent des teneurs faibles en MO (1,3 % de COT maximum) pour une zone d'upwelling, ce qui indique une forte dégradation de la MO le long de la colonne d'eau : les faibles teneurs à la base correspondent à un niveau de mer très bas (- 110 m il y a 11000 ans). Le maximum de productivité est atteint pendant l'Optimum Atlantique (6000 à 8 000 ans), suivi d'une plus forte variabilité. Les autres paramètres, montrent une MO à l'interface des types II et III, c'est-à-dire marine (très oxydée) avec une influence terrestre. La partie supérieure de la carotte (1500 - 6000) montre une contribution marine plus importante, confirmée par la réduction vers la surface du rapport C/N : ceci peut indiquer un renforcement de la fréquence ou de l'intensité de l'upwelling.

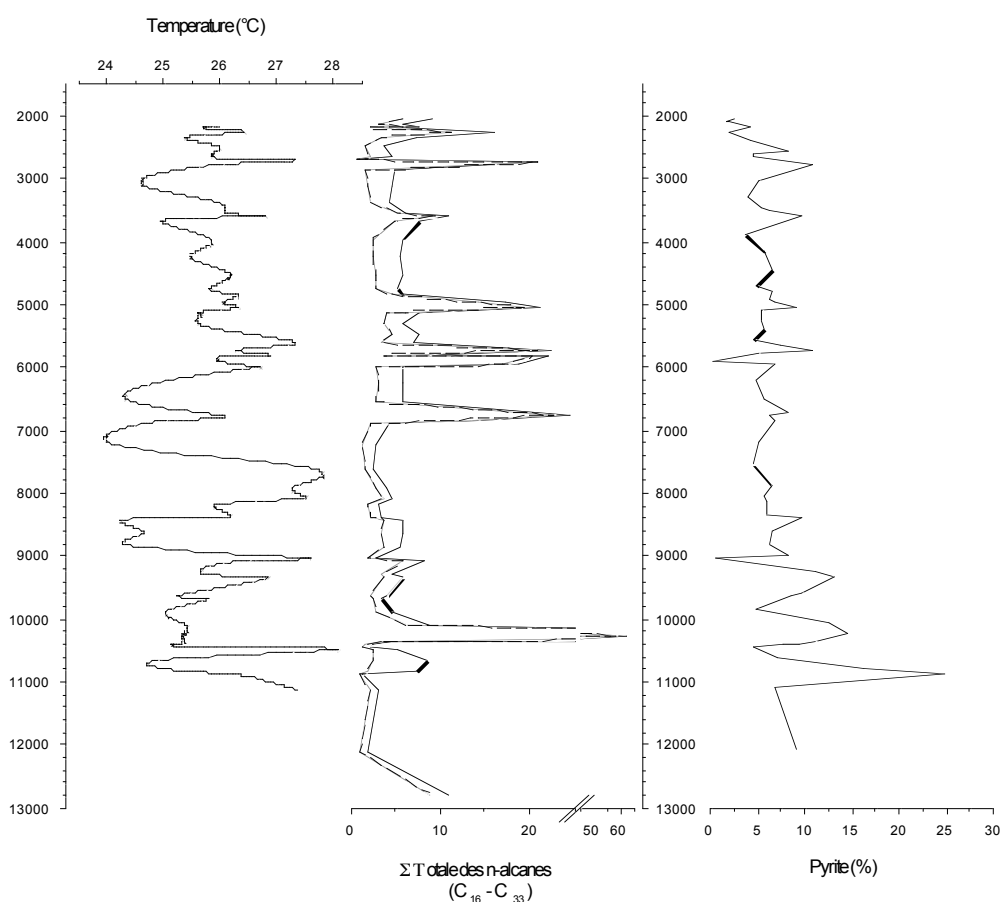


Figure III- 7 : En fonction de l'âge cal. BP est représenté à gauche les températures de surface marine fourni par l'UK37 des alcénones, au milieu la représentation quantitative en ng/g de sédiment des alcanes long et du total des alcanes montrant que la fraction d'alcane est essentiellement représenté par les chaînes longues. Puis à droite le pourcentage en pyrite du palynofaciès. .

La pyrite est présente sur toute la carotte ce qui prouve que le sédiment était anoxique tout le temps. Les sédiments non laminés de ces carottes, pouvaient laisser penser à un environnement complètement oxygéné et bioturbé. La présence de la pyrite avec des fréquences parfois élevées tend à prouver le contraire et laisse à penser qu'au moins une

partie des sédiments superficiels étaient anoxiques, diminuant ainsi le temps de transit de la MO dans cette zone oxygénée.

Les analyses UK₃₇ des alcénones montrent des températures à la surface analogues à celles de l'actuel courant du Brésil (24 à 28°C) (figure III-7) : les épisodes d'upwelling étant de courte durée et restreints à une saison, les signaux de l'upwelling sont "dilués" dans la moyenne annuelle des températures. Toutefois des épisodes de refroidissement à 24-25,5°C sont à noter. Sur cette figure les n- Alcanes montrent une importante contribution terrestre sous forme probablement de pulsations de l'érosion sur le continent. Il s'agit probablement d'apport en provenance du continent, grâce à des épisodes de très fortes précipitations charriant une grande quantité de végétaux supérieurs vers la plateforme continentale. Cette hypothèse est corroborée par la proximité du fleuve Paraíba do Sul au Nord du Cabo São Tomé. Ces épisodes peuvent être liés à l'intensification de la Zone de Convergence Atlantique Sud, apportant des fronts froids et une augmentation de l'activité des courants océaniques froids comme le montre la concordance des signaux de la température de surface marine et la concentration des biomarqueurs des végétaux supérieurs (n-alcanes à chaînes longues). L'augmentation de cette concentration coïncide avec les phases de refroidissement des eaux. Le palynofaciès confirme ces résultats et souligne pendant ces mêmes périodes une augmentation des apports en cuticules et membranes fraîches et bien préservées. La comparaison des indices sur la parité des n-alcanes obtenus et ceux qu'on retrouve dans la littérature nous apporte des indications supplémentaires. Ces indices montrent que le matériel organique détritique de signature continentale est un matériel plus ancien et remanié. Il s'agit d'apport de sédiments provenant de la plateforme marine au niveau de la marge, probablement transportés latéralement par les courants océaniques sous l'influence des fronts froids de l'Atlantique sud qui se trouvent sur leur situation la plus au nord.

L'interprétation et la rédaction des publications sont en cours. La soutenance de cette thèse est prévue pour juin 2008. Les ambitions futures sont de comparer les processus de sédimentation de la matière organique des deux environnements d'upwelling de part et d'autre de l'Amérique du Sud et surtout de déterminer les variations climatiques enregistrées, leurs variabilités et ce qui fait l'originalité de ce sujet, leurs interconnexions.

III-2-1-2- sur des *box cores* ayant archivé les 500 derniers ans

Il s'agit de travaux réalisés en géochimie organique globale et moléculaire et en pétrographie organique des sédiments de la plateforme péruvienne. Cette étude s'est focalisée sur la période de temps la plus récente de ces archives à savoir les derniers 500 ans (Gutiérrez et *al.*, 2006). L'objectif était d'étudier pour la première fois les variations qu'ont subies l'écosystème et l'environnement océaniques de ces upwellings durant cette période récente de la sédimentation. Deux *box-cores* prélevés sur deux zones de sédiments océaniques Pisco et Callao situées sur la plateforme centrale péruvienne (même zone que les carottes longues présentées dans les paragraphes précédents) ont été étudiés. Le contenu organique des sédiments a été caractérisé par des analyses globales en terme de qualité, de type et de quantité. Des observations palynofaciès et leurs quantifications absolues ont permis de tracer l'évolution quantitative des différents constituants organiques.

Les données Rock-Eval (figure III-8) vont dans le sens de l'imagerie X et des analyses des minéraux et des éléments en traces et montrent un changement environnemental radical entre le Petit Âge Glaciaire et l'Actuel. Ceci montre que la sédimentation organique des 500 dernières années dans ces upwellings du Pérou se subdivise en deux phases majeures d'activités et de variabilités distinctes. Ces deux phases expriment le passage de la fin du Petit âge Glaciaire à la situation sédimentaire actuelle. Ce passage s'accompagne d'une intensification régionale des courants océaniques profonds et une production organique plus importante.

Il est vrai que les variabilités quantitatives de la MO, sur une période aussi courte avec une Zone à Minimum d'Oxygène (ZOM) permanente, reflètent essentiellement la productivité de l'upwelling. La variabilité qualitative (conditions de dégradation-préservation) ne peut être mise en cause dans ce cas. La présence de fort COT après 1820 (âge calendaire) est donc à mettre en relation avec une intensification de l'upwelling après le Petit Âge Glaciaire. La baisse notable du COT peut signifier une baisse de la productivité de l'upwelling. Ce qui suppose que les « Alizé » et la circulation océanique côtière (courant de Humboldt) étaient probablement moins actifs pendant le Petit Âge Glaciaire comparé à la situation actuelle.

Ce changement important vers les années 1820, avec ses deux grandes phases sédimentaires majeures, a été enregistré à l'échelle de toute la plateforme du Pérou puisqu'il se retrouve sur deux sites très éloignés, l'un en face de Pisco (au Sud) et l'autre de Callao (au Nord) deux localités péruviennes. Des phases d'oxygénation remarquables ont été enregistrées par les paramètres de qualité de la MO de la phase post Petit âge Glaciaire et particulièrement sur le site le plus profond, celui de Pisco. Ces analyses quantitatives et qualitatives nous ont également révélé deux types de périodicité qui s'ajoutent à ces

événements oxygénés : une cyclicité de courte période (décennale en moyenne) incluse dans des périodes plus longues d'en moyenne 100 ans.

Ces résultats globaux nous ont permis de proposer des conclusions importantes sur l'activité de ce système (Gutierrez et al., 2006 ; Sifeddine et al., accepté).

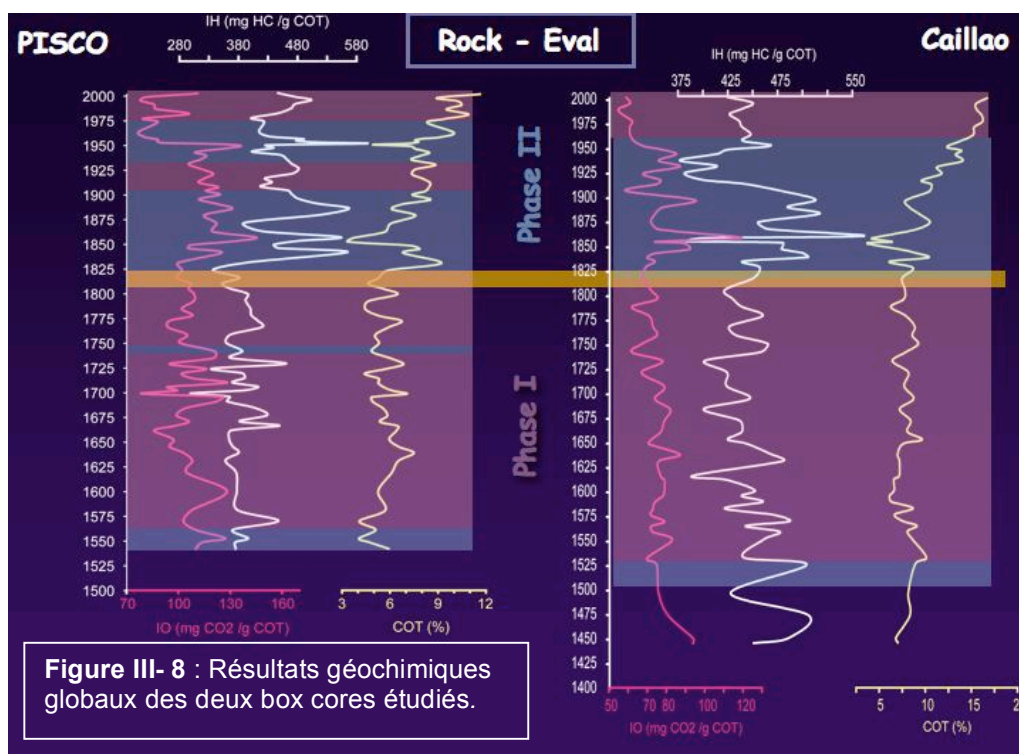


Figure III- 8 : Résultats géochimiques globaux des deux box cores étudiés.

D'autres événements particuliers ont été enregistrés au cours de ces deux phases et des interprétations ont été proposées.

Les analyses moléculaires effectuées sur des échantillons représentatifs des deux phases, ont permis d'aboutir à de nouvelles conclusions concernant les sites étudiés (Callao et Pisco) et les conditions environnementales qui y régnaient. Ces analyses ont été réalisées sur les extraits lipidiques et par pyrolyse flash (figure III-9) du kérogène isolé de la roche. Les chromatogrammes de la fraction neutre des extraits organiques permettent une distinction qualitative entre les deux sites. Sur le site de Callao, la MO présente une origine mixte avec un apport continental important et une contribution phytoplanctonique faible. La MO du site de Pisco quand à elle est essentiellement phytoplanctonique. Les marqueurs moléculaires plaident plus pour des produits organiques issus de diatomées ou de bactéries. Ces analyses révèlent également une différence moléculaire sensible entre les deux périodes. Ainsi, la Phase 2, post Petit Âge Glaciaire est notablement plus riche en composés fonctionnalisés oxygénés comme les esters d'acides gras, les alkyl-ol et alkyl-on...

Ces résultats approfondis en géochimie moléculaire ont montré l'existence de périodes d'oxygénation plus fréquentes durant le dernier siècle probablement en relation avec

l'augmentation de la fréquence des événements El Niño pendant cette phase (Boussafir et al., 2007). En effet, El Niño peut jouer un rôle sur la qualité de la fossilisation des MO produites. Les phases de réchauffement des années El Niño liées à la baisse de l'activité des alizés provoquent un déplacement en profondeur de la thermocline, de l'halocline et surtout de l'oxycline dans cette région. Ceci déplace la ZMO en profondeur provoquant ainsi pendant ces périodes la fossilisation de MO plus oxygénées. Les fractions organiques riches en composés hydrocarbonés, comme en témoigne leur fort IH présentent également des Indices IO- RE anormalement haut dans ce cas. L'une des explications possibles est l'existence probable du mécanisme de préservation décrit au laboratoire de Claude Largeau et de Sylvie Derenne à savoir la préservation « oxydative ». Dans ce cas précis, et contrairement à la description de ce mécanisme uniquement basé sur l'analyse moléculaire, nous avons ici un cas où l'oxygénation est associée à une augmentation de la qualité hydrogénée de la MO et corroborée par les analyses moléculaires. Les échantillons sont également riches en composé hydrocarboné linéaire et oxygéné observés sur les chromatogrammes obtenus sur les extraits lipidiques et sur les pyrolysats.

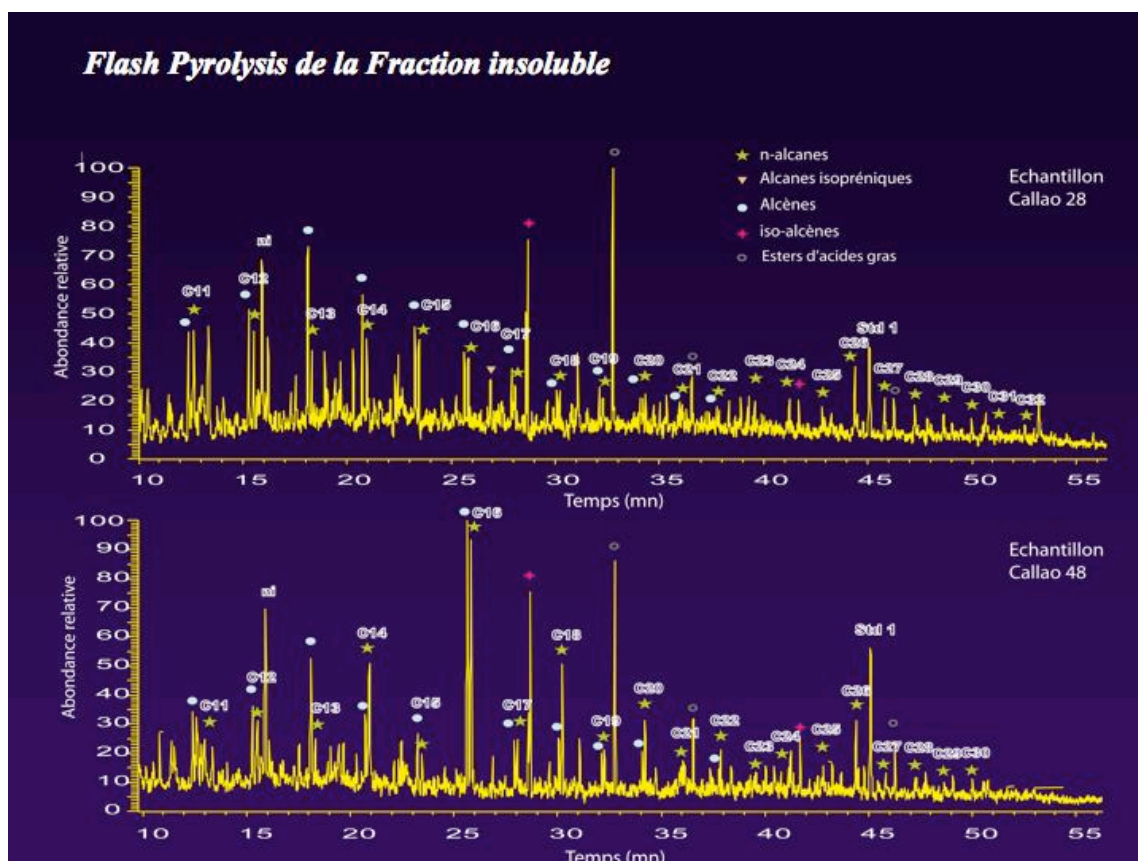


Figure III-9 : Exemple de chromatogramme obtenu par pyro/GC/MS sur deux échantillons, représentatifs d'une phase d'oxygénation dans la ZMO et d'une phase dite « normale », du site de Callao (Boussafir et al., 2007)

L'étude des n- alcanes de la fraction lipidique montre l'absence totale de distribution typiquement algale. Ce qui est surprenant, vu la richesse des zones d'upwelling en productivité phytoplanctonique et notamment l'upwelling du Pérou, considéré comme le plus productif au monde. Seules les alcanes des cires cuticulaire des plantes continentales se retrouvent dans l'extrait lipidique. La pyrolyse flash est venue par la suite apporter des éléments de réponse à ce sujet. La distribution des n-alcanes produits par pyrolyse des kérogènes insolubles, montre un mode en C17, C19 typique des produits algaires. Ce qui montre que dans des sédiments frais et jeunes la signature moléculaire obtenue à partir des extraits peut être dans certain cas trompeuse. L'accès à l'information stockée dans la MO insoluble devient indispensable. L'apport phytoplanctonique se retrouve sous forme particulière non-extractible probablement bien liée à la fraction minérale et plus particulièrement la fraction argileuse.

L'origine de la différence d'apport organique existant entre les deux sites est à mettre en relation avec la situation géographique. Les apports continentaux sont importants sur Callao car ce site le moins profond et le plus proche du continent que celui de Pisco. Ces deux paramètres géographiques jouent évidemment un rôle important dans le type et la quantité d'apport organique sur ce site. C'est pour cette raison que les fluctuations rencontrées dans les apports continentaux sont très bien enregistrées sur ce site. Les variations d'humidité sur le continent, synchrones avec les phases d'oxygénation sont probablement à l'origine des fluctuations d'apport détritique. Ce qui est logique car pendant les phases El Nino les régions habituellement sèches connaissent une augmentation importante de la pluviosité et donc des ruissellements qui amplifient les apports en sédiments. Ceci montre clairement l'intérêt de multiplier les sites pour filtrer le message lié aux événements climatiques et océanographiques de celui qui serait lié à un effet de site (particularité géographique unique d'un site ou d'un bassin). La seule étude de Pisco (plus profond et plus loin de la côte) ne nous permettait pas de conclure sur les fluctuations d'humidité qu'a connues le continent.

III-2-2- Cas de la marge continentale namibienne (Lüderitz, Atlantique Sud-Est) : impacts des variations climatiques sur la paléoprodutivité

Il s'agit du deuxième aspect de la thèse réalisé par L. Pichevin soutenu en 2004. L'objectif de cette partie multimarqueurs était de fournir une meilleure compréhension du rôle joué par le système d'upwellings du Benguela vis-à-vis de la séquestration du carbone au cours des deux derniers cycles climatiques. Il est utile de rappeler que les sédiments de la pente continentale namibienne sont riches en matières organiques (MO), bien que les processus sédimentaires soient exclusivement hémipélagiques. En plus de la caractérisation

des mécanismes de préservation à l'origine de la fossilisation de la MO et de sa distribution en haut et en bas de pente, au large de la cellule de Lüderitz (25°6S) présenté dans la partie II de ce rapport d'HdR, le deuxième objectif était de suivre les variations quantitative et qualitative des MO exportées et par conséquent de la paléoproduktivité pendant le dernier cycle climatique. Les analyses moléculaires, spectroscopiques, pétrographiques nous ont montré que l'enfouissement du carbone organique était plus efficace pendant les périodes glaciaires du fait de flux de MO accrus vers le sédiment (figure III-10). Ces flux agissaient positivement sur l'initiation de mécanismes de fossilisation tels que la sulfuration naturelle grâce à un apport accru en MO métabolisable. Par ailleurs, des associations organo-minérales dans la colonne d'eau ont été responsables de la protection pendant le transport d'une quantité non négligeable de MO métabolisable, et assuré son accumulation sur la pente inférieure. Les teneurs en carbone organique varient au rythme des cycles glaciaires-interglaciaires. (Pichevin et al. 2004). Par ailleurs, nous avons montré que le taux de MO préservée de manière nanoscopiquement amorphe par le mécanisme de sulfuration dans le sédiment est proportionnel aux COT. Le fonctionnement de l'upwelling était renforcé pendant ces périodes froides où les vents alizés, considérés comme moteurs de l'upwelling, et l'apport en nutriment était plus efficace.

La qualité pétrologène de la matière organique accumulée est restée d'une assez bonne qualité et constante sur la pente supérieure quelle que soit la période climatique considérée, mais plus faible et variable sur la pente inférieure. La distribution spatio-temporelle de la qualité de la MO a été mise en relation avec la distribution des modes de préservation, eux-mêmes conditionnés par les flux de MO en provenance de la surface.

Les enregistrements du signal isotopique de l'azote acquis par ailleurs, révèlent une structure compartimentée de l'upwelling de Lüderitz et l'existence d'un découplage de la dynamique des nutriments et de la productivité entre une cellule de plateau, toujours très active, et une cellule de rupture de pente, plus sensible aux variations climatiques. Ce découplage jette un nouvel éclairage sur les raisons de la distribution de la qualité de la MO sur la pente.

Les variations temporelle et spatiale des flux de MO intégrant le sédiment dépendent des fluctuations de la productivité et du niveau marin relatif, ces deux paramètres étant eux mêmes contrôlés par le climat. Les variations eustatiques ont partiellement gouverné l'exportation de carbone organique vers la pente continentale supérieure en déplaçant vers le large la zone de productivité maximum pendant les bas niveaux marins. Par ailleurs, la relative constance du signal isotopique de l'azote, de la carotte de haut de pente a montré que la productivité de la cellule côtière n'a pas drastiquement variée entre les phases

glaciaires et interglaciaires. Ainsi, le comportement de cette zone eutrophe de l'océan vis-à-vis de la séquestration du carbone ne se serait pas profondément modifié au rythme des variations climatiques et aurait, par conséquent, joué un rôle négligeable dans les fluctuations du CO₂ atmosphérique. La cellule de rupture de pente semble au contraire avoir oscillé entre des conditions plutôt oligotrophes pendant les phases interglaciaires, à mésotrophes voire eutrophes, pendant les stades glaciaires.

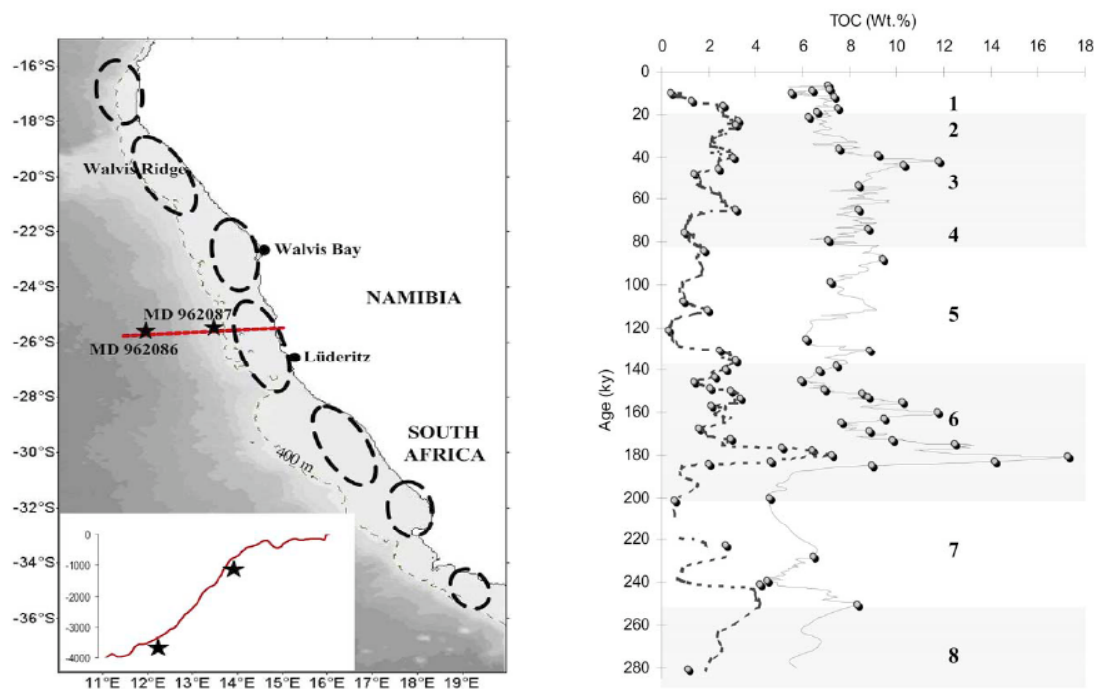


Figure III- 10 : A gauche la carte de situation des carottes, topographie de la pente de Lüderitz et bathymétrie. La courbe de niveau en pointillé représente la profondeur de rupture de pente de la plateforme. Les ellipses représentent les cellules d'upwelling. A droite Les teneurs en COT en fonction de l'âge des sédiments pour MD962086 (carotte de bas de pente en pointillé) et MD962087 (plus haut sur la pente en trait plein) les points gris représentent les échantillons observés en palynofaciès. Les stades isotopiques glaciaires 2, 3, 4, 6 et 8 sont surlignés par la bande grise et les stades isotopiques 1, 5 et 7 par les bandes blanches. La séquestration du carbone organique était plus efficace pendant les phases glaciaires au niveau de la pente continentale de cet upwelling (Pichevin et al., 2004).

La productivité d'un upwelling est à la fois gouvernée par le taux de résurgence et la richesse en nutriments des eaux de subsurface. La seconde partie de ce travail nous a révélé que la productivité, soutenue par l'apport de nitrate en surface, n'est que partiellement contrôlée par la force des alizés. Plusieurs travaux concordent avec les résultats obtenus, et montrent que les advections de masses d'eaux angolaises, indiennes et l'utilisation des nutriments en Antarctique conditionnent l'alimentation en nitrate et silicium, et par voie de conséquence le rendement et la nature de la production primaire de l'upwelling à l'échelle des cycles climatiques. En effet l'étude granulométrique et statistique des sédiments silicoclastiques d'origine éolienne, réalisé par Laetitia Pichevin, a permis la reconstruction

des variations de la force des alizés avec une résolution inférieure au millier d'années. En outre, le marqueur de force des vents, en accord avec les variations de température de surface (SST), constitue un témoin fidèle des variations de l'activité physique de l'upwelling aux échelles orbitales. On considère généralement qu'une relation simple existe entre la productivité du système d'upwellings du Benguela et la force des alizés - ceci a été montré à l'échelle annuelle (Holmes et al., 2002). Ce travail de thèse nous a permis de réviser ce postulat de base en examinant les variations de productivité, de force des vents et de disponibilité en nutriments aux échelles orbitales. La comparaison entre le signal isotopique de l'azote sédimentaire et les indicateurs de productivité, d'une part, et les marqueurs d'intensité physique de l'upwelling (SSTs et taille des particules éoliennes) d'autre part, révèle que, sur des périodes de plusieurs milliers d'années, l'approvisionnement en nitrate vers la zone photique était contrôlé par la richesse en nitrate des eaux centrales plutôt que par l'intensité des vents. Les fortes productivités associées à une disponibilité en nitrate importante pendant la transition 3/2 et le stade isotopique 6.6 ont été attribuées à l'apport d'eaux riches en nitrate en provenance du bassin Angolais. Au contraire, la pompe biologique de carbone constituée par le système d'upwellings du Benguela était affaiblie pendant les interglaciaires (en particulier les déglaciations et les optima climatiques) du fait d'une advection plus massive d'eau indienne provenant partiellement d'une zone dénitrifiante particulièrement active aux périodes considérées. Ainsi, la dénitrification dans les zones d'oxygène minimum est susceptible d'influencer le bilan en nitrate et la productivité des autres régions de l'océan, comme le système du Benguela. Or, les mécanismes modulant la perte en azote par dénitrification ne sont pas encore entièrement compris.

En conclusion de ce travail, qu'on peut considérer comme un exemple réussi d'étude organosédimentaire appliquée aux archives quaternaires récentes, on peut dire que la compréhension des mécanismes permettant la fossilisation et l'enfouissement du carbone organique et le suivi quantitatif et qualitatif de la MO au cours des phases climatiques passées sont intimement liées. Cette étude a marqué une étape dans la compréhension des dynamiques biologique et physique du système d'upwellings du Benguela. Ce dernier est caractérisé par une grande complexité liée à la morphologie du plateau (compartimentation *cross-shore* de l'upwelling) ainsi qu'à la position de ce système dans les circulations océaniques générale (circulation thermohaline) et régionale (proximité du bassin Angolais et de l'océan austral). Notre étude démontre que des modifications sensibles de la circulation générale ou des comportements physique et/ou biochimique des autres zones productives «adjacentes» (océan austral) et même lointaines (océan nord indien) ont des répercussions notables sur la productivité de ce système et l'accumulation sédimentaire de la matière organique sur la pente continentale.

IV- CONCLUSIONS ET PERSPECTIVES DE LA PARTIE III :

Les travaux de recherches réalisés sur la calibration du signal organique sont fragmentaires et rares et méritent un regain d'intérêt de la part des organiciens. L'une des conclusions qu'on peut tirer des premières études réalisées jusqu'à présent est que le potentiel de recherche de cette problématique est vaste et des développements sont possibles à la fois dans le domaine pétrographique que géochimique.

D'un point de vue pétrographique, les résultats obtenus sur le nouvel indice de gélification (somme des MO gélifiées et en cours de gélification sur le total des fractions organiques) et sa relation avec l'épaisseur de la tranche d'eau lacustre, expression du temps de transfert des fractions organiques lignocellulosiques en milieu aquatique, sont encourageants mais mérite d'être confirmés par d'autres études sur d'autres environnements lacustres. De la même manière les résultats géochimiques réalisés sur le Lac Pavin, notamment moléculaires, montrent qu'il serait intéressant de coupler systématiquement les investigations réalisées sur les sédiments de surface avec celles réalisées sur les producteurs organiques potentiels et leurs produits de dégradation prélevés dans la colonne d'eau. Le couplage systématique de la calibration organique et des processus de fossilisation actuelle avec l'étude des archives enregistrées dans le même environnement sédimentaire devrait faire l'objet de grand programme scientifique associant les communautés des biogéochimistes, pétrographes, et biologistes afin d'une part d'assurer le suivi des transformations que subit la MO depuis la zone de production jusqu'aux sédiments. Et d'autre part de comprendre comment le signal peut être altéré ou révélé par la diagenèse. La découverte de nouveaux marqueurs organiques sera d'une grande utilité pour le décryptage de l'information environnementale et ou climatique que les archives sédimentaires sont disposées à nous dévoiler.

Cette deuxième partie du mémoire rejoint la première sur le rôle que jouent les argiles et les fractions minérales en général dans le transfert de la MO vers les sédiments. L'étude des particules organiques en cours de sédimentation, recueillies dans la colonne d'eau, dans la couche néphéloïde et à l'interface sédimentaire, permettrait de préciser les mécanismes d'association entre argile et matière organique dans la zone d'étude et le lien existant entre la neige marine et les agrégats organiques associés et observés en microscopies photonique puis électronique. Elle permet également de suivre les marqueurs sources et leur transformation le long de la colonne d'eau. Là encore un exemple où l'aspect calibration ne peut être dissocié de la problématique préservation de la MO en environnement actuel.

L'une des questions que se posaient et se posent toujours les géochimistes organiciens, et pour laquelle la calibration en milieu actuel peut apporter une réponse, est celle concernant la relation qui existerait entre la concentration dans les sédiments d'un biomarqueur et la densité réelle des organismes producteurs de ces mêmes molécules. Il est évident que les différents biomarqueurs ne sont pas produits de la même façon et dans les mêmes proportions quels que soient les organismes sources. La pratique du géochimiste dans l'état actuel des connaissances, part de l'hypothèse de l'uniformité de synthèse des molécules entre les différents producteurs organiques. L'interprétation d'un indice paléoenvironnemental est donc limitée par les processus qui contrôlent sa production, auquel s'ajoute les transformations au cours du transport et les processus de son archivage.

Les travaux basés sur la MO comme outil nous a révélé sa grande sensibilité envers les reconstitutions paléoclimatique et paléoenvironnementale. Les résultats obtenus permettent de tirer des conclusions importantes sur le régime sédimentaire de la MO et l'influence des changements climatiques sur ce régime. L'exemple des boxes cores des sédiments des 500 dernières années de la marge péruvienne a révélé pour la première fois un changement paléoocéanographique important à partir de la fin du Petit Âge Glaciaire. Une augmentation de la productivité organique et des phases d'oxygénation très fréquentes observées sur la qualité de la MO, reflétant des fluctuations paléoocéanographiques importantes qui avait pour effet le balancement fréquent de l'OMZ depuis la fin du LGM. Ces balancements ont été interprétés pour la première fois comme une accélération d'événement de type El Niño depuis cette période.

Les travaux réalisés sur le dernier cycle climatique enregistré par les sédiments de la pente continentale de l'upwelling du Benguela nous ont montré que la productivité et l'enfouissement du carbone qui s'en suit étaient plus importants au cours des phases glaciaires comparées aux phases interglaciaires. Les upwellings et leurs moteurs jouent un rôle important, mais la disponibilité des nutriments dépend également de la disponibilité des nitrates en relation directe avec la dénitrification s'opérant en basse latitude. Les travaux réalisés sur l'upwelling sud-africain suggèrent d'étudier plus systématiquement les zones de transition entre régions océaniques eutrophes et oligotrophes, leur réponse vis-à-vis des changements climatiques, ainsi que le forçage potentiel qu'elles exercent sur le flux de carbone ; l'ensemble de ces critères semblant pertinents au vu de nos résultats.

Il est vrai que vérifier l'existence d'un tel couplage entre hautes et basses latitudes et examiner son impact potentiel sur le climat nécessite le développement d'études intégrées

sur l'Océan Austral et les upwellings des basses latitudes sud.

Les résultats obtenus en milieu lacustre et notamment du Lac Caço ont permis la découverte de biomarqueurs spécifiques de sécheresse : l'Onocérane et de nombreux autres composés polycycliques de végétaux supérieurs permettant de suivre l'évolution des biomasses du bassin lacustre. Le couplage avec le D/H moléculaire sur des acides gras produits par les végétaux supérieurs, utilisé pour la première fois en milieu tropical, a fourni des informations précieuses sur l'évolution de la paléohumidité et de l'évapotranspiration depuis le dernier maximum glaciaire. Cette étude montre que la recherche de biomarqueurs spécifiques des sources organiques ainsi que des marqueurs climatiques (paléotempératures, paléohumidité, paléosalinité...), devrait être l'un des objectifs majeurs de nos travaux futurs. Certains de ces marqueurs climatiques comme les alcénones pour les paléotempératures de surface existent déjà pour le milieu marin (Zhao 1995 et références associées), mais le challenge scientifique futur reste le développement des marqueurs en milieux lacustres. Ces données climatiques manquent cruellement dans les environnements continentaux où les influences des variabilités climatiques de différent ordre sont très mal connues. Les perspectives sur ce sujet sont très nombreuses et des pistes sont actuellement en cours d'études. Parmi celles-ci l'utilisation des Tétraéthers lipidiques des Crénarchéotes (bactéries du picoplancton) pour les paléotempératures et la recherche des producteurs éventuels des alcénones retrouvés à plusieurs reprises dans les sédiments lacustres afin de les calibrer et d'en faire un analogue aux alcénones d'*Emiliana huxleyi*, coccolitophoridées utilisé en biogéochimie moléculaire en milieu marin.

On peut dire qu'en domaine lacustre, beaucoup reste à faire. Le Lac Caço a été un cadre d'étude original car la matière organique que recèle ses sédiments est principalement issue de végétaux supérieurs. Toutefois, des approches similaires, mettant en jeu des signatures en triterpènes pentacycliques et d'autres marqueurs spécifiques, doivent être envisagées sur d'autres sites pour vérifier la présence des PTME et de l'onocérane. Ce champ d'investigation apparaît prometteur en termes de reconstitutions paléoenvironnementales. L'originalité du Lac Caço ne doit pas rester comme un cas isolé, un cas particulier voire une exception. Les travaux de calibration et d'identification réalisés dans le cadre de la thèse de J. Jacob nous a révélé la difficulté de découvrir de nouveaux biomarqueurs et surtout la difficulté de les valider chimiquement. Le préalable essentiel à de nouvelles voies de recherche dans le domaine des biomarqueurs est l'identification plus précise de certains composés fossilisés. Les problèmes liés à leur identification rendent également nécessaire la mise à disposition de la communauté scientifique, de critères d'identification de ces molécules. En plus de données synthétiques, le "monde" des biomarqueurs manque cruellement de composés de référence pour les valider.

Dans les années à venir, l'effort devrait donc porter sur la synthèse de ces composés et leur mise à disposition du plus grand nombre, en collaboration avec des laboratoires de synthèse chimique.

Pour finir avec les perspectives, le dernier point concernant les biomarqueurs en général et les triterpènes pentacycliques en particulier est lié aux développements ces dernières années de la caractérisation isotopique de molécules isolées des matrices sédimentaires, soit par extraction chimique, soit par pyrolyse. Ces analyses, mettant en oeuvre à la fois les isotopes stables du carbone et de l'hydrogène ($\delta^{13}\text{C}$, $\delta\text{D}/\text{H}$), le ^{14}C et le $\delta^{18}\text{O}$ (sur la cellulose et les monomères de lignine) sont très prometteuses dans le cadre de reconstitutions paléoenvironnementales et paléoclimatiques. Il est en effet possible, par ce biais, d'établir des proxies paléoenvironnementaux (pCO_2 , paléo-précipitations...).

Ces études portent pour le moment sur des composés dont les sources peuvent être multiples (n-alcanes, n-alcools...). Leur application aux triterpènes pentacycliques dans le cadre de reconstitutions paléoenvironnementales/paléoclimatiques n'a pas encore été tentée, ce qui ouvre ici encore des perspectives très intéressantes. Il est en effet rare de disposer de marqueurs moléculaires aussi spécifiques des organismes producteurs, ceux-ci pouvant être limités à une espèce pour les PTME comme pour l'onocérane. Des relations aussi étroites entre fossile moléculaire et organisme précurseur sont pour le moment circonscrites en domaine marin aux alcénones, synthétisées par le coccolithe *Emiliana huxleyi* et en domaine lacustre aux botryococcènes, produits par *Botryococcus braunii*. La découverte de biomarqueurs spécifiques d'une famille, d'un genre ou d'une espèce de végétaux supérieurs est donc une première dans les sédiments.

L'un des exemples pertinents est l'utilité que peuvent avoir les informations portées par l'isotopie de molécules spécifiques de végétaux supérieurs contenus dans les apports organiques continentaux aux sédiments de plateforme et de pente continentales, notamment au niveau des zones d'upwellings. Le déchiffrement de l'information sur la productivité phytoplanctonique autochtone marine serait couplé aux informations sur les paléoprécipitations enregistrées par l'isotopie moléculaire des biomarqueurs spécifiques des végétaux produits sur le continent comme les triterpanes pentacycliques des zones (ou périodes) humides ou l'onocérane qui serait produit dans un contexte ou (événement) climatique sec.

Références citées dans la partie III :

- Allen J.R.M., Brandt U., Brauer A., Hubberten H.W., Huntley B., Keller J., Kraml M., Mackensen A., Mingram J., Negendank J.F. W., Nowaczyk N.R., Oberhansli H., Watts W.A., Wulf S., Zolitschka B., (1999) - Rapid environmental changes in southern Europe during the last glacial period, *Nature* 400, 740–743.
- Austin W.E.N., Bard E., Hunt J.B., Kroon D., Peacock J.D., (1995) - The ^{14}C age of the Icelandic Vedde Ash: implications for Younger Dryas marine reservoir age corrections, *Radiocarbon* 37, 53–62.
- Bard E., Arnold M., Hamelin B., Tisnerat-Laborde N., Cabioch G., (1998) -Radiocarbon calibration by means of mass spectrometric $^{230}\text{Th}/^{234}\text{U}$ and ^{14}C ages of corals. An updated data base including samples from Barbados, Mururoa and Tahiti, *Radiocarbon* 40, 1085–1092.
- Bard E., Arnold M., Mangerud J., Paterné M., Labeyrie L., Duprat J., Melieres M.A., Sonstegaard E., Duplessy J.-C., (1994) - The North-Atlantic atmosphere-sea surface ^{14}C gradient during the Younger Dryas climatic event, *Earth Planet. Sci. Lett.* 126, 275–287.
- Bard E., Correction of accelerator mass spectrometry (1988) - ^{14}C ages measured in planktonic foraminifera: Paleoceanographic implications, *Paleoceanography* 3, 635–645.
- Bard E., Ménot-Combes G., Rostek F., (2004c) - Present status of radiocarbon calibration and comparison records based on polynesian corals and Iberian Margin sediments, *Radiocarbon* 46, 1–14.
- Bard E., Rostek F., Ménot-Combes G., (2004b) - Radiocarbon calibration beyond 20000 ^{14}C yr BP, by means of planktonic foraminifera of the Iberian Margin, *Quat. Res.* 61 (2), 204–214.
- Bard E., Rostek F., Ménot-Combes G., (2006) - Chronologie des variations climatiques rapides pendant la dernière période glaciaire C. R. Palevol 5, 13–19
- Bard E., Rostek F., Ménot-Combes G., better (2004a) A radiocarbon clock, *Science* 303 178–179.
- Bard E., Rostek F., Turon J.-L., Gendreau S., (2000) - Hydrological impact of Heinrich events in the subtropical Northeast Atlantic, *Science* 289, 1321–1324.
- Bond G., Broecker W., Johnsen S., McManus J., Labeyrie L., Jouzel J., Bonani G., (1993) - Correlations between climate records from North-Atlantic sediments and Greenland ice, *Nature* 365, 143–147.
- Boussafir M., Laggoun-Défarge F., Derenne S. & Largeau C. (2000) - Bulk and pyrolytic studies of insoluble organic matter from Tririvakely lake sediments (Interglacial-like and last maximum glacial stages). *Applied Pyrolysis*, 2000, Sevilla, p. 107
- Boussafir M., Foudi M., Jacob J. Disnar J.-R., Sifeddine A., Spadano Albuquerque A.-L (2003) - Petrography and bulk geochemistry studies of organic matter from actual surface sediments of Lake Caço (Maranhão, Brasil) ». Relation ship between early diagenesis and organic sedimentation of lacustrine filling. the 21st Int. Meeting Org. Geochem., 8-12 september 2003, Krakow, Poland.
- Boussafir M., Drouin S., Albéric P., Durand A., (2005) - Calibration of organic signal in sedimentary lacustrine records. Molecular comparison between actual and producers, dissolved organic matter and sedimentary organic matter (Lac, Pavin, France), IMOG 2005 Seville

- Boussafir M., Sifeddine A., Sasias M., Gutierrez D., Ortlieb L., Durand A. (2007) - Apport de la géochimie et de la pétrographie organique dans l'étude des sédiments déposés au cours des cinq derniers siècles sur la plateforme péruvienne. ASF 2007, Caen
- Colinvaux, P.A., De Oliveira, P.E. et Bush, M.B., (2000) - Amazonian and neotropical plant communities on glacial time-scales: The failure of the aridity and refuge hypotheses. *Quaternary Science Reviews* **19**, 141-169.
- Cruz Jr., F.W., Burns, S.J., Karmann, I., Sharp, W.D., Vuille, M., Cardoso, A.O., Ferrari, J.A., Silva Dias, P.L., Viana Jr, O., (2005). Insolation-driven changes in atmospheric circulation over the past 116,000 years in subtropical Brazil. *Nature* **434**, 63–66.
- Dansgaard W., Johnsen S.J., Clausen H.B., Dahl-Jensen D., Gundestrup N. S., Hammer C.U., Hvidberg C.S., Steffensen J.P., Sveinbjörnsdottir A.E., Jouzel J., Bond G., (1993) - Evidence for general instability of past climate from a 250-kyr ice-core record, *Nature* **364**, 218–220.
- Dansgaard W., White J.W.C., Johnsen S.J., (1989) - The abrupt termination of the Younger Dryas climate event, *Nature* **339**, 532–534.
- Dowdeswell J.A., Maslin M.A., Andrews J.T., McCave I.N., (1995) - Iceberg production, debris rafting, and the extent and thickness of Heinrich layers (H-1, H-2) in North-Atlantic sediments, *Geology* **23**, 301–304.
- Drouin S. (2007) Rôle des phyllosilicates dans la préservation et la fossilisation de la Matière Organique pétrologène Thèse soutenue à l'Université de Orléans
- Ganopolski A., Rahmstorf S., (2001) - Rapid changes of glacial climate simulated in a coupled climate model, *Nature* **409**, 153–158.
- Genty D., Blamart D., Ouahdi R., Gilmour M., Baker A., Jouzel J., Van-Exter S., (2003) - Precise dating of Dansgaard–Oeschger climate oscillations in Western Europe from stalagmite data, *Nature* **421**, 833–837.
- Goslar T., Arnold M., Bard E., Kuc T., Pazdur M.F., Ralskajasiewiczowa M., Rozanski K., Tisnerat N., Walanus A., Wicik B., Wieckowski K., (1995) - High-concentration of atmospheric ^{14}C during the Younger Dryas cold episode, *Nature* **377**, 414–417.
- Gurgel, M.H., Sifeddine, A. Lallier-Vergès, E., Boussafir, M. et Jacob, J., (2005) - Holocene Paleooceanographic Conditions of Cabo Frio Upwelling System (Rio de Janeiro / Brazil). As Inferred by Bulk and Molecular Geochemical Approach From Sedimentary Organic Matter. AGU Fall Meeting, San Francisco, Décembre 2005
- Gurgel, M. H. C.; Boussafir, M. ; Sifeddine, A. ; Lallier-Vergès, E. (2007) - Enregistrements moléculaires de la matière organique sédimentaire de l'upwelling de Cabo Frio (SE Brésil) au cours de l'Holocène. In: 11ème Congrès Français de Sédimentologie, 2007, Caen - France. Livre des Résumés. Paris : Associations des Sédimentologues Français, 2007. v. 57. p. 154.
- Gutiérrez D, Sifeddine A., Reyss J. L., Vargas G., Velazco F., Salvattecchi R., Ferreira, Ortlieb L., Field D., Baumgartner, Boussafir M., Boucher H., Valdès J., Marinovic L., Soler P., & Tapia P. (2006) Anoxic sediment off Central Peru record interannual to multidecadal changes of climate and upwelling ecosystem during the last two centuries. *Advances in Geosciences*, **6**, 119-125,
- Heinrich H., (1988) - Origin and consequences of cyclic ice rafting in the Northeast Atlantic ocean during the past 130 000 years, *Quat. Res.* **29**, 143–152.
- Holmes E., Lavik G., Fischer G., Segl M., Ruhland G., and Wefer G. (2002) Seasonal variability of delta N-15 in sinking particles in the Benguela upwelling region. *Deep-Sea Research Part I-Oceanographic Research Papers* **49**, 377-394.

- Huang, Y., Shuman, B., Wang, Y., Webb III, T., 2002. Hydrogen isotope ratios of palmitic acid in lacustrine sediments record late Quaternary climate variations. *Geology* 30, 1103–1106.
- Huang, Y., Shuman, B., Wang, Y., Webb III, T., 2004. Hydrogen isotope ratios of individual lipids in lake sediments as novel tracers of climatic and environmental change: a surface sediment test. *J. Paleolimnol.* 31, 363-375.
- Huang, Y., Street-Perrott, F.A., Perrott, F.A., Metzger, P., Eglinton, G., 1999. Glacial-interglacial environmental changes inferred from the molecular and compound-specific $\delta^{13}\text{C}$ analyses of sediments from Sacred Lake, Mt. Kenya. *Geochim. Cosmochim. Acta.* 63, 1383–1404.
- Jacob, J., 2003. Enregistrement des variations paléoenvironnementales depuis 20000 ans dans le Nord Est du Brésil (Lac Caço) par les triterpènes et autres marqueurs organiques. PhD thesis, Université d'Orléans, 296p.
- Jacob, J., Disnar, J.R., Boussafir, M., Sifeddine, A., Albuquerque, A.L.S., Turcq, B., 2004a. Major environmental changes recorded by lacustrine sedimentary organic matter since the Last Glacial Maximum under the tropics (Lagoa do Caçó, NE Brazil). *Palaeogeogr., Palaeoclim., Palaeoeco.* 205, 183-197.
- Jacob, J., Disnar, J.R., Boussafir, M., Ledru B. M., Albuquerque, A.L.S., Sifeddine, A. et Turcq, B., (2004b) Onocerane testifies to dry climatic events during the Quaternary in the Tropics. *Organic Geochemistry*, 35, 289-297.
- Jacob, J., Disnar, J.R., Boussafir, M., Sifeddine, A., Albuquerque, A.L.S., Turcq, B., 2005. Pentacyclic triterpene methyl ethers in recent lacustrine sediments (Lagoa do Caçó, Brazil). *Org. Geochem.* 36, 449-461.
- Jacob, J., Disnar, J.R., Boussafir, M., Albuquerque, A.L.S., Sifeddine, A. et Turcq, B., (2007a). Contrasted distributions of triterpene derivatives in the sediments of Lake Caçó reflect paleoenvironmental changes during the last 20,000 yrs in NE Brazil. *Organic Geochemistry* 38, 180-197.
- Jacob, J., Huang, Y., Disnar, J.R., Sifeddine, Boussafir, M., A., Albuquerque, A.L.S., Turcq, B., (2007b). Paleohydrological changes during the last deglaciation in Northern Brazil. *Quaternary Science Reviews* 26, 1004-1015
- Pailler D., Bard E., (2002) - High-frequency paleoceanographic changes during the past 140 000 years recorded by the organic matter in sediments off the Iberian Margin, *Palaeogeogr. Palaeoclimatol. Palaeoecol.* 181, 431–452.
- Peterson, L.C., Haug, G.H., Hughen, K.A., Ro^ohl, U., 2000. Rapid changes in the hydrologic cycle of the Tropical Atlantic during the Last Glacial. *Science* 290, 1947–1951.
- Pichevin L. (2004) - Sédimentation organique profonde sur la marge continentale namibienne (Lüderitz, Atlantique Sud-Est) : impacts des variations climatiques sur la paléoproduktivité, Thèse de l'Université Bordeaux.
- Rosell-Mele A., Maslin M.A., Maxwell J.R., Schaeffer P., (1997) - Biomarker evidence for Heinrich events, *Geochim. Cosmochim. Acta* 61, 1671–1678.
- Salgado-Labouriau, M.L., (1997)- Late Quaternary palaeoclimate in the savannas of South America. *Journal of Quaternary Science* 12/5, 371-379.
- Sifeddine, A., Albuquerque, A.L.S., Ledru, M-P., Turcq, B., Knoppers, B., Martin, L., Zamboni de Mello, W., Passenau, H., Landim Dominguez, J.M., Campello Cordeiro, R., Abrao, J.J., Bittencourt, A.C., 2003. A 21000 cal years paleoclimatic record from Caçó Lake, northern Brazil: evidence from sedimentary and pollen analyses. *Palaeogeogr., Palaeoclim., Palaeoeco.* 189, 25-34.

- Sifeddine, A., Bertaux, J., Mourguiart, Ph., Disnar, J.R., Laggoun-Défarge, F., 1998. Etude de la sédimentation lacustre d'un site de forêt d'altitude des Andes centrales (Bolivie). Implications Paléoclimatiques. *B. Soc. Geol. Fr.* 169, 395-402.
- Sifeddine, A., Gutierrez, D., Ortlieb, L., Boucher, H., Velazco, F., Field, D., Vargas, G., Boussafir, M., Salvattecchi, R., Ferreira, V., García, M., Valdes, J., Caquineau, S., Mandeng Yogo, M., Cetin, F., Solis, J., Soler, P., Baumgartner, T. (2007) - Laminated sediments off the Central Peruvian Coast record changes in terrestrial runoff, water mass oxygenation and upwelling productivity over recent centuries. *Progress in oceanography*. Sous press
- Sifeddine, A., Martin, L., Turcq, B., Volkmer-Ribeiro, C., Soubiès, F., Campello Cordeiro, R., Suguio, K., 2001. Variations of the Amazonian rainforest environment: a sedimentological record covering 30,000 years. *Palaeogeogr., Palaeoclim., Palaeoeco.* 168, 221-235.
- Stoecker, T.F., 2003. South dials north. *Nature* 424, 496–499.
- Wang, X., Auler, A.S., Edwards, R.L., Cheng, H., Cristalli, P., Smart, P.L., Richards, D.A., Shen, C.-C., 2004. Wet periods in northeastern Brazil over the past 210 kyr linked to distant climate anomalies. *Nature* 432, 740–743.
- Zhao M., Beveridge N.A.S., Shackleton N.J., Sarnthein M., Eglinton G., (1995) Molecular stratigraphy of cores off Northwest Africa – sea-surface temperature history over the last 80 ka, *Paleoceanography* 10, 661–675.

PARTIE IV

AUTRES ACTIONS DE RECHERCHES:

- I- UNE ROCHE MERE,
- II- UN CHARBON,
- III- UNE ROCHE RESERVOIR
- ET IV- UN SOL

(Publications pour la partie IV : Annexes 8, 9 et 15)

I- UNE ROCHE MERE :**La sédimentation organique du Cénomano-Turonien du nord-ouest de l'Afrique :
Une comparaison entre le bassin de Tarfaya au Maroc et le bassin du Sénégal.**

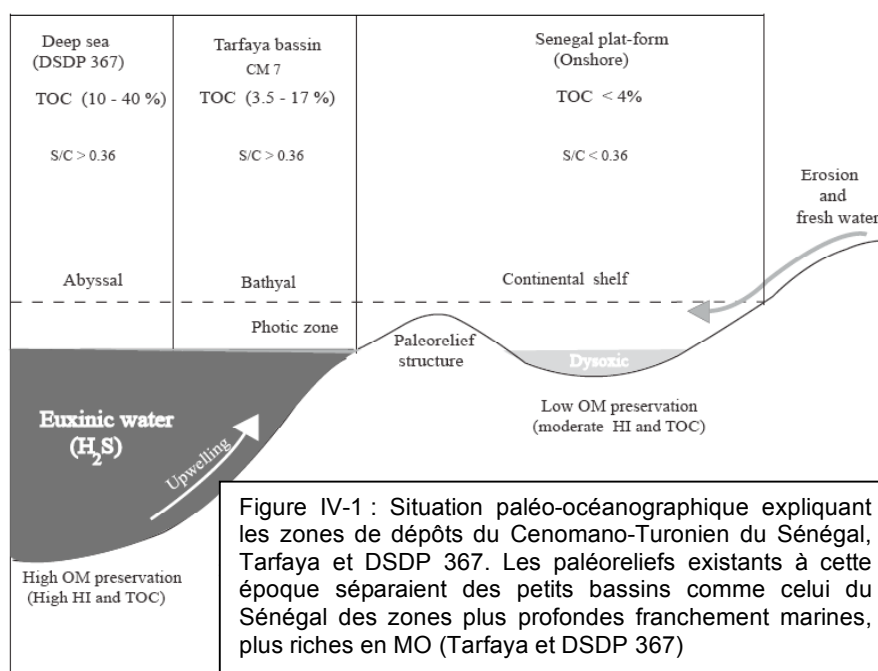
Cette partie du mémoire concerne ma participation à l'encadrement de la thèse de Nzoussi-Mbassani Pierre soutenu en 2003 et co-dirigé par J.R Disnar et F. Laggoun-Défarge à Orléans. Ma participation concerne l'étude géochimique moléculaire notamment par pyrolyse flash de la fraction insoluble de la MO. L'objectif était de caractériser la MO des dépôts de black-shales du Cénomano-Turonien du bassin du Sénégal afin de préciser les conditions environnementales de leur accumulation. Une collaboration avec Nadia Khamli enseignante de l'Université de Tétouan (Maroc) nous a permis de comparer l'environnement de dépôt du bassin étudié à celui de Tarfaya au Maroc. Les travaux de thèse ont permis entre autres de montrer que les conditions présumées anoxiques, de façon globale et à l'échelle de toute la marge atlantique du Nord Ouest de l'Afrique, sur ces dépôts de Black Shales, n'ont pas réellement affecté la totalité des bassins de cette zone géographique pendant la période étudiée. Le modèle proposé relance le débat qui oppose les partisans d'un premier rôle joué par l'anoxie (conditions de préservation) à ceux qui pensent par contre que c'est la productivité primaire qui induit l'anoxie. Dans le cadre de ce travail, nous avons considéré que le meilleur moyen d'approcher ce problème était de faire une comparaison entre des séries contemporaines ayant connu une évolution géodynamique voisine.

La problématique de sédimentation organique du Cénomano-turonien a été élargie grâce à ce travail à l'ensemble de la marge Nord-Atlantique. L'approche consistait donc à comparer l'expression du Cénomano-turonien observée sur la plate-forme sénégalaise à un autre mode d'expression rencontré dans le bassin de Tarfaya au Maroc. Ensuite cette confrontation a été étendue à l'ensemble de la marge, grâce aux données de forages DSDP. Les résultats obtenus nous ont permis de distinguer deux faciès majeurs dépendant des conditions de dépôt. Un premier faciès à faible teneur en carbone organique (<4%) dont la pétrographie et l'analyse moléculaire montraient une matière organique mixte terrestre et marine, et dont les conditions de dépôt correspondent à un environnement suboxique ($S/C < 0,36$), soumis à un flux détritique considérable. Le deuxième faciès majeur présente des teneurs en carbone organique élevées : en moyenne plus de 9%, pouvant localement atteindre plus de 17%. Ici, la matière organique qui est homogène et d'origine marine, présente des IH élevés dénotant d'excellentes conditions de préservation. Cette caractéristique s'accorde avec des teneurs en soufre elles aussi élevées ($S/C > 0,36$) indiquant des conditions de préservation anoxique. De telles conditions ont notamment été favorables à un processus de sulfuration souligné par l'abondance des composés organosoufrés observés sur les pyro-chromatogrammes. Les caractéristiques de ce deuxième faciès sont presque similaires à ceux qui sont observées au niveau d'autres

environnements profonds (Sud Casamance, DSDP 367). La comparaison entre ces environnements anciens, et des modèles actuels de sédimentation conduit à émettre des réserves sur le concept de forte productivité fréquemment évoqué pour expliquer de façon générale le dépôt des "black – shales".

On peut donc dire que la distribution des formations cénomano-turonniennes et leur richesse en carbone organique semblent dépendre plus de la paléogéographie que d'un supposé mécanisme uniforme de sédimentation ou d'anoxie générale. Ainsi les niveaux déposés dans les environnements de plateforme apparaissent moins riches en matière organique que ceux qui se sont déposés en haut voire en bas de pente.

Les facteurs locaux et notamment les apports détritiques, l'influence de courants littoraux oxygénés, la sédimentation d'une matière organique mixte, constituent les traits caractéristiques majeurs des faciès de plateforme. En revanche, les faciès des milieux plus profonds sont caractérisés par une prédominance de matière organique phytoplanctonique, avec une signature moléculaire dominée par des composés organo-soufrés. Au Céno-mano-Turonien, la productivité primaire de la zone d'étude était relativement faible par rapport aux zones d'upwelling actuelles. Il est ainsi difficile d'imaginer que le phénomène d'upwelling ait été déterminant dans le processus d'accumulation de black shales. La distribution des faciès organiques durant cette époque contraste avec les observations qui peuvent être faites sur les milieux océaniques actuels. Ainsi le modèle de sédimentation proposé à l'issue de cette étude (Nzoussi-Mbassani et al. 2003), suggère l'existence de bassins sédimentaires isolés séparés par des paléoreliefs où des structures hautes héritées de la phase de rifting, limitant les échanges entre les domaines profonds et la plate-forme continentale,



II- UN CHARBON :

Altération diagénétique et post-diagénétique (thermicité, oxydation) des charbons carbonifères du Massif Central français (Saint-Etienne, Graissessac et autres lieux)

Cette étude a été réalisée dans le cadre du DEA puis de la thèse de Yoann Copard co-encadré par Jean Robert Disnar et moi-même et soutenue publiquement le 22 février 2002. L'objectif principal était d'étudier l'origine hydrothermale ou supergène de l'altération des charbons humiques du Massif Central Français. Les résultats obtenus au DEA sur l'étude des deux paramètres de rang classiques de la matière organique, c'est-à-dire le pouvoir réflecteur de la vitrinite (R_o , en %) et le T_{max} (°C) de la pyrolyse Rock-Eval 6 (RE6), nous a permis d'émettre une hypothèse sur la circulation de fluides chauds et oxydants post houillification et ayant affecté des charbons du Carbonifère supérieur, de divers bassins intramontagneux du Massif Central français (Copard et al., 2000). Cette interprétation se basait principalement sur des valeurs anormalement fortes du T_{max} par rapport à la réflectance, conduisant à une information contradictoire en terme de stade de maturité de ces charbons. De surcroît, ces valeurs anormalement fortes du T_{max} s'accompagnaient fréquemment par de fortes valeurs de l'Indice d'Oxygène RE6 et de faibles valeurs d'Indice d'Hydrogène. De précédentes études ayant montré la stabilité du T_{max} en pareil cas, nous avons (?) exclu que ces phénomènes aient pu résulter d'un processus d'altération supergène. Il a donc été logiquement proposé que la distorsion de ces paramètres de rang, devait nécessairement impliquer un événement à la fois thermique et oxydant ayant permis de faire évoluer le T_{max} et conjointement l'IH et l'IORE6.

Outre le comportement inhabituel du T_{max} , les observations pétrographiques effectuées sur ces charbons (figure IV-2) ont aussi révélé des micro-fracturations sur les vitrinites accompagnées ou non de franges de plus faible réflectance que le coeur de la particule. Ces observations uniquement effectuées sur ces charbons, nous ont amené à suggérer que ces critères pétrographiques étaient attribuables aux événements thermiques et oxydants précédemment incriminés. Malgré toutes ces concordances, une analogie entre les stigmates observés et des marques d'altération supergène nous a conduit à reconsidérer notre hypothèse du départ. En effet, il semblerait que les circulations chaudes incriminées affectent préférentiellement, voire spécifiquement certains charbons de haut rang caractérisés par un $R_o > 1,5\%$. En revanche, les charbons de bas rang ($0,5 < R_o < 0,9\%$) ne montrent pas d'élévation du T_{max} mais une simple diminution de l'IH et une augmentation de l'IO classiquement attribuables à une altération supergène (Copard et al., 2000).

À l'exception du T_{max} et du IH dont l'augmentation et la diminution respective évoquent un phénomène thermique, l'ensemble des autres paramètres géochimiques et pétrographiques, s'accordent avec une stricte oxydation des dits charbons anomaliques. Le

fait que ce type d'altération affecte sélectivement des charbons de rang élevé (ainsi que des charbons matures très altérés comme ceux d'Argentat), conduit donc à envisager une éventuelle influence du rang de la MO sur la sensibilité du T_{max} vis à vis d'une oxydation de basse température. Cette constatation est confortée par l'homogénéité du comportement des paramètres géochimiques, des pyrogrammes et des spectres micro-IRTF, des échantillons anomaux, prélevés pourtant dans des cadres géographiques éloignés.

Contrairement à ces échantillons, d'autres qui ne présentaient qu'une anomalie de T_{max} (ainsi que de IH) ont vraisemblablement enregistré un phénomène hyperthermique qui peut être lié cette fois aux conditions géothermiques des bassins dans lesquels ils ont été prélevés, par le biais de venues hydrothermales, voire par la mise en place d'une intrusion magmatique. Afin de tenter de mieux préciser les conditions dans lesquelles s'est effectuée l'oxydation invoquée ci-dessus, nous avons étudié la structure de la MO et ses différents groupes fonctionnels, à la fois dans ces charbons anomaux et dans leur référence non altérée. Globalement, tous les charbons altérés montrent des spectres micro-IRTF identiques. L'analyse des spectres des échantillons et des produits de divers traitements infligés à certains d'entre eux (extraction alcaline, pyrolyse...) ont permis de préciser la nature et l'abondance relative de leurs principaux groupes fonctionnels. Les groupes carboxyliques et/ou les carboxylates sont les groupes caractéristiques principaux des échantillons anomaux. Ces données fournissent donc bien un argument, voire une signature de la présence d'acides carboxyliques dans les échantillons présentant de forts IORE6. Ce résultat paraissant désormais indiscutable, l'ensemble des échantillons examinés au cours du DEA, n'ont probablement pas enregistré une quelconque venue hydrothermale, mais ont plus vraisemblablement subi un processus d'oxydation supergène.

L'étude moléculaire a confirmé l'étroite similitude entre les effets des processus thermiques et oxydants, notamment sur la fraction aromatique. Ces effets se marquent par une altération préférentielle des hydrocarbures aromatiques à 3 voire 4 cycles, de faibles masses moléculaires, par rapport à ceux qui comportent plus de 4 cycles. Ces résultats impliquent donc que la première étape de l'oxydation est caractérisée par une consommation de molécules aromatiques de petites tailles (et d'aliphatiques) tandis que la seconde se caractérise par une dégradation / déstructuration plus lente de molécules de masse plus imposante aboutissant à une déstructuration des graphènes des USB. Enfin, et bien que la fraction aliphatique soit également la cible privilégiée de l'oxydation, nous avons également mis en évidence une dégradation préférentielle des n-alcanes (mode en n-C22) à la périphérie des USB par rapport à ceux qui sont protégés stériquement dans la structure du charbon (n-C27).

Ainsi, à l'échelle des paramètres RE6 (IH et T_{max}), il apparaît une nette similitude

entre l'effet de l'oxydation et ceux produits par une dégradation thermique. Celle-ci est confortée par l'influence comparable que ces deux processus paraissent avoir sur les hydrocarbures aliphatiques et aromatiques libérés par la pyrolyse *off-line* d'échantillons diversement altérés.

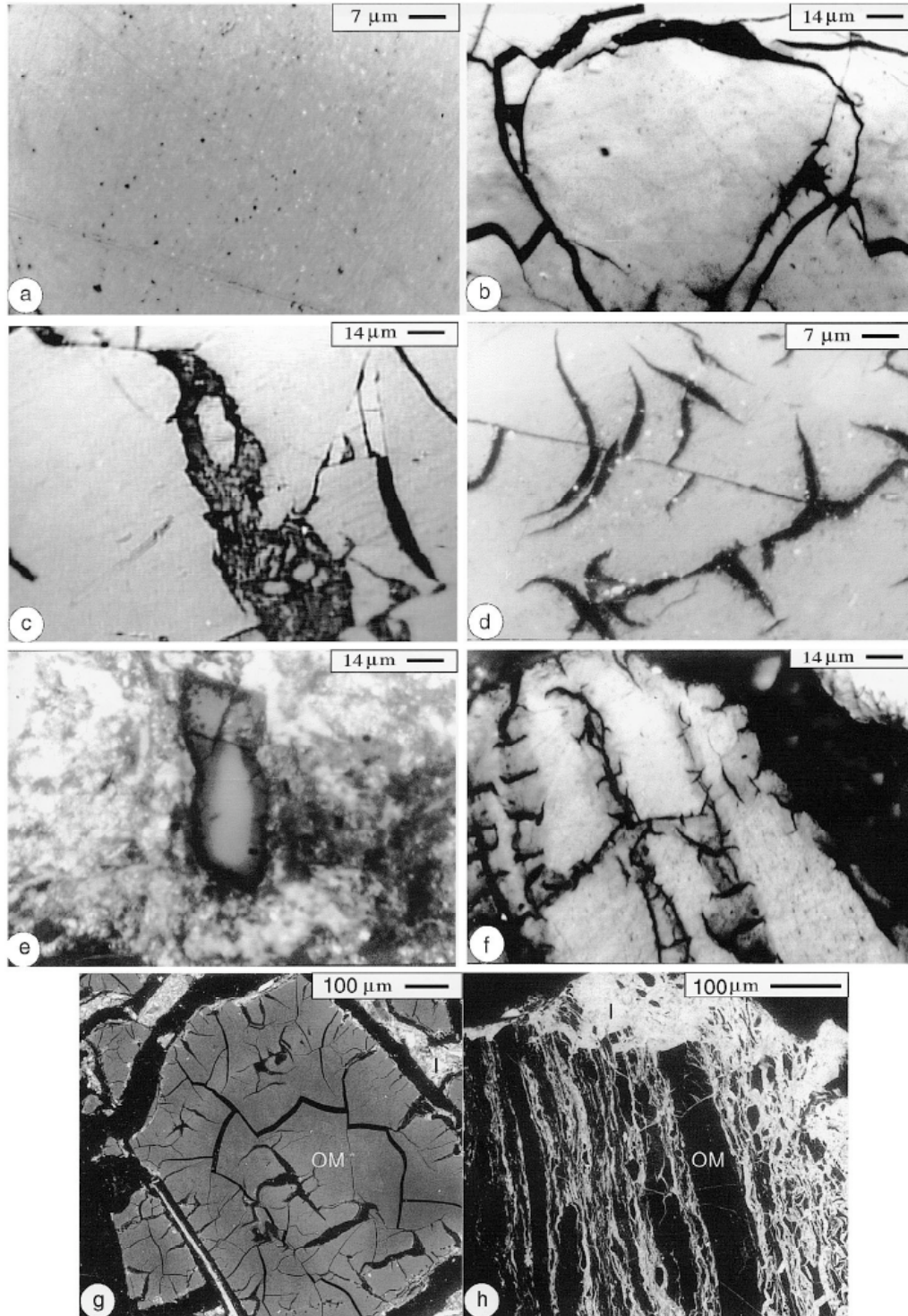


Figure IV-2 : Pétrographie des charbons étudiés montrant la variété des fracturations observées dans les différents échantillons étudiés. Les zonations de réflectance, (taches plus ou moins claires ou en franges) liées essentiellement à l'altération supergène sont observables sur certains clichés.

III- UNE ROCHE RESERVOIR

Formation et distribution des pyrobitumes dans un réservoir gréseux Cambro-Ordovicien, « Fahud Salt Basin, Nord Oman »

Ce sujet traité à la suite d'une collaboration sur un projet piloté par l'Institut Français du Pétrole et dirigé par Alain Huc et Bernard Carpentier sur des roches réservoirs de la province pétrolière omanaise. La partie géochimique et la modélisation cinétique de la maturation des bitumes ont été réalisées par Romain Debard dans le cadre d'un contrat d'ingénieur sortant de l'école des pétroles et moteur de l'IFP. Ma participation concernait la caractérisation pétrographique (Figure IV-3) des différents bitumes solides et de leurs stades de maturité. L'un des objectifs était d'étudier la relation entre porosité et remplissage bitumineux.

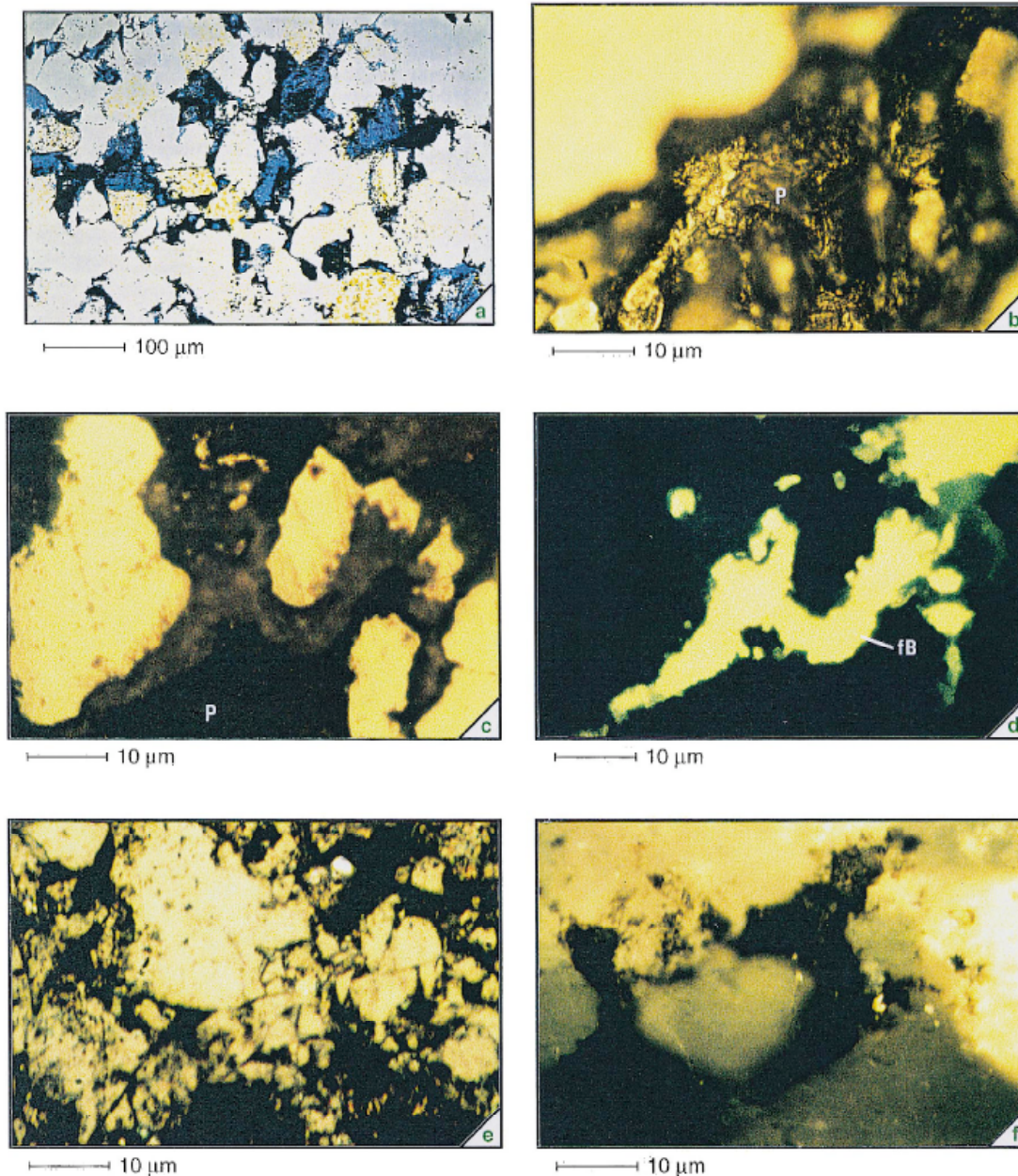
Le sujet était fortement motivé par la tendance actuelle de l'industrie pétrolière à cibler des prospections à des profondeurs et des températures de plus en plus élevées. Ceci a encouragé des recherches importantes sur la stabilité thermique du pétrole et de son évolution éventuelle en pyrobitumes ainsi que la relation de ces bitumes avec la qualité du réservoir. Le début du craquage du pétrole est encore un sujet très débattu à l'heure actuelle. Des études montrent que ce craquage commence pour certaines huiles très tôt, à des températures aussi basses que 140°C (Schenk et Horsfield, 1995). La perte massive d'hydrogène au cours du craquage du pétrole implique que, mis à part la production du gaz, des produits très aromatiques, des résidus carbonés insolubles et des pyrobitumes, sont générés. Ces dépôts de pyrobitumes peuvent fortement dégrader la qualité du réservoir par le colmatage de la porosité et de la perméabilité de la roche. Ce qui constitue un risque majeur dans l'exploration et l'exploitation d'hydrocarbures dans de nombreuses provinces pétrolières. C'est le cas par exemple du Nord de l'Oman où le pyrobitume est souvent identifié dans des examens microscopiques de routine de lames minces de roches provenant de plusieurs puits d'exploration. Ces puits très profonds ont atteint des roches-réservoirs où la porosité est à un tel point remplie par les bitumes que même la production du gaz est compromise. Le but de ce travail était d'étudier la nature, le type et le mode de formation de ces bitumes rencontrés dans les réservoirs gréseux de Barik composés de dépôt fluvio-deltaïques du Cambro-Ordovicien du bassin de Salt Fahud en Oman.

Ces grès-réservoirs contiennent du bitume qui peut occuper jusqu'à 40% de la porosité. Dans le puits Jaleel-1, ce bitume a été isolé selon la procédure habituelle d'isolation et de concentration du kérogène puis analysé par RMN, analyse élémentaire et mesures de la densité. Ce bitume isolé de la roche nous a montré (1) une structure hautement aromatique en RMN soit 75% C.Aro, et un rapport atomique H/C de 0,65 ; (2) Une très haute teneur en soufre de 4,2% ; et (3) Une densité relativement haute avoisinant 1.3-1.4 g/cm³.

L'insolubilité et la réflectance mesurées et comparées au profil obtenu sur des vitrinites montre une valeur moyenne de PRb de 1,2%, soit l'équivalent d'environ 0,9 à 1% PRv. Cette valeur est caractéristique d'un pyrobitume de faible maturité.

La confrontation des données quantitatives obtenues par l'analyse Rock-Eval à celle de la densité ont permis de calculer le volume réel de ces pyrobitumes dans la roche et de l'exprimer en fonction du pourcentage de porosité. Il a été constaté que le volume occupé par les pyrobitumes montre une corrélation négative avec la porosité totale, ce qui indique que les pores intergrains de petites tailles sont plus envahis par le bitume que les grands. Enfin, les essais de pyrolyse sous système fermé, effectués sur les huiles contenant une quantité de composés NSO variés, indiquent que le pétrole in situ doit avoir une très haute teneur en composés lourds NSO pour qu'il puisse générer une aussi grosse quantité de pyrobitumes dans les pores. Ces observations nous ont permis de montrer que le pétrole précurseur de l'actuel pyrobitume est un pétrole très lourd qui a vraisemblablement subi une biodégradation importante. La modélisation du bassin montre que le réservoir était déjà rempli de pétrole pendant la période du Dévonien. Un important « *uplift* » a rapproché ce pétrole accumulé près de la surface au cours du Carbonifère puis a été enfoui de façon régulière jusqu'à sa position actuelle vers 4500 m, soit à 140°C (Loosveld et *al.*, 1996).

Ce scénario proposé par la modélisation et qui suggère un certain temps de résidence du pétrole à une faible profondeur, tout près de la surface renforce l'hypothèse de la biodégradation. La modélisation numérique fournie par le modèle cinétique de craquage de l'IFP, montre que la formation du pyrobitume de Jaleel 1 est un événement très récent. Les inclusions de pyrobitumes dans les franges de croissance de la silice diagénétique contenant des inclusions fluides, donne une limite supérieure de température pour le début de formation de pyrobitumes en accord avec le résultat de cette modélisation cinétique.



a = thin section

d = fluorescence light

b = natural light

e = pyrobitumen concentrate, reflected light

c = natural light

f = pyrobitumen inclusion in quartz, reflected light

P = Pyrobitumen

fB = fluorescent Bitumen

Figure IV-3 : Pétrographie des lames minces non couvertes de la roche réservoir Jaleel1 observée sous différents modes photoniques (lumière naturelle transmise a, lumière naturelle incidente (b, c et e) et excitation ultraviolet pour la fluorescence en d et f (Huc et *al.*, 2000). Cette planche photos nous montre deux types de bitumes l'un fluorescent (photo d) l'autre non (photo f). La porosité a été colorée en bleu et montre que les pores sont obturés par des ménisques en bitumes fluorescents. La microporosité quant à elle est bien remplie.

IV- UN SOL :

Origines, types et transformation diagénétique des matières organiques associées à des unités structurales d'un sol riche en éléments traces métalliques (La Châtre, Massif Central Français).

Ce sujet traité sous ma direction dans le cadre d'un Master de recherche à Orléans et réalisé par Céline Laréché s'intégrait dans le cadre d'un projet « PNSE¹-ACI-Ecologie quantitative » dirigé par Sophie Cornu de l'INRA d'Orléans (45). Ce projet intitulé « Influence de la structure du sol sur la distribution des éléments en traces et des microorganismes dans les sols - conséquences environnementales », avait deux objectifs principaux :

- L'étude simultanée, à l'échelle de l'élément structural, maillon élémentaire de la structure des sols, de la distribution spatiale des éléments chimiques majeurs et traces (Eléments Traces Métalliques : ETM), de la porosité, des microorganismes et de la matière organique d'un horizon profond d'un sol de la région de La Châtre.

- L'étude des transferts en éléments majeurs et en ETM dans les solutions qui percolent à la fois au sein des éléments structuraux et de l'horizon.

Notre travail, pour le situer par rapport à l'ensemble de ce projet, s'est consacré à l'étude, à l'échelle de l'élément structural, de la fraction organique de ce sol par les moyens de la pétrographie et de la géochimie organique. Les échantillons sur lesquels s'est portée notre étude sont des agrégats issus d'un horizon profond d'un sol naturellement riche en éléments traces métalliques (ETM). La caractérisation des matières organiques (MO) présentes au sein des agrégats et dans leur périphérie nous a révélé des différences significatives concernant les quantités, le type et l'état diagénétique de la fraction organique entre les compartiments extérieurs et intérieurs des agrégats. Les méthodes d'analyses géochimiques globales, le Rock-Eval et le LECO, ont montré que l'extérieur est le compartiment le plus riche en carbone organique. L'étude pétrographique a affiné ce premier résultat en mettant en évidence un meilleur état de conservation de la MO dans l'extérieur des agrégats, le cœur rougeâtre contenant essentiellement des composés organiques oxydés. Les résultats de la Microscopie Electronique à Balayage (MEB) et à Transmission (MET), qui a permis de caractériser l'ultrastucture de la MO, vont dans le sens des résultats du palynofaciès. Quant aux travaux visant à rechercher les éventuelles relations entre la distribution des ETM et la MO, les résultats obtenus au MEB et au MET à l'échelle nanométrique n'ont révélé aucune concentration d'espèces métalliques dans la MO.

Les cations sont vraisemblablement adsorbés aux groupements fonctionnels des composés organiques et restent non visibles à l'échelle usuelle des observations pétrographiques. Les résultats de l'extraction séquentielle visant à isoler la fraction organique de l'échantillon prouvent bien l'existence de cette fraction métallique associée à la matière organique.

En ce qui concerne les objectifs secondaires, et notamment celui consistant à comprendre le transfert de la matière organique de la surface vers les horizons profonds, les résultats du Palynofaciès, mettant en évidence un extérieur plus riche en éléments figurés, laissent envisager un apport direct de MO fraîche par les conduits racinaires et les fentes de dessiccation en périodes estivales. Enfin, compte tenu de la stabilité du carbone présent à l'intérieur des agrégats, ce milieu apparaît être un des réservoirs possibles du « carbone manquant » du cycle du carbone.

Références citées dans la partie IV

- Copard Y. (2002) - Altération diagénétique et post-diagénétique (thermicité, oxydation) des charbons carbonifères du Massif Central français (Saint-Etienne, Graissessac et autres lieux). Thèse de l'Université d'Orléans 247p.
- Copard Y., Disnar J.-R., Becq-Giraudon J.-F., Boussafir M. (2000) - Evidence and effects of fluid circulation on organic matter in intramontane coalfields (Massif central, France). *International Journal Coal Geology*, 44, 49-68.
- Huc A.Y., Nederlof P., Debarre R., Carpentier B., Boussafir M., Laggoun-Défarge F. (2000) Pyrobitumen occurrence and formation in a Cambro-Ordovician sandstone reservoir, Fahud Salt Basin, North Oman *Chemical Geology*, 168, 99-112.
- Laréché C., (2003) Natures, types et états diagénétiques des Matières Organiques associées aux éléments structuraux d'un sol riche en Eléments Traces Métalliques. Rapport de Master recherche FluxEnv. Université d'Orléans.
- Loosveld, R.J.H., Bell, A., Terken, J.J.M., 1996. The tectonic evolution of interior Oman. *Geo. Arabia* 1 1., 28–51.
- Nzoussi-Mbassani P. (2003) - Le Cenomano-Turonien de l'Atlantique-Nord (Bassin du Sénégal) environnement de dépôts et évolutions diagénétique. Thèse de l'université d'Orléans.
- Nzoussi-Mbassani P., Khamli N., Disnar J.R., Laggoun-Défarge F., Boussafir M. (2005) - Cenomanian–Turonian organic sedimentation in North-West Africa: A comparison between the Tarfaya (Morocco) and Senegal Basins *Sedimentary Geology*, 177, 271–295
- Schenk, H.J., Horsfield, B., (1995) - Simulating the conversion of oil into gas in reservoirs: the influence of frequency factors on kinetic prediction. In: Selected Papers from the 17th International Meeting on Organic Geochemistry, 4th–8th September, San Sebastian, Spain, A.I.G.O.A.. pp. 1102–1103.

PARTIE V

PROGRAMME DE RECHERCHE

ARCHIVES SEDIMENTAIRES DES ZONES D'UPWELLING DU PACIFIQUE EST:

**BIOGEOCHIMIE ET CALIBRATION DES BIOMARQUEURS
PALEOCEANOGRAPHIQUES ET PALEOCLIMATIQUES**



Baie de Mejillones au nord du Chili, Lieu de vie et de sciences. *Photo M. Boussafir*

I- SITUATION DU PROJET

Ces dernières années, la notion de « variabilité climatique » s'est imposée jusque dans les hebdomadaires et quotidiens grand public. La sensibilisation, du monde politique et de l'opinion publique aux changements climatiques globaux et/ou régionaux, au protocole de Kyoto et aux dérèglements météorologiques récents (canicule, incendies de grandes ampleur, fortes précipitations, cyclones dévastateurs, etc...), est allée de pair avec un intérêt croissant, de la part de diverses communautés scientifiques, pour ce concept de « variabilité climatique », de fluctuations du climat, et d'événements extrêmes.

Comprendre les mécanismes majeurs qui génèrent les oscillations climatiques et déterminent les modes des variations du climat, pour prédire l'évolution de leurs impacts sur l'environnement et être en mesure de gérer leurs conséquences sociétales est ainsi devenu un objectif majeur de recherche. La compréhension des mécanismes de la machine climatique impose de documenter sa variabilité naturelle et de déchiffrer les systèmes complexes de rétroactions liés aux activités humaines. Les données instrumentales des dernières décennies ont permis de décrire différents modes d'oscillation du climat aux fréquences saisonnière, décennale ou pluri-décennales (NAO, SOI, DA, PDO) et de préciser divers systèmes de téléconnexions. Cependant ces mesures instrumentales sont souvent d'une durée trop courte pour appréhender la gamme de variabilité naturelle du climat, au cours des derniers siècles (Petit Age Glaciaire, par ex.). A fortiori sur des périodes plus anciennes (derniers millénaires, Holocène, interglaciaires) la reconstitution des variations climatiques passées requiert des méthodes et techniques d'analyses spécifiques.

Toutes les régions du monde sont affectées par des perturbations climatiques liées aux interactions entre l'océan et l'atmosphère, mais **les régions tropicales** sont particulièrement vulnérables aux anomalies climatiques car elles s'y manifestent par une large amplitude des contrastes climatiques. Alors que l'origine des grands changements climatiques, aux échelles millénaires, est classiquement recherchée dans l'Atlantique Nord, la communauté scientifique s'interroge sur le rôle des tropiques dans la dynamique climatique, notamment en ce qui concerne les variations de flux de chaleur et de vapeur d'eau (Peterson *et al.*, 2000). Peterson *et al.* (2000) supposent par exemple qu'à l'échelle millénaire les variations du cycle hydrologique en zone tropicale participent à la modulation de la circulation thermohaline et donc à la régulation du climat global. Sur des échelles de temps plus courtes, Hoerling *et al.* (2001) considèrent que les variations abruptes du climat dans l'Atlantique Nord (NAO) depuis les années cinquante trouvent en partie leur origine dans les variations atmosphériques induites par les anomalies de température à la surface de l'océan tropical. A l'échelle millénaire, comme à l'échelle décennale ou interannuelle, **les**

tropiques semblent donc jouer un rôle clé mais encore mal compris sur la variabilité climatique naturelle. C'est sur cette région climatique que le choix s'est porté pour ce projet.

Dans le cadre des études paléoclimatiques à l'échelle millénaire-séculaire, s'appuyant sur des séries sédimentaires lacustres ou des carottes forées dans des massifs coraliens, les études actuelles cherchent à reconstituer, par une approche paléoenvironnementale, des climats moyens du passé et leur évolution. Les flux sédimentaires, les diagrammes polliniques, ou des associations de microfaune (foraminifères, par ex.) renseignent sur les paysages, ou les conditions de milieu (lacustre, marin, terrestre) qui reflètent des conditions climatiques moyennes, lesquelles peuvent, ou non, manifester des changements, abrupts ou lents. L'analyse de cette variabilité, révélée par divers indicateurs, conduit à des interprétations sur les facteurs forçants du climat et les modalités des variations observées.

Dans les cas où les archives étudiées et les proxies utilisés sont susceptibles de fournir des informations à haute résolution temporelle (saisonnière, annuelle), comme par exemple dans les spéléothèmes, les carottes coralliennes, les coquilles de mollusques ou les sédiments « varvés », il est théoriquement possible de reconstituer des variations à haute fréquence des conditions de milieu. Il faut toutefois s'assurer que les matériaux analysés n'ont pas subi de modifications diagénétiques et que les proxies « calibrés » dans des matériaux actuels sont effectivement utilisables pour la reconstitution de conditions climatiques passées. Mon projet s'intéressera à cet aspect des recherches paléoclimatologiques, qui n'a pas toujours été traité avec tout le détail souhaitable. Ceci sera abordé par des approches expérimentales spécifiques. Il s'agit par exemple de caractériser les composants biogéochimiques ou biologiques de lamines sédimentaires et de l'étude des transformations diagénétiques que ces composants peuvent subir au cours du temps, après leur dépôt ou leur formation. Il est à noter que les transformations subies par ces composants notamment organiques peuvent, en elles-mêmes, être utilisées pour caractériser des modifications du milieu, constituant ainsi également des proxies de changements de conditions climatiques ou océanographiques.

Les effets de la bioturbation constituent l'une des principales limitations rencontrée dans l'étude de la variabilité des conditions océanographiques et climatiques à très haute résolution temporelle à partir des sédiments marins. Ainsi, il n'est qu'exceptionnellement possible d'obtenir des carottes marines qui permettent d'étudier la variabilité du climat à un pas de temps interannuel, ou qui soient susceptibles d'avoir enregistré des indices pertinents d'occurrence d'événements El Niño individuels. Ce sont des conditions d'anoxie poussées et permanentes qui rendent possibles une sédimentation laminée et une préservation ultérieure de ces sédiments à l'abri des phénomènes de bioturbation. De ce point de vue, plusieurs bassins sédimentaires localisés sur le **plateau continental de la**

marge Pérou-Chili présentent un ensemble de conditions favorables pour la **reconstitution à haute résolution** de l'évolution océano-climatique des derniers milliers d'années.

II- ARGUMENTATION SUR LE CHOIX DU SITE ET DES METHODES

II-1 choix de la zone d'études

L'Est de l'Océan Pacifique, le long de la côte sud-américaine est marqué par des conditions océaniques et climatiques très particulières. Les vents de l'extrémité est de l'Anticyclone du Pacifique Sud soufflent le long des côtes d'Amérique du Sud et sont renforcés par le Courant d'Humboldt de direction sud/nord, repoussent les eaux de surface vers le large, et induisent de nombreux centres de remontée d'eaux profondes. Ces cellules d'upwelling se succèdent tout au long des marges du Pérou et du Chili et font de ce littoral l'un des plus productifs au monde. La productivité phytoplanctonique y est en moyenne très élevée ($> 200 \text{ g C.m}^{-2}.\text{an}^{-1}$; Levin *et al.*, 2003) avec des pics de productivité primaire dans les zones de remontée (upwelling). La décomposition des substances organiques dans la colonne d'eau et sur le fond aboutit à l'apparition d'une Zone à Minimum d'Oxygène (ZMO) entre 100 et 500 m au-dessous des cellules d'upwelling. Comme cette ZMO inhibe alors le développement du benthos, il peut y avoir formation de sédiments laminés.

Pour suivre l'évolution des proxies de paléo-oxygénation, paléotempérature de la colonne d'eau, paléocirculations et leurs conséquences sur la paléoprodutivité, il faut disposer d'un enregistrement de haute résolution temporelle non-perturbé et d'un marqueur (organique ou minéral) de qualité qui dispose de proxies performants. En l'absence d'enregistrement marin de type carottes coralliennes dans le Pacifique tropical, mon choix, guidé par l'exceptionnelle qualité de l'enregistrement déjà observée dans mes études antérieures (taux de sédimentation important ; lamines non perturbées, richesse en matières organiques), s'est porté sur les archives sédimentaires des cellules d'upwelling du Pacifique Est, situées au large des côtes péruviennes et chiliennes. L'outil choisi est celui de l'enregistrement organique et particulièrement moléculaire. Cet outil paléoclimatique a fait ses preuves d'efficacité cette dernière décennie.

Le choix de travailler sur des zones d'upwelling est justifié par le fait que les sédiments marins qui s'y sont accumulés fournissent de bonnes informations sur l'évolution au cours du temps des conditions océanographiques (Martinez *et al.*, 2000; Bertrand *et al.* 2003). Dans des circonstances très favorables, les sédiments de ces zones peuvent enregistrer l'évolution des conditions physico-chimiques de la colonne d'eau avec une très haute résolution temporelle. En fonction du taux de sédimentation et des processus biologiques locaux, les séquences sédimentaires peuvent fournir des enregistrements dont la résolution temporelle peut atteindre l'année, la dizaine d'années ou la centaine d'années. Dans ce type d'environnement, le contenu en carbone organique peut constituer 10% du sédiment total

(Libes, 1992; Hedges & Keil, 1995) alors que la valeur moyenne océanique varie entre 0.2 et 0.4 % (Duan, 2000). Les variations d'intensité du système influencent en grande partie les variations de productivité, comme celles des diatomées (Schwartzlose et al., 1999, Gutierrez et al., 2006). Le site choisi présente une productivité et un taux de sédimentation élevé (2mm /an environ) et permet d'avoir un enregistrement de haute résolution des fluctuations de l'écosystème (Schwartzlose et al., 1999, Gutierrez et al., 2005), ce qui est particulièrement adapté à l'objectif de ce projet

II-2- Importance du marqueur biogéochimique :

II-2-1 L'outil MO dans les problématiques paléoenvironnementales et paléoclimatiques

Le sédiment enregistre plusieurs types d'informations liées à l'origine, la quantité et l'état de préservation des fractions organo-minérales. En effet, certains organismes ayant des cycles de vie très courts, à l'exemple des diatomées et de certaines algues, répondent plus rapidement aux changements des conditions physiques et chimiques du milieu, ce qui permet l'archivage rapide dans les sédiments des variabilités environnementales. De la même manière, l'état et le degré de préservation des fractions organiques et leurs minéralisations nous renseignent aussi sur les conditions physico-chimiques du milieu de dépôt (Température, pH, oxygénation, productivité....).

Au travers de la caractérisation et de la quantification des constituants d'origine continentale: minéraux et organiques détritiques, on peut facilement accéder aux modalités de transport jusqu'au bassin de sédimentation. La préservation de la matière organique dans les sédiments marins est principalement contrôlée par la quantité de la biomasse produite dans la zone euphotique et par les processus de dégradation qui ont lieu dans la zone photique le long de la colonne d'eau et dans les sédiments (Murria & Kuivila, 1990; Lallier-Vergès et al., 1991, 1993a; Bertrand et al., 1993a; Tribovillard et al., 1994; Ransom et al., 1998; Ganeshram et al., 1999; Duan, 2000). Les conditions redox qui règnent dans ces milieux sont le résultat des caractéristiques de la masse d'eau et de la consommation de l'oxygène par les activités microbiennes. Plusieurs travaux (Hedges & Keil, 1995; Boussafir et al. 1995, Boussafir & Lallier-Vergès, 1997; Lallier-Vergès et al., 1998; Lükge et al., 1999; Vetö et al., 2000) ont montré qu'il existe de nombreux facteurs qui contrôlent la qualité et la quantité de la matière organique contenue dans les sédiments, tels que la production primaire, le taux de sédimentation, l'oxygénation de la zone de contact eau-sédiment, les caractéristiques de la colonne d'eau et la distance de la côte. Bien que des synergies entre ces facteurs soient vraisemblables, il n'y a pas de consensus dans la définition des mécanismes qui contrôlent ces facteurs. Des auteurs comme Reimers (1989), Pedersen &

Calvert (1990), Calvert *et al.* (1992; 1996), Bertrand et Lallier-Vergès, (1993 b) pensent que la productivité a l'influence la plus importante dans la préservation de la matière organique, alors que pour d'autres auteurs, tels que Didyk *et al.* (1978), Hollander *et al.* (1992), Ingall *et al.* (1994), Jones & Manning (1994), ce sont les quantités d'oxygène dissous qui sont les principaux facteurs.

La MO sédimentaire étudiée parallèlement à l'analyse du contenu pollinique des sédiments s'est révélée depuis une quinzaine d'années un outil très puissant. De nombreuses études menées notamment par l'équipe « Matière Organique » de l'Institut des Sciences de la Terre d'Orléans, sur la base de l'analyse couplée pétrographique à différentes échelles d'observation et géochimie globale et moléculaire de la MO, appliquée à des séries mésozoïques, néogènes et quaternaires ont ainsi démontré la sensibilité de la composition organique aux variations du climat. Le carbone organique total, le degré de préservation textural et chimique de cette MO, le rapport entre MO détritique et MO aquatique, les proportions de MO remaniée des sols ou des formations géologiques environnantes sont autant de paramètres permettant de révéler l'hétérogénéité climatique de certaines périodes, comme l'Holocène, et de préciser certains événements climatiques abrupts (Lallier-Vergès *et al.*, 1993b ; Sifeddine *et al.*, 1996 ; Rosell-Mele *et al.*, 1997 ; Meyers et Lallier-Vergès, 1999 ; Manalt *et al.*, 2001 ; Noël *et al.*, 2001 ; Paillet *et al.* 2002; Meyers, 2003 ; Jacob *et al.*, 2004,).

Par l'observation au microscope (palynofacies), certains chercheurs ont mis en évidence par l'identification de micro charbons de bois l'existence de feux de forêts en Amazonie (Turcq *et al.*, 1998) et en Europe (Lallier-Vergès, 1993b) témoins de fortes sécheresses climatiques. Un autre indice de l'utilisation de la matière organique comme marqueur climatique est la présence dans les sédiments enfouis au fond des lacs de matière organique d'origine pédologique interprétée comme témoin de phases de déstabilisation du couvert végétal et d'augmentation de l'érosion des bassins versants durant des événements de forte précipitation (Lallier-Vergès *et al.*, 1993b; Sifeddine *et al.*, 1996). Plusieurs travaux ont montré aussi que certains types de matière organique amorphe, reflètent l'installation des phases de forte productivité souvent à la faveur de remontées du niveau lacustre. Outre les études pétrographiques, les proxies géochimiques élémentaires, isotopiques et moléculaires ont, durant ces dernières années, elles aussi démontré leur potentiel quant à leur utilisation comme marqueur paléoclimatique.

II-2-2 Pourquoi les biomarqueurs organosédimentaires dans ce projet ?

La complexité biochimique de la matière organique recèle une grande richesse d'information, en partie conservée lors de la fossilisation, que l'analyse moléculaire permet de discriminer. Parmi les différentes familles biochimiques (acides aminés, sucres, acides nucléiques) les lipides constituent la famille biochimique la plus diversifiée. Cette diversité se traduit dans les sédiments et roches par des cortèges moléculaires comportant à chaque analyse chromatographique plusieurs centaines de composés différents. Les travaux réalisés par les phytochimistes ont permis de préciser les filiations entre certains lipides fossiles et leurs organismes producteurs. Ceci se traduit par une panoplie sans cesse croissante de biomarqueurs spécifiques des différentes communautés ayant peuplé les bassins versants et les colonnes d'eau lacustre et marine.

La diversité des cortèges moléculaires préservés dans les sédiments permet une vision intégrée des différents compartiments (colonne d'eau, substratum et bassin versant) et de leurs contributions respectives au sédiment. En effet, l'outil moléculaire, beaucoup plus riche en informations que l'analyse globale de la MO, renseigne sur les sources organiques et les états de préservation des constituants organiques alors que l'approche globale (étude combinée Rock-Eval / Palynofaciès) permet la quantification des flux organiques terrestres (paléo-érosion) et des flux organiques aquatiques (paléo-production) à haute résolution. Ces deux approches seront systématiquement couplées dans ce projet.

Au cours du cycle géologique, la matière organique biologique subit d'importantes transformations qui conduisent à la dégradation des molécules. Cependant, les lipides, molécules plus stables, gardent leur identité biologique malgré les différentes transformations moléculaires qu'elles subissent au cours du temps et de l'enfouissement au sein des bassins sédimentaires. Cette fraction moléculaire est relativement biorésistante puisqu'on retrouve des lipides préservés dans des sédiments datés de l'Archéen (Brocks et *al.*, 1999). Certaines de ces molécules subissent des altérations de structure qui peuvent renseigner sur les conditions physico-chimiques ayant affecté les milieux où elles ont été produites, transportées et sédimentées.

Ce projet s'intéresse à l'étude des processus intervenant au cours de l'exportation de la MO marine à travers la zone photique et la zone de minimum d'oxygène en vue de la calibration du signal moléculaire enregistré dans les sédiments. Les transformations structurales et/ou fonctionnelles de ces biomolécules seront analysées et leurs significations en termes d'évolution des conditions physico-chimiques de la colonne d'eau seront établies (oxygénation, température, salinité ...etc.).

Ces mêmes molécules, appelées biomarqueurs, seront recherchées dans les sédiments et utilisées comme proxies afin de reconstituer les paléoproduktivités, paléooxygénations et paléotempératures ainsi que la variabilité de la circulation océanique.

II-3 Résumé du projet et de ses objectifs

Plusieurs programmes tentent de suivre l'évolution des enregistrements sédimentaires dans le but de reconstituer le climat et les paléocirculations océaniques dans cette zone particulièrement intéressante du Pacifique Est où les interactions océan /atmosphère sont des plus importantes. Mon projet se démarque de ces différents travaux car il couple sur le même site l'étude de l'enregistrement sédimentaire et la calibration du signal et donc de l'enregistreur. De ce fait il se présente en deux parties principales:

(1) *La première partie concerne l'exploitation d'archives sédimentaires à haute résolution temporelle et la validation de proxies climatiques pour les divers types de variabilité climatique. L'objectif est de reconstituer les variabilités et les oscillations des upwellings, des courants océaniques qui les influencent et des conditions environnementales voire climatiques enregistrées dans le Pacifique tropical au large de l'Amérique du Sud. Pour atteindre cet objectif majeur, des enregistrements moléculaires à haute résolution seront obtenus sur les séries sédimentaires carottées. Cette première approche permettra de suivre les variations quantitatives et qualitatives des organismes sources produits (paléoproduktivité) et de suivre l'évolution des conditions physicochimiques du milieu (paramètre d'oxydation de la MO, de dégradation ou d'anoxie). Cette partie concernera en premier lieu (à court et moyen terme) la côte occidentale de l'Amérique du Sud. Il s'agira d'étudier deux types de prélèvements : - des box-cores pour la partie la plus récente généralement perturbée par les carottages à piston et recouvrant les 500 dernières années, - des carottes de sédiment dans des zones où le faciès est laminé et la stratigraphie bien préservée. L'objectif final est de contribuer activement à la compréhension des mécanismes climatiques opérant à différentes échelles de temps (annuelle, décennale, séculaire). Les triterpanes pentacyclique (marqueurs des apports végétaux supérieurs) seront analysés et quantifiés. Les mesures isotopique du D/H moléculaire sur ces marqueurs venant du*

continent permettront d'apporter des suppléments d'informations en terme de paléoprécipitation sur les terres.

(2) La deuxième partie du projet sera menée parallèlement. Elle consiste en une étude de calibration des marqueurs moléculaires qui concerne également le D/H moléculaire mesuré sur des biomarqueurs de végétaux supérieurs. Elle sera entreprise en essayant de suivre ces marqueurs depuis leur production jusqu'à leur accumulation dans les sédiments. Cette démarche implique un volet relativement important d'expérimentation en matière de calibration de proxies dans des conditions actuelles sur des échantillons prélevés (pièges à sédiments (équipements disponibles à l'IRD-Bondy), pièges de molécules dissoutes « équipement disponible à l'ISTO », sommets de boîte-cores...), mais également par des expérimentations *in vivo* le long de la colonne. En effet, l'étude des processus diagénétiques précoces affectant ces molécules sera entreprise à différentes profondeurs de la colonne d'eau : dans la zone photique oxygénée et dans la ZMO. Cette étude permettra ainsi de simuler les processus de dégradation et de géopolymérisation des molécules organiques dans leur milieu naturel.

Les analyses isotopiques du D/H sur des biomarqueurs de végétaux supérieurs nécessiteront un développement méthodologique lourd et une calibration préalable du fractionnement isotopique en milieu marin liée au filtre de la diagenèse précoce. Les pièges mis en oeuvre pour les expérimentations des interactions argiles MO dans la colonne d'eau du Lac Pavin (thèse S. Drouin) s'avèreront utiles pour ce type d'expérimentation.

L'objectif ultime de cette calibration est de déchiffrer le signal moléculaire complexe, de filtrer l'effet de la diagenèse et de rechercher à calibrer de nouveaux proxies biogéochimiques documentant les reconstitutions des paléo-oxygénations et des paléo-circulations.

II-4 Zones d'étude et collaborations

Ce projet va concerner deux régions de la marge pacifique de l'Amérique du Sud :

La première correspond à la plateforme centrale péruvienne entre Lima et Pisco, où l'équipe PALEOTROPIQUE a initié début 2003 un projet de collaboration avec l'IMARPE (Institut de la Mer du Pérou) intitulé **PALEOPECES** (Enregistrements paléocéanographiques de haute résolution dans les sédiments de la zone de minimum d'oxygène du Pérou central).

La seconde région concerne la baie de Mejillones où l'équipe PALEOTROPIQUE collabore avec l'ISTO en travaillant, depuis une dizaine d'années, en collaboration avec des partenaires chiliens sur l'étude des conditions de paléo-oxygénation et de paléo-productivité durant les 2000 dernières années dans le cadre d'un projet de coopération entre l'Université Antofagasta (Chili) et l'IRD intitulé **PALEOBAME** (PALEOocéanographie de la BAIE de

MEjillones). Ce programme qui se termine actuellement est remplacé par VARCLIMAT (*VARIabilidad de las condiciones océano-CLImáticas en el Norte de Chile, con énfasis en registros sedimentarios MARinos*).

L'insertion ancienne de l'UR PALEOTROPIQUE de l'IRD dans des réseaux scientifiques en Amérique du sud et sa connaissance du terrain garantit la bonne conduite de ce projet. Les expérimentations et études de calibration et validation des divers proxies climatiques utilisées, nécessitent toute une organisation et une logistique sur place, au Pérou et au Chili. Ceci se fera en étroite collaboration avec les partenaires péruviens et chiliens.

II-4-1 Plateforme Centrale du Pérou.

Participants en France :

L. Ortlieb (DR1, Paléotropique, IRD) ; A. Sifeddine (DR2, Paléotropique, IRD) ; F. LeCornec (IR1, Paléotropique, IRD) ; M. Mandeng Yogo (IE, Paléotropique, IRD) ; M. Garcia (AI, Paléotropique, IRD) ; C. Pierre (DR2, LOCEAN) ; P. Soler (DR1, LOCEAN) ; E. Vergès. (DR2, ISTO. Université d'Orléans) ; M. Boussafir (MCF, ISTO, Université d'Orléans) ; I. Bouloubassi (CR, LOCEAN, Université Paris VI) ;

Participants péruviens assurant également la logistique surplace dont les carottages et l'embarquement à la mer:

D. Gutierrez (CR, IMARPE) ; F. Velzco (IR, IMARPE) ; S. Mayor (TR, IMARPE) ; J. Solis (TR, IMARPE)

Participants Chiliens : J. Valdes (MC, Université d'Antofagasta) ; G. Vargas (MC, Université du Chili)

La marge centrale du Pérou est caractérisée par un intense upwelling, le plus productif de la région. L'écosystème de cet upwelling se caractérise par la présence d'une ZMO situé entre 100-500m, entretenu par la circulation du courant sub-superficiel du Pérou (CSP) et par la respiration de la matière organique. La ZMO peut atteindre la plateforme continentale et affectée directement les processus de l'environnement benthique. La présence de la ZMO empêche les bioturbations et facilite la préservation des sédiments et l'enregistrement à haute résolution du contenu organique. Des zones de haute concentration de carbones organiques ont été localisées sur cette marge péruvienne. Le COT peut atteindre les 10% sur certaines lamines du sédiment. Ces zones riches en sédiments laminés et préservés, qui intéressent particulièrement ce projet, se concentrent dans la partie central de l'upwelling péruvien en face des localités de Pisco et de Callao. Ce sont les zones cibles pour nos prélèvements et nos expérimentations *in situ*.

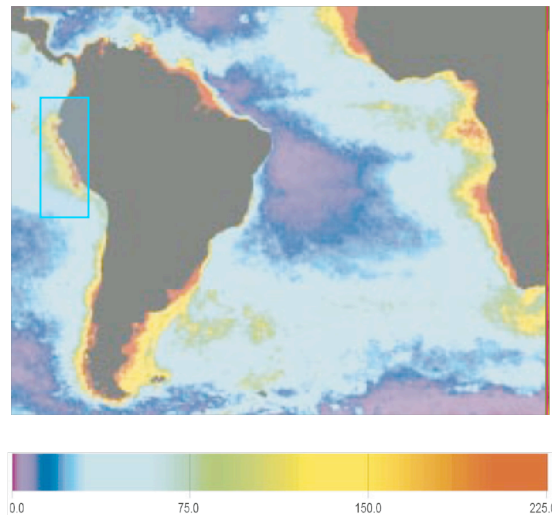


Figure V-1 : Situation de la zone d'étude. Apports annuels moyen en carbone photosynthétique (g C/m^2) (d'après Falkowski et al., 1998). Les valeurs les plus hautes sont situées en zone d'upwelling.

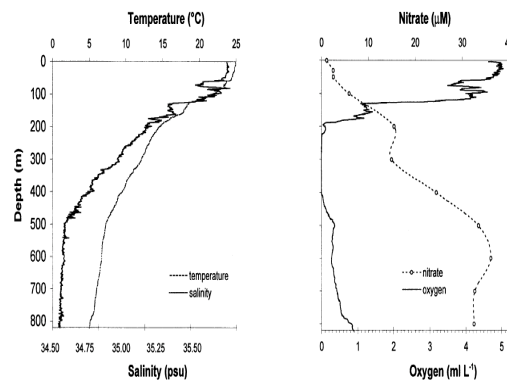


Figure V-2 : Variation de la Température ($^{\circ}\text{C}$), Salinité (psu), Nitrate (μM) et l'oxygène dissous (ml.L^{-1}) le long de la colonne d'eau de la zone d'étude (Levin et al., 2003).

II-4-2 La Baie de Mejillones (Nord Chili).

Participants en France :

L. Ortlieb (DR1, Paléotropique, IRD) ; A. Sifeddine (DR2, Paléotropique, IRD) ; E. Vergès. (DR1, ISTO. Université d'Orléans) ; I. Bouloubassi (LOCEAN, Université Paris VI)

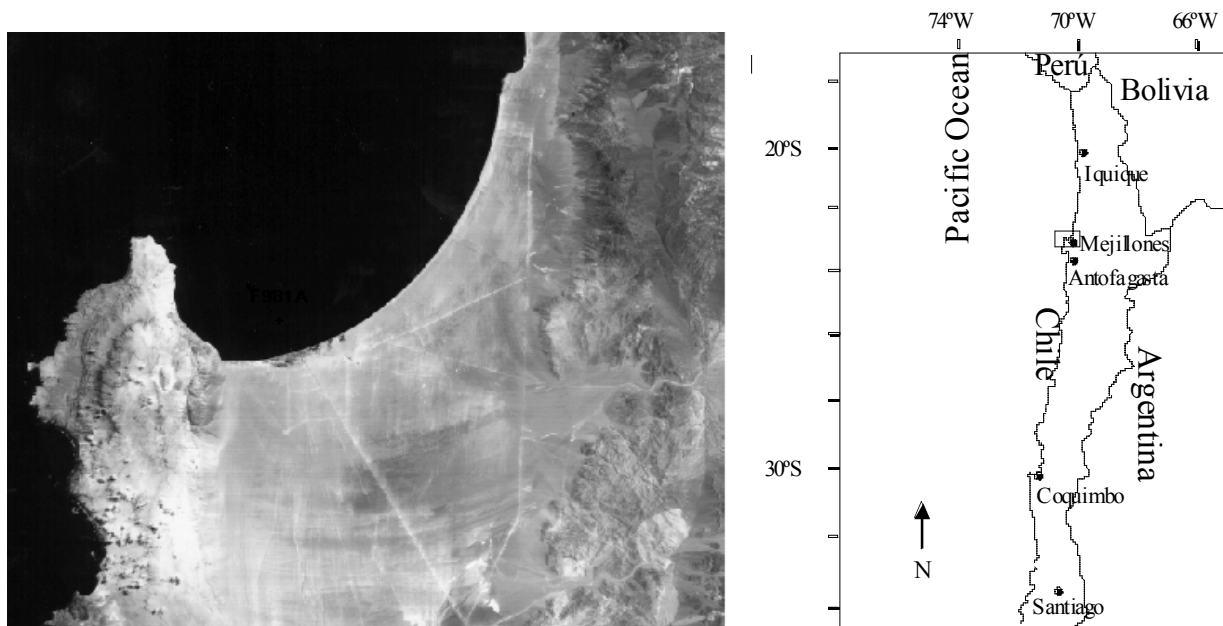
Participants chiliens et logistique sur place:

J. Valdès (Université d'Antofagasta) ; G. Vargas (Université du Chili)

Le climat d'extrême aridité (désert d'Atacama) de la côte nord chilienne associé au courant froid de "Humboldt", provoque des conditions climatiques particulières, caractérisées par des précipitations de moins de 10 mm/an. Dans cette zone, le système de remontée d'eaux profondes de Punta Angamos (23°S) est reconnu comme un des plus productifs de la côte chilienne et pour cette raison, il a fait l'objet de plusieurs études (Escribano, 1998;

Gonzalez *et al.*, 1998; Escribano & Hidalgo, 2000). La baie de Mejillones fait partie de ce système. C'est un bassin de dépôt situé au-dessous d'une zone de très haute productivité primaire. Dans cette baie, l'apport en matériel détritique est très faible et représenté essentiellement par des apports éoliens (Vargas, 1998). Les taux de productivité primaire dans la baie sont de l'ordre de $138 \text{ mg C m}^{-3}\text{an}^{-1}$ (Rodríguez *et al.*, 1986). Les profils de l'oxygène dissous obtenus pour une colonne d'eau durant un cycle annuel montrent que la zone de minimum d'oxygène est située à des profondeurs supérieures à 50 m (Valdés, 1998; Escribano, 1998). Ces conditions expliquent la richesse des sédiments en matière organique dominée par les diatomées (Ortlieb *et al.* 1994; Valdés, 1998).

Figure V-3 : Situation du site de la baie de Mejillones



III- METHODOLOGIE & ADEQUATION DU PROJET

III- 1 Méthodologie :

Dans le but d'une meilleure interprétation des données, la matière organique des sédiments des carottes prélevées dans le cadre de ce projet sera caractérisée par différentes approches géochimiques appuyées par des observations pétrographiques. Les approches géochimiques seront globales (quantitative COT, et qualitative IH & IO de la MO par Rock-Eval) et moléculaires (Biomarqueurs lipidiques, et isotopie moléculaire).. Toutes les méthodes d'études de la MO décrites en partie IV de ce mémoire seront mise en œuvre pour ce projet et réalisée par E. Vergès, J. Jacob et moi même. (Pour la description des

méthodes de pétrologie organique appliquées, se reporter à la partie précédente de ce mémoire).

Les observations pétrographiques à différentes échelles (Microscopie photonique, MEB, Cryo MEB) nous aideront à caractériser l'origine et l'état de préservation des différentes fractions organiques allochtones et autochtones. L'étude des Palynofaciès (Combaz, 1980) nous permettra de caractériser l'ensemble des constituants organiques particuliers et d'identifier et quantifier les différents éléments figurés et amorphes. Cette quantification aboutira au calcul des apports (allochtone/autochtone), ce qui permettra d'estimer en association avec les teneurs en COT, le long de la colonne sédimentaire, la paléoproduktivité au niveau de l'upwelling et les influences des apports continentaux. Dans le cas des sédiments laminés, l'analyse d'image et les observations à très haute résolution sur du matériel brut (CryoMEB) permettront d'aboutir à une meilleure définition du faciès et une caractérisation *in situ* de la matière organique. Les analyses palynofaciès seront réalisées par E. Vergès et moi même.

S'ajoutant à ces études de la MO, d'autres analyses se feront en collaboration.

- Les analyses minéralogiques (RX, IR), et des éléments majeurs et en trace : UR Paléotropique de l'IRD ; les collègues impliqués sont Bruno Turcq, et Abdelfettah Siffeddine.
- La cartographie RX des carottes, et l'analyse de l'azote et de ses isotopes : Le laboratoire d'océanographie EPOC de l'Université de Bordeaux I. Les collègues impliqués sont, Philippe Bertrand et Philippe Martinez.

III-2 Adéquation du projet au programme de l'ISTO et à ses moyens analytiques

Parmi les cinq grand programmes qui structurent l'ISTO, mon projet s'inscrira dans le programme POM (Processus Organo-Minéraux) qui fédère la plus grande partie des projets pilotés par l'équipe MO à Orléans. Il s'intégrera plus particulièrement au sous-programme DynaMO (**D**ynamique de la **M**atière **O**rganique) qui vise les sujets relatifs à la calibration de marqueurs organiques en environnement actuel, à l'étude des processus et des forçages permettant d'affiner les reconstitutions paléoclimatiques et paléoenvironnementales.

D'un point de vue technique, ce projet pourra s'appuyer sur un panel analytique sans équivalent dans l'environnement scientifique et académique en France pour l'étude des biomarqueurs moléculaires. Ce pannel a été enrichi par l'acquisition récente d'un couplage chromatographie en phase liquide - spectromètre isotopique (HPLC-IRMS) et la perspective très proche d'acquisition d'une interface de couplage de l'IRMS avec une chromatographie

en phase gazeuse (GC-IRMS). Cet appareil nous permettra la mesure des isotopes du carbone, de l'hydrogène et de l'oxygène sur des biomarqueurs lipidiques isolées par chromatographie en phase gazeuse.

III-4 Apport de ce projet à la communauté nationale et Internationale

Même si la thématique scientifique de ce projet est par elle-même parfaitement intégrée aux objectifs de l'ISTO et de l'IRD, je souhaiterais continuer la formation, de jeunes doctorants et chercheurs du Sud, orientée vers la biogéochimie organosédimentaire. J'ai l'intention de participer au développement de la coopération sud-sud mise en place par l'équipe PALEOTROPIQUE au Pérou, Chili et Brésil. Cette coopération vise à encourager les échanges entre professeurs et de contribuer à la formation de jeunes chercheurs. Cette action a débuté en septembre 2003 et s'est concrétisée par la formation de plusieurs étudiants dont une thèse à Orléans et de chercheur Chilien et brésilien. Cette thèse (de Marcio Da Costa Curgel) est financée par le Ministère de l'Education Nationale bresilien (CAPES) et soutenue par le programme DynaMO de POM de l'ISTO et de PALEOTROPIQUE de l'IRD .

Même si ce projet est essentiellement centré sur l'Amérique du Sud, il contribuera, par les objectifs scientifiques qu'il s'est fixé, à apporter des nouvelles données pour une meilleure compréhension des processus biogéochimiques des systèmes d'Upwelling d'Amérique du Sud à des fins de reconstitutions paléoclimatiques. Mais aussi, des réponses à un certain nombre de questions que se pose la communauté scientifique qui travaille en Afrique de l'Ouest notamment sur les cellules d'upwellings du Benguela et des Canaries.

Il est clair que ce projet, dont l'objectif est de reconstituer les conditions paléo-océanographiques par les approches biogéochimiques, va apporter une contribution importante au volet Paléo du projet incitatif encouragé par l'IRD et ainsi que la JEAJ de l'IRD MIXPALEO sur le système du Humboldt (Productivité, Oxygénation et Circulation) et dont l'ISTO à travers E. Vergès et moi-même est l'un des acteurs primordiaux. Ce système est considéré comme une priorité régionale des actions de coopération entre l'IRD, l'ISTO et les pays du Sud.

Ce projet s'intègre également dans les prospectives définies pour la division SIC : "Les matières organiques, compartiment et acteur essentiel des processus environnementaux", en particulier dans la réflexion engagée sur l'identification et la calibration de traceurs des processus biogéochimiques portés par les matières organiques.

Du point de vue de la compréhension des processus de sédimentation de la matière organique dans les systèmes d'upwelling, ce projet, par sa spécificité géographique, va apporter une plus value aux études réalisées à l'échelle nationale dans le système de Benguela et dans celui des Canaries par l'équipe d'EPOC (Bordeaux1). Dans cet objectif, en collaboration avec mes collègues de l'équipe EPOC de Bordeaux 1 et ceux de l'Institut des Sciences de la Terre d'Orléans, j'ai l'intention de contribuer à la mise en place d'un groupe de réflexion internationale avec mes collègues chiliens et péruviens **« sur les processus biogéochimiques de la matière organique dans les systèmes d'upwelling »** afin de coordonner nos actions et mieux cibler les objectifs prioritaires. La multidisciplinarité ici est bien justifiée dans la mesure où elle est au service d'objectifs multiples : Calibration du signal organique, interaction organominérale, processus de sédimentation, diagenèse organique dans la colonne d'eau et dans les sédiments, reconstitution paleoocéanographique, paléoclimat, pêche et paloproductivité des upwellings en faune marine

Références citées dans la partie V :

- Bertrand P., Lallier-Vergès E., Boussafir M., (1993a) - Enhancement of accumulation and anoxic degradation of organic matter controlled by cyclic productivity : a model. *Org. Geochem.*, 22(3-5), 511-520.
- Bertrand P., Lallier-Vergès E., (1993b) - Past sedimentary organic matter accumulation and degradation controlled by productivity. *Nature*, 364, 786-788.
- Bertrand P., Pedersen T., Schneider, Shimmield G., Lallier-Vergès E., Disnar J.R., Massias, Villanueva, Tribouillard N.P., Huc Y., Giraud, Pierre C., Venec-Perret M.N. (2003) - Organic-rich sediments in ventilated deep-sea environments : climate, sea-level and trophic changes. 108 (C2), 30-45,
- Boussafir M., Gelin F., Lallier-Vergès E., Derenne S., Bertrand P. & Largeau C. (1995) - Electron microscopy and pyrolysis of kerogens from the Kimmeridge Clay Formation, UK : source organisms, preservation process and origin of microcycles. *Geochimica Cosmochimica Acta* 59, pp. 3731-3747.
- Boussafir M., Lallier-Vergès E., (1997) - Accumulation of organic matter in the Kimmeridge Clay Formation (KCF) : an update fossilisation model for marine petroleum source-rocks. *Marine and Petroleum Geology*, 14(1), 75-83.
- Brocks, J.J., Logan, G.A., Buick, R. et Summons, R.E., (1999)- Archean Molecular Fossils and the Early Rise of Eukaryotes. *Science* 285, 1033-1036.
- Calvert S., Bustin, R., & Pedersen, T., (1992) - Lack of evidence for enhanced preservation of sedimentary organic matter in the oxygen minimum of the Gulf of California. *Geology* 20: 757-760.
- Calvert S., Bustin, R., Ingall, E., (1996) - Influence of water column anoxia and sediment supply on the burial and preservation of organic carbon in marine shales. *Geochimica et Cosmochimica Acta*. 60(9): 1577-1593.
- Combaz A., (1980) - *Les kérogènes vus au microscope*. In Kérogène – Insoluble Organic Matter from Sedimentary Rocks. B. Durand, édition Technips, Paris, pp. 55-87.

- Didyk, B., Simoneit, B., Brassell, S., Eglinton, G., (1978) - Organic geochemical indicators of paleoenvironmental conditions of sedimentation. *Nature* 272 (5660): 216-222.
- Duan, Y., 2000. Organic geochemistry of recent marine sediments from the Nansha Sea, China. *Org Geochem.*, 31: 159-167
- Escribano, R., Hidalgo, P., (2000) - Spatial distribution of copepods in the north of the Humboldt Current region off Chile during coastal upwelling. *J. Mar. Biol. ASS. U. K.*, 80: 1-8.
- Escribano, R., (1998) - Population dynamics of *Calanus chilensis* in the Chilean Eastern Boundary Humboldt Current. *Fish. Oceanogr.* 7 (3/4): 245-251.
- Falkowski, P. G., Barber, R. T., Smetacek, V. (1998) - "Biogeochemical Controls and Feedbacks on Ocean Primary Production." *Science* 281, 200-206. Ganeshram R.S,
- Ganeshram R. S., Calvert S. E., Pedersen T. F., Cowie G. L., (1999) - Factors controlling the burial of organic carbon in laminated and bioturbated sediments off NW Mexico implications for hydrocarbon preservation. *Geochimica et Cosmochimica Acta*, 63, 11-12, 1723-1734
- Gonzalez, H., Daneri, G., Figueroa, D., Iriarte, J., Lefevre, N., Pizarro, G., Quiñines, R., Sobarzo, M., Troncoso, A., (1998) - Producción Primaria y su destino en la trama trófica pelágica y océano profundo e intercambio océano-atmósfera de CO₂ en la zona norte de la corriente de Humboldt (23° S): posibles efectos del evento El Niño, 1997-98 en Chile. *Revista Chilena de Historia Natural* 71: 429-458.
- Gutiérrez D, Sifeddine A., Reyss J. L., Vargas G., Velazco F., Salvatelli R., Ferreira, Ortlieb L., Field D., Baumgartner, Boussafir M., Boucher H., Valdès J., Marinovic L., Soler P., & Tapia P. (2006) - Anoxic sediment off Central Peru record interannual to multidecadal changes of climate and upwelling ecosystem during the last two centuries. *Advances in Geosciences*, 6, 119-125,
- Hedges, J., Keil, R., (1995) - Sedimentary organic matter preservation: an assessment and speculative synthesis. *Marine Chemistry*, 49: 81-115.
- Hollander, D., McKenzie, J., Ten Haven, H., (1992) - A 200 year sedimentary record of progressive eutrophication in lake Greifen (Switzerland): Implications for the origin of organic-carbon-rich sediments. *Geology* 20: 825-828.
- Hoerling M.P., Hurrell J. W., Xu T., (2001) - Tropical Origins for Recent North Atlantic Climate Change, *Science*, 292, 5514, 90 - 92
- Ingall, E., Jahnke, R., (1994) - Evidence for enhanced phosphorus regeneration from marine sediments overlain by oxygen depleted waters. *Geochimica et Cosmochimica Acta*, 58(11): 2571-2575.
- Jacob, J., Disnar, J.R., Boussafir, M., Sifeddine, A., Albuquerque, A.L.S. et Turcq, B., (2004) - Major environmental changes recorded by lacustrine sedimentary organic matter since the Last Glacial Maximum under the tropics (Lagoa do Caçó, NE Brazil). *Palaeogeography, Palaeoclimatology, Palaeoecology* 205, 183-197.
- Jones, B., Manning, D., (1994) - Comparison of geochemical indices used for the interpretation of paleoredox conditions in ancient mudstones. *Chemical Geology* 111: 111-129.
- Lallier-Vergès E., Bertrand P., Desprairies A., Berner U., (1991) - Geochemical and optical investigations on degradation processes affecting organic matter in Celebes Basin sediments. In: Silver E., Rangin C., van Breymann M., (Eds.), *Proceedings of the Ocean Drilling Program, Scientific Results, ODP, 124, 239-247.*

- Lallier-Vergès, E., Hayes, J., Boussafir, M., Zaback, D., Tribovillard, N., Connan, J., Bertrand, P., (1993a) - Productivity-induced sulphur enrichment of hydrocarbon-rich sediments from the Kimmeridge Clay Formation. *Chemical Geology*, 134(4), 177-188.
- Lallier-Vergès, E., Sifeddine, A., De Beaulieu, J. L., Reille, M., Tribovillard, N., Bertrand, P., Mongenot, T., Thouveny, N., Disnar, J.-R. et Guillet, B., (1993b) - Sensibilité de la sédimentation organique aux variations climatiques du Tardi-Würm et de l'Holocène; le lac du Bouchet (Haute-Loire, France). *Bulletin de la Société Géologique de France* 164, 661-673.
- Lallier-Vergès, E., Martinez, P., Bertrand, P., Rabouille, C., Relexans, J.C., Keravis, D., (1998) - Sedimentation, reworking and preservation of organic matter in surficial sediments of the N-W african upwelling system. *Mineralogical Magazine*, vol. 62A, 846-847.
- Levin, L.A., Rathburn, A.E.R., Gutiérrez, D., Muñoz, P., Shankle, A. (2003) - Bioturbation by symbiont-bearing annelids in near-anoxic sediments: Implications for biofacies models and paleo-oxygen assessments. *Palaeogeography, Palaeoclimatology, Palaeoecology*. 199, 120-140.
- Libes, S., (1992) - An introduction to marine biogeochemistry. John Wiley & Sons, Inc., New York: 289 p.
- Lükge, A., Boussafir, M., Lallier-Vergès, E., Littke, R., (1999) - Comparative study of organic matter preservation in immature sediments along the continental margins of Peru and Oman. Part I: Results of petrographical and bulk geochemical data. *Org. Geochem.* 24(4), 437-451.
- Manalt, F., Beck, C., Disnar, J. R., Deconinck, J.-F., Recourt, P., (2001) - Evolution of clay mineral assemblages and organic matter in the Late glacial-Holocene sedimentary infill of Lake Annecy (Northwestern Alps) : paleoenvironmental implications. *Journal of Paleolimnology* 25, 179-192.
- Martinez, P., Bertrand, P., Calvert, S.E., Pedersen, T.F., Shimmield, G.B., Lallier-Vergès, E., Fontugne, M., (2000) - Spatial variations in nutrient utilization, production and diagenesis in the sediments of a coastal upwelling regime (NW Africa): Implications for the paleoceanographic record". *Journal of Marine Research*. 58:5.
- Meyers, P.A. et Lallier-Vergès, E., (1999) - Lacustrine sedimentary organic matter records of late quaternary paleoclimates. *Journal of Paleolimnology* 21, 345–372.
- Meyers, P.A., (2003) - Applications of organic geochemistry to paleolimnological reconstructions: a summary of examples from the Laurentian Great Lakes. *Organic Geochemistry* 34, 261-289.
- Murria J., Kuivila K., (1990) - Organic matter diagenesis in the northeast Pacific: transition from aerobic red clay to suboxic hemipelagic sediments. *Deep-Sea Research*, 37(1), 59-80.
- Noël, H., Brauer, A., Garbolino, E., Lallier-Vergès, E., de Beaulieu, J.L, Disnar, J.R., (2001) - Sedimentary organic matter as a marker of soil erosion during the last millenia (Annecy Lake). *Journal of Paleolimnology*, 25, 229-244.
- Ortlieb, L. Zúñiga, O., Follegati, R. Escribano, R., Kong, I., Rodríguez, L., Mourguiart, Ph., Valdes, J., Iratchet, P., (1994) - Paleocceanografía de la Bahía de Mejillones del Sur (Antofagasta, Chile): Resultados preliminares para el último milenio. *Estudios Oceanológicos* 13: 45-55.
- Pailler D., Bard E., (2002) - High-frequency paleoceanographic changes during the past 140 000 years recorded by the organic matter in sediments off the Iberian Margin, *Palaeogeogr. Palaeoclimatol. Palaeoecol.* 181, 431–452.

- Pedersen, T., Calvert, S., (1990) - Anoxia vs. productivity: What controls the formation of organic-carbon-rich sediments and sedimentary rocks?. *Am. Assoc. Pet. Geol. Bull.*, 74: 454-466.
- Peterson C. J. (2000) - Catastrophic wind damage to North American forests and the potential impact of climate change. *The Science of The Total Environment*, Volume 262, Issue 3, 15 November 2000, Pages 287-311
- Ransom B., Kim D., Kastner M., Wainwright S., 1998. Organic matter preservation on continental slope: Importance of mineralogy and surface area. *Geochem. Et Cosmochem. Acta*, 62(8), 1329-1345.
- Reimers, C., (1989) - Control of benthic fluxes by particulate supply. In: Berger, W. H., et al., (eds.), *Productivity of the ocean: Past and present*, Life Sci. Res. Rep., Vol. 44, Wiley & Sons: 217-234.
- Rodríguez, L., Zarate, O., Oyarce, E., (1986) - Producción primaria del fitoplancton y su relación con la temperatura, oxígeno, nutrientes y salinidad en la bahía de Mejillones del Sur. *Rev. Biol. Mar.* 22 (1): 75-96.
- Rosell-Mele A., Maslin M.A., Maxwell J.R., Schaeffer P., (1997) - Biomarker evidence for Heinrich events, *Geochim. Cosmochim. Acta* 61, 1671–1678.
- Schwartzlose, R., Alheit, J., Bakun, A., Baumgartner, T., Cloete, R., Crawford, R., Fletcher, W., Green-ruiz, Y., Hagen, E., Kawasaki, T., Lluch-Belda, D., Lluch-cota, S., Maccall, A., Matsuura, Y., Nevarez-Martinez, M., Parrish, R., Roy, C., Serra, R., Shust, K., Ward, N., and Zuzunaga, J., (1999) - Worldwide large-scale fluctuations of sardine and anchovy populations, *S. Afr. J. Mar. Sci.*, 21, 289–347,
- Sifeddine, A., Bertrand, Ph., Lallier-Vergès, E., Patience, A., (1996) - The relationships between lacustrine organic sedimentation and palaeoclimatic variations. Lac du Bouchet, Massif Central, France. *Quat. Sci. Rev.* 15, 203– 211.
- Tribovillard, N., Desprairies A., Lallier-Vergès E., Bertrand P., Moureau N., Ramdani A., Ramanampisoa L., (1994) - Geochemical study of organic-matter rich cycles from the Kimmeridge Clay Formation of Yorkshire (UK) : productivity versus anoxia. *Pal. Pal.* 108, 165-181.
- Turcq, B., Sifeddine, A., Martin, L., Absy, M.L., Soubies, F., Suguio, K., Volkmer-Ribeiro, C. (1998) - Amazonian Rainforest Fires: a lacustrine record of 7000 years. *Ambio* , 27, 2, 139-142.
- Valdés, J. (1998) - Evolución oceanográfica reciente de la Bahía Mejillones del Sur (23° S). Evidencia geoquímica en sedimentos marinos. Tesis Doctoral, Centro EULA-Chile Universidad de Concepción. 114 p.
- Vargas, (1998) - Approches méthodologiques en paléocéanographie réalisées à partir de carottes de la Baie de Mejillones, Chile (23°S). Diplôme d'Etudes Approfondies, Université Bordeaux, Bordeaux, France. 32pp.
- Vetö I., Hetenyi M., Hamor-Vido M., Hufnagel H., Haas J., (2000) - Anaerobic degradation of organic matter controlled by productivity variation in a restricted Late Triassic basin. *Organic. Geochemistry*. 31. 439-452.

PARTIE VI

NOTICE INDIVIDUELLE ET LISTES DES PUBLICATIONS

I- NOTICE INDIVIDUELLE

MOHAMMED BOUSSAFIR

Né le 5 novembre 1964 à Fes, Maroc

Nationalité française, Marié trois enfants

Adresse personnelle : N°12, route de Mer, Isy, 41 370 JOSNES

Téléphone : 0238494738

e-Mail : Mohammed.Boussafir@univ-orleans.fr

Fonction : Maître de Conférences C.N., nomination en sept. 97, titularisation en sept. 99

Etablissement d'affectation : UFR Sciences, Université d'Orléans, BP 6759, 45067, Orléans cedex-2

Titres universitaires :

- DEA Géosciences de L'Ecole et Observatoire de Physique du Globe et du Centre de Géochimie de Surface de Strasbourg. Juin 1991, Mention Assez-Bien.
- Doctorat de l'Université d'Orléans. Soutenue le 4 Novembre 1994. Mention Très Honorable Avec Félicitations du Jury.

I-1 Encadrements de la recherche :

Au cours de la dizaine d'année de mon activité d'enseignant chercheur j'ai :

- co-encadré 4 thèses et participé à l'encadrement de 8 thèses (12 Thèses au total)
- Proposé et encadré 6 sujets en Master recherche
- Proposé et encadré 6 sujets de recherche en Master 1 et 1 stage de fin d'études d'ingénieur.

Encadrement sur une partie du sujet de la thèse :

- 1) Andreas Lükge (1992-1995) -
Comparative study of organic matter preservation in immature sediments along the continental margins of Peru and Oman-
Thèse Université de Zulich, Allemagne.
- 2) Thierry Mongenot (1994-1998)
Études pétrographiques et géochimiques d'un dépôt sédimentaire très riche en soufre organique (Orbagnoux, Kimméridgien supérieur) - reconstitution paléoenvironnementale - mécanisme de préservation de la matière organique -
Thèse de l'Université d'Orléans.
- 3) Sonia Bourdon (1995-1999)
Approches micromorphologiques et moléculaires de la diagenèse précoce de la matière organique dans une tourbière à Cypéracées en milieu tropical (Tritrivakely, Madagascar). Implications paléoenvironnementales.
Thèse de l'Université d'Orléans.

- 4) Valérie Salmon (1996-1999)
Modes d'accumulation de la matière organique dans des "black shales" et des silex du Cénomanién d'Italie Centrale. Rôle des minéraux et des processus diagénétiques.
Doctorat de l'école des mines de Paris
- 5) Nicolas Buillit 1997-2000
Marqueurs organiques et stratigraphie génétique. Cas du prisme fluvio-deltaïque campanien du groupe du Mesa Verde, Colorado, EUA.
Thèse de l'Université d'Orléans.
- 6) Yoan Copard (1998-2002)
Altération diagénétique et post-diaogénétique (thermicité, oxydation) des charbons carbonifères du Massif Central français (Saint-Etienne, Graissessac et autres lieux)
Thèse de l'Université d'Orléans.
- 7) Pierre Nzoussi (1999-2003)
Le Cenomano-Turonien de l'Atlantique-Nord (Bassin du Sénégal) environnement de dépôts et évolutions diagénétique. Thèse de l'université d'Orléans.
- 8) Yann Graz (2005-2008) Production et devenir du carbone organique fossile libéré par les altérations mécaniques et chimiques des formations marneuses : approches locales et globales
Thèse de l'Université d'Orléans.
- 9) Renata Zocatelli (2005-2008)
Enregistrement des variations palioenvironnementales au cours de l'holocène dans le Nord-Est du Brésil.
Thèse de l'Université Fédérale de Fluminense (État de Rio de Janeiro, Brésil).

Co-encadrement sur la totalité du sujet de la thèse :

- 10) Jeremy JACOB (1999-2003)
Enregistrement des variations palioenvironnementales depuis 20000 ans dans le Nord-Est du Brésil (Lac Cago) par les triterphnes et autres marqueurs organiques.
Thèse de l'Université d'Orléans.
- 11) Laetitia Pichevin (2000- 2004)
Sédimentation organique profonde sur la marge continentale namibienne (Lüderitz, Atlantique Sud-Est) : impacts des variations climatiques sur la paléoproduktivité
Thèse de l'Université Bordeaux.
- 12) Sylvain Drouin (2003-2007) Rôle des phyllosilicates dans la préservation et la fossilisation de la Matière Organique pétrologène Thèse soutenue à l'Université de Orléans
- 13) Marcio Gurgel (2004-2008)
Processus organo-sédimentaires sous deux systèmes d'upwellings contrastés de l'Amérique du Sud : Les cas des côtes centrales du Brésil et du Pérou.
Considerations paléocéanographiques et paléoclimatiques.
Thèse de l'Université d'Orléans.

Encadrement de 6 étudiants en DEA et Master Recherche

- 1) Meye M. (1999) *Evaluation du potentiel pétrolier des différentes roches mères du bassin du Viking Graben. DEA 3GS, Orléans. DEA 3GS (Lille, Orsay, Orléans)*
- 2) Copard Y. (2000) *DEA 3GS, Altération hydrothermale des charbons carbonifères du Massif Central Français. DEA 3GS (Lille, Orsay, Orléans)*

- 3) Rouet I. (2001) Caractérisation de la fraction organique (graphite ou pyrobitume) des quartzites hercyniennes de Bretagne Méridionale. Origine et évolution diagénétique des bitumes d'un ancien réservoir à hydrocarbures (DEA Géosystème, Orléans).
- 4) Foudi M. (2002). *Distribution et état de préservation de la matière organique des sédiments superficiels du Lac Caço (État de Maranhão, Brésil)*, (DEA Géosystème, Orléans)
- 5) Laréché C., (2003) Natures, types et états diagénétiques des Matières Organiques associées aux éléments structuraux d'un sol riche en Eléments Traces Métalliques. Master recherche, FluxEnv. Université d'Orléans.
- 6) Belhassine K., 2006, Sédimentation organique subactuelle du système d'upwelling de la plateforme centrale du Pérou. Géochimie globale et pétrographie organique. Master recherche, FluxEnv. Université d'Orléans.

Encadrement de 6 stages de recherche du Master1 et 1 stage d'ingénieur:

- 1) Yann Jéhanno (1998) Apport de la pétrographie organique dans la caractérisation des roches-réservoirs pétrolières. Stage de fin du cursus d'ingénieur. Option gestion et exploitation des ressources géologiques de l'Ecole Supérieure de l'Energie et des Matériaux.
- 2) Martial Meye (1999) *Evaluation du potentiel pétrolier des différentes roches mères du bassin du Viking Graben. Maîtrise de géologie fondamentale et appliquée d'Orléans*
- 3) Isabelle Rouet (2000) Caractérisation de la fraction organique (graphite ou pyrobitume) des quartzites hercyniennes de Bretagne Méridionale. Maîtrise de géologie fondamentale et appliquée d'Orléans
- 4) Pouradier Adrien (2001). Mise au point d'une méthode de séparation de la fraction neutre d'extraits organiques de sédiments lacustres récents. Mémoire de recherche de Maîtrise de Sciences de la Terre, Université d'Orléans.
- 5) Claire Trouvé (2001) Analyse pétrographique des particules organiques d'une série lacustre récente du Brésil. Comparaison avec la géochimie. Maîtrise de géologie fondamentale et appliquée d'Orléans
- 6) Etienne Taffoureau (2005) Sédimentation organique subactuelle du système d'upwelling de la plateforme centrale du Pérou. Analyses rock-Eval et palynofaciès. Master1. Master géosciences et environnement d'Orléans
- 7) Marion Sasias (2007) Caractérisation moléculaire de la matière organique représentative de deux phases sédimentologiques distinctes, observée dans les sédiments de surface de l'upwelling Péruvien. Master géosciences et environnement d'Orléans

I-2 Résumé des activités d'enseignements

Charges en heures équivalent TD et discipline enseignées:

Ma charge d'enseignement représente une moyenne annuelle d'environ 260 h équivalent TD, ce qui correspond à une charge qui avoisine 1,5 fois le service statutaire. Le manque d'encadrement en géologie sédimentaire et en géodynamique externe à Orléans oblige certains

d'entre nous à dépasser le service minimum. C'est le cas général de la plupart des disciplines de l'UFR sciences à Orléans mais aussi des autres Universités.

Tableau récapitulatif ma charge d'enseignement en Heures équivalentes TD* :

Années scolaires	DEUG	2 ^{ème} cycle	3 ^{ème} cycle	Total eqTD
97-98	146	66	21	233
98-99	146	92	26	264
99-00	153	73	26	252
00-01	146	76	71	238
01-02	113	74	71	258
02-03	128	104	30	262
03-04	88	110	81	279
04-05Délégation CNRS.....			
05-06	91	119	46	256
06-07	91	116	63	270
07-08	101	116	57	274

(Rappel : 3 heure TP = 2h eqTD ; 2h de Cours = 3h eqTD ; 1h TD = 1h eqTD)

Voici en détail les domaines dans lesquels j'enseigne actuellement :

- Géologie générale et géodynamique externe en DEUG première année.
- Pétrologie sédimentaire en DEUG deuxième année, pour les Master de géologie fondamentale et appliquée (ST), et les Master de Biologie option Sciences de la Terre (filiale enseignements).
- Sédimentation et diagenèse de la MO en Licence de Géologie, Licence de Biologie et licence pluridisciplinaire.
- Géochimie globale et pétrographie organique, géochimie moléculaire, sédimentation et diagenèse (précoce et tardive) de la MO en Master 1.
- Biogéochimie moléculaire en environnements sédimentaires et son utilité dans la reconstitution paléoenvironnementale et paléoclimatique : Etude de cas (Argile du Kimméridgien d'Angleterre, upwelling Namibien, upwelling péruvien, sédiments lacustres) pour le Master2 Recherche FLUXENV d'Orléans.

Responsabilités pédagogiques :

- De 1997 à 2002 : président de jury de 3 modules d'enseignements (ST202, ST302, ST702)

- En 2002-2003 : président de jury de 4 modules d'enseignements (ST202, ST302, ST702 et ST803)
- Responsable du module optionnel de sédimentation et diagenèse de la MO pour :
 - le DEA 3GS commun aux universités de Lille, Orsay et Orléans (1997 à 2001) puis d'Orsay jusqu'en 2003
 - puis pour le DEA géosystèmes gestion et ressources d'Orléans -Tours (2001 à 2003)
 et Master Recherche Flux-ENV d'Orléans (2003 à 2008)
- Participation au JURY de Soutenance : J'ai participé à deux Jury de thèses (Jérémy Jacob et Sylvain Drouin) et à tous les jurys des Masters recherches depuis ma nomination comme Maître de Conférences en 1997 (Soit environ une cinquantaine de jurys d'étudiants Master 2)

I-3 Participations aux programmes nationaux et internationaux

- Participation à l'ANR PerFluid piloté par Xavier Bourra
- Programme National Sols et érosion- ACI Ecologie quantitative piloté par Sophie Cornu de l'INRA d'Orléans.
- Participation au GdR 942 CNRS « processus organominéraux en environnements sédimentaires » dans le cadre de ma thèse et après la thèse. Le sujet concernait l'origine et mode de fossilisation de la MO des argiles du Kimméridgien d'Angleterre.
- Participation au GdR Marges. Plus particulièrement à l'atelier MO de ce GdR coordonné par François Baudin. Ma participation dans cet atelier a concerné l'étude de l'origine et de l'état de préservation de la MO dans des environnements d'upwellings actuels : relation sédimentation organique et fluctuations climatiques quaternaires dans ces environnements hautement producteurs.
- Participation à différents programmes internationaux de l'IRD, en Amérique du Sud, parmi lesquels :

1. Brésil

- AIMPACT (IRD-CNPq) : 2000-2003- Analyses Intégrées des Marqueurs et imPACT
- PALEOTROPIQUE (IRD-CNPq) : 2004-2006 - PALEOenvironnements TROPICAUX et variabilités climatiQUES
- CLIMPACT 2007-2010- **CLIMAt** passé dans les régions troPicales d'Amérique du Sud : Variabilité, **Tendances**, impacts – Enjeux pour le Futur. **CLIMPACT**.

2. Chili :

- PALEOBAME : PALEOcéanographie de la BAie de MEjillones (IRD-Université d'Antofagasta .Chili) : (1992-2006)
- VARCLIMA : Variabilité des conditions océano-climatiques dans le nord du Chili en insistant sur les enregistrements sédimentaires marins (VARCLIMA).

3. Pérou

- PALEOPECES : Enregistrements paléocéanographiques de haute résolution dans les sédiments de la zone de minimum d'oxygène du Pérou central, porté par l'IRD, l'IMARPE avec la collaboration de l'ISTO

I - 4 Activité d'animation scientifique et d'administration de la recherche

- Responsable du laboratoire de Géochimie Organique Moléculaire de l'ISTO (UMR6113) entre (2000 et 2006) :

Responsable du parc analytique : matériel de préparation au laboratoire et des équipements d'analyses du laboratoire (Chromatographie en phase Gazeuse « CG », *Flash-Pyrolysis* associé à un couplage CG/double spectrométrie de masse pour l'analyse des biomarqueurs lipidiques et des sucres,

- Membre du comité d'organisation du 8^{ème} congrès (ASF) à Orléans, édition de septembre 2001.
- Membre de la commission des spécialistes 35-36 de l'université d'Orléans
- Revues d'articles soumis à publication pour des revues internationales.
- Membre du bureau d'administration du département de géologie et de l'environnement de l'Université d'Orléans (trésorier 2001 - 2006).

I - 5 Développement de technique de laboratoire

- Mise au point à Orléans d'un mécanisme de Pyrolyse *off-line* de la MO sédimentaire. Cette méthode nous permet d'accéder à la composition moléculaire de la MO insoluble.
- Mise au point d'un *protocole de prélèvement par micromanipulation* sous stéréomicroscope pour concentrer différents groupes de constituants sédimentaires destinées à des analyses géochimiques et/ou pétrographiques, et permettant ainsi de s'affranchir des problèmes d'analyses moyennées liées aux mélanges.
- Mise au point d'un *protocole de fixation et de coloration* de la matière organique (MO) isolée et d'échantillons argileux destinés aux observations *pétrographiques en microscopie électronique à transmission* : texture ultra fine de la matière organique et du réseau organo-minéral d'une roche.
- Projet d'acquisition d'un équipement analytique mi-Lourd : J'ai pu obtenir en 1999 un financement nous permettant l'acquisition du dernier appareil de chromatographie en phase gazeuse couplée à une double spectrométrie de masse (GC/MS/MS). Le

financement obtenu (100% de la demande : une partie région et une partie INSU) m'a permis de compléter ce système par un pyrolyseur *on-line*, flash avec un système de chauffage dit Point de Curie permettant d'accéder à la composition moléculaire de la MO insoluble.

- J'ai également participé à la demande d'acquisition d'une HPLC/IRMS pour notre laboratoire. Appareil actuellement en fonctionnement à l'ISTO et permettant d'accéder à la composition isotopique du carbone, d'oxygène et d'azote de molécule séparé au préalable.
- Mise au point de pièges permettant les interactions organo-minérales *in-situ* entre la MO dissoute, des eaux naturelles marines et lacustres à différentes profondeurs, et les argiles.

I- 6 Coopération industrielles et valorisation

- 3 Contrats de recherche avec la société **GTM** construction.

Ces trois contrats concernaient des caractérisations pétrographiques à différentes échelles de sédiments marneux en provenance de chantiers autoroutiers de la société GTM. Les marnes utilisées comme couche de forme pour les autoroutes provoquent parfois des grandes détériorations des chaussées et une perte financière très importante. Les objectifs principaux de ces contrats étaient de mettre en évidence les agents responsables de cette détérioration.

II- LISTE COMPLETE DES PUBLICATIONS

Thèse :

Boussafir M. (1994) Microtexture et structure ultrafine des roches et matières organiques pétroliques : Nature et mode de fossilisation de la MO dans les séries organosédimentaires cycliques du Kimméridgien d'Angleterre. Thèse de l'Université d'Orléans

Bilan de la production scientifique

Types	Rang A	Rang B et résumés étendus	Congrès
Total	20	18	63

I-1 Publication de RANG A avec comité de lecture

- 1) SIFEDDINE, A., GUTIERREZ, D., ORTLIEB, L., BOUCHER, H., VELAZCO, F., FIELD, D., VARGAS, G., **BOUSSAFIR, M.**, SALVATTECI, R., FERREIRA, V., GARCIA, M., VALDES, J., CAQUINEAU, S., MANDENG YOGO, M., CETIN, F., SOLIS, J., SOLER, P., BAUMGARTNER, T. (2007)
Laminated sediments off the Central Peruvian Coast record changes in terrestrial

- runoff, water mass oxygenation and upwelling productivity over recent centuries.
Accepté pour publication dans Progress in oceanography.
- 2) JACOB, J., HUANG, Y., DISNAR, J.R., SIFEDDINE, **BOUSSAFIR, M.**, A., ALBUQUERQUE, A.L.S., TURCQ, B., (2007).
Paleohydrological changes during the last deglaciation in Northern Brazil.
Quaternary Science Reviews 26, 1004-1015
 - 3) JACOB, J., DISNAR, J.R., **BOUSSAFIR, M.**, ALBUQUERQUE, A.L.S., SIFEDDINE, A. ET TURCQ, B., (2007).
Contrasted distributions of triterpene derivatives in the sediments of Lake Caçó reflect paleoenvironmental changes during the last 20,000 yrs in NE Brazil.
Organic Geochemistry 38, 180-197.
 - 4) GUTIERREZ D, SIFEDDINE A., REYSS J. L., VARGAS G., VELAZCO F., SALVATTECI R., FERREIRA, ORTLIEB L., FIELD D., BAUMGARTNER, **BOUSSAFIR M.**, BOUCHER H., VALDES J., MARINOVIC L., SOLER P., & TAPIA P. (2006)
Anoxic sediment off Central Peru record interannual to multidecadal changes of climate and upwelling ecosystem during the last two centuries.
Advances in Geosciences, 6, 119-125,
 - 5) NZOUSSI P., KHAMLI N., DISNAR J.-R., LAGGOUN-DÉFARGE F., **BOUSSAFIR M.** (2005)
Cenomanian-Turonian organic sedimentation in North-Western Africa : a comparison between Tarfaya (Morocco) and Senegalo-Mauritanian (Senegal) Basins.
Sedimentary Geology, 177, 3-4, 271-295.
 - 6) JACOB J., DISNAR J.-R., **BOUSSAFIR M.**, SPADANO ALBUQUERQUE A.L., SIFEDDINE A., TURCQ B. (2005) ⁵
Pentacyclic triterpene methyl ethers in recent lacustrine sediments (Lago do Caço, Brazil).
Organic Geochemistry, 36, 449-461.
 - 7) JACOB J., DISNAR J.-R., **BOUSSAFIR M.**, LEDRU M.P., ALBUQUERQUE A.L.S., TURCQ B. (2004)
Onocerane testifies to dry climatic events during the Quaternary in the Tropics.
Organic Geochemistry, 35, 289-297.
 - 8) JACOB J., DISNAR J.-R., **BOUSSAFIR M.**, SIFEDDINE A., TURCQ B., ALBUQUERQUE A.L.S. (2004)
Major environmental changes recorded by lacustrine sedimentary organic matter since the Last Glacial Maximum under the tropics (Lagoa do Caço, NE Brazil).
Palaeogeography Palaeoclimatology Palaeoecology, 205, 183-187.
 - 9) PICHEVIN L., BERTRAND P., **BOUSSAFIR M.**, DISNAR J.-R. (2004)
Organic matter accumulation and preservation controls in a deep sea modern environment: an example from Namibian slope sediments.
Organic Geochemistry, 35, 5, 543-559.
 - 10) COPARD Y., DISNAR J.-R., BECQ-GIRAUDON J.-F., **BOUSSAFIR M.** (2000)
Evidence and effects of fluid circulation on organic matter in intramontane coalfields (Massif central, France).
International Journal Coal Geology, 44, 49-68.
 - 11) HUC A.Y., NEDERLOF P., DEBARRE R., CARPENTIER B., **BOUSSAFIR M.**, LAGGOUN-DÉFARGE F. (2000)
Pyrobitumen occurrence and formation in a Cambro-Ordovician sandstone reservoir,

- Fahud Salt Basin, North Oman
Chemical Geology, 168, 99-112..
- 12) **BOUSSAFIR M.**, LALLIER-VERGÈS E. (1997)
Accumulation of organic matter in the Kimmeridge Clay formation (KCF): an update fossilisation model for marine petroleum source-rocks.
Marine and Petroleum Geology, 14, 1, 75-83.
- 13) LALLIER-VERGÈS E., HAYES J., **BOUSSAFIR M.**, ZABACK D., TRIBOVILLARD N., CONNAN J., BERTRAND P. (1997)
Productivity-induced sulphur enrichment of hydrocarbon-rich sediments from the Kimmeridge Clay Formation.
Chemical Geology, 134, 4, 277-288.
- 14) MONGENOT T., **BOUSSAFIR M.**, DERENNE S., LALLIER-VERGÈS E., LARGEAU C., TRIBOVILLARD N. (1997)
Sulphur-rich organic matter from bituminous laminites of Orbagnoux (France, upper Kimmeridgian); the role of early vulcanization.
Bulletin de la Société Géologique de France, 168, 3, 331-341.
- 15) LÜCKGE A., **BOUSSAFIR M.**, LALLIER-VERGÈS E. & LITCKE R. (1996)
Comparative study of organic matter preservation in immature sediments along the continental margins of Peru and Oman. Part I : Results of petrographical and bulk geochemical data.
Organic Geochemistry. 24, pp.437-451.
- 16) GELIN F., **BOUSSAFIR M.**, DERENNE S., LARGEAU C. & BERTRAND P. (1995)
Study of qualitative and quantitative variations in kerogen chemical structure along a microcycle: correlation with ultrastructural features In: "Organic matter accumulation: The Organic Cyclicities of the Kimmeridge Clay Formation (Yorkshire , G.B.) and the Recent Maar Sediments (Lac du Bouchet)". E. Lallier-Vergès, N. Tribovillard & P. Bertrand (eds.). Springer-Verlag, Heidelberg.
Lecture Notes in Earth Sciences 57, pp. 31-47.
- 17) **BOUSSAFIR M.**, LALLIER-VERGÈS E., BERTRAND P. & BADAUT-TRAUTH D. (1995)
SEM and TEM studies of organic matter and source rock microfacies from a short-term organic cycle of kimmeridgian source-rocks. In: "Organic matter accumulation: The Organic Cyclicities of the Kimmeridge Clay Formation (Yorkshire , G.B.) and the Recent Maar Sediments (Lac du Bouchet)". E. Lallier-Vergès, N. Tribovillard & P. Bertrand (eds.). Springer-Verlag, Heidelberg.
Lecture Notes in Earth Sciences 57, pp. 15-30.
- 18) **BOUSSAFIR M.**, GELIN F., LALLIER-VERGÈS E., DERENNE S., BERTRAND P. & LARGEAU C. (1995)
Electron microscopy and pyrolysis of kerogens from the Kimmeridge Clay Formation, UK : source organisms, preservation process and origin of microcycles.
Geochimica Cosmochimica Acta 59, pp. 3731-3747.
- 19) BERTRAND P., LALLIER-VERGÈS E. & **BOUSSAFIR M.** (1994)
Enhancement of both accumulation and anoxic degradation of organic carbon controlled by cyclic productivity: a model.
Organic Geochemistry 22, pp. 511-520.
- 20) **BOUSSAFIR M.**, LALLIER-VERGÈS E., BERTRAND P. & BADAUT-TRAUTH D. (1994)
Structure ultrafine de la matière organique des roches mères du Kimméridgien du Yorkshire. *Bulletin de la Société Géologique de France*, t. 165, n°4, pp.355-363.

2008 en préparation

JACOB, J., DISNAR, J.R., **BOUSSAFIR**, M., KERAVIS, D., ALBUQUERQUE, A.L.S., SIFEDDINE, A. ET TURCQ, B. More to gain from Rock Eval analysis in paleoclimate reconstructions? A case study from the Lateglacial in Northern Brazil.
En préparation pour Journal of Applied Pyrolysis.

BOUSSAFIR, M, JACOB J. DISNAR J-R., SIFEDDINE A.
Petrography and bulk geochemistry studies of organic matter from actual surface sediments of Lake Caço (Maranhão, Brasil) ». *En préparation pour Organic Geochemistry.*,

M. BOUSSAFIR, S. DERENNE, F. LAGGOUN-DÉFARGE & C. LARGEAU
Geochemical and petrographical studies of insoluble organic matter from sediments, representing interglacial-like and last glacial maximum stages. (Tritrivakely Lake, Madagascar)
En préparation pour Organic Geochemistry.,

BOUSSAFIR M., SOPHIE CORNU, LARÉCHÉ C., & ISABELLE COUSIN
Origins, types and diagenetic transformation of organic matters associated to structural units of a metallic trace elements rich soil.
En préparation pour Geoderma. ?

BOUSSAFIR M., DROUIN S., ALBÉRIC P., DURAND A., (2005) Calibration of organic signal in sedimentary lacustrine records. Molecular comparison between actual producers, dissolved organic matter and sedimentary organic matter (Lac, Pavin, France),
En préparation pour Geochimica Cosmochimica Acta

DROUIN S., **BOUSSAFIR M.**, ROBERT J. L., ALBÉRIC P., DURAND A.
In vitro experiments of carboxylic acids sorption on synthetic clays in natural marine water. Implication on organic clayey rich sedimentation

GURGEL M.H.C., **BOUSSAFIR M.**, SIFEDDINE A., LALLIER-VERGÈS E. Holocene evolution of sea surface temperature from coastal SE Atlantic (23°S) - Cabo Frio, Brazil.
En préparation pour Geochimica Cosmochimica Acta

GURGEL M.H.C., **BOUSSAFIR M.**, SIFEDDINE A., LALLIER-VERGÈS E. - Holocene organic sedimentation at Cabo Frio upwelling cell (SE shelf of Brazil): Bulk geochemical and petrographical approach. *En préparation pour Organic Géochem.*

GURGEL M.H.C., **BOUSSAFIR M.**, SIFEDDINE A., LALLIER-VERGÈS E. Holocene organic sedimentation at Cabo Frio upwelling cell (SE shelf of Brazil): Molecular approach. Marine geology

Y. GRAZ, CHRISTIAN DI-GIOVANNI, YOANN COPARD, **M. BOUSSAFIR** MARCEL ELIE, PIERRE FAURE, JEAN LÉVÊQUE, RAYMOND MICHELS, JEAN-EMMANUEL OLLIVIER - Fossil organic matter occurrence in modern environments: optical, geochemical and isotopic evidences. *En preparation.*

I-2 Publications de Rang B : revues scientifiques à faible *citation-index* et résumés étendus

LALLIER-VERGÈS E., **BOUSSAFIR M.**, BERTRAND M. & BADAUT-TRAUTH D. (1993) - Selective preservation of various organic matters as assessed by STEM studies on

- a cyclic productivity-controlled sedimentary series (Kimmeridge Clay Formation). *Organic Geochemistry*, 16th Int. Meeting of EAOG, Falch Hurtigtrykk, Oslo. (ed. Kjell Oygard), pp. 384-387,
- BOUSSAFIR M.**, LALLIER-VERGES E., BERTRAND P. & BADAUT-TRAUTH D. (1994) - Etude ultrastructurale de matières organiques micro-prélevées dans les roches de la "Kimmeridgian Clay Formation". *Bull. Centre Rech. Expl. Prod. Elf-Aquitaine*, vol. spéc. n°18, pp. 275-278.
- LALLIER-VERGÈS E., BERTRAND P., TRIBOVILLARD N., HAYES J., **BOUSSAFIR M.**, ZABACK D., & CONNAN J. (1994) - Productivity-induced Sulfur enrichment of organic-rich sediments. "The Geochemistry and petrography of kerogens / macerals". *The Amer. Chem. Soc. Bull.*
- LALLIER-VERGES E., BERTRAND P., **BOUSSAFIR M.**, TRIBOVILLARD N.P. & DESPRAIRIES A. (1994) - La productivité: facteur majeur contrôlant les cyclicités en carbone organique à courte période des roches kimméridgiennes du Yorkshire (U.K.). *Bull. Centre Rech. Expl. Prod. Elf-Aquitaine*, vol. spéc. n°18, pp. 157-158.
- GELIN F., **BOUSSAFIR M.**, LALLIER-VERGÈS E., DERENNE S., BERTRAND P. & LARGEAU C. (1995) - Pyrolytic and electron microscopy studies of kerogen in a microcycle of the Kimmeridge Clay Formation. In "Organic Geochemistry : developments and applications to energy, climate, environment and human history (J. O. Grimalt et C. Dorronsoro, eds). A.I.G.O.A., Donostia. pp.131-133.
- HUC A.Y., NEDERLOI P., DEBARRE, R. CARPENTIER B., **BOUSSAFIR M.** & LAGGOUN-DÉFARGE F. (1997) - Detection, characterisation and generation modelling of pyrobitumen in Haima reservoirs in North Oman. 18th Int. Meet. on Org. Geochem., 1997. EAOG Maastricht ed.
- BOUSSAFIR M.**, LAGGOUN-DÉFARGE F., DERENNE S. & LARGEAU C. (2000) - Bulk and pyrolytic studies of insoluble organic matter from Tririvakely lake sediments (Interglacial-like and last maximum glacial stages). *Applied Pyrolysis*, 2000, Sevilla., p. 107.
- COPARD Y., DISNAR J. R., BECQ-GIRAUDON J.-F. & **BOUSSAFIR M.** (2001) - Can low temperature oxidation of high rank coal mimic Thermal alteration ? , 20th Internat. Meeting on Organic Geochemistry, Nancy, pp. 407-408.
- JACOB J., DISNAR J.-R., **BOUSSAFIR M.**, SIFEDDINE A., ALBUQUERQUE A.L.S. & TURCQ B. (2001) - Organic geochemistry record of paleoenvironmental and diagenetic conditions in sediments from a tropical lake (Lagoa de Caço, Brazil), 20th Internat. Meeting on Organic Geochemistry, Nancy, pp. 209-210.
- JACOB, J., DISNAR J.-R., **BOUSSAFIR M.** ET SIFEDDINE A., (2002) - Pentacyclic Triterpene Methyl Ethers (PTME): a new class of biomarkers to trace Gramineae in tropical settings? *Ancient Biomolecules*. Vol. 4/3, pp. 119..
- JACOB J., DISNAR J.-R., **BOUSSAFIR M.**, LEDRU M-P, SIFEDDINE A., SPADANO ALBUQUERQUE A-L & TURCQ B (2003) - Pentacyclic triterpene methyl ethers (PTME) in sediments of Lake Caço (NE Brazil). Plant sources and diagenetic behaviour. *IMOG 2003*, Krakow. pp. 325-326
- BOUSSAFIR M.**, FOU DI M., JACOB J. DISNAR J.-R., SIFEDDINE A., SPADANO ALBUQUERQUE A-L (2003) - Petrography and bulk geochemistry studies of organic matter from actual surface sediments of Lake Caço (Maranhão, Brasil) ». Relation ship between early diagenesis and organic sedimentation of lacustrine filling. *IMOG 2003*, Krakow, pp. 266-267

- BOUSSAFIR M.**, DROUIN S., ALBÉRIC P., DURAND A., (2005) - Calibration of organic signal in sedimentary lacustrine records. Molecular comparison between actual and producers, dissolved organic matter and sedimentary organic matter (Lac, Pavin, France), IMOG 2005 Seville. pp. 754-755
- JACOB, J., DISNAR, J.R., **BOUSSAFIR, M.**, KÉRAVIS, D., SIFEDDINE, A., ALBUQUERQUE, A.L.S. ET TURCQ, B., (2005) - Rapid paleoenvironmental variations in NE Brazil during the Lateglacial. Insights from TpS_2 , S_3CO_2 and S_3CO Rock Eval parameters. IMOG 2005, Séville. pp. 865-866
- DROUIN S., **BOUSSAFIR M.**, ROBERT J.-L., ALBÉRIC P., Durand A., (2005) Sorption of Organic Matter on clay minerals in aquatic system and influence on sedimentary organic preservation. An example of lacustrine environment (Lac Pavin, France), IMOG 2005 Seville pp. 967-968
- DROUIN S., **BOUSSAFIR M.**, ROBERT J.-L., ALBÉRIC P., Durand A., (2007) - Sorption of organic matter on clay minerals in aquatic system : Influence on sedimentary organic preservation. An exemple of a lacustrine environment (Lac Pavin, France), The 23rd International Meeting on Organic Geochemistry, Torquay, England, septembre 2007, IMOG 2007. pp. 17-18
- BOUSSAFIR M.** & LALLIER-VERGES E., (2007) - Les mécanismes de préservation de la MO des sédiments ou comment la MO arrive à se fossiliser dans les sédiments. Géochronique, Magazine des géosciences. Spéciale Matière organique. Vol. 104, pp 23-24
- BOUSSAFIR M.** (2007) - Rôle des argiles dans la préservation de la MO pétrologène. Géochronique, Magazine des géosciences. Spéciale Matière organique. Vol. 104, pp 25

1-3 Participations à des congrès

1992

- 1) LALLIER-VERGÈS E., BERTRAND P. & **BOUSSAFIR M.** (1992) - High resolution study of an organic-carbon cycle in the Kimmeridge rocks of Yorkshire (GB): I - Source and Preservation of organic carbon. Sequence stratigraphy of European Basins. 18-20 mai 1992, Dijon.
- 2) LALLIER-VERGÈS E., BERTRAND P., **BOUSSAFIR M.**, TRIBOVILLARD N. & DESPRAIRIES A. (1992) - Productivity as a major control of short-term organic cyclicity in the Kimmeridge rocks of Yorkshire (U.K.). 4th International Conference on Palaeoceanography, Kiel, 21-25 sept. 1992.

1993

- 3) **BOUSSAFIR M.**, LALLIER-VERGES E., BERTRAND P. & BADAUT-TRAUTH D. (1993) - Ultrastructure des matières organiques micro-prélevées dans des sédiments de la "Kimmeridgian Clay Formation" (Yorkshire, UK). IX colloque des Pétrographes Organ. Francoph., Pau, 17-18 juin 1993.
- 4) **BOUSSAFIR M.**, LALLIER-VERGES E., BERTRAND P. & BADAUT-TRAUTH D. (1993) - Etude ultrastructurale du contenu organique des roches sédimentaires d'âge Kimméridgien (Yorkshire, UK). Colloque Soc. Fr. Microsc. Electr., Villeurbanne-Lyon, 30 juin -2 juillet 1993.
- 5) **BOUSSAFIR M.**, LALLIER-VERGES E., BERTRAND P. & BADAUT-TRAUTH D. (1993) - Structure ultrafine des roches et matières organiques pétrologènes. Origine et mode de fossilisation de la matière organique. Colloque de fin d'activité du GdR 942. Maison de la SGF, le 7 déc. 1993.

- 6) LALLIER-VERGÈS E., **BOUSSAFIR M.**, BERTRAND P. & BADAUT-TRAUTH D. (1993) - Selective preservation of various organic matters as assessed by STEM studies on a cyclic productivity-controlled sedimentary series (Kimmeridge Clay Formation). 16th international meeting of organic geochemistry, Stavanger, 20-24 sept. 1993.

1994

- 7) LALLIER-VERGES E., BERTRAND P., **BOUSSAFIR M.**, TRIBOVILLARD N.P. & DESPRAIRIES A. (1994)- La productivité: facteur majeur contrôlant les cyclicités en carbone organique à courte période des roches kimméridgiennes du Yorkshire (U.K.). IX colloque des Pétrographes Organ. Francoph., Pau.

1995

- 8) **BOUSSAFIR M.** & LALLIER-VERGES E. (1995) - Nature and preservation state of organic matter in sediments: origin of the short term organic carbon content cyclicités in the Kimmeridge Clay Formation (Yorkshire, UK). Int. Assoc. Sedim., 16th European Meeting, Aix les Bains, 24-26 avril 1995.
- 9) GELIN F., **BOUSSAFIR M.**, LALLIER-VERGES E., DERENNE S., BERTRAND P. & LARGEAU C. (1995) - Pyrolytic and electron microscopy studies of Kerogen in a microcycle of the Kimmeridge Clay formation. 17th Int. Meeting of EAOG. San Sebastian, sept. 1995

1996

- 10) BAUDIN F., TRIBOVILLARD N. P., LAGGOUN-DÉFARGE F., **BOUSSAFIR M.**, LICHTFOUSE E., MONOD O. & GARDIN S. (1996) - Environnement de dépôt d'un niveau carbonaté noir du Kimméridgien (Formation d'Akkuyu, SW Turquie). Coll. Sédimentologie de la matière organique, Paris 11&12 décembre 1996.
- 11) **BOUSSAFIR M.**, LAGGOUN-DEFARGE F., DERENNE S. & C. LARGEAU (1996) - Recherche de marqueurs organiques ultrastructuraux et moléculaires dans des sédiments lacustres récents représentant deux stades climatiques différents : glaciaire et interglaciaire. (Lac Tritrivakely, Madagascar). 16^{ème} Réunion des Sciences de la Terre, X^{ème} Coll. des Pétrographes Organiciens Francophones, Orléans, 10 - 12 Avril 1996.
- 12) MONGENOT T., **BOUSSAFIR M.**, LALLIER-VERGES E., TRIBOVILLARD N. P., S. DERENNE & C. LARGEAU (1996) - Étude pétrographiques et géochimiques des laminites bitumineuses d'orbagnoux (France, Kimméridgien supérieur) 16^{ème} Réunion des Sciences de la Terre, X^{ème} Coll. des Pétrographes organiciens francophones, Orléans, 10 - 12 Avril 1996.
- 13) MONGENOT T., DERENNE S., TRIBOVILLARD N. P., LALLIER-VERGES E., **BOUSSAFIR M.**, LARGEAU C & J. CONNAN (1996) - Vulcanisation naturelle et préservation de la matière organique -L'exemple des laminites bitumineuses d'Orbagnoux (France, Kimméridgien supérieur). Coll. Sédimentologie de la matière organique, Paris 11&12 décembre 1996.

1997

- 14) HUC A.Y., NEDERLOI P., DEBARRE, R. CARPENTIER B., **BOUSSAFIR M.** & LAGGOUN-DÉFARGE F. (1997) - Detection, characterisation and generation modelling of pyrobitumen in Haima reservoirs in North Oman. 18th Int. Meet. on Org. Geochem., Maastricht, Sept. 22-26, 1997.

1999

- 15) COPARD Y., DISNAR J. R., BECQ-GIRAUDON J.-F., & **BOUSSAFIR M.** (1999) - Paléothermicité des bassins permo-carbonifères du Massif Central français : houillification et altération hydrothermale mises en évidence par l'analyse de la matière organique. 7^{ème} congrès de l'ASF, 15-17 nov., Nancy. Rés. pp. 85-86.

2000

- 16) **BOUSSAFIR M.**, LAGGOUN-DEFARGE F., DERENNE S. & LARGEAU C. (2000) - Bulk and pyrolytic studies of insoluble organic matter from Tririvakely lake sediments (Interglacial-like and last maximum glacial stages). *14th Int. Symp. on Analytical and Applied Pyrolysis*, 2-6 avril 2000, Sevilla, Espagne. Rés. p. 107.

2001

- 17) **BOUSSAFIR M.**, LAGGOUN-DEFARGE F., DERENNE S. ET LARGEAU C. (2001) - Composition géochimique et pétrographique des matières organiques de sédiments lacustres représentant deux stades climatiques distincts (le lac Tririvakely, Madagascar) 8^{ème} congrès ASF, Orléans 12-14 novembre 2001, p. 531.
- 18) COPARD Y., DISNAR J. R., BECQ-GIRAUDON J.-F. & **BOUSSAFIR M.** (2001) - Can low temperature oxidation of high rank coal mimic Thermal alteration ? , 20th Internat. Meeting on Organic Geochemistry, Nancy 10-14 sept. 2001., abst. 2, pp. 407-408.
- 19) JACOB J., DISNAR J. R., **BOUSSAFIR M.**, SIFEDDINE A., ALBUQUERQUE A.L. & TURCQ B. (2001) - Enregistrement des variations paléoenvironnementales durant le Quaternaire récent en domaine intertropical (Lac Caço, Brésil) : apports de la géochimie organique globale et moléculaire, 8^{ème} congrès ASF, Orléans 12-14 novembre 2001, rés. p. 199.
- 20) JACOB J., DISNAR J.-R., **BOUSSAFIR M.**, SIFEDDINE A., ALBUQUERQUE A.L.S. & TURCQ B. (2001) - Organic geochemistry record of paleoenvironmental and diagenetic conditions in sediments from a tropical lake (Lagoa de Caço, Brazil), 20th Internat. Meeting on Organic Geochemistry, Nancy 10-14 sept. 2001.
- 21) SIFEDDINE A., ALBUQUERQUE A.L., TURCQ B., JACOB J., **BOUSSAFIR M.**, DISNAR JR. & ABRAO J. (2001) - La sédimentation organo-minérale marqueur des changements environnementaux et climatiques au Nord-Est du Brésil (Lac Caço, Maranhao, Brésil) durant les 21,000 ans CAL BP, 8^{ème} congrès ASF, Orléans 12-14 novembre 2001, rés. p. 339

2002

- 22) PICHEVIN L., **BOUSSAFIR M.** & BERTRAND P., (2002) - Organic matter accumulation of Lüderitz, Benguela upwelling system. Control of climatic variations, sea level change and organic matter flux. Congrès AGU.
- 23) JACOB J., DISNAR J.-R., **BOUSSAFIR M.**, & SIFEDDINE A. (2002) - Pentacyclic Triterpene Methyl Ethers (PTME): a new class of biomarkers that illustrate Gramineae in tropical settings. B.O.G.nnbgt&y S., Newcastle (UK), July 2002. Best Poster Award.
- 24) SIFEDDINE, A., TURCQ, B., CARDOSO, A., SPADANO ALBUQUERQUE, A.L., LEDRU, M.-P., JACOB, J., CAMPELLO CORDEIRO, R., **BOUSSAFIR, M.**, DISNAR, J.R. & ABRÃO, J.J., (2002) - La sédimentation organo-minérale lacustre durant les 21 000 ans CAL BP (Lac Caço, Maranhão, Brésil). Implications environnementales et paléoclimatiques. Colloque International Quaternaire 3, « Événements rapides, instabilités, changements culturels au quaternaire » (Aix en Provence, 24-26 janv. 2002), Abstr. Vol., p. 56

2003

- 25) COPARD Y., DISNAR J.R., **BOUSSAFIR M.** (2003) - Analogies between the effects of low temperature weathering and thermal alteration on the structure and the composition of mature coals. the 21st Int. Meeting Org. Geochem., 8-12 september 2003, Krakow, Poland.
- 26) JACOB J., DISNAR J-R., . **BOUSSAFIR M.**, LEDRU M-P, SIFEDDINE A., SPADANO ALBUQUERQUE A-L & TURCQ B (2003) - Pentacyclic triterpene methyl ethers (PTME) in sediments of Lake Caço (NE Brazil). Plant sources and diagenetic behaviour. 21st Int. Meeting Org. Geochem., 8-12 september 2003, Krakow, Poland.
- 27) JACOB J., DISNAR J-R., **BOUSSAFIR M.**, LEDRU M-P, SIFEDDINE A., SPADANO ALBUQUERQUE A-L AND TURCQ B (2003) - Onocerane I witnesses to dry climatic phases at the end of Last Glacial Maximum and during the Younger Dryas in Northern Brazil. the 21st Int. Meeting Org. Geochem., 8-12 september 2003, Krakow, Poland.
- 28) JACOB, J., DISNAR, J.R., **BOUSSAFIR, M.**, SIFEDDINE, A., ALBUQUERQUE, A.L.S. ET TURCQ, B., (2003) - Paleoenvironmental record of the last 20,000 years in north-eastern Brazil (Lake Caçó, Maranhão State): Insights from Rock Eval pyrolysis. 3rd International Limnogeology Congress, March 29 - April 2, 2003, Tucson, Arizona.
- 29) JACOB, J., DISNAR, J.R., **BOUSSAFIR, M.**, LEDRU, M.-P., SIFEDDINE, A., ALBUQUERQUE, A.L.S. ET TURCQ, B., (2003) - New higher plant biomarkers for deciphering past vegetational successions in continental Quaternary tropical sedimentary series. 3rd International Limnogeology Congress, March 29 - April 2, 2003, Tucson, Arizona.
- 30) **BOUSSAFIR M.**, FOU DI M., JACOB J. DISNAR J-R., SIFEDDINE A., SPADANO ALBUQUERQUE A-L (2003) - Petrography and bulk geochemistry studies of organic matter from actual surface sediments of Lake Caço (Maranhão, Brasil) ». Relation ship between early diagenesis and organic sedimentation of lacustrine filling. the 21st Int. Meeting Org. Geochem., 8-12 september 2003, Krakow, Poland.
- 31) **BOUSSAFIR M.**, JACOB J. DISNAR J-R., SIFEDDINE A., (2003) Etude pétrographique et géochimique de la MO des sédiments de surface actuelle du Lac Caço (Maranhão, Bresil) ». Relation entre la diagenèse précoce, remplissage organique du lac et calibration des archives sédimentaires. Congrès ASF 2003, Bordeaux
- 32) JACOB, J. DISNAR, J.R., **BOUSSAFIR, M.**, SIFEDDINE, A., ALBUQUERQUE, A.L.S. ET TURCQ, B., (2003) - Nouveaux Marqueurs moléculaires témoins des successions végétales en domaine tropical. Exemple du Lac Caço (Nord Est du Brésil) depuis le DMG. ASF Bordeaux, 2003.

2004

- 33) GURGEL, M. H. G., SIFEDDINE, A., LALLIER-VERGÈS, E., **BOUSSAFIR, M.** & KERAVIDS, D., (2004) - Bulk organic parameters from Cabo Frio (Rio de Janeiro - Brasil) upwelling system cores during the last ~ 8.000 years. First results. 4th International Symposium Environmental Geochemistry in Tropical Countries (October 25-29, Buzios, Brésil). Abstr. Vol.: 297 (poster).
- 34) GURGEL, M.H.C., SIFEDDINE, A., LALLIERS-VERGÈS, E., **BOUSSAFIR, M.**, VALDÈS, J. & ORTLIEB, L., (2004) - Organic sedimentation processes under two different upwelling systems over 23°S South American margins. 8th International conference on Paleoceanography An Ocean View of Global Change. 5-10 September 2004. Biarritz. France.
- 35) BAUDIN F., BLANKE R., PICHEVIN L., TRANIER J., BERTRAND P., DISNAR J.-R., LALLIER-VERGÈS E., VAN BUCHEM F., **BOUSSAFIR M.**, FROHLICH F. ET AL (2004) - Recent

sedimentation of organic matter along the SE Atlantic Margin : A key for understanding deep offshore petroleum source rocks. EAGE 66th Conference & Exhibition - (2004) -

- 36) JACOB, J., DISNAR, J.-R., & **BOUSSAFIR, M.**, (2004) - Biomarqueurs et isotopie moléculaire dans les archives lacustres : acquis récents et perspectives d'application. Séance spécialisée de la Société Géologique de France : "Archives lacustres en domaine tempéré", 4 février 2004, Paris.
- 37) JACOB, J., DISNAR, J.R., HUANG, Y., **BOUSSAFIR, M.**, SIFEDDINE, A., ALBUQUERQUE, A.L.S. ET TURCQ, B., (2004) - Deciphering past climates from ancient molecules preserved in lake sediments. 21ème congrès de la Société Française de Spectrométrie de Masse, Strasbourg, 14-17 septembre 2004.
- 38) BLANKE R., PICHEVIN L., TRANIER J., BAUDIN F., BERTRAND P., DISNAR J.R., LALLIER-VERGES E., VAN BUCHEM F., GIRAUDEAU J., **BOUSSAFIR M.**, FRÖHLICH F., MARTINEZ P., MALAIZE B. & KERAVID D.(2004) - Recent organic-rich deep sedimentation of Southwest Africa: keys for understanding the deep offshore petroleum source-rock distribution. 32th international Geological Congress. Florence du 20-28 Août 2004

2005

- 39) GURGEL, M.H.C., LALLIER-VERGES, E., SIFEDDINE, A., **BOUSSAFIR M.**, JACOB, J. & VALDES, J., (2005) - La matière organique des archives sédimentaires marines : évolution des marqueurs paléoenvironnementaux et paléoclimatiques (Amérique du Sud). Congrès international des sédimentologues Français. 09-16 Octobre 2005. Hyères. France.
- 40) GURGEL, M.H.C., SIFEDDINE, A., VERGES, E., **BOUSSAFIR, M.**, JACOB, J. ET VALDES, (2005) - J. La matière organique sédimentaire de deux zones d'upwelling sud-américaines : évolution des marqueurs. Congrès de l'ASF, Giens, 11-13 octobre 2005.
- 41) GURGEL, M.H., SIFEDDINE, A. LALLIER-VERGES, E., **BOUSSAFIR, M.** ET JACOB, J., (2005) - Holocene Paleooceanographic Conditions of Cabo Frio Upwelling System (Rio de Janeiro / Brazil). As Inferred by Bulk and Molecular Geochemical Approach From Sedimentary Organic Matter. AGU Fall Meeting, San Francisco, Décembre 2005.
- 42) GUTIERREZ, D., SIFEDDINE, A., ORTLIEB, L., VELAZCO, F., BAUMGARTNER, T., REYSS, J.L., VARGAS, G., SALVATECCI, R., TAPIA, P., FIELD, D., FERREIRA, V., VALDES, J., SOLÍS, J., SOLER, P., **BOUSSAFIR, M.**, TAFFOUREAU, E., BOUCHER, H., MANDENG, M. & BOULOUBASSI. I., (2005) - Secular to interannual climatic and oceanographic changes in the Peruvian upwelling ecosystem revealed by multiproxies sedimentary records of the past 250 years preserved in the continental margin. Eos Trans. AGU, 86(52), Fall Meet. Suppl., Abstract.
- 43) GUTIERREZ, D., SIFEDDINE, A., ORTLIEB, L., VELAZCO, F., FERREIRA, V., BAUMGARTNER, T., SALVATECCI, R., **BOUSSAFIR, M.**, VARGAS, G., SOLER, P. & VALDES J., (2005) - Sedimentary and bulk organic composition of anoxic sediments off Central Peru record interannual to multidecadal changes of climate and upwelling ecosystem functioning during the past few centuries. Congrès international de l'Assoc. des Sédimentologues Français (09-16 Octobre 2005, Hyères).
- 44) GUTIERREZ, D. SIFEDDINE, A., REYSS, J.L., VARGAS, G., VELAZCO, F., SALVATECCI, R., FERREIRA, V., ORTLIEB, L., BAUMGARTNER, T., **BOUSSAFIR, M.**, BOUCHER, H., VALDES, J., MARINOVIC, L., SOLER, P., FIELD, D. & TAPIA, P., (2005) - Decadal to interannual paleoceanographic records of the past 200 years in anoxic sediments off central Peru. 1st Alexander von Humboldt International Conference on "The El Niño phenomenon and its global impact" (Guayaquil, Ecuador, may 2005).

- 45) **BOUSSAFIR M.**, DROUIN S., ALBÉRIC P., DURAND A., (2005) - Calibration of organic signal in sedimentary lacustrine records. Molecular comparison between actual and producers, dissolved organic matter and sedimentary organic matter (Lac, Pavin, France), IMOG 2005 Seville
- 46) JACOB, J., DISNAR, J.R., **BOUSSAFIR, M.**, KÉRAVIS, D., SIFEDDINE, A., ALBUQUERQUE, A.L.S. ET TURCQ, B., (2005) - Rapid paleoenvironmental variations in NE Brazil during the Lateglacial. Insights from TpS2, S3CO₂ and S3CO Rock Eval parameters. 22nd IMOG meeting, Séville, Espagne, septembre 2005.
- 47) DROUIN S., **BOUSSAFIR M.**, ROBERT J.-L., ALBERIC P., (2005) - Rôle des interactions argilo-organiques dans la préservation de la Matière Organique en environnement sédimentaire : Exemple d'un environnement lacustre (le lac Pavin, France), ASF 2005 Presqu'île de Giens (communication orale)
- 48) DROUIN S., **BOUSSAFIR M.**, ROBERT J.-L., ALBÉRIC P., Durand A., (2005) - Sorption of Organic Matter on clay minerals in aquatic system and influence on sedimentary organic preservation. An example of lacustrine environment (Lac Pavin, France), IMOG 2005 Seville
- 49) DROUIN S., ROBERT J.-L., **BOUSSAFIR M.**, ALBERIC P., (2005) - Rôle des interactions argilo-organiques dans la préservation des Matières Organiques en environnement lacustre (le Lac Pavin, France), GFA 2005 à l'Ecole des Mines

2006

- 50) BAUDIN F., BERTRAND P., PICHEVIN L., BLANKE R., TRANIER J., DISNAR J.-R., LALLIER-VERGES E., VAN BUCHEM F., **BOUSSAFIR M.**, MARTINEZ P. ET AL (2006) - Sédimentation organique profonde associée au système d'upwelling du Courant de Benguela (Atlantique Sud-est) : de la molécule à la modélisation. Réunion des Sciences de la Terre, Dijon : France (2006) -
- 51) DROUIN S., ROBERT J.-L., **BOUSSAFIR M.**, ALBÉRIC P., DURAND A., (2006) - Sorption of Organic Matter on clay minerals in aquatic system: influence on sedimentary organic preservation. An example of a lacustrine environment (Lac Pavin, France) (2006), GFA-the Clay Minerals Society, Île d'Oléron (communication orale)
- 52) DROUIN S., **BOUSSAFIR M.**, ROBERT J.-L., ALBERIC P., DURAND A., (2006) - Rôle des argiles dans la préservation de la Matière Organique : exemple d'un environnement lacustre (le Lac Pavin, France), Réseau Matière Organique 2006 Carqueiranne

2007

- 53) GURGEL M., SIFEDDINE A., LALLIER-VERGES E., **BOUSSAFIR M.** (2007) - Enregistrement multi-marqueurs de l'évolution de la matière organique sédimentaire de la zone d'upwelling de Cabo Frio (SE Brésil) au cours de l'Holocène. Les Journées Paléocéanographiques, Paris : France (2007)
- 54) GURGEL, M. H. C.; GUTIERREZ, D.; SIFEDDINE, A.; BOUSSAFIR, M.; VERGES, E; ORTLIEB, L.; DURAND, D.; VELAZCO, F. (2007) - Inferences on marine paleo-productivity and paleo-oxygenation off Callao (12°S) during the Holocene. Primer Congreso de Ciencias del Mar del Peru, Lambayeque, 27 - 30 de Novembre 2007.
- 55) GURGEL, M. H. C.; BOUSSAFIR, M. ; SIFEDDINE, A. ; VERGES, E. (2007) - Enregistrements moléculaires de la matière organique sédimentaire de l'upwelling de Cabo Frio (SE Brésil) au cours de l'Holocène. In: 11ème Congrès Français de Sédimentologie, 2007, Caen - France. Livre des Résumés. Paris : Associations des Sédimentologistes Français, 2007. v. 57. p. 154-154.
- 56) GURGEL, M. H. C. ; SIFEDDINE, A. ; VERGES, E. ; BOUSSAFIR, M. . (2007) - Enregistrement multi-marqueurs de l'évolution de la matière organique sédimentaire de la zone d'upwelling de Cabo Frio (SE Brésil) au cours de l'Holocène. In:

Journées Paléocéanographiques, 2007, Paris - França. Programme et Résumés.
Paris : Programa IMAGES, 2007. –

- 57) DROUIN S., BOUSSAFIR M., ROBERT J.-L., ALBÉRIC P., Durand A., (2007) - Sorption of organic matter on clay minerals in aquatic system : Influence on sedimentary organic preservation. An exemple of a lacustrine environment (Lac Pavin, France), The 23rd International Meeting on Organic Geochemistry, Torquay, England, septembre 2007, IMOG 2007
- 58) BOUSSAFIR, M., SIFEDDINE, A., SASIAS M., GUTIERREZ, D., ORTLIEB L., DURAND A. (2007) - Apport de la géochimie et de la pétrographie organique dans l'étude des sédiments déposés au cours des cinq derniers siècles sur la plateforme péruvienne. ASF, Septembre 2007 Caen
- 59) DROUIN S., BOUSSAFIR M., ROBERT J.-L., ALBERIC P., Durand A., (2007) - Rôle des argiles dans le transfert des Matières Organiques vers les sédiments : Un modèle présenté sur l'exemple d'un environnement lacustre, ASF, Septembre 2007 Caen
- 60) GRAZ Y., DI-GIOVANNI C., COPARD Y., ALBERIC P., BAILLIF P., BOUSSAFIR M., ELIE M., FAURE P., GOUIN J., LAGGOUN-DEFARGE F., LEVEQUE J., MATHYS N., MICHELS R., (2007) - Le devenir du carbone organique fossile libéré par l'altération des roches sédimentaires : application aux bassins versants expérimentaux de Draix. Yann à ASF, Septembre 2007 Caen.
- 61) SIFEDDINE A., GUTIERREZ D., ORTLIEB L., VELAZCO F., FILED D., BOUCHER H., GARCIA M., MANDENG YOGO M., BOUSSAFIR M, SALVATTECI R, SOLER P., (2007) – Multi proxies of oceanographic and climate changes during the little ice age in laminated sediments of the central peruvian margin. ASF, Septembre 2007 Caen.
- Prévus en 2008
- 62) GRAZ Y., DI-GIOVANNI C., COPARD Y., ALBERIC P., BAILLIF P., BOUSSAFIR M., ELIE M., FAURE P., LAGGOUN-DEFARGE F., LÉVEQUE J., MATHYS N., MICHELS R. (2008) - The fate of the fossil organic carbon released from marls weathering: application to the experimental watersheds of Draix, Congrès EUG, 2008
- 63) SIFEDDINE A., GUTIÉRREZ D., GURGEL M., GARCÍA M., ORTLIEB L., BOUSSAFIR M., VELAZCO F., BOUCHER H., CAQUINEAU S. AND VALDÉS J. (2008) - Interdecadal to Centennial variability of paleoproductivity and redox conditions in the Peruvian continental margin during the last two millennia, Cannaries Meeting.2008

HABILITATION À DIRIGER DES RECHERCHES

PRESENTÉE À

L'UNIVERSITÉ D'ORLÉANS

PAR

MOHAMMED BOUSSAFIR

PARTIE VII

ANNEXES :

EXEMPLAIRES DE QUELQUES PUBLICATIONS

Soutenue publiquement le 27 Juin 2008

Devant le Jury composé de :

M. François BAUDIN,	Professeur à l'Université de Paris VI (Rapporteur)
M. Raymond MICHELS ,	Chargé de Recherche (HdR) à l'Université de Nancy I (Rapporteur)
M. Luc ORTLIEB ,	Directeur de recherche à l'IRD (Rapporteur)
Mme Sylvie DERENNE	Directeur de Recherche à BIOEMCO Paris (Examineur)
Mme Elisabeth VERGES	Directeur de recherche à l'ISTO (Examineur)
M. Ary BRUAND	Professeur à l'université d'Orléans (Examineur)
M. Abdelfettah SIFEDDINE	Directeur de Recherche à l'IRD (Examineur)



Enhancement of accumulation and anoxic degradation of organic matter controlled by cyclic productivity: a model

PHILIPPE BERTRAND,* ELISABETH LALLIER-VERGES and MOHAMMED BOUSSAFIR
GDR 942 & URA 724 du CNRS, Université d'Orléans, 45067 Orléans Cedex 2, France

Abstract—The aim of the study is to determine the relative influences of the genetic sources, the export efficiency, and the anaerobic degradation of organic carbon as factors controlling short-term cyclic organic-rich sedimentation in areas of high marine productivity. A cyclic organic sequence of the Kimmeridge Clay Formation of Yorkshire (U.K) was studied as an example of ancient sedimentation. This formation outcropping in the Cleveland basin near Marton is known as a lateral equivalent of the major oil source rock unit of the North Sea. On the basis of petrographic and geochemical results, a new model is proposed to explain the short-term cyclic sedimentation of organic carbon under continuously anoxic bottom conditions.

The model assumes that the cyclicity is primarily controlled by variations of mineral-free phytoplanktonic productivity. Such variations are thought to induce changes in carbon recycling in the photic zone so that the export efficiency of the metabolizable organic matter is modified. A high sulphate reduction intensity relative to the organic matter flux is observed for the highest productivity periods, which also reflects an enhancement of export efficiency. As the redox conditions did not change significantly, such variations in sulphate reduction intensity must be attributed not only to quantitative variations in the export productivity, but also to its qualitative variations, with more metabolizable organic matter reaching the anoxic domain during high productivity periods. Biosedimentary processes depending on productivity, such as aggregation, are thought to play an important role in reducing the transit time of metabolizable organic matter to the sediment. Finally, the model implies that the amplitude of export productivity variations probably were larger than that of TOC variations recorded in sediment which are mainly due to biologically refractory organic matter from plankton.

Key words—source rock deposition, model, Kimmeridge Clay Formation, cyclicity, anoxic conditions, sulphate reduction, productivity

INTRODUCTION

Organic-rich sedimentary series frequently show short-term cyclic fluctuations in their quantitative and qualitative organic content. This had been reported for ancient marine sediments such as the Kimmeridge Clay Formation of the North Sea and adjacent areas (Oschmann, 1988; Herbin *et al.*, 1991), the Cenomanian–Turonian shales of the Atlantic and Tethys (Herbin *et al.*, 1987; Crumières *et al.*, 1990), the Oligocene evaporites of the Mulhouse basin (Blanc-Valleron *et al.*, 1991) as well as for modern Quaternary analogs such as the Oman and Peru margin sediments (Prell *et al.*, 1989; Wefer *et al.*, 1990).

In modern sediments, for which a very high chronostratigraphic resolution can be obtained, fluctuations in organic carbon burial have often been recognized as being climatically controlled, and a correlation between organic carbon burial, insolation and ice volumes can be recognized (Lyle, 1988). The only argument to draw such a conclusion for ancient sediments is that, broadly evaluated, the frequency of

the fluctuations in organic content generally is of the same order of magnitude (≤ 0.1 Ma) as the main orbital periods forcing isolation.

As variations of global climate cannot be directly assessed from ice volume ($\delta^{18}\text{O}$ stratigraphy) for ancient organic-rich sediments, this type of study has been restricted to comparing the influences of factors possibly forced by local climate and oceanographic conditions as consequences of global forcing. The factors are marine productivity and terrestrial inputs as possible sources for organic carbon, dilution by detrital or biogenic minerals, and the redox conditions as a possible factor of enhanced preservation (Demaison and Moore, 1980; de Graciansky *et al.*, 1984). With respect to these questions, the use of high resolution sampling combined with petrographic and geochemical approaches has allowed us to propose a new model to explain the fluctuations in organic content for margin environments with high productivity.

The study has been performed on an organic cycle of the Kimmeridge Clay Formation in Yorkshire. This formation is a lateral equivalent of the major oil source rock unit of the North Sea. It consists of alternating organic-rich shales and marls deposited in marginal shallow water and under low energy conditions (Myers and Wignall, 1987; Scotchman, 1987;

*Present address: Department of Geology and Oceanography, Université de Bordeaux I, avenue des Facultés, 33405 Talence Cedex, France.

Wignall, 1989; Miller, 1990), and reveals a cyclic distribution of organic content (Herbin *et al.*, 1991). One of these microcycles, about 1 m thick and representing about 30 kyr of sedimentation, has been investigated by petrographical and geochemical analyses with respect to mineral and organic components (90 samples from a 120 cm long core section) in order to characterize the cycle in detail. The cycle is located in the Eudoxus zone of the Marton-87 borehole. Qualitative results related to genetic sources, nature of export fluxes, and anaerobic degradation of organic matter are discussed. Most of the results have already been reported by Pradier *et al.* (1992), Ramanampisoa *et al.* (1992) and Tribouillard *et al.* (1992). The aim of this paper is mainly to present and discuss the interpretations, assumptions and principles in order to establish a model.

AMOUNT AND GEOCHEMICAL TYPE OF ORGANIC CARBON

The organic sequence is shown as a total organic carbon content (TOC) and hydrogen index (HI) vs depth representation (Fig. 1). The TOC values range between 1.8 and 9.5 weight % of dry sediment with the lowest values at the beginning of the cycle. The middle part is characterized by the highest TOC values but also by abrupt fluctuations of large amplitude, whereas the beginning and the end of the cycle exhibit relatively constant TOC values.

For TOC values between 1.8 and 4% TOC, corresponding to the beginning (1.8–2.2% TOC) and to the end of the cycle (2.2–4% TOC), the HI and TOC values are positively correlated. For TOC values above 4%, corresponding to the middle part of the cycle, the HI values tend to reach a maximum around 550–600 mg HC/g Corg although TOC varies largely. These HI values do not correspond to terrestrial organic matter from higher plants, but imply the

presence of hydrogen-rich material such as algae, spores or cuticles. Some points with very high HI values from 600 to 800 mg HC/g Corg probably correspond to brief and exceptional events superimposed on the normal cycle. Up to now, the nature of these events has not been unveiled.

SOURCES OF ORGANIC CARBON AND REDOX ENVIRONMENT

The mineralogical and major elements studies of Tribouillard *et al.* (1992) have shown that the inorganic fraction is mainly composed of silico-clastic minerals (clays and quartz) and coccolith-derived carbonates, and that the TOC variations cannot be an effect of dilution by these minerals. Moreover, the petrographic examination of palynofacies has revealed only a minor proportion of lignitic terrestrial debris along the sequence which is unable to explain the TOC variations (Ramanampisoa *et al.*, 1992). It can be inferred from this that the TOC variations originate either from changes in the marine productivity-related organic supply to the sediment or from modifications in organic matter burial efficiency. As indicated below, the answer has partially been provided by petrographic studies, IR spectroscopy and trace elements geochemistry.

Palynofacies examination indicates that the optically structureless organic matter, which is often reported to have a marine origin in such sediments, predominates over structured palynodebris. Four categories have been clearly distinguished within the structureless organic matter, mainly according to its coloration: brown; orange; black to dark brown; yellow to translucent (Ramanampisoa *et al.*, 1992). The proportion of the orange type varies considerably (from 1 to 60% vol.) and it is the only type that correlates with the TOC variations. On the other hand, the macerals, i.e. individualized organic

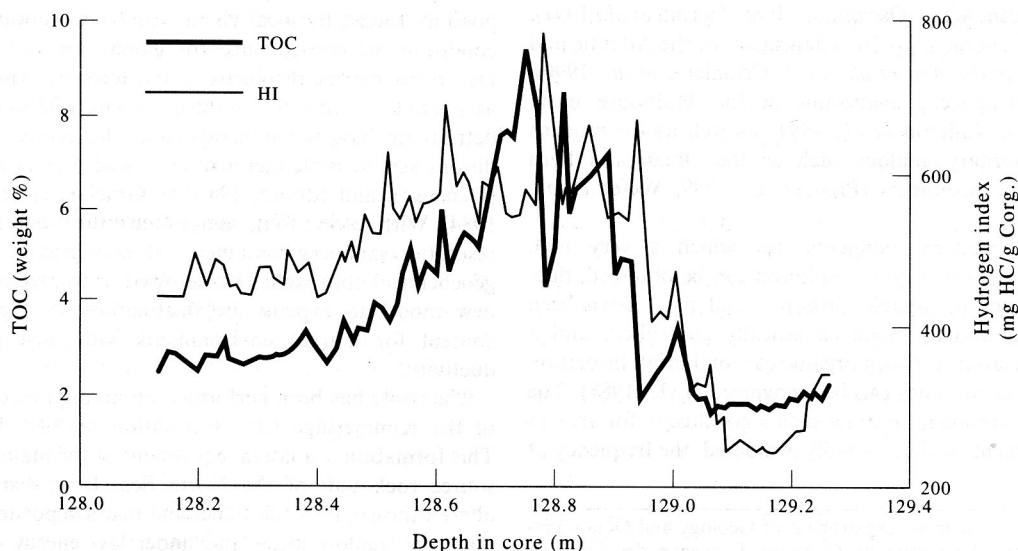


Fig. 1. TOC and hydrogen index profiles along the studied sequence.

particles as observed in incident light on polished sections, are mainly composed of fluorescent bodies, some of them being clearly recognizable as algal bodies (Pradier *et al.*, 1992). As for the structureless organic matter, different types of fluorescent macerals were distinguished, one of these, the so called "brown bodies" because of their coloration in fluorescence, shows the best correlation with TOC variations. Because of the covariance between the orange amorphous organic matter and the brown bodies, we assume that the latter are mainly derived from the former, and do not occur as recognizable algae in palynofacies. Moreover, T.E.M. studies on particles optically selected from palynofacies indicate that the amorphous organic matter is mainly composed of resistant ultralaminae (Lallier-Vergès *et al.*, 1993) similar to those derived from planktonic algal material as described by Largeau *et al.* (1990).

A supplementary argument in favour of productivity variations has been provided by IR spectroscopy of kerogens (IRFT) and trace elements geochemistry (Tribovillard *et al.*, 1992) which tend to indicate that variations in the depositional environment have been weak. This is consistent with the fact that observations of the sedimentary microfacies show no differences. Especially, no bioturbation occurs whatever the TOC in the cycle may be. This indicates that anaerobic conditions have been continuously prevailing in the water column overlying the water-sediment interface.

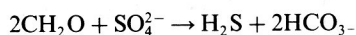
SULPHATE REDUCTION

Recent studies showed that biogenic sulphate reduction is one of the most efficient diagenetic processes affecting organic matter preservation in modern marine sediments. As much as 50% of the organic matter degradation could be due to this process (Thode-Andersen and Jørgensen, 1989). As a consequence of bacterial sulphate reduction and subsequent trapping of sulphur, reduced sulphur is often concentrated in organic-rich marine sediments (Holser and Kaplan, 1966; Berner, 1970). The quantities of sulphur trapped commonly exceed amounts of sulphate initially present in pore waters, implying that additional sulphate is transported into the sediments via diffusion and/or advection (Goldhaber and Kaplan, 1980; Jørgensen, 1979; Aller, 1984; Chanton *et al.*, 1987) or that significant sulphate reduction occurs above or at the water-sediment interface.

The amount of sulphur trapped in marine sediments can therefore be regarded as a good indicator to assess the organic carbon oxidized by sulphate reduction. Such assessment further requires the evaluation of the fraction of sulphur retained as reduced sulphur and the fraction internally recycled due to oxidizing agents other than sulphate. From unpublished isotope studies ($\delta^{34}\text{S}$) we know that the minimum for sulphate retention ranges between 30 and 50% (J. Hayes, personal communication). In the

following discussion and modelling, we assume that the sulphur has been retained with a constant efficiency of 30%.

Taking into account the stoichiometry proposed for sulphate reduction by Berner and Raiswell (1984)



we can write

$$C_{\text{ox}} \geq 0.75S_{\text{sed}}$$

where C_{ox} and S_{sed} denote masses of organic carbon oxidized by sulphate reduction and reduced sulphur trapped in sediment respectively. The inequality (\geq) represents the uncertainty about the efficiency with which reduced sulphur has been retained.

With respect to sulphate reduction, C_{ox} is related to an initial and a residual organic carbon masses, C_i and C_r respectively,

$$C_i = C_r + C_{\text{ox}}$$

A sulphate reduction index (SRI) can be defined as

$$\text{SRI} = C_i/C_r \text{ (Lallier-Vergès } et al., 1993)$$

A simple calculation indicates that SRI, which is strictly a mass or a flux ratio, can reasonably be calculated using total sulphur content for S_{sed} and total organic carbon content (TOC) for C_r . Indeed, the effect of the sulphur retention on the sediment composition is weak relative to the total mass of initial sediment.

Variations of the SRI values vs depth are represented together with TOC in Fig. 2. This shows clearly that sulphate reduction was stronger during the high productivity period corresponding to the middle part of the sequence. This result can also be petrographically observed through the higher frequency of pyrite framboids occurring within the organic matter (Lallier-Vergès *et al.*, 1993). Elemental analysis of the kerogen + sulphides fraction (after HF-HCl treatment) allows us to calculate and compare the amounts of sulphur trapped as iron sulphides and organic compounds (Fig. 3). The good correlation between sulphur as iron sulphide and TOC denotes that easily reducible iron species have always been available, and that sulphur has been preferentially trapped in this form (mainly pyrite) all along the cycle. The same conclusion has been reached by determining the Degree of Pyritization (D.O.P.) (Tribovillard *et al.*, 1994). High SRI values are also observed at the beginning of the cycle where the supply of organic matter should have been lower. In this interval, sulphur occurs mainly as massive pyrite within foraminifer tests. We assume that the degraded organic matter was mainly zooplanktonic and that the transfer downward was favoured by the size of mineral tests. This phenomenon does not play a significant role in the control of the cycle. All these SRI variations are discussed and modelled below.

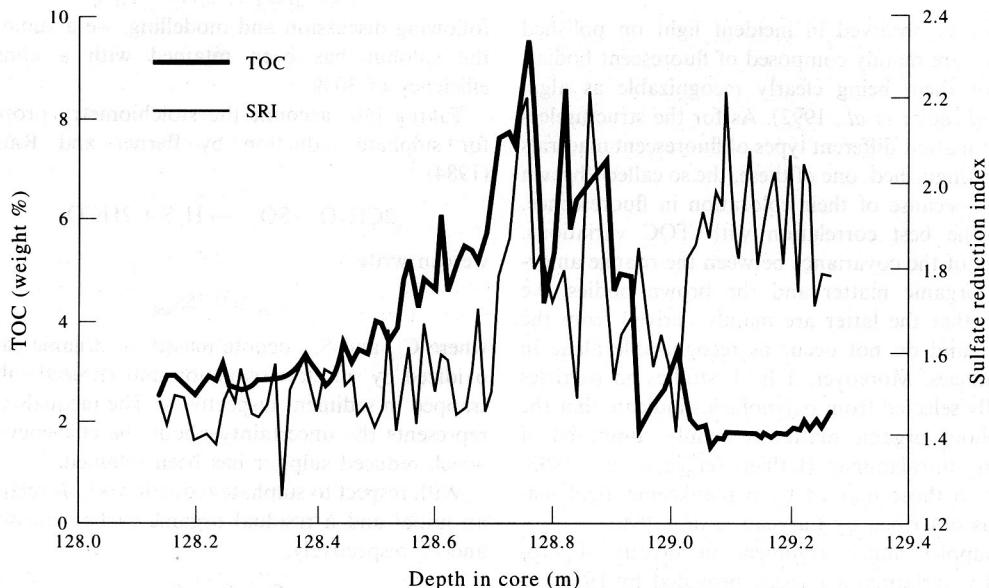


Fig. 2. Sulphate Reduction Index (SRI) and TOC profiles along the studied sequence.

DISCUSSION

As previously shown, the variations in redox conditions have been very weak during the cycle (Tribovillard *et al.*, 1992). Consequently, variations in sulphate reduction can be interpreted in terms of sulphate access or of changes in nature of organic matter supply more than in redox conditions (Bertrand and Lallier-Vergès, 1993).

Two arguments are in favour of a weakly restricted sulphate access for this cycle. The first one is the absence of bioturbation all along the sequence, which means that the redox boundary was maintained above the water-sediment interface. In such conditions, sulphate availability is only restricted by diffusion in water and not by porosity or permeability

of the sediment. The second argument is that the maximum of sulphate reduction occurred when the organic accumulation was at maximum because of high productivity-related inputs. In these conditions, the organic particles have been more rapidly buried so that access to sulphate could have been more restricted than during the other periods. If the nature of organic matter supply did not change, the result should be a weaker sulphate reduction which is opposed to the observed facts. This means that metabolizable organic matter is rapidly degraded by sulphate reduction at or above the water-sediment interface and that the sulphate availability is not restricted. Therefore, the sulphate access should have a small influence on sulphate reduction in comparison to variations in the nature of organic matter supply.

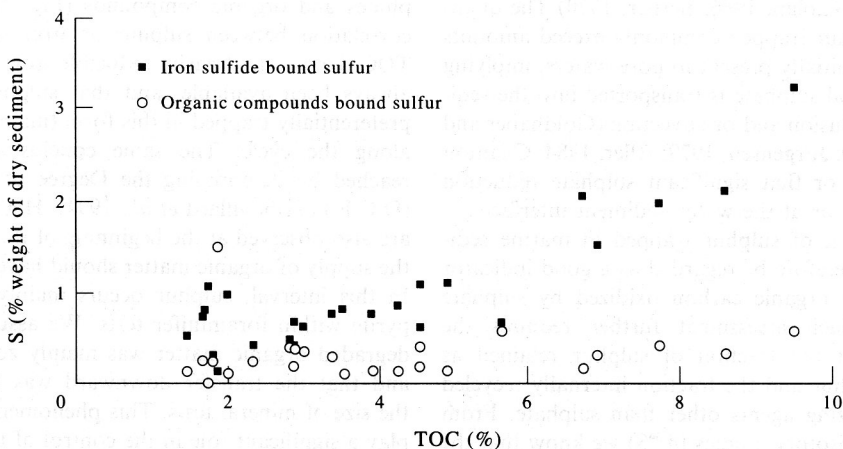


Fig. 3. Concentrations of the main sulphur forms calculated from elemental analysis of HF-HCl resistant fraction (organic matter and sulphides).

Supply of organic matter consists of both refractory and metabolizable organic flux. The metabolizable flux is reflected by the sulphate reduction indices (mainly pyrite), while refractory material can be observed through different petrographic investigations. The refractory character can be biologically inherited as for exins, cuticles, and other protective membranes, or it is acquired through an aerobic degradation which leads to carbonaceous residue such as inertinite. These occurrences of refractory material are easily recognizable in optical microscopy. Another type of refractory material has recently been described by transmitted electron microscopy studies (Raynaud *et al.*, 1990; Largeau *et al.*, 1990). It consists of ultralaminar biological structures (algal or bacterial membranes) which are usually counted as structureless organic matter in palynofacies studies. All these types were recognized in our palynofacies samples (Ramanampisoa *et al.*, 1992; Lallier-Vergès *et al.*, 1994) as well as strictly structureless material (i.e. even in T.E.M. observations). This kind of gelified material is also considered to be refractory as the samples were severely treated by acids for organic matter isolation. Most of the metabolizable part, which is hydrolysable, is therefore probably released during this treatment. The gelified refractory material could result from the incomplete metabolization of individual molecules, i.e. not engaged in biological organs such as membranes, but having parts able to resist the biodegradation.

Changes in sulphate reduction intensity are thought to be mainly due to variations of the planktonic fluxes because the land plant debris is a minor proportion and exhibits only small variations relatively to sulphate reduction intensity. Results on present marine productivity and export (Berger *et al.*, 1989; Betzer *et al.*, 1984) indicate that the export efficiency increases as the marine productivity increases because of lower recycling in the photic zone. Variability in primary production due to varying nutrient injection involves a lack of co-adapted autotrophs, heterotrophs and decomposers. Nutrient injection, which is largely determined by wind stress subject to seasonal, interannual or long-term climatic changes, stimulates rapid growth of autotrophs which will bloom, not being grazed sufficiently to prevent exponential increase. As a consequence, the new productivity, i.e. the part of productivity which escapes the recycling in the photic zone and which therefore can be exported out, is concentrated in organic matter from autotroph species and is enriched in metabolizable organic matter. In addition, the export of metabolizable organic matter is favoured by aggregate formation which is more important during high productivity periods (Wefer, 1989). With regard to our study, such a mechanism would reduce the transit time of metabolizable organic matter down to the sediment and the aggregates themselves might serve as micro-environments for early anoxic degradation.

A NUMERICAL SIMULATION

The previous interpretations can be mathematically modelled. In turn, the modelled values can be compared to the measured ones as a supplementary argument in favour of the validity of interpretations. In addition, the model provides new ways for reconstructing the palaeoproductivities in such environments.

The proposed model, which is a mass balance model, simulates a sediment composition from initial fluxes at the redox interface (Fig. 4). The redox interface should not be considered as a stratigraphic concept because anoxic micro-environments might exist within particles in the photic zone or in the oxic water column. For this reason, the anoxic domain is called "anaerosphere". The particulate fluxes reaching the redox interface can be mineral and organic fluxes from both planktonic productivity and detrital inputs.

According to analytical results, the model assumes that the primary factor of the cyclicity is phytoplanktonic productivity variations. These variations are imposed into the model by a flux of refractory organic matter which is considered to be a linear function of the productivity, assuming that the proportion of the refractory material in the living biomass is nearly constant when the productivity changes.

The metabolizable organic matter flux is calculated as a function of the refractory organic matter flux in such a way that the metabolizable to refractory ratio increases as the productivity increases, as indicated in Fig. 5. When the productivity is still moderate (1–5% TOC), the organic flux to the redox interface is mainly composed of refractory organic matter because the metabolizable material is highly degraded in the photic zone and thus, the refractory flux increases more rapidly than the metabolizable one as the productivity increases. This can be expressed by the following mathematical expression which is a combination between a linear term and an exponential term:

$$F_m = k_1 + (k_2 \cdot Fr) \cdot \exp(-k_3/Fr) \quad (\text{Fig. 5})$$

where

- F_m is the total metabolizable organic matter flux (from plankton) to the redox interface, with a CH_2O mean stoichiometry (Berner and Raiswell, 1984); Fr is considered as a linear function of productivity,
- Fr is the planktonic refractory organic matter flux, with a $\text{CH}_{1.5}\text{O}_{0.05}$ mean stoichiometry (type I kerogen, Durand and Monin, 1980), i.e. a mean carbon content of 84%,
- k_1 is the metabolizable organic matter flux reaching the anoxic domain even under low and moderate productivity conditions; as previously mentioned, this flux could be related to the sinking of zooplankton such as foraminifers; as

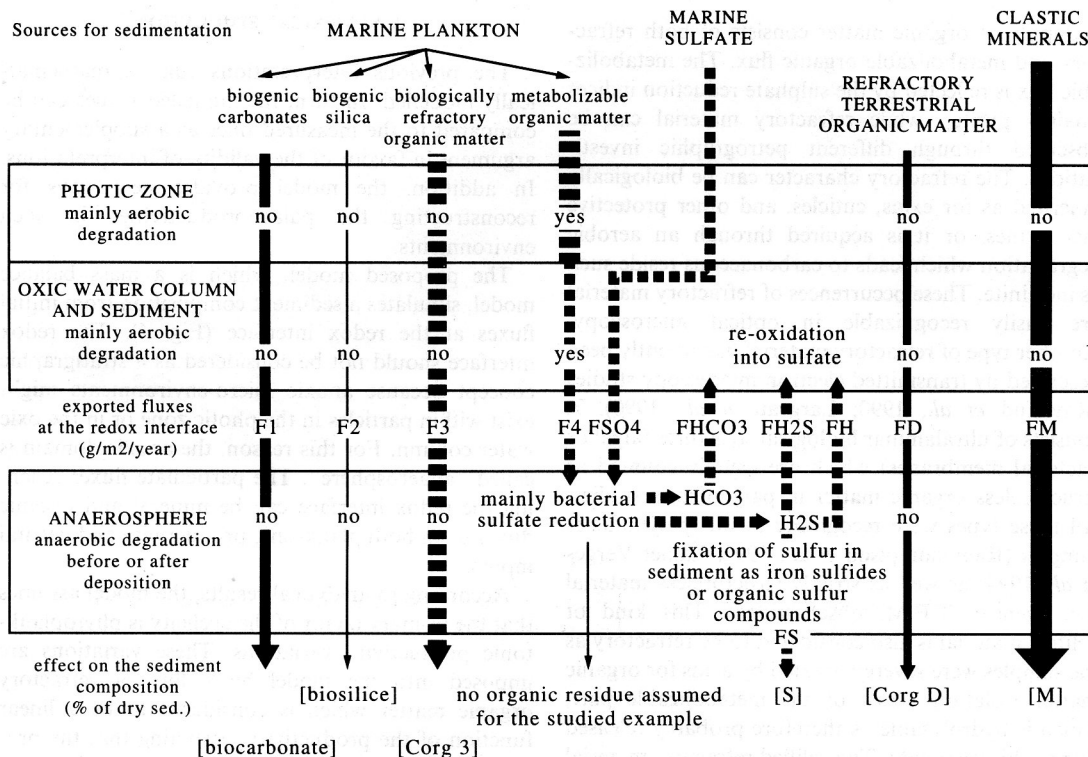


Fig. 4. Basic scheme for the mass balance model.

a simplification, this minor flux is considered to be constant,

- k₂ is the maximum metabolizable to refractory planktonic flux ratio obtained when the export productivity is maximum, and probably linked to the metabolizable to refractory ratio in the living phytoplanktonic biomass
- k₃ is a coefficient which presumably character-

izes the recycling efficiency of the organic matter in the photic zone; this coefficient is considered to be constant for the studied example.

When the productivity is low, both the linear and exponential terms tend to zero, expressing the fact that most of the metabolizable organic matter is aerobically recycled within the photic zone, except

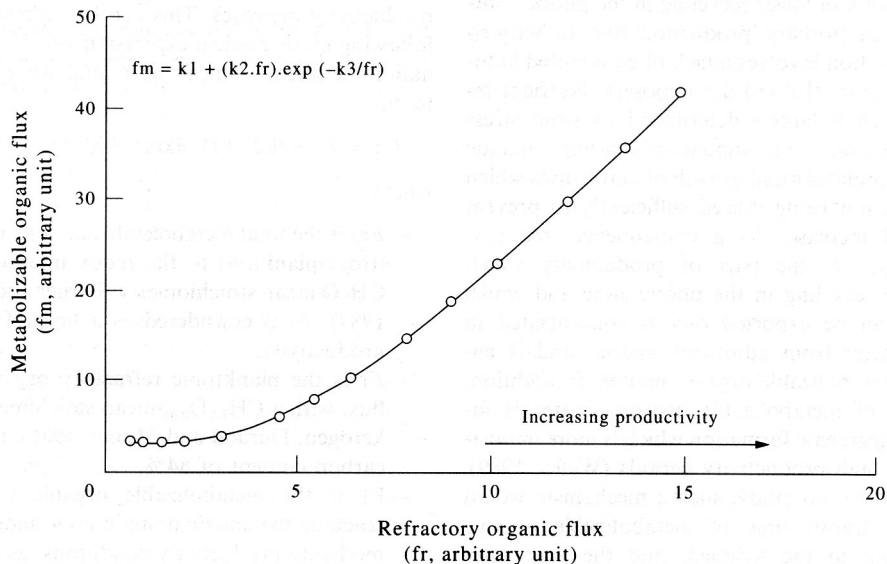


Fig. 5. The modelled relationship between the metabolizable and refractory organic matter flux from phytoplanktonic productivity to the redox interface (after Bertrand and Lallier-Vergès, 1993).

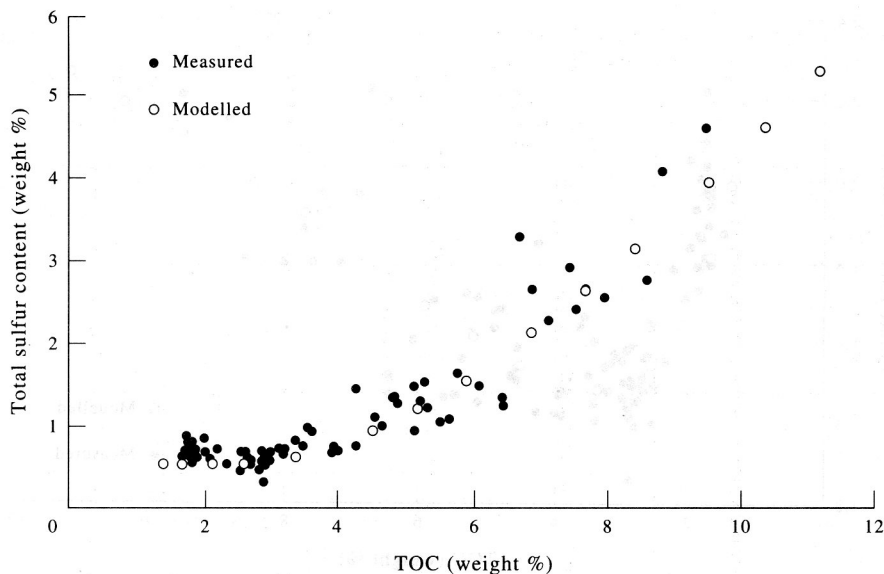


Fig. 6. Total sulphur content vs TOC for both the measured and modelled data (after Bertrand and Lallier-Vergès, 1993).

the k_1 flux to anoxic microenvironments which is anaerobically degraded. When the productivity is high, the exponential term increases so that the export metabolizable flux tends to a linear function of the productivity. The latter situation corresponds to a maximum export efficiency which is probably different for different areas (latitude, water depth, type of productivity).

The variations in detrital organic and mineral fluxes and of the biogenic mineral fluxes are assumed to be negligible relative to the organic flux variations from planktonic productivity. These invariant fluxes are each adjusted relative to the others in such a way that they give a correction simulation of the sediment composition when productivity is lowest. A mean carbon content of 85% has been attributed to the terrestrial refractory organic flux (Winans and Crelling, 1984), which is mainly composed of inertinite.

The model assumes that sulphate reduction is the dominant organic matter degradation process beyond the redox front, and that the metabolizable organic flux reaching this front is totally consumed by sulphate reduction (sulphate access being not restricted). This basic principle turns our model into a selective preservation pathway model, where the balance between oxic and anoxic degradation is primarily controlled by the phytoplanktonic productivity and associated recycling in the photic zone.

The downward and upward dissolved fluxes, which are induced by diagenetic processes, are numerically controlled by F_m according to the sulphate reduction stoichiometry and the boundary hypothesis that 70% of H_2S released by sulphate reduction escapes the sediment. An upward hydrogen flux is necessary to

respect mass balance. This flux probably combines with HCO_3^- flux to give water and carbon dioxide.

As shown on Figs 6 to 8, the modelling results can be adjusted to the measured ones by giving characteristic values for the k_1 , k_2 and k_3 constants. The relationship between TOC and sulphur content (Fig. 6) can be regarded as a reflection of the relative variations of the metabolizable flux and the refractory flux. The TOC is mainly controlled by the flux of refractory organic matter, while the sulphur content is mainly controlled by the flux of metabolizable organic matter to the redox interface. The relationship between sulphate reduction index and TOC (Fig. 7) derives from that between S and TOC. When TOC is high, the sulphate reduction intensity relative to the organic flux is also high because of an enhanced export efficiency of metabolizable organic matter from planktonic productivity. When productivity is lowest (in the cycle), the sulphate reduction intensity is high presumably because of a higher relative influence of early sulphate reduction due to rapid sinking of metabolizable organic matter within particles of dead zooplankton such as foraminifera. By using specific hydrogen index values for the refractory organic fraction, it is also possible to simulate the relationship between hydrogen index and TOC (Fig. 8). The shape of the curve results from the dilution of the inertinite flux by the increasing phytoplanktonic refractory flux. The slight decrease in the measured hydrogen index for high TOC could indicate that sulphate reduction results in minor formation of carbonaceous residue with low hydrogen index. This hypothesis can also be satisfactorily simulated by introducing a residual carbon flux proportional to the metabolized carbon flux.

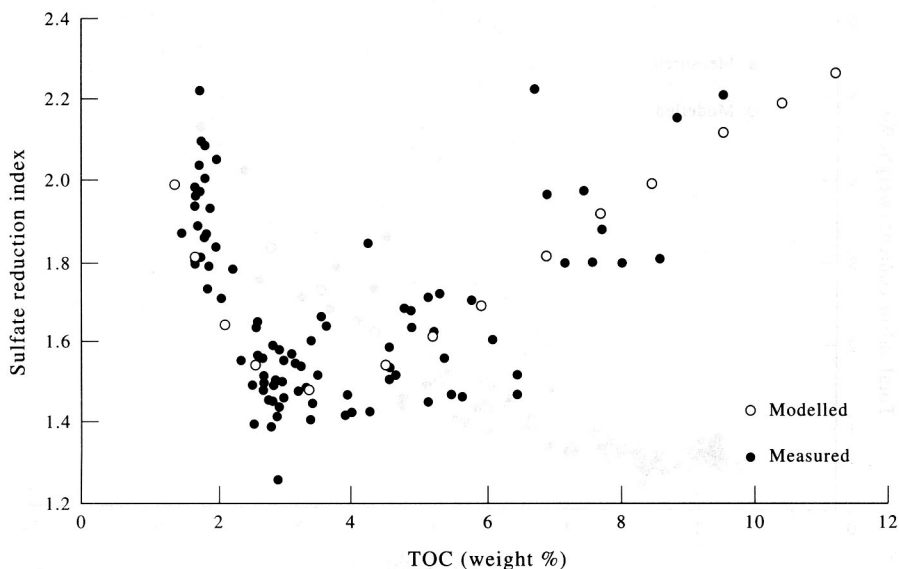


Fig. 7. Sulphate Reduction Index vs TOC for both measured and modelled data (after Bertrand and Lallier-Vergès, 1993).

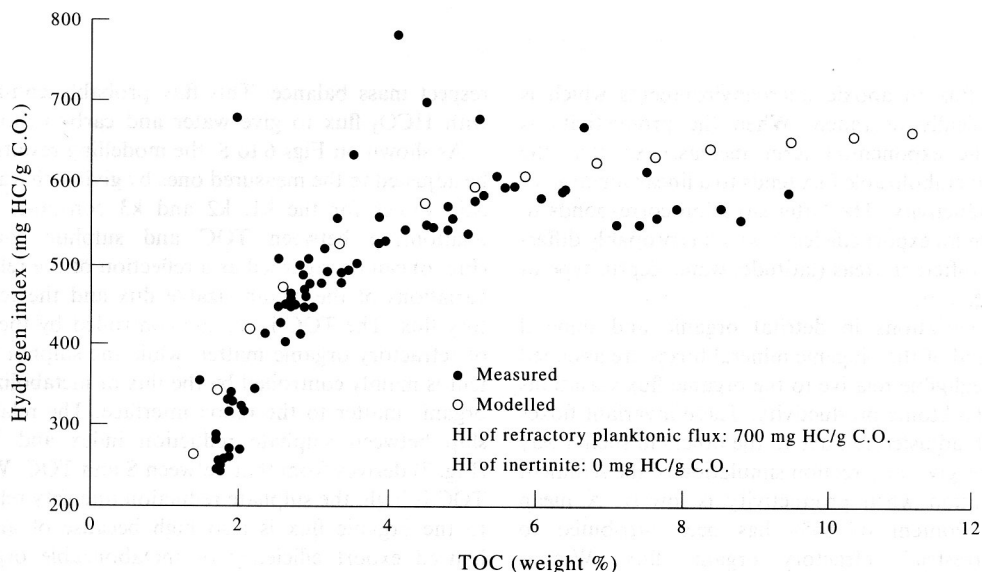


Fig. 8. Hydrogen Index vs TOC for both measured and modelled data.

CONCLUSIONS

As the proposed model is able to numerically simulate the evolution of the most important geochemical parameters with respect to the observed cyclicity (TOC, S, HI) the following conclusions can be considered as realistic.

(1) Cyclic variations of productivity together with selective preservation of refractory organic matter are able to explain the formation of cyclic organic-rich sedimentary series in margin and low energy environments, without marked changes in anoxia; such a conclusion is an agreement with the results of Calvert and Pedersen (1992) and Pedersen *et al.* (1992), who studied modern sediments.

(2) An increasing organic accumulation (of the refractory material) can combine with increasing diagenetic degradation (of the metabolizable material), and is thus not *a priori* a sign of an enhanced preservation of the organic matter flux, even in the absence of dilution effects.

In addition, the model leads to new ways of relating the organic carbon content of marine sediments to palaeoproductivity variations throughout glacial-interglacial successions.

Acknowledgements—This work was performed in the collaborative research group GdR 942 “Relations et Processus Organo-Minéraux en Environnements Sédimentaires” (CNRS, IFP, CFP Total, Elf Aquitaine, URA 724 de

l'Université d'Orléans et URA 723 de l'Université de Paris Sud). We are indebted to all participants of this group for their scientific, analytical and financial support. We thank also Dr Throndsen and a second anonymous reviewer for their constructive comments and suggestions.

REFERENCES

- Aller R. C. (1984) The importance of relict burrow structures and burrow irrigation in controlling solute distributions. *Geochim. Cosmochim. Acta* **48**, 1929–1934.
- Berger W. H., Smetacek V. S. and Wefer G. (1989) *Report of the Dahlem Workshop on Productivity of the Oceans: Present and Past*, 471 p. Wiley, Berlin.
- Berner R. A. (1970) Sedimentary pyrite formation. *Am. J. Sci.* **268**, 1–23.
- Berner R. A. and Raiswell R. (1984) Burial of organic carbon and pyrite sulfur in sediments over Phanerozoic time: a new theory. *Geochim. Cosmochim. Acta* **47**, 855–862.
- Bertrand P. and Lallier-Vergès E. (1993) Past sedimentary organic matter accumulation and degradation controlled by productivity. *Nature* **364**, 786–788.
- Betzler P.R., Showers W. J., Laws E. A., Winn C. D., DiTullio G. R. and Kroopnick P.M. (1984) Primary productivity and particles fluxes on a transect of the equator at 135°W in the Pacific Ocean. *Deep-Sea Res.* **31**, 1–11.
- Blanc-Valleron M. M., Gely J. P., Schuler M., Dany F. and Ansart M. (1991) La matière organique associée aux évaporites de la base du Sel IV (Oligocène inférieur) du bassin de Mulhouse (Alsace, France). *Bull. Soc. Géol. Fr.* **162**, 113–122.
- Calvert S. E. and Pedersen T. F. (1992) Organic carbon accumulation and preservation in marine sediments: how important is anoxia? In *Organic Matter: Productivity, Accumulation, and Preservation in Recent and Ancient Sediments* (Edited by Whelan J. and Farrington J. W.), pp. 231–263. Columbia University Press, U.S.A.
- Chanton J. P., Martens C. S. and Goldhaber M. B. (1987) Biogeochemical cycling in a organic-rich coastal marine basin. 7. Sulfur mass balance, oxygen uptake and sulphide retention. *Geochim. Cosmochim. Acta* **51**, 1187–1199.
- Crumières J. P., Crumières-Ayraud C., Espitalié J. and Cotillon P. (1990) Global and regional controls on potential source-rock deposition and preservation: the Cenomanian–Turonian Oceanic Anoxic Event (CTOAE) on the European Thethyan margin (southeastern France). In: *Deposition of Organic Facies: AAPG Studies in Geology* (Edited by Huc A.), vol. 30, pp. 107–118.
- Demaison G. J. and Moore G. T. (1980) Anoxic environments and oil source bed genesis. *AAPG Bull.* **64**, 1179–1209.
- Durand B. and Monin J. C. (1980). Elemental analysis of kerogens (C, H, O, N, S, Fe). In *Kerogen*, (Edited by Durand B.) pp. 113–142. Éd. Technip, Paris.
- Goldhaber M.B. and Kaplan I.R. (1980). Mechanisms of sulfur incorporation and isotope fractionation during early diagenesis in sediments of the Gulf of California. *Marine Chem.* **9**, 95–143.
- de Graciansky P.-C., Deroo G., Herbin J.-P., Montadert L., Müller C., Shaaf A. and Sigal J. (1984) Ocean-wide stagnation episode in the late Cretaceous. *Nature* **308**, 346–349.
- Herbin J. P., Masure E. and Roucaché J. (1987) Cretaceous formations from the lower continental rise off cape Hatteras: organic geochemistry, dinoflagellate cysts, and the Cenomanian/Turonian boundary event at Sites 603 (Leg 93) and 605 (Leg 11). *Init. Repts. Deep Sea Drill. Prof.* **XCII**, 1139–1162
- Herbin J. P., Müller C., Geysant J. R., Mélières F. and Penn I. E. (1991) Hétérogénéité quantitative et qualitative de la matière organique dans les argiles du Val de Pickering (Yorkshire, U.K.): cadre sédimentologique et stratigraphique. *Rev. Inst. Franç. Pétr.* **46**, 675–712.
- Holser W. T. and Kaplan I. R. (1966) Isotope geochemistry of sedimentary sulphates. *Chem. Geol.* **1**, 93–135.
- Jørgensen B. B. (1979) A theoretical model of the stable sulfur isotope distribution in marine sediments. *Geochim. Cosmochim. Acta.* **43**, 363–374.
- Lallier-Vergès E., Bertrand P. and Desprairies A. (1993) Organic matter composition and sulfate reduction intensity in Oman Margin sediments. *Marine Geol.* **112**, 57–69.
- Lallier-Vergès E., Boussafir M., Bertrand P. and Badaut-Trauth D. (1994) Selective preservation of various organic matters as assessed by STEM studies on a cyclic productivity-controlled sedimentary series (Kimmeridge Clay Formation, U.K.) Extended abstract at the *International Meeting on Organic Geochemistry*, Stavanger, September 1993 (Edited by K. Øygard), pp. 384–388.
- Largeau C., Derenne S., Casadevall E., Berkaloff C., Corolleur M., Lugardon B., Raynaud J. F. and Connan J. (1990) Occurrence and origin of “ultralaminar” structures in “amorphous” kerogens of various source rocks and oil shales. In *Advances in Organic Geochemistry 1989* (Edited by Durand B. and Behar F.), pp. 889–895. Pergamon Press, Oxford, U.K.
- Lyle M. (1988) Climatically forced organic carbon burial in equatorial Atlantic and Pacific Oceans. *Nature* **335**, 529–532.
- Miller R. G. (1990) A palaeoceanographic approach to the Kimmeridge Clay Formation. In *Deposition of Organic Facies, AAPG Studies in Geology* (Edited by Huc A.) vol. 30, pp. 13–26.
- Myers K. J. and Wignall P. B. (1987) Understanding Jurassic organic-rich mudrocks? New concepts using gamma-ray spectrometry and palaeoecology: examples from the Kimmeridge Clay of Dorset and the Jet Rock of Yorkshire. In *Marine Clastic Sedimentology* (Edited by Leggett J. K. and Zuffa G. G.) pp. 172–189. Graham & Trotman, London.
- Oschmann W. (1988) Kimmeridge clay sedimentation—a new cyclic model. *Palaeogeogr. Paleoclimatol. Palaeoecol.* **65**, 217–251.
- Pedersen T. F., Shimmield G. B. and Price N. B. (1992) Lack of enhanced preservation of organic matter in sediments under the oxygen minimum on the Oman margin. *Geochim. Cosmochim. Acta* **56**, 545–551.
- Pradier B., Ramanampisoa L. and Bertrand P. (1992) Etude à haute résolution d'un cycle de carbone organique des argiles du Kimméridgien du Yorkshire (Grande Bretagne): relation entre composition pétrographique du contenu organique observé in situ, teneur en carbone organique et qualité pétrologène. *C. R. Acad. Sci. Paris Serie II*, **315** 187–192.
- Prell W. L., Niitsuma N. and shipboard scientific party (1989) *Proc. ODP, Init. Repts.*, vol. 117. College Station, Texas.
- Ramanampisoa L., Bertrand P., Disnar J. R., Lallier-Vergès E., Pradier B. and Tribouillard N. P. (1992) Etude à haute résolution d'un cycle de carbone organique des argiles du Kimméridgien du Yorkshire (Grande Bretagne): résultats préliminaires de géochimie et de pétrographie organique. *C. R. Acad. Sci., Paris, Serie II*, **314**, 1493–1498.
- Raynaud J.-F., Lugardon B. and Lacrampe-Couloume G. (1990) Lamellar structures and bacteria as main components of the amorphous organic matter of source rocks. *Bull. Centre Rech. Expl.-Prod. Elf-Aquitaine, Pau* **13**, 1–21.
- Scotchman I. C. (1987) Diagenesis of the Kimmeridge Clay, onshore U.K. *J. Geol. Soc. London*, **146**, 285–303.
- Thode-Andersen S. and Jørgensen B. B. (1989). Sulphate reduction and the formation of ³⁵S-labeled FeS, FeS₂, and S in coastal marine sediments. *Limnol Oceanogr.* **34**, 793–806.

- Tribovillard N., Desprairies A., Bertrand P., Lallier-Vergès E., Disnar J. R. and Pradier B. (1992) Etude à haute résolution d'un cycle du carbone organique de roches kimméridgiennes du Yorkshire (Grande-Bretagne): minéralogie et géochimie (résultats préliminaires). *C. R. Acad. Sci., Paris* **1**, 314, *Série II*, 923–930.
- Tribovillard N., Desprairies A., Lallier-Vergès E., Bertrand P., Moureau N., Ramdani A., Ramanampisoa L. (1994) Geochemical study of organic-rich cycles from the Kimmeridge Clay Formation of Yorkshire (G.B.): productivity versus anoxia. *Palaeogeogr. Palaeoclim. Palaeoecol.* **108**, 165–181.
- Wefer G. (1989) Particle flux in the oceans: effects of episodic production. In *Report of the Dahlem Workshop on productivity of the oceans: present and past*, Berlin 1988 (Edited by Berger W. H., Smetacek V. S. and Wefer G.), pp. 139–154, Wiley, New York.
- Wefer G., Heinze P. and Suess E. (1990) Stratigraphy and sedimentation rates from oxygen isotope composition, organic carbon content, and grain-size distribution at the Peru upwelling region: Holes 680B and 686B. In *Proc. ODP, Scientific Results* (Edited by Suess E., von Huene R. *et al.*), Vol. 112, 355–367.
- Wignall P. B. (1989) Sedimentary dynamics of the Kimmeridge Clay: tempests and earthquakes. *J. Geol. Soc. London* **146**, 273–284.
- Winans R. E. and Crelling J. C. (1984) *Chemistry and Characterization of Coal Macerals* (Edited by Winans R. E. and Crelling J. C.), ACS symposium series 252, 184 p.

Structure ultrafine de la matière organique des roches mères du Kimméridgien du Yorkshire (UK)

par MOHAMMED BOUSSAFIR*¹, ELISABETH LALLIER-VERGÈS*¹,
PHILIPPE BERTRAND**¹ et DENISE BADAUT-TRAUTH***¹

Mots clés. – Cycle de carbone organique, Kérogène, Matière organique amorphe, Ultrastructure, Sulfato-réduction.

Résumé. – La matière organique isolée des roches sédimentaires, après destruction de la matière minérale, et observée au microscope optique en lumière transmise (palynofaciès), montre l'existence d'un ensemble de matières organiques amorphes dominantes. Ce travail réalisé sur des échantillons provenant de la formation de la Kimmeridge Clay (Angleterre) propose :

- 1 – l'identification en microscopie électronique à transmission de ces matières organiques, après microprélèvement sous stéréomicroscope ;
- 2 – la distribution de ces ultrastructures dans la matière organique totale, replacée dans la logique des cyclicités organiques de cette formation.

La matière organique amorphe orangée du palynofaciès présente une structure interne nanoscopiquement amorphe parfaitement homogène. Elle se présente comme un gel, semblable en tous points aux lamines diffuses observées dans les coupes ultraminces de la matière organique totale. Témoin d'une productivité phytoplanctonique accrue, elle est accompagnée d'une sulfato-réduction intense. Elle est interprétée comme le résultat d'une gélification précoce de matière organique phytoplanctonique originelle.

La matière organique amorphe brune du palynofaciès présente en majorité des ultralaminae, interprétées comme les parties bio-résistantes d'organismes phytoplanctoniques dont la fraction métabolisable associée a été dégradée en partie avant le dépôt.

La matière organique amorphe noire du palynofaciès contient une grande diversité d'ultrastructures dans lesquelles dominent les débris ligneux auxquels sont associés des matières organiques de diverses origines. Les empreintes de coccolithes, de quartz et d'argiles qui lui sont associées témoignent d'une étroite association avec la fraction minérale et suggèrent que cette matière organique constitue la fraction organique de la matrice organo-minérale de la roche.

The ultrafine structure of organic matter from Kimmeridgian source-rocks of Yorkshire (UK)

Key words. – Organic carbon cycle, Kerogen, Amorphous organic matter, Ultrastructure, Sulphate reduction.

Abstract. – Isolated organic material from sedimentary rocks, after destruction of minerals and observation under optical microscope in transmitted light (palynofaciès) shows the existence of various amorphous organic materials. This work deals with the identification of this organic material. Organic material microsampled with stereomicroscope is studied by transmission electron microscopy. Results are interpreted with respect to the sedimentology of the depositional cycle.

The orange amorphous organic matter exhibits an internal structure nanoscopically amorphous and perfectly homogeneous. It exists as a gelatinous form closely resembling the lamellar diffuse amorphous organic matter observed in the ultrathin sections of total organic material. As a proof of a phytoplanktonic productivity, it is accompanied by an intense sulphate reduction. It is interpreted as the result of an early gelification process of the original phytoplanktonic material.

The brown amorphous organic matter is mainly represented by ultralaminae, interpreted as the bio-resistant parts of planktonic organisms of which the metabolisable fraction was partly degraded before deposition.

The black amorphous organic matter contains a large diversity of ultra-structures dominated by lignaceous debris. This amorphous organic matter, contains organic materials of diverse origin including imprints from coccoliths, quartz and clays. The close association with the mineral fraction would suggest that this material constitutes the organic fraction of the organo-mineral groundmass of the original rock.

Abridged English version

The organic matter is incorporated in the sediment after more or less important bacterial degradation. The two principal processes of organic matter preservation are the formation of geopolymers by degradation and polycondensation, and the selective preservation of bioresistant structures or resistant macromolecules.

This work is essentially based on ultrastructural study of isolated organic matter. It forms part of a larger scientific framework concerning the pre- and syn-diagenetic history of organic matter in short-term sedimentary cyclicity of the Kimmeridgian clays of Yorkshire. For this, an organic carbon cycle (approximately 1,20 m) was sampled from Marton 87 cores (fig. 1 & 2) and a multidisciplinary study was completed on these samples. This cyclicity essentially represents a variation in the quantity of organic matter "TOC varying from 1,8 to 9,5%" associated with a variation in the geochemical quality "HI varying from 200 to 800 mg HC/g C-org" [Ramanampisoa *et al.*, 1992] and petrographical quality [Pradier and Bertrand, 1992; Ramanampisoa *et al.*, 1992].

Optical analysis of the palynofaciès allowed identification, in addition to the constituents derived from the terrestrial biomass and zooplankton, of three principal types of amorphous organic matter (AOM) classed depending on their colour and texture : orange AOM (pl. Ia), brown AOM (pl. Ic) and black AOM (pl. 1e). Quantification of the palynofaciès throughout the cycle illustrates the existence of a strong correspondence between the variations in HI and those of the orange AOM throughout the microcycle (fig. 3).

* URA 724 du CNRS, Université d'Orléans, 45067 Orléans cedex.

** URA 197 du CNRS, Université Bordeaux 1, 33405 Talence cedex.

*** URA 723 du CNRS, Museum d'Histoire Naturelle de Paris, 53, rue Buffon, 75005 Paris.

1. GdR 942 du CNRS. Relations et Processus Organo-minéraux en Environnements Sédimentaires. (CNRS – Université d'Orléans – Université d'Orsay – CFP, Total – IFP – SNEAP).

Manuscrit déposé le 7 octobre 1993 ; accepté le 9 février 1994.

The concentration of each AOM was accomplished using a micromanipulator on the palynological preparation followed by preparation for observation under transmission electron microscope (TEM) [Boussafir *et al.*, 1994]. The results are the following :

(1) the orange AOM has a nanoscopically amorphous (perfectly homogeneous) texture without any apparent structures even at high TEM magnifications (pl. Ib);

(2) the brown AOM is mainly composed of laminar structures "ultralaminæ", more or less elongated and always with a regular thickness (50 to 400 nm) (pl. Id) which is generally greater than a cellular membrane (7,5 to 12 nm). These ultralaminar structures have already been observed by many researchers [Raynaud *et al.*, 1988; Largeau *et al.*, 1990; Derenne *et al.*, 1991; Lugardon *et al.*, 1991; Derenne *et al.*, 1993] who consistently quote the thickness of these ultralaminations as being smaller than 60 nm;

(3) the black AOM contains a large diversity of ultrastructurally different fragments dominated by the ligno-cellulosic debris (pl. If). Associated with these detritic inclusions, one finds some granular organic matter, some small particles of nanoscopically AOM (pl. 1f) and some ultralaminar structures.

In order to assess the distribution of the organic material observed under TEM throughout the carbon microcycle eight representative samples of the microcycle were chosen to study the ultrathin sections of their total organic matter (tab. 1, fig. 4). Observation of these samples allowed the identification of the previously described ultrastructures. Nevertheless, two categories of nanoscopically AOM have been characterized :

— firstly, large massive homogeneous areas with a strong electron contrast (pl. II-a). These zones, when compacted, form a homogeneous "gel" corresponding to the orange AOM. Within this nanoscopically AOM, one distinguishes some anastomosed zones with discontinuous linear structures, the diffuse laminations (pl. II-b). One also finds in these zones some pyrite in diverse assemblages (pl. II-g & h) as well as some detritic debris (pl. II-c);

— secondly, regions of AOM, less homogeneous and with a weaker electron contrast than the previous category, with a speckled aspect (more or less granular) and without any particular form (pl. II-d).

The semi-quantification of the observed ultrastructures form four large groups (fig. 5) and show that the samples at the centre of cycle, with the highest TOC, are also those which have the greatest proportion of pyrite and AOM. However, the samples from the beginning and the end of the cycle are weak in pyrite and AOM, but have abundant ultralaminæ.

Electron microscope studies have shown that the nanoscopically AOM, represented by the orange AOM in palynofacies, is dominant in the levels richest in organic carbon. This organic matter originates from the gelification of the remains of phytoplanktonic organic matter which is deposited in the form of algal mats and which forms large surfaces parallel to the stratification. The ultrastructural studies of the total organic matter have underlined the role that sulphate reduction, which is more intense in the middle of the cycle than at the beginning or the end, has played in the generation of orange AOM.

These results confirm the hypothesis that the cyclicity of the organic carbon in the Kimmeridgian is mainly due to variations in the biological productivity.

The accumulation of the bio-resistant organic matter (ultralaminæ, lignaceous debris) responded to a weaker phytoplanktonic exportation (beginning and end of the cycle) and to a selective preservation of bio-macromolecules already existing in the living organisms.

The parallel increase in the TOC and HI of an AOM rich in pyrite and organic sulphur was in response to a greater exportation from the photic zone (strong phytoplanktonic production) of metabolizable organic matter favouring the sulphate-reduction.

As the sulphate-reduction was not limited [Tribouillard *et al.*, 1994], the nanoscopically particular or diffuse AOM should represent the resistant fraction which is formed mainly by lipides. This should explain its high hydrocarbon potential.

I. – INTRODUCTION

Les organismes qui sont à l'origine de la matière organique des roches sédimentaires sont de nature et de compositions diverses. La matière organique est incorporée dans les sédiments après avoir subi une dégradation bactérienne plus ou moins intense faisant intervenir différents processus dont les deux principaux actuellement reconnus sont la formation de géopolymères par dégradation suivie de polycondensation et la préservation sélective de structures biologiquement résistantes ou de macromolécules résistantes.

Cette matière organique fossile, lorsqu'elle est isolée de la roche après destruction de la matrice minérale par attaques acides, peut être observée au microscope optique en lumière transmise (palynofaciès). Elle se présente alors sous deux grands ensembles de composants palynologiques [Combaz, 1980] :

— un ensemble de matières organiques amorphes (MOA) qui regroupe différentes particules organiques biologiquement indéfinies,

— un ensemble de particules structurées, encore appelées éléments figurés, qui regroupe les débris végétaux terrestres, les microfossiles marins ainsi que quelques rares vestiges animaux.

Dans cet article, le terme amorphe est utilisé pour décrire toute matière organique qui ne montre aucune structure en microscopie optique.

Majoritaires dans la plupart des kérogènes, les matières organiques amorphes représentent parfois la quasi totalité de la matière organique des roches-mères [Combaz, 1980]. Leur observation pétrographique se trouve toutefois limitée par le faible pouvoir de résolution du microscope photonique par rapport à la taille des particules. La mise en œuvre d'une nouvelle méthodologie et d'outils plus performants (microscope électronique à transmission ou MET d'un pouvoir de résolution d'environ 500 fois plus important que celui de la microscopie optique) est devenue indispensable à une meilleure connaissance de ces constituants organiques et plus particulièrement de leurs processus de préservation.

Les premiers travaux consacrés à l'ultrastructure des kérogènes datent de 1988 [Raynaud *et al.*]. Ces auteurs ont travaillé sur une sélection d'une quarantaine d'échantillons de roches mères et ont mis en évidence un certain nombre d'ultrastructures dans lesquelles dominaient des structures dites « membranaires ». Des « membranes » fossiles et des structures tubulaires avaient été observées auparavant par Degens *et al.* [1970] dans des sédiments holocènes de la

HDR M. Boussafir, juin 2008, pages 158

mer Noire. Mais ces auteurs ne proposaient pas d'explication sur l'origine des « membranes » et ils attribuaient les structures tubulaires à des réarrangements de fragments membranaires de cellules eucaryotiques non identifiées, sous l'influence de fluctuations de l'environnement ionique dans le milieu de dépôt.

D'autres auteurs ont examiné la composition et l'origine de ces « membranes », appelées « ultralaminae » [Largeau *et al.*, 1990b; Derenne *et al.*, 1991, 1992 a, b, c, 1993]. Sur la base d'études moléculaires, ces auteurs ont montré que les ultralaminae correspondaient à de fines parois externes de micro-algues. Des expériences d'hydrolyse en milieu acide sur des cultures de diverses micro-algues, ont permis d'en isoler un résidu. Ce dernier observé par microscopie électronique a montré des structures ultralaminaires similaires à celles observées par Raynaud *et al.* [1988] et Lugaardon *et al.* [1991] dans la matière organique isolée de roches mères. Ces études avaient pour objectif essentiel la connaissance de la composition du kérogène.

Le présent travail propose des résultats complémentaires à partir d'une démarche doublement originale.

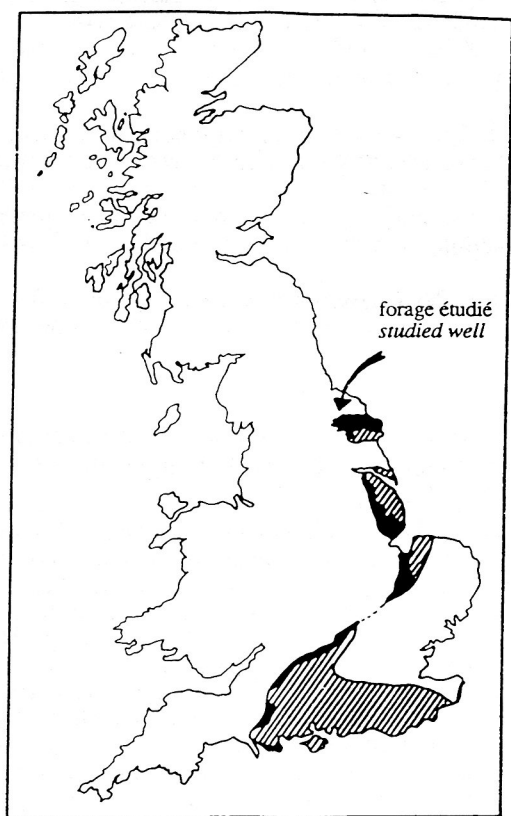
La première, essentiellement analytique, permet de s'affranchir du doute de la représentativité des études MET par rapport aux études optiques. Pour cela, nous avons mis au point une technique de prélèvement par micro-manipulateur sous stéréomicroscope permettant de prélever avec précision les différentes particules de matière organique amorphe

dans le résidu palynologique de roches-mères [Boussafir *et al.*, 1994].

La seconde permet d'inscrire ces recherches dans un cadre scientifique plus large qui concerne la préservation de la matière organique dans les cyclicités sédimentaires à court-terme. Pour cela, des échantillons ont été sélectionnés le long d'un cycle de carbone organique (forage Marton, Kimméridgien du Yorkshire, Grande Bretagne) pour examiner la variation de leur état de préservation, en relation avec la variation quantitative du carbone.

II. - ECHANTILLONS ET MÉTHODES D'ÉTUDE

Les échantillons proviennent des argiles noires du Kimméridgien du Yorkshire, considérées comme l'équivalent latéral de l'unité de roche-mère qui fournit l'essentiel des hydrocarbures de la mer du Nord. Elles sont généralement constituées d'alternances d'argilites noires riches en matière organique et de marnes avec quelques lentilles calcaires coccolithiques. Dix zones d'ammonites ont été distinguées dans le Kimméridgien du Yorkshire [Herbin *et al.*, 1991]. Un cycle de carbone organique d'une puissance de 1,20 m, situé dans la zone à Eudoxus, soit environ 30 000 ans de sédimentation, a été prélevé sur la carotte du forage Marton 87 (fig. 1 et 2).



■ Kimmeridge Clay Formation à l'affleurement
Kimmeridge Clay Formation outcrops
▨ Kimmeridge Clay Formation dans le sous-sol
Kimmeridge Clay Formation subcrops

FIG. 1. - La formation des argiles du Kimméridgien à l'affleurement et dans le sous-sol en Grande-Bretagne; emplacement du forage étudié.

FIG. 1. - The Kimmeridge Clay Formation (outcrop and subcrop) and location of the studied well.

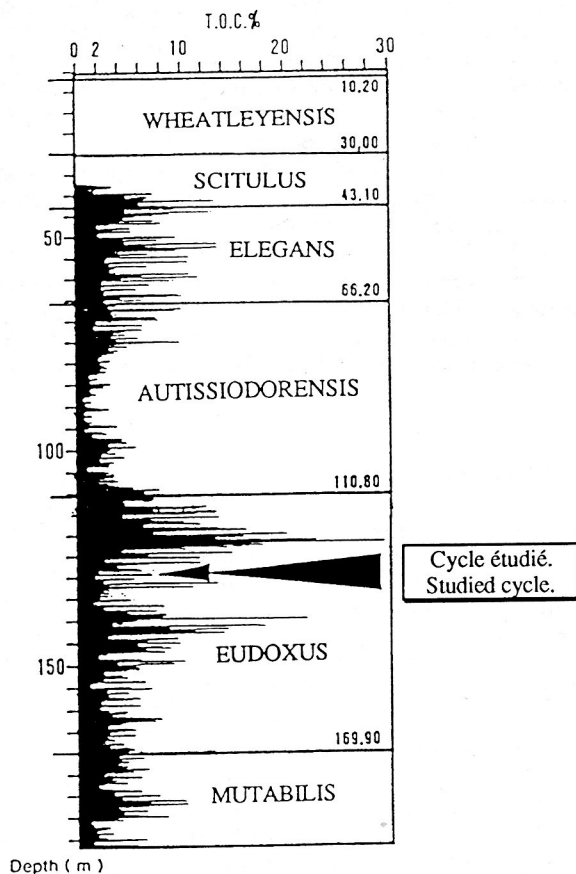


FIG. 2. - Evolution de la teneur en carbone organique total le long du puits Marton 87 et localisation du cycle étudié [d'après Herbin *et al.*, 1991].

FIG. 2. - Evolution of the total organic carbon in Marton-87 borehole and location of the studied cycle [after Herbin *et al.*, 1991].

Dans le but de rechercher les phénomènes à l'origine de cette cyclicité, une étude à haute résolution a été réalisée sur le cycle choisi [Pradier et Bertrand, 1992; Ramanampisoa *et al.*, 1992; Tribovillard *et al.*, 1992; Bertrand et Lallier-Vergès, 1993]. Cette cyclicité se traduit essentiellement par une variation de quantité de matière organique (carbone organique total ou COT variant de 1,7

à 9,5%), associée à une variation de la qualité géochimique (index d'hydrogène ou IH variant d'environ 250 à 800 mg HC/g C org) et pétrographique.

L'analyse optique des palynofaciès (matière organique totale isolée de la roche par attaques HCl-HF (MOT)) a révélé trois types principaux de matières organiques amorphes (MOA);

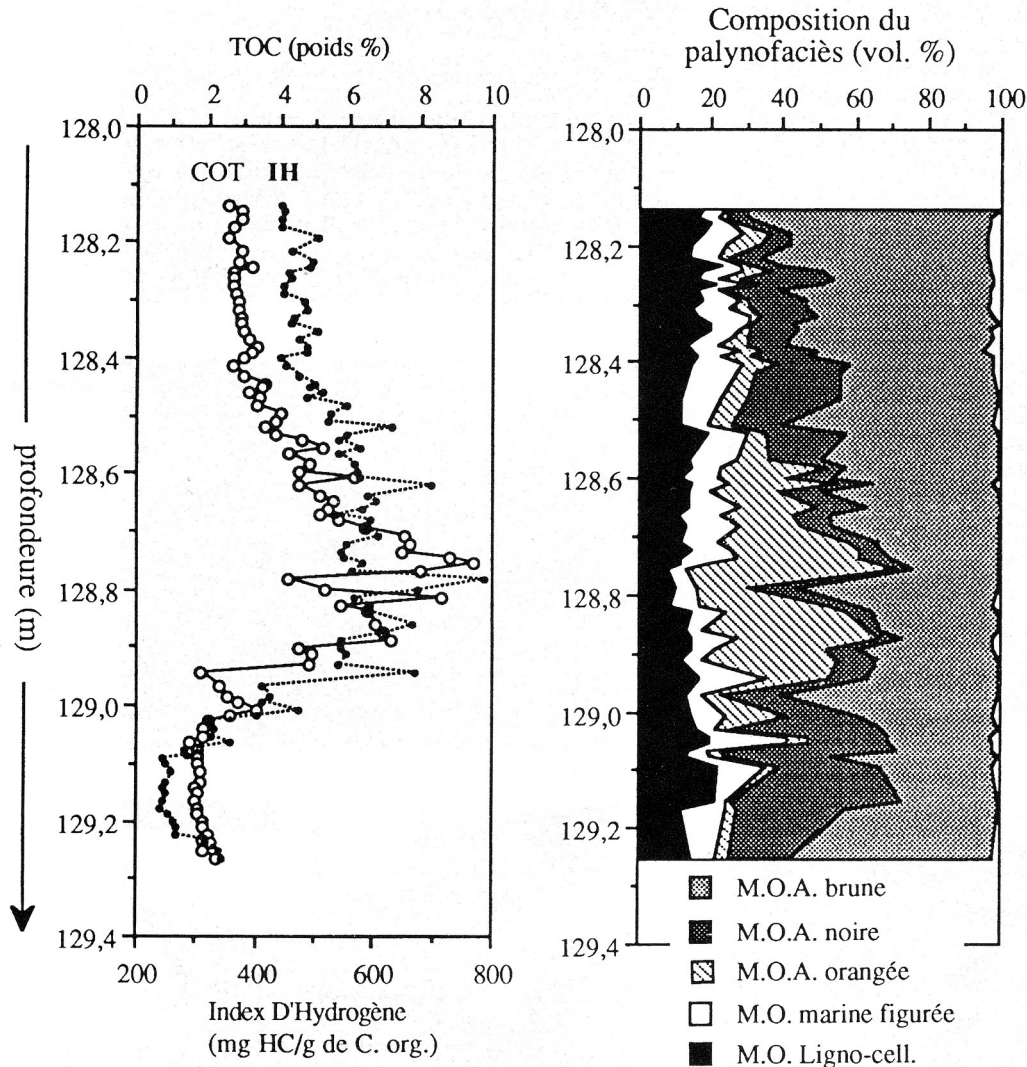


FIG. 3. - Variation de la composition du palynofaciès, du COT et de l'IH le long du microcycle étudié.

FIG. 3. - Variation of palynofaciès composition, TOC and HI in the studied microcycle.

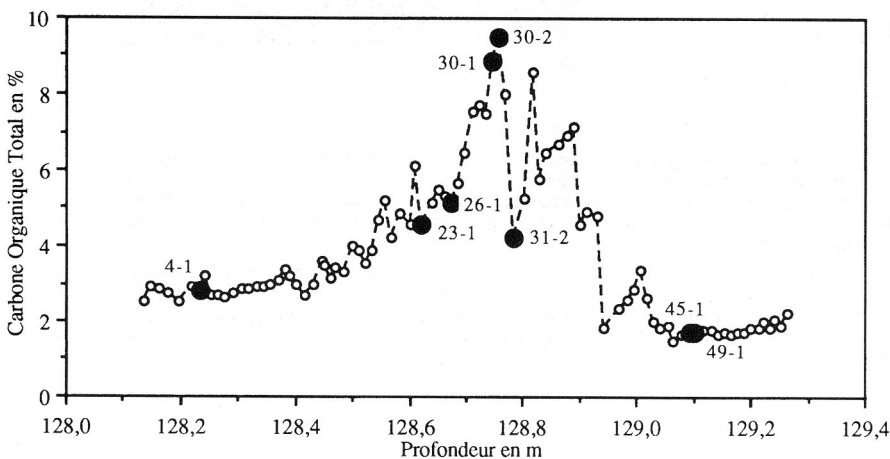
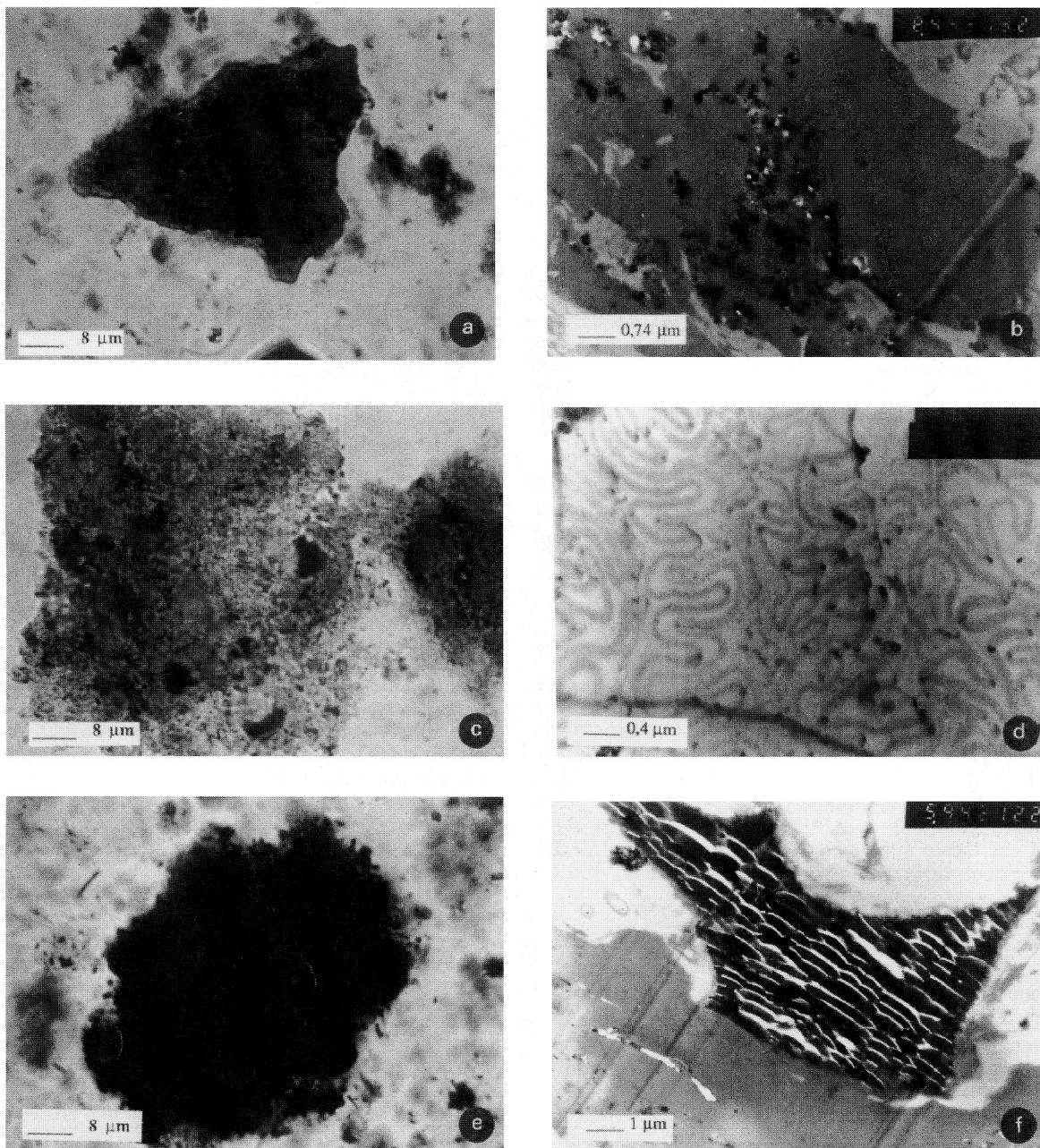


FIG. 4. - Localisation des huit échantillons étudiés sur le cycle du carbone organique total.

FIG. 4. - The location of the eight studied samples in the cycle of total organic carbon.



PL. I. – Ultrastructures des trois types de matières organiques amorphes microprélevées : (a) matière organique amorphe orangée observée en microscopie photonique ; (b) matière organique amorphe orangée observée au MET ; (c) matière organique amorphe brune observée en microscopie photonique ; (d) structures ultralaminaires de la matière organique amorphe brune observée au MET ; (e) matière organique amorphe noire observée en microscopie photonique ; (f) ultrastructure caractéristique de la matière organique amorphe observée au MET.

PL. I. – *Ultrastructures of the three types of the microsampled amorphous organic matter : (a) orange amorphous organic matter observed with light microscopy ; (b) orange amorphous organic matter of the palynofacies observed by TEM ; (c) brown amorphous organic matter observed by light microscopy ; (d) ultralamellar structures of brown amorphous organic matter observed by TEM ; (e) black amorphous organic matter observed by light microscopy ; (f) typical ultrastructures of black amorphous organic matter observed by TEM.*

— une MOA orangée avec des limites franches et une apparence gélifiée, se présentant sous la forme de plaquettes, au stéréomicroscope ;

— une MOA brune, généralement floconneuse avec des limites floues ;

— une MOA noire, à l'aspect gélifié ou floconneux.

La figure 3 résume les résultats de la quantification palynologique le long du cycle. On constate qu'une bonne correspondance existe entre les variations de l'IH et les proportions de la MOA orangée tout le long du microcycle. L'augmentation du COT coïncide avec l'apparition de cette MOA orangée.

L'ensemble des résultats concernant les fractions organique et minérale aboutit à la conclusion selon laquelle l'origine de cette cyclicité serait liée à une variation de la production phytoplanctonique, plus particulièrement à une variation des flux organiques exportés depuis la zone photique.

Des concentrés de chacune des MOA ont été isolés à partir de la préparation palynologique de l'échantillon le plus riche en carbone organique en suspension dans l'eau. Ces concentrés sont pré-inclus dans la gélose agar-agar sous stéréomicroscope ; préfixés dans l'aldéhyde formique, fixés au tétr oxyde d'osmium, déshydratés dans des bains de concentration progressivement croissante de 10 jusqu'à 100 % d'acétone, avec une durée qui varie de 5 à 15 mn selon les bains, puis immédiatement inclus, de façon progressive, dans la résine époxy 812.

Les moulages polymérisés dans une étuve à 60°C, ont été taillés en sommets pyramidaux faisant une surface d'environ 1/3 de mm², puis coupés à l'ultramicrotome à l'aide d'un couteau de diamant, en sections ultraminces d'environ 500 Å d'épaisseur. Les sections ont été placées sur des grilles de 3 mm de diamètre, puis observées au MET.

Pour étudier la répartition des matières organiques le long du cycle de COT, huit échantillons ont été sélectionnés (tab. I, fig. 4) selon leur teneur en carbone organique total (COT), leur index d'hydrogène (IH) et leur indice de sulfato-réduction (ISR). On remarque que l'échantillon 23-1 présente un potentiel pétrologène (IH) anormalement élevé. Il a été étudié pour observer s'il y a une éventuelle différence ultrastructurale avec les échantillons voisins. L'indice de sulfato-réduction [Lallier-Vergès *et al.*, 1993a, 1993b], calculé à partir des teneurs en soufre total et en COT du sédiment permet de préciser l'intensité de la dégradation par sulfato-réduction subie par la matière organique déposée. Sa répartition le long du cycle de carbone organique souligne une forte dégradation de la matière organique en milieu du cycle [Lallier-Vergès *et al.*, 1993c].

Le terme de matière organique totale ou MOT désigne pour cette partie de l'étude, la totalité du résidu organique obtenu après attaques acides HCl/HF. La MOT est constituée de matières organiques variées (figurées et amorphes) ainsi que de sulfures. Des quantités millimétriques de cette matière organique totale ont été prélevées sous stéréomicroscope et ont subi la même préparation que les concentrés de matière organique amorphe, pour être étudiés au MET.

TABLE I. – Carbone organique total (COT en %), index d'hydrogène (IH en mg HC/g C org) et indice de sulfato-réduction (ISR) des huit échantillons étudiés au MET.

TABLE I. – Total organic carbon, hydrogen index and sulphate-reduction index of the eight samples studied by TEM.

profondeur. (m)	échantillon n°	COT	IH	ISR
128,233	4-1	2,80	495	1,12
128,622	23-1	4,55	696	1,18
128,672	26-1	5,12	535	1,21
128,746	30-1	8,84	550	1,34
128,755	30-2	9,51	582	1,36
128,785	31-2	4,25	785	1,25
129,093	45-1	1,74	243	1,27
129,101	49-1	1,71	254	1,31

III. – PRINCIPAUX RÉSULTATS

A) Les matières organiques microprélevées

Les observations ultrastructurales menées sur les concentrés des différentes MOA apportent les résultats suivants.

1) La MOA orangée (pl. I-a) présente une texture nanoscopiquement amorphe parfaitement homogène sans aucune structure apparente au grandissement du MET. Les particules apparaissent avec des limites franches (pl. I-b).

2) La MOA brune (pl. I-c) présente en majorité des structures d'aspect laminaire plus ou moins étendus, d'épaisseur toujours régulière (50 à 400 nm) : ce sont les ultralaminae (pl. I-d).

3) La MOA noire (pl. I-e) contient une grande diversité de fragments à ultrastructure différente dans lesquels dominent les débris ligno-cellulosiques (pl. I-f). À côté de ces inclusions détritiques, on retrouve de la matière organique granulaire, de la matière organique nanoscopiquement amorphe en petites particules ou en lamines diffuses et quelques structures ultralaminaires.

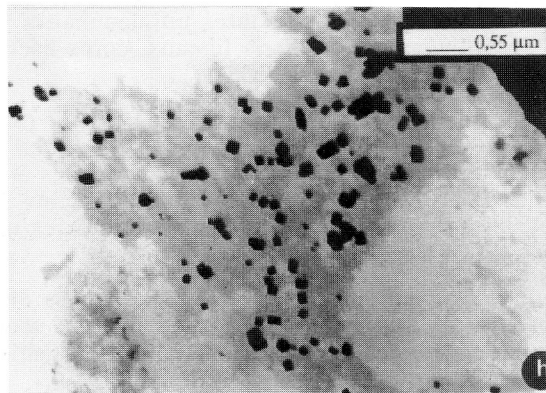
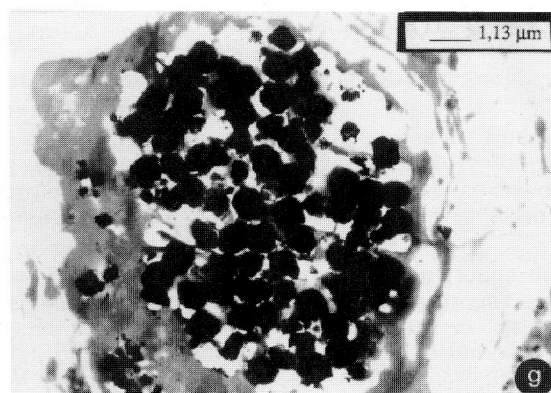
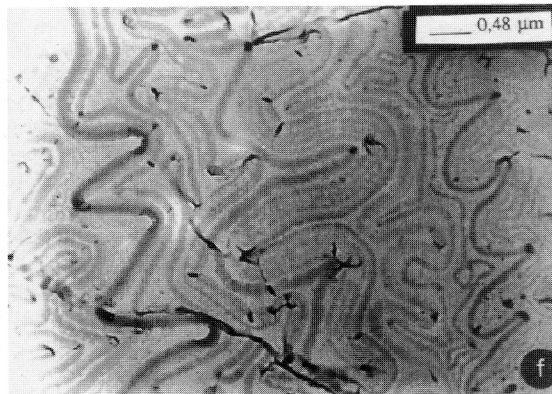
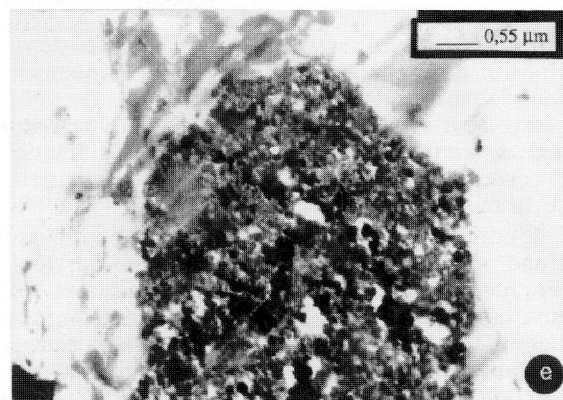
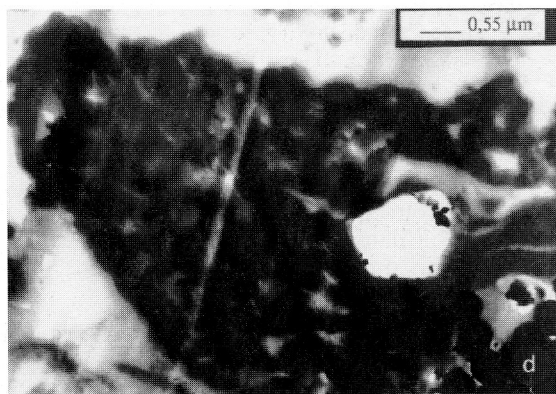
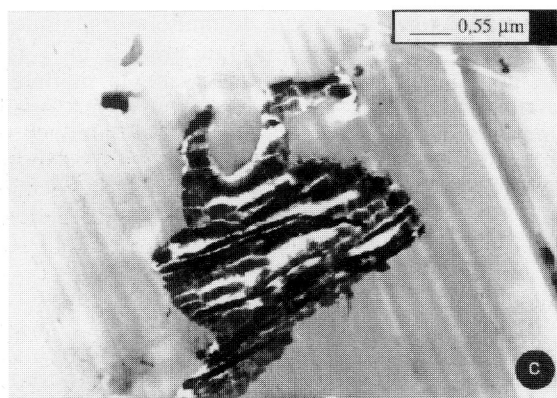
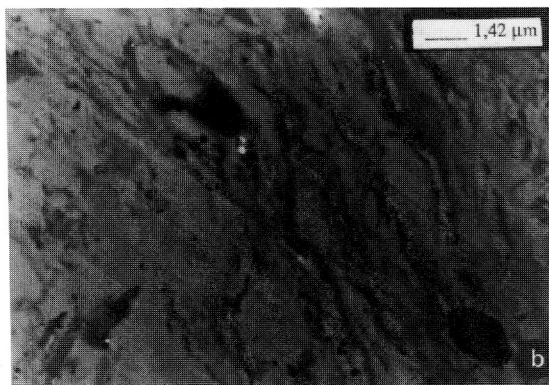
B) Répartition des ultrastructures le long du cycle de carbone organique

Les observations au microscope électronique de la matière organique totale ont permis de distinguer les tendances suivantes.

La matière nanoscopiquement amorphe, correspondant à la MOA orangée, constitue de grandes plages homogènes massives avec un fort contraste (pl. II-a), desquelles se dégagent des zones anastomosées avec des structures linéaires discontinues : les lamines diffuses (pl. II-b). On retrouve aussi dans ces zones de la pyrite sous divers assemblages ainsi que des débris détritiques (pl. II-c) et des empreintes de minéraux. Certaines plages de MOA sont moins homo-

PL. II. – Différentes ultrastructures observées au MET dans la matière organique totale : (a) matière organique nanoscopiquement amorphe et homogène (MOnA), et inclusion de trois framboïdes de pyrite ; (b) zone de matière organique amorphe diffuse ; (c) débris ligneux au sein d'une MOnA ; (d) matière organique à fort contraste, d'aspect tacheté, plus ou moins granulaire, dans laquelle on devine quelques parois épaisses ; (e) matière organique granulaire formée de sphérules agglomérées, les analyses *in-situ* indiquent la présence de C, S et Fe ; (f) structure ultralaminaire d'épaisseur toujours régulière en lamelles parallèles et continues ; (g) framboïde de pyrite ; (h) pyrites en cristaux automorphes (250 nm) dans la MOnA.

PL. II. – Various ultrastructures of the total organic matter observed in TEM : (a) nanoscopically amorphous and perfectly homogeneous organic matter with inclusions of pyrite framboïds ; (b) diffuse amorphous organic matter ; (c) ligneous fragments in the nanoscopically amorphous organic material ; (d) organic material with a high contrast, more or less granular with some faint visible thick cellwalls ; (e) granular organic material with aggregated spherules ; EDAX analyses indicate the occurrence of C, S and Fe ; (f) ultralaminar structures, parallel and continuous, and with regular thickness ; (g) pyrite framboïds ; (h) pyrite crystals (250 nm) in nanoscopically amorphous organic matter.



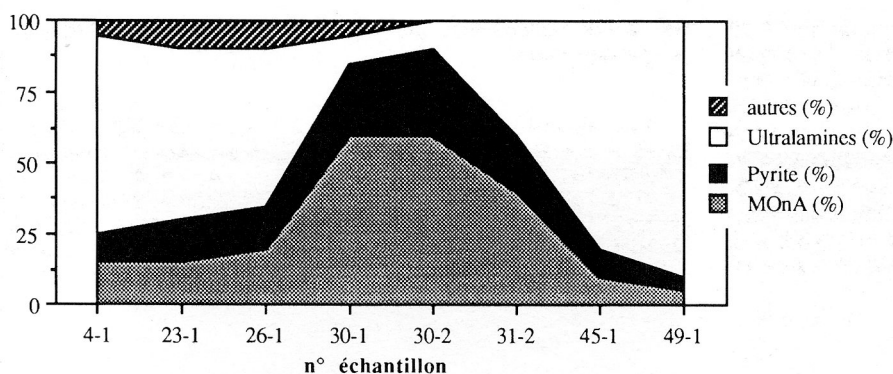


FIG. 5. – Evolution le long du cycle des fréquences des différentes ultrastructures observées dans la matière organique totale.

FIG. 5. – *Semiquantitative evolution along the cycle of the different ultrastructures observed in the total organic matter.*

gènes et présentent un aspect tacheté (plus ou moins granulaire) (pl. II-d).

Les lamines diffuses et la MOA déchiquetée se présentent comme une matrice enrobant la pyrite, les minéraux et les tests d'organismes (dissous ici par les attaques chimiques).

En plus de la matière organique nanoscopiquement amorphe (MOnA), on observe des zones granulaires qui se distinguent par leur aspect en granules agglomérés de façon jointive et par leur densité électronique, généralement plus élevée. Ces amas granulaires forment des zones d'environ 5 µm de long, et se trouvent le plus souvent dispersés dans la MOA homogène ou dans les lamines diffuses. Les granules élémentaires plus ou moins sphériques ont une taille variant entre 10 et 150 nm (pl. II-e).

Les structures ultralaminaires (pl. II-f) ont une épaisseur variant entre 50 et 400 nm. A ce titre, elles sont légèrement différentes de celles décrites par Largeau *et al.* [1990 a et b], Derenne *et al.* [1991], Lugardon *et al.* [1991] dont l'épaisseur est < 60 nm. Par ailleurs, ces lamines sont parallèles et continues, et ne présentent aucun caractère de triple membrane.

Etant donné le type d'attaques (HCl-HF) subies par les échantillons, les seuls minéraux présents sont les sulfures. La pyrite est localisée dans la matière organique nanoscopiquement amorphe et ses lamines diffuses. Plusieurs habitus cristallins ont été distingués : de petits cristaux automorphes (de 0,5 à 1,5 µm) isolés peu fréquents, des assemblages quelconques de microcristaux ≤ 250 nm (pl. II-h), et enfin des assemblages framboïdaux (1 µm et 5 µm) très abondants (pl. II-g), formés de microcristaux dont la taille varie de 100 à 500 nm.

La figure 5 présente les fréquences d'apparition des différentes ultrastructures observées, regroupées en quatre grands ensembles : les matières organiques nanoscopiquement amorphes, la pyrite, les structures ultralaminaires et l'ensemble « MOA granulaire, débris ligneux, corps bactériiformes... », le long du cycle de COT.

On remarque que les échantillons du milieu du cycle (30-1 et 30-2) – les plus riches en carbone organique total – sont aussi ceux qui contiennent les fréquences les plus élevées en pyrite et en MOnA. Les échantillons de début et de fin de cycle sont, de ce fait, enrichis en structures ultralaminaires.

L'échantillon 23-1, qui possède un IH anormalement élevé (696 mg HC/g Corg), présente des ultrastructures semblables à celles des échantillons voisins. Ce potentiel pétrologène élevé reste pour l'instant inexpliqué.

IV. – DISCUSSION

L'étude des différents types de matières organiques amorphes au MET montre que chaque type défini en palynofaciès présente une ultrastructure spécifique et correspond de ce fait à un type de matière organique déterminé.

La MOA orangée se présente comme un gel nanoscopiquement amorphe. L'observation de la matière organique totale a révélé que les plaquettes de MOA orangée possédaient la même ultrastructure que les lamines diffuses de la matrice organo-minérale. Ces structures continues semblent constituer le réseau organique de la roche [Boussafir *et al.*, 1994] rejoignant en cela des observations récentes effectuées sur les matières organiques étudiées *in situ* dans les roches du Kimméridgien du Dorset (travaux en cours). Les apports minéraux et la compaction confèreraient à certaines des particules leur aspect en plaquettes. La pyrite est uniquement associée à ce type de matière organique.

La MOA brune ultralaminaire correspondrait, par similitude avec les résultats de Largeau *et al.* [1990 a] à des biopolymères résistants issus d'organismes phytoplanctoniques.

La MOA noire, constituée de fragments de diverses origines et de matière organique nanoscopiquement amorphe, dans laquelle on trouve des empreintes de coccolithes, de quartz et d'argile (pl. I-f), témoigne d'une étroite association de cette matière organique avec la fraction minérale et correspondrait donc à l'ensemble de la matière organique de la matrice organo-minérale.

L'enrichissement en COT étant par ailleurs le résultat d'une augmentation de la production phytoplanctonique [Pradier et Bertrand, 1992; Ramanampisoa *et al.*, 1992; Tribovillard *et al.*, 1992, Bertrand et Lallier-Vergès, 1993], la matière organique nanoscopiquement amorphe serait donc le constituant organique majeur témoignant de cette productivité.

V. – CONCLUSION

Nous proposons donc l'interprétation suivante :

— le début et la fin du cycle seraient les témoins d'un apport organique riche en constituants biorésistants (ultralamines) dont la matière organique métabolisable associée a été en partie consommée avant le dépôt (moins de sulfures), peut-être également par des processus oxydiques ;

— le milieu de cycle riche en sulfures correspondrait à un apport plus important en matière organique métabolisable favorisant la sulfato-réduction. Si on admet que la totalité de la matière organique métabolisable a été consommée par sulfato-réduction, puisque celle-ci n'était pas limitée [Tribovillard *et al.*, 1994], la MOnA, en parti-

cules ou diffuse, représenterait la fraction moléculaire résistante à la sulfato-réduction (principalement lipidique). Cela expliquerait son fort potentiel pétrologène. Cette fraction moléculaire aurait acquis son caractère résistant au travers de la dégradation bactérienne du phytoplancton et de la préservation sélective de macromolécules dérivant de bactéries : les bactéranes [Le Berre *et al.*, 1991]. L'ultrastructure homogène de cette matière organique, similaire à celle observée dans des bactéranes actuelles ou isolées de kérogènes, est donc interprétée comme le résultat d'une gé-

lification bactérienne précoce de la matière phytoplanctonique originelle.

Remerciements. – Ce travail a été financé par le GdR 942 du CNRS : Relations et Processus Organo-minéraux en Environnements Sédimentaires (CNRS – Université d'Orléans – Université d'Orsay – CFP, Total – IFP – SNEAP) et par la Région Centre (allocation d'étude). Nous tenons à remercier plus particulièrement Dominique Jalabert du Service Commun de Microscopie Electronique de l'Université d'Orléans, pour son soutien technique.

Références

- BERTRAND P. & LALLIER-VERGÈS E. (1993). – Past sedimentary organic matter accumulation and degradation controlled by productivity. – *Nature*, **364**, 786-788.
- BOUSSAFIR M., LALLIER-VERGÈS E., BERTRAND P. & BADAUT-TRAUTH D. (1994). – Etude ultrastructurale de matières organiques micro-prélevées dans les roches de la «Kimmeridgian Clay Formation» (Yorkshire, UK). – *Bull. Centres Rech. Explor. Prod. Elf-Aquitaine* (sous presse).
- COMBAZ A. (1980). – Les kérogènes vus au microscope. In : B. DURAND Kerogen. – Technip, Paris.
- DEGENS F.T., WATSON S. & REMSEN C. (1970). – Fossil membranes and cell-wall fragments from a 7000 year-old Black Sea sediment. – *Science*, **168**, 1207-1208.
- DERENNE S., LARGEAU C., CASADEVALL E., BERKALOFF C. & ROUSSEAU B. (1991). – Chemical evidence of kerogen formation in source rocks and oil shales via selective preservation of thin resistant outer walls of microalgae : origin of ultralaminae. – *Geochim. Cosmochim. Acta*, **55**, 1041-1050.
- DERENNE S., LE BERRE F., LARGEAU C., HATCHER P., CONNAN J. & RAYNAUD J.F. (1992a). – Formation of ultralaminae in marine kerogens via selective preservation of thin resistant outer walls of microalgae. – *Org. Geochem.*, **19**, 345-350.
- DERENNE S., LARGEAU C. & HATCHER P.G. (1992b). – Structure of *Chlorella fusca* algaenan : relationships with ultralaminae in lacustrine kerogens ; species- and environment-dependent variations in the composition of fossil ultralaminae. – *Org. Geochem.*, **18**, 4, 417-422.
- DERENNE S., LARGEAU C., CASADEVALL E., BERKALOFF C., ROUSSEAU B., WILHELM C. & HATCHER P.G. (1992c). – Non-hydrolysable macromolecular constituents from outer walls of *Chlorella fusca* and *Nanochlorum eucaryotum*. – *Phytochemistry*, **31**, 6, 1923-1929.
- DERENNE S., LARGEAU C. & TAULELLE F. (1993). – Occurrence of non-hydrolysable amides in the macromolecular constituent of *Scenedesmus quadricauda* cell wall as revealed by ¹⁵N NMR : Origin of *n*-alkylnitriles in pyrolysates of ultralaminae-containing kerogens. – *Geochim. Cosmochim. Acta.*, **57**, 851-857.
- HERBIN J.P., MÜLLER C., GEYSSANT J.R., MÉLIÈRES F. & PENN I.E. (1991). – Hétérogénéité quantitative et qualitative de la matière organique dans les argiles du Kimméridgien du Val de Pickering (Yorkshire, UK). Cadre sédimentologique et stratigraphique. – *Rev. IFP*, **46**, 675-713.
- LALLIER-VERGÈS E., BERTRAND P. & DESPRAIRIES A. (1993a). – Organic matter composition and sulfate reduction intensity in Oman margin sediments. – *Mar. Geol.*, **112**, 57-69.
- LALLIER-VERGÈS E., BERTRAND P., HUC A.Y., BÜCKEL D. & TREMBLAY P. (1993b). – Control of the preservation of organic matter by productivity and sulfate reduction in marine anoxic sediments : Kimmeridgian shales from Dorset (UK). – *Mar. Petrol. Geol.*, **10**, 600-605.
- LALLIER-VERGÈS E., BOUSSAFIR M., BERTRAND P. & BADAUT-TRAUTH D. (1993c). – Selective preservation of various organic matter types as assessed by STEM studies on a cyclic productivity-controlled sedimentary series (Kimmeridge Clay Formation). – In : *Advances in Organic Geochemistry 1993*, 16th Meeting of E.A.O.G., 384-388.
- LARGEAU C., DERENNE S., CASADEVALL E., BERKALOFF C., COROLLEUR M., LAGARDON B., RAYNAUD J.F. & CONNAN J. (1990a). – Occurrence and origin of ultralaminar structures in "amorphous" kerogens from various source-rocks and oil-shales. In : B. DURAND and F. BEHAR, *Advances in organic geochemistry 1989*. – Org. Geochem., 889-896.
- LARGEAU C., DERENNE S., CLAIRAY C., CASADEVALL E., RAYNAUD J.F., LUGARDON B., BERKALOFF C., COROLLEUR M. & ROUSSEAU B. (1990b). – Characterisation of various kerogens by scanning electron microscopy (SEM) and transmission electron microscopy (TEM) – Morphological relationships with resistant outer walls in extant micro-organisms. – *Meded. Rijks Geol. Dienst*, **45**, 91-101.
- LE BERRE F., DERENNE S., LARGEAU C., CONNAN J. & BERKALOFF C. (1991). – Occurrence of non-hydrolysable, macromolecular, walls constituents in bacteria. Geochemical implications. In : D.A.C. MANNING, *Organic geochemistry : Advances and applications in energy and the natural environment*. – Univ. Press, Manchester, 428-431.
- LUGARDON B., RAYNAUD J.F. & HUSSON P. (1991). – Données ultrastructurales sur la matière organique amorphe des kérogènes. – *Palyonoscience*, **1**, 69-88.
- PRADIER B. & BERTRAND P. (1992). – Etude à haute résolution d'un cycle de carbone organique des argiles du Kimméridgien du Yorkshire (GB) : relation entre composition pétrographique du contenu organique observé *in-situ*, teneur en carbone organique et qualité pétrologène. – *C.R. Acad. Sci.*, Paris, **315**, II, 187-192.
- RAMANAMPISOA L., BERTRAND P., DISNAR J.R., LALLIER-VERGÈS E., PRADIER B. & TRIBOVILLARD N.P. (1992). – Etude à haute résolution d'un cycle de carbone organique des argiles du Kimméridgien du Yorkshire (GB) : résultats préliminaires de géochimie et de pétrographie organique. – *C.R. Acad. Sci.*, Paris, **314**, II, 1493-1498.
- RAYNAUD J.F., LUGARDON B. & LACRAMPE-COULOUME G. (1988). – Observation de membranes fossiles dans la matière organique « amorphe » de roches-mères de pétrole. – *C.R. Acad. Sci.*, Paris, **307**, 1703-1709.
- TRIBOVILLARD N.P., DESPRAIRIES A., BERTRAND P., LALLIER-VERGÈS E., DISNAR J.R. & PRADIER B. (1992). – Etude à haute résolution d'un cycle de carbone organique de roches kimméridgiennes du Yorkshire (GB) : minéralogie et géochimie (résultats préliminaires). – *C.R. Acad. Sci.*, Paris, **314**, II, 923-930.
- TRIBOVILLARD N.P., DESPRAIRIES A., LALLIER-VERGÈS E., BERTRAND P., MOUREAU N., RAMDANI A. & RAMANAMPISOA L. (1994). – Geochemical study of organic-rich cycles in the Kimmeridge Clay Formation of Yorkshire (GB) : productivity vs. anoxia. – *Palaeogeogr., Palaeoclimatol., Palaeoecol.*, **108**, 165-181.



0016-7037(95)00273-1

Electron microscopy and pyrolysis of kerogens from the Kimmeridge Clay Formation, UK: Source organisms, preservation processes, and origin of microcycles

M. BOUSSAFIR,¹ F. GELIN,² E. LALLIER-VERGÈS,¹ S. DERENNE,² P. BERTRAND,^{1,*} and C. LARGEAU²

¹Université d'Orléans, URA CNRS 724, Dépt. des Sciences de la Terre, F-45067 Orléans cedex, France

²Laboratoire de Chimie Bioorganique et Organique Physique, URA CNRS 1381, Ecole Nationale Supérieure de Chimie de Paris, 11 rue Pierre et Marie Curie, F-75231 Paris cedex 05, France

(Received November 29, 1994; accepted in revised form June 9, 1995)

Abstract—Recent studies revealed short-term cyclic variations (microcycles) in total organic carbon (TOC) and the hydrogen index (HI) in the Kimmeridge Clay Formation, an organic-rich deposit considered to be a lateral equivalent of the main source rocks of the North Sea. In addition, three different types of organic matter that all appear to be amorphous when observed by light microscopy (AOM) were recognized. Together, these AOM types account for over 80% of total kerogen and their relative abundances show large variations along each microcycle. In the present work, transmission electron microscopy (TEM) observations were carried out on samples (whole kerogens, kerogen subfractions only comprising a single type of AOM, selected rock fragments) corresponding to typical points within a microcycle and obtained via high resolution sampling. The nature and the relative abundances of the products generated by Curie-point Py–GC–MS and off-line pyrolyses of isolated kerogens were also determined for two selected samples corresponding to the beginning and the top of the microcycle. Combination of such ultrastructural observations, including some semiquantitative studies, and the analysis of pyrolysis products allowed (1) determination of the ultrastructural features of the three AOM types thus providing what we believe to be the first example of correlations between light microscopy (palynofacies, *in situ* maceral analysis) and TEM observations on “amorphous” fossil materials; (2) identification of the source organisms and elucidation of the mode of formation of the different AOM types in the Kimmeridge Clay; (3) explanation of the variations in their relative abundances taking place along a microcycle and establishment of tight correlations with TOC and HI changes; and (4) explanation of the origin of the microcyclic variations in kerogen quantity (TOC) and quality (HI) occurring in the Kimmeridge Clay Formation. Interrelationships between primary productivity, sulphate reduction intensity, and lipid “vulcanization” likely played a major role in the control of such variations.

1. INTRODUCTION

The aim of this work was to gain information on kerogen genesis and source organisms in the Kimmeridge Clay and on the origin of the short-term cyclic variations, in both kerogen quantity and quality, occurring in this formation. Kimmeridge Clay is a marine deposit, with alternating organic-rich shales and marls, considered as a lateral equivalent of the main source rocks of the North Sea. This Upper Jurassic formation, up to five hundred meters thick, outcrops in Britain as a belt stretching from Dorset to Yorkshire (Williams and Douglas, 1980). It is generally considered that the Kimmeridge Clay was deposited below wave base under a shallow shelf regime (Tyson et al., 1979) during a period of maximum eustatic rise and transgression (Gallois, 1976). Depositional conditions were mainly controlled by the topography of the basin and sedimentation and subsidence rates. The onshore basin topography led to the sedimentation of organic matter-rich mudstones and to anoxic conditions in restricted areas only (Tribouillard et al., 1994). Previous studies on the bulk chemical features of Kimmeridge Clay kerogens, chiefly based on elemental analyses and pyrolyses (Williams and Douglas, 1980, 1983; Farrimond et al., 1984; Pfendt, 1984; Eglinton et al., 1986, 1988a,b), showed a type II material with a low degree

of maturity, consistent with a maximal burial depth around 1,500 m (Williams, 1986). In addition, a recent bitumen examination pointed to an important contribution of algae along with a minor contribution of land-derived organic material (Ramanampisoa and Disnar, 1994).

Recently, high resolution measurements of total organic carbon (TOC) on Kimmeridge Clay cores from three boreholes in the Cleveland basin (Yorkshire, UK) revealed a conspicuous feature (Herbin et al., 1991, 1993). Pronounced, short-term, cyclic variations in TOC were observed with each microcycle corresponding to about 30,000 years. Moreover, it was noted (Ramanampisoa et al., 1992) that the hydrogen index (HI) also exhibits substantial cyclic variation along with TOC. As a result of such parallel, wave-shaped, changes in TOC and HI, the oil potential of the Kimmeridge Clay formation shows a sharp maximum at the top of each cycle.

The first petrographic observations carried out on Kimmeridge Clay kerogens, by light and UV fluorescence microscopy (Tyson et al., 1979; Williams and Douglas, 1980; Smith, 1984), indicated a marked predominance of a seemingly structureless matter with bituminite as the main maceral according to Williams and Douglas (1980). A low contribution of recognizable elements, mainly of a terrestrial origin (humic material), was also noted (Bertrand et al., 1990; Huc et al., 1992). Examinations by transmitted and reflected light microscopy were recently carried out on kerogens obtained via high resolution sampling of a microcycle, from one of the

* Present address: Université Bordeaux I, URA CNRS 197 Géologie & Océanographie, F-33405 Talence cedex, France

three boreholes previously studied by Herbin et al. (1991, 1993): Cleveland basin, Marton 87 well (Ramanampisoa et al., 1992; Pradier and Bertrand, 1992). The palynofacies study (transmitted light microscopy) revealed that the dominant "amorphous" organic material (AOM, over 80% of total organic matter) is in fact comprised of three distinct types of particles that can be characterized by differences in texture and color: orange homogeneous flakes with sharp edges (orange AOM, Fig. 1a); brown heterogeneous flocks with fuzzy outlines (brown AOM, Fig. 1b); opaque aggregates (black AOM, Fig. 1c). It was observed that important differences in the relative abundances of the three above types take place along the cycle. Moreover, Ramanampisoa et al. (1992) noted a strong parallel between the variations in TOC and HI values, on the one hand, and the abundance of orange AOM on the other hand. The beginning and the end of the cycle are thus characterized by a predominance of the black and brown AOMs associated with land-derived debris, whereas the peak (or top) of the cycle, where maximum TOC and HI occur, shows a major contribution of orange AOM.

The purposes of the present study were therefore to derive information on (1) the ultrastructural and chemical features, the source organisms, and the mode of formation of these different types of so-called "amorphous organic matter" (AOM), (2) the origin of the substantial variations in AOM relative abundances occurring along the microcycle, (3) the relationships between such variations and TOC and HI changes, and (4) the cause(s) of the cyclic variations observed in the Kimmeridge Clay. The conclusions obtained from the study may also aid in understanding the factors that control organic matter quantity (TOC) and quality (HI) in marine sediments in general. To this end, transmission electron microscopy observations (TEM) and pyrolytic studies were carried out on isolated kerogens, corresponding to typical points from the above Kimmeridge Clay microcycle. Bulk kerogens and kerogen subfractions, obtained by micromanipulation and only comprising a single type of AOM particles, were both examined by TEM. Additionally, in situ TEM observations were also directly performed on untreated rock fragments.

2. EXPERIMENTAL

2.1. Samples

The studied microcycle (90 cm thick, corresponding to about 30,000 years, depth in the core 128.2 to 129.1 m) was sampled in the Eudoxus zone of the Marton 87 borehole, Pickering Vale, Cleveland Basin, Yorkshire, UK (Herbin et al., 1991). The corresponding geologic section is discussed in Herbin et al. (1991, 1993), Tribouillard et al. (1994), and Desprairies et al. (1995). TOC values range from ca. 2% (beginning and end of the microcycle) to 9.5% at the top of the microcycle and HI from ca. 250 to ca. 780 mg of hydrocarbons/g of organic carbon (Ramanampisoa et al., 1992). The microfacies observed by light microscopy (reflected light and UV excitation on polished sections) is laminated throughout the cycle and no bioturbation features are observed. The distribution of the organic matter appears to be relatively heterogeneous. In samples with relatively low TOC values, the organic matter is comprised predominantly of small irregular or angular particles, from 5 to 20 μm in size, identified as inertinite. For samples with TOC values > 4%, the microfacies are characterized by an increase in size and abundance of more or less continuous elongated organic particles (up to 500 μm) which are largely predominant at the peak of the cycle; when studied by re-

flected light they appear as bituminite maceral (Pradier and Bertrand, 1992). For the highest TOC values, the organic matter tends to form thick laminations and to occur within the mineral matrix in greater amounts.

The eight samples examined were selected on the basis of previous light microscopy and Rock-Eval high resolution studies (centimetric scale) carried out by Ramanampisoa et al. (1992). These samples correspond to the beginning of the cycle (128.23 m), the section encompassing the increasing TOC values (128.62 and 128.67 m), the top of the cycle (128.74 and 128.75 m), the section covering decreasing TOC values (128.79 m), and the end of the cycle (129.09 and 129.1 m). In agreement with the previously stated occurrence of low maturity type II material in the Kimmeridge Clay, elemental analysis indicated atomic H/C ratios of 1.1 to 1.2 for the selected kerogens.

Kerogens used for petrographic and pyrolytic studies were isolated from these different rock samples via the classical HF/HCl treatment. Direct TEM observations were then carried out on whole kerogens and on handpicked kerogen subfractions comprising only a single type of AOM. The subfractions were obtained by picking out AOM particles under a stereomicroscope, with a microsyringe coupled to a micromanipulator, from aqueous suspensions of whole isolated kerogens (Boussafir et al., 1994a). Fragments of untreated rocks dominated by a single type of maceral (e.g., bituminite), or by the organomineral matrix, were also selected by light microscopy, from polished sections, for in-situ TEM observations.

All the above materials (whole kerogens, kerogen subfractions, and selected rock fragments) were fixed in osmium tetroxide, embedded in resin, cut with an ultramicrotome, and stained as described in Boussafir et al. (1994b) prior to TEM examination using a STEM Jeol 100 CX.

2.2. Pyrolyses

"Off-line" pyrolyses and identification of pyrolysis products were performed according to Largeau et al. (1986). Briefly, kerogens are firstly heated at 300°C for 20 min so as to eliminate adsorbed compounds by thermovaporization and, after extraction with $\text{CHCl}_3/\text{MeOH}$ (2/1), the insoluble residue is pyrolysed at 400°C for 2 h under a helium flow. The released products are trapped in CHCl_3 at -5°C , separated by column chromatography on activity 2 alumina into three fractions of increasing polarity by eluting with hexane, toluene, and methanol, respectively. The hexane-eluted, low polarity products are further separated into three subfractions by TLC on $\text{SiO}_2\text{-AgNO}_3$ (10%). The various pyrolysate fractions thus obtained were analysed by GC-MS (DB1 capillary column, 60 m \times 0.25 mm i.d., oven heated from 120 to 260°C at 4°C/min). Curie point pyrolysis-gas chromatography-mass spectrometry (Py-GC-MS) was performed as described in Derenne et al. (1992a) using a Curie point pyrolyser (FOM3-LX) and a ferromagnetic wire with a Curie temperature of 610°C.

3. RESULTS AND DISCUSSION

3.1. Electron Microscopy

A first series of TEM observations on whole isolated kerogens, corresponding to typical points of the microcycle, revealed the presence of various ultrastructures in the eight samples examined: a massive, gel-like, amorphous material; very thin lamellae; small ligneous debris; a granular material; and a diffuse amorphous material (Fig. 2). The above ultrastructures were shown to occur all along the microcycle but sharp differences in their relative abundances were noted. A semi-quantitative study was therefore carried out by examining, for each kerogen sample, 60 to 75 ultrathin sections. The gel-like material was thus shown to exhibit large changes in relative abundances that parallel TOC and HI variations (and hence variations in orange AOM relative contribution). This structureless material is only a minor constituent at the end and the beginning of the cycle (about 5 to 10% of total AOM)

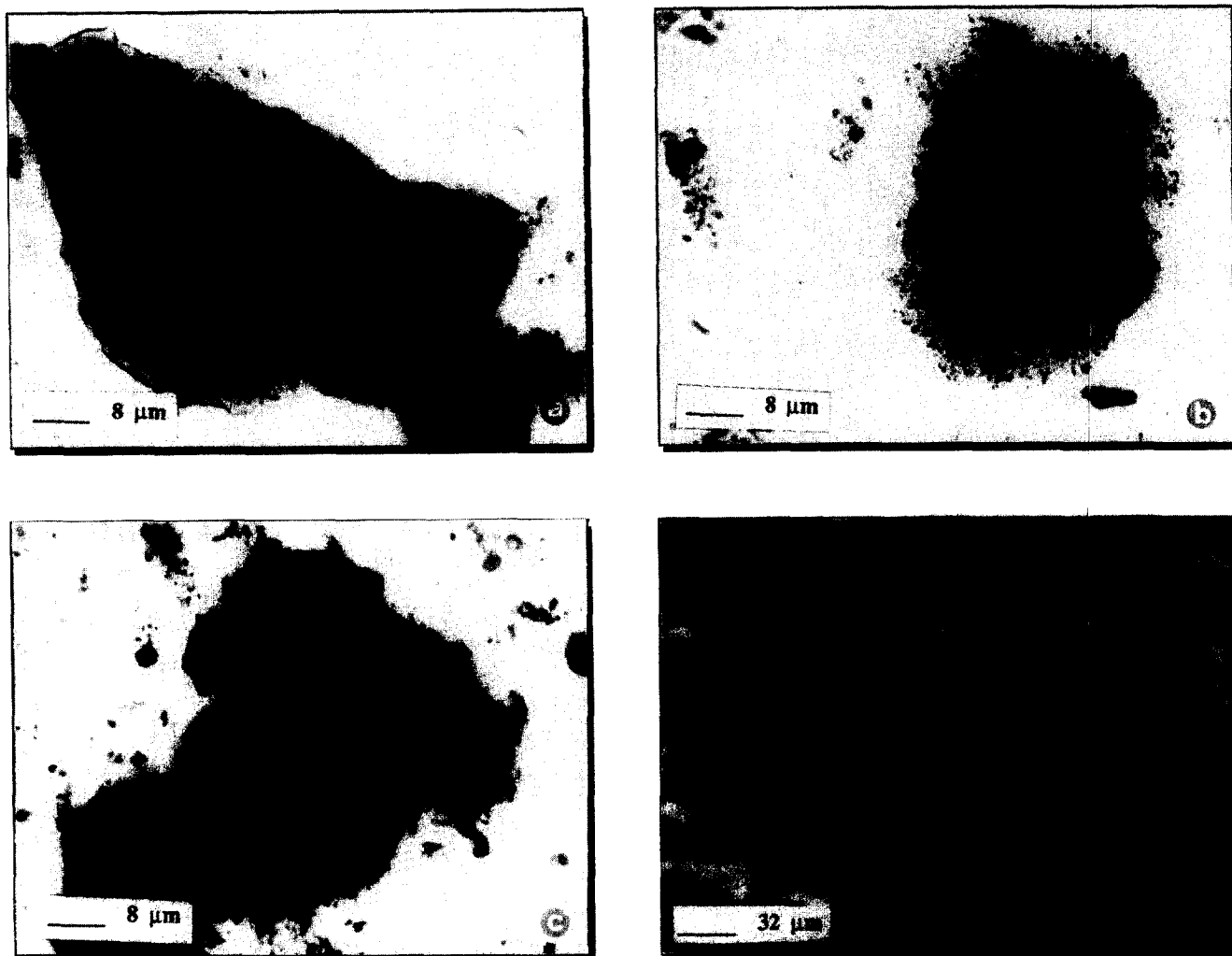


FIG. 1. The three different types of AOM observed in transmitted light microscopy (palynofacies) from Kimmeridge Clay isolated kerogens: (1a) orange AOM; (1b) brown AOM; (1c) black AOM; (1d) Elongated organic particles of bituminite "b" associated with framboidal pyrite "fp" as seen by reflected light (UV excitation) in the microtexture of high-TOC samples.

but markedly predominates at the top (up to 75%). Reverse changes in relative abundances were noted, along the micro-cycle, for other types of ultrastructures (lamellae, ligneous debris) and the latter are only abundant at the end and the beginning of the cycle. The above semiquantitative features suggested that tight correlations may occur between the three types of AOM, previously detected by transmitted light microscopy (palynofacies), and the different ultrastructures identified at higher magnification in the present TEM study. The occurrence of such correlations was fully confirmed by TEM examination of kerogen subfractions, composed of a single type of AOM, obtained by picking out particles under the light microscope.

In fact, when taken together, the above TEM observations indicate the following.

- 1) The orange AOM corresponds to the massive gel-like material. This material is characterized by a completely homogeneous texture without any apparent biological structures and it appears truly amorphous, even at a very high magnification (up to $\times 80,000$). That this material is a discrete entity is suggested by well-defined, distinct edges (Fig. 2a). The orange AOM can therefore be defined as a "nanoscopically amorphous organic matter." Such a material is often associated with pyrite crystals and framboids (Fig. 2b). In addition, Electron Energy Loss Spectrometry (EELS) pin-point analyses (Boussafir et al., 1995) showed that the orange AOM contains substantial amounts of organic sulphur (atomic S/C ratios of 0.9 to 1.1).
- 2) The brown AOM corresponds to very thin lamellae with a regular thickness ranging from 50 to 400 nm (Fig. 2c). Similar structures, with thickness up to 60 nm, were previously observed, by TEM, in a number of kerogens isolated from source rocks and oil shales (Raynaud et al., 1988; Largeau et al., 1990a,b; Lugardon et al., 1991; Derenne et al., 1991a, 1993) and termed ultralaminae (Largeau et al., 1990a). No pyrite and no organic sulphur were detected in the brown AOM.
- 3) The black AOM corresponds to a mixture dominated by minute ligneous debris (Fig. 2d) and also comprises a dif-

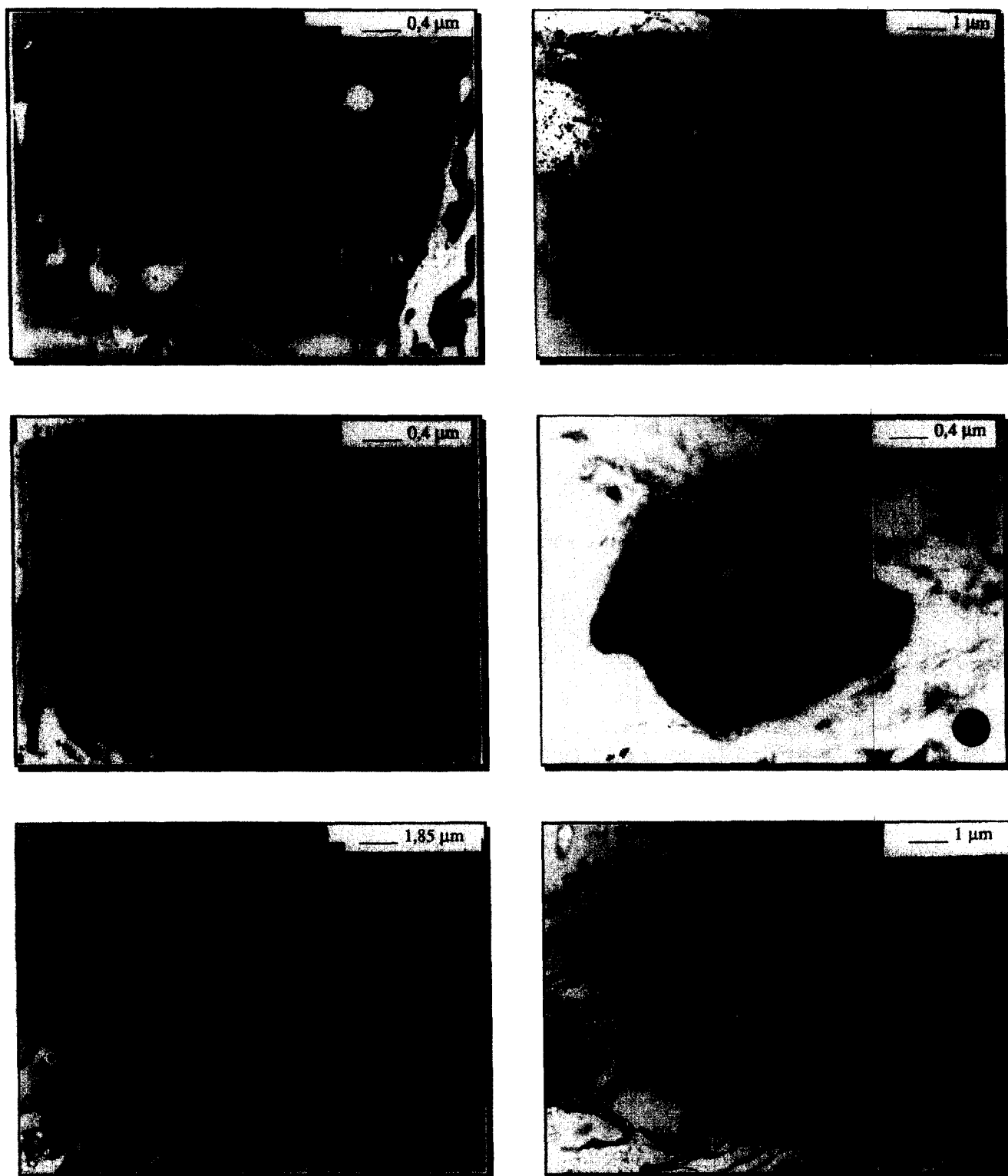


FIG. 2. Main types of ultrastructures observed by TEM in Kimmeridge Clay isolated kerogens: (2a, 2b) massive, gel-like, nanoscopically amorphous organic matter associated with pyrite (P), corresponding to the orange AOM, the electron-lucent areas are voids originating from the elimination of mineral constituents during kerogen isolation; (2c) ultralaminae corresponding to the brown AOM; (2d) ligneous debris (major constituents of the black AOM); (2e, 2f) diffuse nanoscopically amorphous matter contributing to the black AOM; this continuous organic network appears as a grey material whereas "ghosts" of minerals (quartz: Q; pyrite: P; clays: Cl; coccolithes: C) are seen as white areas. In 2f pyrite has been eliminated via nitric acid treatment.

fuse nanoscopically amorphous material; low amounts of granular organic matter are also detected. The amorphous diffuse material was closely associated with mineral constituents in the untreated rock and built an organic network within the mineral groundmass. This network is well preserved following mineral elimination by chemical leaching (Fig. 2e, f). Such a preservation reveals the occurrence of a continuous organic network exhibiting a high degree of cohesion.

The above TEM observations thus revealed major ultrastructural differences between the three types of AOM identified by transmitted light microscopy. The orange AOM is truly amorphous whereas the brown and black forms of AOM comprise well-defined structures that could not be detected by light microscopy. The combination of TEM examination on whole kerogens and on kerogen subfractions obtained by micromanipulation thus provided what we believe to be the first example of correlations between "amorphous" organic materials identified in palynofacies studies and ultrastructures observed by TEM. Moreover, close relationships can be noted between the relative abundances of these different ultrastructures and TOC and HI values (Fig. 3).

Finally, in-situ TEM observations were carried out on rock fragments selected by light microscopy from polished sections. The purpose of these observations was (1) to attempt

a correlation between the main ultrastructures identified above by TEM in isolated kerogens (and hence the AOM types observed in palynofacies studies) and the macerals identified by light microscopy from polished sections of untreated rock samples and (2) to examine the association of these macerals with the mineral constituents. Selected bituminite particles, when observed by TEM, show a massive nanoscopically amorphous gel-like organic matter (Fig. 4a) embedding clay particles and pyrite framboids (Fig. 4b). In addition, previous analyses performed by X-ray mapping (Lallier-Vergès et al., 1993a) revealed a specific enrichment in organic sulphur within bituminite particles from the Kimmeridge Clay. Bituminite and the orange AOM therefore exhibit the same lack of ultrastructure, the same close association with sulphur, and the same variability in relative abundances along the microcycle. The bituminite maceral thus appears to correspond to the orange AOM observed in palynofacies studies. In sharp contrast, the ultralaminar structures (and hence the brown AOM) do not correspond to any recognizable macerals. They are thought to be dispersed in the organo-mineral matrix and thus difficult to be identified by light microscopy from polished sections. The ligneous debris observed in the black AOM present the same morphology at high magnification and the same ultrastructural features as inertinite macerals. Because of their small size (about 1 μm), these debris were not detected by light microscopy.

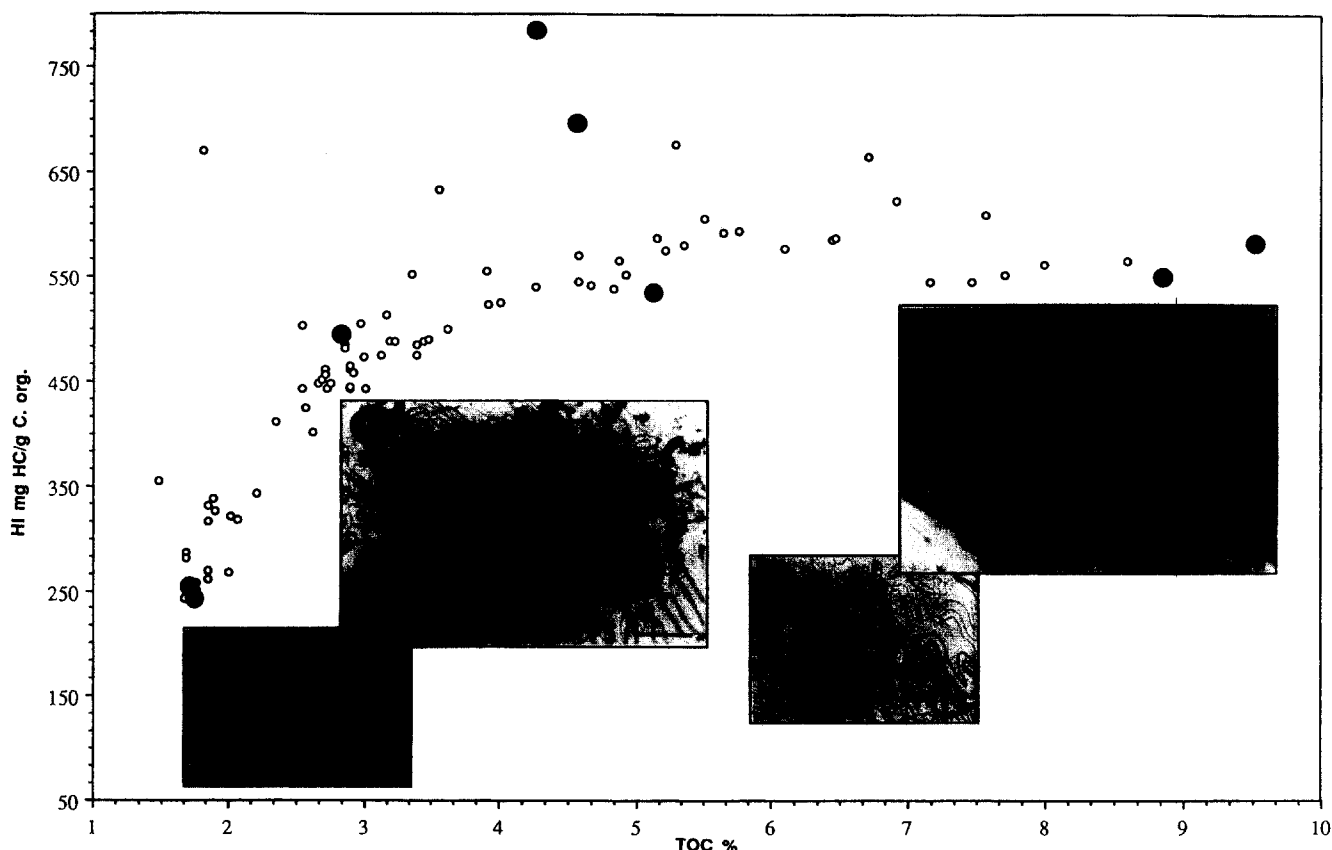


FIG. 3. Main ultrastructures identified by TEM in Kimmeridge Clay isolated kerogens and relationships with TOC and HI variations along the microcycle (after Lallier-Vergès et al., 1993a). Filled circles represent the samples studied by TEM. Ultralaminar (b, c) and minute ligneous debris (a) dominate in samples with relatively low TOC values while the massive amorphous matter (d) is predominant in kerogens with higher TOC.

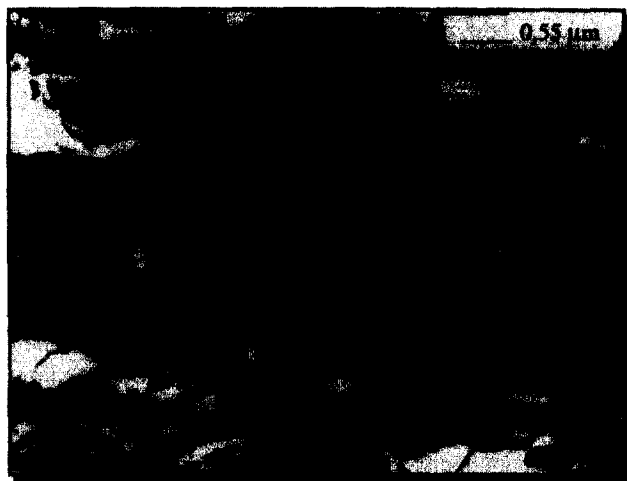


FIG. 4. In-situ TEM observations of bituminite-rich rock fragments revealing the nanoscopically amorphous nature of bituminite (B) and its close association with clays (Cl). Such a close association between clays and bituminite has been described in other source-rock samples (Bishop and Philp, 1994).

Further studies were carried out by pyrolysis so as to examine the chemical features, the source organisms, and the mode of formation of the different constituents identified above in Kimmeridge Clay AOMs.

3.2. Pyrolyses

On the basis of the above petrographic results, two samples termed B (128.23 m) and T (128.75 m) were selected for pyrolytic studies; they correspond to the beginning and the top of the microcycle, respectively. Sample B is thus characterized by lower values for TOC and HI (1.8% and 255 mg HC/g C_{org}) when compared to T (9.5% and 582 mg HC/g C_{org}).

3.2.1. Curie-point Py-GC-MS of isolated kerogens

GC-MS analysis of the 610°C flash pyrolysates revealed complex mixtures of products dominated by doublets corresponding to *n*-alkanes and *n*-alk-1-enes from C_7 to C_{30} (Fig. 5). These two dominant series show maxima around C_{15} , no significant difference in their distributions, and relative intensities was noted between kerogens B and T. These observations indicate an abundant contribution of long polymethylene chains in both samples. The GC-MS traces also show the presence of a large number of compounds eluting between the alkane/alkene doublets. These compounds correspond, as indicated for some of them on Fig. 5, to series of alkylated thiophenes, alkylated phenols, alkylated benzenes, and to additional series of linear/branched, (un)saturated hydrocarbons. The major difference between B and T flash pyrolysates is to be found in the higher relative abundance of thiophenic compounds for T. This difference can be assessed from the thiophene index: $ThI = [2,3\text{-dimethylthiophene}]/[\text{non-1-ene} + 1,2\text{-dimethylbenzene}]$. This ratio is known to provide a convenient way for a rapid estimation of organic sulphur content in kerogens (Eglinton et al., 1990). A significantly higher ratio is indeed noted (0.22 instead of 0.12) from T pyrolysate when compared to B, thus indicating a larger contribution of

sulphur-containing moieties in the former sample. Such a difference is also supported by bulk elemental analyses and the atomic S_{org}/C ratio is about twice as high for T.

3.2.2. Off-line pyrolyses of isolated kerogens

Due to the very high complexity of the effluents produced upon thermal degradation of kerogens B and T, "off-line" pyrolyses were also carried out so as to obtain further information on the generated products. Prior to GC-MS analyses the crude pyrolysate was separated by column chromatography into three fractions (low polarity products, medium polarity products, and polar products) accounting for about 35, 25, and 40% of the total pyrolysates, respectively. Thereafter the low polarity, hexane-eluted fraction was further separated by TLC on SiO_2-AgNO_3 and the polar methanol-eluted fraction was separated by extraction into acid and non-acid compounds.

3.2.3. Low polarity products

The different series of compounds identified in the low polarity fractions are reported in Table 1 along with their distributions and relative abundances. In addition to the already mentioned *n*-alkanes and *n*-alk-1-enes series, a number of other homologous series were identified. They comprise various types of branched alkanes, normal unsaturated hydrocarbons, and compounds with long normal alkyl chains associated with a cyclopentyl, a cyclohexyl, a benzene, a thiophene, a benzothiophene, or a naphthalene ring (in addition the benzene and thiophene rings can be substituted by one or two methyl groups). Despite the occurrence of these different types of cyclic units, the identification of the low polarity pyrolysis products confirms the important contribution of long $(CH_2)_n$ chains to both B and T kerogens. Indeed it can be noted that (1) each fraction is dominated by a series corresponding to normal compounds and that other series of acyclic unbranched products also occur in substantial amounts, (2) the cyclic structures are always associated with long normal

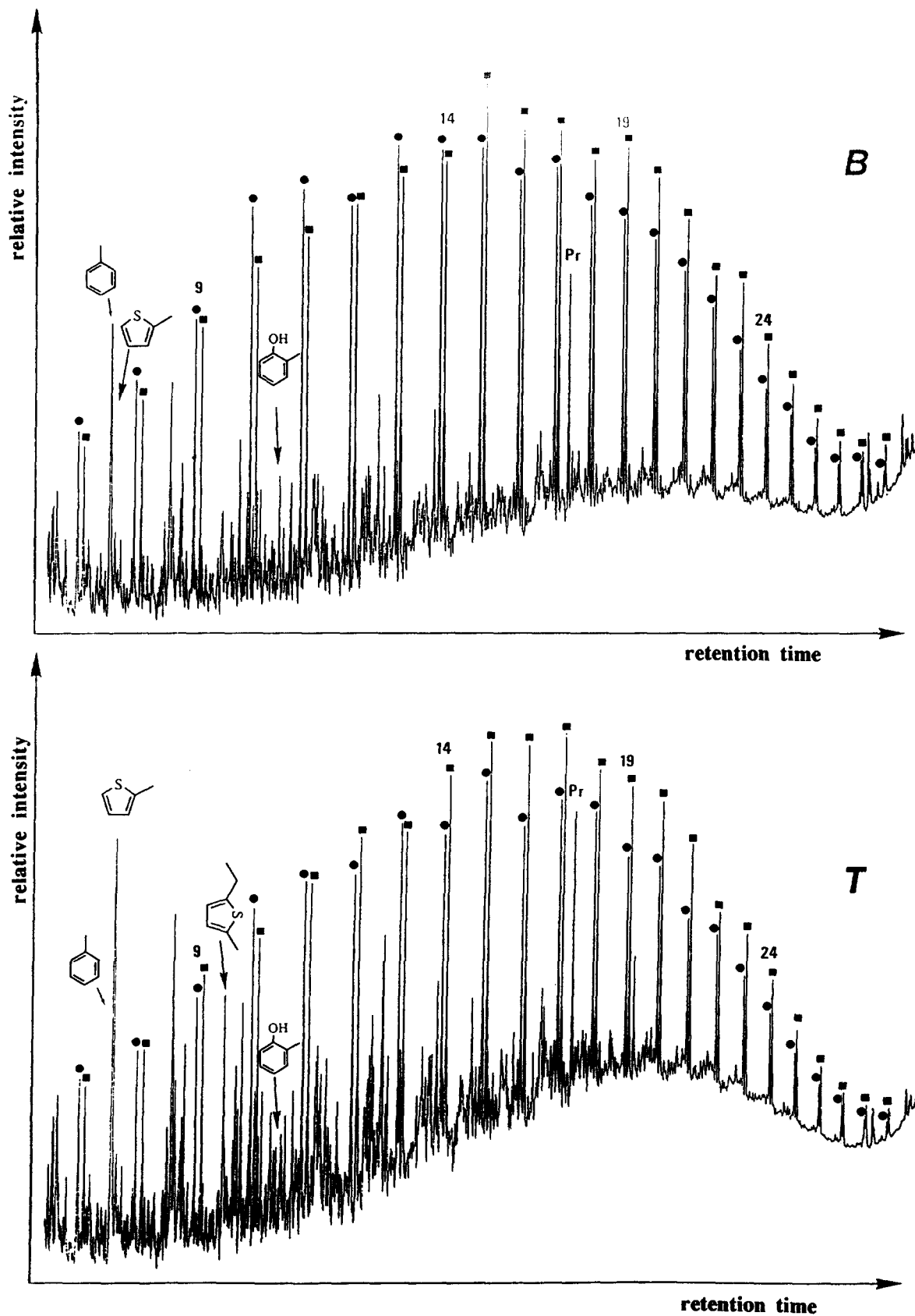


FIG. 5. Total ion current (TIC) traces of the flash pyrolysates of kerogens **B** and **T**. Filled circles and filled squares indicate the homologous series of *n*-alk-1-enes and *n*-alkanes, respectively. Numbers indicate their chain length. The structure of some major compounds is indicated and Pr designates prist-1-ene.

Table 1. Nature and relative abundances of the homologous series of low polarity compounds identified in the 400°C pyrolysates of kerogens B and T.^a

	<u>B</u>		<u>T</u>	
	constituents	r. a.	constituents	r. a.
<i>n</i> -alkanes	C14-C31 (C17)	1	C12-C30 (C15)	1
isoprenoid alkanes	C15-C20 (C18)	0.16	C15-C20 (C18)	0.23
dimethylalkanes I ^b	C17-C31 (C25)	0.08	n.d.	—
dimethylalkanes II ^b	C15-C31 (C21)	0.05	n.d.	—
3-methylalkanes	C14-C30 (C20)	0.10	C13-C22 (C15)	0.04
<i>n</i> -alkylcyclopentanes	C14-C26 (C20)	0.27	n.d.	—
<i>n</i> -alkylcyclohexanes	C14-C25 (C19)	0.05	C12-C23 (C14)	0.13
<i>n</i> -alkenes (E)	C14-C26 (C17)	1	C13-C25 (C15)	1
<i>n</i> -alkadienes ^c	C14-C24 (C17)	0.52	C12-C22 (C15)	0.62
<i>n</i> -alkylbenzenes	C14-C22 (C16)	0.16	C12-C18 (C14)	0.35
<i>n</i> -alkyltoluenes	C14-C23 (C16)	0.18	C12-C21 (C15)	0.28
<i>n</i> -alkyldimethylbenzenes	C14-C20 (C16)	0.16	C12-C18 (C14)	0.33
2- <i>n</i> -alkylthiophenes	C12-C24 (C14)	0.15	C10-C24 (C12)	0.65
2- <i>n</i> -alkyl,5-methylthiophenes	C12-C24 (C14)	0.33	C10-C20 (C12)	0.86
<i>n</i> -alkyl, dimethylthiophenes	C12-C24 (C15)	0.06	C10-C20 (C12)	0.28
<i>n</i> -alk-1-enes	C14-C28 (C18)	1	C12-C28 (C15)	1
<i>n</i> -alkenes (Z)	C14-C25 (C18)	0.09	n.d.	—
<i>n</i> -alkadienes ^c	C14-C22 (C18)	0.08	C12-C18 (C14)	0.11
<i>n</i> -alkylbenzothiophenes	C8-C12	trace	C8-C12 (C11)	0.40
<i>n</i> -alkylnaphthalenes	C10-C14	trace	C10-C14 (C12)	0.15

^aIdentifications were carried out following further separation of the hexane-eluted compounds into three fractions by TLC. r.a.: relative abundances of the homologous series calculated with respect to the predominant series of each fraction (ratios of maxima); the bracketed values correspond to the maximum of the series. ^bBased on their mass spectra, these compounds correspond either to 3,7-dimethylalkanes or to 3, ω -7-dimethylalkanes (series I) and either to 3,5-dimethylalkanes or to 3, ω -5-dimethylalkanes (series II). ^cDouble bond positions could not be determined. The alkadienes series of the second and third fractions exhibit different retention times and do not correspond to α,ω -alkadienes. n.d.: not detected.

alkyl chains, and (3) the abundant series of alkylmethylthiophenes corresponds to the isomer (2-alkyl,5-methyl) with a “normal carbon skeleton”, i.e., to compounds derived from sulphur incorporation in unbranched precursors (Sinninghe-Damsté et al., 1989; Sinninghe-Damsté and de Leeuw, 1990). This major contribution of long polymethylenic chains was confirmed, as shown thereafter, by analysis of the toluene- and methanol-eluted fraction of B and T pyrolysates; it is also consistent with previous studies on Kimmeridge Clay kerogens from the Dorset area using solid state ¹³C NMR spectrometry and RuO₄ oxidation (Boucher et al., 1990).

As discussed below, the abundance and the nature of the organic sulphur compounds (OSC) generated from samples B and T provide important information. As shown in Table 1, although the same series with similar distributions are observed in both cases, much larger relative amounts of OSC

are always obtained from T. In agreement with flash pyrolyses, the latter kerogen therefore comprises a markedly higher contribution of sulphur-containing moieties. This difference can be also illustrated by comparison of the two mass chromatograms of *m/z* 111 of the total pyrolysates of B and T (Fig. 6), highlighting the series of 2-*n*-alkyl, 5-methylthiophenes, and *n*-alk-1-enes.

It is well documented that a rapid incorporation of sulphur into various functionalized lipids takes place during early diagenesis in the presence of reduced sulphur species (reviewed in Sinninghe-Damsté and de Leeuw, 1990). Such an incorporation occurs in lipids comprising carbon-carbon double bonds but also, as recently demonstrated, in ketones and aldehydes (Schouten et al., 1994; Krein and Aizenshtat, 1994). Due to this “natural vulcanization,” the above lipids can become tightly associated via covalent bonds within insoluble

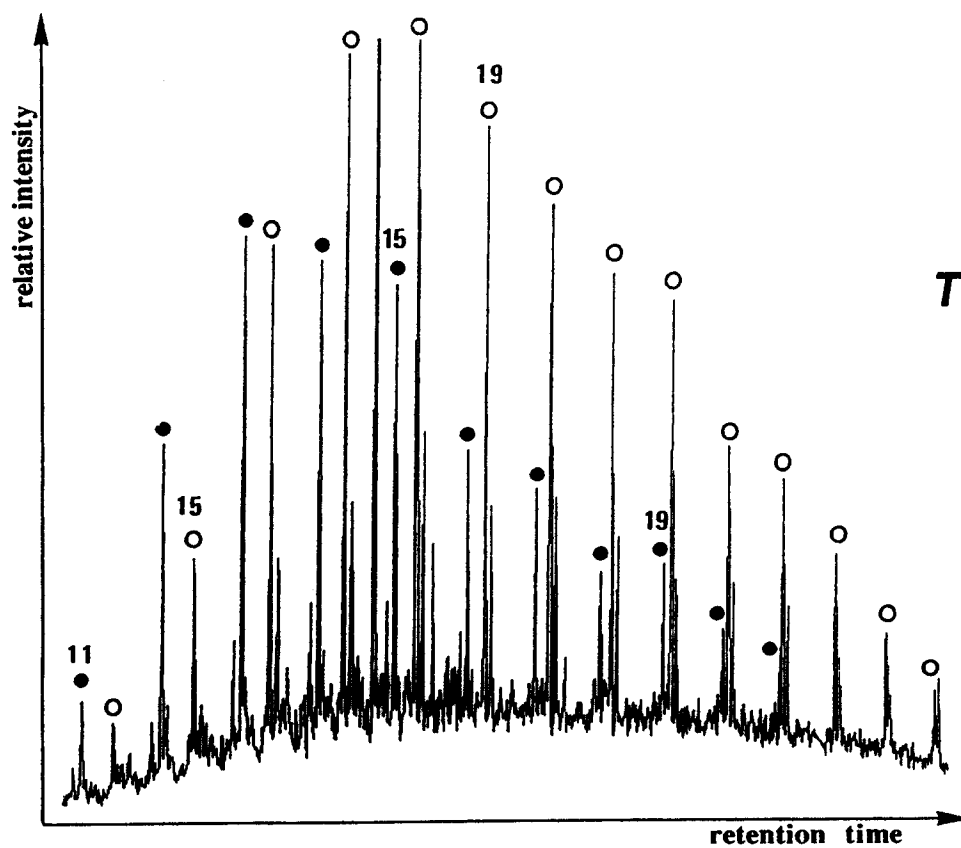
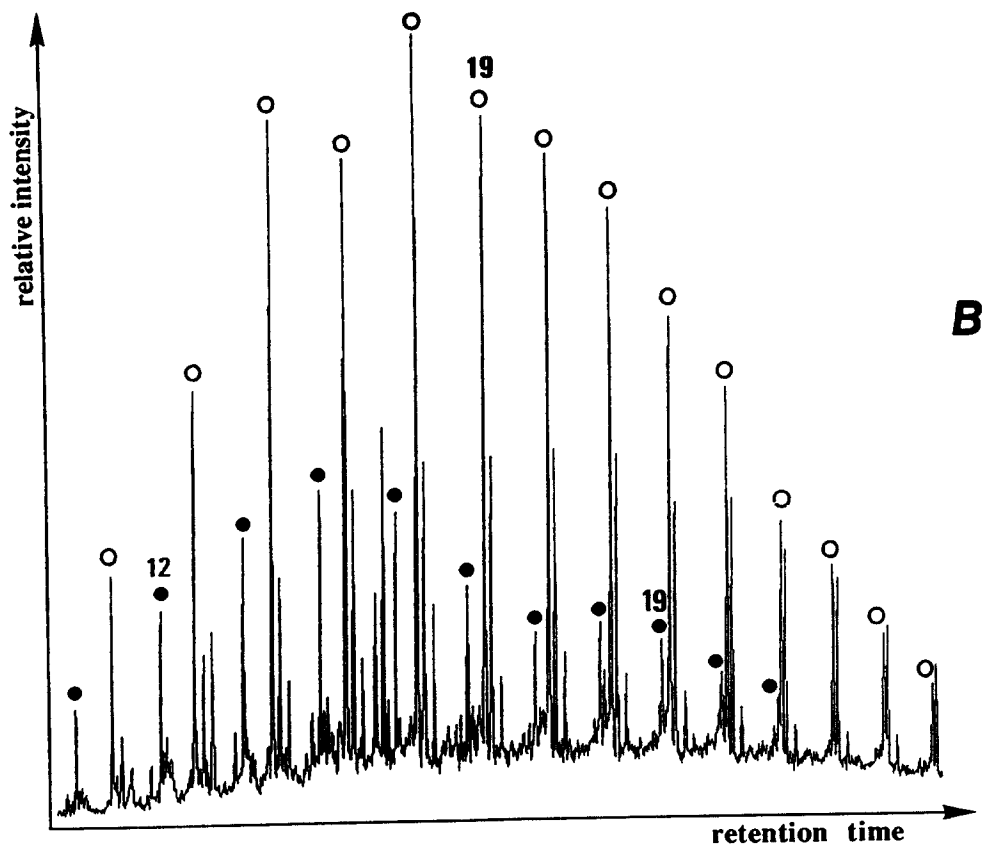


FIG. 6. Mass chromatograms of m/z 111 revealing the homologous series of 2-*n*-alkyl, 5-methylthiophenes (filled circles) and *n*-alk-1-enes (empty circles) in the total "off-line" pyrolysates of kerogens T and B. Numbers indicate the length of the alkyl chains.

Table 2. Nature and relative abundances of the homologous series of medium polarity compounds identified in the 400°C pyrolysates of kerogens B and T.^a

	<u>B</u>		<u>T</u>	
	constituents	r.a.	constituents	r.a.
<i>n</i> -alkan-2-ones	C ₁₄ -C ₃₁ (C ₁₇)	1	C ₁₀ -C ₂₃ (C ₁₃)	1
branched alkyl, methylketones ^b	n.d.	—	C ₁₁ -C ₂₁ (C ₁₃)	0.3
<i>n</i> -alkyl, ethylketones	n.d.	—	C ₁₀ -C ₂₅ (C ₁₃)	0.2
<i>n</i> -alkylnitriles	C ₁₁ -C ₂₁ (C ₁₄)	0.8	trace	—
alkylated indoles	C ₉ -C ₁₂	0.9	C ₉ -C ₁₁	0.1
alkylated quinolines	C ₁₀ -C ₁₂	0.15	C ₁₀ -C ₁₃	0.3

^a Toluene-eluted compounds. r.a.: relative abundance of the homologous series calculated with respect to the predominant series (ratios of maxima). n.d.: not detected. The bracketed values correspond to the maximum of each series

^b The methyl branch is not on carbon 3, but its precise location was not established.

macromolecular structures. As a result such lipids are likely to be protected against microbial mineralization and thus to efficiently contribute to kerogen formation (Sinninghe-Damsté et al., 1989). The main outcome of sulphur incorporation may therefore be to strongly reduce the degradation that would take place if these lipids remained in a free state. Regarding morphological features, the “vulcanization” process should lead to amorphous kerogen fractions. As already emphasized, the orange AOM that occurs in Kimmeridge Clay kerogens appears truly amorphous when examined by TEM; it is often associated with pyrite and pin-point analyses indicated a substantial content of organic sulphur. In addition, its relative abundance sharply increases with TOC and is at a maximum at the top of the cycle, what is to say for sample T. Moreover, as just discussed, the level of organic sulphur-containing moieties is higher in kerogen T when compared to B. Finally, it is noted that the different series of OSC generated both from B and T are commonly found in the pyrolysates of kerogens which formed via sulphur incorporation into lipids. Taken together, the morphological and chemical features described above therefore strongly point to the formation of the orange AOM occurring in Kimmeridge Clay kerogens via lipid “vulcanization.” The nature of the OSC generated upon pyrolysis indicate that such lipids were dominated by products comprising long polymethyleneic chains as commonly noted, for example, in the total lipid fraction of most microalgae. This formation pathway for the orange AOM is also consistent with previous observations on T_{\max} obtained by Rock-Eval pyrolyses (Ramanampisoa and Disnar, 1994) which indicated a slight but regular increase in T_{\max} when TOC decreases in the microcycle (422°C for sample T and 427°C for B). Differences in maturity could not be responsible for T_{\max} variations over this short-term cycle since no hydrothermal or volcanic alterations occurred and the above differences were considered as reflecting changes in the degree of organic sulphur content. In fact, it is well documented that sulphur-sulphur and sulphur-carbon bonds are much weaker than carbon-carbon bonds (Orr, 1986), thus facilitating thermal degradation.

Indeed, it was previously reported that samples with the highest ThI also show the lowest T_{\max} values (Eglinton et al., 1989). A higher content of orange AOM thus likely accounts for the lower T_{\max} observed in kerogen T when compared to B.

3.2.4. Medium polarity products

The compound series occurring in the toluene-eluted fraction of B and T pyrolysates are reported in Table 2. In both cases the fraction is dominated by a series of *n*-alkan-2-ones. This type of ketone was observed in the pyrolysates of all the algaenans so far examined and, also, of all the kerogens known to be derived from the selective preservation of these resistant biomacromolecules (e.g., Largeau et al., 1986; Flaviano et al., 1994). The thermal cleavage of the ether bridges linking some of the hydrocarbon chains building up the macromolecular skeleton of algaenans accounts for the formation of the ketones (Gelin et al., 1993). Substantial amounts of aromatic, N-containing products, corresponding to series of substituted indoles and quinolines, are also formed from B and T. However, these compounds have not been so far related to a specific type of source organism and biomolecules; thus, the significance of their abundant presence in both pyrolysates has yet to be established.

Normal alkylnitriles are also generated in substantial amounts from kerogen B where they account for ca. 6% of the total pyrolysate; in sharp contrast, these compounds are not clearly detected in the case of sample T. It is now well documented that such nitriles are specific pyrolysis products of the algaenans building up the thin resistant outer walls of numerous species of green microalgae (Derenne et al., 1991a, 1992b). Unlike the *n*-alkan-2-ones mentioned above, these *n*-alkylnitriles are not produced from all types of algaenan and a complete absence of such compounds was previously noted in the case of species (*Botryococcus braunii* and *Tetraedron minimum*) exhibiting thick resistant outer walls. These nitriles were also systematically detected in the pyroly-

sates of ultralaminae-containing kerogens. Indeed as previously shown, the latter structures, which can only be identified by electron microscopy, originate from the selective preservation of thin resistant outer walls of microalgae (Derenne et al., 1991a, 1992c). It was also observed that important differences in *n*-alkylnitrile distribution occur depending on whether the examined samples, i.e., algaenan-composed thin outer walls from extant green microalgae and ultralaminae-containing kerogens, are of a marine or lacustrine origin (Derenne et al., 1992d). With regard to Kimmeridge Clay kerogens, light microscopy and TEM observations revealed a major contribution of brown AOM in kerogen **B** and the bulk of this brown material appears to be composed of lamellar structures reminiscent of ultralaminae. The nature and the origin of these lamellar structures was ascertained, from the pyrolysis experiments, by (1) the relatively abundant presence of *n*-alkylnitriles in sample **B** pyrolysate and (2) the identical distribution of these nitriles when compared to those generated from ultralaminae-containing marine kerogens and from thin algaenan-composed outer walls of extant marine microalgae. These morphological and chemical features observed from kerogen **B** therefore clearly indicate that the brown AOM of the Kimmeridge Clay was formed via the selective preservation of thin resistant microalgal walls. The difficulty of clearly establishing the presence of *n*-alkylnitriles in **T** pyrolysate reflects the relatively low level of brown AOM in this kerogen.

Insoluble and nonhydrolysable macromolecular constituents have been recently shown to also occur in some species of bacteria (Le Berre et al., 1991; Flaviano et al., 1994). As observed for algaenans, the so-called bacterans are located in cell walls. However the skeleton of the cell wall of these bacteria is chiefly composed of hydrolysable macromolecules like peptidoglycans. Accordingly bacterans, when isolated after drastic base and acid hydrolyses, appear as amorphous materials. Similarly, the selective preservation of bacterans results in the formation of amorphous kerogen fractions. Indeed, close chemical relationships have been established between some bacterans and kerogens dominated by nanoscopically amorphous organic matter, as shown by TEM observations (Flaviano et al., 1994). As discussed above, sample **T** is characterized by a low contribution of selectively preserved algal material whereas such constituents played a major role in kerogen **B** formation. Pyrolysis results also point to a substantial contribution of bacteran selective preservation in the genesis of the latter kerogen. Thus, the low polarity fraction of **B** pyrolysate is characterized by the presence of significant amounts of dimethylalkanes (series I) and 3-methylalkanes (Table 1). These two series were previously detected, with similar relative abundances and distributions (odd-carbon-numbered dimethylalkanes and even-carbon-numbered 3-methylalkanes), in pyrolysates of bacterans and derived kerogens (Flaviano et al., 1994). Sample **B** constituents originating from the selective preservation of bacterans should appear as an amorphous material. Accordingly, such constituents are likely to be associated with the amorphous matrix occurring in the black and/or in the brown organic matter and embedding ligneous debris or minerals and ultralaminae, respectively. In agreement with the low contribution of black and brown matter in kerogen **T**, bacteran-related

products are not detected, or in much lower amounts, in the pyrolysate of this sample (Table 1).

3.2.5. Polar products

Fatty acids. The nature and the relative abundances of the fatty acids generated upon pyrolysis of kerogens **B** and **T** are illustrated in Fig. 7. In both cases, the acid fraction is dominated by palmitic acid and also comprises substantial levels of stearic and *n*-C₂₂ saturated acid. The main series in these fractions thus corresponds to C₁₄-C₂₄ normal saturated acids that are characterized by a very strong predominance of the even-carbon-numbered compounds, with Carbon Preference Indexes (CPI)[†] of 0.12 and 0.10 from samples **B** and **T**, respectively. Substantial amounts of normal monounsaturated C₁₆ and C₁₈ acid are also observed, along with low levels of diunsaturated C₁₈ acids including the $\omega(9)$ cis, $\omega(12)$ cis isomer (linoleic acid). A very low contribution of branched, iso and anteiso, saturated C₁₇ compounds is also noted. Comparison of **B** and **T** (Fig. 7) reveals almost identical compositions regarding both their nature and their relative abundances, for the acids released upon pyrolysis.

Fatty acids from extant microalgae and higher plants are generally characterized by a marked predominance of even normal fatty acids, comprising substantial amounts of unsaturated compounds along with saturated acids. However, it is well documented that fatty acids, especially the unsaturated ones, are highly sensitive to microbial degradation. Accordingly, both fatty acids esterified into lipid structures and occurring in a free form are markedly altered during early diagenesis as reflected by a sharp decrease in the predominance of the even compounds and a nearly complete disappearance of the unsaturated acids. Nevertheless, it has been recently shown that fatty acids can escape to diagenetic degradations when they are included, as esters, in insoluble and non-hydrolysable macromolecules like algaenans (Largeau et al., 1986; Kawamura et al., 1986; Fukushima and Ishiwatari, 1988; Derenne et al., 1991b). Such "tightly bound" fatty acids can only be released by a thermal stress and the corresponding ester moieties remain nearly unaffected following diagenesis owing to the very efficient protection provided by the macromolecular network. As a result, the fatty acid fractions generated by pyrolysis of kerogens derived from algaenan selective preservation are characterized by a very low level of alteration.

Fatty acids may also be protected from diagenetic degradation via a second way, based on sulphur incorporation. As already stressed, if "vulcanization" reactions take place during early diagenesis, various lipids can be involved in the formation of insoluble macromolecular structures. Such lipids, including their fatty acid moieties, are then efficiently protected and, owing to this acquired resistance, they will only undergo negligible alterations after the "vulcanization" step.

The presence in kerogen pyrolysates of fatty acids which distribution reveals a low level of alteration should therefore reflect a contribution of the selective preservation of algaenans and/or the occurrence of a fast "vulcanization" dur-

[†] Calculated according to Bray and Evans (1961).

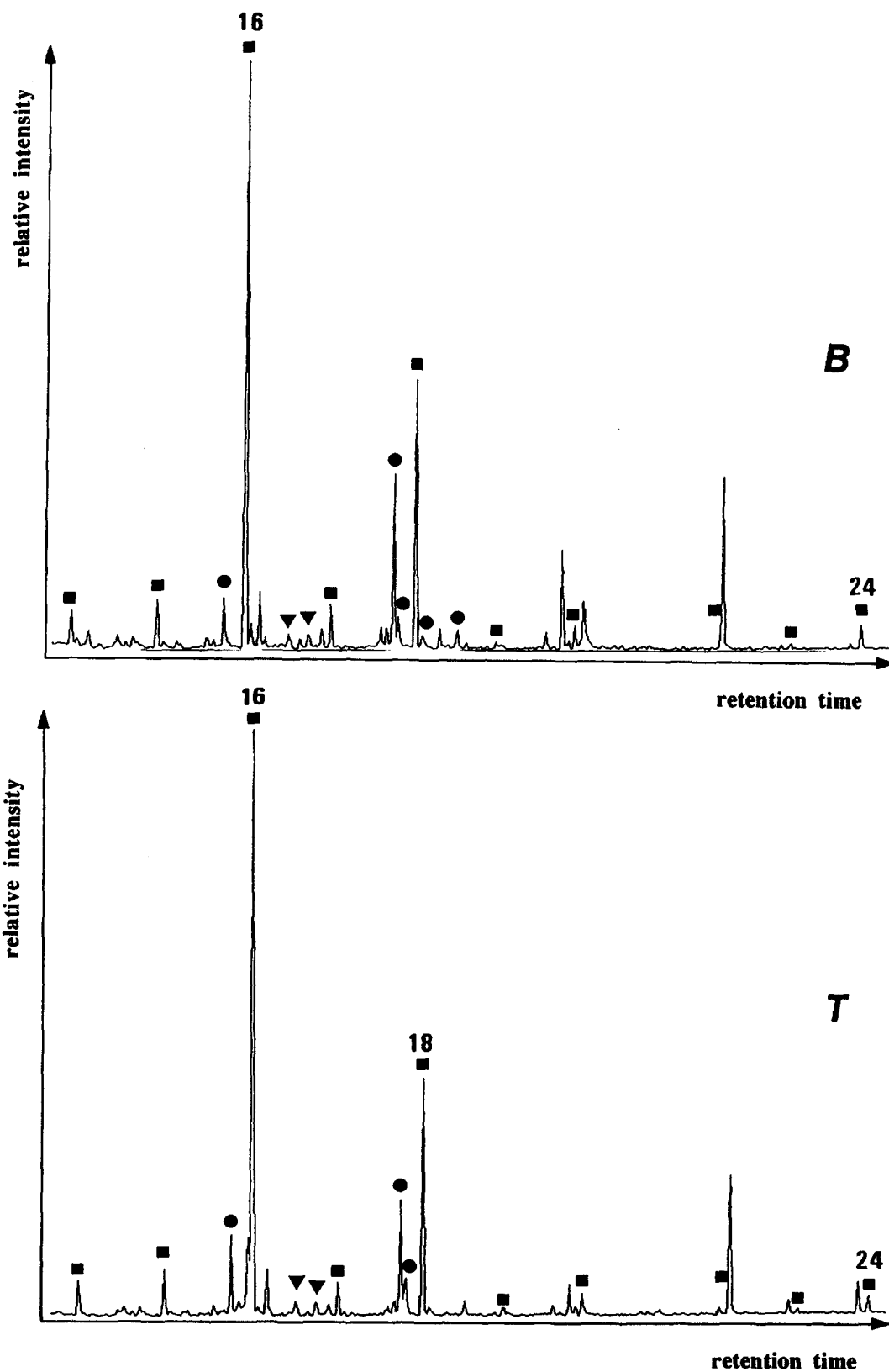


FIG. 7. TIC traces of the acid fractions from "off-line" pyrolysates of samples B and T. Filled squares and circles indicate saturated and unsaturated fatty acids, respectively; filled triangles indicate branched saturated acids.

ing early diagenesis. In fact, these two mechanisms of fatty acid protection appear to be important in B and T kerogens, respectively. The very low level of alteration observed in the acid fractions of their pyrolysates is thus consistent with (1) the formation of the brown AOM, that predominates in B, via algaenan selective preservation and (2) the formation of the orange AOM, accounting for the bulk of T, via lipid "vulcanization".

Non-acid compounds. GC-MS analysis of the non-acid polar fractions only indicated the presence of phenolic compounds. Their distribution is illustrated in Fig. 8 in the case of kerogen B. A similar distribution is also observed from sample T although the relative abundance of these phenols is substantially lower (1.5–2 times), as shown by comparison of the GC traces of the crude pyrolysates. A number of phenols, including series of alkyl-substituted compounds, are generated upon pyrolysis of both B and T. However, the sub-fractions are dominated by mono- and dimethyl products. The latter phenols are well known as typical pyrolysis products of diagenetically altered lignins (Nip et al., 1987). As already discussed, electron microscopy observations on picked out particles showed the prevalence of minute ligneous debris in the black AOM. In addition, the latter material is relatively

more abundant in sample B than in T. Such features, added to the above results on the nature and abundance of phenols in pyrolysates, indicate that a part of the black AOM of Kimmeridge Clay kerogens is of a terrestrial origin and is derived from lignins.

The information obtained from the electron microscopy and pyrolytic studies, on the ultrastructure, the source organisms, and the mechanism of formation of the different types of AOM in the Kimmeridge Clay are summarized in Table 3. Based on these results, and on the variations in AOM relative abundances, a general scheme accounting for the occurrence of TOC and HI microcycles in the Kimmeridge Clay Formation can be established.

3.3. Origin of TOC and HI Cycles

Previous studies indicated that cyclic variations in the Kimmeridge Clay can result neither from changes in redox conditions (because bottomwater remained continuously anoxic during deposition, as shown by the lack of bioturbation and the analysis of inorganic trace elements), nor from changes in the extent of organic matter dilution by detrital and/or biogenic minerals (Tribouillard et al., 1992, 1994; Bertrand and

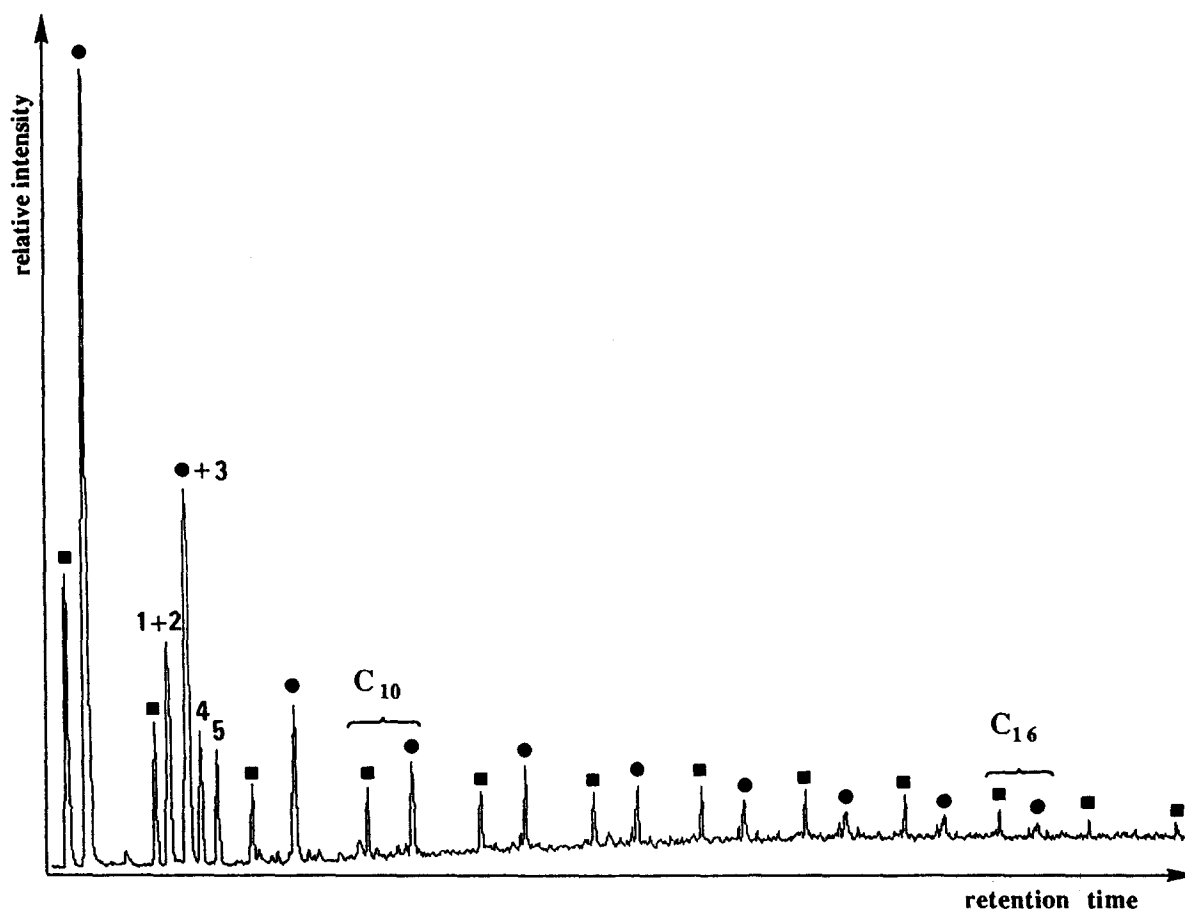


FIG. 8. Summed mass chromatogram of m/z 107 + 108 revealing the distribution of n -alkylphenols in the total "off-line" pyrolysate of sample B. Filled squares indicate the homologous series of *ortho*- n -alkylphenols and filled circles indicate the homologous series of the coeluting *meta*- and *para*- n -alkylphenols. Numbers correspond to the following dimethylphenols: 1 = 2,4-dimethylphenol; 2 = 2,5-dimethylphenol; 3 = 3,5-dimethylphenol; 4 = 2,3-dimethylphenol; 5 = 3,4-dimethylphenol. A similar mass chromatogram was obtained for kerogen T.

Table 3. Relationships between the ultrastructural features, the typical pyrolysis products and the origin of the different types of AOM occurring in Kimmeridge Clay kerogens.

Ultrastructure and AOM type	Typical pyrolysis products *	Process of formation
Massive nanoscopically amorphous orange AOM	Organic sulphur compounds	Lipid "vulcanization"
Ultralaminae of brown AOM	Alkyl nitriles	Algaenan selective preservation
Minute ligneous debris of black AOM	Alkylphenols	Altered lignin preservation
Nanoscopically amorphous matrix of brown and/or black AOM	Branched alkanes	Contribution of bacteran selective preservation

* Fatty acids cannot be related with a given AOM type; they can be associated with any fraction described in this Table except the lignin-derived debris in the black AOM.

Lallier-Vergès, 1993). Accordingly, the typical cycles occurring in the Kimmeridge Clay probably reflect changes in the primary productivity of phytoplanktonic species without mineral tests (Bertrand and Lallier-Vergès, 1993; Bertrand et al., 1994). In addition, examination of kaolinite distribution, also carried out on Kimmeridge Clay samples from the Marton 87 borehole, pointed to a climatic origin for the above changes in primary productivity (Desprairies et al., 1995).

It is well documented that increasing phytoplankton productivity is associated with faster sinking rates (Wefer, 1989). The resultant higher export to deep water is due to the formation of aggregates and flakes (Jackson, 1990). As a result, a larger proportion of the degradable constituents of the primary microalgal biomass can escape mineralization in the upper part of the water column and thus reach the oxic-anoxic interface. This increasing supply of metabolizable organic matter to anoxic bottomwater should promote a prolific growth of sulphate-reducing bacteria (an ubiquitous group of microorganisms in anoxic environments containing both sulphate and organic matter sources, Widdel, 1988; Trudinger, 1992; Elsgaard et al., 1994), hence an intense production of hydrogen sulphide. The latter will rapidly react with available iron to generate iron sulphides; however, a part may react with various lipids according to the already mentioned "vulcanization" process. Lipidic compounds that, otherwise, would be heavily degraded may escape mineralization via this process. Owing to such an acquired resistance, the above lipids will contribute to kerogen formation and a large increase in TOC in the corresponding sediments is thus achieved. (This is also supported by a recent study by Lallier-Vergès et al., (1994) concerned with sulphur content in the Kimmeridge Clay (total S, organic S, pyrite) and suggesting an important role for sulphate reduction intensity in controlling organic matter accumulation). All these interrelationships between primary productivity, sinking rates, and sulphate-reduction intensity, and the resulting control on TOC values, as illustrated in Fig. 9, are fully consistent with the present morphological and chemical results. Thus, an increasing "vulcanization" should be reflected by the formation of high TOC sediments

with an abundant content of orange AOM, as observed at the top of the cycle. Moreover, the morphology of the orange AOM particles and their close association with sulphate-reduction markers (iron sulphides) and clays indicate that such a material was probably generated very early as flocks or mats.

As shown in Fig. 9, decreasing primary productivity will result in lower sinking rates. Extensive mineralization of the degradable constituents of microalgae will therefore take place in the oxic part of the water column. Accordingly, only a weak sulphate reduction intensity will develop in anoxic bottomwater. Under these conditions the amount of buried organic matter will be relatively low and chiefly comprised of biomacromolecules exhibiting a high intrinsic resistance to diagenetic degradations such as the refractory constituents of algal cell-walls and (to a lesser extent) lignins. Indeed, the kerogen samples corresponding to relatively low TOCs, i.e., at the beginning and the end of the cycle, exhibit a low content of orange AOM and are dominated by the brown and black AOMs.

The interrelationships illustrated in Fig. 9 can also account for the cyclic changes in HI occurring, along with TOC variations, in the Kimmeridge Clay Formation. Thus, the high HI values observed at the top of the TOC cycle result from the marked predominance of the orange AOM. The latter, being derived from sulphur incorporation into long chain lipids, should be characterized by a high oil generation potential. Resistant biomacromolecules from algal cell walls are known to be highly aliphatic. As a result, the relatively abundant presence of brown, ultralaminae-composed AOM in kerogen samples with lower TOC, corresponding to the beginning and the end of the cycle, will favour high values for HI. In sharp contrast the black AOM, mainly derived from lignins, shall be characterized by extremely low HI. The substantial contribution of this material in the samples with lower TOC account for their relatively low HI. Moreover, in such samples with TOC values around 2%, a mineral matrix effect (Espitalié et al., 1980; Katz, 1983) may also contribute to HI lowering.

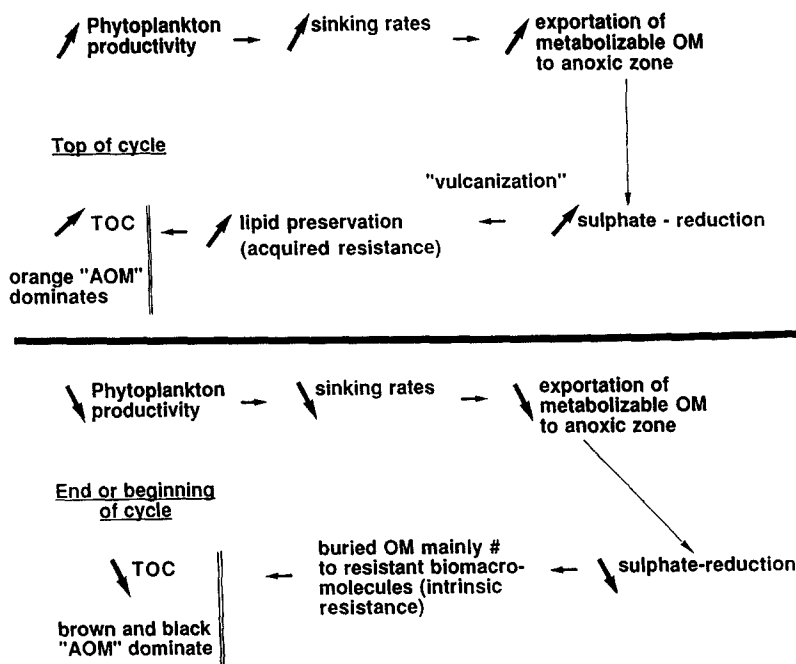


FIG. 9. Postulated relationships between primary productivity, sulphate reduction intensity, TOC and HI microcyclic variations, and the dominant type(s) of AOM in Kimmeridge Clay kerogens.

4. CONCLUSIONS

The combination of high resolution sampling of a Kimmeridge Clay microcycle, of transmission electron microscopy observations on total isolated kerogens, on handpicked kerogen particles and on untreated rock fragments, along with flash and off-line pyrolytic studies allowed:

- 1) Precise information to be derived on the morphological features of the three types of so-called "amorphous" organic matter previously defined by light microscopy in the Kimmeridge Clay. The orange AOM is truly amorphous whereas the brown AOM is chiefly composed of ultralaminae and the black AOM of minute ligneous debris embedded within a diffuse nanoscopically amorphous matrix. It was also shown that the maceral bituminite, observed in situ from polished sections, corresponds to the orange AOM identified in palynofacies studies.
- 2) Elucidation of the sources and modes of formation of the three above types of organic matter. The orange AOM originates from sulphur incorporation into lipids, whereas the brown AOM is derived from the selective preservation of algaenan-composed thin outer walls of microalgae. The black AOM is likely to be highly heterogeneous and it was shown to comprise contributions from altered lignins and selectively preserved bacterans.
- 3) Explanation of (1) the large changes in the relative abundances of the three types of AOM occurring, in Kimmeridge Clay kerogens, along a ca. 30,000 years microcycle and (2) the origin of the parallel, cyclic, wave-shaped variations in kerogen quantity (TOC) and quality (HI) typical of the Kimmeridge Clay Formation. Such variations stemmed from modifications in primary productivity rate. However, the production of microalgal biomass did not exert a direct and simple control on TOC and HI. In fact,

the extent of lipid "vulcanization" was probably a major parameter that strongly amplified the effects of primary productivity variations originating from global environmental changes. The values of TOC and HI and the relative abundances of the different types of AOM in the Kimmeridge Clay appear therefore to be controlled by a balance between a number of interrelated processes concerned both with the nature of the deposited biomass and deposition conditions: (1) the extent of terrestrial material contribution (minute ligneous debris of the black material), (2) the level of resistant biomacromolecules in the source microorganisms (algaenans and bacterans forming, via selective preservation, the bulk of the brown material (ultralaminae), and a part of the amorphous matrix of the black and/or brown AOM's, respectively), and (3) the intensity of lipid "vulcanization" leading to the orange material. This intensity being controlled by several factors including the amount of metabolizable organic matter reaching the oxic-anoxic interface, the occurrence of suitable conditions, in anoxic bottomwater, allowing for a prolific growth of sulphate-reducers and a somewhat limited supply of iron so that the produced H_2S is not entirely trapped as pyrite. Finally, the first of the above parameters is determined, in turn, by the depth of the oxic part of the water column and by primary productivity-controlled sinking rates. The OM accumulated in the Kimmeridge Clay thus chiefly originates from the contributions of both macromolecular compounds with a high intrinsic resistance to diagenetic degradations, like algaenans, bacterans and lignins, and lipidic components that acquired a resistant nature via "vulcanization." Kerogen quality (HI) reflects the balance between these different contributions, high HI values being promoted by large levels of "vulcanized" lipids, and/or selectively preserved algaenans.

Acknowledgments—Financial support was provided by the Research Group GdR 942 (CNRS, IFP, Total, Elf Aquitaine, Universités d'Orléans et de Paris-Sud). A special thank is devoted to all the scientists of this Research Group. We are also indebted to D. Jalabert from the "Service central de microscopie électronique de l'Université d'Orléans" for its technical assistance. Dr. J. W. de Leeuw (NIOZ, Netherlands) is gratefully acknowledged for permitting access to the Py-GC-MS instrument. We are grateful to the reviewers, Drs. T. I. Eglinton, B. Horsfield and S. W. Imbus and the Associate Editor for constructive comments.

Editorial handling: J. T. Senftle

REFERENCES

- Bertrand P. and Lallier-Vergès E. (1993) Past sedimentary organic matter accumulation and degradation controlled by productivity. *Nature* **364**, 786–788.
- Bertrand P. et al. (1990) Examples of spatial relationships between organic matter and mineral groundmass in the microstructure of the organic-rich Dorset Formation rocks (Great Britain). *Org. Geochem.* **16**, 661–675.
- Bertrand P., Lallier-Vergès E., and Boussafir M. (1994) Enhancement of both accumulation and anoxic degradation of organic carbon controlled by cyclic productivity: a model. *Org. Geochem.* **22**, 511–520.
- Bishop A. N. and Philp R. P. (1994) The potential for amorphous kerogen formation via adsorption of organic material at mineral surfaces. 207th American chemical Society 1994, National Meeting, March 13–18, San Diego, CA, USA.
- Boucher R. J., Standen G., Patience R. L., and Eglinton G. (1990) Molecular characterisation of kerogen from the Kimmeridge clay formation by mild selective chemical degradation and solid state ¹³C-NMR. *Org. Geochem.* **16**, 951–958.
- Boussafir M., Lallier-Vergès E., Bertrand P., and Badaut-Trauth D. (1994a) Etude ultrastructurale de matières organiques micro-prélevées dans les roches de la "Kimmeridge Clay Formation" (Yorkshire, UK). *Bull. Centres Rech. Explor. Prod. Elf-Aquitaine*, pp. 275–277.
- Boussafir M., Lallier-Vergès E., Bertrand P., and Badaut-Trauth D. (1994b) Structure ultrafine de la matière organique des roches mères du kimméridgien du Yorkshire (UK). *Bull. de la Soc. Géol. de Fr.* **165**, 355–363.
- Boussafir M., Lallier-Vergès E., Bertrand P., and Badaut-Trauth D. (1995) SEM and TEM studies on isolated organic matter and rock microfacies from a short-term organic cycle of the Kimmeridge Clay Formation (Yorkshire, G.B.). *Lecture Notes in Earth Science Series* **57**, pp. 15–30. Springer-Verlag.
- Bray E. E. and Evans E. D. (1961) Distribution of *n*-paraffins as a clue to recognition of source beds. *Geochim. Cosmochim. Acta* **22**, 2–15.
- Derenne S., Largeau C., Casadevall E., Berkaloff C., and Rousseau B. (1991a) Chemical evidence of kerogen formation in source rocks and oil shales via selective preservation of thin resistant outer walls of microalgae: Origin of ultralaminae. *Geochim. Cosmochim. Acta* **55**, 1041–1050.
- Derenne S., Largeau C., and Casadevall E. (1991b) Occurrence of tightly bound isoprenoid acids in an algal, resistant biomacromolecule: possible geochemical implications. *Org. Geochem.* **17**, 597–602.
- Derenne S. et al. (1992a) Similar morphological and chemical variations of *Gloeocapsomorpha prisca* in Ordovician sediments and cultured *Botryococcus braunii* as a response to changes in salinity. *Org. Geochem.* **19**, 299–313.
- Derenne S., Largeau C., Berkaloff C., Rousseau B., Wilhelm C., and Hatcher P. G. (1992b) Non-hydrolysable macromolecular constituents from outer walls of *Chlorella fusca* and *Nanochlorum eucaryotum*. *Phytochemistry* **31**, 1923–1929.
- Derenne S., Largeau C., and Hatcher P. G. (1992c) Structure of *Chlorella fusca* algaenan: Relationships with ultralaminae in lacustrine kerogens; species- and environment-dependent variations in the composition of fossil ultralaminae. *Org. Geochem.* **18**, 417–422.
- Derenne S., Le Berre F., Largeau C., Hatcher P., Connan J., and Raynaud J. F. (1992d) Formation of ultralaminae in marine kerogens via selective preservation of thin resistant outer walls of microalgae. *Org. Geochem.* **19**, 345–350.
- Derenne S., Largeau C., and Taulelle F. (1993) Elucidation, via solid-state ¹⁵N NMR, of the origin of the alkylnitriles generated upon pyrolysis of ultralaminae-containing kerogens. In *Organic Geochemistry* (ed. K. Øygard), pp. 766–770. Falch Hurtigtrykk.
- Desprairies A., Bachaoui M., Ramdani A., and Tribovillard N. P. (1995) Clay diagenesis in organic-rich cycles from the Kimmeridge Clay Formation of Yorkshire (G. B.): implication for palaeoclimatic interpretations. In *Lecture Notes in Earth Sciences* **57**, pp. 63–91. Springer-Verlag.
- Eglinton T. I., Rowland S. J., Curtis C. D., and Douglas A. G. (1986) Kerogen-mineral reactions at raised temperatures in the presence of water. *Org. Geochem.* **10**, 1041–1052.
- Eglinton T. I., Douglas A. G., and Rowland S. J. (1988a) Release of aliphatic, aromatic and sulphur compounds from Kimmeridge kerogen by hydrous pyrolysis: A quantitative study. *Org. Geochem.* **13**, 655–663.
- Eglinton T. I., Philp R. P., and Rowland S. J. (1988b) Flash pyrolysis of artificially matured kerogens from the Kimmeridge Clay (U.K.). *Org. Geochem.* **12**, 33–41.
- Eglinton T. I., Sinninghe-Damsté J. S., Kohnen M. E. L., de Leeuw J. W., Larter S. R., and Patience R. L. (1989) Analysis of maturity-related changes in the organic sulfur composition of kerogens by flash pyrolysis-gas chromatography. In *Geochemistry of Sulfur in Fossil Fuels* (ed. W. L. Orr and C. M. White); *ACS Symposium Series* **429**, pp. 529–565. Amer. Chem. Soc.
- Eglinton T. I., Sinninghe-Damsté J. S., Kohnen M. E. L., and de Leeuw J. W. (1990) Rapid estimation of the organic sulphur content of kerogens, coals and asphaltenes by pyrolysis-gas chromatography. *Fuel* **69**, 1394–1404.
- Elsgaard L., Isaksen M. F., Jørgensen B. B., Alayse A.-M., and Jannasch H. W. (1994) Microbial sulfate reduction in deep-sea sediments at the Guaymas Basin hydrothermal vent area: Influence of temperature and substrates. *Geochim. Cosmochim. Acta* **58**, 3335–3343.
- Espitalié J., Madec M., and Tissot B. (1980) Role of mineral matrix in kerogen pyrolysis: influence on petroleum generation and migration. *AAPG Bull.* **64**, 59–66.
- Farrimond P. et al. (1984) Organic geochemical study of the Upper Kimmeridge Clay of the Dorset type area. *Mar. Petrol. Geol.* **1**, 340–354.
- Flaviano C., Le Berre F., Derenne S., Largeau C., and Connan J. (1994) First indications of the formation of kerogen amorphous fractions by Selective Preservation. Role of non-hydrolysable macromolecular constituents of Eubacterial cell walls. *Org. Geochem.* **22**, 759–771.
- Fukushima K. and Ishiwatari R. (1988) Geochemical significance of lipids and lipid-derived substructures interlaced in kerogen. *Org. Geochem.* **12**, 509–518.
- Gallois R. W. (1976) Coccolith blooms in the Kimmeridge Clay and origin of the North Sea oil. *Nature* **259**, 473–475.
- Gelin F. et al. (1993) Mechanisms of flash pyrolysis of ether lipids isolated from the green microalga *Botryococcus braunii* race A. *J. Anal. Appl. Pyrolysis* **27**, 155–168.
- Herbin J. P., Geysant J. R., Müller C., Mélières F., le groupe YOR-KIM, and Penn I. E. (1991) Hétérogénéité quantitative et qualitative de la matière organique dans les argiles du Kimméridgien du val de Pickering (Yorkshire, UK). Cadre sédimentologique et stratigraphique. *Rev. Inst. Fr. Pétrol.* **46**, 1–39.
- Herbin J. P., Müller C., Geysant J. R., Mélières F., and Penn I. E. (1993) Variation of the Distribution of organic matter within a transgressive system tract: Kimmeridge Clay (Jurassic), England. In *AAPG 1993 "Petroleum source rocks in a sequence stratigraphic framework"* (ed. B. Katz and L. Pratt), pp. 67–100.
- Huc A. Y., Lallier-Vergès E., Bertrand P., Carpentier B., and Hollander D. J. (1992) Organic matter response to change of depositional environment in Kimmeridgian shales, Dorset, U.K. In *Organic Matter: Productivity, Accumulation and Preservation of Organic Matter in Recent and Ancient Sediments* (ed. J. Whelan and J. Farrington), pp. 469–486. Columbia Univ. Press.

- Jackson G. A. (1990) A model of the formation of marine algal flocs by physical coagulation processes. *Deep-Sea Res.* **37**, 1197–1211.
- Katz B. J. (1983) Limitations of "Rock-Eval" pyrolysis for typing organic matter. *Org. Geochem.* **4**, 195–199.
- Kawamura K., Tannenbaum E., Huizinga B. J., and Kaplan I. R. (1986) Long-chain carboxylic acids in pyrolysates of Green River kerogen. In *Advances in Organic Geochemistry 1985* (ed. D. Leythaeuser and J. Rullkötter); *Org. Geochem.* **10**, 1059–1065. Pergamon.
- Krein E. B. and Aizenshtat Z. (1994) The formation of isoprenoid sulfur compounds during diagenesis: simulated sulfur incorporation and thermal transformation. *Org. Geochem.* **21**, 1015–1025.
- Lallier-Vergés E., Boussafir M., Bertrand P., and Badaut-Trauth D. (1993a) Selective preservation of various organic matter types as assessed by STEM studies on a cyclic productivity-controlled sedimentary series (Kimmeridge Clay Formation). In *Organic Geochemistry: Poster sessions from the 16th International Meeting on Organic Geochemistry, Stavanger, 1993* (ed. K. Øygard), pp. 384–386. Falch Hurtigtrykk.
- Lallier-Vergés E., Bertrand P., Büchel D., Huc A. Y., and Tremblay P. (1993b) Control of the preservation of organic matter by productivity and sulphate reduction in Kimmeridgian shales from Dorset (UK). *Mar. Petrol. Geol.* **10**, 600–605.
- Lallier-Vergés E. et al. (1994) Productivity-induced sulfur enrichment of organic-rich sediments. 207th American Chemical Society 1994, National Meeting—March 13–18, San Diego, CA, USA.
- Largeau C., Derenne S., Casadevall E., Kadouri A., and Sellier N. (1986) Pyrolysis of immature Torbanite and of the resistant biopolymer (PRBA) isolated from extant alga *Botryococcus braunii*. Mechanism of formation and structure of Torbanite. In *Advances in Organic Geochemistry 1985* (ed. D. Leythaeuser and J. Rullkötter); *Org. Geochem.* **10**, 1023–1032. Pergamon.
- Largeau C. et al. (1990a) Occurrence and origin of ultralaminar structures in "amorphous" kerogens from various source-rocks and oil-shales. In *Advances in Organic Geochemistry 1989* (ed. B. Durand and F. Behar), pp. 889–896. Pergamon.
- Largeau C. et al. (1990b) Characterization of various kerogens by Scanning Electron Microscopy (SEM) and Transmission Electron Microscopy (TEM)—Morphological relationships with resistant outer walls in extant microorganisms. *Meded. Rijks Geol. Dienst.* **45**, 91–101.
- Le Berre F., Derenne S., Largeau C., Connan J., and Berkaloff C. (1991) Occurrence of non-hydrolysable, macromolecular, wall constituents in bacteria. Geochemical implications. In *Organic Geochemistry Advances and Applications in Energy and the Natural Environment* (ed. D. A. C. Manning), pp. 428–431. Manchester Univ. Press.
- Lugardon B., Raynaud J. F., and Husson P. (1991) Données ultra-structurales sur la matière organique amorphe des kérogènes. *Palyoscience* **1**, 69–88.
- Nip M., de Leeuw J. W., and Schenck P. A. (1987) Structural characterization of coals, coal macerals and their precursors by pyrolysis-gas chromatography and pyrolysis-gas chromatography-mass spectrometry. *Coal Sci. Technol.* **11**, 89–92.
- Orr W. L. (1986) Kerogen/asphaltene/sulfur relationships in sulfur-rich Monterey oils. *Org. Geochem.* **10**, 499–516.
- Pfendt P. A. (1984) Comparison of the general chemical nature of various kerogens based on their reactivities towards bromine. *Org. Geochem.* **6**, 383–390.
- Pradier B. and Bertrand P. (1992) Etude à haute résolution d'un cycle de carbone organique des argiles du Kimméridgien du Yorkshire (GB): relation entre composition pétrographique du contenu organique observé in-situ, teneur en carbone organique et qualité pétrologène. *C.R. Acad. Sc. Paris* **315**, 187–192.
- Ramanampisoa L. and Disnar J. R. (1994) Primary control of paleo-production on organic matter preservation and accumulation in the Kimmeridge rocks of Yorkshire (UK). *Org. Geochem.* **21**, 1153–1167.
- Ramanampisoa L., Bertrand P., Disnar J. R., Lallier-Vergés E., Pradier B., and Tribouillard N. P. (1992) Etude à haute résolution d'un cycle de carbone organique des argiles du Kimméridgien du Yorkshire (GB): résultats préliminaires de géochimie et de pétrographie organique. *C. R. Acad. Sc. Paris* **314**, 1493–1498.
- Raynaud J. F., Lugardon B., and Lacrampe-Couloume G. (1988) Observation de membranes fossiles dans la matière organique "amorphe" de roches-mères de pétrole. *C. R. Acad. Sci. Paris* **307**, 1703–1709.
- Schouten S., van Driel G. B., Sinninghe-Damsté J. S., and de Leeuw J. W. (1994) Natural sulphurization of ketones and aldehydes: A key reaction in the formation of organic sulphur compounds. *Geochim. Cosmochim. Acta* **57**, 5111–5116.
- Sinninghe-Damsté J. S. and de Leeuw J. W. (1990) Analysis, structure and geochemical significance of organically-bound sulphur in the geosphere: State of the art and future research. In *Advances in Organic Geochemistry 1989* (ed. B. Durand and F. Behar); *Org. Geochem.* **16**, 1077–1101. Pergamon.
- Sinninghe-Damsté J. S., Eglinton T. I., de Leeuw J. W., and Schenck P. A. (1989) Organic sulphur in macromolecular sedimentary organic matter: I. Structure and origin of sulphur-containing moieties in kerogens, asphaltenes and coals as revealed by flash pyrolysis. *Geochim. Cosmochim. Acta* **53**, 873–889.
- Smith P. M. R. (1984) The use of fluorescence microscopy in the characterisation of amorphous organic matter. *Org. Geochem.* **6**, 839–845.
- Tribouillard N. P., Desprairies A., Bertrand P., Lallier-Vergés E., Disnard J.-R., and Pradier B. (1992) Etude à haute résolution d'un cycle du carbone organique de roches kimméridgiennes du Yorkshire (Grande-Bretagne): minéralogie et géochimie (résultats préliminaires). *C. R. Acad. Sci. Paris* **314** (II), 923–930.
- Tribouillard N. P. et al. (1994) Geochemical study of organic matter rich cycles from the Kimmeridge Clay Formation of Yorkshire (UK): productivity versus anoxia. *Palaeogeogr. Palaeoclim. Palaeoecol.* **108**, 165–181.
- Trudinger P. A. (1992) Bacteria sulfate reduction: Current status and possible origin. In *Early Organic Evolution: Implications for Mineral and Energy Resources* (ed. M. Schidlowski et al.), pp. 367–377. Springer-Verlag.
- Tyson R. V., Wilson R. C. L., and Downie C. (1979) A stratified water column environmental model for the type Kimmeridge Clay. *Nature* **277**, 377–380.
- Wefer G. (1989) Particles flux in the Oceans: effects of episodic production. In *Report of the Dahlem Workshop on Productivity of the Oceans: Present and Past* (ed. W. H. Berger, V. S. Smetacek, and G. Wefer), pp. 139–154. Wiley.
- Widdel F. (1988) Microbiology and ecology of sulfate- and sulfur-reducing bacteria. In *Biology of Anaerobic Organisms* (ed. J. B. Zehnder), pp. 469–585. Wiley.
- Williams P. F. V. (1986) Petroleum Geochemistry of the Kimmeridge Clay of onshore southern and eastern England. *Mar. Petrol. Geol.* **3**, 258–281.
- Williams P. F. V. and Douglas A. G. (1980) A preliminary organic geochemical investigation of the Kimmeridgian oil shales. In *Advances in Organic Geochemistry 1979* (ed. A. G. Douglas and J. R. Maxwell), pp. 531–545. Pergamon.
- Williams P. F. V. and Douglas A. G. (1983) The effect of lithologic variation on organic geochemistry in the Kimmeridge Clay, Britain. In *Advances in Organic Geochemistry 1981* (ed. M. Bjorøy et al.), pp. 568–575. Pergamon.



Comparative study of organic matter preservation in immature sediments along the continental margins of Peru and Oman. Part I: Results of petrographical and bulk geochemical data

ANDREAS LÜCKGE,¹ MOHAMMED BOUSSAFIR,²
ELISABETH LALLIER-VERGÈS² and RALF LITCKE¹

¹Forschungszentrum Jülich GmbH (KFA), Institut für Chemie und Dynamik der Geosphäre (ICG-4), D-52425, Jülich, Germany and ²URA 724-FR 09 du CNRS, Université d'Orléans, Dépt. des Sciences de la Terre, F-45067, Orléans Cedex, France

Abstract—Detailed petrographical and bulk geochemical investigations of organic matter (OM) have been performed on sediments deposited below or close to upwelling areas offshore Peru (ODP-Leg 112; Sites 679, 681, 688) and Oman (ODP-Leg 117; Sites 720, 723, 724) in order to obtain a quantitative understanding of its accumulation and degradation. Microscopical as well as nanoscopical investigations reveal that the OM in sediments affected by upwelling mechanisms mainly (up to 98%) consists of unstructured (amorphous) organic aggregates without any apparent biological structures. In sediments which are not or to a lesser extent affected by upwelling (Site 720) terrestrial OM predominates.

Organic carbon (TOC) contents are highly variable and range between 9.8% in sediments deposited below upwelling cells and 0.2% in sediments outside the upwelling zone. The TOC/sulphur ratios of the sediments scatter widely. The samples from the deep-water locations (Sites 688 and 720), show C/S-ratios of "normal" marine sediments, whereas at the other locations no correlation or even a negative correlation between sulphur and TOC concentration exists. In most of the upwelling-influenced sediments OM contains a significant amount of sulphur. The incorporation of sulphur into the OM followed microbial sulphate reduction and occurred in the upper meters of the sedimentary column. Below, OM is still present in vast amounts and relatively hydrogen-rich, but is nevertheless non-metabolizable and becomes the limiting factor for bacterial sulphate reduction.

According to mass balance calculations 90–99% of the OM produced in the photic zone was remineralized and 1–3% was consumed by microbial sulphate reduction. The aerobic and anaerobic processes have greatly affected degradation and conservation of OM. Copyright © 1996 Elsevier Science Ltd

Key words—sulphur in immature sediments, sulphate reduction, unstructured (amorphous) organic matter, organic petrology, upwelling

INTRODUCTION

In general, marine sediments are lean in organic carbon (TOC). "Normal" marine deep-sea sediments usually contain less than 0.2% TOC (McIver, 1975). In contrast sediments from upwelling areas are characterised by significantly higher TOC contents, which are generally greater than 1%. In the case of coastal upwelling, surface ocean water, triggered by atmospheric and oceanic circulation, is driven offshore and is replaced by deep water enriched in nutrients. This replenishment of surface waters leads to an increased fertility resulting in a high primary productivity. The high primary productivity enhances the flux of organic particles sinking through the water column and results in an increased accumulation of organic matter (OM) in sediments below the upwelling cells. In addition, the high bioproductivity favours, by the decay of OM, a depletion of dissolved oxygen and results in stable and extended oxygen-minimum-zones (OMZ).

In this study we have compared sediments from two of the most prominent Neogene coastal

upwelling regions, from offshore Peru and Oman. The strong trade winds along the Peruvian coast result in a persistent upwelling which creates one of the most productive areas in modern day oceans (Heinze and Wefer, 1992) with primary productivity rates of about 200 gC/m²/a. In contrast, upwelling in the Arabian Sea caused by strong monsoonal southwest winds occurs from June to September. Similarly to the case of the Peruvian upwelling area, the annual productivity rates reach up to 200 gC/m²/a. This contrasts with "normal" marine conditions characterized by a primary production of only 20–60 gC/m²/a (Berger, 1989) for most areas. Besides primary productivity, bulk sedimentation rates as well as early diagenetic conditions have an important impact controlling the preservation and accumulation of TOC-rich sediments. Under oxygen-deficient conditions prevailing in upwelling areas microbial sulphate reduction processes play a significant role in the accumulation of OM (Calvert and Pedersen, 1992).

In this paper we present new petrographical and geochemical data in order to elucidate the factors

controlling the accumulation of OM in sediments deposited below or close to upwelling areas. Furthermore, the areal distribution of OM quantity, quality and the vertical distribution at selected locations (boreholes) are discussed. Special emphasis will be given to the net effect of bacterial sulphate reduction. Finally, mass balance calculations are presented which give insight into the rate of total OM degradation at the various sites. In a subsequent publication, aspects of kerogen pyrolysis as well as molecular geochemical data will be discussed for the same set of samples.

Geological background

This study examines sediments deposited below upwelling cells which were recovered during ODP-Leg 112 offshore Peru (Suess *et al.*, 1988) and ODP-Leg 117 (Prell *et al.*, 1989) offshore Oman. Twenty-nine samples were collected from Sites 679, 681, 688 (Peru; Fig. 1a) and 64 samples from Sites 720, 723 and 724 (Oman; Fig. 1b).

The most landward Peruvian Site 681 (Hole B) is located in the Salaverry Basin at a water depth of 150.5 m. This site is nearest to the present upwelling centers. At Site 681, the sediment/water interface lies close to the upper boundary of the OMZ. Samples were taken from the lithological Units I–III as defined in Suess *et al.* (1988). The sediments of Unit I are dominantly composed of laminated, olive-gray diatomaceous muds. The diatoms are enriched in thin yellow-brown layers. Below the laminated muds with high biogenic silica contents (up to 40%), more bioturbated sediments containing higher proportions of clastic components are present. Unit I stratigraphically belongs to the Holocene/Pleistocene and has a thickness of 35 m. Unit II (Pleistocene) is characterized by a higher amount of bioturbated sediments and a higher input of sandy and silty material. Unit III is of Pleistocene age and is dominated by olive-gray, laminated diatomaceous muds interbedded with thin, more terrigenously influenced, bioturbated intervals. The unit reaches from 97 to 135 meters below sea floor (mbsf).

The sediments at Site 679 (Hole D) were deposited within an intense oxygen-minimum-zone. Site 679 is located in the Lima Basin at the seaward edge on the upper slope of the Peruvian margin at a present water depth of 439.5 m. Samples were taken from the (lithologically separated) Units I–III as defined in Suess *et al.* (1988). The Quaternary and Pliocene samples of Unit I and Unit II consist mainly of olive-gray to black, TOC-rich, foraminifer-bearing and diatomaceous mud, which show partly massive and partly laminated sequences. The Pliocene to Miocene Unit III (102–236 m depth) is composed of clayey and silty diatomaceous muds. These hemipelagic sediments are interbedded with sandy and silty sections, which are of shallow marine origin.

Site 688 (Holes A and E) is situated in the forearc basin off Peru on the lower continental slope at a

water depth of 3830 m and below the OMZ. The sedimentary sequence of 745 m thickness can be divided into three lithologic units. Unit I is of Holocene to Pleistocene age and is characterized by the predominance of olive-gray to dark-gray, TOC-rich diatomaceous ooze, interlayered with turbidites in the upper part of the section. Unit I also shows bioturbated intervals indicating that these sediments were deposited under more oxygenated water conditions. Below 338 m, Unit II (Pliocene to Miocene) consists of dark-gray diatomaceous mudstones. Unit III (Eocene) comprises sediments rich in terrigenous components. This unit extends from 595 to 769 m depth. In contrast to Units I and II the absence of diatoms is striking within this unit.

The sediments drilled in the Arabian Sea were taken from cores of the Oman margin (Sites 723 and 724). They are directly influenced by upwelling processes. For comparison sediments were selected from the adjacent, distal Indus Fan (Site 720) which are not or to a lesser degree affected by upwelling.

Site 724 (Holes B and C) is situated at a water depth of 600 m in the upper slope basin on the continental margin within the center of the OMZ. The penetrated sediments are of Holocene to early Pliocene age and comprise a sequence of calcareous, black to olive clayey silts. At the Pliocene/Pleistocene boundary an interval (216–220 mbsf) enriched in diatoms and radiolarians associated with high TOC contents was found. The occurrence of these siliceous organisms coincides with lamination implying anoxic or oxygen-deficient conditions in the bottom water.

Site 723 was drilled in an upper slope basin at a water depth of 808 m and is positioned within the OMZ. The whole sequence which is of Holocene to uppermost Pliocene age is lithologically uniform. These TOC-rich 432 m thick sediments are composed of foraminifer-bearing, marly nannofossil ooze and olive-gray, calcareous, clayey silts. The partly laminated Pliocene and lower Pleistocene sediments indicate low oxygen contents of the bottom water during deposition.

Site 720 (Hole A) is located on the middle Indus Fan at a water depth of 4045 m. The penetrated sequence of Holocene to Pleistocene sediments can be subdivided lithologically into two TOC-poor units. Unit I is dominated by pelagic nannofossil ooze interbedded with turbidites whereas Unit II, starting at 17 m depth, is characterized by a high clastic, turbidite input intercalated with thin nannofossil ooze layers.

EXPERIMENTAL METHODS

The sediment samples were dried at 40°C for 12 h. Part of the material was embedded in epoxy resin for microscopic studies in incident light. The surfaces of the impregnated blocks were ground flat and polished. The determination of the maceral

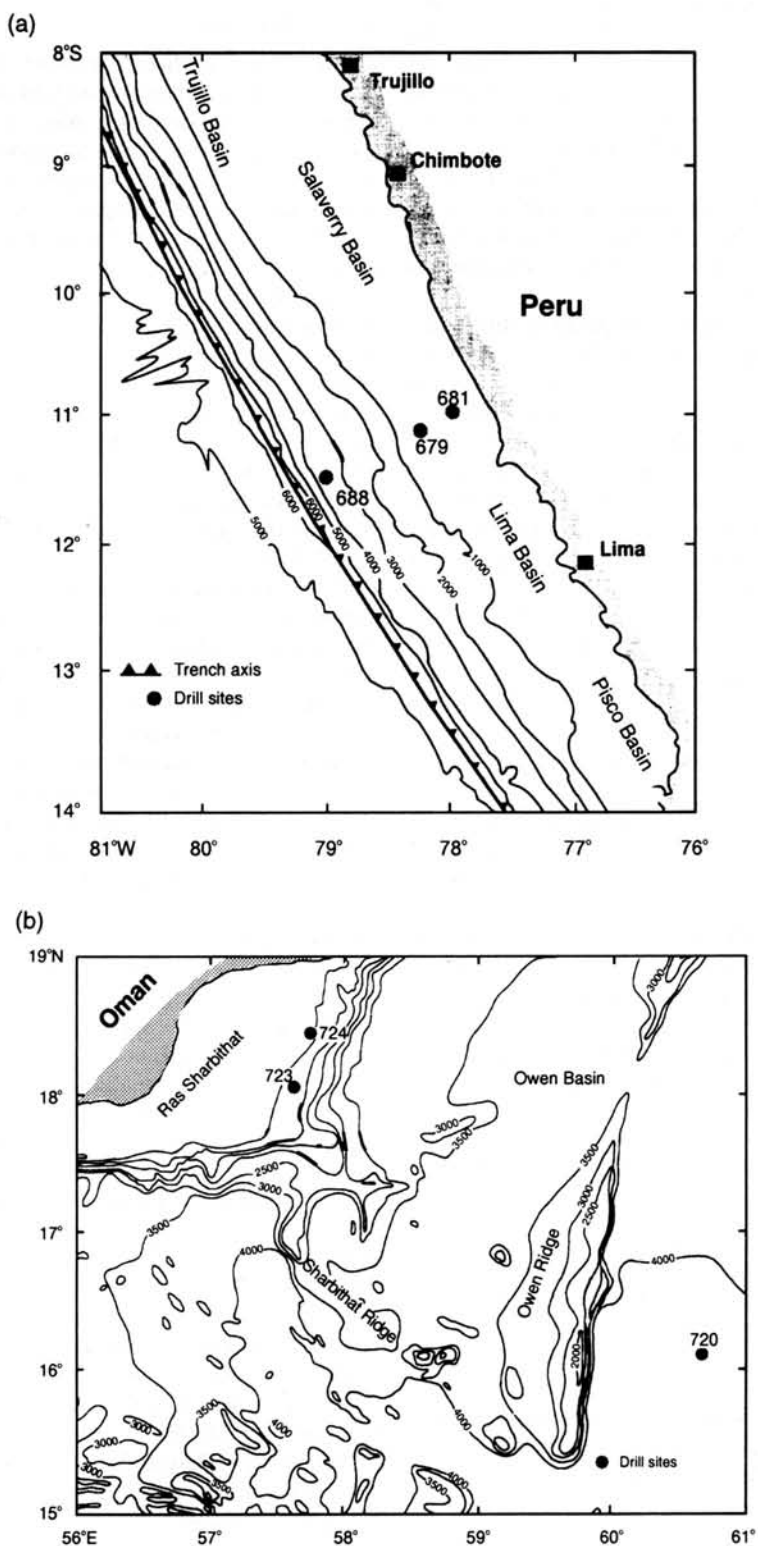


Fig. 1. (A) Location map of Sites 679, 681 and 688 drilled during Leg 112 of the "Ocean Drilling Program" offshore Peru. (B) Location map of Sites 720, 723 and 724 drilled during Leg 117 of the "Ocean Drilling Program" offshore Oman.

composition followed the classification of Stach (1982) using reflected white and fluorescence light (UV-excitation) microscopy. In addition, nine samples were observed under a transmission electron microscope (TEM). For that purpose, sediment samples were fixed by Osmium Tetroxyde and after stepwise dehydration with acetone they were progressively impregnated with epon 812 resin. Ultrathin sections (500 Å in thickness) were obtained using an ultramicrotome equipped with a diamond knife. Details of the analytical procedure are described in Boussafir *et al.* (1995).

Kerogen concentrates were prepared by stirring the samples in hydrochloric acid (25%) for 2 h. After washing and neutralization with distilled water the samples were treated with a mixture of hydrochloric (25%) and hydrofluoric (48%) acid and stirred for 16 h. Afterwards they were washed and neutralized again. Part of the dried OM was used for microscopic studies (incident light) as described above. Another part was prepared for palynofacies investigations in transmitted light (Bertrand *et al.*, 1990).

Organic carbon (TOC) and sulphur (S) contents were measured by combustion under oxygen flow using a LECO IR-112 carbon analyzer. Iron concentrations were determined for kerogen concentrates by X-ray fluorescence (XRF) analysis, using a RIGAKU, SMAX spectrophotometer.

Rock-Eval pyrolysis was performed using a Rock-Eval-II analyzer (GEOCOM). Fundamentals and more details of this method are described in Espitalié *et al.* (1977) and Tissot and Welte (1984).

The calculation of mass accumulation rates of total organic carbon (MARTOC) according to van Andel *et al.* (1975) can be used to obtain further insight into the supply and preservation of OM (Stein *et al.*, 1989). The sedimentation rate and physical data necessary for this calculation were taken from Suess *et al.* (1988) and Prell *et al.* (1989).

$$MARTOC = TOC/100 * SR * (WBD - 1.025Po/100)$$

where

MARTOC = mass accumulation rate of total organic carbon (g/m²/a)

TOC = total organic carbon (wt%)

SR = mean sedimentation rate (cm/a)

WBD = wet bulk density (g/cm³)

Po = porosity

The calculation of sulphate reduction indices (SRI) as presented by Lallier-Vergès *et al.* (1993) can be used to estimate the amount of the TOC consumed by sulphate reduction.

$$SRI = \%initial\ org.C / \%residual\ org.C$$

where

% initial org.C = metabolizable org.C + non metabolizable org.C

% residual org.C = %TOC

RESULTS

Organic petrology

The organic particles identified in incident light mainly consist of unstructured OM of marine origin, alginites and liptodetrinites. Also, terrestrial organic particles such as vitrinites, inertinites and liptinites similar to those derived from spores and pollen grains were observed. The filamentous alginites of 15–30 µm length or fragments of algae show orange to yellow fluorescence colours (Fig. 2A). Liptodetrinites appear as brightly fluorescing particles of round or oval shape with a maximum diameter of 15 µm. Generally, the terrigenous vitrinites and inertinites are smaller than 10 µm in diameter. The largest vitrinite fragments (up to 80 µm) occur at the Peruvian margin. Spores and pollen grains in very small amounts were observed at all locations.

A typical petrographical feature of all samples from the two upwelling areas—with the exception of Site 720—is that the OM is mainly composed of unstructured organic aggregates as described by ten Haven *et al.* (1990) and Bertrand *et al.* (1990). Palynofacies studies as well as microscopical observations of the whole sediment and the kerogen concentrates indicate that most of the OM in the Peru and Oman sediments are not present as well-defined macerals. OM dominantly occurs as dark-brown to orange-brown fluorescing material of variable size and irregular shape (Fig. 2B) and brownish cloudy or fluffy aggregates as seen in transmitted light. It represents between 86 and 98% (volume percentage) of the total visible OM at the Peru and Oman sites. At Site 723 the unstructured OM is frequently associated with pyrite framboids, whereas at Site 724 in the samples with lower TOC contents, pyrite mainly occurs in foraminiferal tests or as single, needle-shaped crystals.

Additionally, we observed at all locations (with the exception of Site 720) small, brown-fluorescing spherules (2–15 µm) similar in shape to pyrite framboids. These spherules possibly represent gelified organic particles, which are considered as precursors of pyrite (Lallier-Vergès *et al.*, 1993; Sawlowicz, 1993).

Only the more sandy or silty intervals in Unit II at Site 681 and Unit III at Site 679 contain slightly enhanced amounts of terrigenous macerals (max. 2–4%). At Site 720 the OM of most samples is dominated by lignaceous debris, according to Bertrand *et al.* (1990), i.e. vitrinite and inertinite (up to 73%; see also Bertrand *et al.*, 1990). Some of these terrestrial components are replaced by pyrite.

Figure 3 shows the relative percentages of unstructured OM and structured marine and terrigenous OM at Site 723. There is little difference between the unstructured and the structured OM ratio in sediments close to the sediment–water interface and those from several hundred meters depth.

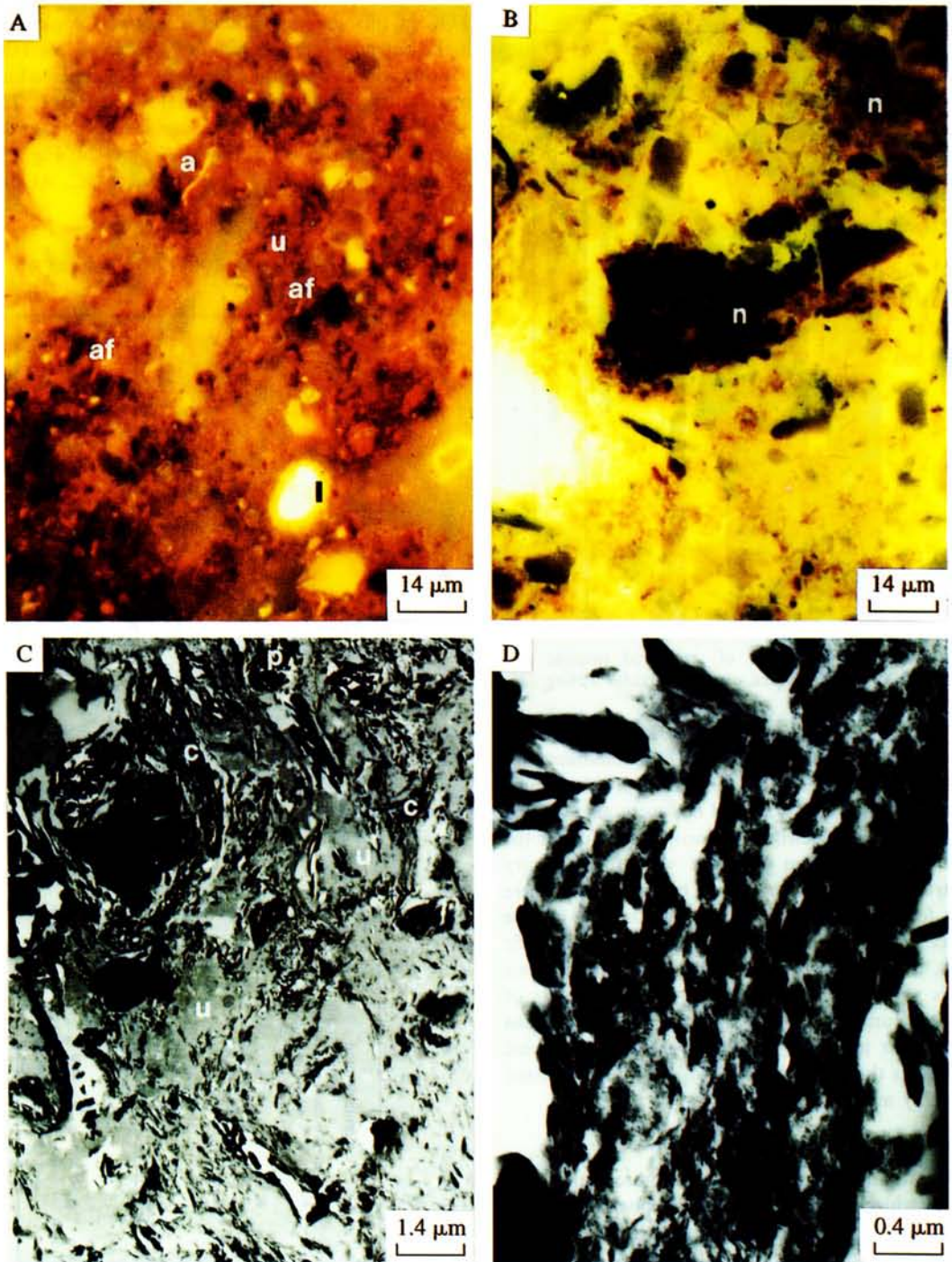


Fig. 2. (A) Alginates and unstructured organic matter in sample 723A, 182.12 mbsf, observed in reflected light (UV excitation). Alginates (a) and fragments of algae (af) show orange and liptodetrinites (l) brightly yellow fluorescence colours, whereas the unstructured organic matter appears as brown aggregates (u). (B) Unstructured organic matter in sample 723A, 65.85 mbsf, observed in reflected light (UV excitation). Dark to middle brown fluorescing patches of organic matter (u) predominate. (C) Larger aggregate of structureless organic matter in sample 724B, 218.62 mbsf, observed by TEM. The unstructured organic matter (u) is associated with clay minerals (c) and pyrite framboids (p). (D) Unstructured (amorphous) organic matter in sample 723A, 362.08 mbsf, observed by TEM. The organic matter is characterized by a granular texture without any apparent biological structures.

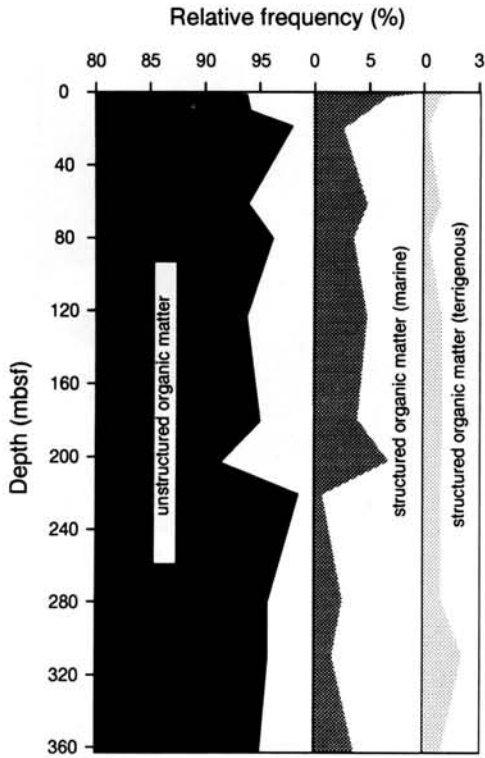


Fig. 3. Relative percentage of structured (marine and terrestrial) and unstructured organic particles at Site 723.

In order to test whether the predominance of unstructured OM is a magnification problem, nine samples of Sites 723, 724 and 688 were also studied by transmission electron microscopy; even under the highest magnification none or very few primary biostructures could be observed; by comparison there were fewer than those observed in shallow marine source rocks such as the Kimmeridge Clay (Boussafir *et al.*, 1995). With the exception of some lignaceous debris and membranes, the OM mainly consists of non-structured aggregates which show homogenous or granular textures (Fig. 2C, D). In these organic aggregates the unstructured OM is frequently mixed with clay minerals.

Elemental analysis and Rock-Eval pyrolysis

The origin and/or the state of preservation and factors which are controlling the deposition of OM can be partly addressed by investigations of its bulk geochemical composition. In this study, the quality and quantity of OM were estimated geochemically by using different analytical methods and parameters: TOC-contents, mass accumulation rates of organic carbon, Rock-Eval pyrolysis data as well as C/S- and S/Fe-ratios measured on kerogen concentrates.

Organic carbon. The TOC concentrations of the studied samples are highly variable. The sediments of Site 720, which is not directly influenced by upwelling, are poor in TOC. The TOC values range between 0.15 and 0.93% and are even higher than 1%

in a few samples analyzed onboard JOIDES Resolution (Fig. 4A). The highest percentages of TOC at this site were found in samples containing high contents of unstructured OM whereas low TOC concentrations were measured in sediments which predominantly contain terrestrial-derived OM. The 49 Holocene to upper Pliocene sediment samples from the Oman margin (Sites 723 and 724; Fig. 4B, C) contain between 0.73 and 9.55% TOC. At Site

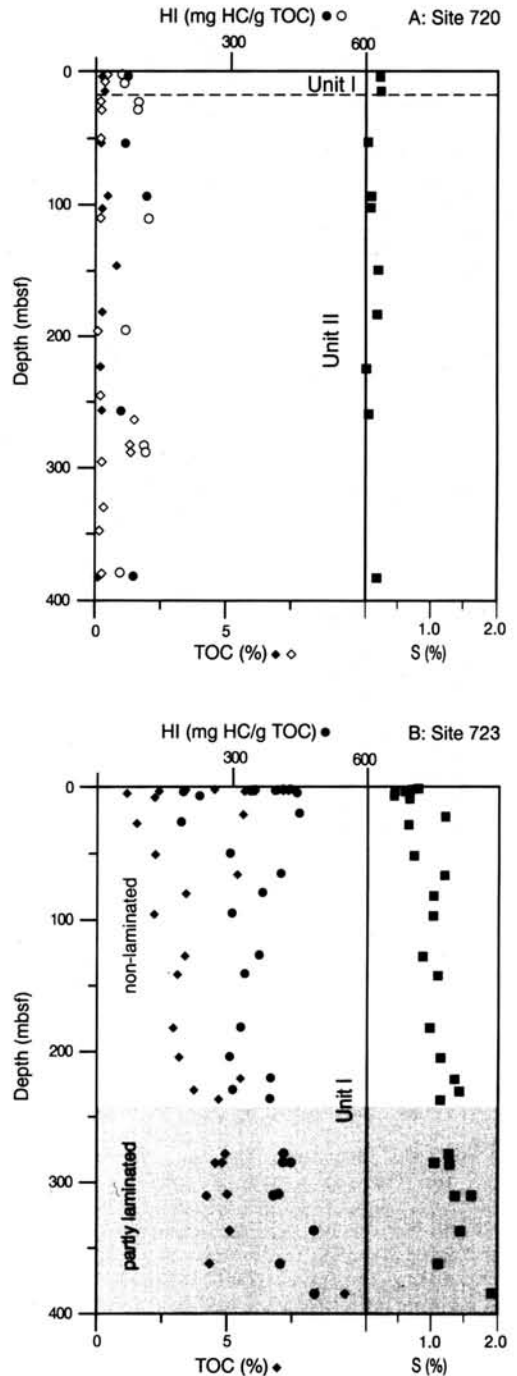


Fig. 4(A,B).

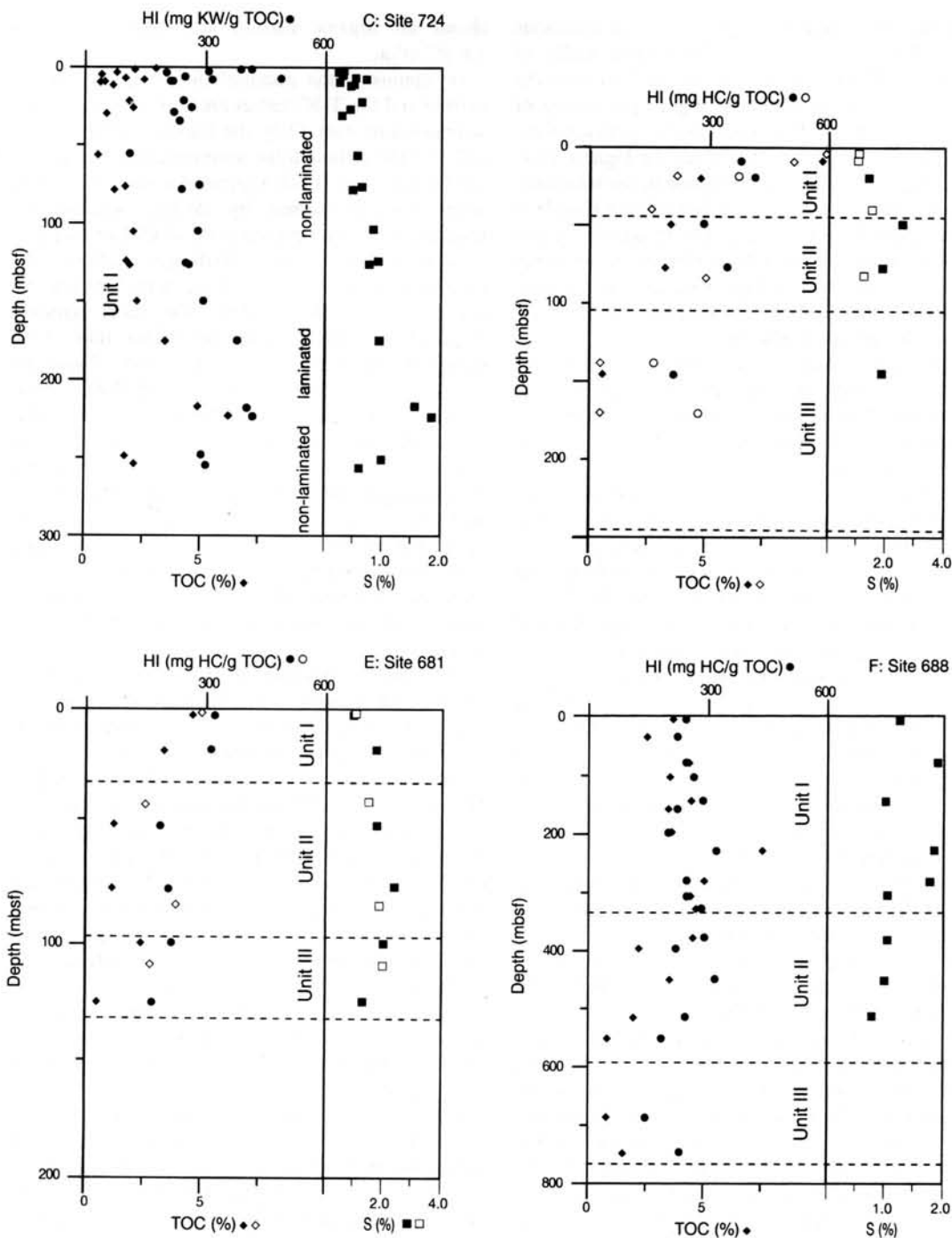


Fig. 4. (A–F) Depth trends of organic carbon, sulphur and hydrogen-index values for Sites 720 (A), 723 (B), 724 (C), 679 (D), 681 (E) and 688 (F). Full symbols represent onshore measurements in our laboratory (Jülich), whereas the open symbols represent measurements taken from the shipboard reports (Suess *et al.*, 1988; Prell *et al.*, 1989). Additional sulphur data were taken from Patience *et al.* (1990).

723 a high value (7.32%) occurs at the top of the sequence (0.02 mbsf), and values decrease rather continuously down to 1.13% at 4.20 mbsf. Below this zone the TOC contents scatter widely (without a clear trend) between 1.51 and 5.59% and reach a maximum of 9.55% at 384.80 mbsf. The sediments at

Site 724 are in general leaner in TOC than those of Site 723. The amount varies between 0.50 and 6.14% and no clear depth trend was observed. The highest values were measured in the samples which are laminated and enriched in diatoms and radiolarians.

At Site 679 there are high TOC concentrations (3.45–9.80%) in the foraminifer-bearing muds of Units I and II and low concentrations (0.63%) in the Miocene sample containing a higher percentage of sand (Unit III; see Fig. 4D). Similar patterns were found at Site 681 (Fig. 4E) where the highest TOC values (up to 4.61%) were measured in the laminated sequence of Unit I. The more bioturbated Unit II is characterized by lower values. The 18 samples of Site 688 can be subdivided into a Pleistocene to upper Miocene sequence with high average TOC concentrations of 4.0% and older sediments with distinctly lower TOC contents (Fig. 4F).

TOC concentrations transformed into mass accumulation rates of TOC can be used for the interpretation of changes in preservation conditions or supply of OM. The accuracy of the calculated accumulation rates greatly depends on the stratigraphic resolution, because physical rock properties and TOC values were measured in great detail. The reproducibility of TOC values is very good, as indicated by a comparison between onshore and shipboard measurements (see Fig. 4A–F). In addition, it must be noted that accumulation rates of TOC are only average values calculated for time intervals of thousands or millions of years.

Accumulation rates are more meaningful, if terrigenous and marine-derived organic carbon can be differentiated (e.g. Stein and Littke, 1990). This differentiation is possible here, based on petrographical observations, which show that—with the exception of Site 720—the marine-derived OM is clearly predominant (> 90%). Therefore, the discussed accumulation rates of total organic carbon are very similar to those of marine organic carbon. The calculations of accumulation rates were not performed for samples of Site 720, because of the abundant occurrence of turbiditic intervals and possible erosional unconformities.

At Site 723 the accumulation rate of organic carbon varies between 2.9 and 9.1 gC/m²/a. The highest rate of 9.1 gC/m²/a was calculated for the laminated samples at the Pleistocene/Pliocene boundary. At the top of Site 723 the organic carbon accumulation rates are on average 4.5 gC/m²/a. In contrast to Site 723, the organic carbon accumulation rate at Site 724 is significantly lower. The values range from 0.9 gC/m²/a at the top to 3.7 gC/m²/a in the laminated part of the site.

At Site 679 the highest organic carbon accumulation rates were found in the Quaternary samples (2.2–6.3 gC/m²/a). The Pliocene and Miocene sediments are characterized by low accumulation rates of only 0.4 gC/m²/a. At Site 681 the accumulation rates of organic carbon are lower (0.8–1.7 gC/m²/a), whereas at Site 688 highly variable rates were calculated. The highest rates (max. 15.1 gC/m²/a) were observed for the diatomaceous muds of early Pleistocene age. The more terrigenous lithology in the upper part of the core

shows an organic carbon accumulation rate of 1.8 gC/m²/a.

In summary, the accumulation rates of organic carbon and the TOC-values are mainly linked to the sedimentation rate. Only the Pliocene of Site 679 is rich in TOC although the sedimentation rate is low. ten Haven *et al.* (1990) suggested a stagnant anoxic water column caused by density stratification resulting in a better preservation of OM at that site.

Rock-Eval pyrolysis. Hydrogen Indices (HI) measured by Rock-Eval pyrolysis range between 300 and 450 (mg HC/g TOC) for most samples (Fig. 4A–F). These values are higher than those observed for typical terrestrial OM (Type III kerogen; < 200–300, e.g. Tissot and Welte, 1984; Littke, 1993) and lower than for typical marine OM from petroleum source rocks (Type II kerogen; 600–900, see Tissot and Welte, 1984; Littke and Sachsenhofer, 1994). HI-values significantly decrease with increasing maturation and petroleum generation. For the sediments discussed here, this finding is, however, insignificant, because the sediments are immature. Vitrinite reflectance values measured on primary vitrinite grains are lower than 0.4% in all sediments.

The lowest HI-values of 100 on average were measured in the sediments of the Indus Fan (Site 720; Fig. 4A) and are due to the relative enrichment of terrigenous organic particles. The intervals with higher contents of unstructured OM show higher HI-values. At Site 723, HI decreases (similar to TOC) within the first 4 m of the sediment from 400 to 200. Below, there is a sequence in which HI-values are 330 on average. In the laminated lower Pleistocene and Pliocene samples a shift to higher values ranging between 380 and 490 was observed (Fig. 4B). HI-values in samples of Site 724 are on average lower (300) than at Site 723. Within the first few meters the HI rapidly decreases from 430 to 200. Below this, the HI-values are at 280 and increase again in the laminated facies at the Pleistocene–Pliocene boundary (Fig. 4C).

The sediments at Site 679 have an average HI-value of 350 (Fig. 4D). The lowest values were detected in the deeper part of the sequence characterized by a strong input of clastic material. At Site 681 the HI-values are higher in the laminated Unit I, than in the units below (Fig. 4E), although the input of terrestrial OM is small, as is obvious from the microscopical investigations. For Site 688 HI-values of 300 on average were observed. The values vary from 150, in more bioturbated sections, to 330 in diatomaceous muds (Fig. 4F).

As it is well-known that HI-values of sediment samples tend to be lower, if TOC-values are low to moderate (Katz, 1983; Peters, 1986; Littke, 1993), Rock-Eval pyrolysis was also performed on selected kerogen concentrates of sediments from all sites. The results obtained for kerogen concentrates indicate a depression of HI-values by only 20–30% for the

respective sediment samples. A much greater effect was found for OI-values (these data are not reported here).

Organic carbon–sulphur–iron. Sulphur (S) contents of the sediments vary between 0.83 and 2.54% for the Peru sites and between 0.04 and 1.95% for the Oman sites. The lowest average values (0.16%) occur at Site 720 (Fig. 4A), whereas highest average values were measured at Site 679 and Site 681 (1.91 and 1.73%; see Fig. 4D and 4E). For Sites 723, 724 and 688 average S concentrations are at 0.95, 0.66 and 1.34% (Fig. 4B, C and F), respectively.

The TOC vs S relationship for the samples is shown in Fig. 5. Figure 5 also includes the empirical relationship between TOC and S (dashed line) for "normal" marine sediments adopted from Berner and Raiswell (1983). Under "normal" marine conditions TOC concentration and S content are positively correlated and the ratio is about 2.8. A positive correlation between TOC and S content is regarded as an indication that the availability of (metabolizable) OM is controlling the S fixation in the sediments (Berner, 1970).

The measured TOC/S ratios exhibit different trends at the studied sites (Fig. 5). At Sites 720 and 724 the ratios are mainly in accordance with the empirical line of Berner and Raiswell (1983). However, at Site 724, there is a successive decrease of the TOC/S ratio in the first few decimeters of the sediment. At the top of the sequence it is 8.5, followed by 6.8 and 4.0 (at a depth of 0.1 and 0.5 m). Below a depth of 1 m the values are nearly constant (average 2.5) over the entire sequence. Thus the data of Site 724 which plot below the dashed line in Fig. 5 are mainly from the uppermost sediments. A similar trend of TOC over S ratios for the uppermost sediments can be observed

at Site 723 (Fig. 5), but the TOC/S ratio averages distinctly higher (4.1). The ratio decreases from 12.2 in the sample close to the sediment–water interface (depth 0.02 mbsf) to values between 2.6 and 4.9 at depth greater than 3 m.

The dissolved sulphate concentrations in the pore water of the studied sediments are displayed in Fig. 6. At the Oman Sites 720, 723 and 724 sulphate concentrations decrease from values of 25 mmol/l to almost zero within the first 50 m, thus indicating a rather final depth for bacterial sulphate reduction.

Because of the smaller number of the investigated Peruvian samples, TOC/S depth trends cannot be described for this area. The TOC/S ratios at Site 688 range from 2.2 to 4.5 and mainly plot along the trend line of Berner and Raiswell (1983). The average TOC/S ratio at Site 679 is 2.1. At Site 681 the lowest ratios (1.3) were established for the deeper interval. The low ratios at Site 681 can be explained by a continued sulphate supply due to the sulphate-bearing brine (see Fig. 6 and Suess *et al.*, 1988). The low sulphate concentration gradient at Site 679 (values of zero are only reached below 170 mbsf) may be due to a very small activity of sulphate-reducing bacteria at this site (see discussion).

To understand the quantitative significance of OM degradation due to sulphate reduction, total S and TOC were compared for the sediments from the two upwelling areas (Fig. 5). TOC/S ratios of the samples from the two deep-water locations (Site 720 and Site 688) roughly plot along the trend line defined by Berner and Raiswell (1983), although absolute concentrations of S and TOC are much higher at Site 688 than at Site 720. No correlation, or even a negative correlation, between TOC and S was, however, observed for sediments from Sites 723, 724, 679, and 681. Similar observations were made by Emeis and Morse (1993) for another set of samples from Site 723. Furthermore, S over TOC values are on average higher in the Peruvian samples from Sites 681 and 679 than in those from the Oman Sites 723 and 724.

Figure 7 shows the concentrations of sulphur and iron in the kerogen concentrates (see also Table 2). The dashed line in this figure displays the ideal pyrite composition. For samples plotting above this line, sulphur will be completely fixed in pyrite. For sediments plotting below the pyrite composition line, it has to be assumed that sulphur is not only present in pyrite, but also in OM. (Alternatively other sulphur-bearing minerals which are not dissolved in HCl and HF could also be present.) Among the samples from Site 679, only the Miocene sample which is characterized by a high content of terrigenous OM plots close to the pyrite line. The S/Fe-ratios in the other samples of Site 679 are clearly higher. The samples of Sites 688, 723, 724 and partly those of Site 681 also plot below the pyrite line indicating significant amounts of sulphur are not bound to pyrite. The two data points of Site 681,

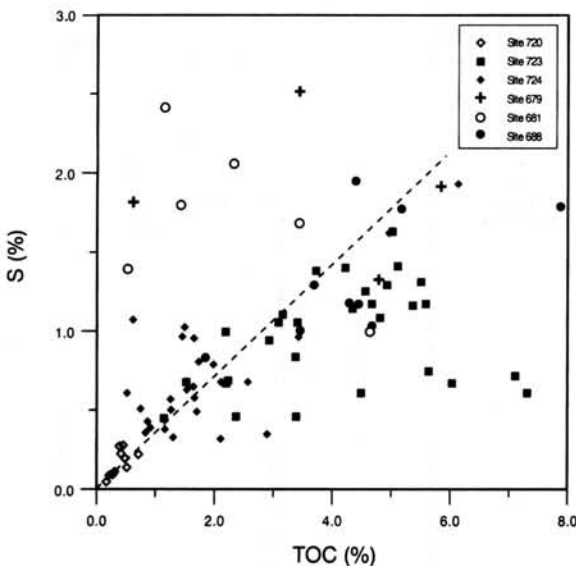


Fig. 5. Organic carbon content (wt%) vs sulphur (wt%) content at the studied locations. The dashed line shows the TOC/S-ratio for "normal-marine" sediments adopted from Berner and Raiswell (1983).

which plot close to the pyrite line correspond to the samples characterized by the lowest TOC/S ratios (see above) and low HI-values. The HI-values of the samples, which are lying close to the pyrite line, are lower than those with high sulphur over iron ratios (Table 2). Thus the S over iron ratios most different from that of pyrite are those of Sites 723, 724, 681 and especially 679. These are the sites which are situated within the major upwelling areas, where the present sediment-water interfaces are within the respective OMZ. The excess S in the sediments from these sites is mainly organic sulphur (which was formed during early diagenesis) as indicated by organic geochemical data which will be presented in Part II of this publication.

The sulphur content of sedimentary sequences can be used to calculate an "original" TOC content. "Original" here refers to the TOC content, before bacterial sulphate reduction began. The limitations of

this calculation are discussed in some detail in Littke *et al.* (1991) and Vetö *et al.* (1994). Lallier-Vergès *et al.* (1993) presented a method to express the amount of consumed carbon using the "sulphate reduction index" (SRI), which is the ratio of "initial" over residual TOC. In reality, this number is an underestimation, because a fraction of the H_2S produced microbially is lost to the bottom waters or oxidized in the sediment (Zaback *et al.*, 1993; Vetö *et al.*, 1994; Lallier-Vergès *et al.*, 1996). Also not taken into account is the part of S which is coupled with methane.

The calculated SRI shows the following patterns: at Site 723, it slightly increases (from 1.1 to 1.2) within the first meters of the sediment, whereas HI and TOC concentrations show decreasing trends (see above). Below this zone, the SRI are nearly constant (1.2) over the entire sequence. For Site 724, we calculated a slightly higher SRI of 1.3 on average,

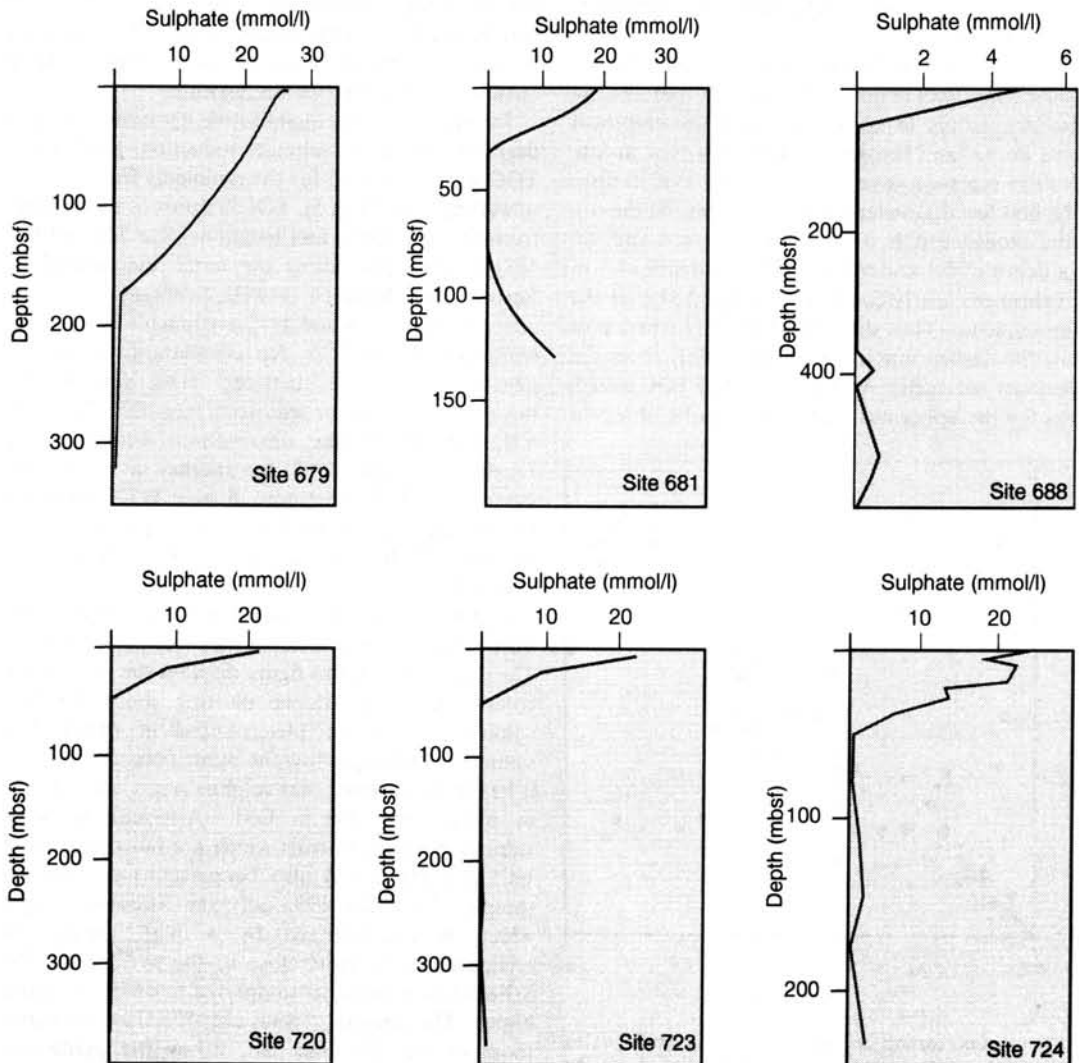


Fig. 6. Concentrations of sulphate with depth at the studied sites using data from Suess *et al.* (1988) and Prell *et al.* (1989).

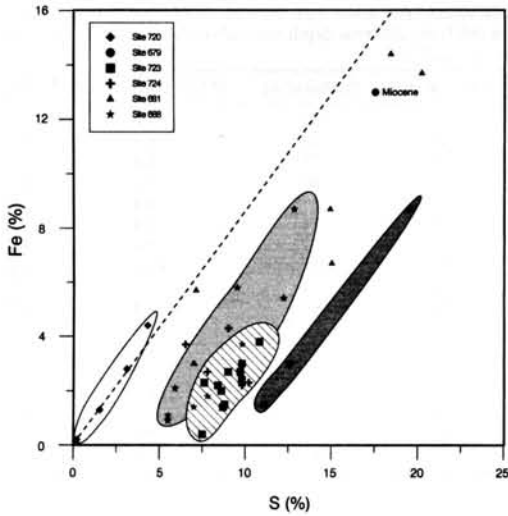


Fig. 7. Sulphur content vs iron content of kerogen concentrates at the studied sites. The dashed line indicates the ideal pyrite composition.

showing the same trend at the top of the borehole as at Site 723. At the Indus Fan (Site 720), highest SRI-values (1.5) were calculated for sediments with high amounts of clastic components (Unit II). These elevated values are probably due to higher iron contents and higher porosities of the sediments leading to an increased access of sulphate. The pelagic nanofossil oozes with higher amounts of unstructured OM possess SRI-values similar to those of Site 723 and Site 724.

For Site 679 the SRI-values are 1.3 on average. In the Miocene, the value is much higher (3.1) which is possibly due to the increased input of clastic sediments with higher iron contents and higher porosities. The calculated indices for the deeper samples at Site 681 are very high (max. 3.0) due to the permanent sulphate supply. Site 688 is characterized by SRI-values ranging between 1.2 and 1.3 in the Pleistocene–Pliocene interval.

DISCUSSION

Bioproductivity vs preservation of organic matter

Phyto- and zooplankton as well as terrigenous organic particles are the most important precursors of sedimentary OM in deep-sea environments. The percentage of most of the terrigenous OM, either derived from higher land plants or resedimented from older, eroded rock sequences, can usually be determined quite accurately by means of incident light petrography, because these particles have a high reflectivity. In most deep-sea sediments, terrigenous OM occurs in high amounts relative to marine-derived OM, mainly because it is—on average—more resistant to degradation processes (Huc, 1988; Littke and Sachsenhofer, 1994 and references therein). In the upwelling sediments of this study, the percentage

of terrestrial OM is small however. This observation is supported by earlier petrographical (Bertrand *et al.*, 1990) and geochemical studies (ten Haven and Rullkötter, 1991; Emeis *et al.*, 1991; ten Haven *et al.*, 1992; Aplin *et al.*, 1992; Eglinton *et al.*, 1993).

Thus, OM derived mostly from phytoplankton is the major source of the sedimentary OM at the two upwelling areas. Fluorescing particles, usually described as alginites are rarely observed in the samples (e.g. Fig. 3) whereas they are characteristic in most marine and lacustrine petroleum source rocks (Tissot and Welte, 1984; Littke, 1993).

OM occurs mainly as unstructured and optically amorphous aggregates in the sediments investigated. Furthermore, even under transmission electron microscopy, only very few biological organic structures were observed. (To avoid misunderstandings it should be mentioned that biologic structures are present and well-visible in great numbers as *inorganic* particles such as diatoms, foraminifers etc.) The same type of OM was described in Kimmeridge source rocks and is characterized, on the basis of combined pyrolytic and ultrastructural studies, as resulting from early sulphur incorporation (vulcanization) in an initially metabolizable OM (Boussafir *et al.*, 1995). This mechanism is responsible for the acquired bioresistant character of the unstructured OM whereas the resistance of structured marine OM (e.g. cell-walls of microalgae) is biologically inherited (Bertrand *et al.*, 1994).

Here, the close association of the unstructured organic material with clays revealed by TEM indicates that the “amorphization” should be a syn-sedimentary process. Whether this “amorphization” took place in the photic zone, where most of the consumption and remineralization of biomass occurs (e.g. Suess, 1980) or at the sediment–water interface remains to be investigated. In any case, some authors have interpreted this association as an early flocculation (in the water column) of labile organic material and clay particles (Bishop and Philp, 1994).

Indeed, the unstructured OM is ultimately derived from planktonic biomass which was produced in the surface waters of the two areas in vast amounts. Typical recent bioproductivity rates are in the order of 200 gC/m²/a in both areas (Berger, 1989). The mass accumulation rates established for the sediments are, however, less than 2–16 gC/m²/a (Table 1). The accumulation rates are in agreement with numbers calculated by ten Haven *et al.* (1990) for the Peruvian upwelling sediments (Site 679) and by ten Haven *et al.* (1992) for their counterparts offshore Oman. These data indicate that between 90 and 99% of the originally produced biomass was degraded in the water column or within the surficial (probably the upper 1–2 m) sediment (Fig. 8). The calculated accumulation rates are average values for long-time intervals. Clearly, the accumulation rates during specific years can be higher or lower.

Table 1. Sedimentation rates (meters per million years), average organic carbon values (TOC), wet bulk densities (WBD), porosities, organic carbon mass accumulation rates (MARTOC), and sulphate reduction indices (SRI) for different depth intervals (mbsf = metres below sea floor) at Sites 679, 681, 688, 723 and 724

Location, depth (mbsf)	Linear Sed. Rate (m/my)	Average TOC (%)	WBD (g/cm ³)	Porosity(%)	MARTOC (gC/m ² /a)	SRI
Site 679, 0–65	140	4.1	1.3	82	2.6	1.3
Site 679, 65–114	20	4.9	1.4	75	0.4	1.3
Site 679, 114–161	80	1.1	1.5	73	0.4	3.1
Site 681, 0–80	80	3.9	1.4	80	1.5	1.3
Site 681, 80–144	80	1.7	1.3	84	0.8	3.0
Site 688, 0–37	98	2.7	1.5	78	1.8	1.2
Site 688, 37–170	135	4.0	1.5	73	4.4	1.3
Site 688, 170–338	350	4.9	1.6	71	15.9	1.3
Site 723, 0–35	187	3.7	1.6	65	3.7	1.2
Site 723, 35–74	128	2.6	1.6	61	3.2	1.2
Site 723, 74–153	239	2.8	1.7	59	6.7	1.2
Site 723, 153–247	150	3.4	1.7	56	4.5	1.2
Site 723, 247–331	187	4.3	1.7	56	8.5	1.2
Site 724, 0–74	73	1.6	1.7	55	1.5	1.3
Site 724, 74–111	58	1.4	1.8	57	1.3	1.3
Site 724, 132–166	142	2.1	1.8	55	3.7	1.3
Site 724, 166–235	48	4.2	1.7	55	1.9	1.3

The role of microbial sulphate reduction

Anaerobic processes such as sulphate-, manganese-, nitrate- and iron-reduction as well as methanogenesis are known to contribute to the degradation of OM in sediments. Among these processes, microbial sulphate reduction is by far the most important within

marine sediments (Jørgensen, 1983; Deming and Baross, 1993), where sulphate concentrations are generally much higher than those occurring in freshwater sediments.

The observed carbon–sulphur–iron relationship is explained as follows: part of the bacterially produced S was incorporated into OM, a process sometimes

Table 2. Organic carbon, sulphur, iron contents, atomic S_{org}/C_{org} ratios and HI-values of kerogen concentrates at the studied Sites 720, 723, 724, 679, 681 and 688

Site/depth (mbsf)	C (%)	S (%)	Fe (%)	S_{org}/C_{org}	HI (mg Hc/g TOC)
720/3.33	6.9	4.3	4.4	—	337
720/58.75	3.9	0.2	0.2	—	58
720/145.35	7.9	3.1	2.8	—	—
720/288.33	16.8	15.2	12.6	0.02	376
723/0.34	55.3	3.7	2.1	0.01	450
723/20.42	49.8	7.5	0.4	0.05	469
723/65.85	49.7	8.7	1.4	0.05	453
723/80.25	47.4	9.7	2.7	0.05	445
723/127.52	47	8.4	2.2	0.05	410
723/141.55	43.4	9	2.7	0.05	432
723/204.36	38.5	7.6	2.3	0.05	396
723/220.75	50.7	8.8	1.5	0.05	452
723/236.61	50.9	8.6	2	0.05	472
723/278.33	52.8	10.8	3.8	0.05	468
723/309.17	51.6	9.8	2.4	0.05	488
723/362.08	54.9	9.8	3	0.04	502
724/38.98	22.9	6.5	3.7	0.04	419
724/79.61	33.9	9	4.3	0.04	377
724/176.84	38.8	7.8	2.7	0.05	419
724/218.62	47.6	9.8	2.2	0.06	427
724/227.30	52.1	10.2	2.3	0.05	450
679/21.68	59	11.1	1.5	0.06	518
679/49.94	46.4	19.5	8.7	0.08	395
679/78.30	55.7	12.6	3	0.06	405
679/143.69	11.9	17.5	13	0.08	223
681/2.81	45.2	7	3	0.03	412
681/16.81	46.8	15	6.7	0.06	382
681/55.82	8.64	7.1	5.7	0.03	235
681/73.44	17	18.4	14.4	0.04	179
681/99.94	23.9	14.9	8.7	0.08	294
681/125.41	18.7	20.2	13.7	0.09	153
688/5.74	32.5	9.5	5.8	0.03	460
688/82.08	44.4	9.8	3.7	0.05	337
688/146.66	40.9	5.5	0.9	0.04	466
688/228.10	54.5	5.5	1.1	0.03	420
688/275.41	52.2	7.8	1.8	0.04	419
688/307.09	53.9	5.9	2.1	0.02	382
688/370.80	49.4	7	1.4	0.04	466
688/453.37	51.3	12.2	5.4	0.04	432
688/521.09	39.2	12.8	8.7	0.03	406

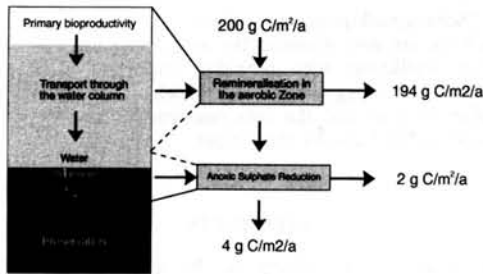


Fig. 8. Mass balance of organic carbon due to remineralization in the oxic zone and sulphate reduction processes for Site 723. Note that this site is situated in a small basin and was therefore much less affected by erosion than other sites along continental margins.

called vulcanization. This incorporation of S into OM is most intense in the Peruvian sediments from Site 679, because all reactive iron has already been consumed (Emeis and Morse, 1993). The formation of organic sulphur was less intense at the Oman Sites 724 and 723. For the latter site, Emeis and Morse showed that reactive iron was still present. Thus, the absence of reactive iron seems to favour organic sulphur formation, but is not a prerequisite.

The samples of the various sites plot along the described lines parallel to the pyrite line (Fig. 7) attesting to a specific and variable sulphur incorporation in the OM at the different sites. Sulphur incorporation has the effect of a transformation of metabolizable into non-metabolizable OM. It is tentatively assumed that sulphate reduction ceased, when a specific maximum value of the organic S/TOC ratio was reached. At this stage, OM (the substrate) became the limiting factor for bacterial sulphate reduction, although it is still present in vast amounts and is rather hydrogen-rich (see HI-values in Fig. 4). Thus, elevated HI-values are not a valid indication for the presence of metabolizable OM. This scenario can well explain the presence of sulphate in the pore water of the respective sediments, e.g. at Sites 723, 679 and 724, as well as the presence of some reactive iron not bound to pyrite (Emeis and Morse, 1993). Especially, the intense early sulphur incorporation into OM at Site 679 may well explain the slowly decreasing sulphate concentration trend at this location (Fig. 6). Similar results are reported by Schulz *et al.* (1994) for the upwelling dominated sediments of the eastern South Atlantic.

At the sites situated below the oxygen-minimum-zone (720 and 688), sulphur incorporation into the OM is a much less important phenomenon (Fig. 7). This difference may indicate that the sulphur incorporation into the OM is a phenomenon mainly occurring only several decimeters or very few meters below the sediment-water interface (Mossmann *et al.*, 1991) where differences between the pore water chemistry and redox potential of upwelling and

non-upwelling sites may be expected. This conclusion is in agreement with earlier work (e.g. Sinninghe Damsté *et al.*, 1989) suggesting an *early* diagenetic incorporation of sulphur into the OM.

The degree of degradation of OM by sulphate reduction can be estimated following the concepts developed by Littke *et al.* (1991), Lallier-Vergès *et al.* (1993, 1996) and Vetö *et al.* (1994). If we assume that all the H_2S generated microbially in the uppermost sediments was fixed (as iron sulphide or in OM) in the sediment, the sulphate reduction indices listed in Table 1 apply. This calculation assumes that no H_2S was lost from the sediments, which may, however, be the case in more porous lithologies. Vetö *et al.* (1994) found indications that this loss of H_2S for non-bioturbated, fine-grained sediments is in the order of almost zero to 45%. If this also holds true for the sediments studied here, the respective carbon losses will be slightly higher than calculated. Whether we incorporate this loss into our calculations or not, a comparison between primary productivity rates, OM accumulation rates, and sulphate reduction rates indicates that most of the OM degradation occurred in the aerobic zone (Fig. 8). As well-established by sediment trap experiments, most of this degradation will have happened within the photic zone or at the sediment-water interface with an additional (smaller) contribution which occurred in the deep water below the photic zone (Suess, 1980).

The high degree of degradation of OM in the aerobic zone is the principal reason for the rather low HI-values of the upwelling sediments studied in this paper when compared to lacustrine and shallow-marine source rocks deposited under anoxic bottom water. In the upwelling areas, the aerobic zone reaches from the surface waters to a depth of several millimeters or a few centimeters into the sediments. In this zone more than 90% of the primarily produced organic carbon was consumed at all sites discussed here (Fig. 8 and Table 1). The exact rate of oxic OM degradation varied, however, in space and time as indicated by more laminated and more bioturbated sediments in each of the investigated sites.

In comparison to many shallow marine deposits, the morphological preservation of the OM is much lower. It is tentatively suggested that this observation is due to the more pronounced degradation of the OM in the aerobic zone at the deep-sea locations. Whether this intense but far from complete degradation generated an ideal type of OM for sulphur incorporation remains to be solved. In any case, the further decomposition of OM below the aerobic zone by bacterial sulphate reduction consumed only about 1–3% of the originally produced organic carbon, but a great proportion of that sedimented at the top of the anaerobic zone (roughly 25–50%). Similar values were previously established for the Lower Toarcian Posidonia Shale (17–32%; Littke *et al.*, 1991).

Furthermore, in terms of quantity and quality of OM, the sediments at Site 688 (which is situated outside of the Peruvian upwelling area and below the oxygen-minimum-zone) seem to be superior or at least equal to those from the upwelling areas. This phenomenon indicates that transport processes such as turbidity and mass flow are of equal importance for OM accumulation and conservation at continental margins as bioproductivity and oxic and anoxic respiration. Such rapid transport and accumulation processes can preserve OM effectively (Degens and Mopper, 1976).

CONCLUSIONS

The results of the organic petrographical and geochemical studies of sediments offshore Peru and Oman can be summarized as follows:

1. The upwelling area sediments are characterized by a predominance of unstructured OM (86–98%) which is derived from degradation of phytoplankton in the water column or close to the sediment–water interface. The degree of this degradation can be estimated by comparing the recent primary productivity rates of TOC and the accumulation rates of organic carbon in the respective sediments. This comparison suggests that between 90 and 99% of the primary organic carbon was remineralized.
2. All samples have experienced a significant bacterial sulphate reduction. Most of the reduced sulphur produced by this process was fixed in pyrite. In addition, most of the sediments also contain a large proportion of organic sulphur.
3. Using published procedures, the amount of organic carbon destroyed by bacterial sulphate reduction was estimated to vary between 1 and 3% of the primarily produced organic carbon. This implies that 20–50% of the OM that reached the anaerobic zone was degraded by sulphate reduction.
4. It is assumed that the incorporation of sulphur transformed metabolizable OM into non-metabolizable OM. This assumption helps to explain the presence of sulphate (in pore waters) and organic matter with high HI-values in some of the investigated sediment sequences.
5. Mass accumulation rates of organic carbon are significantly higher in one deep-marine site outside the upwelling area offshore Peru than within the upwelling area. This observation further supports the theory that sediment transport processes (e.g. turbidity flow) are of equal importance to organic matter accumulation along continental margins as bioproductivity in surface waters.

Acknowledgements—Our study greatly benefitted from the analytical support by the technical staff of the institutes in Jülich (ICG-4 and ZCH) and Orléans (URA 724-FR09 CNRS). The Deutsche Forschungsgemeinschaft provided financial support (Grant No. Li 618/1) in the framework of

the “Schwerpunktprogramm” Ocean Drilling Program for which we are very grateful. We would also like to thank Jürgen Rullkötter who provided important ideas and concepts, H. Clegg and H. S. Poelchau for editing the English version and the two constructive reviewers, R. Buscaill and I. Vetö for their input.

REFERENCES

- van Andel T. H., Heath G. R. and Moore T. C. (1975) Cenozoic history and paleoceanography of the central equatorial Pacific Ocean. *Mem. Geol. Soc. Am.* **143**.
- Aplin A. C., Bishop A. N., Clayton C. J., Kearsley A. T., Mossman J.-R., Patience R. L., Rees A. W. G. and Rowland S. J. (1992) A lamina-scale geochemical and sedimentological study of sediments from the Peru Margin (Site 680, ODP Leg 112). In *Upwelling Systems: Evolution Since the Early Miocene* (Edited by Summerhayes C. P., Prell W. L. and Emeis K. C.), *Geol. Soc. Spec. Publ.* **64**, 131–149.
- Berger W. H. (1989) Global maps of ocean productivity. In *Productivity of the Ocean: Present and Past* (Edited by Berger W. H., Smetacek V. S. and Wefer G.), *Dahlem Workshop Reports, Life Sciences Research Report* **44**, 429–456.
- Berner R. A. (1970) Sedimentary pyrite formation. *Am. J. Sci.* **268**, 1–23.
- Berner R. A. and Raiswell R. (1983) Burial of organic carbon and pyrite sulfur in sediments over Phanerozoic time: a new theory. *Geochim. Cosmochim. Acta* **48**, 606–615.
- Bertrand P., Lallier-Vergès E. and Grall H. (1990) Organic petrology of Quarternary and Neogene sediments from North Indian Ocean (ODP, Leg 117): amount, type and preservation of organic matter. *Proceedings of the Ocean Drilling Program, Scientific Results* (Edited by Prell W. L., Niitsuma N. *et al.*) **117**, 587–594.
- Bertrand P., Lallier-Vergès E. and Boussafir M. (1994) Enhancement of both accumulation and anoxic degradation of organic carbon controlled by cyclic productivity: a model. *Org. Geochem.* **22**, 511–520.
- Bishop A. N. and Philp R. P. (1994) The potential for amorphous kerogen formation via adsorption of organic material at mineral surfaces. 207th Amer. Chem. Soc. (1994) National Meeting, San Diego, March 13–18.
- Boussafir M., Gelin F., Lallier-Vergès E., Derenne S., Bertrand P. and Largeau C. (1995) Origin and preservation processes of organic material in the short-term organic cyclicities of the KCF (G.B.) attested by TEM, SEM and molecular studies. *Geochim. Cosmochim. Acta* **59**, 3731–3748.
- Calvert S. E. and Pedersen T. F. (1992) Organic carbon accumulation and preservation in marine sediments: how important is anoxia? In *Organic Matter, Productivity, Accumulation and Preservation in Recent and Ancient Sediments* (Edited by Whelan J. K. and Farrington J. W.) pp. 231–263. Columbia Univ. Press.
- Degens E. T. and Mopper K. (1976) Factors controlling the distribution and early diagenesis of organic material in marine sediments. In *Chemical Oceanography* (Edited by Riley J. P. and Chester R.) **6**, 60–114.
- Deming J. W. and Baross J. A. (1993) The early diagenesis of organic matter: bacterial activity. In *Organic Geochemistry—Principles and Applications* (Edited by Engel M. H. and Macko S. A.) pp. 119–144. Plenum Press.
- Eglinton T. I., Irvine J. E., Vairavamurthy A., Zhou W. and Manowitz B. (1993) Formation and diagenesis of macromolecular organic sulfur in Peru Margin sediments. *Org. Geochem.* **22**, 781–799.

- Emeis K.-C., Whelan J. K. and Tarafa M. (1991) Sedimentary and geochemical expressions of oxic and anoxic conditions on the Peru Shelf. In *Modern and Ancient Continental Shelf Anoxia* (Edited by Tyson R. V. and Pearson T. H.), *Geol. Soc. Spec. Publ.* **58**, 155–170.
- Emeis K.-C. and Morse J. W. (1993) Zur Systematik der Kohlenstoff-Schwefel-Eisen-Verhältnisse in Auftriebsedimenten. *Geol. Rundschau* **82**, 604–618.
- Espalià J., Laporte J. L., Madec M., Marquis F., Leplat P., Paulet J. and Boutefeu A. (1977) Méthode rapide de caractérisation des roches mères, de leur potentiel pétrolier et de leur degré d'évolution. *Rev. Inst. Franç. Pét.* **32**, 23–42.
- ten Haven H. L., Littke R., Rullkötter J., Stein R. and Welte D. H. (1990) Accumulation rates and composition of organic matter in Late Cenozoic sediments underlying the active upwelling area off Peru. In *Proceedings of the Ocean Drilling Program, Scientific Results* (Edited by Suess E., von Huene R. et al.), **112**, 591–605.
- ten Haven H. L. and Rullkötter J. (1991) Preliminary lipid analysis of sediments recovered during Leg 117. In *Proceedings of the Ocean Drilling Program, Scientific Results* (Edited by Prell W. L., Niitsuma N. et al.), **117**, 561–570.
- ten Haven H. L., Eglinton G., Farrimond P., Kohnen M. E. L., Poynter J. G., Rullkötter J. and Welte D. H. (1992) Variations in the content and composition of organic matter in sediments underlying active upwelling regimes: a study from ODP Legs 108, 112, and 117. In *Upwelling Systems: Evolution Since the Early Miocene* (Edited by Summerhayes C. P., Prell W. L. and Emeis K. C.), *Geol. Soc. Spec. Publ.* **64**, 229–246.
- Heinze P. M. and Wefer G. (1992) The history of coastal upwelling off Peru (11 S, ODP Leg 112, Site 680B) over the past 650000 years. In *Upwelling Systems: Evolution Since the Early Miocene* (Edited by Summerhayes C. P., Prell W. L. and Emeis K. C.), *Geol. Soc. Spec. Publ.* **64**, 451–462.
- Huc A. Y. (1988) Sedimentology of organic matter. In *Humic Substances and their Role in the Environment* (Edited by Frimmel F. H. and Christman R. F.) pp. 215–243. 5th Dahlem Conf.
- Jørgensen B. B. (1983) Processes at the sediment–water interface. In *The Major Biogeochemical Cycles and their Interaction* (Edited by Bolin B. and Cook R. B.), *SCOPE Rep.* **21**, 477–515.
- Katz B. J. (1983) Limitations of “Rock-Eval” pyrolysis for typing organic matter. *Org. Geochem.* **4**, 195–199.
- Lallier-Vergès E., Bertrand P. and Desprairies A. (1993) Organic matter composition and sulfate reduction intensity in Oman Margin sediments. *Mar. Geol.* **112**, 57–69.
- Lallier-Vergès E., Hayes J. M., Boussafir M., Zaback D., Tribouillard N. P., Connan J. and Bertrand P. (1996) Productivity-induced sulphur enrichment of hydrocarbon-rich sediments from the Kimmeridge Clay Formation. *Chem. Geol.* (in press).
- Littke R. (1993) *Deposition, Diagenesis, and Weathering of Organic Matter-Rich Sediments*. Springer, Heidelberg, 216 pp.
- Littke R., Baker D. R., Leythaeuser D. and Rullkötter J. (1991) Keys to the depositional history of the Posidonia Shale (Toarcian) in the Hils syncline, northern Germany. In *Modern and Ancient Continental Shelf Anoxia* (Edited by Tyson R. V. and Pearson T. H.), *Geol. Soc. Spec. Publ.* **58**, 311–334.
- Littke R. and Sachsenhofer R. F. (1994) Organic petrology of deep sea sediments: a compilation of results from the ocean drilling program and the deep sea drilling project. *Energy and Fuel* **8**, 1498–1512.
- McIver R. (1975) Hydrocarbon occurrence from JOIDES Deep Sea Drilling Project. *Proc. World Petr. Congr.* **9**, 269–280.
- Mossman J.-R., Aplin A. C., Curtis C. D. and Coleman M. L. (1991) Geochemistry of inorganic and organic sulphur in organic-rich sediments from the Peru margin. *Geochim. Cosmochim. Acta* **55**, 3581–3595.
- Patience R. L., Clayton C. J., Kearsley A. T., Rowland S. J., Bishop A. N., Rees A. W. G., Bibby K. G. and Hopper A. C. (1990) An integrated biochemical, geochemical, and sedimentological study of organic diagenesis in sediments from Leg 112. In *Proceedings of the Ocean Drilling Program, Scientific Results* (Edited by Suess E., von Huene R. et al.), **112**, 135–153.
- Peters K. E. (1986) Guidelines for evaluating petroleum source rocks using programmed pyrolysis. *Am. Assoc. Petr. Geol. Bull.* **70**, 318–329.
- Prell W. L., Niitsuma N. et al. (1989) *Proceedings of the Ocean Drilling Program, Initial Reports 117*, College Station, TX (Ocean Drilling Program).
- Sawłowicz Z. (1993) Pyrite framboids and their development: a new conceptual mechanism. *Geol. Rundschau* **82**, 604–618.
- Schulz H. D., Dahmke A., Schinzel U., Wallmann K. and Zabel M. (1994) Early diagenetic processes, fluxes, and reaction rates in sediments of the South Atlantic. *Geochim. Cosmochim. Acta* **58**, 2041–2060.
- Sinninghe Damsté J. S., Eglinton T. I., De Leeuw J. W. and Schenck P. A. (1989) Organic sulphur in macromolecular sedimentary organic matter: I. Structure and origin of sulphur-containing moieties in kerogen, asphaltenes and coal as revealed by flash pyrolysis. *Geochim. Cosmochim. Acta* **53**, 389–415.
- Stach E. (1982) The macerals of coal. In *Stach's Textbook of Coal Petrology* (Edited by Stach E. et al.) pp. 87–139.
- Stein R., ten Haven H. L., Littke R., Rullkötter J. and Welte D. H. (1989) Accumulation of marine and terrigenous organic carbon at upwelling Site 658 and nonupwelling Sites 657 and 659: implications for the reconstruction of paleoenvironments in the eastern subtropical Atlantic through Late Cenozoic times. In *Proceedings of the Ocean Drilling Program, Scientific Results* (Edited by Ruddiman W., Sarnthein M. et al.) **108**, 361–385.
- Stein R. and Littke R. (1990) Organic-carbon-rich sediments and palaeoenvironment: results from Baffin Bay (ODP-Leg 105) and the upwelling area off northwest Africa (ODP-Leg 108). In *Deposition of Organic Facies* (Edited by Huc A. Y.), *Amer. Assoc. Petr. Geol. Stud. Geol.* **30**, 41–56.
- Suess E. (1980) Particulate organic carbon flux in the oceans—surface productivity and oxygen utilization. *Nature* **288**, 260–263.
- Suess E., von Huene R. et al. (1988) *Proceedings of the Ocean Drilling Program, Initial Reports 112*, College Station, TX (Ocean Drilling Program).
- Tissot B. P. and Welte D. H. (1984) *Petroleum Formation and Occurrence*, 2nd edn. Springer, Berlin, 699 pp.
- Vetö I., Hetényi M., Demény A. and Hertelendi E. (1994) Hydrogen index as reflecting intensity of sulphidic diagenesis in non-bioturbated, shaly sediments. *Org. Geochem.* **22**, 299–310.
- Zaback D. A., Pratt L. M. and Hayes J. M. (1993) Transport and reduction of sulphate and immobilisation of sulphide in marine black shales. *Geology* **21**, 141–144.



Chemical Geology 134 (1997) 277–288

**CHEMICAL
GEOLOGY**
INCLUDING
ISOTOPE GEOSCIENCE

Productivity-induced sulphur enrichment of hydrocarbon-rich sediments from the Kimmeridge Clay Formation

E. Lallier-Vergès^a, J.M. Hayes^b, M. Boussafir^a, D.A. Zaback^b, N.P. Tribovillard^c,
J. Connan^d, P. Bertrand^{a,*,1}

^a URA 724 – FR 09 CNRS, Université d'Orléans, F-47067 Orléans, France

^b BioGeochemical Laboratories, Indiana University, Bloomington, IN 47405, USA

^c URA 723 du CNRS, Université de Paris-Sud, F-91405 Orsay, France

^d ELF-Aquitaine, F-64000 Pau, France

Received 7 July 1995; accepted 6 May 1996

Abstract

This work aims to highlight the relationship between primary productivity, sulphate reduction and organic carbon preservation in cyclic marine sediments from the Kimmeridge Clay Formation. A concomitant increase of the total sulphur content with the preserved organic content (TOC), shows the progressive supply of both metabolisable organic matter and resistant organic matter is linked to primary productivity. However, variations in sulphate reduction efficiency, based on elemental abundance and isotopic composition of sulphur, reveal that the proportion of metabolisable vs. resistant organic matter has varied along the cycles. This is interpreted in terms of the variation in organic delivery. Organic sulphur content is found to be proportional to the organic matter content, whereas concentrations of pyritic sulphur are constant at very high (> 10% TOC) values. This result is explained by a limitation of available iron for pyritisation at times of very high organic flux. Under such conditions, HS⁻ in excess could be responsible for the early formation of organo-sulphur compounds and thus for the preservation of highly aliphatic (i.e. lipid-rich) organic matter.

Keywords: Kimmeridge Clay; Oil shale; Biological processes; Sulphur isotopes; Organic sulphur; Pyrite

1. Introduction

The Kimmeridge Clay Formation (KCF) is a marine deposit composed of alternating organic-rich shales and marls that is considered as the lateral equivalent of the main source-rocks of the North

Sea. These immature formations outcrop on the south coast of England (Dorset) whereas others were drilled in the Cleveland Basin (Yorkshire, England) by the YORKIM Group (Herbin et al., 1991). Extended previous studies on the organic-rich shales from the KCF sites have evidenced the cyclic accumulation of organic matter through the time, with periods of several orders. The cyclicity concerns both the abundance and the geochemical quality of the organic matter (Herbin et al., 1993). The prominent role played by primary productivity in this cyclic organic

* Corresponding author.

¹ Present address: URA 197 du CNRS, Université de Bordeaux I, 33405 Talence, France.

accumulation has already been demonstrated (Bertrand and Lallier-Vergès, 1993). Moreover the study of the mineral phases (i.e. clays) and trace-element distribution has shown: (1) that the mineral contribution was constant throughout the cycles; (2) that the water column was oxygenated; and (3) that depositional conditions were anoxic and unchanged during the time of deposition for both cycles (Tribouillard et al., 1992, 1994). Petrographical and geochemical parameters show that this organic matter presents both a well-preserved hydrocarbon content (Ramanampisoa and Disnar, 1994) and a strong degradation by sulphate-reducing bacteria (Bertrand et al., 1994). Reduced sulphur is concentrated in these organic-rich sediments as a consequence of bacterial sulphate reduction and subsequent formation of sulphides (Berner, 1970). The present paper

focuses on the role of sulphate reduction in the cyclic accumulation of highly aliphatic organic matter. The measurement of total sulphur content, the isotopic composition of sulphur and the speciation of sulphides have been performed to specify the different occurrences of sulphur enrichment, the variability of sulphate reduction intensity and the different processes which led to its trapping during early diagenesis.

Two short-term depositional cycles of the Kimmeridgian series from the Cleveland Basin have been sampled at centimetre intervals (Marton 87 Hole). Each cycle represents ~ 30 kyr; both are situated in the Eudoxus Zone (Herbin et al., 1991). One (CYCLE 1) is at the base of an organic megacycle, the other (CYCLE 2) at the peak of the same megacycle (Fig. 1).

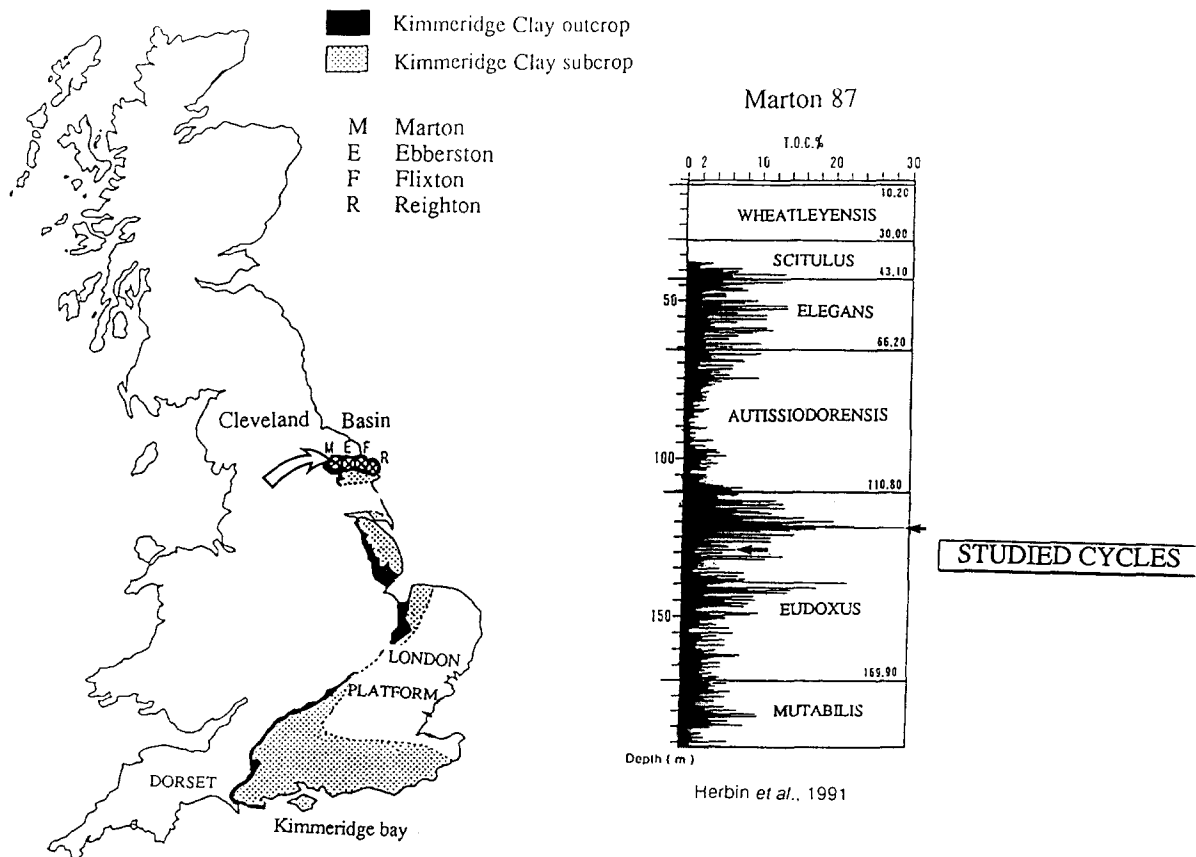


Fig. 1. Main outcrops of the Kimmeridge Clay Formation in England and vertical distribution of TOC contents (wt%) in Marton 87 Hole (after Herbin et al., 1991). The two short-term organic cycles studied are indicated by arrows.

2. Samples and methods

The total organic carbon content (TOC) and hydrogen index (HI) were obtained by Rock Eval pyrolysis performed on powdered rock samples (Espitalié et al., 1985).

The total sulphur content of the rocks was determined using both a LECO induction furnace system and energy-dispersive spectrometry coupled to a scanning electron microscope (SEM–EDS) analysis of homogenised and pressed powders (the analyses were normalised for total oxides = 100%, considering their H₂O content, %TOC and %TIC). The organic sulphur content and the pyrite sulphur content were also measured using two independent

methods. The first method involved analysis of Fe and S contents in residues after HF–HCl digestion, assumed to contain only organic matter and sulphides, according to Middelburg, 1991. The second method employed a “GSA” (GEOELF–Sulphur–Analyser). This is a self-contained system utilising the combined thermal extraction and programmed pyrolysis to liberate sulphur, which is measured by a chemiluminescence detector. This system provides data on free elemental sulphur, organically bound sulphur in kerogen and finally, inorganic sulphur (Jensen et al., 1994). The sum of the three forms of sulphur is considered as the total sulphur. Data are presented in Tables 1 and 2.

The isotopic composition of total sulphur was

Table 1
CYCLE 1

Sample No.	Depth in the core (m)	TOC (wt%)	Total S (wt%)			$\delta^{34}\text{S}$ (‰ vs. CDT)	f_s	Pyrite S (wt%)		Pyrite S (wt%)	
			EDS	LECO	GSA			TOM	GSA	TOM	GSA
1-2	128.149	2.89	0.50					0.68		0.19	
2-2	128.195	2.54	0.40	1.07	0.41	–17.00	0.43		0.276	0.276	0.132
4-1	128.233	2.82	0.44					0.46		0.40	
8-1	128.292	2.74	0.50	1.03	0.54	–12.30	0.51		0.418		0.119
10-2	128.343	2.89	0.30					0.42		0.37	
13-1	128.401	3.00	0.55	1.01	0.49	–13.80	0.49	0.62	0.372	0.35	0.115
18-1	128.509	3.91	0.73					0.76		0.13	
18-2	128.522	3.55	0.94					0.80		0.11	
22-1	128.600	4.56	0.92					0.63		0.40	
23-1	128.622	4.55	1.07					1.06		0.19	
27-1	128.683	5.64	1.04					0.68		0.58	
29-1	128.724	7.70	2.69					1.95		0.39	
30-2	128.755	9.51	4.59	7.60	3.24	–19.00	0.40	3.23	2.371	0.56	0.868
31-2	128.785	4.25	1.43	1.92	1.35	–23.75	0.32	0.84	0.951	0.14	0.394
33-1	128.817	8.59	2.75	3.64	2.08	–25.00	0.30	2.09	1.511	0.32	0.571
35-1	128.862	6.71	3.28					2.03		0.15	
35-2	128.876	6.91	2.65	3.00	1.70	–23.75	0.32	1.52	1.309	0.28	0.388
36-2	128.901	4.56	0.97	1.44	1.00	–22.00	0.35		0.781		0.219
37-1	128.912	4.91	1.25					1.10		0.14	
38-2	128.944	1.81	0.62					0.32		0.24	
39-1	128.968	2.34	0.52					0.41		0.23	
41-1	129.008	3.38	0.55					0.75		0.29	
42-1	129.029	2.01	0.67					0.97		0.10	
43-2	129.065	1.47	0.51	1.28	2.62	–16.00	0.45	0.53	2.195	0.12	0.423
44-1	129.077	1.68	0.66					0.74		0.24	
45-1	129.093	1.74	0.85					1.07		0.01	
49-2	129.187	1.71	0.55					0.82		0.01	
50-1	129.200	1.84	0.80	1.54	0.60	–18.50	0.41		0.503		0.101
52-2	129.252	1.88	0.59					0.14		1.50	

Total sulphur content was analysed by using three different techniques: EDS coupled to a SEM ($\pm 0.05\%$), a LECO system ($\pm 0.02\%$) and a GSA system (GEOELF–Sulphur–Analyser) ($\pm 0.02\%$). Pyrite and organic sulphur data were obtained by two methods: measurements of S and Fe in total organic matter (TOM) with an accuracy $\pm 0.01\%$ and GSA with an accuracy $\pm 0.02\%$

Table 2
CYCLE 2

Sample No.	Depth in the core (m)	TOC (wt%)	Total S (wt%)			Pyrite S (TOM) (wt%)	Organic S (TOM) (wt%)
			EDS	LECO	GSA		
43	121.04	8.58	3.76			2.08	0.57
41	121.07	17.02	5.15			2.56	0.98
33	121.17	7.39	2.24			2.22	0.37
30	121.21	9.49	3.16	3.42	3.88		
26	121.26	15.62	4.31			2.17	0.84
24	121.28	9.18	6.13			2.08	0.46
22	121.30	16.86	4.67	4.89	5.43		
21	121.35	13.66	4.87			2.16	0.66
19	121.38	31.37	10.76			1.82	2.96
17	121.42	28.94	10.80			2.15	2.46
16	121.43	28.47	9.98	7.61	10.24	2.43	2.24
15	121.44	20.04	6.99			2.58	2.21
14	121.46	14.05	6.22	8.02	8.26	0.95	0.89
9	121.51	8.87	3.46	4.41	4.21		
7	121.53	9.40	3.38			2.27	0.52
4	121.57	5.53	1.22	1.97	1.24		
3	121.58	4.99	0.85			1.04	0.55
1	121.60	4.73	0.81	1.23	0.78		

Total sulphur content was analysed by using three different techniques: EDS coupled to a SEM ($\pm 0.05\%$), a LECO system ($\pm 0.02\%$) and a GSA system (GEOELF-Sulphur-Analyser) ($\pm 0.02\%$). Pyrite and organic sulphur data were obtained by measurements of S and Fe in total organic matter (TOM) with an accuracy $\pm 0.01\%$.

determined as described in Zaback and Pratt (1992). A "LECO" type C/S-244 automatic analysis system, was used for quantitative determination of total sulphur and for preparation of SO_2 for analysis of ^{34}S in total sulphur. Amounts of SO_2 were measured spectrophotometrically and a portion of the SO_2 was trapped for mass spectrometric analysis with a Nuclide model 6–60 (Ripley and Al-Jassar, 1987). The accuracy of the procedure was confirmed by comparison of results with mass-balanced contributions from individual sulphur phases and with results of conventional total-sulphur analyses.

The standard deviation of replicate analyses of total sulphur was better than 0.3% . Replicate analysis of the NBS-123 ZnS standard, for which the accepted $\delta^{34}\text{S}$ CDT value is $+17.32\%$, yielded an average δ value of $+17.35\%$ and $\sigma = 0.16\%$ ($n = 5$).

3. Results

The sediments of the first short-term cycle contain total organic carbon contents (TOC) between 2% and

10%, and hydrogen indices (HI) between 150 and 650 mg HC/g TOC. The second cycle has TOC values between 4% and 30%, and HI values ranging from 300 to 800 mg HC/g TOC. Both cycles show a strong positive correlation between quantity and quality of the organic matter, as illustrated by TOC and HI variations (Fig. 2).

As described by Boussafir et al. (1995a,b), the petrographical study of organic matter from the same samples, using transmission electron microscopy techniques (TEM), showed different organic ultrastructures to be associated with respect to the TOC and HI values of the samples. Both ultrastructural and molecular features of these samples are summarised in a model which accounts for the accumulation of marine hydrocarbon-rich organic matter (Boussafir and Lallier-Vergès, 1996). TEM investigations demonstrated that samples with low values of TOC and HI are characterised by a bio-resistant organic matter which mainly consists of ultralaminated material and lignaceous minute debris in minor quantities. The ultralaminae are the result of the selective preservation of bio-resistant microalgal cell-walls as shown by the presence of *n*-alkylnitriles

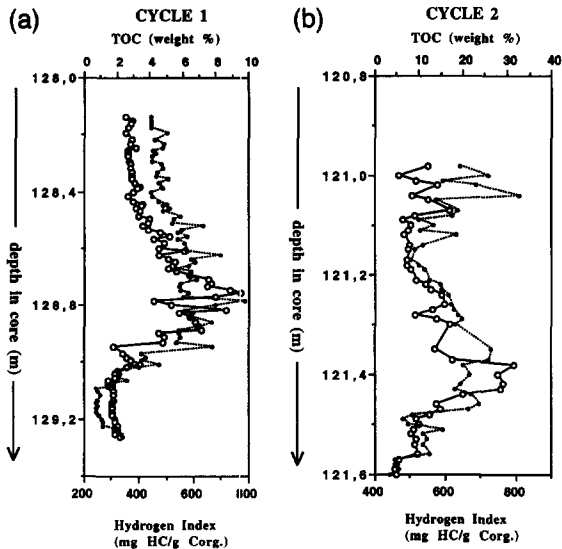


Fig. 2. Distributions of TOC (wt%; open circles) and HI (mg HC/g TOC; filled squares) values along the two cycles.

in the pyrolysis products (Derenne et al., 1992) while the lignaceous debris are the product of the selective preservation of resistant higher-plant material (also evidenced by the occurrence of phenols in the pyrolysis products). In contrast, samples with high values of TOC and HI are mainly characterised by a nanoscopically amorphous organic matter in which the resistant character is thought to have been inherited due the early incorporation of sulphur. This natural vulcanisation of lipid-rich molecules (Sinninghe-Damsté et al., 1989) has been previously demonstrated on same samples by the study of pyrolytic products (Boussafir et al., 1995b).

3.1. Estimation of sulphate reduction intensity

The sulphur measurements from the three methods are generally consistent, but tend to show some discrepancy for the highest values of sulphur. The relationship between the data obtained from EDS system and those obtained by LECO and GSA systems is presented in Fig. 3a and b for CYCLE 1. Because of the good correlation of EDS data with both LECO and GSA results, the sulphur contents for the 60 samples studied were analysed by EDS system, which is an accurate method, easier to perform than the other ones.

In all cases, there is a positive relationship between sulphur content and TOC (Fig. 4). This well-known correlation, first defined by Berner and Raiswell (1983), describes the microbial sulphate reduction process. The greater the amount of metabolisable organic matter available to sulphate-reducing bacteria, the higher the intensity of sulphate reduction and thus the amount of accumulated sulphides and resistant organic matter. Fig. 5 illustrates this linear relationship for both cycles, based on EDS measurements only. For high TOC values, the points

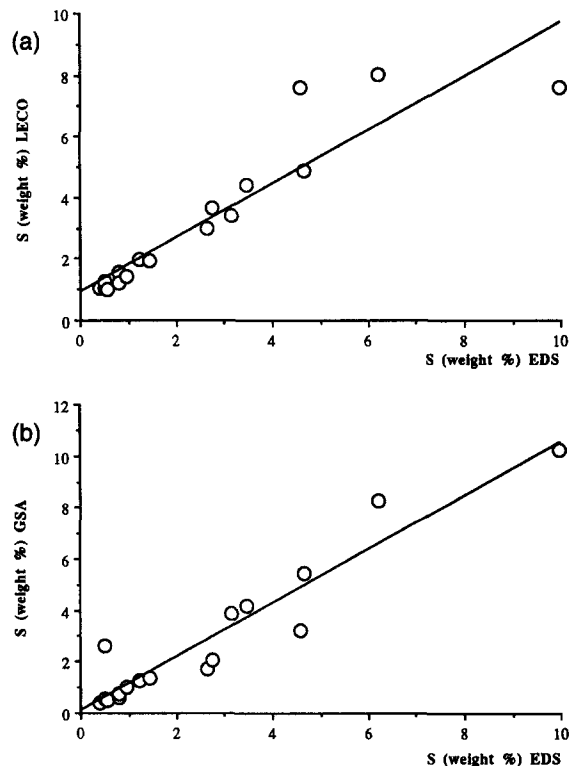


Fig. 3. a. Comparison of total sulphur content results (wt%) obtained by EDS system (X-ray energy-dispersive spectrometry) coupled to a SEM and LECO system for CYCLE 1 samples. The equation of the regression line is $y = 0.94 + 0.88x$ with $r^2 = 0.845$.

b. Comparison of total sulphur content results (wt%) obtained by EDS system (X-ray energy-dispersive spectrometry) coupled to a SEM and a GSA system (GEOELF-Sulphur-Analyser). The equation of the regression line is $y = -0.17 + 1.09x$ with $r^2 = 0.937$. One sample exhibits a high S content (= 2.62%) with GSA system, whereas EDS system gives 0.51% but this is due to the occurrence of a large-sized fragment of pyritic ammonite in the sample which was analysed by GSA system.

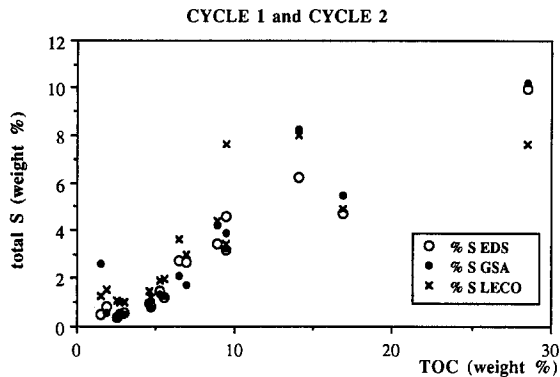


Fig. 4. Total sulphur content (wt%) vs. TOC (wt%) in CYCLE 1. Sulphur was analysed by using three different techniques: LECO system, GSA system (GEOELF-Sulphur-Analyser), EDS system (X-ray energy-dispersive spectrometry) coupled to a SEM (see Table 1).

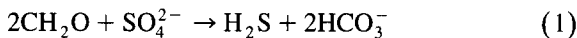
are located under the Berner and Raiswell’s line, that may indicate a slight decrease in the activity of microbial sulphate reduction. This is interpreted as a progressive limitation of sulphate (or other metabolites) for sulphate-reducing bacteria (Pedersen and Calvert, 1990; Lallier-Vergès et al., 1993a). The parallel organic enrichment is due to the accumulation of resistant organic matter, which the resistant character has been inherited or acquired through bacterial degradation.

Each mole of sulphide formed represents the oxidation of approximately two moles of organic carbon (Berner and Raiswell, 1983). Depending on the efficiency with which hydrogen sulphide is retained,

each mole of sedimentary sulphide therefore represents at least two moles of organic carbon initially present in the sediment (considerably more if retention of sulphide has been poor). In order to estimate the extent of S trapping in the sediment, two independent approaches have been attempted. The first approach which takes into account the stoichiometry of the sulphate reduction equation, is based on the calculation of a “sulphate reduction index” (SRI) obtained from the determination of total sulphur and TOC contents present in the sediment. The second approach takes into account the possible variation of HS⁻ retention and is based on the isotopic composition of the total-reduced-sulphur pool.

3.1.1. Sulphate reduction index (SRI)

We determined the SRI, as defined in Lallier-Vergès et al. (1993a,b), on the basis of the sulphate reduction reaction:



$$\text{SRI} = \frac{(\% \text{ initial organic carbon})}{(\% \text{ preserved organic carbon})}$$

Initial organic carbon was calculated as the sum of preserved organic carbon (i.e. TOC) and oxidised organic carbon utilising the sulphur contents and the above stoichiometric equation. The relationship between SRI and TOC, presented for the two cycles studied (Fig. 6), attests that organic matter quality, in terms of the ratio of metabolisable/refractory carbon delivered to the sediments, has varied along the two

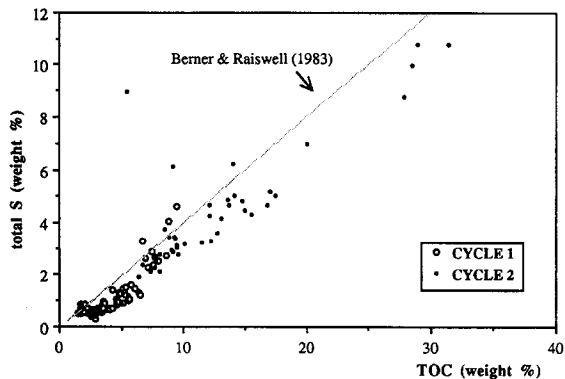


Fig. 5. Total sulphur content (wt%) vs. TOC (wt%) for CYCLE 1 and CYCLE 2. Sulphur contents were obtained by using energy-dispersive spectrometry coupled to a SEM on homogenised powders.

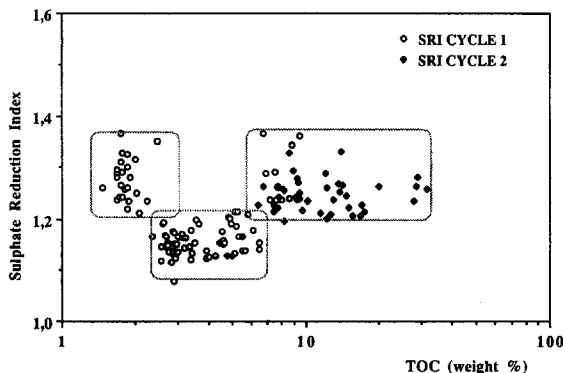


Fig. 6. Sulphate reduction index (SRI) vs. TOC (wt%) for CYCLE 1 and CYCLE 2. Sulphur contents were obtained by using energy-dispersive spectrometry coupled to a SEM on homogenised powders.

cycles. This variation shows within the three envelopes of points, different distinct trends discussed below.

3.1.2. Calculation of HS⁻ retention

The rate of HS⁻ retention in the sediment has been calculated on the basis of δ³⁴S measurements of total sedimentary sulphur. Measured values of δ for total sulphur reflect depletion in ³⁴S relative to seawater sulphate. The magnitude of that depletion can be expressed in terms of an overall fractionation factor, α₀:

$$\alpha_0 = (\delta_{sw} + 1000) / (\delta_{sed} + 1000)$$

where sw and sed designate seawater sulphate and sedimentary sulphide, respectively. The value of δ_{sw} was about +16.3‰ at the Kimmeridgian time as suggested by data from Claypool et al. (1980) and Holser et al. (1988).

According to Zaback and Pratt (1992) and Zaback et al. (1993), α₀ is controlled by isotope effects and by relative flows of sulphur in the system (see Fig. 7), where α₁ is the fractionation factor associated with dissimilatory reduction of sulphate by bacteria and the Φ terms are flux of sulphur in moles per unit of time.

Once HS⁻ has been formed, its commitment to pathway 3 (immobilisation) or to pathway 4 (re-oxidation) will depend mainly on the direction in which it diffuses (towards O₂ or away from O₂). In this study, the partially oxidised intermediates such as thiosulphates, polythionates and polysulphides, which are important in explaining the mobility of reduced sulphur in sedimentary pore waters and es-

tablishing the overall fractionation between sulphate and sulphide, are not considered as far as the aim of this study only concerns the overall mass and redox balances and does not deal properly with mechanisms underlying sulphate reduction and isotopic fractionation.

Since there is no significant isotopic effect expected with diffusion, according to Zaback et al. (1993), the division of sulphur between pathways 3 and 4 would not be associated with any isotopic fractionation. Thus, if δ₃ is equal to δ₄, then δ₃ and δ₄ must also be equal to δ₂ and to δ_{sed}, and the mass-balance equations become simply:

$$\begin{aligned} \text{For total sulphur:} \quad & \Phi_1 = \Phi_5 + \Phi_3 \\ \text{For } ^{34}\text{S:} \quad & \Phi_1 \delta_{sw} = \Phi_5 \delta_{pw} + \Phi_3 \delta_{sed} \end{aligned}$$

where δ_{pw} is the isotopic composition of pore-water sulphate.

Rearrangements of these expressions yields

$$\alpha_0 = f_s + (1 - f_s) \alpha_1$$

where f_s is Φ₃/Φ₁, that is the fraction of incoming sulphate that is immobilised or trapped in the sediment. Here values of f_s have been calculated from measured values of α₀ and α₁ = 1.060.

This parameter was obtained for ten samples of CYCLE 1 (Fig. 8a). From these observed variations in f_s, it is clear that efficiency of retention of sulphide varied, being minimal when supply of organic material was greatest. This variation occurring in a single cycle (1 m thick) may reflect variations in delivered organic matter in terms of metabolisable/refractory carbon ratio. This idea is also supported by SRI variations and petrographical results.

3.2. Sulphide speciation and iron availability

Sulphur speciation has been examined to specify the mechanisms of sulphur enrichment of the sediments. The sulphur content vs. TOC diagram for CYCLE 1 (Fig. 9) shows the comparison of pyrite sulphur and organic sulphur contents, analysed by both the methods used. In spite of some discrepancies between the results of each method, the general trends of sulphur species vs. TOC are comparable. Comparison between the two cycles was made using sulphur and iron determinations in the total organic

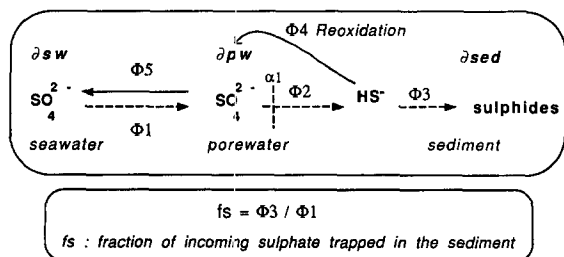


Fig. 7. Schematic illustrating isotope effects and relative flows of sulphur at the sediment–water interface, occurring during reduction of sulphates and fixation of sulphides.

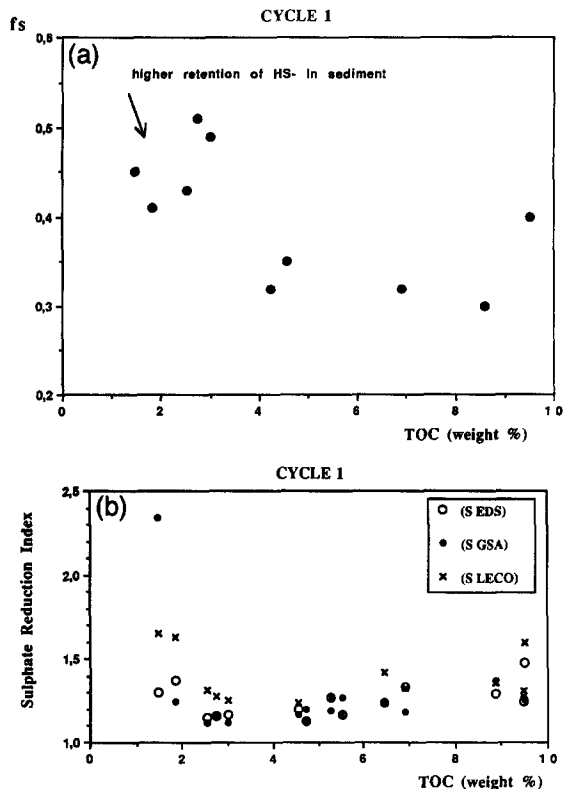


Fig. 8. a. f_s (HS^- retention) vs. TOC (wt%) for CYCLE 1. b. Sulphate reduction index (SRI) vs. TOC (wt%) for CYCLE 1. Sulphur was analysed by using three different techniques: LECO system, GSA system (GEOELF-Sulphur-Analyser), and EDS system (X-ray energy-dispersive spectrometry) coupled to a SEM. One sample exhibits a very high SRI (~ 2.4). This is due to the occurrence of a large-sized fragment of pyritic ammonite in the sample which was analysed by the GSA system.

matter (TOM) isolated by HF–HCl (Fig. 10a and b). In CYCLE 1, pyritic sulphur is always greater than organic sulphur and, as a consequence, the general trend of pyritic sulphur vs. TOC is similar to that of total sulphur content. In CYCLE 2, pyritic sulphur reaches a plateau between 10% and 15% TOC, and remains nearly constant. At the same time, organic sulphur increases proportionally with increased TOC and indeed becomes greater than the pyritic sulphur content at the highest TOC values. This result is in accordance with previous studies on the organic-rich sediments from the Kimmeridge Clay Formation of Dorset, south England (Lallier-Vergès et al., 1993b).

The degree of pyritisation, DOP, has been determined on the basis of iron analyses. It consists of the

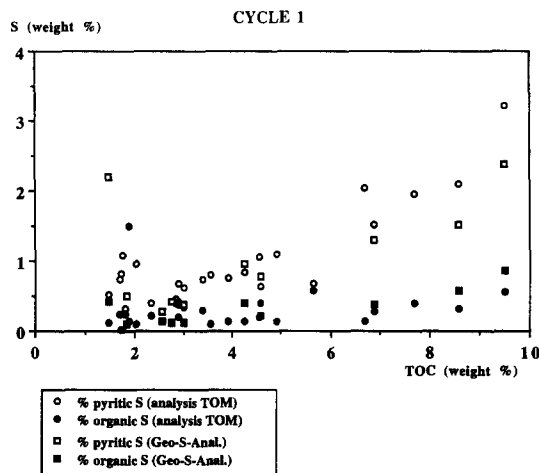


Fig. 9. Organic and pyrite sulphur contents (wt%) vs. TOC (wt%) for CYCLE 1. Comparison of data obtained by the two methods: GSA and measurements of S and Fe in total organic matter.

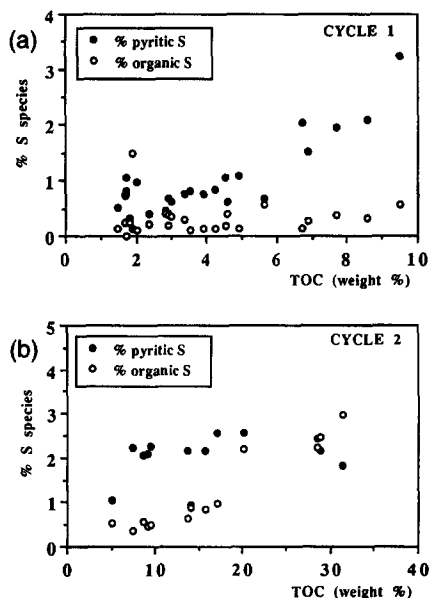


Fig. 10. a. Organic and pyrite sulphur contents (wt%) vs. TOC (wt%) for CYCLE 1. Data obtained by measurements of S and Fe in total organic matter. b. Organic and pyrite sulphur contents (wt%) vs. TOC (wt%) for CYCLE 2. Data obtained by measurements of S and Fe in total organic matter.

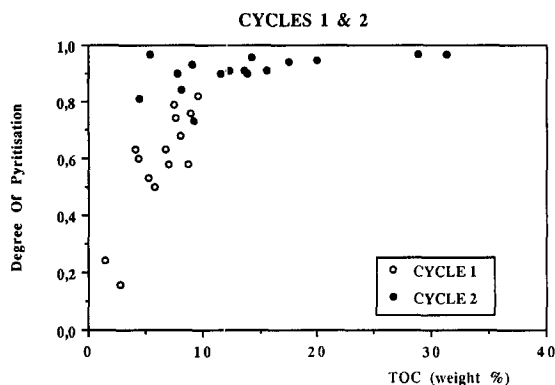


Fig. 11. Degree of pyritisation (DOP) vs. TOC (wt%) for CYCLE 1 and CYCLE 2, after Tribovillard et al. (1994). In samples from CYCLE 2, DOP is close to 1, showing the limitation of pyrite formation.

ratio between reduced iron content and total reactive iron content and is thought to estimate the extent to which the initial potentially reactive iron has been transformed in pyrite (Berner, 1970; Raiswell et al., 1988). The DOP is plotted vs. TOC contents on Fig. 11, for samples from both the cycles. When this ratio is < 1 , it is considered that available iron was not a limiting factor for pyritisation, as is the case for CYCLE 1. On the contrary, when the ratio approaches unity, as is the case for CYCLE 2, the available iron is considered to have been the limiting factor for pyritisation (Tribovillard et al., 1994). This leads to the conclusion that the availability of reactive iron was limited above TOC values ranging around 7%, which in turn, resulted in excess HS^- and favoured incorporation of sulphur into organic matter.

4. Discussion

We have compared our results with the present functioning of the well-constrained marine photic zone. These studies indicate that when primary productivity is low, most of the phytoplankton is recycled in the photic zone due to the action of the grazing. Due to the increase of assimilation efficiency, the ratio between export and total production decreases when total production decreases (Aksnes and Wassman, 1993). Only a small amount of organic matter escapes from the photic zone and is delivered to the sediments. In contrast, high primary

productivity periods are characterised by the inability of the grazers to recycle the total produced organic matter. The phytoplankton may form large flocs which are rapidly delivered downwards the sediment–water interface (Wefer, 1989; Jackson, 1990). The particle flux rate may exceed consumption rate. These flocs are associated with algal blooms, nowadays mainly diatoms. The formation of these aggregates is related to the production of mucilages composed of polysaccharides, which increase the proportion of labile organic matter in the delivered organic matter.

Fig. 8a and b show, respectively, the variations of f_s values and SRI (calculated by elemental abundances) vs. TOC. SRI variations represent the variations of delivered metabolisable organic matter vs. resistant organic matter. f_s is considered to represent the fraction of sulphate imported to the system that is retained as reduced sulphur, either as pyrite or organically-bound sulphur. Minimum values of f_s ($\rightarrow 0$) occur when only a small fraction of the sulphate imported from the water column is retained in the sediment. High values of f_s ($\rightarrow 1$) indicate situations in which nearly all imported sulphate has been retained as sedimentary sulphur.

For sediments exhibiting low TOC values ($< 2\%$ or 3%), the SRI increases with decreasing TOC (Fig. 8b). Surprisingly, in these low-TOC samples, which also have low HI values (Fig. 2) and low sulphur contents (Fig. 5), the retention of HS^- is high as indicated by the maximum values of f_s (Fig. 8a). In these sediments, the marine organic matter is mainly composed of bio-resistant organic matter (lipid-rich algal cell-walls). All these results indicate that the amount of organic matter delivered towards the water–sediment interface, was low and poor in metabolisable organic matter. Nearly all the available metabolisable organic matter has been oxidised before deposition. This high SRI in samples having low TOC and sulphur contents is unexpected. It is here tentatively explained by an additional input of metabolisable organic matter derived from biological species which do not contain any resistant lipid-rich organic matter and consequently do not accumulate organic matter as TOC. This is mostly the case for zooplankton and nekton. Indeed, thin section studies show that the samples with the highest SRI have the greatest microfossil content, mainly foraminifers,

ammonites and bivalves, whose skeletons have been partially or totally replaced by pyrite. Moreover, these skeletal remains increase the porosity of the sediment, in which reducing micro-environments mainly develop. This trend has already been described in Oman Margin sediments (Lallier-Vergès et al., 1993a). Here, the occurrence of pelagic grazers, attested by zooplankton skeletons and pellets, also suggest a low primary productivity, as far as the ratio between grazing and production in the photic zone is higher during periods of lower productivity (Aksnes and Wassman, 1993).

For TOC values increasing from ~2–3% to ~6–7%, the SRI values are low and mostly constant. In this range of values, total sulphur contents also increase (Fig. 5). This result shows the degradation of a constant part of metabolisable organic matter delivered to the sediment. Indeed, the petrographical study of organic matter of these sediments revealed the progressive diminution of structured bio-resistant organic matter and the correlative increase of amorphous organic matter. Pyrite framboids are mostly associated to this amorphous organic matter. The amount of pyrite sulphur also increases in this interval of TOC values (Fig. 10a and b).

Above ~6–7% TOC, the SRI is still high (Fig. 6); this domain also corresponds to increasing total sulphur contents. This trend suggests that the proportion of metabolisable organic matter associated with the bio-resistant organic matter, increased with the rate of delivery of organic matter. In these samples, f_s is minimum (Fig. 8a). It is thought that the real variations in delivery of metabolisable organic material to the sediment were even greater than apparent from the variations in carbon + sulphur contents. Parallel geochemical studies also indicate that for these sediments, the 6% TOC value is a threshold value above which the molecular composition of bitumen is different (Ramanampisoa and Disnar, 1994). TEM observations reveal that this organic matter is strictly composed by a nanoscopically amorphous organic matter enriched in organic sulphur and closely associated with clays (smectites). Indeed, the molecular composition of the kerogen shows that labile lipid-rich compounds have been preserved from microbial degradation by early incorporation of sulphur (Boussafir et al., 1995b). This early ‘‘vulcanisation’’ is probably greatly favoured

by the limitation of available iron species, as seen by the distribution of DOP (Fig. 11).

5. Conclusions

Within the cycles, the rate and quality of organic matter delivered from the photic zone to the sediment varied through the time such that concentrations of accumulated organic carbon vary as a function of depth in the core. For total sedimentary sulphur, there are concomitant variations not only in concentration but also in isotopic composition. It is therefore required that sedimentary processes changed in response to variations in the input of organic carbon. Specifically, differences in the rate and chemical composition of delivered organic matter are thought to have influenced microbial sulphate reduction intensity (as indicated by SRI values) and efficiency (as seen by isotopic composition of sulphur). As a result, the sulphate reduction process would be ruled by the availability of organic matter for sulphate-reducing bacteria in which the variations along the cycle led to various HS^- retentions compared to the useful sulphate pool.

In summary, we propose a model to explain the cyclicity of both sulphide and organic matter contents in relation to primary productivity variations. Fig. 12 summarises the different stages envisioning link between primary productivity and sediment composition in terms of organic carbon, hydrocarbon, sulphur contents and SRI.

As primary productivity of phytoplankton abundance increases, a point is reached where delivered organic flux increases dramatically and becomes dominated by metabolisable organic matter (probably derived from organic flocs associated with coccolite blooms). This situation is the reverse of a low productivity regime in which the grazer action dominates the organic delivery. In the latter case, we propose the idea that the grazing action may locally favour the sulphate reduction (high SRI) in the sediments, despite the low amount of labile organic matter exported from the photic zone, both by supplying some metabolisable organic matter present into the mineral tests and also by creating local strongly reducing environments into the skeletons.

A sudden and intense increase of the organic flux

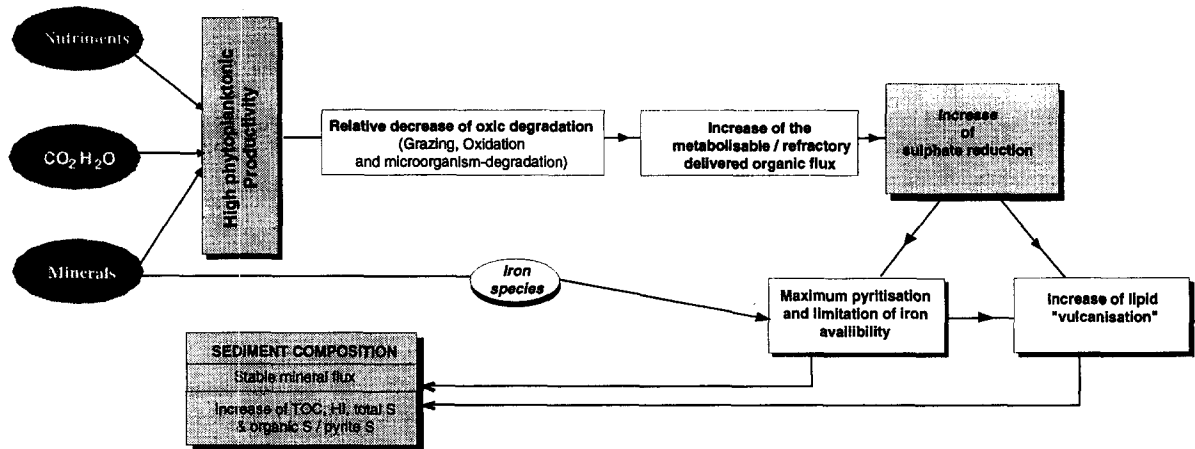


Fig. 12. Schematic summarising proposed inter-related processes linking primary productivity, sulphate reduction and HC-enriched organic matter preservation to account for the variability of organic composition of Kimmeridgian series. The relative intensity of each step is represented using arrows.

results in an increased SRI due to the additional supply of metabolisable organic matter. Moreover the increased organic supply has a global diluting action on the mineral supply and thus, on the reactive iron relative availability. The combination of these two processes result in the formation of excess HS^- , which may lead to the early vulcanisation of labile lipidic organic matter (Sinninghe-Damsté et al., 1989), the latter being derived from phytoplankton and microalgae as indicated by the molecular studies of this organic matter (Boussafir et al., 1995a,b).

All these interactive processes influence the final sedimentary organic content, oil potential, sulphur content and speciation. If primary productivity variations are considered to be the dominant parameter in driving the organic cyclicity, other parameters may play a critical role in determining organic accumulation by influencing degradation efficiencies. Examples include the type of specific primary productivity, the ratio of organic flux to mineral flux, that means the various weathering on land linked to climatic and sea-level variations.

Acknowledgements

The authors wish to acknowledge the "Groupe-ment de Recherche 942" of the Centre National de

la Recherche Scientifique for its financial support. This group was formed by CNRS, Université d'Orléans, Université de Paris-Sud, IFP, TOTAL-CFP and ELF-Aquitaine. Special thanks are devoted to J.R. Disnar (URA 724 CNRS, Orléans) for providing and discussing Rock Eval data.

References

- Aksnes, D.L. and Wassman, P., 1993. Modeling the significance of zooplankton grazing for export production. *Limnol. Oceanogr.*, 38(5): 978–985.
- Berner, R.A., 1970. Sedimentary pyrite formation: an update. *Am. J. Sci.*, 268: 1–23.
- Berner, R.A. and Raiswell, R., 1983. Burial of organic carbon and pyrite sulphur in sediments over Phanerozoic time: a new theory. *Geochim. Cosmochim. Acta*, 47: 855–862.
- Bertrand, P. and Lallier-Vergès, E., 1993. Past sedimentary organic matter accumulation and degradation controlled by productivity. *Nature (London)*, 364: 786–788.
- Bertrand, P., Lallier-Vergès, E. and Boussafir, M., 1994. A major control of cyclic organic sedimentation in marine anoxic depositional conditions: the productivity-related organic fluxes to redox interface. *Org. Geochem.*, 22: 511–520.
- Boussafir, M. and Lallier-Vergès, E., 1996. Accumulation of organic matter in the Kimmeridge Clay Formation (KCF): an update fossilisation model for petroleum source-rocks. *Mar. Pet. Geol.* (in press).
- Boussafir, M., Lallier-Vergès, E., Bertrand, P. and Badaut-Trauth, D., 1995a. SEM and TEM studies of organic matter and source rock microfacies from a short-term organic cycle of Kimmeridgian source-rocks. In: E. Lallier-Vergès, N.P. Tri-

- bovillard and P. Bertrand (Editors), *Organic Matter Accumulation. Lecture Notes in Earth Sciences*, 57. Springer, Heidelberg, pp. 15–30.
- Boussafir, M., Gelin, F., Lallier-Vergès, E., Derenne, S., Bertrand, P. and Largeau, C., 1995b. Electron Microscopy and pyrolysis of kerogens from the Kimmeridge Clay Formation (UK): source of organisms, preservation processes and origin of microcycles. *Geochim. Cosmochim. Acta*, 59: 3731–3747.
- Claypool, G.E., Holser, W.T., Kaplan, L.R., Sakai, H. and Zak, L., 1980. The age curves of sulfur and oxygen isotopes in marine sulfate and their mutual interpretation. *Chem. Geol.*, 28: 199–260.
- Derenne, S., Le Berre, F., Largeau, C., Hatcher, P., Connan, J. and Raynaud, J.F., 1992. Formation of ultralaminar in marine kerogens via selective preservation of thin resistant outer walls of microalgae. *Org. Geochem.*, 19: 345–350.
- Espitalié, J., Deroo, G. and Marquis, F., 1985. La pyrolyse Rock Eval et ses applications, Part B. *Rev. Inst. Fr. Pét.*, 40(6): 563–579.
- Herbin, J.P., Müller, C., Geysant, C., Mélières, J.R., Penn, F. and the YORKIM Group (IFP), 1991. Hétérogénéité quantitative et qualitative de la matière organique dans les argiles du Val de Pickering (Yorkshire, U.K.): cadre sédimentologique et stratigraphique. *Rev. Inst. Fr. Pét.*, 46(6): 675–712.
- Herbin, J.P., Geysant, J.R., Mélières, F., Müller, C., Penn, I.E. and YORKIM Group, 1993b. Variation of the distribution of organic matter within a transgressive system tract: Kimmeridge Clay (Jurassic), England. In: B. Katz and L. Pratt (Editors), *Petroleum Source Rocks in a Sequence Stratigraphic Framework*. Am. Assoc. Pet. Geol., Stud. Geol., pp. 67–99.
- Holser, W.T., Schidlowski, M., Mackenzie, F.T. and Maynard, J.B., 1988. Geochemical cycles of carbon and sulfur. In: C.B. Gregor, R.M. Garrels, F.T. Mackenzie and J.B. Maynard (Editors), *Chemical Cycles in the Evolution of the Earth*. Wiley, New York, N.Y., pp. 105–173.
- Jackson, G.A., 1990. A model of the formation of marine algal flocs by physical coagulation processes. *Deep-Sea Res.*, 37(8): 1197–1211.
- Jensen, H., Connan, J., Bjorøy, M., Hall, K. and Ferriday, I.L., 1994. GEOELF sulphur analyser (GSA), a new instrument for rapid screening of organic and mineral sulphur in coals. *Bull. Cent. Rech. Explor.-Prod. Elf-Aquitaine*, 18: 287–288.
- Lallier-Vergès, E., Bertrand, P., and Desprairies, A., 1993a. Organic matter composition and sulphate reduction intensity in Oman margin sediments. *Mar. Geol.*, 112: 57–69.
- Lallier-Vergès, E., Bertrand, P., Huc, A.Y., Tremblay, P. and Bückel, D., 1993b. Control of the preservation of organic matter by productivity and sulphate reduction in marine anoxic sediments: Kimmeridgian shales from Dorset (U.K.). *Mar. Pet. Geol.*, 10: 600–605.
- Middelburg, J.J., 1991. Organic carbon, sulphur and iron in recent semi-euxinic sediments from sediments of Kau Bay, Indonesia. *Geochim. Cosmochim. Acta*, 55: 815–828.
- Pedersen, T.F. and Calvert, S.E., 1990. Anoxia vs. productivity: What controls the formation of organic-carbon rich sediments and sedimentary rocks? *Am. Assoc. Pet. Geol. Bull.*, 74: 454–466.
- Raiswell, R., Buckley, F., Berner, R.A. and Anderson, T.F., 1988. Degree of pyritization as a palaeoenvironmental indicator of bottom water oxygenation. *J. Sediment. Petrol.*, 58: 812–819.
- Ramanampisoa, L. and Disnar, J.R., 1994. Primary control of paleoproduction on organic matter preservation and accumulation in the Kimmeridge rocks of Yorkshire. *Org. Geochem.*, 21: 1153–1167.
- Ripley, E.M. and Al-Jassar, T., 1987. Sulfur and oxygen isotopic studies of melt–country rock interaction, Babitt Cu–Ni deposit, Duluth Complex, Minnesota. *Econ. Geol.*, 82: 87–107.
- Sinninghe-Damsté, J.S., Rijpstra, W.I., Kock-Van Dalen, A.C., de Leeuw, J.W. and Schenck, P.A., 1989. Quenching of labile functionalised lipids by inorganic sulphur species: evidence for the formation of sedimentary organic sulphur compounds at the early stages of diagenesis. *Geochim. Cosmochim. Acta*, 55: 1343–1355.
- Tribovillard, N.P., Desprairies, A., Bertrand, P., Lallier-Vergès, E., Disnar, J.R. and Pradier, B., 1992. Étude à haute résolution d'un cycle du carbone organique de roches kimmeridgiennes du Yorkshire (GB): minéralogie et géochimie (résultats préliminaires). *C.R. Acad. Sci., Paris*, 314(9): 923–930.
- Tribovillard, N.P., Desprairies, A., Lallier-Vergès, E., Bertrand, P., Moureau, N., Ramdani, A. and Ramanampisoa, L., 1994. Geochemical study of organic matter rich cycles from the Kimmeridge Clay Formation of Yorkshire (UK): productivity versus anoxia. *Palaeogeogr., Palaeoclimatol., Palaeoecol.*, 108: 165–181.
- Wefer, G., 1989. Particle flux in the oceans: effects of episodic production In: W.H. Berger, V.S. Smetacek and G. Wefer (Editors), *Report of the Dahlem Workshop on Productivity of the Oceans: Present and Past*, Berlin 1988. Wiley, Chichester, pp. 139–154.
- Zaback, D.A. and Pratt, L.M., 1992. Isotopic composition and speciation of sulphur in the Miocene Monterey Formation: Re-evaluation of sulphur reactions during early diagenesis in marine environments. *Geochim. Cosmochim. Acta*, 56: 763–774.
- Zaback, D.A., Pratt, L.M. and Hayes, J.M., 1993. Transport and reduction of sulphate and immobilisation of sulphide in marine black shales. *Geology*, 21: 141–144.

Accumulation of organic matter in the Kimmeridge Clay Formation (KCF): an update fossilisation model for marine petroleum source-rocks

Mohammed Boussafir and Elisabeth Lallier-Vergès

URA 724-FR09 CNRS, Laboratoire de Géologie de la Matière Organique, Université d'Orléans, B.P. 6759, F-45067 Orléans cedex 2, France

Received 18 December 1995; revised 26 August 1996; accepted 25 September 1996

A model for marine source-rocks based on previous microtextural and molecular characterisation of the immature organic matter from the KCF (UK) is developed, illustrating the relationship between the type of primary producers, the nature of organic matter (metabolisable or bio-resistant) delivered to the sedimentary environment and the mechanisms of organic matter fossilisation. The fossilisation occurs because one of the following factors prevails: (a) The inherited bio-resistant character of the initial organic matter in the case of (i) a selective preservation sensu stricto when both the biological structure and the molecular composition are well preserved, and (ii) a re-organisation of resistant bio-macromolecules selectively preserved when only the molecular composition is conserved. (b) The acquisition of bio-resistance, as in the case of (iii) natural vulcanisation, which produces a homogeneous and nanoscopically amorphous organic matter. The latter is hydrogen-rich and its genesis depends on the rate of delivery of metabolisable organic matter to the oxic-anoxic boundary. This is determined by primary productivity-controlled sinking rates and, as a consequence, by the occurrence in bottom waters of conditions promoting a prolific growth of sulphate-reducers along with a somewhat limited supply of iron so that H₂S is not entirely trapped as pyrite. (c) The accumulation of hydrogen-rich organic matter in such source-rocks is not only due to the phytoplanktonic and micro-algal origin of natural bio-macromolecules, but also to sulphate-reduction which protects a part of the oil potential of deposited organic matter. © 1997 Elsevier Science Ltd. All rights reserved.

Keywords: Kimmeridge Clay; primary production; sulphate reduction; amorphous organic matter; selective preservation; natural vulcanisation

The 'preservation' of sedimentary organic matter (OM) in sedimentary rocks is a general concept used by petrographers, geochemists and sedimentologists in different ways. For sedimentologists, the preserved fraction of the organic matter is that defined relative to the recycled organic carbon and corresponds to the total sedimentary organic carbon (TOC%). For petrographers, OM is 'well preserved' when the biological textures are still visible, whereas for geochemists, it is only 'well preserved' when it is hydrogen-rich and has a good capacity to generate hydrocarbon molecules at the stage of catagenesis during sediment burial.

The organic origin of sedimentary hydrocarbons is now generally accepted (Durand, 1980; Tissot and Welte, 1984; Bordenave and Durand, 1993). However, debates concerning the general sedimentology of OM and in particular the genetic origin of petroleum source rocks, rage on. Two main interpretative models, involving different mechanisms of preservation for the accumulation of sedimentary OM, have already been proposed:

1. a first model is based on a diagenetic fragmentation of the bio-macromolecules of the OM. Monomers are transformed by re-organisation into a group of humic substances which, as a whole, further evolve into a

group termed 'geopolymers' as a result of polycondensation (Tissot and Welte, 1984).

2. a second model is based on two concepts: selective preservation and natural vulcanisation of sedimentary OM. Indeed, certain bio-macromolecules, are inherently resistant and they participate in the formation of kerogen. This concept is therefore named the 'selective preservation' of resistant bio-macromolecules (Largeau *et al.*, 1984; Tegelaar *et al.*, 1989; Tegelaar, 1990; Derenne *et al.*, 1991). Sulphur-containing organic components in kerogen, can be formed by early natural vulcanisation of the lipids (Sinningh-Damsté *et al.*, 1989).

Finally, the discussion also concerns the concept of anoxicity which is considered either as the primary parameter involved in the accumulation of OM in sediments (Demaison and Moore, 1980) or as a consequence of high primary productivity which is thus considered as the primary parameter (Calvert and Pedersen, 1992).

Generally, the study of fossilised organic matter, isolated from the rock and observed under transmitted light microscopy (palynofacies), shows two organic sets: biologically unstructured organic matter called amorphous organic matter (AOM), which often represents almost all

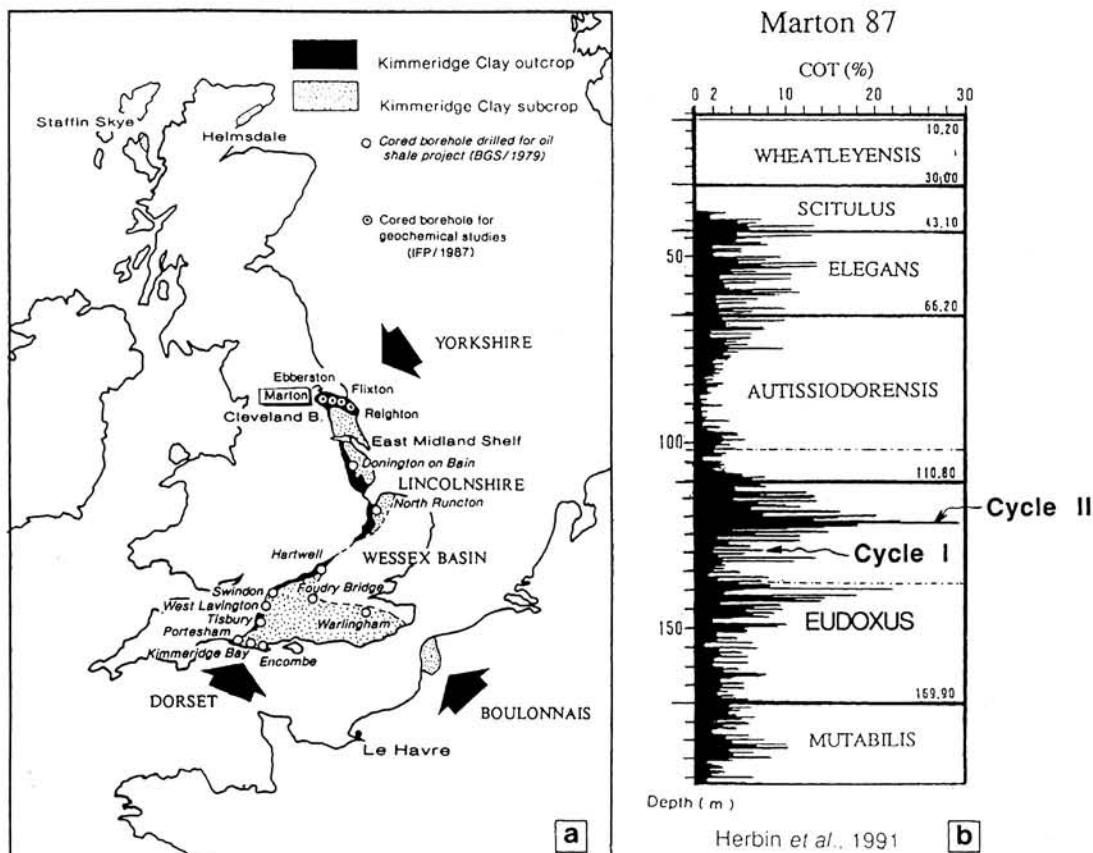


Figure 1 (a) Situation of studied sites. (b) Downcore distribution of TOC values in Marton Borehole (Cleveland Basin)

of the kerogen in many source rocks (Combaz, 1980); and fragments with recognisable biological structure. The origin and the mode of formation of the AOM is a very topical subject. The development of more powerful tools, such as the electron microscope and pyrolytic geochemical methods, has facilitated a better understanding of the genesis of this OM.

The objective of this paper is to discuss these concepts concerning the origin, the formation pathways and the state of preservation of the OM in sediments in the light of observations made on samples of the Kimmeridge Clay from the Cleveland Basin boreholes and from the Dorset outcrops (UK), then to propose a model for the fossilisation of the OM that we think to be applicable to other organic rich marine sediments.

Organic content: origin and preservation processes

High resolution Total Organic Carbon (TOC) and Hydrogen Index (HI) measurements on cores of the Kimmeridge Clay Formation (KCF) from boreholes in the Cleveland Basin (Yorkshire, UK) (Figure 1) and from Dorset outcrops show a parallel wave-shaped cyclic variation in kerogen quantity and quality (Cox and Gallois, 1981; Herbin *et al.*, 1991; Huc *et al.*, 1992). Two organic carbon cycles (each approximately one metre thick) were sampled from Marton 87 cores (Figure 1) and a multidisciplinary study was completed on these samples. These marine sedimentary rocks exhibit TOC values ranging from about 1.5% to 30% and HI values ranging between ≈ 200 and $\approx 800 \text{ mg HC g}^{-1} \text{ org.C}$ in the Cleveland Basin (Marton Hole). In the Dorset area, highest

TOC and HI values may attain, respectively $\approx 48\%$ and $\approx 800 \text{ mg HC g}^{-1} \text{ org.C}$ (Figure 2a). These deposits are the lateral immature equivalents of the kimmeridgian source-rocks which furnished a large part of the North Sea oil.

Transmitted light microscopical examination (paly-nofacies analysis) allows identification of the organic components and evaluation of their relative proportions (Ramanampisoa *et al.*, 1992; Boussafir *et al.*, 1994). This organic matter is mainly composed of three distinct types of AOM (up to 90% of the total KC kerogen), with a minor contribution of structured constituents derived from the terrestrial biomass and zooplankton. The most abundant type of AOM is represented by orange homogeneous flakes with sharp edges 'orange AOM'. AOM also occurs as brownish heterogeneous flocs 'brown AOM' and opaque aggregates 'black AOM'. The relative abundance of these different types of AOM exhibit large changes along the microcycle: variations in the proportions of 'orange AOM' account for the organic carbon cyclicity encountered in the KCF (Figure 2b).

Ultrastructural observations by transmission electron microscope (TEM) on the whole kerogen and on kerogen sub-fractions prepared by micromanipulation and containing a single type of AOM particles were performed (Boussafir *et al.*, 1994, 1995a). Using methods developed by Largeau *et al.* (1986), additional chemical studies by molecular gas chromatography and mass spectrometry (GC-MS) analysis of 'off-line' pyrolysis products were also performed (Boussafir *et al.*, 1995b). The results obtained by this approach combining with observations

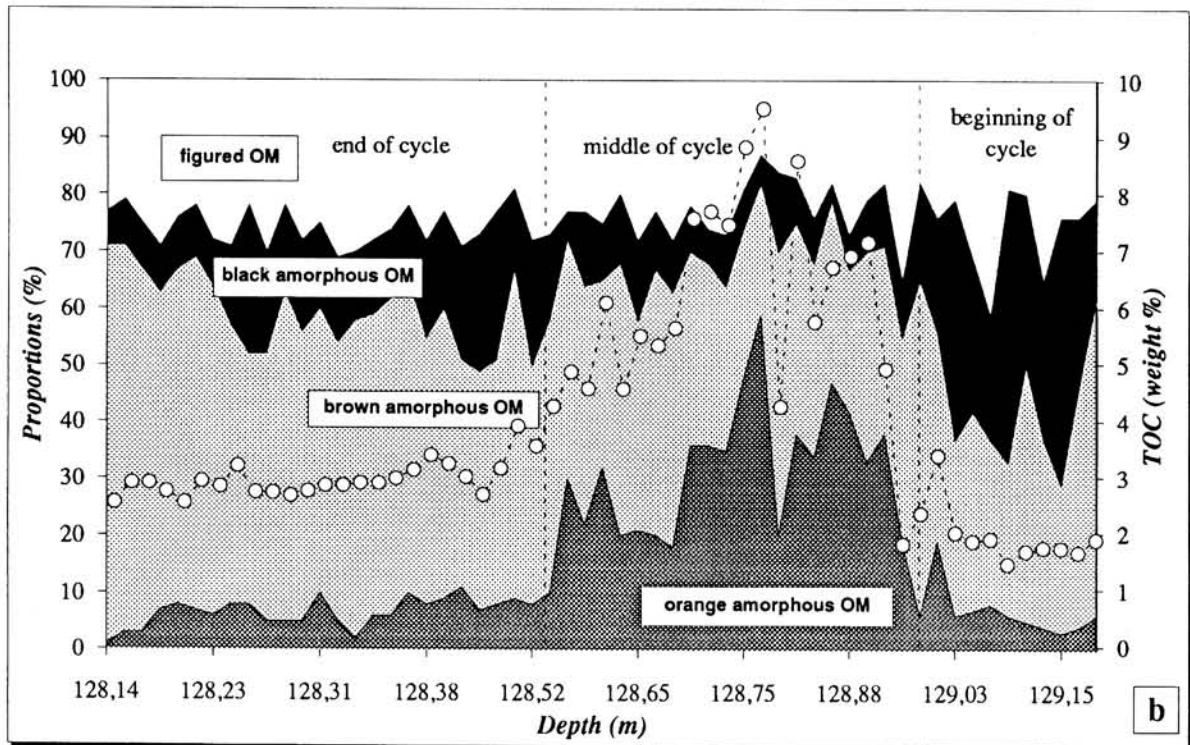
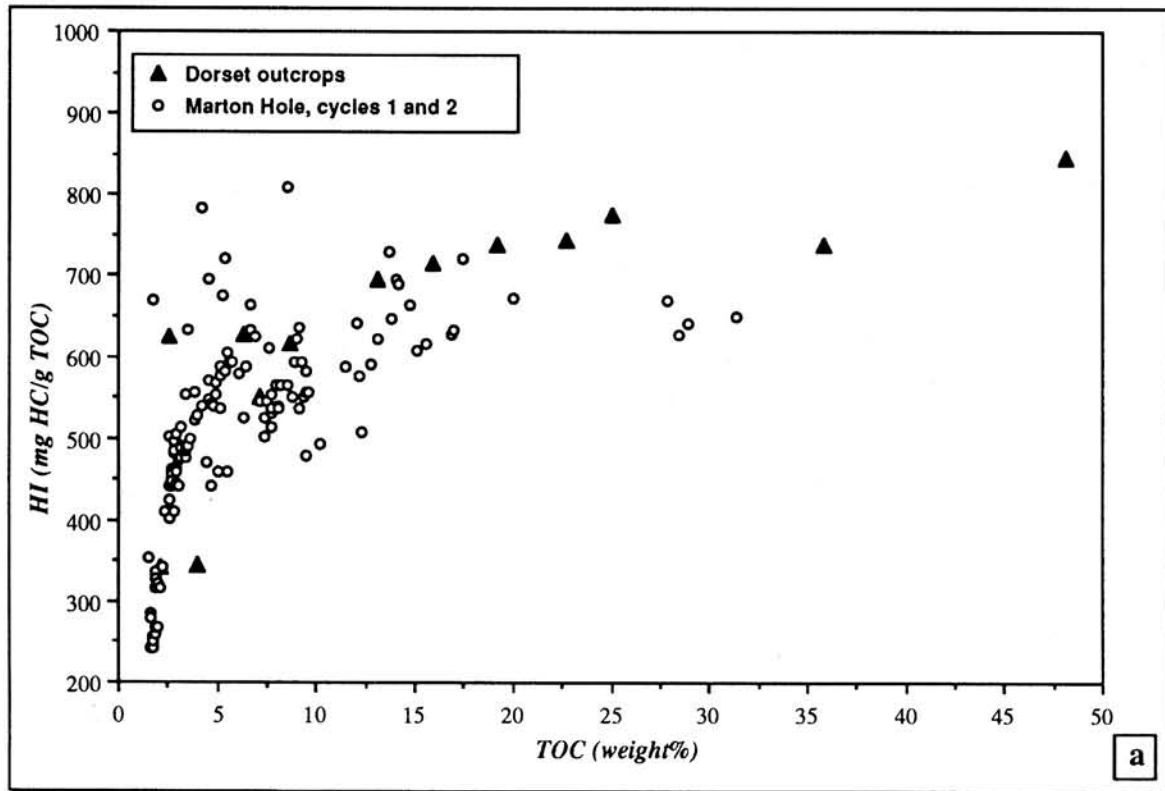


Figure 2 (a) Relationship between organic matter quantities (TOC %) and geochemical quality of organic matter (HI mg HC g⁻¹ org. C). (b) Downcore evolution of the palynofacies composition and TOC contents (open circles) along cycle 1 of Marton Hole. The variations of proportions of 'orange AOM' account for the organic carbon cyclicity. Similar results were obtained for the cycle 2 of Marton Hole and samples from Dorset

by TEM displayed three main mechanisms involved in the OM preservation.

sensu-stricto selective preservation

'Selective preservation' of initial structures or bio-macromolecules represents the main process of fossilisation for OM in the sediments with low TOC contents which are characterized by the very low content of orange AOM. This process seems to be directly responsible for the deposition of structured organic matter, which is more abundant in such sediments. It was demonstrated by the following observations:

1. The occurrence of optically well preserved organic structures (terrestrial organic debris, zooclasts and algae).
2. The presence of ultralaminar structures (*Figure 3a*) in the 'brown AOM'. The molecular analysis of the samples richest in these ultralaminae showed the presence of substantial amounts of *n*-alkylnitriles (*Figure 3b*). Similar structures termed 'ultralaminae' were previously detected in other source rocks and oil shales by Raynaud *et al.* (1988), Largeau *et al.* (1990a) Derenne *et al.* (1991, 1992). Molecular studies by Largeau *et al.* (1990b) and Derenne *et al.* (1991, 1993) showed that *n*-alkylnitriles were specific pyrolysis products of ultralaminae-containing kerogen. The origin of such components has been determined by Berkaloff *et al.* (1983) and Largeau *et al.* (1984) who proved that this 'brown AOM' was formed by the selective preservation of resistant cell-walls of green microalgae.
3. The presence of dominant lignaceous debris in several types of organic ultrafine structures in the 'black AOM' (*Figure 3c*). Phenolic compounds are generated from all samples but in higher relative abundance ($ca \times 2$) from the samples richest in 'black AOM' (i.e. low TOC samples) (*Figure 3e*). These phenols are dominated by typical pyrolysis products of diagenetically-altered lignins (mono- and di-methyl compounds).

Re-organisation of selectively preserved macromolecules

'Selective preservation' is also involved in the formation of the diffuse and nanoscopically amorphous organic matter observed by TEM in the 'black AOM' (*Figure 3d*), which produces by pyrolysis, branched alkanes believed to be derived from bacterian macromolecules. Organic matter with such resistant bio-macromolecules have been called 'bacteranes' by Largeau *et al.* (1990b) and also presents an amorphous and diffuse ultrastructure. This type of OM is part of the optically defined 'black AOM' and is thought to be formed by selective preservation and re-organisation of bio-macromolecules or 'bacteranes', without any preservation of initial biological structures.

Natural vulcanisation

'Natural vulcanisation' is the major preservation process observed in sediments with high TOC values. It is thought to have contributed to the formation of the 'orange AOM' which has a nanoscopically amorphous (perfectly homogeneous) texture without any biological structure even at high magnification (*Figure 3f*). This OM probably has a phytoplanktonic origin and is hydrogen rich, as

attested by the study of bitumens from 'orange AOM' containing samples (Ramanampisoa and Disnar, 1994). GC-MS analyses of the 'orange AOM'-rich kerogens showed a very high relative abundance of thiophenic compounds (*Figure 3g*) typical of organic matter formed by incorporation of sulphur or 'natural vulcanisation'. This process therefore provides a high resistance to some molecules which, otherwise, would be heavily degraded during early diagenesis. The lipidic composition explains the high hydrocarbon potential of such samples. Orange AOM from the KCF probably derives from planktonic species with considerable proportions of metabolisable OM which here, despite their lability, have been preserved from degradation by sulphur incorporation.

Relationship between preservation and sulphate reduction

The mineralisation of OM into CO₂ and H₂O in oxic environments, leaves no direct trace in the sediment as the compounds formed are not retained. Conversely, the presence of reduced sulphur (mineral and/or organic sulphides) in the anoxic sediments shows that OM has been degraded by sulphate reduction. Several factors are crucial for sulphate reduction: availability of metabolisable OM, reducing agent (bacteria), sulphate (supplied from sea water) and available iron for pyritisation (Berner, 1984).

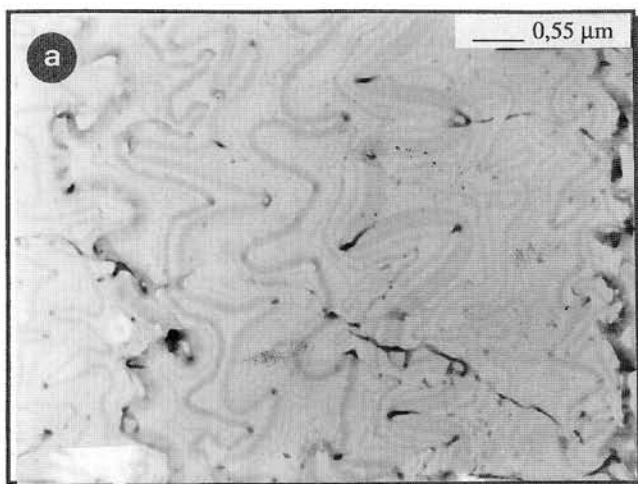
The role of sulphate reduction in the cyclic accumulation of OM in the KCF has been discussed by Bertrand and Lallier-Vergès (1993), Lallier-Vergès *et al.* (1993, in press) and Bertrand *et al.* (1994). The elemental sulphur contents of sediments are assumed to reflect the amounts of carbon mineralised by anaerobic processes, according to the equation (1) of sulphate reduction (Berner and Raiswell, 1983).

$$2 \text{CH}_2\text{O} + \text{SO}_4^{2-} \rightarrow \text{H}_2\text{S} + 2 \text{HCO}_3^- \quad (1)$$

This type of evaluation, taking into account the possible diffusion of HS⁻ and variable sulphur occurrences, showed that the relative proportions of metabolised OM (degraded by sulphate reduction) and accumulated OM were variable along the organic cycles, indicating that the intensity of sulphate reduction had changed through time.

Sediments with high TOC values (*Figure 4a*), representing the middle of the cycles, are those which have the greatest contents of reduced sulphur (Lallier-Vergès *et al.*, 1995). This indicates that a large proportion of the metabolisable organic matter entered the anoxic zone and promoted a high activity of sulphate reducers. These high sulphur contents are accompanied by high organic sulphur contents, more abundant than pyritic sulphur ones (*Figure 4b*). The pyritisation was limited because easily reducible iron was not abundant enough compared to the amounts of HS⁻ produced by sulphate reduction (Tribouillard *et al.*, 1994). In the very organic-rich sediments from the Dorset area, it was shown that the pyritisation process as well as sulphate reduction was limited (*Figure 2b & c*); this is interpreted as a progressively limited access to sea-water sulphate (Lallier-Vergès *et al.*, 1993).

Most of the samples with low TOC contents have low contents of sulphur, the largest part being as pyrite (org.S/pyr.S ratio >1). This suggests that very low amounts of metabolisable organic matter entered the anoxic domain. It was always lower than the availability



b	low TOC contents		high TOC contents	
	constituents	r.a.	constituents	r.a.
<i>n</i> -alkylmethylketones	C ₁₄ -C ₃₁ (C ₁₇)	1	C ₁₀ -C ₂₃ (C ₁₃)	1
branched alkylmethylketones	n.d.	—	C ₁₁ -C ₂₁ (C ₁₃)	0.3
<i>n</i> -alkylethylketones	n.d.	—	C ₁₀ -C ₂₅ (C ₁₃)	0.2
<i>n</i> -alkylnitriles	C ₁₁ -C ₂₁ (C ₁₄)	0.8	n.d.	—
ethylalkanoates	n.d.	—	C ₁₂ -C ₂₂ (C ₁₈)	traces
alkylated indoles	C ₉ -C ₁₂	0.9	C ₉ -C ₁₁	0.1
alkylated quinolines	C ₁₀ -C ₁₂	0.15	C ₁₀ -C ₁₃	0.3

r.a.: relative abundance of the homologous series calculated with respect to the predominant series. n.d.: not detected. The bracketed values correspond to the maximum of each series.

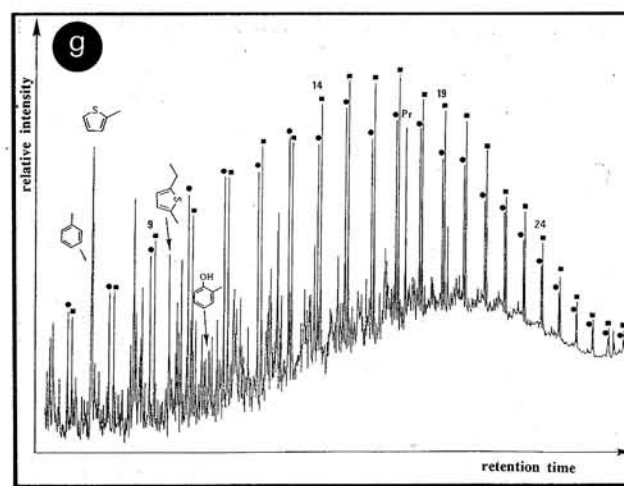
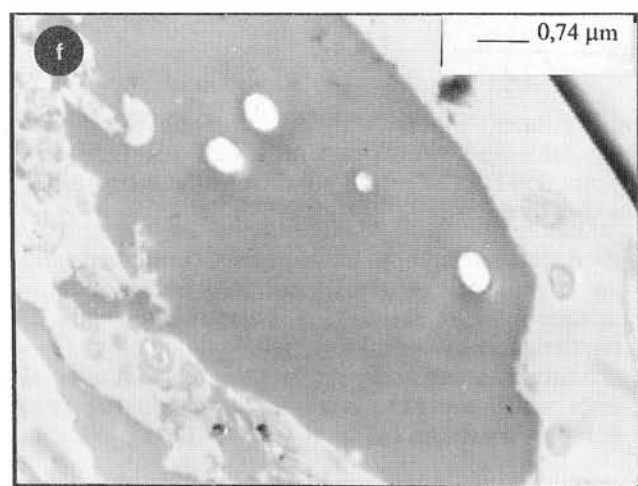
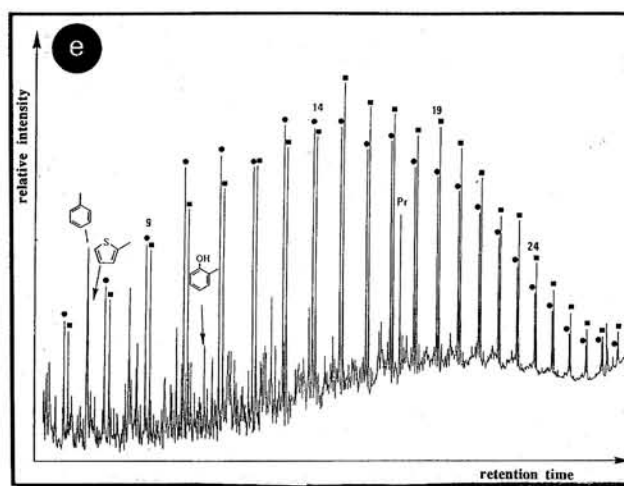
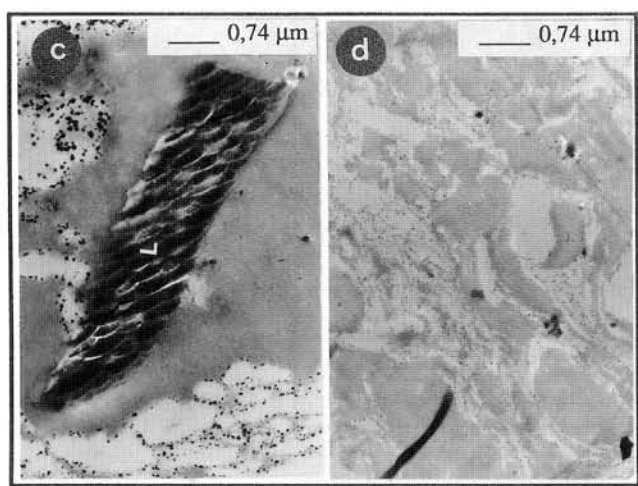


Figure 3 (a) TEM micrograph of ultralaminae (i.e. brown AOM). (b) Nature and relative abundances of homologous series of toluene-eluted compounds identified in the 400°C pyrolysates of total kerogens. (c) and (d) TEM micrographs of lignaceous debris and diffuse amorphous OM (i.e. opaque AOM). (e) Total ion current traces of the flash pyrolysates of kerogens of low TOC samples. Numbers indicate their chain length. The structure of some major compounds is indicated and Pr designates prist-1-ene. (f) TEM micrograph of nanoscopically amorphous OM (i.e. orange AOM). (g) Idem *Figure 3e* for high TOC samples. *Figure 3(b, e & g)* are after Boussafir *et al.*, 1995b

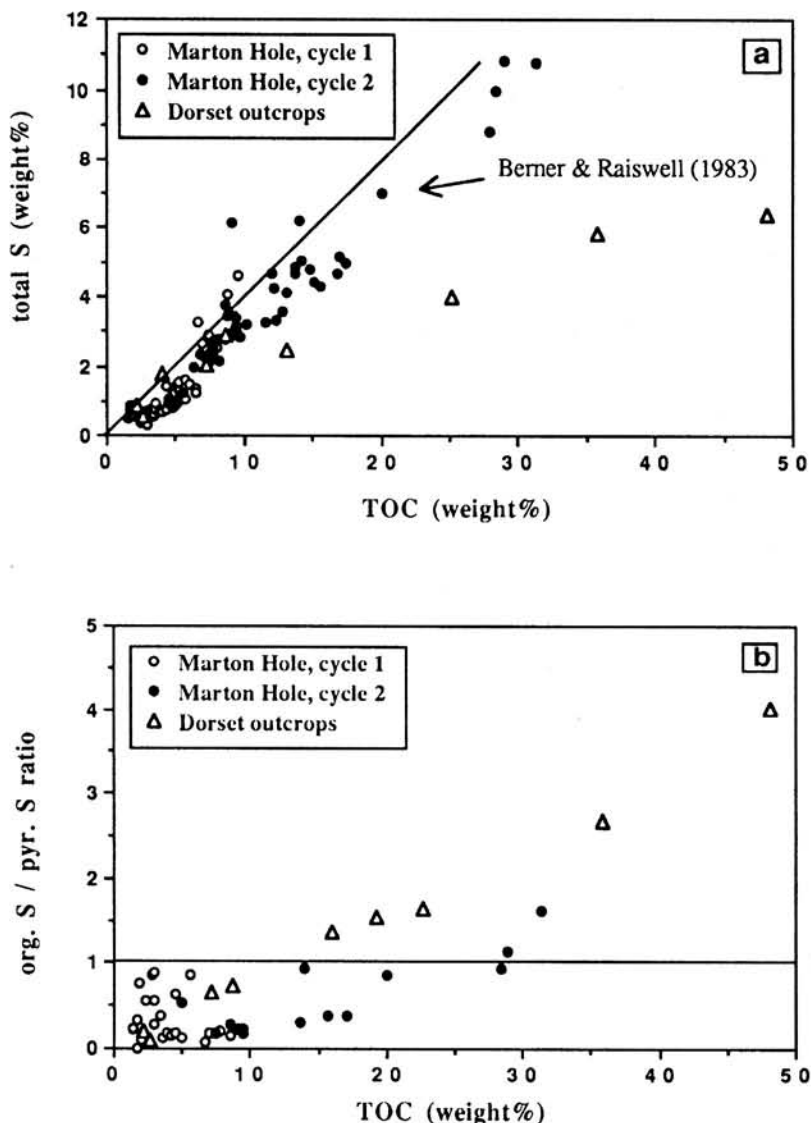


Figure 4 (a) Positive correlation between total sulphur contents (%) and TOC (%). (b) Organic sulphur/pyritic sulphur ratio versus TOC values (%). Organic sulphur is the dominant sulphidic form for samples with TOC > 15% (Dorset outcrops) and TOC > 25% (Marton Holes)

of iron and sulphates so that neither sulphate reduction or pyritisation were ever limited.

A model of organic matter preservation

The different ultrastructures and mechanisms (as described above) responsible for the accumulation of the Kimmeridge Clay kerogen, have been integrated into a general interpretative model for the fossilisation of marine hydrogen-rich organic matter. This model also takes into account the recent results obtained by marine biologists on the biological and physico-chemical processes occurring in the photic zone. It could be considered as a working hypothesis for the study of other marine source rocks of petroleum.

This model (Figure 5) begins with biological primary production, which is the precursor parameter initiating organic accumulation. Primary organic productivity depends on several parameters, such as temperature, light, water-column stability and nutrient supply. The main producers of OM in the marine environment are unicellular phytoplanktonic organisms such as diatoms,

dinoflagellates, green algae, cyanophytes, phytoflagellates and nanoflora (for review see Lalli and Parsons, 1993). The model subdivides these organisms into two groups:

1. producers having both labile organic compounds and an 'organic test' naturally enriched in lipidic bioresistant macromolecules (e.g. protective cell-walls of microalgae, phytoplankton...).
2. producers having no lipidic 'organic test' but mineral ones which are rich in labile organic matter (e.g. diatoms, coccolites...).

In parallel with this phytoplanktonic production, bacterial production occurs both in the production zone and at the sediment-water interface. Bacteria play a dual role in the organic sedimentation: they are involved in the cycle at the level of the biodegradation of the OM but also at the level of the production of bacterial OM (Smith *et al.*, 1976).

A very small amount of the produced OM escapes recycling. This recycling begins in the photic zone due to

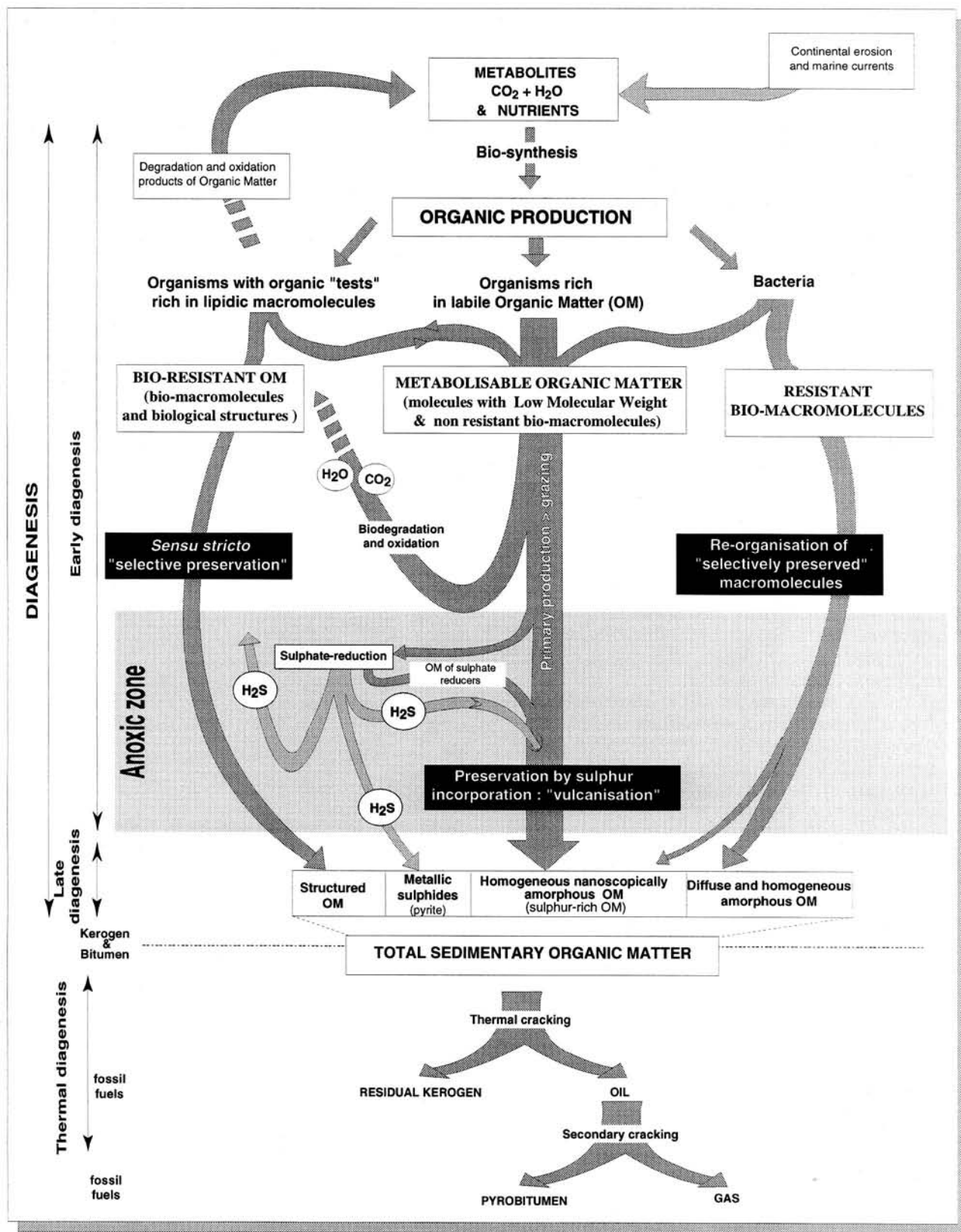


Figure 5 A fossilisation model for organic matter of source-rocks. This interpretative model takes into account the different source organisms linked to the primary production, the nature of delivered organic matter and the mechanisms of preservation involved in the fossilisation of hydrocarbon-rich sedimentary organic matter. (The size of arrows is approximate and not exactly proportional to the relative organic fluxes)

the grazing of the phytoplankton by the zooplankton (Peinert *et al.*, 1987) and to oxidation. Biological models (Wakeham *et al.*, 1984a, 1984b) show that during high primary productivity periods, the formation of mucilage around the cells and the aggregation of such particles (so called 'flocs') increase the chances of preservation of labile OM during export to deep water. In our model, we include two types of delivered OM: one is 'metabolisable' OM and the other one is a bio-resistant organic fraction.

All the organisms produced contribute to the flux of metabolisable OM exported to the sea floor. Organisms with organic 'tests' and bacteria possess naturally bio-resistant bio-macromolecules. In the first case, selective preservation *sensu-stricto* preserves both biological and molecular structures: microalgae cell-walls (ultralaminae), dinocysts and, also including terrestrial OM. In the case of bacteria, the preservation process acts as a re-organisation of 'selectively preserved' molecules. Only the molecular structure is preserved, whereas the texture appears nanoscopically amorphous as diffuse OM in the microtexture of the rock.

The metabolisable OM (represented by the central arrow on the figure) is generally recycled in the oxic zone by grazing activity. During periods of very high productivity, metabolisable OM entering the anoxic domain allows the development of sulphate reducing micro-organisms, which are the main cause of the OM degradation in the marine environment (Jørgensen, 1978; Berner, 1980, 1984; Boudreau and Westrich, 1984). Most of H₂S produced diffuses from the sediments and tends to be removed from the system in the direction of upper beds or even into the water column, where it is re-oxidised (Coleman, 1985; Curtis, 1980, 1987).

When reactive metals are present in sea water and/or the sediment, part of the H₂S reacts to form sulphides of which the most common is pyrite (Berner and Raiswell, 1983; Berner and Westrich, 1985). Excess HS⁻ is incorporated in part of the metabolisable OM as organo-sulphur compounds. This OM acquires a bioresistant character by natural vulcanisation, and is preserved as perfectly amorphous and homogeneous OM at the nanometric scale (i.e. 'orange AOM').

Under favourable thermal conditions, this fossilised organic matter may be further degraded by generating liquid and gaseous hydrocarbons, through the cracking of its macro-molecules during the stage of catagenesis.

Conclusions

This model brings together a variety of phenomena ranging from marine biological production and fossilisation of the produced organisms. The main organic precursors, the nature of the deposited organic matter and the main mechanisms involved in OM accumulation have been determined by detailed molecular and textural studies of different organic constituents from the KCF and it has been demonstrated that the primary parameter for OM accumulation is organic productivity. However, subsequent anoxic conditions favour preservation of hydrocarbon rich OM.

The kerogen of KCF is composed of several types of organic constituents for which three major mechanisms of preservation were recognised:

1. a selective preservation mechanism *sensu-stricto* which leads to the preservation of both biological and

molecular structures, namely algal cell-walls and land-derived higher plant debris. This mechanism is thought to have occurred during low-productivity periods during which the amount of metabolisable organic matter was completely degraded under both oxic and anoxic conditions.

2. a re-organisation of bioresistant macromolecules which were selectively preserved (bacterans) without any preservation of the biological structure (diffuse amorphous organic matter).
3. an acquired bioresistance by natural vulcanisation of lipids, which results in a nanoscopically amorphous OM rich in S-compounds. This mechanism characterises high productivity periods during which large amounts of delivered metabolisable organic matter favour the production of HS by sulphate reducers and the incorporation of excess HS in the organic matter.

The oil potential of KCF kerogens reflects both the chemical nature of produced OM and the mechanisms of its preservation. High HI values are related to large amounts of resistant algal constituents (micro-algae) and/or large amounts of vulcanised metabolisable organic matter. This may explain the general trend of different source-rocks which exhibit correlatively high values of organic carbon, hydrocarbon moieties and sulphur contents.

Acknowledgements

We are indebted to our colleagues of the Research Group (GdR 942) of CNRS (France) for their scientific contribution. Special thanks are due to Dr Ph. Bertrand (Université Bordeaux I, France), Dr C. Largeau (Ecole Nationale Supérieure de Chimie, Paris, France) and Dr J. R. Disnar (URA 724, Université d'Orléans, France) for their fruitful collaboration.

References

- Berkaloff, C., Casadevall, E., Largeau, C., Metzger, P., Peracca, S. and Virlet, J. (1983) The resistant polymer of the walls of the hydrocarbon-rich alga *Botryococcus braunii*. *Phytochemistry* **22**, 389–397
- Berner, R. A. (1980) Early diagenesis: A theoretical approach. Princeton University Press, N. J.
- Berner, R. A. (1984) Sedimentary pyrite formation: an update. *Geochimica et Cosmochimica Acta* **48**, 605–615
- Berner, R. and Raiswell, R. (1983) Burial of organic carbon and pyrite sulphur in sediments over Phanerozoic time: a new theory. *Geochimica et Cosmochimica Acta* **47**, 855–862
- Berner, R. A. and Westrich, J. T. (1985) Bioturbation and the early diagenesis of carbon and sulphur. *American Journal of Science* **285**, 193–206
- Bertrand, P. and Lallier-Vergès, E. (1993) Past sedimentary organic matter accumulation and degradation controlled by productivity. *Nature* **364**, 786–788
- Bertrand, P., Lallier-Vergès, E. and Boussafir, M. (1994) Enhancement of both accumulation and anoxic degradation of organic carbon controlled by cyclic productivity: a model. *Organic Geochemistry* **22**, 511–520
- Bordenave, M. L. and Durand, B. (1993) Evolution of ideas and concepts in geochemistry. In *Applied Petroleum Geochemistry*, ed. M. L. Bordenave, pp. 5–14. Editions Technip, Paris
- Boudreau B. P. and Westrich J. T. (1984) The dependance of bacterial sulphate reduction on sulphate concentration in marine sediments. *Geochimica et Cosmochimica Acta* **48**, 2503–2516
- Boussafir, M., Lallier-Vergès, E., Bertrand, P. and Badaut-Trauth, D. (1994) Structure ultrafine de la matière organique des roches mères du kimméridgien du Yorkshire (UK). *Bulletin of the Geological Society France* **165**, 355–363

- Boussafir, M., Lallier-Vergès, E., Bertrand, P. and Badaut-Trauth, D. SEM and TEM studies on isolated organic matter and rock microfacies from a short-term organic cycle of the Kimmeridge Clay Formation (Yorkshire, G. B.). In *Organic matter accumulation*, eds E. Lallier-Vergès, N. P. Tribovillard and P. Bertrand, Vol. 57, 15–30. *Lecture Notes in Earth Sciences*, Springer, Heidelberg
- Boussafir, M., Gelin, F., Lallier-Vergès, E., Derenne, S., Bertrand, P. and Largeau, C. (1995) Electron microscopy and pyrolysis of kerogen from the Kimmeridge Clay Formation (U. K.). Source organisms, preservation processes and origin of microcycles. *Geochimica et Cosmochimica Acta* 59, 3731–3747
- Calvert, S. E. and Pedersen, T. F. (1992) Organic carbon preservation and accumulation in marine sediments: How important is the anoxia? In *Productivity, Accumulation, and Preservation of Organic Matter in Recent and Ancient Sediments*, eds J. Whelan and J. Farrington, pp. 241–263. Columbia University Press, New York
- Coleman, M. L. (1985) Geochemistry of diagenetic non silicate minerals: kinetic considerations. *Philosophical Transactions of the Royal Society London* 315, 39–56
- Combaz, A. (1980) Les kérogènes vus au microscope. In *Kerogen*, ed. B. Durand, pp. 55–87. Technip, Paris
- Cox, B. M. and Gallois, R. W. (1981) The stratigraphy of the Kimmeridge Clay of Dorset type area and its correlation with some other Kimmeridgian sequences. *Report of the Institute of Geological Science* 80, 1–31
- Curtis, C. D. (1980) Diagenetic alteration in black shale fabrics. *Journal of the Geological Society London* 137, 189–194
- Curtis, C. D. (1987) Données récentes sur les réactions entre matières organiques et substances minérales dans les sédiments et sur leurs conséquences minéralogiques. *Mémoires de la Geological Society, France* 151, 127–141
- Demaison, G. J. and Moore, G. T. (1980) Anoxic environments and Oil source Bed Genesis. *A.A.P.G. Bulletin* 64, 1179–1209
- Derenne, S., Largeau, C., Casadevall, E., Berkaloff, C. and Rousseau, B. (1991) Chemical evidence of kerogen formation in source rocks and oil shales via selective preservation of thin resistant outer walls of microalgae: Origin of ultralaminae. *Geochimica et Cosmochimica Acta* 55, 1041–1050
- Derenne, S., Le Berre, F., Largeau, C., Hatcher, P., Connan, J. and Raynaud, J. F. (1992) Formation of ultralaminae in marine kerogens via selective preservation of thin resistant outer walls of microalgae. *Organic Geochemistry* 19, 345–350
- Derenne, S., Largeau, C. and Taulelle, F. (1993) Occurrence of non-hydrolysable amides in the macromolecular constituent of *Scenedesmus quadricauda* cell-wall as revealed by ¹⁵N NMR: Origin of *n*-alkylnitriles in pyrolysates of ultralaminae-containing kerogens. *Geochimica et Cosmochimica Acta* 57, 851–857
- Durand, B. (1980) *Kerogen: Insoluble organic matter from sedimentary rocks*, ed B. Durand. Technip, Paris
- Herbin, J. P., Müller, C., Geyssant, J. R., Melières, F. and Penn, I. E. (1991) Hétérogénéité quantitative et qualitative de la matière organique dans les argiles du Val de Pickering (Yorkshire, U. K.) cadre sédimentologique et stratigraphique. *Review of the Institut France Pétrology* 46, 675–712
- Huc, A. Y., Lallier-Vergès, E., Bertrand, P., Carpentier, B. and Hollander, D. J. (1992) Organic matter response to change of depositional environment in Kimmeridgian shales, Dorset, UK In *Productivity, Accumulation, and Preservation of Organic Matter in Recent and Ancient Sediments*, eds J. Whelan and J. Farrington, pp. 469–486. Columbia University Press, New York
- Jørgensen, B. B. (1978) A comparison of methods for the quantification of bacterial sulphate reduction in coastal marine sediments. *Geomicrobiology Journal* 1, 49–64
- Lalli and Parsons (1993) *Biogeochemical Oceanography: An Introduction*. Pergamon Press
- Lallier-Vergès, E., Bertrand, P., Huc, A. Y., Büchel, D. and Tremblay, P. (1993) Control of the preservation of organic matter by productivity and sulphate reduction in Kimmeridgian shales from Dorset (UK). *Marine and Petroleum Geology* 10, 600–605
- Lallier-Vergès, E., Tribovillard, N. P. and Bertrand, P. (1995) Organic matter accumulation: The Organic Cyclicities of the Kimmeridge Clay Formation (Yorkshire, G. B.) and the Recent Maar Sediments (Lac du Bouchet). In *Lecture Notes in Earth Sciences*, eds E. Lallier-Vergès, N. P. Tribovillard and P. Bertrand. Vol. 57, 187pp. Springer
- Lallier-Vergès, E., Hayes, J., Boussafir, M., Zaback, D. A., Tribovillard, N. P., Bertrand, P., and Connan, J. (in press) Productivity-induced sulphur enrichment of organic-rich sediments. *Chemical Geology*
- Largeau, C., Casadevall, E., Kadouri, A. and Metzger, P. (1984) Formation of botryococcus-derived kerogens. Comparative study of immature torbanites and of the extant alga *Botryococcus braunii*. *Organic Geochemistry* 6, 327–332
- Largeau, C., Derenne, S., Casadevall, E., Kadouri, A. and Sellier, N. (1986) Pyrolysis of immature torbanite and of the resistant bio-polymers (PRBA) isolated from extant alga *Botryococcus braunii*. Mechanisms of formation and structure of Torbanite. (1986) In *Advances in Organic Geochemistry 1987*, eds D. Leythaeuser and J. Rullkötter. *Organic Geochemistry* 10, 1023–1032
- Largeau, C., Derenne, S., Casadevall, E., Berkaloff, C., Corolleur, M., Lugardon, B., Raynaud, J. F. and Connan, J. (1990a) Occurrence and origin of ultralamina structures in 'amorphous' kerogens from various source-rocks and oil-shales. In *Advances in Organic Geochemistry 1989*, eds B. Durand and F. Behar, *Organic Geochemistry*, pp. 889–896
- Largeau, C., Derenne, S., Clairay, C., Casadevall, E., Raynaud, J. F., Lugardon, B., Berkaloff, C., Corolleur, M. and Rousseau, B. (1990) Characterisation of various kerogens by scanning electron microscopy (SEM) and transmission electron microscopy (TEM) — Morphological relationships with resistant outer walls in extant micro-organisms. *Meded. Rijks Geol. Dienst* 45, 91–101
- Peinert, R., Bathman, V., Von Bodingen, B. and Noji, T. (1987) The impact of grazing on spring phytoplankton growth and sedimentation in the Norwegian current. *Mitt. Geologie. Paläontologie Institute University, Hambourg* 62, 149–164
- Ramanampisoa, L., Bertrand, P., Disnar, J. R., Lallier-Vergès, E., Pradier, B. and Tribovillard, N. P. (1992) Etude à haute résolution d'un cycle de carbone organique des argiles du Kimmeridgien du Yorkshire (GB): résultats préliminaires de géochimie et de pétrographie organique. *C. R. Academy of Science, Paris* 314, 1493–1498
- Ramanampisoa, L. and Disnar, J. R. (1994) Primary control of paleoproduction on organic matter preservation and accumulation in the Kimmeridge rocks of Yorkshire (U.K.). *Organic Geochemistry* 21, 1153–1167
- Raynaud, J. F., Lugardon, B. and Lacrampe-Couloume, G. (1988) Observation de membranes fossiles dans la matière organique 'amorphe' de roches-mères de pétrole. *C. R. Academy of Science, Paris* 307, 1703–1709
- Sinninghe-Damsté, J. S., Rijpstra, W. I., Kock-Van Dalen, A. C., de Leeuw, J. W. and Schenk, P. A. (1989) Quenching of labile functionalized lipids by inorganic sulphur species: Evidence for the formation of sedimentary organic sulphur compounds at the early stages of diagenesis. *Geochimica et Cosmochimica Acta* 55, 1343–1355
- Smith, W. O., Barber, R. T. and Huntsman, S. A. (1976) Primary production of the coast of northwest Africa: excretion of dissolved organic matter and its heterotrophic uptake. *Deep-Sea Research* 24, 35–47
- Tegelaar, E. W., de Leeuw, J. W., Derenne, S. and Largeau, C. (1989) A reappraisal of kerogen formation. *Geochimica et Cosmochimica Acta* 53, 3103–3106
- Tegelaar, E. W. (1990) Resistant bio-macromolecules in morphologically characterized constituents of kerogen: a key to the relationship between biomass and fossil fuels. Ph.D. Thesis, Amsterdam University
- Tissot, B. P. and Welte, D. H. (1984) *Petroleum formation and occurrence*, 2nd edition. Springer
- Tribovillard, N. P., Desprairies, A., Lallier-Vergès, E., Bertrand, P., Disnar, J. R., Pradier, B. and Moureau, N. (1994) Geochemical study of organic-rich cycles from the Kimmeridge Clay Formation of Yorkshire. *Palaeogeography, Palaeoclimatology, Palaeoecology* 108, 165–181
- Wakeham, S. G., Farrington, J. W. and Gagosian, R. B. (1984) Variability in lipid flux and composition of particulate organic matter in the Peru upwelling region. *Organic Geochemistry* 6, 204–215
- Wakeham, S. G., Farrington, J. W. and Gagosian, R. B. (1984) Geochemistry of particulate organic matter in the oceans: results from sediment trap experiments. *Deep-Sea Research* 31, 509–528

Sulphur-rich organic matter from bituminous laminites of Orbagnoux (France, Upper Kimmeridgian). The role of early vulcanization

by THIERRY MONGENOT*, MOHAMMED BOUSSAFIR**, SYLVIE DERENNE***,
ELISABETH LALLIER-VERGES**, CLAUDE LARGEAU*** and NICOLAS-PIERRE TRIBOVILLARD*

Key words. – Kimmeridgian, Laminated facies, Kerogen, Amorphous organic matter, Natural vulcanization, Organic-sulphur compounds, Coccolithophorids.

Abstract. – Upper Kimmeridgian bituminous laminites outcrop in the southern Jura Mountains at Orbagnoux and the field section comprises five calcareous facies. Organic matter (OM) in all these facies shows high hydrogen index values (from 780 to 960 mg "HC"/g TOC) whereas only four are OM-rich (TOC between 2 and 8.6%). A combination of petrographical and geochemical methods was applied to analyse a representative sample of one of the most OM-rich facies (dark parallel laminae).

Transmitted-light microscopy and UV excitation microscopy indicated the presence of two lamellar organic constituents: a dominant orange one with an intense yellow-green fluorescence and a minor dark, non-fluorescing one. Backscattering scanning electron microscopy (BSEM) also revealed the occurrence of an organic network closely associated with the micritic matrix. The palynological residue consists of gel-like OM which is amorphous even when observed by transmission electron microscopy (TEM).

Sulphur-mapping and energy dispersive spectrometry indicated that this element is solely associated with the OM. A high S-content is observed in both the organic lamellar constituents and in the organic network.

All these petrographical features of the organic material in dark parallel laminae suggest a minor role of the selective preservation pathway whereas vulcanization of lipids probably played a major role. Such a process would explain the highly aliphatic nature of the kerogen. "Off-line" pyrolysis released mostly organic sulphur compounds (OSC), thus confirming the major contribution of vulcanized lipids. S-incorporation allowed these lipids to escape bacterial degradation. Moreover, the macromolecular compounds thus formed can survive strongly oxidic, post-depositional conditions due to temporary and occasional sediment emergences. Nevertheless, the latter conditions should have induced some alterations reflected by the presence of the dark organic constituent.

Analyses of pyrolysis products indicated that the vulcanized lipids were chiefly of algal origin. Since coccolithophorids constitute the mineral matrix, they could have provided the bulk of these lipids.

La matière organique riche en soufre des laminites bitumineuses d'Orbagnoux (France, Kimméridgien supérieur). Le rôle de la vulcanisation naturelle

Mots clés. – Kimmeridgien, Faciès laminés, Kérogène, Matière organique amorphe, Vulcanisation naturelle, Composés organo-soufrés, Coccolithophoridés

Résumé. – Les laminites bitumineuses d'âge kimméridgien supérieur affleurant à Orbagnoux dans le Jura méridional français sont constituées de cinq faciès carbonatés. La matière organique (MO) de ces faciès possède des valeurs d'indice hydrogène toujours très élevées (de 780 à 960 mg "HC"/g COT) alors que seuls quatre faciès sont riches en carbone organique (COT compris entre 2 et 8,6%). Une combinaison de méthodes pétrographiques et géochimiques a été appliquée sur un échantillon représentatif de l'un des faciès les plus riches en carbone organique (laminés parallèles sombres). Deux types de constituants organiques lamellaires ont été mis en évidence en lumière naturelle transmise ainsi qu'en lumière ultraviolette réfléchie: une forme prédominante, orange, possédant une fluorescence jaune-vert et une forme relativement moins abondante, sombre, non fluorescente. La microscopie électronique à balayage en mode rétrodiffusé montre qu'il existe également un réseau organique finement associé à la matrice micritique. Le résidu palynologique est constitué par de la matière organique orangée gélifiée, nanoscopiquement amorphe en microscopie électronique à transmission. La cartographie du soufre et la spectrométrie par dispersion d'énergie indiquent que le soufre est uniquement associé à la matière organique. Le contenu en soufre des deux constituants organiques lamellaires et du réseau est toujours très élevé.

L'étude pétrographique suggère un rôle mineur pour la préservation sélective dans la formation du kérogène étudié provenant de lamines parallèles sombres. En revanche, le processus de vulcanisation des lipides a probablement joué un rôle majeur. En outre, ce processus expliquerait la nature hautement aliphatique du kérogène. La pyrolyse "off-line" du kérogène a délivré principalement des composés organo-soufrés confirmant une contribution majeure des lipides vulcanisés. L'incorporation de soufre dans ces lipides leur a permis d'échapper à la dégradation bactérienne. De plus, les composés macromoléculaires ainsi formés résisteraient à des conditions relativement oxydiques, postsédimentaires, dues à l'émergence temporaire et occasionnelle du sédiment. Ces conditions oxydantes ont dû induire néanmoins des altérations de la matière organique, reflétées par la présence des constituants organiques sombres.

L'analyse des produits de pyrolyse indique que les lipides vulcanisés seraient principalement d'origine algale; les coccolithophoridés, constituant unique de la matrice minérale du sédiment, auraient pu fournir l'essentiel de ces lipides.

VERSION FRANÇAISE ABRÉGÉE

L'accumulation de la matière organique dans les sédiments est gouvernée, outre par le classique schéma dégradation/recondensation, par deux processus: la préservation sélective [Largeau *et al.*, 1986; Tegelaar *et al.*, 1989] et la vulcanisation de la MO [Sinninghe Damsté *et al.*, 1988 et 1989]. Brièvement, le processus de préservation sélective est lié à l'existence dans des organismes vivants de biopolymères résistants et localisés dans les parois externes des cellules. Ils sont ensuite sélectivement préservés lors de la diagenèse précoce et donc préférentiellement enrichis dans le sédiment. Dans ce cas, des morphologies héritées d'organismes sources sont reconnaissables sur des coupes ultraminces du résidu palynologique. La vulcanisation naturelle de la MO, c'est à dire l'incorporation de soufre dans des lipides fonctionnalisés (alcènes, cétones et aldéhydes) se produit lorsque le milieu est anoxique, qu'une population de bactéries sulfato-réductrices s'est

* Géochimie des Roches sédimentaires, URA CNRS 723, Université Paris-Sud, Bât. 504, 91405 Orsay cedex, France.

** URPO, CNRS 724, Université d'Orléans, 45067 Orléans cedex 2, France.

*** CBOP, URA CNRS 1381, ENSCP, 11 rue Pierre et Marie Curie, 75231 Paris cedex 05, France.

Manuscrit déposé le 5 août 1996; accepté après révision le 14 janvier 1997.

développée (production de H₂S) et que la quantité de fer réactif disponible est faible. Le soufre s'incorpore alors dans des lipides au niveau des insaturations et leur permet d'échapper à la dégradation bactérienne en formant des réseaux macromoléculaires. Ce mode de formation conduit à des kérogènes amorphes possédant un fort potentiel pétrologène.

Le propos de cette étude est l'articulation de ces processus lors du dépôt des laminites bitumineuses dans le paléolagon d'Orbagnoux (Jura méridional français) au Kimméridgien supérieur. Les laminites bitumineuses sont constituées par cinq faciès [Cayeux, 1935; Bernier *et al.*, 1972], quatre étant riches en MO (carbone organique total : de 2 à 8,6%) : calcaires massifs, lamines parallèles sombres et claires et lamines ondulées sombres. Ces quatre faciès possèdent également une matrice carbonatée constituée exclusivement de coccolithes. Le cinquième faciès (lamines ondulées claires) est lié au développement de tapis cyanobactériens; il est pauvre en MO. Alors que la teneur en carbone organique varie, les valeurs de IH sont toujours très élevées (entre 780 et 960 mg "HC"/g COT), témoignant du caractère fortement aliphatique de la MO, quel que soit le type de faciès.

Parallèlement à l'étude des processus d'accumulation de la MO il sera intéressant de statuer sur de possibles organismes sources ayant fourni du matériel lors de la formation du kérogène.

L'étude s'est plus particulièrement portée sur un des faciès les plus riches en MO : les lamines parallèles sombres. Une combinaison de méthodes incluant de la pétrographie organique (microscopie photonique et électronique, cartographie élémentaire) et de la géochimie organique (résonance magnétique nucléaire du ¹³C à l'état solide et pyrolyse "off-line") a été appliquée à un échantillon représentatif de ce faciès.

Observée en lumière naturelle transmise, la MO d'une lamine parallèle sombre se présente sous la forme de structures lamellaires orangées ou noires, respectivement jaune-vert et sombres en lumière ultraviolette réfléchie. Une troisième forme de MO est mise en évidence par la microscopie électronique à balayage en mode rétrodiffusé : il s'agit d'un réseau organique intimement lié à la matrice carbonatée. Une faible contribution continentale au kérogène est également à signaler (vitrinite et inertinite < 3% des constituants organiques).

La cartographie du soufre effectuée sur des sections polies indique que cet élément est uniquement localisé dans la MO. L'enrichissement en soufre semble relativement élevé dans les deux types de structures lamellaires et dans le réseau organique.

Le résidu palynologique est constitué par au moins 95% de MO gélifiée, orangée, plus ou moins plane et apparaissant nanoscopiquement amorphe en coupes ultramines. Des plages parfaitement homogènes (attribuées aux structures lamellaires) et des zones contenant de nombreuses cavités (correspondant au réseau organique) se distinguent, bien qu'il n'existe pas de limites nettes entre elles. En fait, il y a un continuum de la MO dans le sédiment.

L'ensemble des observations démontre que la préservation sélective n'a dû être qu'un phénomène mineur dans la formation du kérogène (aucune structure héritée visible). Des particules nanoscopiquement amorphes associées à de fortes teneurs en soufre ont été décrites dans la formation du Kimmeridge Clay [Boussafir *et al.*, 1995a]. Ces particules tiraient leur origine du processus de vulcanisation. De même, à Orbagnoux, la vulcanisation a probablement joué un rôle essentiel dans la formation du kérogène des lamines parallèles sombres. Il en ressort que de fortes teneurs en soufre organique associées à la présence de MO nanoscopiquement amorphe peuvent être considérées comme des indicateurs de vulcanisation naturelle dans un environnement et donc de la sulfato-réduction.

Comme un seul type de particule de MO a été observé dans le résidu palynologique, il est probable que les deux types de structures lamellaires organiques observés dans l'échantillon brut soient constitués de matériel nanoscopiquement amorphe. Cependant, la présence de ces structures lamellaires sombres et orangées traduirait l'oxydation différentielle de particules de même origine sous l'action de variations locales du potentiel redox. En effet, l'examen de lames minces souligne l'existence de périodes relativement oxydantes dans le sédiment et dans la colonne d'eau (clastes d'organismes benthiques de milieux oxygénés; pseudomorphoses de gypse liées à des émergences temporaires et occasionnelles du sédiment) alternant avec des épisodes réducteurs (présence d'isorenieratane observé par Sinninghe Damsté *et al.* [1995]). Il en résulte que le kérogène formé par vulcanisation de lipides durant les périodes les plus réductrices a survécu pendant les épisodes oxydiques. La vulcanisation conférerait donc non seulement une résistance à la dégradation bactérienne mais aussi vis à vis de conditions redox différentes de celles du milieu d'accumulation.

La pyrolyse "off-line" a libéré une grande quantité de composés organo-soufrés (COS) confirmant ainsi le rôle tenu par la vulcanisation naturelle de lipides dans la formation du kérogène étudié. De plus, la désulfuration des effluents de pyrolyse a révélé une nette prédominance dans le pyrolysateur des COS possédant un squelette carboné linéaire. Un tel type de squelette indiquerait une origine algale du matériel organique lors de la formation du kérogène. Cette origine algale pourrait être liée aux coccolithophoridés constituant la matrice minérale des lamines parallèles sombres d'Orbagnoux. Dans ce cas, le paléolagon d'Orbagnoux serait un des rares sites où la sédimentation de coccolithes, dont le matériel organique paraît normalement très labile, s'est accompagnée d'une accumulation de MO, la vulcanisation des lipides protégeant de la dégradation ce matériel.

L'utilisation combinée de méthodes pétrographiques et géochimiques a donc mis en évidence que : (i) le kérogène des lamines parallèles sombres est composé de deux types de structures organiques lamellaires, orangées et sombres, et d'un réseau organique étroitement associé à la matrice minérale; (ii) le soufre est exclusivement lié à la MO; le contenu en soufre des divers constituants du kérogène est très élevé; (iii) le résidu palynologique est composé de MO gélifiée nanoscopiquement amorphe; (iv) la vulcanisation de lipides a joué un rôle majeur lors de la formation du kérogène étudié et ceci étant confirmé par la présence de nombreux COS dans les produits de pyrolyse; (v) du matériel nanoscopiquement amorphe et de fortes teneurs en soufre sont les témoins de la vulcanisation et donc de la sulfato-réduction; (vi) la vulcanisation protège la MO sédimentaire d'altérations liées à des variations locales du potentiel redox. Ces variations locales expliquant certainement la couleur sombre (liée à l'oxydation) de l'un des constituants organiques; (vii) les coccolithophoridés formant la matrice carbonatée sont une source probable des lipides vulcanisés lors de la formation du kérogène.

INTRODUCTION

Organic matter (OM)-rich Kimmeridgian sediments have been identified at several places in the French southern Jura Mountains (fig. 1). These deposits were formed during Upper Kimmeridgian – Beckeri ammonite zone – [Bernier, 1984], on a carbonate platform, behind a reef, in isolated hollows. The outcrop near the village of Orbagnoux (French map IGN 1/25000 n° 3330 Seyssel ouest) exhibits five different calcareous facies, previously described by several authors [Cayeux, 1935; Gubler and Louis, 1956; Bernier *et al.*, 1972; Tribovillard *et al.*, 1991]. These facies (massive limestones, dark or light parallel laminae and dark or light undulated laminae) show large differences in total organic carbon (TOC) content. Massive limestones, dark or light parallel laminae and dark undulated ones, have a coccolithic matrix and relatively high organic carbon contents (> 2%). The organic-matter-richest samples correspond to dark laminae (up to 8.6%). On the contrary, light undulated laminae are characterized by low TOC values (< 1%). The latter facies is related to cyanobacterial mat developments (stromatolites) as shown by the presence of endolithic filaments [Tribovillard *et al.*, 1991]. This facies is also characterized by a lack of coccolithophorids.

Whilst TOC values strongly vary with facies, hydrogen indices (HI) are always high (780 to 960 mg “HC”/g TOC)¹ and occur in the same range. Such values suggest a highly aliphatic nature of the organic matter, independent of facies.

In the present paper, we examine one of the most organic carbon-rich facies: the dark parallel laminae. The study is based upon a representative sample of such a facies characterized by a high TOC content (7.19%) and a high HI value (909 mg “HC”/g TOC). The elemental com-

position of the palynological residue isolated from this sample is (wt%): C (68.07), H (8.06), Fe (0.38), S (16.72) and the H/C atomic ratio is thus of 1.42; the $\delta^{13}\text{C}$ of the OM content is -26.4‰ PDB.

The goal of this study is to derive information on preservation and accumulation pathway (degradation/recondensation and/or selective preservation and/or natural vulcanization) of aliphatic OM in dark parallel laminae. To this end, we used various scales of petrological observations (transmitted and reflected-light microscopy, backscattered and transmission electron microscopy) to obtain a complete description of OM. Parallel geochemical studies by spectroscopic and pyrolytic methods were also carried out to obtain information on the chemical structure of the kerogen in order to determine the mode of accumulation and the source organisms.

METHODS AND SAMPLING

Petrographical investigations

Light microscopy

The organic matter was described directly from thin sections of the rocks by transmitted-light microscopy and polished section by natural reflected-light and UV excitation. In addition, the sample was treated with HF/HCl and the organic residue and the associated metal sulfides were observed in transmitted-light microscopy (palynofacies).

Transmission electron microscopy

Transmission electron microscopy (TEM) observations were carried out on the palynological residues. The latter were fixed in osmium tetroxide, embedded in resin, cut with an ultramicrotome and sometimes stained by uranyl acetate prior to TEM examination using a STEM JEOL 100 CX according to Boussafir *et al.* [1995a]. Sulphur analyses were performed on ultrathin sections using an energy dispersive spectrometer (EDS) coupled to STEM.

Backscattered electron microscopy and elemental mapping

Backscattered scanning electron microscopy (BSEM) observations and analyses were performed on polished sections covered with a thin carbon film, using a Philips 505 microscope coupled with an EDS analysis system. The individual elemental maps (Ca and S) were established using a Si(Li) detector equipped with a Be conventional window (7.5 μm thickness), a source feed of 15 keV and an analysis time of 0.4 s for each pixel. Each map was obtained by the scanning of 128×128 pixels.

Geochemical analysis

Solid-state ^{13}C nuclear magnetic resonance spectroscopy

A solid-state ^{13}C nuclear magnetic resonance spectrum was obtained on a Bruker CXP300 spectrometer operating at 75.47 MHz with combined high-power proton decoupling and CP-MAS sequence. A double-bearing probe was used, and the rotation frequency was 4 kHz. The contact time was 1 ms with a delay between successive sequences of 2 ms.

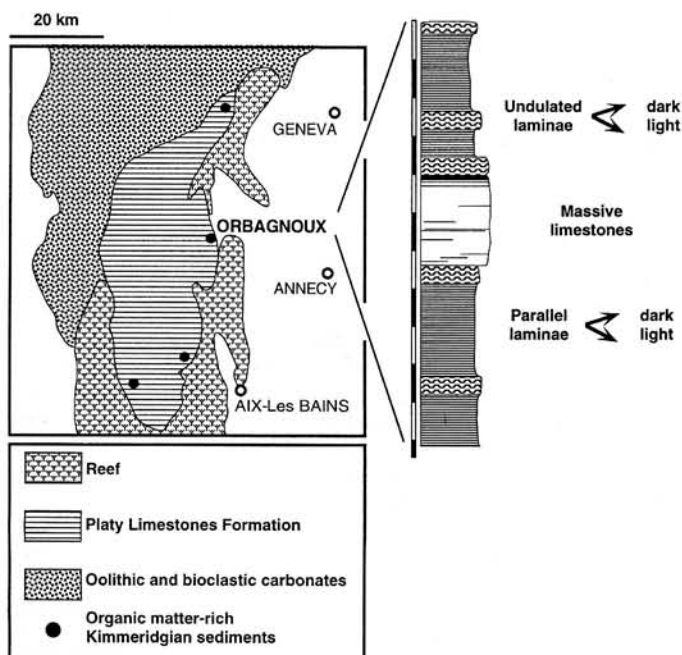


FIG. 1. – Location map and field section of Orbagnoux.

FIG. 1. – Localisation et coupe lithologique d'Orbagnoux.

¹ As shown by subsequent chemical studies, the products generated by pyrolysis, corresponding to the S2 peak of Rock-Eval, are mainly composed of organic sulphur compounds.

Pyrolysis

"Off-line" pyrolysis was performed according to Largeau *et al.* [1986]. Briefly, palynological residue was extracted once with $\text{CHCl}_3/\text{MeOH}$ (2/1). Then the kerogen was heated at 300 °C for 20 min to eliminate adsorbed compounds by thermovaporization and, after extraction with $\text{CHCl}_3/\text{MeOH}$ (2/1), the insoluble residue was pyrolysed at 400 °C for 1 h under a helium flow. The released products were trapped in CHCl_3 at -5 °C and separated by column chromatography on activity-2 alumina into three fractions of increasing polarity by eluting with heptane, toluene and methanol, respectively.

Raney nickel desulphurization and hydrogenation

According to Sinninghe Damsté *et al.* [1988], the toluene fraction was dissolved in 4 ml of ethanol with 0.5 ml of a suspension of Raney nickel. The mixture was refluxed 1.5 h under nitrogen. Desulphurized products were isolated after three successive centrifugations in dichloromethane. The extracts were washed with NaCl-saturated water, dried with Na_2SO_4 and evaporated to dryness. The extracts were dissolved again in 5 ml of ethylacetate, 5 mg of PtO_2 and 2 drops of acetic acid were added and hydrogen was bubbled through the solution for 1 h. Lastly, water, acid and reduced platinum were removed on a $\text{Na}_2\text{SO}_4/\text{Na}_2\text{CO}_3$ (1/1) column.

Gas chromatography-Mass spectrometry

Gas chromatography-mass spectrometry (GC/MS) was carried out on a Hewlett-Packard 5890 gas chromatograph interfaced to a 5989A Hewlett-Packard mass spectrometer operated at 70 eV. The gas chromatograph was equipped with a CPSil 5 CB (film thickness: 0.4 μm) column. Helium was the carrier gas. The oven was heated from 100 °C to 300 °C at 4 °C min^{-1} .

RESULTS & DISCUSSION

Thin and polished sections

Thin sections (pl. Ia), observed under a transmitted-light microscope, reveal two types of organic constituents (relative abundance ca 85/15), within a dark-brown to yellow-brown biomicrite. The major one appears as orange lamellar structures (up to 10 μm thick and with a length reaching several hundred μm) and the less abundant constituent as dark lamellae (up to 10 μm thick and at most 200 μm in length).

Under ultraviolet excitation (pl. Ib), on polished sections, the former type of organic particle shows a yellow to yellow-green fluorescence whereas the second one does not fluoresce. The occurrence of a yellow fluorescence for the particles corresponding to the major type of organic constituent is consistent with a highly aliphatic nature, reflected by high HI values for the bulk OM [Bertrand *et al.*, 1986].

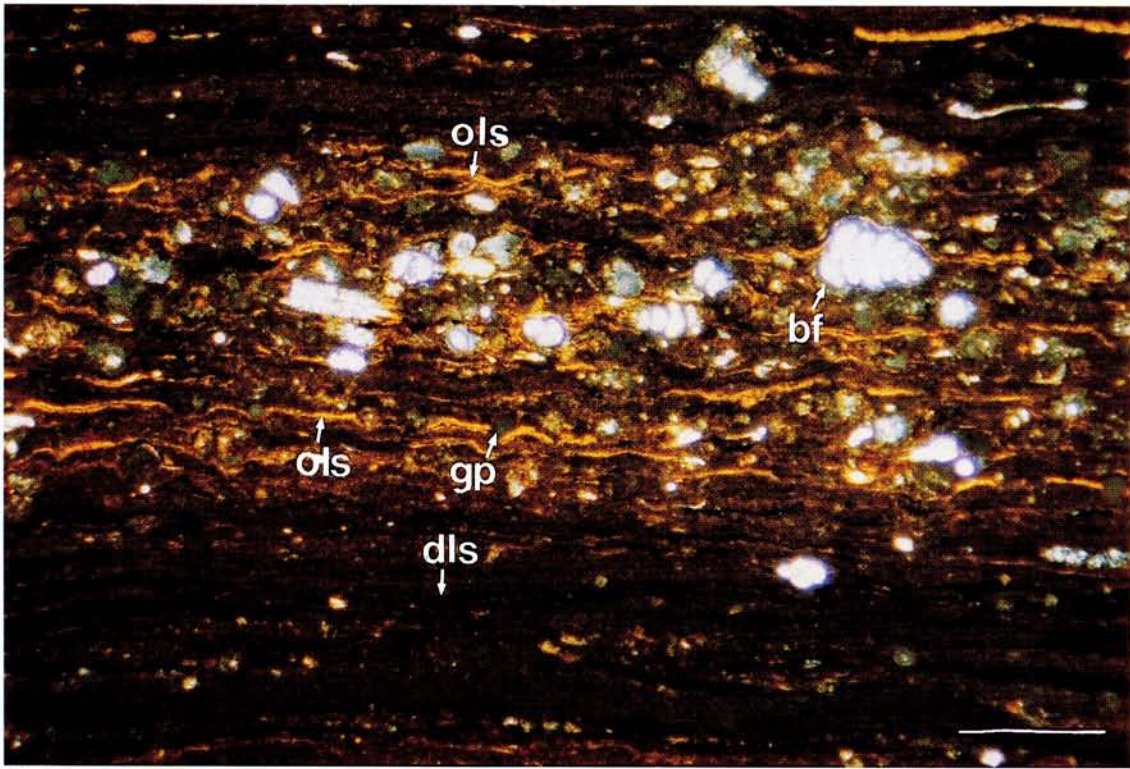
Finally, observations of the polished sections under natural and UV reflected-light indicate that vitrinite and inertinite only occur in very small amount (at most 3% of total organic constituents) thus indicating a low continental contribution.

Two areas of a polished section were selected for back-scattered scanning microscopy (BSEM) observations to determine how the OM is distributed within the sediment. These areas contain the two types of organic lamellar constituents described above. When examined by BSEM the

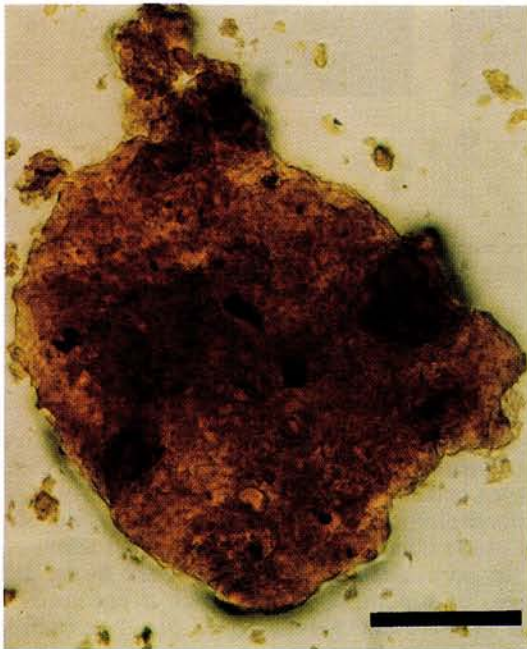
OM obviously appears in a black color and the carbonates are grey. Homogeneous grey zones are constituted by carbonates and dark elongated homogeneous zones (figs. 2a and 2d) should correspond to organic lamellar structures. However, this method does not allow to differentiate the two organic constituents identified above by light microscopy. Nevertheless, these BSEM observations show that scattered OM exists between successive lamellar structures (figs. 2a and 2d) and build a continuous network. Based on this morphological feature, the fluorescence detected in some micrite layers using ultraviolet excitation should correspond to the diffuse OM.

Mapping of calcium and sulphur, using SEM coupled with electron dispersive spectrometry (EDS), was performed on the same areas. As expected (figs. 2b and 2e), the highest Ca contents (dark-grey to dark color in the figures) are related to purely calcareous zones while the zones without Ca (in white color on the figures) correspond to the OM. S-mapping (figs. 2c and 2f) shows that the main portion of the sulphur is associated with the lamellar OM. Nevertheless, sulphur also occurs in intermediate zones which appear as mixed zones for calcium and sulphur where the latter is associated with diffuse OM. In fact, a very low content of pyrite was indicated by Fe elemental analysis in samples corresponding to the dark parallel laminae facies [Mongenot *et al.*, 1996]. Accordingly, the mixed zones contain scattered sulphur-rich OM forming a network within carbonates. Such observations, therefore, give evidence that sulphur almost exclusively corresponds to organic sulphur and is homogeneously distributed in the OM. This is consistent with the result obtained from Geoelf Sulphur Analyser [J. Connan, personal communication] which indicates a lack of elemental sulphur ($\text{SS3 peak} = 0 \text{ S}_{\text{mineral}}/\text{g sample}$) for dark parallel laminae. Indeed, the organic sulphur to organic carbon atomic ratio is around 0.09, a relatively high value. Nevertheless, as observed above, fluorescence results reveal important differences between the two types of organic particles. This should reflect either intrinsic differences (source organisms and/or mode of formation) or a differential evolution of initially identical particles due to local alterations.

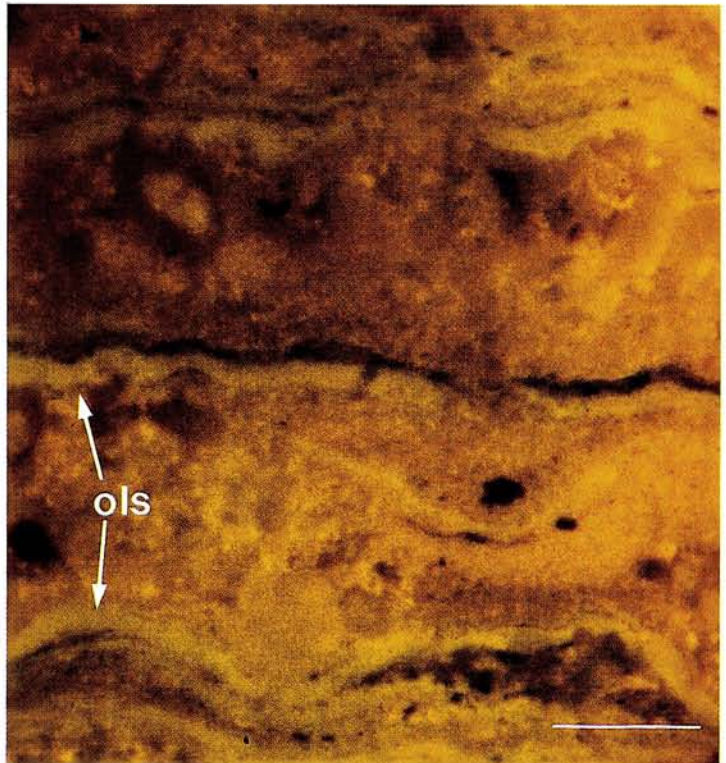
The second hypothesis is consistent with the occurrence of changes in redox potential within the water column and/or the sediment during the setting phase. In fact the biomicrite in the dark parallel laminae contains numerous clasts of oxygen-depending organisms - echinoderms, lamellibranchiata and brachiopods, ostracods, miliolidea, benthic foraminifera and algal thallus - [Tribouillard *et al.*, 1991 and 1992; Mongenot *et al.*, 1996]. Based on the identification in the extracts of isorenieratane (a compound derived from a specific carotenoid of green photosynthetic bacteria), it was recently concluded that the bottom part of the water column was anoxic during the deposition of the Orbagnoux sediments [Sinninghe Damsté *et al.*, 1995]. In fact, the present observations indicate alternations of periods during which the bottom water was at least dysoxic and others when anoxia was reached and green photosynthetic sulphur bacteria were growing. The occurrence of such alternations is supported by the analysis of redox-sensitive trace elements which have recorded these events [Mongenot *et al.*, 1996]. Moreover, the occurrence of oxic events within the sediment was indicated by the presence of pseudomorphs with shapes indicating that they likely correspond to gypsum pseudomorphs. In addition, the low level of detrital material, and hence of metals capable of forming sulphides, like pyrite, makes it unlikely that such pseudomorphs originated from sulphides. Gypsum crystals need a local oversaturation and/or a relatively high redox potential to be formed. In the case of Orbagnoux, as ob-



a



c



b

PLATE 1. Dark parallel lamina observed (a) in transmitted-light microscopy (thin section, scale bar : 0.5 mm) and (b) under UV excitation (polished section, scale bar : 0.1 mm); (c) gel-like OM (palynological residue, scale bar : 0.06 mm). (dls) dark lamellar structures; (ols) orange lamellar structures; (gp) gypsum pseudomorphs; (bf) benthic foraminifera.

PL. 1. *Lamine parallèle sombre observée (a) en lumière naturelle transmise (lame mince, barre d'échelle : 0,5 mm) et (b) en lumière ultraviolette réfléchie (section polie, barre d'échelle : 0,06 mm). (dls) structures lamellaires sombres; (ols) structures lamellaires orangées; (gp) pseudomorphoses de gypse; (bf) foraminifères benthiques.*

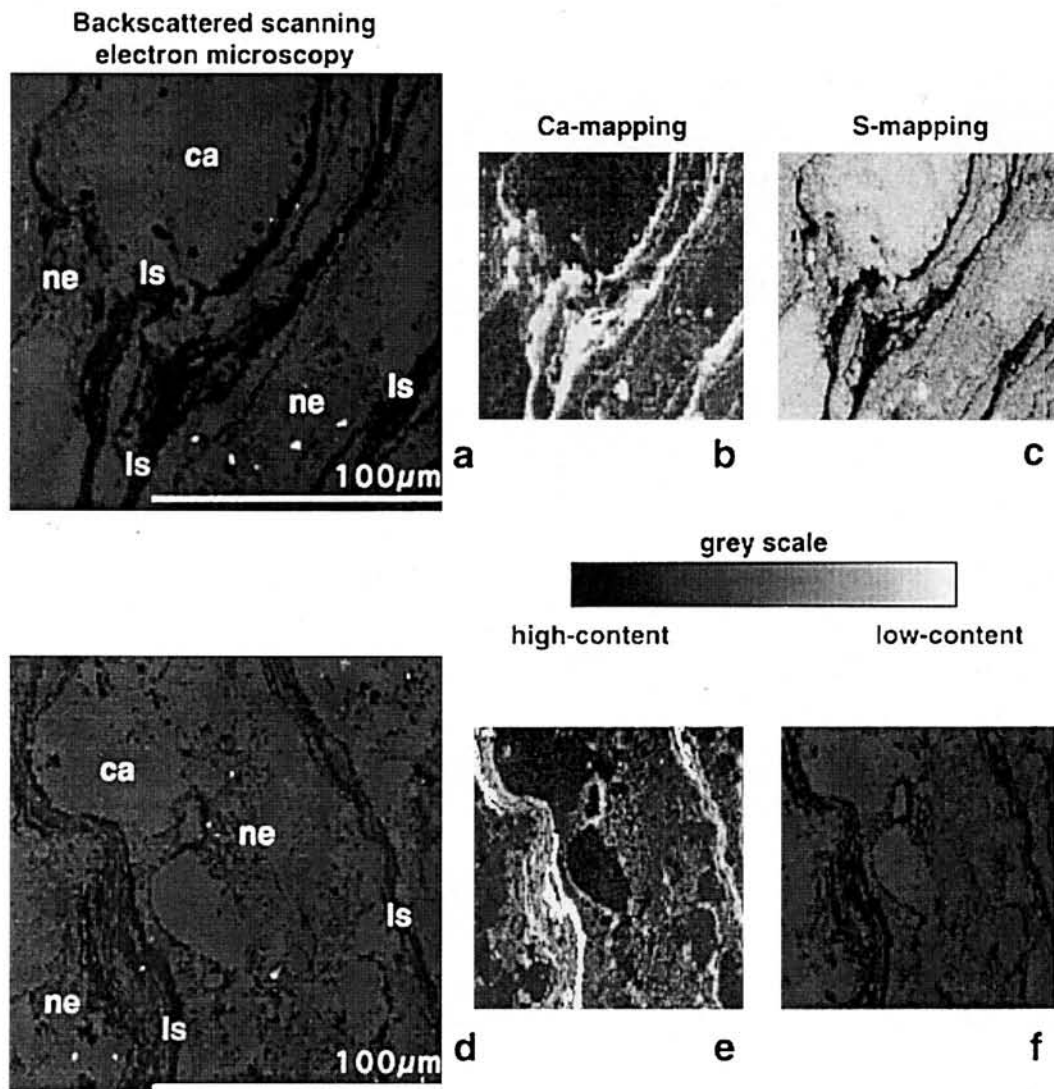


FIG. 2. – Backscattered scanning electron microscopy and elemental mapping of (a) an area with green fluorescing lamellar structures and (d) an area with dark organic constituents; (b) and (e) Ca-mapping of the two areas; (c) and (f) S-mapping of the two areas. ca : pure carbonates; ls : lamellar structures; ne : organic network.

FIG. 2. – Microscopie électronique à balayage en mode rétrodiffusé et cartographie élémentaire (a) d'une zone contenant seulement la structure lamellaire fluorescente en vert et (d) d'une zone riche en constituants organiques noirs. (b) et (e) localisation du calcium dans ces deux zones; (c) et (f) distribution du soufre dans ces mêmes zones. ca : carbonates purs; ls : structures lamellaires; ne : réseau organique.

served by Brosse *et al.* [1990] for the Triassic Noto Formation, gypsum growth seems related to sediment quasi-emergence, *i.e.* to subaerial exposure of the sediment as indicated by the presence of mudcracks and fenestrae [Tribouillard *et al.*, 1991; Mongenot *et al.*, 1997]. As a result, some postdepositional or syndepositional alteration could have occurred locally and could have affected some particles.

Palynological residue

Light microscopy observations of palynological residues allow the identification of kerogen components. The kerogen isolated from the dark parallel laminae appears to be constituted of at least 95% of flat to granular gel-like orange OM (pl. 1c) forming particles with sharp edges. This palynological residue was also examined by TEM. The kerogen was thus shown to be entirely composed of nanoscopically amorphous OM (AOM). This AOM corresponds

either to massive perfectly homogeneous material (fig. 3a) or to porous material characterized by numerous voids of various shapes and sizes (fig. 3b). According to their extent and their morphological features, the massive zones should correspond to the lamellar structures described above. Consequently, the porous zones should be related to the diffuse OM and voids to mineral imprints. No clear-cut limit exists between the massive and porous zones (fig. 3c), both form a continuous organic network.

Such amorphous texture strongly suggests a negligible contribution of the selective preservation pathway [Tegelaar *et al.*, 1989]. The kerogens originating from the latter pathway commonly retain some of the morphological features of the source organisms such as ultralaminae [Largeau *et al.*, 1990]. The latter correspond to outer-walls of microalgae. They are constituted of biopolymers resistant to bacterial degradation which are thus preferentially preserved during early diagenesis and relatively enriched within sediments.

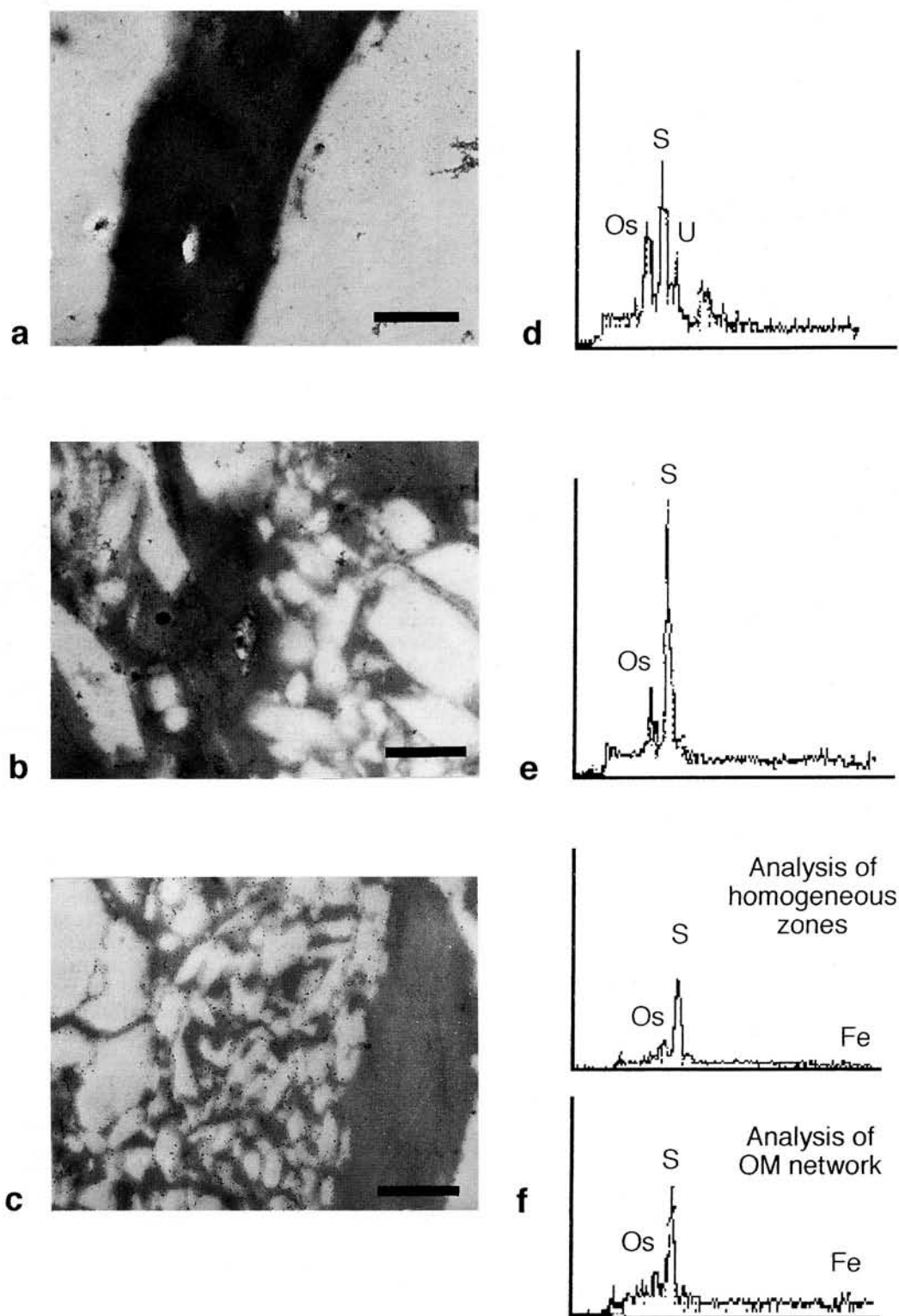


FIG. 3. – Ultrastructures of OM particles. (a) homogeneous zone; (b) zone with voids; (c) occurrence of the two zones in a single particle. Scale bar : 0.8 μ m. (d), (e) and (f) EDS analyses of the corresponding zones. Os and U are due to the fixation in osmium tetroxide and the staining with uranyl acetate of OM respectively. The relatively high S-content in each zone likely reflects S-incorporation into lipids during early diagenesis.

FIG. 3. – Ultrastructure de la MO. (a) zone homogène; (b) zone contenant de nombreux vides; (c) coexistence des deux zones dans une même particule. barre d'échelle : 0,8 μ m. (d), (e) et (f) analyses EDS des zones. Os et U sont respectivement dus à la fixation de l'échantillon par le tétraoxyde d'osmium et à la coloration de la préparation par l'acétate d'uranyle. La forte teneur en S dans chaque zone traduit l'incorporation de S dans des lipides pendant la diagenèse précoce.

Although two types of particles were identified from thin and polished sections, only one type of particle is observed in the palynofacies. The gel-like OM (light microscopy) and the AOM (TEM) observed from the palynological residue in fact correspond to fragments of both types of organic particles associated with diffuse OM.

Sulphur enrichment

Pin-point sulphur analyses on nanoscopically amorphous OM particles, using EDS coupled to TEM, indicate that all these particles are S-rich (figs. 3d, 3e, 3f) which is in agreement with the results from S-mapping (EDS-SEM).

In the Kimmeridge Clay Formation, the S-rich nanoscopically amorphous OM forming homogeneous zones was shown to derive from a natural vulcanization process [Boussafir *et al.*, 1995a; Gelin *et al.*, 1995]. The authors assumed that such a process occurred in the early stages of diagenesis probably in the water column and/or at the water-sediment interface.

Natural vulcanization results from sulphur incorporation into lipids, during early diagenesis, leading to a macromolecular material [Sinninghe Damsté *et al.*, 1989; Hofmann *et al.*, 1992; Adam *et al.*, 1993; Eglinton *et al.*, 1994]. Two conditions shall be fulfilled for this process to be important in kerogen formation: (i) a prolific growth of sulphate-reducing bacteria (triggered by anoxic conditions and an abundance of metabolizable OM) and (ii) the lack or a relatively low level of available reactive iron [Tribouillard *et al.*, 1994]. Under these conditions the H₂S produced by the bacteria will not be trapped as pyrite by iron species but will react with various lipidic compounds. This sulphur incorporation will allow lipids (such as alkenes, ketones and/or aldehydes), known as sensitive to early diagenetic degradation, to escape mineralization. Sulphur is added to double bonds and, depending on their positions and nature, either intermolecular or intramolecular S-linkages are formed. The vulcanization process yields amorphous macromolecular materials with a lipidic character and therefore exhibiting high values of HI. According to our results (high S-content and nanoscopically amorphous texture of the OM) this process should have played a major role in the formation of OM in dark parallel laminae.

The above morphological investigations on dark parallel laminae pointed to a major role of vulcanization in OM preservation. Geochemical investigations were performed to test such a feature and to examine the possible contribution of other minor processes (selective preservation and/or degradation/recondensation). In addition geochemical analyses could provide information on the source organisms which were implicated in kerogen formation.

Solid-state ¹³C nuclear magnetic resonance (NMR) spectroscopy

This spectroscopic method allows to derive information on the nature and abundance of the various functional groups occurring in insoluble macromolecular structures. The observations were carried out on the isolated kerogen. The spectrum (fig. 4) is characterized by the predominance of a peak at 30 ppm assigned to carbons in polymethylenic chains with a shoulder at 15 ppm (methyl groups). This important contribution of aliphatic carbon is consistent with the high values of HI. Several shoulders from 36 to 60 ppm and a peak at 75 ppm are assigned to carbon atoms linked to sulphur. A substantial contribution of olefinic and/or aromatic bonds is also noted.

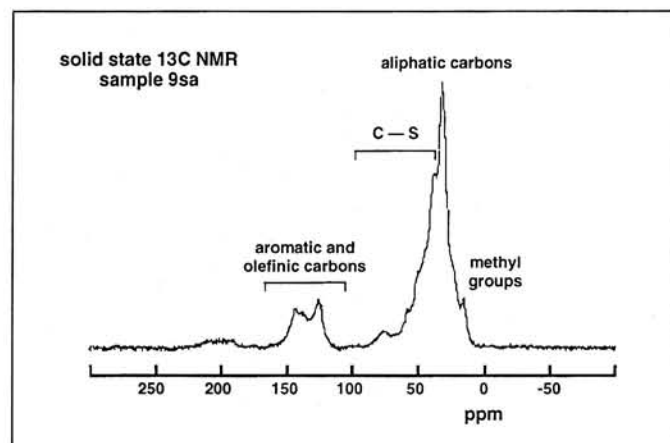


FIG. 4. – Solid-state ¹³C NMR of the kerogen from a sample of dark parallel laminae.

FIG. 4. – Résonance magnétique nucléaire ¹³C à l'état solide d'un kérogène provenant de lamines parallèles sombres.

“Off-line” pyrolysis

The isolated kerogen was submitted to successive pyrolyses at 300 °C and 400 °C. A relatively weak weight loss (9.4 % of the initial OM) was observed at 300 °C but an efficient cracking took place at 400 °C (weight loss of 62.6 %). Moreover, at 300 °C the released compounds mostly correspond to volatile products (the recovered effluents accounting for less than 0.4 % of the initial OM) while most of the pyrolysis products released at 400 °C are of medium volatility and therefore trapped into chloroform (54.2 % of the initial OM). This 400 °C pyrolysate contains structural information on the initial kerogen and was therefore studied. To this end, it was separated, by column chromatography on alumina, into three successive fractions eluted with heptane, toluene and methanol, accounting for 10.5, 27 and 8 wt % of the pyrolysate, respectively.

A complete discussion of the composition of these fractions will be reported elsewhere. Therefore, only a part of the results, corresponding to the toluene-eluted fraction, are briefly described here so as to illustrate the main conclusions derived from the chemical study in connection with the petrographic observations. All three fractions are mostly composed of organic sulphur compounds (OSC), as indicated below for the medium polarity (toluene-eluted) compounds. In fact, the total ion current (TIC) of the toluene fraction only shows a hump with very few well-resolved peaks (fig. 5a). Based on mass spectrometry data the latter peaks are assigned to homologous series of alkylated methylbithiophenes ($m/z = 193$) and alkylated vinylbenzothiophenes ($m/z = 173$). This hump reflects the occurrence of an extremely complex mixture of OSC, as demonstrated by desulphurization and hydrogenation. Following these two reactions, sulphur is completely eliminated and the saturations are reduced. As a result, all the OSC which were derived from sulphur incorporation, in lipids based on the same carbon skeleton, are thus transformed into a single hydrocarbon. The combination of these two reactions, which can be considered in some way as the reverse of the vulcanization process, shall therefore result in a remarkable simplification when applied to OSC mix-

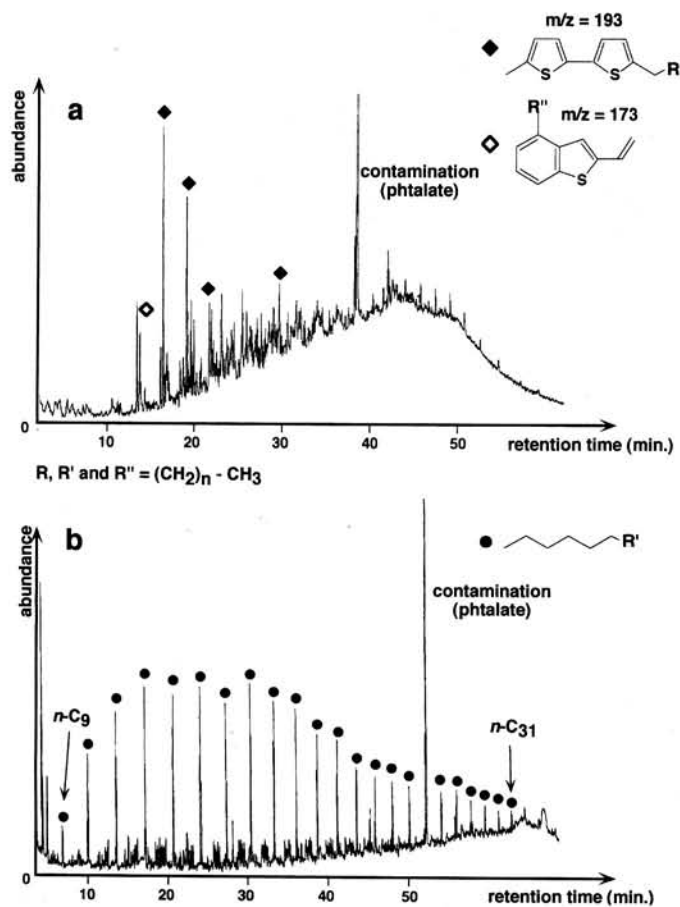


FIG. 5. – Total ion current of the toluene-eluted fraction before (a) and after (b) desulphurization and hydrogenation.

FIG. 5. – Courant ionique total de la fraction éluee au toluène avant (a) et après (b) désulfuration et hydrogénation.

tures. Indeed, the TIC of the toluene-eluted fraction after desulphurization and hydrogenation appears very simple (fig. 5b). This chromatogram is dominated by a series of well-resolved peaks identified as C₉-C₃₁ *n*-alkanes. Such a series did not occur in the fraction prior to desulphurization, as expected based on its polarity and confirmed by GC/MS (selective ion detection at $m/z = 57$). Similar results were obtained for the other two fractions (heptane- and methanol-eluted). The pyrolysate of the kerogen from dark parallel laminae therefore appears to be largely dominated by OSC. This high abundance of OSC confirms the major role of lipid "vulcanization" during early diagenesis. The bulk of the kerogen in dark parallel laminae originates from this pathway. This is also consistent with previously reported geochemical data on the extracts of various Orbagnoux samples. Gas-chromatography coupled with mass spectrometry analysis of these extracts revealed the occurrence of substantial amounts of OSC resulting from sulphur incorporation into free lipids [Gorin *et al.*, 1989; Hopfgartner, 1991; van Kaam-Peters *et al.*, 1995]. However, their level of cross-linking via S-linkages was not high enough to make them insoluble in organic solvents. The insoluble AOM is likely to represent a further stage of cross-linking. Taken together these observations indicate a very high rate of vulcanization during deposition of the dark parallel laminae in Orbagnoux sediments.

As stressed above, strong variations in redox conditions took place during deposition and subsequent burial of Orbagnoux sediments. The presence of gypsum pseudomorphs reveals that the dark parallel laminae locally encountered post-depositional oxic conditions as the result of emergence or quasi-emergence of the overlying sediment layers. The fact that a continuous network of S-rich OM was nevertheless retained in this facies indicates that vulcanized lipids can survive not only bacterial degradation but also a wide range of redox conditions. Nevertheless, substantial alterations should then occur in such macromolecular compounds as probably reflected by the occurrence of the dark maceral. Indeed, when the OM surrounding gypsum pseudomorphs is carefully examined, it can be noted that the area in contact with the crystal usually corresponds to the dark portion of the OM.

An algal source of OM?

The predominance of the *n*-alkanes in the hydrocarbon mixture obtained after desulphurization and hydrogenation demonstrates that most of the OSC of the pyrolysate exhibit a linear carbon skeleton. This points to a major contribution of algal lipids during kerogen formation. As already indicated, coccolithophorid hard parts entirely constitute the matrix in the dark parallel laminae as in three other Orbagnoux facies. It is known that coccolithophorids have contributed to sedimentation, and the nature of the Orbagnoux facies reflects their development [Tribovillard *et al.*, 1991 and 1992]. The absence of coccolithophorid production allowed the development of cyanobacteria (light undulated laminae facies). Reversely, a high rate of sedimentation related to a relatively high production of coccoliths prevented the development of cyanobacterial mats (massive limestones, dark and light parallel laminae and dark undulated laminae). Thereby, a major role of coccolithophorids in kerogen formation can be put forward for the dark parallel laminae. However, no direct evidence of such a role was reported although some previous studies suspected a contribution of coccolithophorid-derived compounds to the formation of other kerogens on the basis of OM and coccolith associations: (i) alternating OM-rich and coccolith-rich thin layers in the Upper Kimmeridgian Bituminous Limestones of Armailles [Busson and Noël, 1972] and from the Kimmeridge Clay Formation [Gallois, 1976; Oschmann, 1988]; (ii) light microscopy observation on amorphous OM with coccolith moulds in Rhetian and younger kerogen [Batten, 1985]; (iii) "algal bodies" with intense blue-green fluorescence and scattered coccoliths in samples from the Jurassic Dorset Formation [Bertrand *et al.*, 1990; Huc *et al.*, 1989]. TEM studies also showed coccolith imprints in the S-rich nanoscopically amorphous OM of the Kimmeridge Clay Formation [Boussafir *et al.*, 1995b].

Further studies on dark parallel laminae, including a precise examination of pyrolysate constituents and their comparison with coccolithophorid lipids, are in progress to test the role of such microalgae in kerogen formation in this facies.

CONCLUSIONS

A combination of petrographical studies (light and electron microscopy) on thin and polished sections and on palynological residue, and EDS analyses (sulphur-mapping) demonstrated that: (i) the kerogen in dark parallel laminae from the Bituminous Laminites of Orbagnoux comprises two types of lamellar organic constituents and an OM network closely associated with a micritic matrix. The very

low contents of vitrinite and inertinite indicate a negligible terrestrial contribution; (ii) sulphur in this facies almost exclusively corresponds to organic sulphur. High S-contents occur in both types of organic constituents and also in the OM network; (iii) the palynological residue is composed at least by 95% of gel-like OM which appears nanoscopically amorphous when observed by TEM. This AOM comprises extended homogeneous zones corresponding to the two organic constituents and diffuse zones with a number of voids related to the network. In addition, the amorphous texture of the OM strongly suggests a negligible role of the selective preservation pathway. On the contrary, a major role was played by the lipid vulcanization pathway in the formation of the kerogen in the dark parallel laminae facies. Therefore, the morphological and geochemical criteria (AOM and high S-content) also observed in other formations would provide a proxy indicator for the occurrence of natural vulcanization in palaeoenvironments.

The assumed role of vulcanization, fully confirmed by spectroscopic and pyrolytic studies, is consistent with high values of HI. The macromolecular compounds thus formed by S-incorporation into lipids are capable of surviving early diagenesis but also strongly oxic, post-depositional conditions probably induced by emergence. Nevertheless some alterations, probably accounting for the formation of the dark lamellar organic constituent, occurred under such con-

ditions. In addition, the geochemical studies indicate that the lipids involved in the vulcanization process were mostly of algal origin.

Coccolithophorid hard parts build up the whole mineral matrix in the dark parallel laminae facies of Orbagnoux. Accordingly the bulk of the vulcanized lipids may originate from this type of microalgae. Orbagnoux sediments could, thus, be an unusual case where an extensive deposition of coccolithophorids is associated with OM accumulation. Classically, the deposition of such algae (*e. g.* in Cretaceous chalks and modern oceanic settings) leads to sediments with a negligible organic matter content. In sharp contrast, owing to an intense natural vulcanization, a substantial part of coccolithophorid organic constituents might have been protected during the formation of the kerogen of Orbagnoux dark parallel laminae.

Acknowledgements. – We are grateful to Dr. J.W. de Leeuw for allowing Th. M. to perform desulphurization at NIOZ. We thank H.M.E. van Kaam-Peters for her help in chemical treatments, D. Jalabert for STEM analyses, P. Tremblay for carrying out BSEM and elemental mapping, Y. Pouet for performing GC-MS and D. Collin, the manager of Orbagnoux mine. We thank Jeol, Leica, Elexience societies and Aimpact program (orstorm) for their financial support. Authors are grateful to Pr. J. Rullkötter and an anonymous reviewer for their help in the improvement of this manuscript.

References

- ADAM P., SCHMID J.C., MYCKE B., STRAZIELLE C., CONNAN J., HUC A., RIVA A. & ALBRECHT P. (1993). – Structural investigation of nonpolar sulfur macromolecules in petroleum. – *Geochim. Cosmochim. Acta*, **57**, 3395-3419.
- BATTEN D.J. (1985). – Coccoliths moulds in sedimentary organic matter and their use in palynofacies analysis. – *J. Micropal.*, **4**, 111-116.
- BERNIER P. (1984). – Les formations carbonatées du Kimméridgien et du Portlandien dans le Jura méridional. Stratigraphie, micropaléontologie et sédimentologie. – *Doc. lab. Géol. Lyon*, **92**, 803 p.
- BERNIER P., BUSSON G., ENAY R. & NOËL D. (1972). – Les calcaires bitumineux d'Armailles, formation laminée du Kimméridgien de la région de Belley (Ain) et leurs conditions de dépôts. – *C.R. Acad. Sci., Paris*, **274**, 2925-2928.
- BERTRAND P., PITTON J.-L. & BERNARD C. (1986). – Fluorescence of sedimentary organic matter in relation to its chemical composition. – *Org. Geochem.*, **10**, 641-647.
- BERTRAND P., LALLIER-VERGÈS E., MARTINEZ L., PRADIER B., TREMBLAY P., HUC A., JOUHANNE R. & TRICART J.-P. (1990). – Examples of spatial relationships between organic matter and mineral groundmass in the microstructure of the organic-rich Dorset Formation rocks, Great Britain. In : B. DURAND & F. BEHAR Eds., *Advances in organic geochemistry, 1989.* – *Org. Geochem.*, **16**, 661-675.
- BOUSSAFIR M., GELIN F., LALLIER-VERGÈS E., DERENNE S., BERTRAND P. & LARGEAU C. (1995a). – Electron microscopy and pyrolysis of kerogens from the Kimmeridge Clay Formation, UK : Source organisms, preservation processes, and origin of microcycles. – *Geochim. Cosmochim. Acta*, **59**, 3731-3747.
- BOUSSAFIR M., LALLIER-VERGÈS E., BERTRAND P. & BADAUT-TRAUTH D. (1995b). – SEM and TEM studies of organic matter and source rock microfacies from a short-term organic cycle of Kimmeridgian source-rocks. In : E. LALLIER-VERGÈS *et al.*, Eds., *Organic matter accumulation. The organic cyclicities of the Kimmeridge Clay Formation (Yorkshire, GB) and the recent maar sediments (lac du Bouchet, France).* – *Lecture Notes in Earth Sciences*, **57**, Springer-Verlag, 15-30.
- BROSSE E., RIVA A., SANTUCCI S., LOREAU J.-P. & FRIXA A. (1990). – Some sedimentological and geochemical characters of the late Triassic Noto Formation, source rock in the Ragusa basin (Sicily). In : B. DURAND and F. BEHAR Eds., *Advances in organic geochemistry 1989.* – *Org. Geochem.*, **16**, 715-734.
- BUSSON G. & NOËL D. (1972). – Sur la constitution et la genèse de divers sédiments finement feuilletés ("laminites") à alternances de calcaires et de matière organique ou argileuse. – *C.R. Acad. Sci., Paris*, **274**, 3172-3175.
- CAYEUX L. (1935). – Les roches sédimentaires de France. Roches carbonatées. – Masson, Paris, 582 p.
- EGLINTON T.I., IRVINE J.E., VAIRAVAMURTHY A., ZHOU W. & MANOWITZ B. (1994). – Formation and diagenesis of macromolecular organic sulfur in Peru margin sediments. – *Org. Geochem.*, **22**, 781-799.
- GALLOIS R.W. (1976). – Coccolith blooms in the Kimmeridge Clay and origin of North Sea oil. – *Nature*, **259**, 473-475.
- GELIN F., BOUSSAFIR M., DERENNE S., LARGEAU C. & BERTRAND P. (1995). – Study of qualitative and quantitative variations in kerogen chemical structure along a microcycle : Correlations with ultrastructural features. In : E. LALLIER-VERGÈS *et al.* Eds., *Organic matter accumulation. The organic cyclicities of the Kimmeridge Clay Formation (Yorkshire, GB) and the recent maar sediments (lac du Bouchet, France).* – *Lecture Notes in Earth Sciences*, **57**, Springer-Verlag, 31-47.
- GORIN G., GÜLAÇAR F. & CORNIOLEY Y. (1989). – Organic geochemistry, palynofacies and palaeoenvironment of Upper Kimmeridgian and Lower Tertiary organic-rich samples in the southern Jura (Ain, France) and subalpine massifs (Haute-Savoie, France). – *Eclogae geol. Helv.*, **82**, 491-515.
- GUBLER Y. & LOUIS M. (1956). – Études d'un certain milieu du Kimméridgien bitumineux de l'Est de la France. – *Rev. Inst. Fr. Pétr.*, **XI**, 1536-1543.
- HOFMANN I.C., HUTCHINSON J., ROBSON J.N., CHICARELLI M.I. & MAXWELL J.R. (1992). – Evidence for sulphide links in a crude oil asphaltene and kerogens from reductive cleavage by lithium in ethylamine. In : C.B. ECKARDT, J.R. MAXWELL, S.R. LARTER and D.A.C. MANNING Eds., *Advances in organic geochemistry 1991.* – *Org. Geochem.*, **19**, 371-387.
- HOPFGARTNER G. (1991). – Géochimie organique : Recherches sur l'extraction de la matière organique des sédiments par des fluides supercritiques – Étude de marqueurs biologiques dans des sédi-

- ments jurassiques du Toarcien. – PhD Thesis, Univ. Geneva, 151 p.
- HUC A.Y., LALLIER-VERGÈS E., BERTRAND Ph., CARPENTIER B. & HOLLANDER D.J. (1989). – Organic matter response to change of depositional environment in Kimmeridgian shales, Dorset, U.K. In : J. WHELAN et J. FARRINGTON Eds., *Organic matter : productivity, accumulation and preservation of organic matter in recent and ancient sediments.* – Columbia University Press, New York, 469-486.
- VAN KAAM-PETERS H.M.E., KÖSTER J., DE LEEUW J.W. & SINNINGHE DAMSTÉ J.S. (1995). – Occurrence of two novel benzothiophene hopanoid families in sediments. – *Org. Geochem.*, **23**, 607-616.
- LARGEAU C., DERENNE S., CASADEVALL E., KADOURI A. & SELLIER N. (1986). – Pyrolysis of immature torbanite and of the resistant biopolymer (PRB torbaniteA) isolated from extant alga *Botryococcus braunii*. Mechanism of formation and structure of torbanite. – *Org. Geochem.*, **10**, 1023-1032.
- LARGEAU C., DERENNE S., CLAIRAY C., CASADEVALL E., RAYNAUD J.-F., LUGARDON B., BERKALOFF C., COROLLEUR M. & ROUSSEAU B. (1990). – Characterization of various kerogens by scanning electron microscopy (SEM) and transmission electron microscopy (TEM) – Relationships with resistant outer-wall in extant microorganisms. – *Meded Rijks Geol.*, **45**, 91-101.
- MONGENOT Th., TRIBOVILLARD N.-P., LALLIER-VERGÈS E., DERENNE S. & LARGEAU C. (1996). – Study of the different facies in laminated organic-rich Kimmeridgian sediments of Orbagnoux (Jura, France): source organisms and depositional environments. – *V.M. Goldschmidt Conference, Heidelberg.* – *J. Conf. Abstr.*, **1**, 408.
- OSCHMANN W. (1988). – Kimmeridge clay sedimentation – a new cyclic model. – *Palaeogeogr., Palaeoclimatol., Palaeoecol.*, **65**, 217-251.
- SINNINGHE DAMSTÉ J.S., RIJSTRA W.I.C., DE LEEUW J.W. & SCHENCK P.A. (1988). – Origin of organic sulphur compounds and sulphur-containing high molecular weight substances in sediments and immature crude oils. – *Org. Geochem.*, **13**, 593-606.
- SINNINGHE DAMSTÉ J.S., EGLINTON T.I., DE LEEUW J.W. & SCHENCK P.A. (1989). – Organic sulphur in macromolecular sedimentary organic matter : I. Structure and origin of sulphur-containing moieties in kerogen, asphaltenes and coal as revealed by flash pyrolysis. – *Geochim. Cosmochim. Acta*, **53**, 873-889.
- SINNINGHE DAMSTÉ J.S., KOOPMANS M.P., KÖSTER J., VAN KAAM-PETERS H.M.E., KENIG F., SCHOUTEN S. & DE LEEUW J.W. (1995). – Molecular palaeontological evidence for photic zone anoxia in past depositional environment. In : J.O. GRIMALT and C. DORRONSORO Eds., *Organic geochemistry : developments and applications to energy, environments and human history.* – A.I.G.O.A., Donostia-San Sebastian, 55-57.
- TEGELAAR E.W., DE LEEUW J.W., DERENNE S. & LARGEAU C. (1989) – A reappraisal of kerogen formation. – *Geochim. Cosmochim. Acta*, **53**, 3103-3106.
- TRIBOVILLARD N.-P., GORIN G., HOPFGARTNER G., MANIVIT H. & BERNIER P. (1991). – Conditions de dépôts et matière organique en milieu lagunaire d'âge kimméridgien du Jura méridional français (résultats préliminaires). – *Eclologiae geol. Helv.*, **84**, 441-461.
- TRIBOVILLARD N.-P., GORIN G., BELIN S., HOPFGARTNER G. & PICHON E. (1992). – Organic-rich biolaminated facies from a Kimmeridgian lagoonal environment in the French southern Jura mountains A way of estimating accumulation rate variations. – *Palaeogeogr., Palaeoclimatol., Palaeoecol.*, **99**, 163-177.
- TRIBOVILLARD N.-P., DESPRAIRIES A., LALLIER-VERGÈS E. & BERTRAND Ph. (1994). – Vulcanization of lipidic organic matter in reactive-iron deficient environments : a possible enhancement for the storage of hydrogen-rich organic matter. – *C.R. Acad. Sci.*, Paris, **319**, 1199-1206.



Pyrobitumen occurrence and formation in a Cambro–Ordovician sandstone reservoir, Fahud Salt Basin, North Oman

Alain Y. Huc ^{a,*}, Peter Nederlof ^b, Romain Debarre ^a, Bernard Carpentier ^a,
 Mohammed Boussafir ^c, Fatima Laggoun-Défarge ^c, Arnaud Lenail-Chouteau ^a,
 Nathalie Bordas-Le Floch ^a

^a *Institut Français du Pétrole, Division Géologie-Geochimie, 1 et 4 Avenue de Bois-Préau, 92852 Rueil-Malmaison, France*

^b *Petroleum Development of Oman, Oman*

^c *Université d'Orléans, UNR 6531 du CNRS, France*

Received 4 March 1999; accepted 7 January 2000

Abstract

The Cambro–Ordovician Barik Sandstone reservoirs in the Fahud Salt Basin in Oman contain bitumen which may fill up to 40% of the porosity. In well Jaleel-1, this bitumen was isolated (according to kerogen procedure) and typed by NMR, elemental analysis and density measurements. The isolated bitumen is characterized by: (1) a highly aromatic character (NMR 75% C_{Aro}, H/C atomic ratio: 0.65), (2) a very high sulphur content (4.2%) and (3) a relatively high density (1.3–1.4 g/cm³). The insolubility and the reflectivity of the bitumen (1.2% Vr) qualify it as a low mature pyrobitumen. The combination of Rock-Eval and density data was used to calculate the actual volume of the pyrobitumen in the rock, as a percentage of porosity. It was found that the pyrobitumen volume shows a negative correlation with total porosity, indicating that small pores are more invaded by bitumen than larger ones. Finally, closed system pyrolysis experiments, performed on oils with different NSO contents, indicate that an in situ oil with a very high content of NSO compounds is required to generate such large amounts of pyrobitumen in the pore system. These observations suggest that the precursor oil of the current pyrobitumen was a very heavy oil tentatively assumed to be the result of a severe biodegradation. Basin modeling shows that the reservoir was charged already in Devonian times. A major uplift brought the oil accumulation near the surface during the Carboniferous and a rather regular burial to the present day position (4500 m, 140°C) (Loosveld et al., 1996). This scenario, involving a residence time at shallow depth, strengthens the biodegradation hypothesis. The numerical modeling, which involves the IFP kinetic model for secondary oil cracking, suggests that pyrobitumen formation is a very recent event. Inclusion of pyrobitumen particles within quartz overgrowth, containing fluid inclusions, provides an upper temperature limit for the beginning of pyrobitumen formation which comforts the result of kinetic modelling. © 2000 Elsevier Science B.V. All rights reserved.

Keywords: Pyrobitumen; Oman; Oil cracking; Biodegradation; Reservoir geochemistry

* Corresponding author. Tel.: +33-1-47-52-60-00; fax: +33-1-47-52-70-19.
E-mail address: a-yves.huc@ifp.fr (A.Y. Huc).

1. Introduction

The current trend in hydrocarbon exploration to target deep, high temperature prospects has encouraged research on the thermal stability of petroleum. The onset of oil cracking is still a matter of debate but has been predicted for certain oils at temperatures as low as 140°C (Schenk and Horsfield, 1995). The hydrogen mass balance of oil cracking implies that apart from gas, a highly aromatic and insoluble carbonaceous residue, pyrobitumen, is generated. Because deposition of pyrobitumen may significantly deteriorate reservoir quality, bitumen plugging is recognized as a major exploration risk in many hydrocarbon provinces. This is the case of North Oman where bitumen is often identified on routine microscopical examination of thin sections and where several exploration wells have penetrated reservoirs

where the porosity is plugged to such an extent that even gas production is impaired.

The purpose of this paper is to investigate the nature and formation of the bitumen occurrences encountered in the Cambro–Ordovician fluvio-de-ltaic Barik Sandstone reservoirs in the Fahud Salt Basin in Oman.

2. Geological setting

The Jaleel prospect belongs to the Fahud basin which is located on the eastern flank of a north–south graben system. The Fahud basin is separated from the Ghaba salt basin, sited in the central graben itself, by the Makarem-Mabrouk High (Figs. 1 and 2). The graben system has been emplaced during Infracambrian time, and is coeval with the rifting

LOCATION MAP, NORTH OMAN

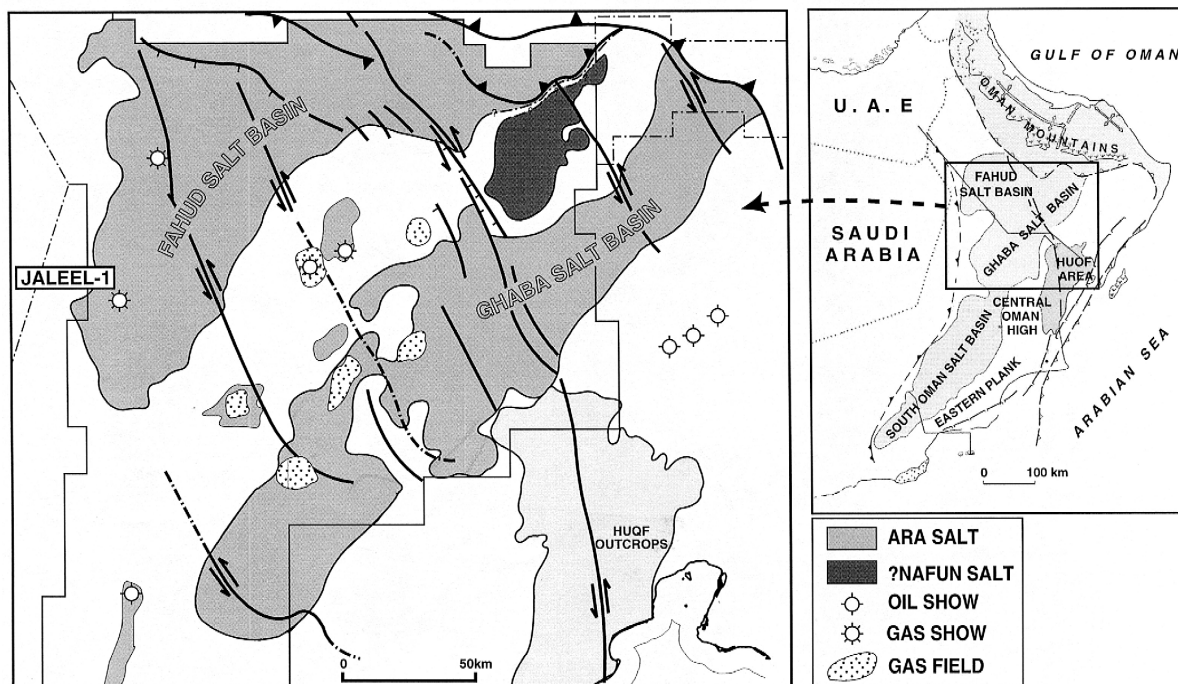


Fig. 1. Location map.

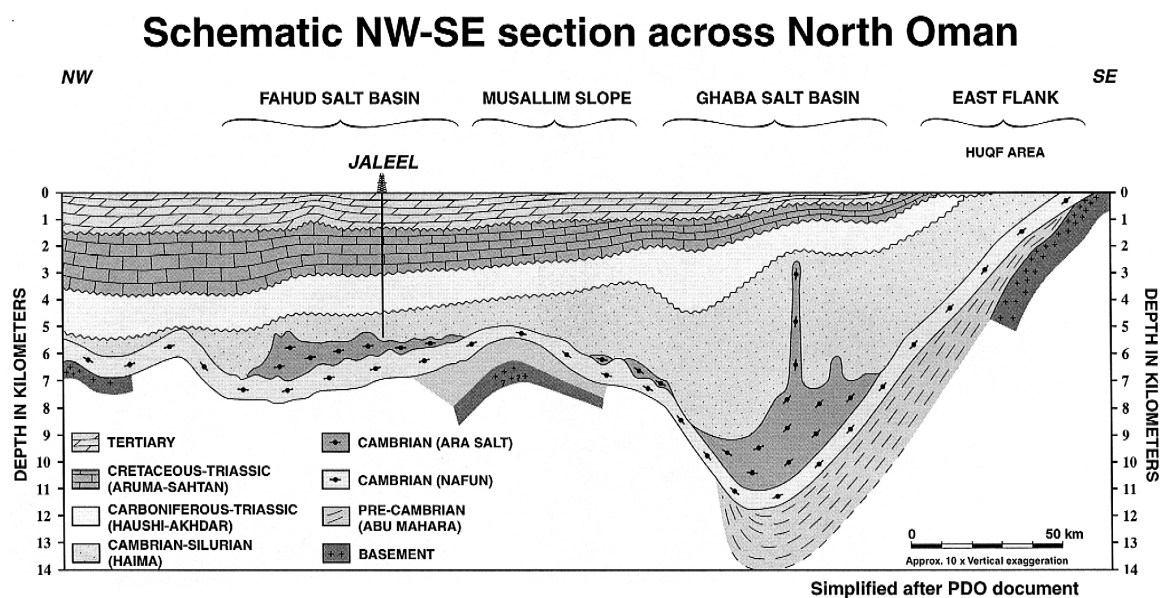


Fig. 2. Schematic NW–SE geological section across North Oman.

phases associated with a sinistral motion along the Najd fault which crosses the Arabian plate along a NW–SE direction from Bani Ghayy basins in Saudi Arabia to southern Oman and northern Yemen (Bejdoun, 1993). This rifting event was followed by a thermal relaxation, accounting for the development of a Cambro–Ordovician sag basin. The fluvio-deltaic Barik sandstone (belonging to the Andam formation and the Haima Super Group) (Fig. 3) constitutes the reservoir of the Jaleel prospect. It was deposited as a part of the sag fill. During this rift-sag cycle, Infracambrian Huqf source rock intervals were buried to a sufficient depth to generate hydrocarbons (probably during the Ordovician). This rift-sag period was followed by an important phase of uplift starting during Devonian time, probably in relation to the doming which preceded the Gondwana break-up and which caused the erosion/non deposition of most of the Silurian–Carboniferous interval. Finally, the Gondwana break-up itself was achieved during the Permian, thus inducing the creation of the north-eastern and southeastern passive margins of the Arabian plate. It results in a renewed subsidence, which was relayed by the creation of a foredeep basin in North Oman, initiated from late Cretaceous, as a

HAIMA SUPERGROUP

Super Group	Group	Formation	Member	Tent. Age	
HAIMA	Safiq	Sahmah		Silurian	
		Hasirah			
		Saih Nihayda		ORDOVICIAN	
	Ghurdun		Middle		
	Mahatta-Humaid	Andam	Barakat Mb.		Late / Early
			Mabrouk Mb.		
			Barik Sst. Mb.		Late
			Al Bashair Mb.		
	Miqrat	Upper Mb.		CAMBRIAN	
		Lower Mb.			
	Amin	Sst./Slt. Mb.		Early / Middle	
		Cgl. Mb.			
Nimr	Undiff.				

Fig. 3. Stratigraphy of the Haima supergroup.

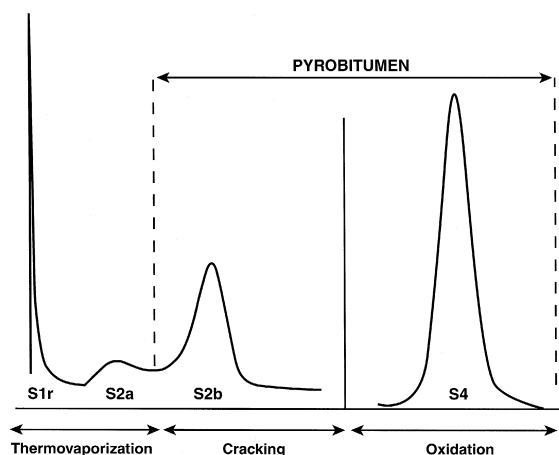


Fig. 4. Rock-Eval pyrogram of a Jaleel rock sample using the “reservoir mode” heating program.

consequence of the formation of Oman Mountains and ophiolites obduction. This continuous subsidence has progressively buried the sediments down to their current depth (Beydoun, 1993; Loosveld et al., 1996).

3. Samples

Twenty-one plugs (JLL1 to JLL21) selected from the 11-m cored section (4560–4571 m) of the Jaleel 1 well were complemented by two cuttings samples respectively assigned to depth intervals: 4480–4560 m (JLLCUT1) and 4571–4636 m (JLLCUT2). As a consequence, the entire set of samples can be considered as representative of a 150-m thick interval of the reservoir. The core samples have been collected at spots where porosity data were available. The two cuttings samples have been separated into two aliquots: one treated as bulk material, the other one, hand picked in order to tentatively sort out different lithological facies.

4. Experimental

Rock-Eval II pyrolysis has been performed on the whole set of samples using the reservoir mode (temperature heating ramp: 10°C/min). Besides the classical S1 peak (light thermovaporizable fraction), this specific mode allows to deconvolute the S2 peak into S2a and S2b peaks which can be respectively assigned to a heavy thermovaporizable fraction and to an actual pyrolyzable fraction (Trabelsi et al., 1994) (Fig. 4). The residual organic carbon is oxidized and the resulting CO₂ is recorded as S4 peak. The total organic carbon (TOC) is calculated from the entire set of generated peaks (Espitalié et al., 1985a,b,c).

According to the Rock-Eval results, two core samples (JLL15 and JLL17) containing sufficient amount of organic carbon (respectively, 2.3% and 1.5% TOC) have been selected for further characterization of the organic phase.

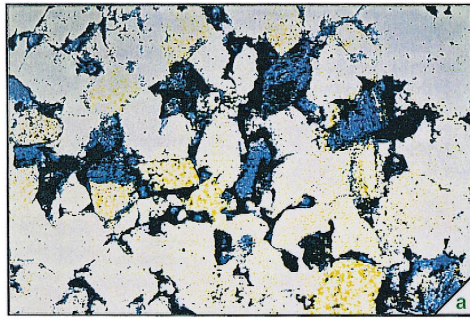
Visual examination has been performed on these two samples, including microscopical observation of polished sections both in natural light (Plate 1b,c) and UV fluorescence (Plate 1d) and determination of reflectance was made on densimetric concentrates (Plate 1e).

The two selected samples have been subjected to solvent extraction using dichloromethane. The resulting extracts were quantified and, after *n*-heptane deasphalting, separated by thin layer chromatography into saturates, aromatics and NSO fractions. The saturates were then analysed by GC and by GC MS on a VG Autospec; *m/z* 191 and *m/z* 217 fragmentograms were extracted for comparison with existing regional data base (Grantham et al., 1990).

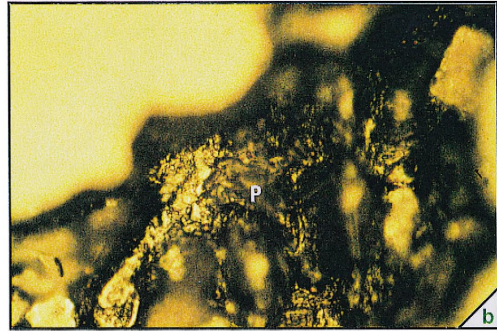
The insoluble organic matter was isolated following the procedure designed for kerogen preparation involving HF/HCl digestion of the mineral matrix (Durand and Nicaise, 1980).

The resulting organic residue was characterized by elemental analysis including C, H, O, N, S, Fe.

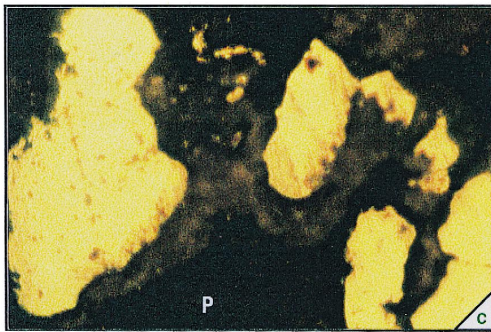
Plate 1. Microphotographs of Jaleel samples: (a) thin section: porosity in blue and pyrobitumen in black; (b) polished section, reflected light: particle of solid bitumen in porosity (quartz in yellow); (c) polished section, reflected light: particle of solid bitumen in porosity (P) and extractable bitumen in brown (see d); (d) polished section, UV light: fluorescent extractable bitumen (fB) corresponding to the brown bitumen in previous microphotograph; (e) polished section, reflected light: particles of solid bitumen resulting from density concentration; (f) polished section, reflected light: pyrobitumen inclusions in quartz.



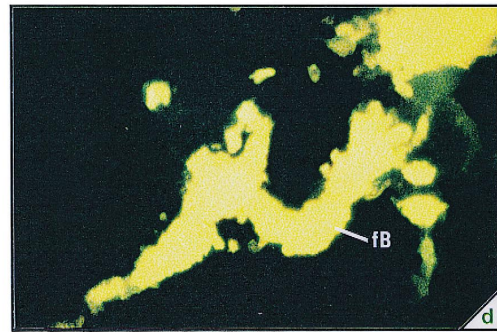
100 μm



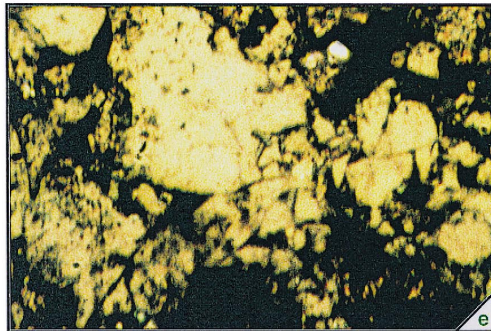
10 μm



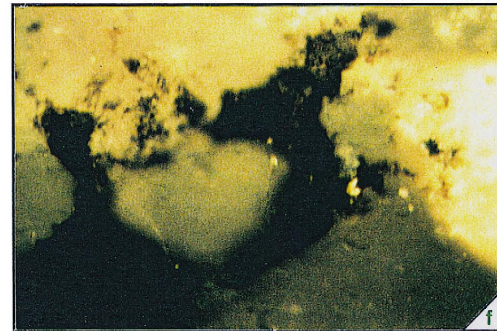
10 μm



10 μm



10 μm



10 μm

a = thin section

d = fluorescence light

b = natural light

e = pyrobitumen concentrate, reflected light

c = natural light

f = pyrobitumen inclusion in quartz, reflected light

P = Pyrobitumen

fB = fluorescent Bitumen

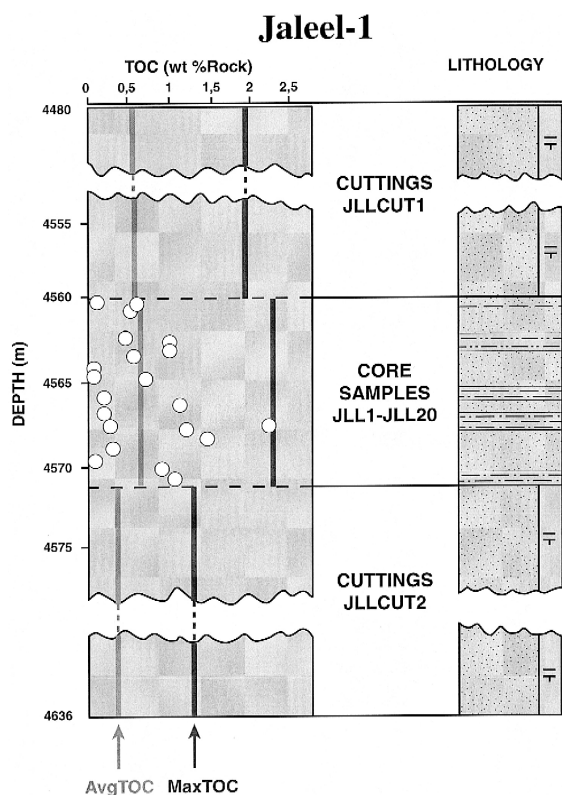


Fig. 5. Total organic carbon (TOC) of the cuttings and core samples.

The occurring pyrite is evaluated by assuming that the entire Fe is involved as pyrite FeS₂. The sulfur, which is not stoichiometrically associated with the pyrite, is considered to be organic sulfur. The remaining minerals including, in these samples, TiO₂ (anastase), ZrSiO₄ (Zircon), KAlSi₃O₈ (feldspar microcline), have been tentatively identified by X-ray diffraction supported by X fluorescence which provided the following lists of major elements: S, Zr, Cl, Ca, Ti, Fe, and minor elements: Si, K, V, Ni. ¹³C

solid state ¹³C NMR of the organic residue was performed on a Bruker instrument MSL 400.

The density of the organic residue was calculated from its weight (corrected from the estimated pyrite and other minerals weight) and volume (corrected from its Helium porosity and assuming that the volume of the minerals can be neglected).

The stable carbon isotope ratio of the extracts and of the insoluble organic residues was measured using a Delta E Finnigan mass spectrometer, and is reported in the usual δ-notation in units per mil (‰) relative to the Pee Dee Belemnite standard (PDB).

$$\delta^{13}\text{C}(\text{‰}) = \left[\left(\frac{R_{\text{sample}}}{R_{\text{PDB}}} \right) - 1 \right] \times 10^3$$

where $R = {}^{13}\text{C}/{}^{12}\text{C}$.

5. Results and discussion

5.1. Organic content

According to Fig. 5, the TOC of the 21 core samples ranges from about < 0.01wt.% to 2.3 wt.%, although most values are between 0.3 wt.% and 1.2 wt.%, and the average value is 0.7 wt.%.

TOC content of bulk cuttings samples (based on 10 aliquots for each sample), although slightly lower than the core samples average, is comparable to this value: 0.5 wt.% (JLLCUT1) and 0.3 wt.% (JLLCUT2). The TOC content of the hand-picked lithological fractions from JLLCUT1 and JLLCUT2 ranges, respectively, from 0.01wt.% to 1.9 wt.% (average 0.5 wt.%) and from 0.01wt.% to 1.2 wt.% (average 0.3 wt.%). Moreover, 90% to 95% of the TOC corresponds to refractory nonpyrolysable organic matter, according to Rock-Eval pyrolysis, for the whole set of samples including core and cuttings material, with hydrogen index ranging between 96 and 113. These data suggest that the organic material

Table 1
Extract composition

Solvent extract (% extractable carbon)	Carbon isotope ratio of the solvent extract δ ¹³ C‰	Saturates % of extract	Aromatics % of extract	Resins % of extract	Asphaltenes % of extract	
JLL15	9	- 31.9	65.5	10.2	21.4	2.9
JLL17	10	- 31.8	73.1	9.8	14.7	2.4

present in the cored section is rather representative (quantitatively and qualitatively) of the organic matter occurring in the entire considered 150-m thick reservoir interval (Fig. 5).

5.2. Bitumen characterization

Upon solvent extraction, JLL15 and JLL17 core samples release, respectively, 9% and 10% of their carbon as extractable material. The composition of the extracts shown on Table 1 is characterized by its relative richness in saturates.

The molecular composition of the extracts, including the significant occurrence of diasteranes, predominance of C27 regular steranes and the abundance of C24 tricyclic terpanes (Fig. 6), together with the isotopic signature of the extracts (Table 1) suggest that they are originating from the regional Q and B source rocks which have been identified by Grantham et al. (1990) and Nederlof et al. (1994) and proposed to be stratigraphically associated with the Ara-salt (at intra and top salt situation).

5.3. Insoluble bitumen characterization

The elemental analysis of the insoluble organic residue is displayed in Table 2. The samples exhibit an unusually high organic sulfur content (4.14%–4.21%) and a low H/C atomic ratio (0.62–0.64) which reflects a high aromaticity.

A direct measurement of the aromaticity is obtained by ^{13}C solid state NMR analysis (Fig. 7), which reveals that aromatic carbon atoms account for 76%–77% of the total carbon atoms.

The insolubility and the aromaticity of this organic material support its identification as pyrobitumen.

However, the insoluble bitumen reflectance measured on the organic concentrates (Plate 1e) of the two samples ($R_o = 1.2\%$) qualifies it as a low maturity pyrobitumen (Hunt, 1995).

The $\delta^{13}\text{C}$ of the pyrobitumen is dramatically lower (by 4‰) than the $\delta^{13}\text{C}$ of the related extracts (Tables 1 and 2). This strongly points to a clear difference in origin for the two organic phases which consequently belong to two separate charges of the reservoir, implying a complex filling history. The current gas content of the reservoir potentially represents a third charge, but since no sample of gas has been collected, no analytical evidence can support this

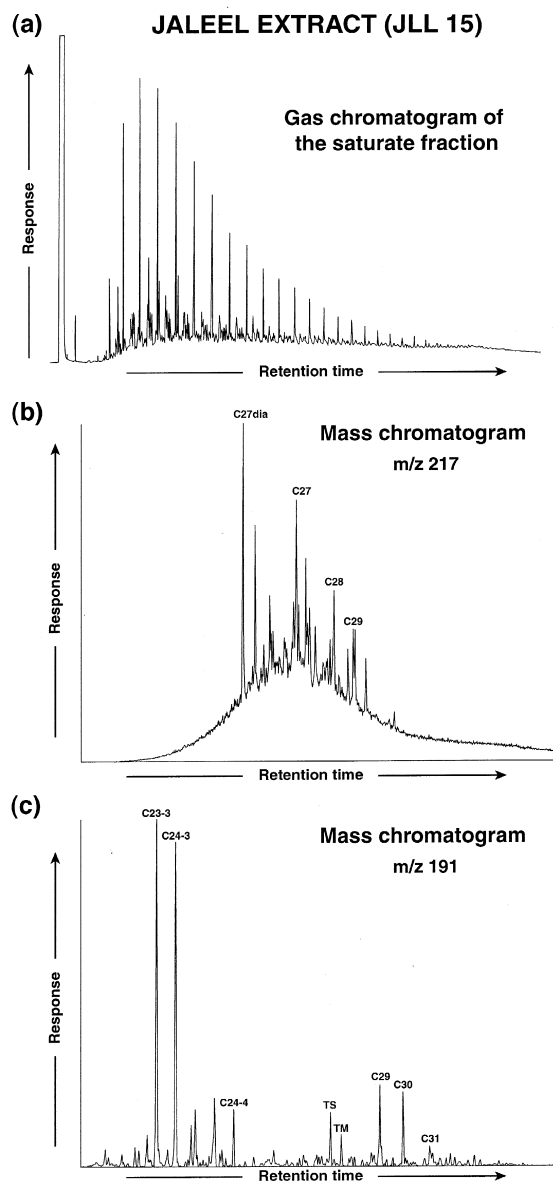


Fig. 6. Gas chromatogram and mass chromatograms ($m/z = 217$ and $m/z = 191$) of a Jalleel rock extract.

assumption. The very light carbon isotope value is characteristic of oils sourced from the so-called Huqf or Nafun infra salt source rock of Precambrian–Infracambrian age. They are probably related to the strong negative excursions of $\delta^{13}\text{C}$ which have been recognized worldwide in both organic matter and

Table 2

Elemental and isotopic composition of the insoluble bitumen

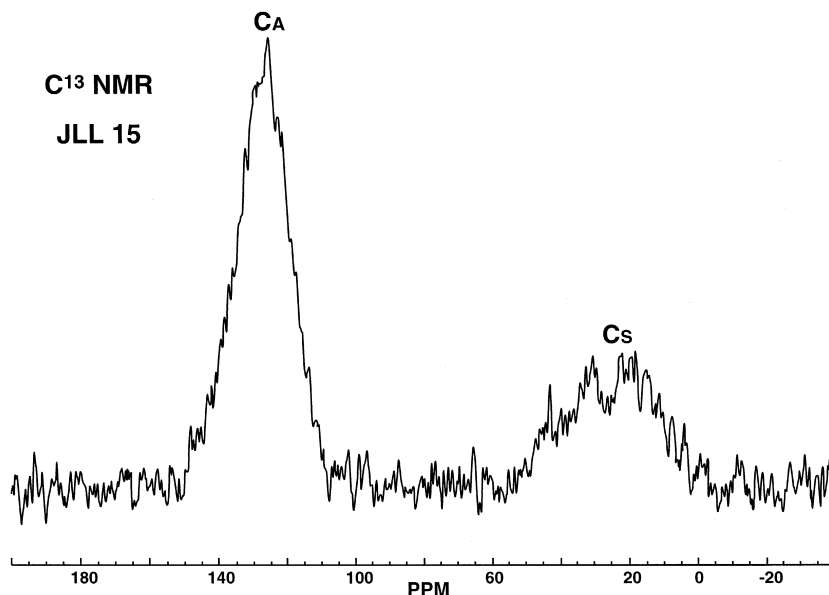
	C (wt.%)	H (wt.%)	N (wt.%)	O (wt.%)	Org S (wt.%)	Fe (wt.%)	Pyrite (wt.%)	Other minerals (wt.%)	H/C	O/C × 100	$\delta^{13}\text{C}$ (‰)
JLL15	88.16	4.59	0.40	2.72	4.14	0.58	1.24	6.40	0.62	2.31	-35.66
JLL17	87.00	4.67	0.87	3.25	4.21	0.90	1.93	7.03	0.64	2.80	-35.86

carbonate within the basal Vendian, uppermost Vendian and early Cambrian (Hsü et al., 1985; Knoll et al., 1986; Magaritz et al., 1986; Kaufman et al., 1991; Burns and Matter, 1993; Narbonne et al., 1994; Kimura et al., 1997). K–Ar dating and numerical basin modeling (Borgomano, personal communication) indicate that the reservoir was initially charged during the Ordovician and that the “Huqf” source rock located in the inferred fetch area was generating hydrocarbons at this time. The isotopic identification of the pyrobitumen in the Jaleel prospect clearly indicates that it is a remnant of this early charge of a “Huqf” oil.

5.4. Habitat of pyrobitumen

Microscopical examination of the reservoir rock (Plate 1a,b) shows that the solid bitumen occurs as

pore lining and pore filling material. Large particles of nonfluorescent pyrobitumen deteriorate the porosity and are associated with subordinate amount of fluorescing material probably related to the extractable organic matter previously identified. Two silicification events occurred in the reservoir. The first one appears as syntaxial overgrowth around the detrital grains, the other one as autigenic quartz crystals in the pores which reflect the occurrence of a latter diagenetic phase. These autigenic quartz grains are surrounded by bitumen and, locally, particles of pyrobitumen are included in diagenetic quartz (Plate 1f). The homogenization temperatures of the related fluid inclusions indicate that the silicification event took place at a temperature comprised between 130°C and 170°C with a mode at 140°C–145°C (Fig. 8). These temperatures must be compared with the

Fig. 7. Solid state ^{13}C NMR of the insoluble bitumen.

FREQUENCY PLOT OF Th DISTRIBUTION IN AUTHIGENIC QUARTZ

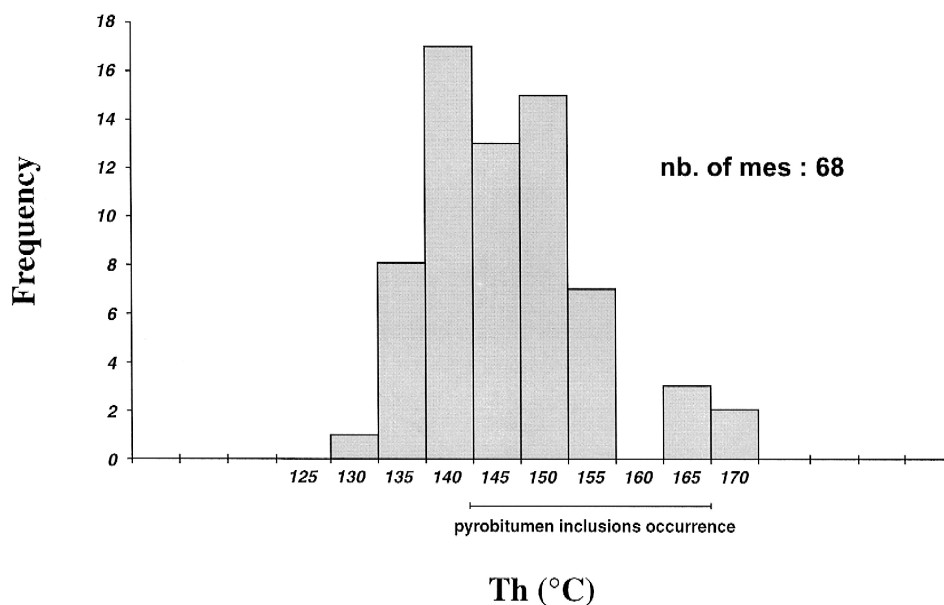


Fig. 8. Histogram of homogenization temperatures of fluid inclusions within quartz inclusions.

present-day reservoir temperature: 145°C suggesting a recent (ongoing?) phenomenon. These observations imply that the onset of pyrobitumen formation pre-dates at least a part of the silicification event. Most probably the two phenomena occurred concomitantly.

In order to evaluate the extent of the pore space alteration, the relative volume of the pyrobitumen within the porosity has been assessed by combining Rock-Eval, porosity, solid bitumen elemental analysis and density data. The Rock-Eval data provide a measurement of the organic carbon content (wt.% TOC) which is converted in wt.% organic matter through the elemental analysis and in vol.% of the porosity (bitumen saturation) through the available petrophysical data and the density of the insoluble bitumen. The latter has been measured to be 1.36 (JLL15) and 1.39 (JLL17). Due to the uncertainty in density determination, resulting from the relatively high mineral content including 1.2%–1.9% pyrite and 6.4%–7% other minerals (Table 2), and the assumption made for density calculation that the volume of ashes is negligible, these values are proba-

bly overestimated. Consequently, a conservative density value of 1.3 has been considered for our calculation.

The results of these calculations are displayed in Fig. 9. Fig. 9a shows the positive relationship between the wt.% pyrobitumen and the total porosity (corrected in order to account for both the measured porosity and the porosity occupied by the bitumen) probably reflecting only the fact that the solid bitumen is associated with the porosity. Fig. 9b shows a negative relationship between the bitumen saturation and the total porosity. This latter trend can be tentatively explained by two types of phenomena.

(a) The relationship is a reflection of various extents of quartz overgrowth differentially reducing the porosity and increasing the relative concentration of bitumen within the porosity. However, according to visual examination of thin sections, the volumetric loss of porosity due to authigenic quartz ranges from 5% to 72% and shows only a very weak correlation with the bitumen saturation (Fig. 9c), implying a subordinate control (if any) of the diagenesis on the observed trend (Fig. 9b). Fig. 9d shows that the

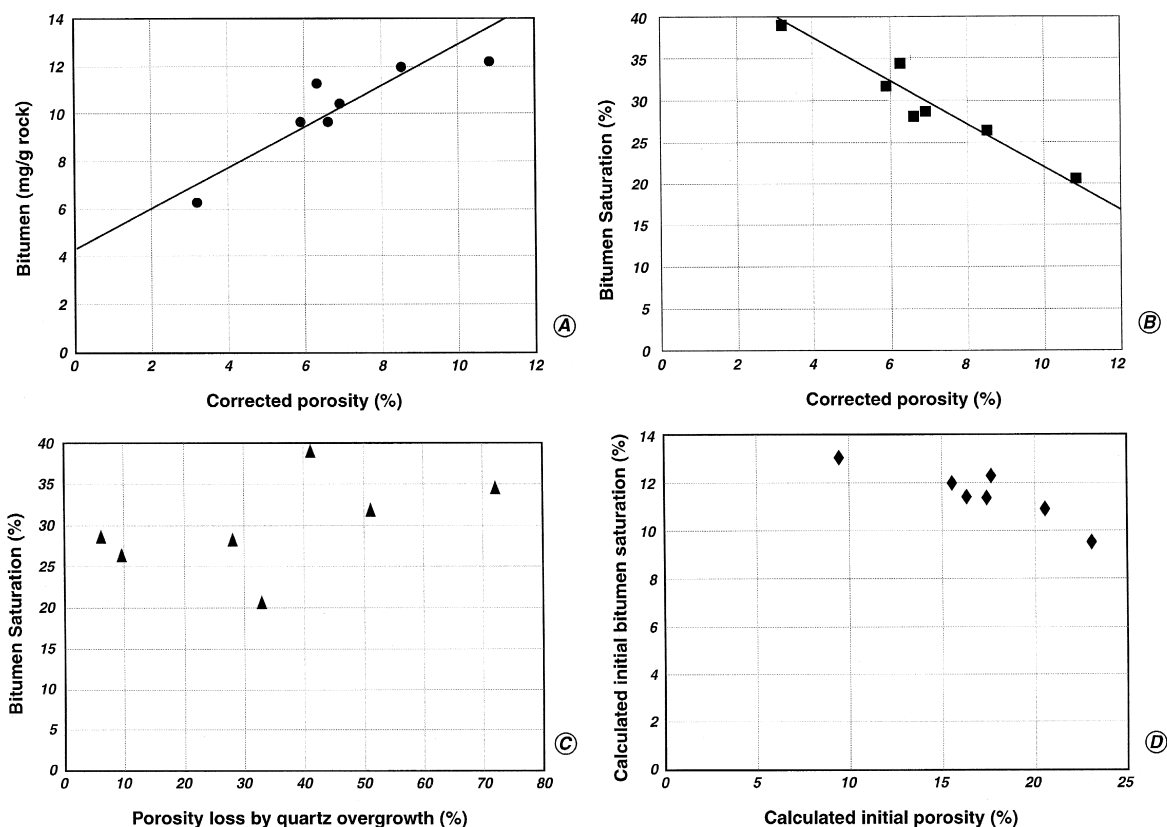


Fig. 9. Relationship between bitumen content and porosity: (a) bitumen (mg/g rock) versus corrected porosity; (b) bitumen saturation (vol.% of porosity) versus corrected porosity; (c) bitumen saturation (vol.% of porosity) versus porosity loss by quartz overgrowth; (d) calculated initial bitumen saturation versus calculated initial porosity.

pyrobitumen saturation in a diagenetic free reservoir should range between 9% and 13%, which is substantially lower than the 20%–40% observed today but which does not change the unusual importance of the bitumen in the considered samples.

(b) Assuming that the reservoir has experienced several charging steps, the initial Huqf charge might have been better preserved within the lowest porosity from being flushed by subsequent oil charging. As a consequence of the importance of the quartz cementation, this hypothesis is difficult to substantiate. However, it is interesting to note that the observed trend still holds when considering the relationship between the “pre-quartz overgrowth” porosity (calculated by adding the corrected porosity and the estimated porosity lost by quartz cementation) and

the “pre-quartz overgrowth” initial bitumen saturation (Fig. 9d).

5.5. Origin of the pyrobitumen

According to laboratory experiments (Behar et al., 1991), the fraction of oil converted to pyrobitumen during the thermal alteration of an oil is related to the initial content in heavy compounds including high molecular weight aromatics, resins and asphaltenes.

In this respect, oil samples from north Oman, including a conventional oil, a biodegraded oil and an asphaltene fraction isolated from the biodegraded oil have been subjected to closed system pyrolysis using the gold tube technology (Behar et al., 1991).

The experimental conditions have been set to an isothermal heating at 375°C during 72 h in order to maximize the pyrobitumen yield at the lowest possible temperature. Results are calculated in terms of bitumen saturation in a porosity assumed to be entirely filled up with the initial oil. The amount of generated pyrobitumen is minute for the conventional oil, around 10% of the porosity for the biodegraded oil as starting material, and around 40% for a reconstructed tar sand (based on the data derived from the isolated asphaltenes pyrolysis) (Fig. 10). Assuming that these pyrolysis experiments are representative of the natural thermal alteration of oils, these data suggest that the oil which was originally in the porosity of the Jaleel prospect should have been a very heavy crude oil to account for the observed 20%–40% volume saturation for the existing pyrobitumen. Even if one considers the porosity reduction due the quartz cementation and calculates a pre-quartz overgrowth bitumen saturation, the val-

ues are lowered to 9%–13% which are still requiring a heavy oil precursor. Such a heavy crude can occur as a result of the biodegradation of an oil charge affecting the whole reservoir or localized at the OWC, or from the local concentration of NSO compounds within the reservoir due to phenomena such as gravitational segregation or deasphalting.

The fact that the pyrobitumen occurrence affects rather uniformly a 150-m reservoir interval (see above), it precludes situations corresponding to local accumulation of NSO compounds (biodegradation at oil–water contact, deasphalting, gravitational segregation, etc.) and points to a general extensive biodegradation of the initial oil charge. Regional backstripping studies provide a burial history of the Jaleel prospect suggesting an uplift event following the Ordovician charging, bringing the reservoir to a shallow depth during the Carboniferous–Permian time leading to leaching of unstable minerals (e.g., feldspar) (Borgomano, personal communication)

EXPERIMENTAL CRACKING OF OILS

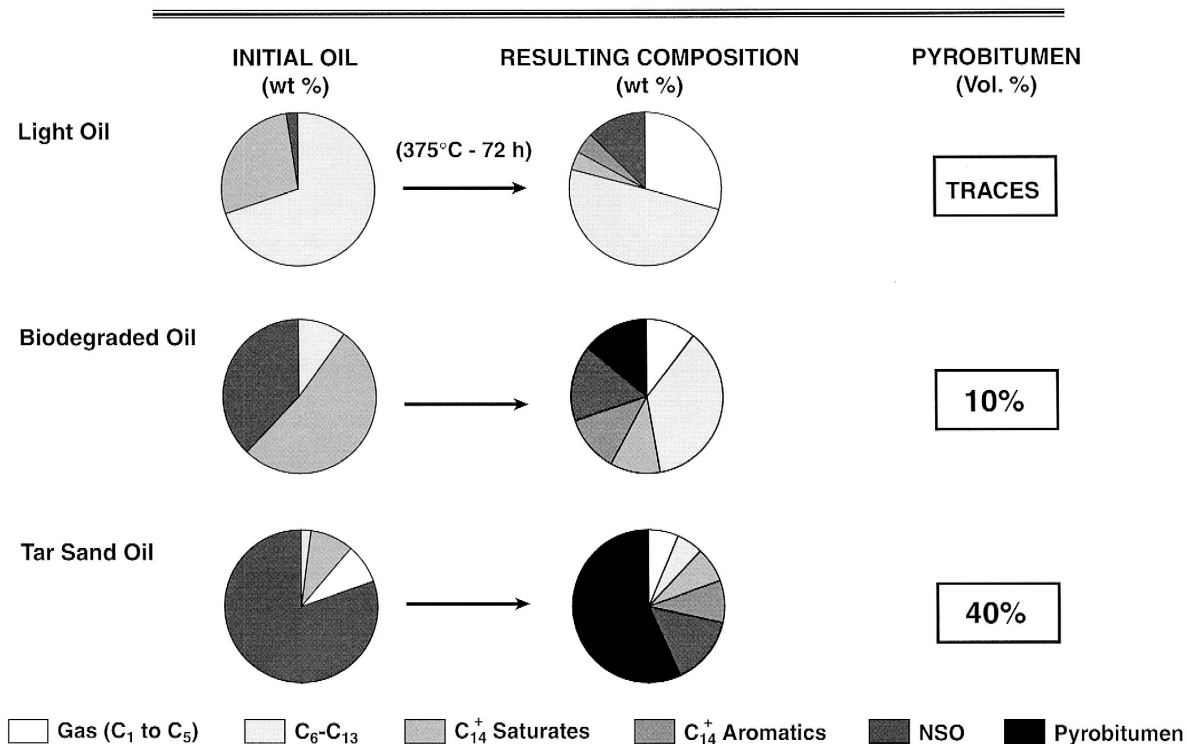


Fig. 10. Experimental cracking of oil: resulting product composition related to initial oil composition.

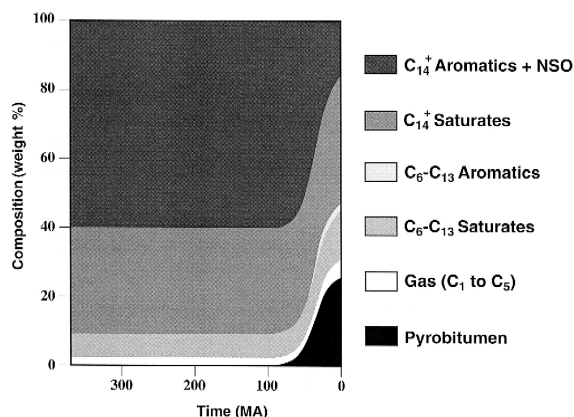


Fig. 11. Numerical modeling of oil composition as a result of natural thermal cracking as a function of time.

probably sufficient for allowing biodegradation to take place. Biodegradation is known to result in sulfur-rich oil (Hunt, 1995). In this respect, the very high sulfur content of the pyrobitumen (> 4%) is consistent with such a phenomenon (Table 2).

5.6. Timing of pyrobitumen formation

In order to model the thermal cracking of the oil, we used the kinetic scheme designed by Behar et al. (1992). This model is based on a unique set of cracking reactions for which fixed kinetic parameters have been determined. The only required input is the composition of the initial oil expressed as chemical classes which have been selected by the authors according to molecular weight and thermal stability, and which can be analytically assessed: methane, BTXN (benzene, toluene, xylenes, naphthalenes) and coke are taken as stable, ethane, C3–C5 saturates, C6–C13 saturates, C14⁺ saturates, C9–C13 aromatics, C14⁺ aromatics, NSO compounds and precoke are taken as unstable (Behar et al., 1991). In order to account for the formation of pyrobitumen, the latter has been defined as the sum of coke and precoke moieties. The model has been applied without any further adjustment according to the burial history and thermal regime of the Jaleel area (PDO data). As shown in Fig. 11, the considered initial oil has been taken as a heavily biodegraded crude in order to account for the observed pore saturation. The result of the simulation suggests that the pyrobitumen for-

mation is a rather recent event, probably initiated around 50 million years ago and still in progress (Fig. 11). This is in agreement with the observed relationship between the pyrobitumen particles and the timing of quartz overgrowth constrained by fluid inclusions data.

6. Conclusion

Based on the available geological and geochemical information, the following scenario is proposed to explain the observed pyrobitumen occurrence in the Jaleel prospect (Fig. 12). Emplacement into the Barik sandstone member of an early charge of oil generated during the Ordovician by a Huqf source rock which was buried as a result of a rifting phase initiated in Infracambrian time. This charging episode was followed by a regional uplift affecting eastern Oman during late Paleozoic and bringing the reservoir to shallow depth where the accumulated oil experienced an extensive biodegradation, resulting in the creation of a very heavy oil deposit (or even in the formation of a tar sand). During the subsequent burial, leading to the present-day depth and associated with the break-up of the Gondwana and the creation of the northeastern and southeastern passive

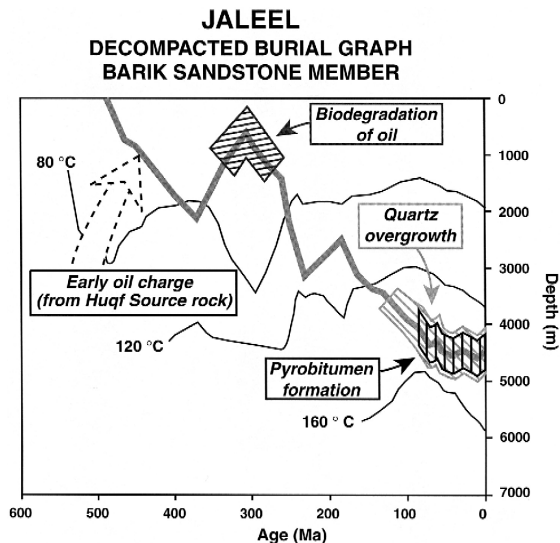


Fig. 12. Proposed scenario for pyrobitumen formation in Jaleel prospect.

margin of the Arabian plate, this heavy oil deposit underwent a progressive heating increase. This latter thermal history eventually resulted in a secondary cracking process in the last ten million years transforming, by disproportionation reactions, the oil into light hydrocarbons (probably lost) and residual insoluble bitumen. The unusual amount of pyrobitumen is inferred to be a direct consequence of the biodegradation event.

The industrial implication of such a scenario is the identification of the two factors controlling the pyrobitumen risk at the regional scale: the charging of the reservoir by a Huqf charge before the regional late-Paleozoic uplift (including timing of source rock maturity and adequate trap structuration) and a sufficient local uplift bringing the considered prospect to a depth allowing the microbial alteration to be effective. Published data indicate that biodegradation can only be significant at a temperature below 80°C (Bernard et al., 1992; Connan et al., 1997), implying, according to the assumed thermal regime (PDO data) a depth shallower than 1000 m. In this respect, the reconstruction of the burial history of a regional prospect is of prime importance for pyrobitumen prediction.

A more general implication of this study is the validation of the secondary cracking model proposed by Behar et al. (1992). As a matter of fact, the model has been applied without any adjustment. The result of the numerical simulation predicts a timing for the pyrobitumen formation which is perfectly corroborated by the factual data provided by the paragenesis examination. Moreover, the co-occurrence of insoluble pyrobitumen and of saturates containing recognizable biomarkers illustrates the predicted difference of stability between the NSO compounds more readily transformed into solid bitumen and the more stable saturated hydrocarbons.

Acknowledgements

We are indebted to J. Amthor, J. Borgomano, J. Terken, and N. Al-Ruwehy for the fruitful discussions. The used petroleum geology of North Oman is the result of the work of many PDO and Shell Geoscientists, who cannot all be mentioned here. We want to extend our appreciation to the comments

made on the first manuscript by J.M. Gaulier, F. Roure and M. Vandenbroucke.

This paper is authorized by the Petroleum Development of Oman LLC and the Ministry of Petroleum and Minerals of Oman. The authors would like to thank the authorities for their permission to publish this paper. This work was supported by the Petroleum Development of Oman.

References

- Behar, F., Kressman, S., Rudkiewicz, J.L., Vandenbroucke, M., 1992. Experimental simulation in a confined system and kinetic modelling of kerogen and oil cracking. *Org. Geochem.* 19 (1–3), 173–189.
- Behar, F., Ungerer, P., Kressman, S., Rudkiewicz, J.L., 1991. Thermal evolution of crude oils in sedimentary basins: experimental simulation in a confined system and kinetic modeling. *Rev. Inst. Franç. Pétrol.* 46 (2), 151–181.
- Bernard, F., Connan, J., Magot, M., 1992. Indigenous microorganisms in connate water of many oil fields: a new tool in exploration and production techniques. In: 67th Annual Conference and Exhibition of the Society of Petroleum Engineers, Washington D.C., USA, 4th–7th October. paper 24811.
- Beydoun, Z.R., 1993. Evolution of the Northeastern Arabian plate margin and shelf: habitat: hydrocarbon habitat and conceptual future potential. *Rev. Inst. Franç. Pétrol.* 48 (4), 311–345.
- Burns, S., Matter, A., 1993. Carbon isotopic record of the latest Proterozoic from Oman. *Ecolgae Geol. Helv.* 86, 595–607.
- Connan, J., Lacrampe-Couloume, G., Magot, M., 1997. Anaerobic biodegradation of petroleum in reservoirs: a widespread phenomenon in nature. In: 18th International Meeting on Organic Geochemistry, Maastricht, The Netherlands, Forschungszentrum Jülich. Book of Abstracts, pp. 5–6, Part 1.
- Durand, B., Nicaise, G., 1980. Procedures for kerogen isolation. In: *Kerogen, Insoluble Organic Matter from Sedimentary Rocks*. Durand, B. (Ed.), Technip, pp. 35–53.
- Espitalié, J., Deroo, G., Marquis, F., 1985a. La pyrolyse Rock-Eval et ses applications: Part 1. *Rev. Inst. Franç. Pétrol.* 40, 563–578.
- Espitalié, J., Deroo, G. et al., 1985b. La pyrolyse Rock-Eval et ses applications: Part 2. *Rev. Inst. Franç. du Pétrol.* 40, 755–784.
- Espitalié, J., Deroo, G. et al., 1985c. La pyrolyse Rock-Eval et ses applications: Part 3. *Rev. Inst. Franç. du Pétrol.* 41, 73–89.
- Grantham, P.J., Lijmbach, G.W.M., Posthuma, J., 1990. Geochemistry of crude oils in Oman. In: Brook, J. (Ed.), *Clastic Petroleum Provinces* 50, pp. 317–328.
- Hsü, K.J., Hedi, O., Gao, J.Y., Su, S., Chen, H., Krahenbuhl, U., 1985. Strangelove ocean before the Cambrian explosion. *Nature* 316, 809–811.
- Hunt, J.M., 1995. In: Freeman, W.H. (Ed.), *Petroleum Geochemistry and Geology*. Freeman, San Francisco, 743 pp.
- Kaufman, A.J., Hayes, J.M., Knoll, A.R., Germs, G.J.B., 1991. Isotopic composition of carbonates and organic carbon from

- Upper Proterozoic successions in Namibia: stratigraphic variation and the effects of diagenesis and metamorphism. *Precambrian Res.* 49, 301–327.
- Kimura, H., Matsumoto, R., Kakuwa, Y., Hamdi, B., Zibaseresht, H., 1997. The Vendian–Cambrian $\delta^{13}\text{C}$ record, North Iran: evidence for overturning of the ocean before the Cambrian explosion. *Earth Planet. Sci. Lett.* 147, E1–E7.
- Knoll, A.R., Hayes, J.M., Kaufman, A.J., Swett, K., Lambert, I.B., 1986. Secular variation in carbon isotopic ratios from Upper Proterozoic successions of Svalvard and East Greenland. *Nature* 321, 832–838.
- Loosveld, R.J.H., Bell, A., Terken, J.J.M., 1996. The tectonic evolution of interior Oman. *Geo. Arabia* 1 (1), 28–51.
- Magaritz, M., Holster, W.T., Kirschvink, J.L., 1986. Carbon isotope events across the Precambrian–Cambrian boundary on the Siberian platform. *Nature* 320, 258–259.
- Narbonne, G.M., Kaufman, A.J., Knoll, A.R., 1994. Integrated chemostratigraphy of the Windermere Supergroup, Northern Canada: implications for Neoproterozoic correlations and early evolution of animals. *GSA Bull.* 106, 1281–1292.
- Nederlof, P.J.R., Gijzen, M.A., Doyle, M.A., 1994. Application of reservoir geochemistry to field appraisal. In: *Gulf Petrolink* edn. Al Husseni, M.I. (Ed.), Middle East Petroleum Geosciences GEO 94 vol. II, pp. 709–722.
- Schenk, H.J., Horsfield, B., 1995. Simulating the conversion of oil into gas in reservoirs: the influence of frequency factors on kinetic prediction. In: *Selected Papers from the 17th International Meeting on Organic Geochemistry*, 4th–8th September, San Sebastian, Spain, A.I.G.O.A., pp. 1102–1103.
- Trabelsi, K., Espitalié, J., Huc, A.Y., 1994. Characterization of extra heavy oil and tar deposits by modified pyrolysis methods. In: *Proceedings of the European Symposium on Heavy Oil Technologies in a wider Euro*, 7th–8th June, Berlin. pp. 30–40.



ELSEVIER

International Journal of Coal Geology 44 (2000) 49–68

International Journal of
coal
geology

www.elsevier.nl/locate/ijcoalgeo

Evidence and effects of fluid circulation on organic matter in intramontane coalfields (Massif Central, France)

Y. Copard ^{a,*}, J.R. Disnar ^{a,1}, J.-F. Becq-Giraudon ^{b,2},
M. Boussafir ^a

^a UMR 6531 and FR 09 du CNRS, Université d'Orléans, 45067 Orléans Cedex, France

^b BRGM, DR / LGM, Av. Claude Guillemin, B.P. 6009, 45060 Orléans, France

Received 19 March 1999; accepted 28 September 1999

Abstract

Recent evidence for a Late Carboniferous hydrothermal event responsible for Au–As mineralization within the Variscan belt of the French Massif Central adds a supplementary episode to the already rather complex thermal history of this area. To better understand this history, 45 coal samples from various sites in the Massif Central were studied petrographically (reflectance analysis) and geochemically (Rock-Eval pyrolysis). The results of this study suggest that the studied coal was buried to 1500 m and that the coalification took place within 25 Ma, probably ending at the boundary between the Early and Late Permian (marked by the Saalic orogeny). Two thermal end-members basins were identified: (i) the Carboniferous of Bosmoreau-les-Mines (Limousin) and West Graissessac (Montagne Noire) showing geothermal paleoflow values between 150 and 180 mW m⁻², and (ii) the Stephanian of Argentat and Détroit de Rodez (SW Massif Central) with values estimated at between 100 and 120 mW m⁻². By plotting the T_{\max} and R_o values on a diagram, the samples were grouped into two populations, the first showing a positive correlation between R_o and T_{\max} and the second with higher T_{\max} values than expected after R_o values. Selected samples of the second group are also characterized by a high Oxygen Index (OI) that increases with T_{\max} . These divergence between R_o and T_{\max} associated with a high OI may be the result of the circulation of slightly oxidizing hot fluids subsequent to coalification. The other kind of R_o – T_{\max} divergence seems to be linked to local, particularly high thermal activity, especially in Graissessac and Bosmoreau basins. It is interpreted as being due to

* Corresponding author. Fax: +33-2-3841-7308; e-mail: yoann.copard@univ-orleans.fr

¹ E-mail: jean-robert.disnar@univ-orleans.fr.

² E-mail: becqgiraud@exchange.brgm.fr.

a difference in response of these two maturity indicators, respectively to the intensity and duration of the thermal events (e.g., short-lived hydrothermal circulation and thermal domes of regional extent). © 2000 Elsevier Science B.V. All rights reserved.

Keywords: Stephanian; Massif Central; coalification anomaly; Rock-Eval; vitrinite reflectance; hot fluid; thermal dome

1. Introduction

After the Devonian–Viséan, the Variscan belt of the French Massif Central was successively subjected to crustal thickening then thinning (Faure and Becq-Giraudon, 1993; Faure, 1995; Faure et al., 1997). Crustal instability following thickening was first marked by a Late Variscan (350 Ma) strike–slip event, and then by a Middle–Late Carboniferous extensional episode (Leloix, 1998). Sedimentary basins then developed along major faults such as the Sillon Houiller Fault and the Argentat Fault (Letourneur, 1953; Marest, 1985; Gelard et al., 1986; Faure and Becq-Giraudon, 1993; Genna et al., 1998). The basement lineaments commonly controlling the distribution and paleogeography of these basins (Faure, 1995) were preferentially adopted as pathways by high-temperature hydrothermal fluids, particularly those responsible for Au–As mineralization within the French Massif Central (Bouchot et al., 1997; Roig et al., 1997). These same fluids probably also affected sediments in basins such as Blanzay–Montceau (Berquer-Gaboreau, 1986) and Meisseix–Singles (Robert et al., 1988). For example, at Blanzay–Montceau, Golitsyn et al. (1997) noted an increase in the coal rank along a single layer towards an active fault that would have controlled heat flow by draining heat-bearing fluids.

One the initial aims of the present study was to determine whether the hydrothermal fluids which circulated during the Middle–Late Carboniferous (Roig et al., 1997) could have affected the coals in the French Massif Central. Accordingly, in this paper, we discuss the thermal activity of the basins analysed (Fig. 1), beginning with the maximum depth of burial of the Carboniferous succession and the duration of coal maturation in the Carboniferous and Permian by the use of two parameters of OM rank, i.e., vitrinite reflectance R_o (%) and T_{max} (°C). Then, we estimated the maximum paleotemperatures experienced by the coal during burial and examined the nature and origin OM maturity anomalies to determine whether they could have been caused by hydrothermal circulations.

2. Samples and methods

2.1. Samples

The study was based on the analysis of 45 grab coal samples collected from outcrop in six Carboniferous intramontane basins, namely: (1) Bosmoreau-les-Mines at the northern end of the Argentat Fault, (2) Lappleau–Maussac, (3) the Carboniferous of

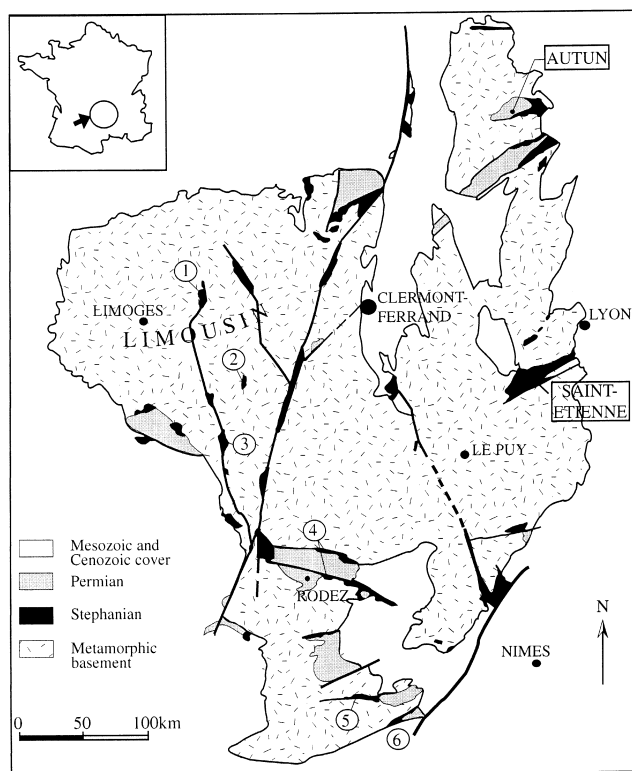


Fig. 1. General map of the Massif Central showing the location of the Carboniferous basins from which the analysed coal samples were collected (adapted from Becq-Giraudon, 1984). 1: Bosmoreau-les-Mines, 2: Lapleau-Maussac, 3: Argentat, 4: Déroit de Rodez, 5: Graissessac, 6: Roujan-Neffiès.

Argentat in Bas-Limousin, (4) Déroit de Rodez, (5) Graissessac, the western continuation of the Permian Lodève basin, and (6) Roujan-Neffiès to the south of the metamorphic domain of the Montagne Noire (Fig. 1).

2.2. Methods

Two rank parameters were recorded for all the samples, R_o (%) and T_{max} (°C) of Rock-Eval pyrolysis. The reflectance was measured using grain polished sections according to the standard method developed by the International Committee of Coal Petrology (ICCP) using a reflected light microscope (LEITZ MPV II) equipped with a monochromator and a photometer. Qualitative petrographic examinations, such as microfracture and oxidation studies, were carried out on whole-rock polished sections.

Some samples (A1, A3 from Argentat and Sé1, Sé2 from Graissessac) were analysed under a scanning electron microscope in backscattered electron mode (SEM/BE) to test for the presence of chemical elements or minerals characteristic of hydrothermal

Table 1
Experimental conditions for Rock-Eval® 6 pyrolysis

	Initial temperature (°C)	Final temperature (°C)	Temperature programming
pyrolysis	300	800	25°C/min
oxidation	400	850	25°C/min

circulation (EDS point analysis) and to examine the fractures within the vitrinite particles.

Rock-Eval pyrolysis was carried out using the Rock-Eval® 6 device of Vinci Technologies according to the conditions given in Table 1. T_{\max} corresponds to the temperature recorded for the S2 pyrolysis peak, i.e., when the emission of hydrocarbon-bearing compounds is at its maximum during thermal cracking of kerogen under inert atmosphere, in linear programming of temperature (Espitalié et al., 1985a,b,c). In addition to T_{\max} , pyrolysis provides values of Total Organic Carbon (TOC) (%), Oxygen Index (OI expressed in mg CO₂/g TOC) and Hydrogen Index (HI expressed in mg HC/g TOC). HI and OI, corresponding respectively to the quantities of hydrocarbons and CO₂ released during pyrolysis, in relation to TOC, are proportional to the hydrogen and oxygen contents of the OM (Espitalié et al., 1985a,b,c; Lafargue et al., 1996).

3. Results

The R_o measurements and pyrolysis results are given in Table 2. We will not discuss here the TOC values which, for the disseminated samples collected at outcrop, simply confirm whether we are dealing with coal sample from a seam or dispersed OM.

3.1. Vitrinite reflectance

The vitrinite reflectance was systematically measured on telocollinite, a submaceral of collinite (Fig. 2a). The coal from the Argentat and Détroit de Rodez basins (Fig. 1) shows R_o values between 0.6 and 1.05% (Table 2) which, according to the North-American classification (ASTM standard), coincides with a rank of high volatile B to A bituminous. Apart from samples Ber3 (R_o 0.92%) and Mé1 (R_o 1.05%) that are characterized by a relatively high R_o attributed to recent meteoric weathering, the Détroit de Rodez coal shows a relatively homogeneous degree of maturity with, however, a slightly higher rank near the southern border. The maturity of these samples is very similar to that of coal from the Decazeville mine (Détroit de Rodez; 0.6 to 0.8%, Ligouis, 1988). With reflectance values between 0.6 and 0.69%, the Argentat coal is given the rank of high volatile B bituminous. Samples LM1, LM2 and LM3 from the base of the Carboniferous of Lapleau–Maussac have reflectance values greater than 1%, with LM3 being slightly more mature than the other two (1.2% compared to 1.03–1.06% for LM1 and LM2). LM4, taken from a younger coal layer, has a lower vitrinite reflectance (0.83%; Table 2). The three samples from the Carboniferous of Roujan-Nef-

Table 2
Rock-Eval pyrolysis and R_o results

Basin	Sample	R_o (%)	Standard deviation	T_{max} (°C)	HI (mgHC/gTOC)	TOC (%)	OI (mgCO ₂ /gTOC)	
Argentat	<i>A.1</i>	0.64	0.084	446	25	25	70.35	
	<i>A.2</i>	0.65	0.102	447	73	73	44.13	
	<i>A.3</i>	0.69	0.069	560	9	19	96.23	
	<i>A.3'</i>	0.60	0.083	506	9	20	62.3	
Bosmoreau-les-Mines	<i>B.1</i>	1.37	0.094	564	25	70.74	2.42	
	<i>B.3</i>	1.43	0.081	562	36	38.77	2.22	
Lapleau-Maussac	<i>LM1</i>	1.06	0.100	486	84	73.8	5.19	
	<i>LM2</i>	1.03	0.088	470	121	52.65	4.69	
	<i>LM3</i>	1.20	0.087	494	94	46.67	10.89	
	<i>LM4</i>	0.83	0.056	500	14	7.52	81.13	
Déroit de Rodez, North border	<i>E1</i>	0.61	0.065	437	189	62.16	6.52	
	<i>E3</i>	0.68	0.090	437	62	15.02	53.36	
	<i>E4</i>	0.67	0.080	434	126	43.95	37.90	
	<i>Pou1</i>	0.66	0.075	430	186	28.02	31.1	
	<i>Pou2</i>	0.61	0.063	444	207	37.64	7.70	
Déroit de Rodez, South border	<i>Ber1</i>	0.71	0.059	437	175	52.02	7.19	
	<i>Ber2</i>	0.80	0.115	441	49	20.55	57.56	
	<i>Ber3</i>	0.92	0.181	444	57	51.92	33.26	
	<i>Ber4</i>	0.77	0.075	485	60	63.59	15.18	
	<i>Ber4'</i>	0.77	0.74	449	31	4.17	49.18	
	<i>Gal</i>	0.73	0.084	438	217	46.1	8.94	
	<i>Ay1</i>	0.63	0.074	447	18	36.72	67.66	
	<i>Mé1</i>	1.05	0.078	442	213	40.38	7.38	
	Roujan-Neffiès	<i>Ro-Né1</i>	1.42	0.099	475	63	23.03	10.86
		<i>Ro-Né2</i>	1.45	0.079	489	68	8.01	12.45
<i>Ro-Né3</i>		1.35	0.044	533	18	6.17	61.42	
East Graissessac	<i>Sé1</i>	1.41	0.108	477	150	44.59	2.91	
	<i>Sé2</i>	1.31	0.087	536	20	46.73	55.58	
	<i>Sé3</i>	1.36	0.079	477	101	13.15	4.17	
	<i>Sé4.1</i>	1.40	0.067	473	118	17.53	4.40	
	<i>Sé4.2</i>	1.40	0.056	472	141	25.73	2.29	
	<i>Sé4.3</i>	1.46	0.073	492	67	48.38	6.99	
	<i>Sé5</i>	1.46	0.065	481	128	47.71	4.44	
	<i>Sé6</i>	1.45	0.068	514	36	47.55	41.53	
	<i>Ray1</i>	1.46	0.111	490	63	50.01	9.9	
	<i>Mou1</i>	1.39	0.094	513	33	54.67	57.9	
	<i>RG1</i>	1.25	0.085	477	128	52.34	5.29	
	<i>RG2</i>	1.20	0.102	560	11	26.4	75.34	
	<i>Sal</i>	1.49	0.095	605	5	32.92	67.09	
<i>Sal'</i>	1.45	0.064	515	10	3.55	60.68		
<i>Roc-Camp1</i>	1.48	0.086	553	29	48.85	50.11		
West Graissessac	<i>Pal</i>	2.05	0.071	610	10	51.77	44.59	
	<i>Cad1</i>	2.05	0.064	604	19	50.96	40.84	
	<i>Cad2</i>	2.15	0.104	600	15	38.93	37.54	

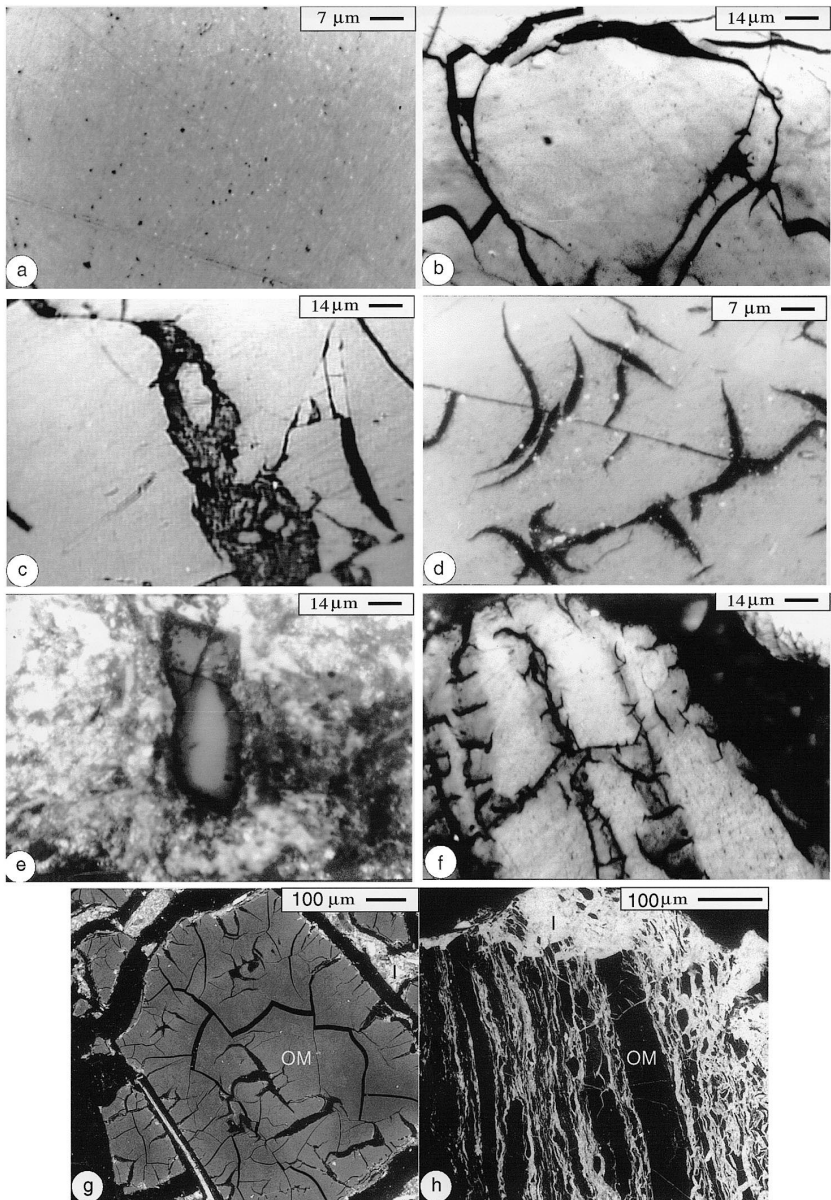


Fig. 2. (a) Telocollinite on which the Ro measurements were carried out (sample Mou1 from East Graissessac and Ro-Né2 from Roujan-Neffiès). (b) I-type microfracturing (sample Ro-Né1 from Roujan-Neffiès and Ber2 from Déroit de Rodez, southern boundary). (c) II-type microfracturing (sample Sé4.3 from East Graissessac). (d) III-type anastomosed microfracturing (sample RG2 from East Graissessac and A3 from Argentat). (e) *b*-type fringes with a lower reflectance (0.4%) than the core (0.6%) (sample A3' from Argentat). (f) *b*-type fringes (0.95% against 1.32% in the core) associated with anastomosed microfracturing (sample Sé2 from East Graissessac). (g) comparison of an oxidized particles, from Argentat (sample A3; (g)) with another one more oxidized, from East Graissessac (sample Sé1; (h)); OM: Organic Matter, l: limestone; (SEM/BE photographs).

fiès show similar vitrinite reflectance values between 1.35% and 1.42% (medium volatile bituminous). Similar values were recorded for the Bosmoreau-les-Mines samples (1.37 and 1.43%), which is in agreement with previous data of Becq-Giraudon and Mazeaud (1981). The coal from the Carboniferous of East Graissessac shows reflectance values between 1.2 and 1.48%, which is in agreement with values recorded by Becq-Giraudon and Gonzalez (1986). These values indicate a coal rank between medium volatile bituminous and low volatile bituminous (Table 2). The coal from West Graissessac, is of a semi-anthracite rank as indicated by reflectance values of the order of 2%.

3.2. Geochemistry

The pyrolysis data presented in Table 2 highlight the marked diversity of the T_{\max} values, as well as HI and OI. Only the T_{\max} values will be considered in this section, and the reader is referred to the general discussion for the HI and OI values. Apart from a few abnormally high values (A3, A3' and Ber4: 560, 506 and 485°C), the samples from the Argentat and Détroit de Rodez basins show T_{\max} values between 435 and 450°C, thus placing them in the first part of the oil window (Espitalié et al., 1985a,b,c). It is noted, particularly for samples A3 and A3' from the Carboniferous of Argentat, that the high T_{\max} values are associated with low HI and high OI values. The coal from the Lapeau–Maussac basin has T_{\max} values between 470°C and 500°C, which corresponds to the beginning of the gas window, i.e., during early metagenesis. The samples from East Graissessac can be divided into two sub-groups based on T_{\max} values: (i) a first group with T_{\max} values similar to those of Lapeau–Maussac (480°C), (ii) a second group characterized by higher T_{\max} values between 515 and 605°C which, as a first approximation, seems to suggest fairly varied maturity stages. In addition to their high T_{\max} values, these samples also show relatively high OI values. The three samples from West Graissessac show homogeneous T_{\max} values between 600 and 610°C, suggesting a degree of maturity corresponding to the end of metagenesis. The T_{\max} value of 533°C measured on coal sample Ro-Né3 from the Carboniferous of Roujan-Neffiès contrasts with the less mature samples Ro-Né1 and 2 from the same basin which have T_{\max} values of about 482°C, indicating the onset of metagenesis.

3.3. Petrographic observations (optical microscope and SEM / BE)

During the petrographic observations we particularly concentrated on characterizing the microfractures and studying the reflectance variations of the vitrinite particles. The following microfracture types were identified (Copard, 1998): (a) type I, mainly affecting vitrinite particles (Fig. 2b), (b) type II, larger than type I, affecting all samples studied, and commonly filled with clay, inertodetrinite, vitrodetrinite, and, in places, liptinite (Fig. 2c), and (c) type III, characterized by their specific anastomosed morphology, mainly affecting vitrinite particles (Fig. 2d). This type, which is only observed in samples with high OI values, represents microfracturing where high-temperature oxidation is likely to occur (Alpern and Maume, 1969). The first two microfracture types were observed in all the studied samples, whereas type III was only observed in samples

A3 and A3' from Argentat, and S  2, Sa1 and RG2 from East Graissessac. Certain vitrinite particles are characterized by fringes that are variably lighter than their cores. These fringes, following Copard (1998), are labelled *a* where they have higher reflectance than the core of the vitrinite particle and *b* where their reflectance is lower. A-type fringes may result from recent meteoric oxidation, whereas *b*-type fringes can be related to early oxidation during coal evolution as testified by Alpern and Maume (1969). B-type fringes (Fig. 2e) were identified in samples A1 and A3' (0.4% in the fringes against 0.6% in the cores), LM1 and LM3 of Lapleau–Maussac (respectively 0.5% and 1% in the fringes against 1% and 1.3% in the cores), Ber1, Ber2 and Ber4' (0.5% against 0.8%), Ay1 (0.4% against 0.6%) and S  2 and S  4.3 (0.95–1% against 1.32–1.46%). Furthermore, the *b*-type fringes observed in sample S  2 were associated with III-type microfractures (Fig. 2f).

4. Discussion

4.1. Thermal activity

As particularly demonstrated by the differences in paleo-heat flow evaluated in the Brive (100 and 120 mW m⁻²) and Bosmoreau-les-Mines (150 and 180 mW m⁻²) basins (Mascl  , 1990, 1998), the Massif Central was subjected to a hyperthermal regime that varied in intensity from site to site. Such variations in the regional thermal field are closely linked to crustal thinning following thickening of the Variscan crust during the Devonian–Carboniferous collisional episodes (Becq-Giraudon and Van Den Driessche, 1993; Faure, 1995). During thinning, the ductile–brittle limit in the crust must have been relatively close to the surface (10 km or less), as demonstrated by microthermometric studies carried out on fluid-inclusion planes in granites of the Haut Limousin (Andr  , 1997). In addition to a decrease in the fluid-trapping depth, these analyses also suggest a drop in the homogenization pressure/temperature pair from Late Stephanian times, which continued through the Autunian. These results seem compatible with the marked decrease in temperature of the circulating hydrothermal fluids (from 350  C to 80–130  C) recorded throughout the Massif Central between Stephanian–Autunian and Saxonian–Thuringian times (Jebrak, 1989). Modelling of the heat-flow evolution at the base of the sediments in the Brive basin indicates a marked decrease in the intensity of this flow from the Late Stephanian (100–120 mW m⁻²) to present day (30 mW m⁻²) (Mascl  , 1998). According to this model, the immaturity of Lias organic matter in this basin can be explained not only by burial of the Mesozoic sediments to less than 1000 m, but also by the low intensity of heat flow compared to that recorded during the Late Paleozoic. All these considerations are consistent with high geothermal paleogradient during the Late Carboniferous (Latouche, 1969; Becq-Giraudon and Gonzalez, 1986; Berquer-Gaboreau, 1986; Robert et al., 1988).

Recent studies (Ligouis, 1988; Wang, 1991; Disnar et al., 1995; Mascl  , 1998) proposed an average paleoburial depth for the Stephanian successions of the order of 1500 m, a depth which seems particularly applicable to the basins of Argentat, Bosmoreau-les-Mines, and D  troit de Rodez (Ligouis, 1988). We adopted this average

paleoburial depth of 1500 m for the Stephanian successions of all the basins studied. On the base of previous results obtained on different basins such as Blanzey–Montceau (Golitsyn et al., 1997), Alès (Wang and Courel, 1993) and Graissessac (Becq-Giraudon and Gonzalez, 1986), the duration of coalification must have been rather short. It is difficult to give a precise figure but there are two geodynamic events which could have ended this evolution: (1) the Saalic orogenic phase (–270 Ma) which marks the Early/Late Permian boundary (Feys, 1989); in this case, the maximum coalification duration would have been 20–25 Ma. (2) The Palatine orogenic phase at the end of the Permian (–245 Ma) which would give a maximum coalification duration of 35–40 Ma.

Because, with the exception of samples A3 and A3' (Table 2), the T_{\max} values recorded in the Détroit de Rodez and Argentat are very similar to those from the Brive basin, we adopted the thermal evolution model applied to the latter basin to the other two. The more mature Bosmoreau-les-Mines samples also seem to agree with the Brive basin model, although with higher heat flows (i.e., 150–180 mW m⁻² at the base of the sediments, Mascle, 1998) during Stephanian–Autunian times.

The T_{\max} values for the Lapeau–Maussac basin are relatively heterogeneous, varying from 470°C to 500°C. Considering the intermediate maturity of those samples, located between that of Argentat, Détroit de Rodez and Bosmoreau-les-Mines, it is possible to envisage heat flows of between 120 and 140 mW m⁻², with the 300 m difference in burial depth between LM4 and the surrounding lithostratigraphically deeper samples being sufficient to explain the difference in vitrinite reflectance (0.83% vs. 1.05% — see Table 2).

The Upper Paleozoic of Roujan-Neffiès was probably subjected, along with the basins of the Cévennes and Ardèche border (Wang and Courel, 1993; Disnar et al., 1995), to a hyperthermal regime. Estimation of the paleo-heat flow is nevertheless difficult due to the prevailing uncertainties concerning the history and burial of this basin. However, as the vitrinite reflectance values are identical to those of Bosmoreau-les-Mines (Table 2), we assume that the Roujan-Neffiès basin was probably subjected to a paleo-heat flow of the same order as that of Bosmoreau.

In the Graissessac basin, if we adopt a burial depth and coalification duration similar to those assumed previously, the degree of coal maturity depends essentially on the structural framework of the basin within which thermal domes developed and on the intensity of the heat flow associated with those domes. Their intensity seems directly linked to the end-Variscan metamorphic cycle that affected the axial zone of the Montagne Noire to the southwest of the basin (Latouche, 1969; Becq-Giraudon and Gonzalez, 1986). Consequently, the thermal domes show increasing intensity the nearer they are to the axial zone. An increase in the coal rank from east to west (Table 3) confirms the spatial distribution and evolution of the intensity of these domes. The paleo-heat flows for West Graissessac are thus estimated at more than 180 mW m⁻² by comparison with the situation in Bosmoreau-les-Mines. Adopting the same conditions, East Graissessac would have been subjected to flows corresponding to those of Lapeau–Maussac if based on T_{\max} , and those of Bosmoreau-les-Mines, if one considers vitrinite reflectance.

Despite the various uncertainties concerning the results and/or their interpretation, there is no doubt that all the studied basins were subjected to a hyperthermal regime,

Table 3

Coal ranks (ASTM standard) based on R_o and T_{max} ; anomalous samples are in bold

Basin and samples	Coal rank (based on R_o)	Coal rank (based on T_{max})
Argentat (A1 and A2)	High Volatile B Bituminous	High Volatile C Bituminous
A3	High Volatile B Bituminous	semi-anthracite
A3'	High Volatile B Bituminous	Low Volatile Bituminous
Bosmoreau-les-Mines B1, B3	Medium Volatile Bituminous	semi-anthracite
Lapleau-Maussac LM1, LM2	High Volatile A Bituminous	Medium Volatile Bituminous
LM3	Medium-Volatile-Bituminous	Medium Volatile Bituminous
LM4	High Volatile A Bituminous	Low Volatile Bituminous
Détroit de Rodez (North)	High Volatile B Bituminous	High Volatile C Bituminous
Détroit de Rodez (South)	High Volatile B/A Bituminous	High Volatile B/C Bituminous
Ber4	High Volatile A Bituminous	Medium Volatile Bituminous
Ber3 and M61	High Volatile A Bituminous	High Volatile B Bituminous
Roujan-Neffiès (Ro-Né1 and 2)	Medium-Volatile-Bituminous	Medium-Volatile-Bituminous
Ro-Né3	Medium Volatile Bituminous	Low-Volatile-Bituminous
East Graissessac	Medium-Volatile-Bituminous	Medium-Volatile-Bituminous
Sé1, 3, 4.1, 4.2, 4.3, 5, RG1		
RG2	Medium Volatile Bituminous	anthracite
Sé6, Mou1, Sa1'	Medium/Low Volatile Bituminous	Low Volatile Bituminous
Sé2, Roc-Camp1	Medium/Low Volatile Bituminous	semi-anthracite
Sa1	Medium/Low Volatile Bituminous	anthracite
West Graissessac	semi-anthracite	anthracite

probably controlled by basement faults dividing them into blocks. Knowledge of the hyperthermal activity thus mainly provides data concerning the tectonic regime at a given time. The Middle Permian Saalic orogeny is the most likely event responsible for interruption of the thermal maturation of the Stephanian coal studied. Local tectonic and erosion data make it possible to deduce a short lived coalification period, of 25 Ma or less.

4.2. Estimation of paleotemperatures recorded by organic matter

Based on heat flow values and the assumed burial depth, the maximum paleotemperatures to which the coal was subjected can be estimated using the three methods described below and their results are presented and compared in Table 4.

(1) The geothermal paleogradients prevailing during coalification was estimated, based on the heat flow values given previously and assuming an average thermal conductivity of $4 \times 10^{-3} \text{ cal cm}^{-1} \text{ s}^{-1} \text{ C}^{-1}$ for the sediments underlying the coal layers. The restrictions of this method are mainly related to the uncertainties concerning the paleo-heat flow extrapolated to the Lapleau–Maussac, Roujan–Neffiès and Graissessac basins. This flow is assumed to have been constant throughout coalification.

Table 4

Comparison between results of the three methods used to characterize the maximum coal paleotemperatures

Basin	Average R_o (%)	Orogeny	Method 1: estimated geothermal gradient	Method 2: based on R_o (Karweil's chart modified by Bostick, 1971)	Method 3: based on T_{min} (Disnar, 1994)
Argentat	0.65	Saalic	$100 \pm 10^\circ\text{C}$	$110 \pm 10^\circ\text{C}$	$117 \pm 10^\circ\text{C}$
Détroit de Rodez	0.70	Palatinian	$100 \pm 10^\circ\text{C}$	$90 \pm 10^\circ\text{C}$	$110 \pm 5^\circ\text{C}$
Lapleau-Maussac	1.05	Saalic	$115 \pm 10^\circ\text{C}$	$140 \pm 10^\circ\text{C}$	$135 \pm 5^\circ\text{C}$
		Palatinian	$115 \pm 10^\circ\text{C}$	$115 \pm 10^\circ\text{C}$	$125 \pm 5^\circ\text{C}$
Bosmoreau Neffiès	1.40	Saalic	$150 \pm 15^\circ\text{C}$	$155 \pm 10^\circ\text{C}$	$168 \pm 10^\circ\text{C}$
East Graissessac		Palatinian	$150 \pm 15^\circ\text{C}$	$125 \pm 10^\circ\text{C}$	$155 \pm 10^\circ\text{C}$
West Graissessac	2.00	Saalic	$170 \pm 10^\circ\text{C}$	$180 \pm 10^\circ\text{C}$	$145 \pm 10^\circ\text{C}$
		Palatinian	$170 \pm 10^\circ\text{C}$	$150 \pm 10^\circ\text{C}$	$135 \pm 10^\circ\text{C}$

Maximum burial, which was reached during the Late Paleozoic (Masclé, 1998), is assumed to be of the order of 1500 m for all the basins.

(2) This method is based on vitrinite reflectance values and on Karweil's time/temperature charts (modified by Bostick, 1971 and in Robert, 1985) where the coalification period is assumed to be the same as the age of the coal. As the samples from any one basin were collected from lithostratigraphically well-defined horizons, it was possible to calculate average reflectance values for each basin (Table 4). Although we have reason to refute this model on the basis that it is too simple, since it obeys a single kinetic (Disnar, 1994), the model nevertheless can be used for comparative purposes as it is based on two samples from Ruhr (Germany) and an exponential law that is compatible with the normal evolution of vitrinite reflectance with depth (e.g., Bostick, 1971).

(3) The third method adopted for this study is based on determining the maximum paleotemperatures of burial (MPTB, Disnar, 1994) calculated from a kinetic parameter known as T_{min} , that is graphically determined from the Rock-Eval S2 pyrolysis peak of OM (Disnar, 1994). An estimated value of a geological thermal gradient, expressed in $^\circ\text{C Ma}^{-1}$. This geological gradient value is equal to the product of the classic geothermal gradient (in $^\circ\text{C km}^{-1}$) by the subsidence rate (in km Ma^{-1}).

The first two methods provided similar paleotemperatures for all the basins except the Lapleau–Maussac basin, which yields a lower paleotemperature using the first method (Table 4). The third method does not seem consistent with the other two, and only the MPTB values for Argentat and Détroit de Rodez seem comparable to the results of Karweil's method and the paleo-heat flow estimations. The high MPTB values for Bosmoreau-les-Mines are associated with samples showing a positive T_{max} anomaly and, consequently, T_{min} . West Graissessac, however, has lower calculated MPTB values than those obtained with the other two methods, despite a positive T_{max} anomaly. In this case, the S2 pyrolysis peaks, which show marked asymmetry, cause the low T_{min} values and consequently the low MPTB values. The dissimilarity of the results obtained with three methods for the Lapleau–Maussac Basin can be explained by the scattered values of the maturity parameters, uncertainties concerning burial depth, the duration of coalification, and heat flow constant values.

4.3. Relationship between the Au–As fluids and the heat flow affecting the Stephanian coal

One of the initial aims of the present study was to determine whether the Au–As fluids circulating during the Middle–Late Carboniferous (Roig et al., 1997) could have affected the Late Stephanian coals in the French Massif Central. At regional scale, a hydrothermal event is contemporaneous with an increased heat flow leading to the production of granite (Bouchot et al., 1997). Consequently, the Au–As bearing fluids would, a priori, have been associated with episodes of magmatism and remobilization of the crust which occurred from 340 to 290 Ma (Costa, 1990) and therefore could have influenced the Stephanian coals.

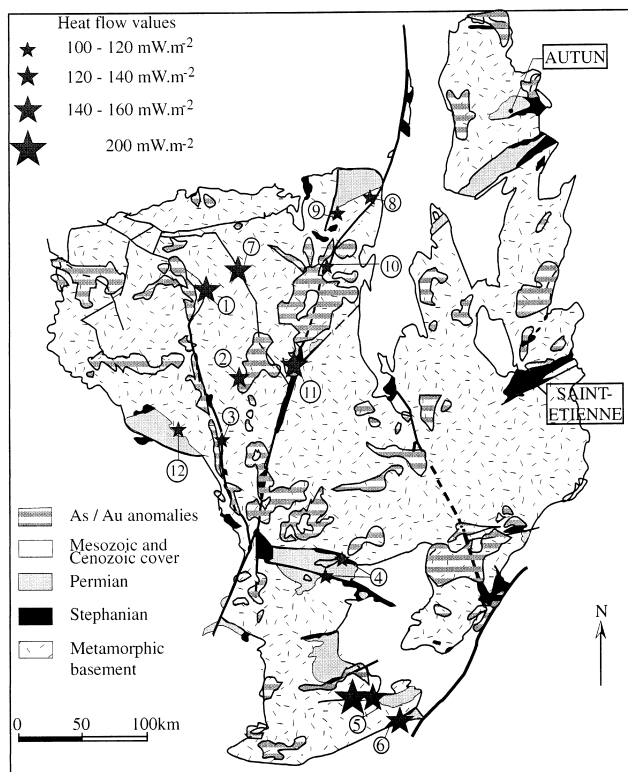


Fig. 3. General map of the Massif Central showing the location of the Carboniferous basins from which the analysed coal samples were collected (adapted from Becq-Giraudon, 1984). 1: Bosmoreau-les-Mines, 2: Lapeau-Maussac, 3: Argentat, 4: Déroit de Rodez, 5: Graissessac, 6: Roujan-Neffiès, 7: Ahun, Saint-Michel-de-Veisse, 8 and 9: Noyant, 10: Saint-Eloy-les-Mines, 11: Meisseix, 12: Brives. Location of the hydrothermal paleofields (As anomaly > 80 ppm, Bouchot et al., 1997); the stars correspond to the heat-flow intensities estimated during the present study — from the smallest to largest star: 100–120 mW m⁻², 120–140 mW m⁻², 160–180 mW m⁻², 200 mW m⁻² (the heat flow rates for basins labelled 7 to 12 are derived from the T_{max} values adopted by Mascle, 1998).

The heat flows, notably the most intense one, have two possible origins: (i) an extremely high geothermal paleogradient associated with a shallow ductile–brittle limit in the crust, and (ii) thermal metamorphism induced by basement metamorphic cycles which, through the creation of thermal domes of varying intensity, are likely to have had a direct effect on the sediments, as observed at Graissessac for example (Becq-Giraudon and Gonzalez, 1986); either origin not excluding the other.

According to the data provided herewith (Tables 2 and 4) and the T_{\max} values for coal determined by Mascle (1998); sites labelled 7–12 in Fig. 3), three basins, namely Bosmoreau–Ahun, Meisseix and Graissessac (Fig. 3), show heat flows of above 160 mW m^{-2} for the Stephanian–Autunian. These areas are thus more likely to have been affected by the circulation of hydrothermal fluids. More specifically, it would seem that the high heat flow envisaged for Bosmoreau–Ahun is genetically related to the production of Variscan (340–290 Ma) granites in the Limousin (western part of Massif Central) and, more particularly, the Millevaches plateau (Ledru et al., 1994). This region would thus have had a shallow ductile–brittle limit in a hot crust, interpreted as a thermal dome of limited extent in the Limousin. By comparing the lowest ranks of Stephanian–Autunian coal in the northeast (Fig. 3. no. 8–9–10) and southwest (Brive–Argentat, Fig. 3. no. 12) of the Limousin with those of Bosmoreau–Ahun, it is suggested that the peak of the hyperthermal event was confined to the Millevaches plateau. However, superposition of the As–Au anomalies and the heat flows onto the same map (Fig. 3) reveals no direct relationship between the emplacement of these two events. This is particularly true for the “hot zone” of the Limousin; the hydrothermal paleofields, responsible for As–Au mineralizations (Bouchot et al., 1997), appear to have developed along the edge of the Millevaches plateau, the hottest area of the Limousin dome. The discovery of gold-bearing pebbles in the Late Stephanian at Alès (Charrier, 1992) and in the Carboniferous at Argentat (Becq-Giraudon et al., 1999; Bouchot et al., 1999) confirms that these hydrothermal paleofields were active before the opening of the Stephanian–Autunian basins and, therefore, that these two events are not contemporaneous.

4.4. Anomalies typology

Plotting of the results on HI/OI diagrams for each basin reveals OM evolution paths that differ from the standard evolution of a transformation under the influence of temperature (Fig. 4). The increase in the OI, accompanied by a decrease in the HI, suggests oxidation of the OM.

By plotting the results on a R_o/T_{\max} reference diagram (Fig. 5, adapted from Teichmüller and Durand, 1983), two groups of samples can be identified.

- A group near the R_o-T_{\max} correlation curve (Fig. 5) comprising the Détroit de Rodez samples (except Ber4), A1 and A2 from Argentat, the East Graissessac samples (with a $T_{\max} < 490^\circ\text{C}$), and Ro-Né1 and 2 from Roujan-Neffiès.

- A group characterized by abnormally high T_{\max} values with respect to R_o ; these two parameters thus provide divergent information concerning the rank of a coal (Table 3). Based on the OI/T_{\max} diagram (Fig. 6), this group can be further subdivided into two sub-groups.

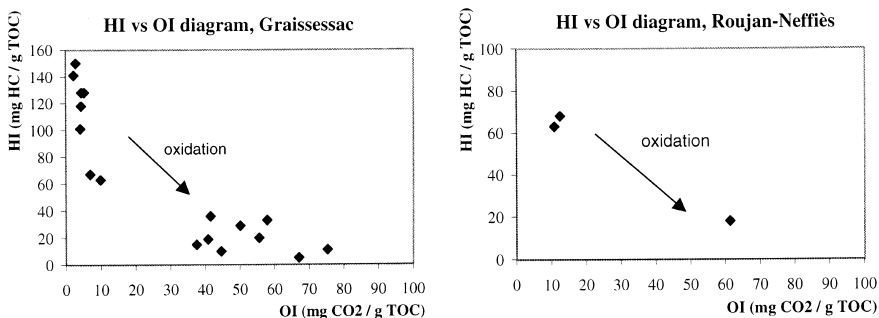


Fig. 4. Relationship between Hydrogen Index and Oxygen for samples from Graissessac and Roujan-Neffiès.

- Samples with diverging R_o and T_{max} accompanied by a positive T_{max}/OI correlation (group 2, Fig. 6), particularly well represented by the East Graissessac samples (with a $T_{max} > 500^\circ\text{C}$), and also by A3 and A3' of Argentat and Ro-Né3 of Roujan-Neffiès. This atypical anomaly can be attributed to the circulation of hot oxidizing fluids likely to cause a simultaneous increase in T_{max} and OI. Furthermore, the data suggest that the evolution of these two parameters can be associated with a slight decrease in R_o .

- Samples with a R_o/T_{max} divergence but no notable increase in OI (group 3, Fig. 6), represented by the Bosmoreau-les-Mines and West Graissessac samples. This R_o/T_{max} divergence, without any sign of oxidation, probably has a purely thermal origin

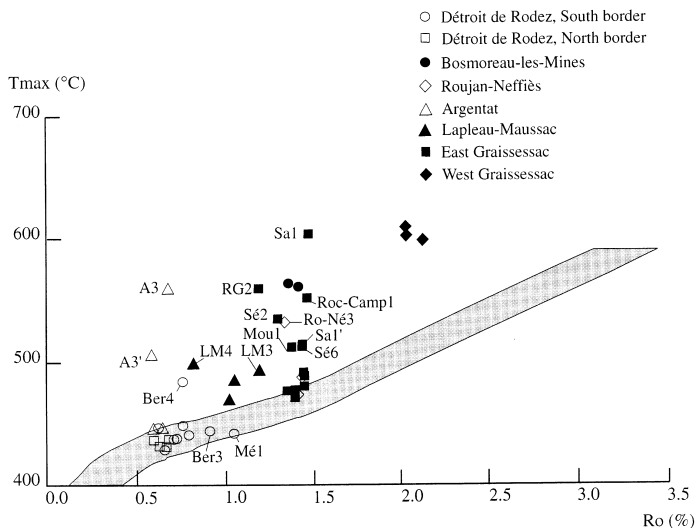


Fig. 5. R_o / T_{max} diagram, the grey area corresponds to the R_o / T_{max} correlation of Teichmüller and Durand (1983).

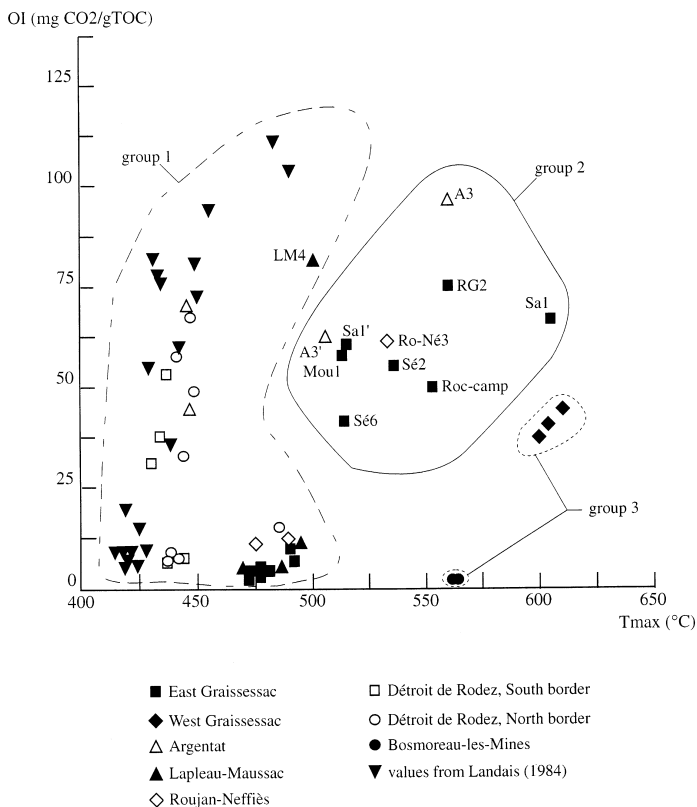


Fig. 6. OI/T_{max} diagram including the values of Landais et al. (1984). Group 1: samples showing no significant T_{max} anomaly, Group 2: samples showing a positive T_{max}/OI correlation, Group 3: samples showing a simple positive T_{max} anomaly with respect to the reference envelope of Teichmüller and Durand (1983), these samples belong to basins with a more intense hyperthermicity.

and consequently, the T_{max} anomaly probably becomes more marked with increasing intensity of the local heat flow.

These two types of anomalies (R_o/T_{max} alone and $R_o/T_{max}/OI$) seem to be superimposed onto the classic thermal maturation process of coal, a priori similar to burial diagenesis, which distorts the interpretation of the parameters considered independently.

A synthesis of the results acquired for the Lapleau–Maussac basin (Table 2) seems difficult to interpret because of a large scatter in R_o , T_{max} and OI values. However, samples LM1 and LM2 are similar to those of Bosmoreau-les-Mines, inasmuch as they have a high T_{max} (compared to R_o), but not necessarily a high OI. Sample LM3, from the same stratigraphic layer as LM1 and LM2, but with a higher R_o , nevertheless poses a problem. The presence of *b*-type fringes suggests that this sample underwent early oxidation (Alpern and Maume, 1969), which had the effect of modifying the reflectance and, to a lesser degree, T_{max} , but not the OI (Copard, 1998).

4.5. Origin of the T_{max}/OI and R_o/T_{max} anomalies

The textural and R_o observations make it possible to exclude alteration related to plutonic intrusion, which would have considerably increased R_o (Goodarzi and Cameron, 1990; Bertrand and Pradier, 1993). Similarly, late meteoric oxidation, as observed in certain samples, is likely to cause an increase in the OI, but not T_{max} (Deroo, 1986).

4.5.1. T_{max}/OI anomaly

Fluid circulation can cause variably complex modifications of OM, with the nature and intensity being governed by fluid temperature and composition, and by the rank of the coal at the onset of the hydrothermal event. Harouna et al. (1993) attributed a marked increase in reflectance, a classic evolution of T_{max} with burial and a decrease in the H/C ratio without variation of the O/C ratio, to the influence of early diagenetic hydrothermal flows of moderate temperature, i.e., too low for the cracking of OM, thus a variation in T_{max} . We can exclude such syn-coalification hydrothermal circulation because the T_{max} of our samples collected from a single lithostratigraphic unit from the same basin should be constant. Furthermore, the high paleo-heat flow that is assumed to have affected the entire Massif Central during the Stephanian–Autunian is not consistent with the circulation of early hydrothermal fluids of moderate-temperature.

We thus envisage late hydrothermal flows probably during and due to the tectonic event affecting the French Massif Central during Upper Carboniferous and Lower Permian. We assume that the fluids were of a higher temperature than that reached during coalification. An increase in T_{max} is only possible if the coal receives sufficient heat to break the molecular bonds that show increased stability with increasing OM maturity (Disnar, 1994). However, the increase in T_{max} that the hot fluids would have caused should be accompanied by a decrease in the OI, as with a classic maturation process, which is not observed here. We can rule out coal alteration by low-temperature fluids, a process essentially reflected by an increase in the OI (Fig. 6; Landais et al., 1984) which is similar comparable to simple oxidation of meteoric type. However, if the fluids involved had been of a moderate oxidizing nature in addition to having a high temperature, they would have probably caused coal transformations identical to those observed. The reasons why this moderately oxidizing thermal event was not recorded by R_o remain to be determined. Two hypotheses can be proposed based on the constancy of the R_o values for the same basin:

(1) According to the Fresnel-Beer formula, the loss of aliphatic chains, which could lead to a thermal maturation process, tends to decrease the refraction index n and thus increase R_o . Conversely, coal oxidation causes the formation of ether, carbonyl and hydroxyl groups (Berkowitz, 1979, van Krevelen, 1981) that have higher molecular refraction indices than the aromatic bonds. We can thus assume that the influence of temperature and oxidation can contradict each other and cause no notable R_o variation.

(2) If we consider the artificial maturation experiments of Monthioux (1986) and Saxby et al. (1986), R_o seems to evolve very slowly under the influence of temperature. Furthermore, George (1992) observed a delay in R_o evolution with respect to that of T_{max} as one approaches a volcanic dyke; the R_o evolution kinetics thus seem slower than those of T_{max} where the OM is subjected to intense thermal events such as dyke intrusion. In our case, the anomalous coal may not have recorded notable R_o variations

during a hyperthermal event, providing that it was of fairly short duration. This process would have occurred after coalification, which agrees fairly well with a reflectance of the altered coal identical to those of the surrounding coal.

The most feasible hypothesis to explain most of the anomalies observed is one involving the circulation of hot, moderately oxidizing fluids after coalification. The presence of *b*-type fringes, marking an alteration of vitrinite particles, does not seem to indicate widespread oxidation of this maceral. Conversely, the III-type microfractures that affect the samples with highly anomalous T_{\max} and OI (A3, RG2, S 2 and Sa1) seem to constitute a criterion of high-temperature OM oxidation. In addition, the SEM results confirm that the more oxidized the sample, the denser the fracture system is (Fig. 2g). The hydrothermal circulation hypothesis, although probable, was not confirmed by the presence of typical minerals.

4.5.2. R_o/T_{\max} anomaly

The abnormally high T_{\max} values compared to R_o , without an increase in the OI, were particularly well represented in the Bosmoreau-les-Mines and West Graissessac basins. Both these sites show extremely high heat flows between 150 mW m^{-2} and 200 mW m^{-2} . The results of the artificial maturation experiments mentioned above suggest a difference in the evolution rate of R_o and T_{\max} . In addition, in the Rhine Graben, Doehl et al. (1974) noted abnormally low vitrinite reflectance values considering the current regional thermal activity. Along the Ard che margin, carbonaceous debris in a Rhaetian layer affected by hydrothermal circulation gave a R_o of 1.57% and an abnormally high T_{\max} value of 539°C against the expected 480°C (Disnar et al., 1997). All these examples point towards the hypothesis that the identified anomalies may result from the reflectance evolution kinetics being slower than those of T_{\max} .

5. Conclusions

– All the studied basins record a hyperthermal event of variable intensity related to the geodynamic conditions prevailing in the Variscan belt during the Stephanian–Autunian. The most intense paleo-heat flows, such as those of the Millevaches plateau (Bosmoreau–Ahun), are probably related to a very hot crust with a shallow ductile–brittle limit and the development of thermal domes of varying extent. The local tectonic and erosion data suggest that the Saalic orogeny (Early/Late Permian boundary) is the most likely event responsible for interruption of coalification of the analysed coal.

– The absence of superposition of the hydrothermal paleofields and the heat flows estimated from the maturity of the Stephanian coal reveals that no direct relationship exists between these two events. The discovery of gold-bearing pebbles at Argentat and Al s confirms that gold mineralization occurred before opening of the basins, and the –300 Ma age (Bouchot et al., 1997) proposed for gold emplacement in the Massif Central thus corresponds to the youngest age for this event.

– The petrographic (R_o) and geochemical (pyrolysis: T_{\max} , OI, HI) analyses have made it possible to identify two types of anomalies that seem to be superimposed on coal maturation and are characterized by either a divergence in the evolution of R_o and T_{\max} associated with a high OI, or by a simple divergence between R_o and T_{\max} for the

same sample. The first type indicates a local thermal and oxidizing character at sample scale, whereas the second reflects a hyperthermal event at regional scale.

We propose two hypotheses for the origin of these anomalies:

(a) R_o/T_{max} divergence associated with a positive OI anomaly, based on the assumption that hot, slightly oxidizing fluids circulated after coalification.

(b) R_o/T_{max} divergence associated with very high hyperthermal activity at basin scale, or better still, tectonic-block scale, interpreted as a first-order chemical reaction velocity differential between R_o and T_{max} .

– Type III anastomosed microfractures, notably observed at Graissessac and Argentat, optically characterize the positive OI anomaly in association with a high T_{max} .

– In summary, this study demonstrates a difference in reaction kinetics for R_o and T_{max} that is related, to varying degrees, to hyperthermal activity affecting a lithologic column under given geodynamic conditions. Interpretation of the observations is thus faced with the problem of oxidation of the coal at different temperatures and the consequences concerning the rank parameters and the reliability for their combined use as maturity indicators. In this respect, if the increase in reflectance is very slow compared to that of T_{max} , it is the latter that more accurately reflects the true rank of the sample.

Acknowledgements

The authors would like to thank Jim Hower, Maria Mastalertz and Paul Robert for their careful rereading of the manuscript which greatly benefitted from their constructive criticisms. This paper is assigned the BRGM scientific contribution no. 99004 and the GéoFrance 3D Program no. 57.

References

- Alpern, B., Maume, F., 1969. Etude pétrographique de l'oxydation naturelle et artificielle des houilles. *Rev. Ind. Miner.* 51 (11), 979–998.
- André, A.S., 1997. Paléochamps de contraintes et paléochamps géothermiques, Exemple des granites tardihercyniens du Nord du Limousin. DEA dissertation, Laboratoire d'Etude des Systèmes Hydrothermaux, University of Nancy, 1, 39 pp.
- Becq-Giraudon, J.F., Gonzalez, G., 1986. Maturation de la matière organique dans le bassin stéphanien de Graissessac (Hérault): liaison entre structure et métamorphisme des charbons; signification régionale, note brève. *Géol. France* 3, 339–344.
- Becq-Giraudon, J.F., Mazeaud, N., 1981. Bassin houiller de Bosmoreau-les-Mines (Creuse), étude géologique. BRGM Report, 81, SGN 291 GEO, 47 pp.
- Becq-Giraudon, J.F., Van Den Driessche, J., 1993. Continuité de la sédimentation entre le Stéphanien et l'Autunien dans le bassin de Graissessac-Lodève (sud du Massif Central): implications tectoniques. *C.R. Acad. Sci. Paris* 317, 939–945, Série II.
- Becq-Giraudon, J.F., Roig, J.Y., Bouchot, V., Milési, J.P., 1999. Internal palaeogeography of the Uer Carboniferous (Stephanian) outliers of Argentat (Massif Central, France): Metallogenic Implications (GéoFrance 3D). Submitted to EUG, 1999.
- Berkowitz, N., 1979. An Introduction to Coal Technology. In: Denton, J. (Ed.), *Energy Science and Engineering: Resources, Technology, Management*. Academic Press, New York, 346 pp.
- Berquer-Gaboreau, Cl., 1986. Pétrologie des charbons de deux bassins limniques du Massif Central français (Blanzay-Montceau et Meisseix). Exemples d'hyperthermies locales. Doctoral thesis, Univ. Lille, 184 pp.

- Bertrand, P., Pradier, B., 1993. Optical methods applied to source rock study. In: Bordenave, M.L. (Ed.), *Applied Petroleum Geochemistry*. Technip, Paris, pp. 281–310.
- Bostick, N.H., 1971. Thermal alteration of clastic organic particles as an indicator of contact and burial metamorphism in sedimentary rocks. *Am. Assoc. Stratigr. Palynologists Proc.*, 2nd, Geoscience Man. 3, 83–92.
- Bouchot, V., Milési, J.P., Lescuyer, J.L., Ledru, P., 1997. Les minéralisations aurifères de la France dans leur cadre géologique autour de 300 Ma. *Chron. Rech. Min* 528, 13–62.
- Bouchot, V., Becq-Giraudon, J.F., Bailly, L., Le Goff, E., Milési, J.P., 1999. Identification of palaeoconglomerate-hosted Au–As bearing pebbles in the Stephanian Argentat basin: geological implications. *J. Conf. Abs.* 4, 478.
- Charrier, J., 1992. Etude des minéralisations aurifères des Cévennes (Massif Central, France) et de leur contexte géologique. Doctoral thesis, Univ. Limoges, unpublished, 271 pp.
- Copard, Y., 1998. Contribution à la mise en évidence de paléocirculations des fluides dans les bassins houillers du Massif Central français par l'analyse de la Matière Organique. BRGM Report GF3D, 94/98, 83 pp.
- Costa, S., 1990. De la collision continentale à l'extension tardi-orogénique: 100 millions d'années d'histoire varisque dans le Massif Central français. Une étude chronologique par la méthode $40\text{ Ar}-39\text{ Ar}$. Doctoral thesis, University of Languedoc, Montpellier, 391 pp.
- Deroo, G., 1986. Altération superficielle de la Matière Organique. IFP Internal Report, unpublished.
- Disnar, J.R., 1994. Determination of maximum paleotemperatures of burial (MPTB) of sedimentary rocks from pyrolysis data on the associated organic matter: basic principles and practical application. *Chemical Geology* 118, 289–299.
- Disnar, J.R., Barsonny, I., Drouet, J., Espitalié, J., Farjanel, G., Marquis, F., Martinez, L., 1995. Géochimie organique et reconstitution de l'histoire thermique et tectono-sédimentaire de la marge ardéchoise (programme GPF; France). In: Résumé des communications de la Séance spécialisée de la S.G.F., du sédim. . . au réservoir, quantification et modélisation de la diagenèse, 6 and 7 November 1995, Poitiers, pp. 73–81.
- Disnar, J.R., Marquis, F., Espitalié, J., Barsonny, I., Drouet, S., Giot, D., 1997. Géochimie organique et reconstitution de l'histoire thermique et tectono-sédimentaire de la marge ardéchoise (programme GPF; France). *Bull. Soc. Géol. France* 168 (1), 73–81.
- Doebel, F., Heling, D., Homann, W., Karweil, J., Teichmüller, M., Welte, D., 1974. Diagenesis of Tertiary clayey sediments and included dispersed organic matter in relationship to geothermics in the upper Rhine Graben. In: *Approaches to Taphrogenesis*, Inter-Union Commission of Geodynamics Scientific Report, Stuttgart 1974, pp. 192–207.
- Espitalié, J., Deroo, G., Marquis, F., 1985a. La pyrolyse Rock-Eval et ses applications. *Rev. Inst. Franç. du Pétr.* 40 (5), 563–579.
- Espitalié, J., Deroo, G., Marquis, F., 1985b. La pyrolyse Rock-Eval et ses applications. *Rev. Inst. Franç. du Pétr.* 40 (6), 755–784.
- Espitalié, J., Deroo, G., Marquis, F., 1985c. La pyrolyse Rock-Eval et ses applications. *Rev. Inst. Franç. du Pétr.* 41 (1), 73–89.
- Faure, M., 1995. Late orogenic Carboniferous extensions in the Variscan French Massif Central. *Tectonics* 14 (1), 132–153.
- Faure, M., Becq-Giraudon, J.F., 1993. Sur la succession des épisodes extensifs au cours du désépaissement carbonifère du Massif Central français. *C.R. Acad. Sci. Paris* 316, 967–973, série II.
- Faure, M., Leloix, C., Roig, J.Y., 1997. L'évolution polycyclique de la chaîne hercynienne. *Bull. Soc. Géol. France* 168 (6), 695–705.
- Feys, R., 1989. Le système permien en Europe. In: *Synthèse Géologique des Bassins Permien Français*. Mém. BRGM 128, 17–22, Orléans.
- Gelard, J.P., Castaing, C., Bonijoly, D., Grolhier, J., 1986. Structure et dynamique de quelques bassins houillers limniques du Massif Central. *Mém. Soc. Géol. France*, N.S. 149, 57–72.
- Genna, A., Roig, J.Y., Debriette, P.J., Bouchot, V., 1998. Le bassin houiller d'Argentat (Massif Central français), conséquence topographique d'un plissement de son substratum varisque. *C.R. Acad. Sci. Paris* 327, 279–284.
- George, S.-C., 1992. Effect of igneous intrusion on the organic geochemistry of a siltstone and an oil shale horizon in the Midland Valley of Scotland. *Org. Geochem.* 18 (5), 705–713.

- Golitsyn, A., Courel, L., Debriette, P., 1997. A fault-related coalification anomaly in the Blanzay–Montceau Coal Basin (Massif Central, France). *Int. J. Coal. Geol.* 33, 209–228.
- Goodarzi, F., Cameron, A.R., 1990. Organic petrology and elemental distribution in thermally altered coals from Telkwa, British Columbian. *Energy Sources* 12, 315–343.
- Harouna, M., Disnar, J.-R., Martinez, L., Trichet, J., 1993. Discrepancies between different organic maturity indicators in a coal series affected by an abnormal thermal event (Visean, Niger). *Chemical Geology* 106, 397–413.
- Jebrak, M., 1989. Le thermalisme au Permien. In: *Synthèse Géologique des Bassins Permien Français*. Mém. BRGM 128, 265–270, Orléans.
- Lafargue, E., Espitalié, J., Marquis, F., Pillot, D., 1996. ROCK EVAL 6 applications in hydrocarbon exploration, production and in soil contamination studies. Conference proceedings: 5th Latin American Congress on Organic Geochemistry, Cancun, October 6–10, 26 pp.
- Landais, P., Monthioux, M., Meunier, J.-D., 1984. Importance of the oxidation/maturation pair in the evolution of humic coals. *Org. Geoch.* 7 (3/4), 249–260.
- Latouche, L., 1969. Existence d'un métamorphisme post-stéphanien dans le bassin de Graissessac et dans la partie nord-est de la zone axiale de la Montagne Noire (Hérault). *C.R. Somm. Soc. Géol. Fr.* 3, 93–94.
- Ledru, P., Costa, S., Echtler, H., 1994. Structure. In: Keppies, J.D. (Ed.), *Pre-Mesozoic Geology in France and related areas*. Springer-Verlag, Berlin, pp. 305–323.
- Leloix, C., 1998. Arguments pour une évolution polycyclique de la chaîne hercynienne, structure des Unités Dévono-dinantiennes du Nord-Est du Massif Central (Brévenne-Bourbonnais-Morvan). Doctoral thesis, Univ. Orléans, 248 pp.
- Letourneur, L., 1953. Le Grand Sillon Houiller du plateau central français. *Bull. Carte. Géol. France*, LI 238, 12–36.
- Ligouis, B., 1988. La grande couche de Bourran du bassin stéphanien de Decazeville (Aveyron), Pétrologie et environnements de dépôt du charbon: genèse d'une veine puissante. Doctoral thesis, Univ. Orléans, 341 pp.
- Marest, D., 1985. Comparaison des évolutions dynamiques des bassins houillers limniques du Limousin: mise en place de modèle de dépôts. Doctoral thesis, Univ. Paris, 268 pp.
- Masclé, A., 1990. Géologie pétrolière des bassins permien français. Comparaison avec les bassins permien du Nord de l'Europe. *Chron. Rech. Min.* 499, 69–86.
- Masclé, A., 1998. Subsidence et thermicité des bassins stéphanien-permien de l'Ouest du Massif Central, rapport provisoire. BRGM Report GF3D, 93/98, 16 pp.
- Monthioux, M., 1986. Maturation naturelle et artificielle d'une série de charbons homogènes. Doctoral thesis, Univ. Orléans, 331 pp.
- Robert, P., 1985. Histoire géothermique et diagenèse organique. *Bull. Centres Rech. Explor-Prod. Elf-Aquitaine*, Dissertation, 345 pp.
- Robert, P., Berquer, C., Courel, L., Kubler, B., Robert, P., 1988. Anomalie thermique précoce dans le bassin houiller stéphanien de Meisseix-Singles, Massif Central français. *Sci. Géol. Bull.* 3/4, 333–349.
- Roig, J.Y., Calgano, P., Bouchot, V., Maluski, H., Faure, M., l'équipe Géofrance 3D Cartographie et Métallogénie du Massif Central, 1997. Modélisation 3D du paléochamp hydrothermal As + Au (330–300 Ma) le long de la faille d'Argentat (Massif Central français). *Chron. Rech. Min.* 528, 63–69.
- Saxby, J.-D., Bennett, A.J.R., Corcoran, J.F., Lambert, D.E., Riley, K.W., 1986. Petroleum generation: simulation over six years of hydrocarbon formation from torbanite and brown coal in a subsiding basin. *Org. Geochem.* 9 (2), 69–81.
- Teichmüller, M., Durand, B., 1983. Fluorescence microscopical rank studies on liptinites and vitrinites in peat and coals, and comparison with results of the Rock-Eval pyrolysis. *Int. J. Coal Geol.* 2, 197–230.
- van Krevelen, D.W., 1981. Coal chemistry, the main chemical reaction processes of coal. In: *Coal Science and Technology* 3. Coal, typology — chemistry — physics — constitution. Elsevier, pp. 155–236.
- Wang, H., 1991. Dynamique sédimentaire, structuration et houillification dans le bassin houiller stéphanien des Cévennes. Doctoral Thesis, University of Bourgogne, Dijon, 266 pp.
- Wang, H., Courel, L., 1993. Houillification dans le bassin houiller stéphanien des Cévennes (France). *Zbl. Geol. Paläont. Teil I* 5, 473–486.

Available online at www.sciencedirect.com

Organic Geochemistry 35 (2004) 543–559

**Organic
Geochemistry**www.elsevier.com/locate/orggeochem

Organic matter accumulation and preservation controls in a deep sea modern environment: an example from Namibian slope sediments

Laetitia Pichevin^{a,*}, Philippe Bertrand^a, Mohammed Boussafir^b,
Jean-Robert Disnar^b

^aDépartement de Géologie et Océanographie, Université Bordeaux I, UMR-CNRS 5805, 33405 Talence Cedex, France

^bLaboratoire de Géologie de la Matière Organique, Institut des Sciences de la Terre d'Orléans (I.S.T.O.), UMR-CNRS 6113, BP 6759, 45067 Orléans Cedex 2, France

Received 3 June 2003; accepted 9 January 2004
(returned to author for revision 2 October 2003)

Abstract

The Lüderitz upwelling cell is presently the most productive area of the Benguela current system and abundant organic matter (OM) accumulates on the adjacent slope sediments even at great water depth. OM from two cores taken on the slope and covering the last 280 kyear was analysed in terms of “petroleum quality” (Rock-Eval), chemical features (FTIR, EDS) and petrographic composition (light microscopy and TEM). These data indicate that the OM is more oxidized at 3606 m water depth than on the upper slope sediments (1029 m) although the petroleum quality of the OM throughout the deep-water core remains surprisingly high for hemipelagic deep-sea sediments (HI = 200–400 mg/g). The petroleum quality of OM accumulated on the upper slope is consistently high: HI averages 450 mg/g. Two petrographic types of OM are distinguishable from microscopic observation, each ascribed to distinctive preservation mechanisms: (1) ‘Granular’ amorphous OM, which dominates in the deep-water core, is formed by organo-mineral aggregates. Aggregation appears to be the primary preservation mode at this depth although is quantitatively limited (maximum TOC value of 4 wt.% of bulk sediment obtained through this process). The ultrastructure of the aggregates highlights an intimate association pattern between sedimentary OM and clays. (2) ‘Gel-like’ nanoscopically amorphous OM (NAOM) largely dominates at 1000 m water depth and contains sulfur. Thus, early diagenetic sulfurization was probably involved in the preservation of this OM, but a contribution from the classical degradation–recondensation pathway cannot be ruled out. Moreover, selective preservation occurred at both sites but represents an insignificant part of the OM.

Organic fluxes mainly control the occurrence and extent of sulfurisation at both water depths by determining the redox conditions at the sea floor. Aggregate formation is limited by both organic and mineral fluxes at the lower slope whereas OM supply is never limiting on the upper slope. Although consistently operating through time at both depths, preservation by organo-mineral association is limited by mineral availability and thus accounts for a relatively minor portion of the OM accumulated on this organic-rich slope. In the case of large organic fluxes, sulfurisation and/or degradation–recondensation is required to obtain TOC contents above 4 wt.% of bulk sediment in the area.

© 2004 Elsevier Ltd. All rights reserved.

* Corresponding author. Tel.: +33-5-40008960; fax: +33-5-4000848.
E-mail address: l.pichevin@epoc.u-bordeaux1.fr (L. Pichevin).

1. Introduction

The degradation of organic matter (OM) spans the journey of dead organisms and detritus as they sink from the euphotic zone through the water column, enter the sediment and are ultimately buried. Degradation processes involve a series of redox reactions that provide electron acceptors for the oxidation of OM by heterotrophs. Oxygen, when present, is energetically favoured over other oxidants and is the first to be consumed. Next, nitrate, Mn/Fe oxides and sulfate are successively consumed in the degradation of any remaining organic compounds (Canfield, 1993).

As in most open ocean regions, the water column overlying the Namibian slope is usually well oxygenated at all depths. However, during highly productive upwelling events, the large amount of exported labile organic matter can cause the rate of O₂ consumption in surface sediments to exceed the supply of dissolved oxygen by diffusion from the bottom water (Calvert and Pedersen, 1993), generating anoxic conditions at the sediment–water interface. Thus, the OM which sediments on the Namibian slope is likely to experience varying degrees of biochemical transformation under oxic, sub-oxic and/or anoxic conditions (Schulz et al., 1994), depending on the flux of labile organic matter that reaches the sea floor.

The aim of this work was to investigate organic matter preservation mechanisms that may have contributed to the high TOC contents measured in slope sediments off Lüderitz, spanning the last 280 kyear. The maximum TOC content in a core from the upper slope (about 1000 m water depth) is ~17% (8% on average) and the maximum value on the lower slope (ca. 3600 m) is as high as 8% (2% on average). The broad range of OC concentrations recorded (from ca. 0.3 to 17.4%) allows the study of various OM preservation states. Moreover, the bathymetric range (1000 vs. 3600 m water depth) and long time scale permit a test of the impact of (1) water depth, in terms of sinking time and distance from the coast, and (2) climate, through sea level and primary productivity changes. Through assessment of petroleum quality, petrographic composition and some chemical features of the OM, we have determined the preservation processes that occurred on the Lüderitz slope and their variation with depth and time.

2. Rationale

Organic compounds exported from the euphotic zone can be classified into two main types by considering their ‘preservation potential’ (Tegelaar et al., 1989). The first consists of labile biomacromolecules, namely polypeptides and polysaccharides which are prone to intense degradation during transit (e.g. Wakeham et al., 1997).

The second, which is resistant or refractory, includes, for example, lignin, tannin and algeenan. The last is found in the cell walls of various algae, e.g. *Botryococcus braunii* and is well preserved in sediments (Derenne et al., 1991, 1997). Although resistant biomacromolecules do not dominate biomass, they become increasingly concentrated with increasing time in the water column or decreasing burial efficiency, while the more labile molecules are degraded (Largeau et al., 1984, 1986, 1989; Hedges et al., 2001).

Labile organic matter can become more resistant owing to chemical transformation during sinking and early diagenesis. The ‘degradation-recondensation’ pathway (Tissot and Welte, 1984) consists of successive and random repolymerization and polycondensation reactions acting on the degradation products (monomers) of the original OM. Another mechanism, the so-called natural sulfurization process, has been well described by Sinninghe-Damsté et al. (1989) and by Lückge et al. (1996, 2002), among others, for both ancient sediments and recent environments. This preservation pathway involves the protective role of newly formed bonds between S and functionalized OM. Under anoxic conditions, inorganic sulfur species produced by sulfate reduction are scavenged by iron to form pyrite. When the amount of sulfides formed exceeds that which can be fixed as pyrite, the surplus may re-oxidize or be incorporated into OM (Lückge et al., 2002). These reactions take place during the early diagenetic stages (Schouten et al., 1994; Wakeham et al., 1995; Adam et al., 2000) and form characteristic molecules such as isoprenoid thiophenes (Sinninghe-Damsté et al., 1989; Kok et al., 2000).

Over the past 20 years, a fourth preservation pathway, the so-called protection by mineral matrix, has been evidenced in soils (Oades, 1988), sedimentary rocks (Salmon et al., 2000) and recent marine sediments (e.g. Mayer et al., 1985; Keil et al., 1994a; Mayer, 1993, 1994, 1999; Ransom et al., 1997; Hedges and Keil, 1999; Armstrong et al., 2002). Suess (1973) noted that the highest organic carbon contents in some recent marine environments correlate with a low mean grain-size of the mineral fraction. Mayer et al. (1988) proposed that high specific surface area, rather than the fine-grained texture of the sediment, inhibits degradation by increasing the amount of OM that could be protected by adsorption on to mineral particles. Mesopore spaces (<10 nm in diameter) and the interstices of siliciclastic particles, which represent 80% of the sediment surface area, constitute the most efficient traps for OM and prevent its degradation by excluding enzymatic hydrolysis (Mayer, 1994; Bock and Mayer, 2000). Among the classic siliciclastic minerals in marine sediments and soils, OM is preferentially associated with clays, (Mayer, 1994; Keil et al., 1994b), especially the Ca-rich clays of the smectite group (Furukawa, 2000). The latter study also showed that OM is associated with the surfaces as

well as being structurally incorporated into clay crystals. OM is not systematically coated on grain surfaces and pores as thin layers or infillings, but can appear as blebs Ransom et al. (1997, 1998a,b). Organo-mineral associations can also occur as alternating organic and clay nanolayers, as evidenced in Cenomanian black shales (Salmon et al., 2000).

3. Study area and sediment composition

The Benguela upwelling system is one of the four major eastern boundary current regions in the world and is characterized by cold, nutrient-rich sub-surface water which upwells owing to prevailing southeasterly trade winds. The upwelling area is composed of several distinct upwelling cells (Lutjeharms and Meeuwis, 1987), distributed from the Angola-Benguela front to the Agulhas retroflection zone, which constitute its northern and southern boundaries, respectively (Fig. 1). Perennially consistent atmospheric conditions maintain the activity of the central Walvis and Lüderitz cells (22–27° S, Shannon and Nelson, 1996) while southern cells show a stronger seasonality. Productivity measured

along the Lüderitz and Walvis coasts is one of the highest in the world and often reaches $350 \text{ gCm}^{-2} \text{ year}^{-1}$ (Behrenfeld and Falkowski, 1997).

A thermal front coincides with the shelf break and constitutes the offshore limit of the upwelling cell, though a filamentous mixing domain streaming up to 1000 km offshore in winter allows highly productive conditions well beyond the front (Lutjeharms and Meeuwis, 1987; Hagen et al., 2001). The most productive zones do not systematically occur within the main upwelling centre but on the outer fringe of the cell (Mollenhauer et al., 2002). It has been documented that, under strong wind-stress conditions, a secondary upwelling cell may occur seaward of the front (Barange and Pillar, 1992; Giraudeau and Bailey, 1995).

The prevailing wind field parallels the coastline. Thus, aeolian transport of detrital material from the arid continent to the ocean is weak and terrigenous input represents a minor fraction of the sediment. Terrigenous organic matter is, therefore, negligible in the cores studied as shown by the $\delta^{13}\text{C}_{\text{org}}$ record ranging from -19.5 to -21.4‰ (Martinez, unpublished data).

4. Analytical methods

4.1. Samples

Sediment sampling was carried out in 1996 on the R/V Marion Dufresne during the NAUSICAA cruise using piston-cores of 40 m length. The first core MD962086 (site 25.8° S, 12.13° E) was located at 3606 m water depth and the MD962087 (25.6° S, 13.38° E) lies under 1029 m water depth, on the upper slope (Fig. 1). Both cores were studied over intervals spanning the last 280 kyear, covering two complete climatic cycles. Sampling resolution for TOC measurements (elemental analysis) and Rock-Eval pyrolysis was 10 cm. Petrographic observations and infrared analyses were performed on a selection of samples chosen by TOC content, petroleum quality and location within a climatic cycle; optimum or transition (Fig. 2 and Table 1).

4.2. Stratigraphy

The age model at site MD962086 was generated by correlation of the benthic foraminifera species *Cibicides wuellerstorfi* $\delta^{18}\text{O}$ records with the SPECMAP reference (Imbrie et al., 1984), as given by Bertrand et al. (2003) with slight modification. No oxygen isotope data were available for MD962087 because of carbonate dissolution. The age model for MD962087 was obtained by seven radiocarbon measurements on tests of mixed planktonic foraminifers (Arizona AMS facility, USA and Gif, France) for the last 40 kyear (Table 2). A polynomial calibration with the Calib 4.3 program

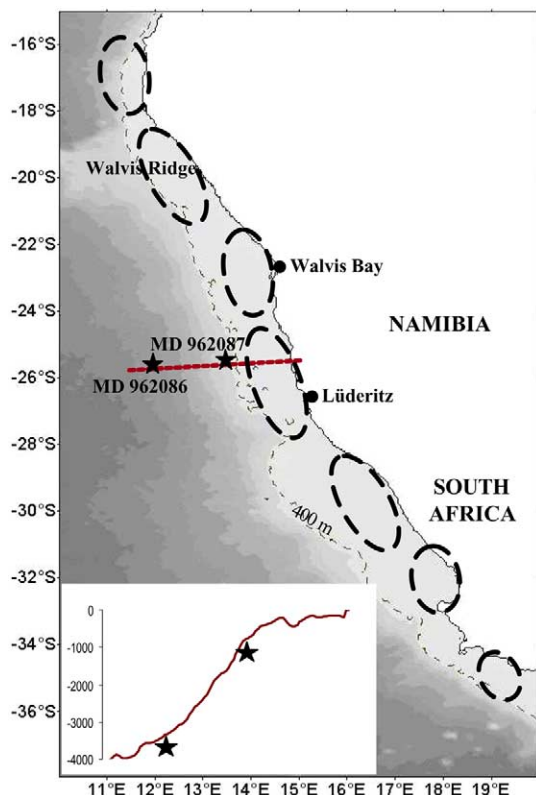


Fig. 1. Core locations, topography of Lüderitz slope and water depths. The dashed isobath underlines the mean depth of the shelf break. The upwelling cells are represented as dashed circles.

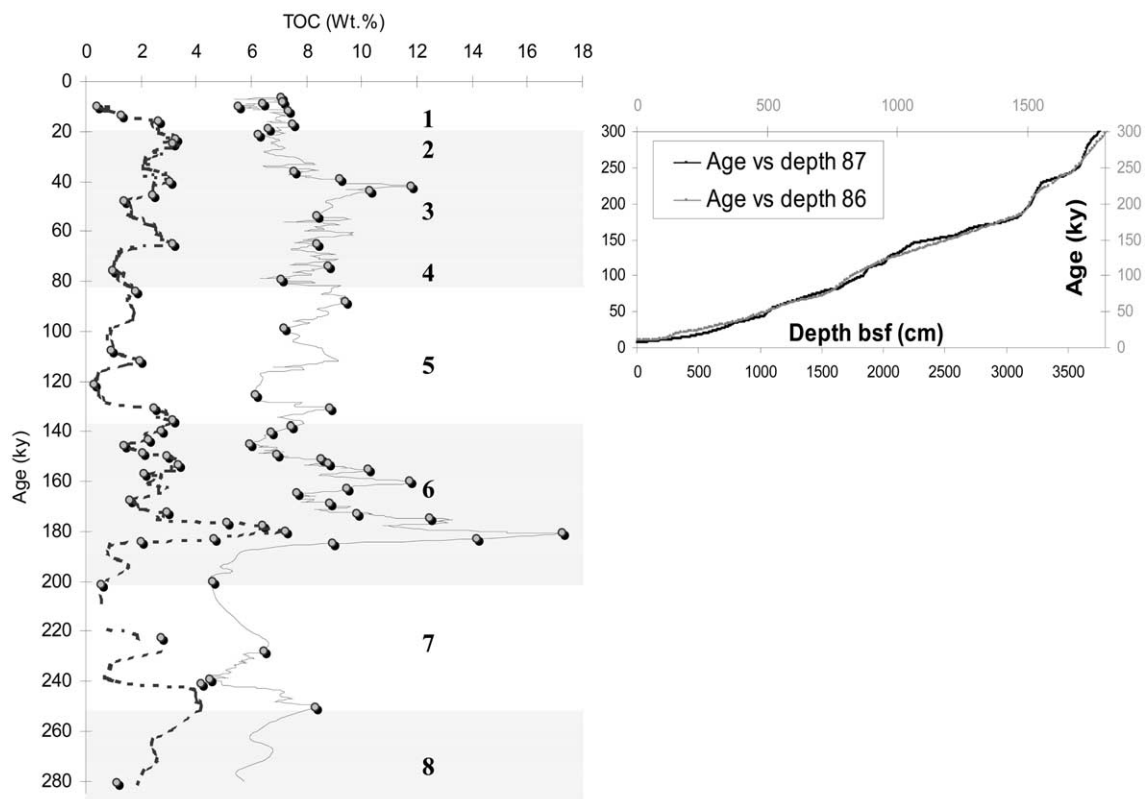


Fig. 2. TOC content vs. age for MD 962086 (dashed line) and MD 962087 (black line). Grey dots represent samples observed by light microscopy. Glacial isotopic stages 2, 3, 4, 6 and 8 are indicated by grey bands, interglacial isotopic stages 1, 5 and 7 by white bands.

Table 1
Chemical parameters and palynological composition of samples observed by TEM

Sample	TOC (wt.%)	HI (mg/g)	NAOM (%)	Aggregate (%)	Iox	Water depth (m)
1343	1.6	229	8	80.6	7.03	3606
1439	7.2	349	37.7	57.6	3.5	3606
1513	0.56	200	6.9	61.9	12.8	3606
120	6.4	424	38.7	55.9	2.02	1029
990	11.8	470	75.2	19.5	1.85	1029
3102	17.3	329	87.7	8.8	1.85	1029

Table 2
Radiocarbon dates (MD962087)

Reference	Depth bsf (cm)	AMS Age (years)	Error (years)	Species	Calendar Age (years)
101 217	2	5820	80	Mixed plankton	6177
101 218	199	10,150	90	Mixed plankton	11,009
AA47 704	366	11,336	75	Mixed plankton	12,738
101 219	450	13,890	120	Mixed plankton	15,843
AA47 703	654	20,220	150	Mixed plankton	23,371
101 220	719	26,100	260	Mixed plankton	30,148
101 221	869	35,010	570	Mixed plankton	40,019

(Stuiver et al., 1998) and a regional reservoir correction of 400 years were applied for all ^{14}C dates. The chronology of earlier stages of MD 962087 was obtained by correlation of TOC and CaCO_3 records with those of MD962098, MD962086 (Lüderitz transect) and GEOB 1712-4 (Walvis Bay, 998 m water depth) published by Kirst et al. (1999).

4.3. Chemical and spectroscopic analyses

Rock-Eval pyrolysis was performed on 40–60 mg of bulk sediment. Hydrogen indices (HI) was determined using a Rock-Eval VI under a He atmosphere, following the commonly used programme for recent sediments: 400 °C for 3 min, followed by a temperature increase at a rate of 30 °C/min to 750 °C. In 10 carbonate-rich samples, CaCO_3 was removed by mild HCl leaching (10% during 1 min) before pyrolysis.

FTIR spectra were obtained on isolated OM samples using a Perkin-Elmer FTIR 16PC spectrometer (following HF/HCl hydrolysis). Each KBr pellet contained 1 mg of isolated OM.

4.4. Petrographic studies

Mineral constituents were eliminated via classical HF/HCl treatment (Durand and Nicaise, 1980). The petrographic features of 72 samples of isolated OM were determined by light microscopy. We obtained qualitative and quantitative descriptions of OM from the shallow and deep cores, i.e. determination of the different organic fractions considering their textural and structural appearance, the contribution of each fraction and pyrite occurrence. The abundance of OM facies was

estimated by counting the fraction of the palynofacies slide covered by each facies.

The next step was performed using transmission electron microscopy (TEM) and elemental diffraction analysis (EDS), which permit observation of the structural patterns and the compositional elements of OM at a very fine scale (to 10 nm). The six samples studied by TEM were fixed in osmium tetroxide and embedded in resin as previously described by Boussafir et al. (1994). They were selected according to light microscopy examination and TOC content. To ensure that the observations were representative, three preparations were made and examined for each sample.

5. Results and interpretation

5.1. Petroleum quality: impact of water depth and OC content

Interestingly, TOC values (wt.%) vary significantly with climate: enhanced TOC generally occurs during glacial periods (Fig. 2) and especially during stage 6.6 at both locations. TOC is always much higher for the upper slope samples. In total, 550 samples of bulk sediment from both cores were analysed by Rock-Eval pyrolysis. The results are shown in Fig. 3. HI (mg/g) represents the mass of hydrocarbon compounds produced by pyrolysis of 1 g of TOC. Here, 99% of the HI values range from 150 to 540 mg/g, which demonstrates the variable petroleum quality of the OM. Schematically, high HI indicates that the contribution of hydrocarbon chains (aliphatic compounds) to the total OM is high.

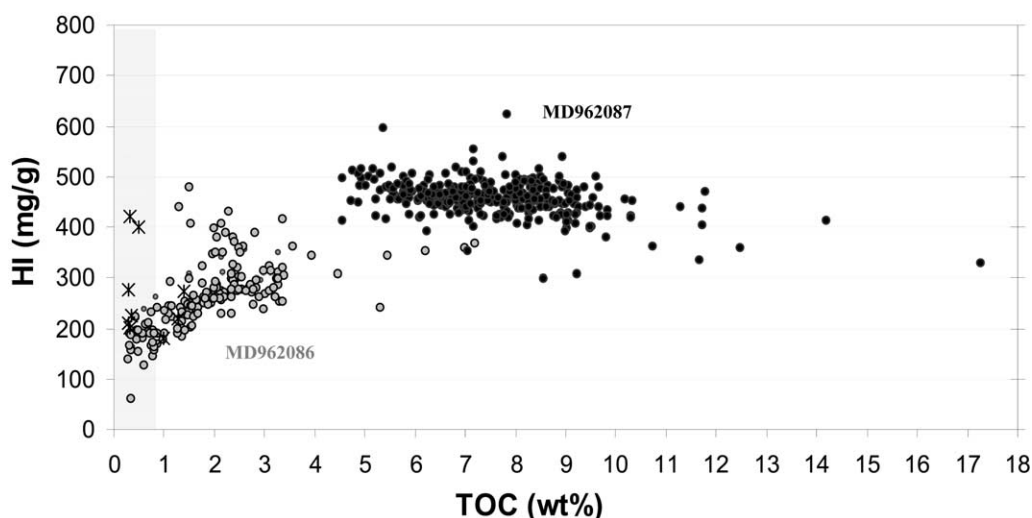


Fig. 3. Hydrogen index (mg/g) vs. TOC (wt.%) for MD 962087 (black) and MD 962086 (grey). High HI indicates more aliphatic compounds. When TOC is under 1%, we assume that HI is underestimated because of carbonate abundance (greater than 70%). Asterisks indicate samples that were examined again after a mild HCl leaching.

As shown in Fig. 3, HI vs. TOC distributions display two different trends depending on the core. The upper slope core MD 962087 shows high, almost constant, HI values (around 450 mg/g) irrespective of the variation in TOC. HI values from the lower slope core (MD 962086) are comparatively lower (50 up to 400) and decrease with decreasing TOC content. The latter core displays the typical decaying trend often described in the literature (e.g. Ramanampisoa and Disnar, 1994). However, when TOC is under 1%, we assume that HI is underestimated because of the abundance of minerals which can trap the effluents released during pyrolysis (Espitalié et al., 1985; Saint-Germès et al., 2002). Ten organic-poor samples from the deep core were gently treated with HCl in order to remove carbonate without substantial OM degradation. The HI values of these carbonate-free samples were much higher than those of the untreated ones (200–420 mg/g instead of 50–150 mg/g). Thus, HI values for the deep core range from about 200 to 400 mg/g even when TOC contents are low (<0.5%) and show a weak positive correlation with TOC. On average, for a given TOC value (%), HI is higher in the shallow core than in the deep core.

T_{\max} data average 411 °C (± 12 and ± 25 °C for MD 962087 and 962086, respectively) in agreement with the low maturity of the OM (Espitalié et al., 1985). Oxygen indices (OI mg/g, the mass of CO₂ produced by pyrolysis of 1 g of TOC) range from 120 to 230 mg/g in the shallow core. For the deep core, higher OI values and a wider range are observed: from 130 to more than 700 mg/g. TOC contents are negatively correlated with OI. The highest OI values (from 300 to 700 mg/g), result, however, partly from the thermal decomposition of carbonates, which releases CO₂.

The above results indicate that, at a given location, the petroleum quality of the OM does not vary greatly over 280 kyr despite large variations in TOC. However, HI is substantially higher in the shallow core than in the deep core. OM that reaches the lower slope has presumably remained longer under oxic conditions than the OM accumulated on the upper slope because (1) sinking time increases with water depth and (2) sedimentation rate decreases with increasing distance from the upwelling centre due to decreasing primary productivity (Hedges et al., 1999).

5.2. Petrographic composition

The following palynofacies analyses were performed on a selection of 72 samples in order to depict the petrographic nature of the OM and its variation with climate and water depth. All the samples yield an overwhelming majority of brown/orange, amorphous OM (AOM), and hardly any recognizable palynomorphs. In general, terrestrial plant detritus only accounts for 1–4% of the palynofacies although an

enrichment in refractory lignocellulosic debris is observed in samples from the lower slope core with very low TOC content (<1.5 wt.%). We assume that the amorphous OM is of marine origin as suggested by the $\delta^{13}\text{C}$ of the OM from MD 962098 averaging -20% (Martinez, unpublished data). Framboidal pyrite or single crystals are always present, testifying to the local, permanent occurrence of anoxic conditions in the sediment. Among the amorphous material, two palynological fractions were distinguished (Fig. 4):

1. The granular AOM appears as a pulverulent material formed by clusters of very thin (infra-micrometric), irregularly sized curds (Fig. 4b). The texture of the granular AOM is finer in the deep core than in the shallow core sediments.
2. The gel-like AOM consists of discrete or aggregate flecks of a few μm , with clear edges. Each fleck is characterized by a homogeneous texture (Fig. 4c). No trace of biological structure is visible within this amorphous material. This feature recalls the orange AOM described for the Kimmeridgian deposits from Yorkshire (Boussafir et al., 1995; Boussafir and Lallier-Vergès, 1996) and Orbagnoux (Mongenot et al., 1999). According to these authors, gel-like AOM was produced by sulfurization.

Gel-like AOM is more abundant in the upper slope core (from 40 to 87%) than in the lower slope core (from 3 to 41%) sediments. As a corollary, granular AOM dominates in the palynofacies of MD 962086. Furthermore, gel-like AOM content increases with increasing TOC content and granular AOM abundance follows the opposite trend.

5.3. TEM observations

TEM observations were made on six samples of isolated OM, selected on the basis of the above results. These OM isolates represent samples with TOC contents ranging from 0.56 to 17.4%, including almost completely granular to almost entirely gel-like AOM. Ultrathin sections of samples 1343, 1439 and 1513 are from the deep core while samples 120, 990 and 3102 come from the shallow core (Table 1). We assume, based on light microscopy observation, that TEM images from samples 3102 and 990 show the nanoscopically amorphous structure of pure gel-like AOM (NAOM), whereas TEM micrographs of samples 1513 and 1343 illustrate the ultrathin structure of granular AOM (Fig. 5). Both types of AOM coexist in samples 120 and 1439, as their TOC contents and petrographic composition are comparable and intermediate. Additionally, EDS analyses were performed on selected OM fractions

(Fig. 6a and b). The EDS spectra show the nature of the major elements of the material.

Gel-like AOM appears as nanoscopically undifferentiated, amorphous smears when viewed by TEM (Fig. 5A, B and C), similar to the orange AOM identified by Boussafir et al. (1995) and Mongenot et al. (1999). Some lamellar structures embedded in NAOM are seen but are not abundant (Fig. 5C and D). These structures are between 7 nm and 50 nm wide and are comparable to the ultralaminae described by Largeau et al. (1989). This indicates that selective preservation exists here but did not play a major role in OM accumulation. Thus, in the ensuing discussion, NAOM will refer to gel-like AOM as this fraction is mainly nanoscopically amorphous. NAOM contains S, as revealed by EDS analysis (Fig. 6a). This suggests preservation by sulfurization, consistent with the conclusions of Boussafir et al. (1995) and Mongenot et al. (1999) concerning the origin of gel-like, orange AOM.

Overall, granular AOM is formed by microaggregates, clusters of microaggregates and pellets. The size and shape of the aggregates vary depending on the core (Fig. 5), i.e. on water depth of deposition, as discussed below. Aggregates are formed by association between OM and clays (principally), as suggested by the presence of Si, Al, Mg, Ca and Na in the particles (Fig. 6b). Thus, the protection by the ‘mineral matrix’ is an operative mode of preservation at both sites but shows two different features depending on the core:

- In the shallow water core, mineral–OM association microfabrics occur as large clay or carbonate aggregates (pellets) of a few μm in

diameter and containing discrete OM blebs of 0.1 μm in size as observed by Ransom et al. (1998b) in samples from the nepheloid layer offshore California. Those pellets are typically observed in sample 120 (Fig. 5E and F)

- In the deep water core, the organo-mineral association is formed by apparently undifferentiated microaggregates (Fig. 5G–J). High magnification ($\times 80,000$) highlights, however, the ultrastructure of the micro-aggregates and reveals that OM is intimately associated with the surface of the clays as well as being in the interlayer spaces (Fig. 5I and K). The clay sheets appear completely embedded within the OM, contrasting with the monolayer clay–OM association traditionally described by Mayer (1994) or Collins et al. (1995), among others. Some pale flecks, tens of nm in size, are also seen in the highly magnified TEM images of deep core samples 1343 and 1513 (Fig. 5G). EDS pin-point analysis of these particles shows the elements of clays and carbonates, which is surprising considering the classic dark appearance of these minerals under an electron beam. We presently do not know if those particles contain any organic compounds or how they have resisted HF/HCl leaching.

OM aggregates were also observed by SEM in recent upwelling sediments from the northwest African slope. Their formation was ascribed to the degradation–recondensation process (Zegouagh et al., 1999). However, when viewed by TEM, this isolated OM appeared nanoscopically amorphous and resembled the NAOM

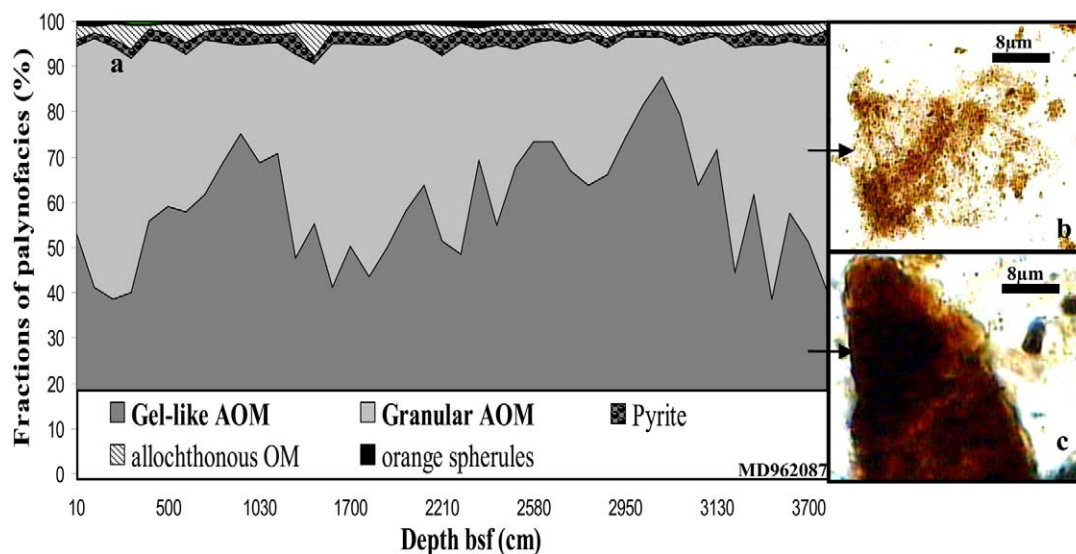


Fig. 4. Light microscopy observations of the isolated OM from MD972087. (a) Palynofacies composition (in% of slide area), (b) Granular Amorphous OM, (c) Gel-like Amorphous OM.

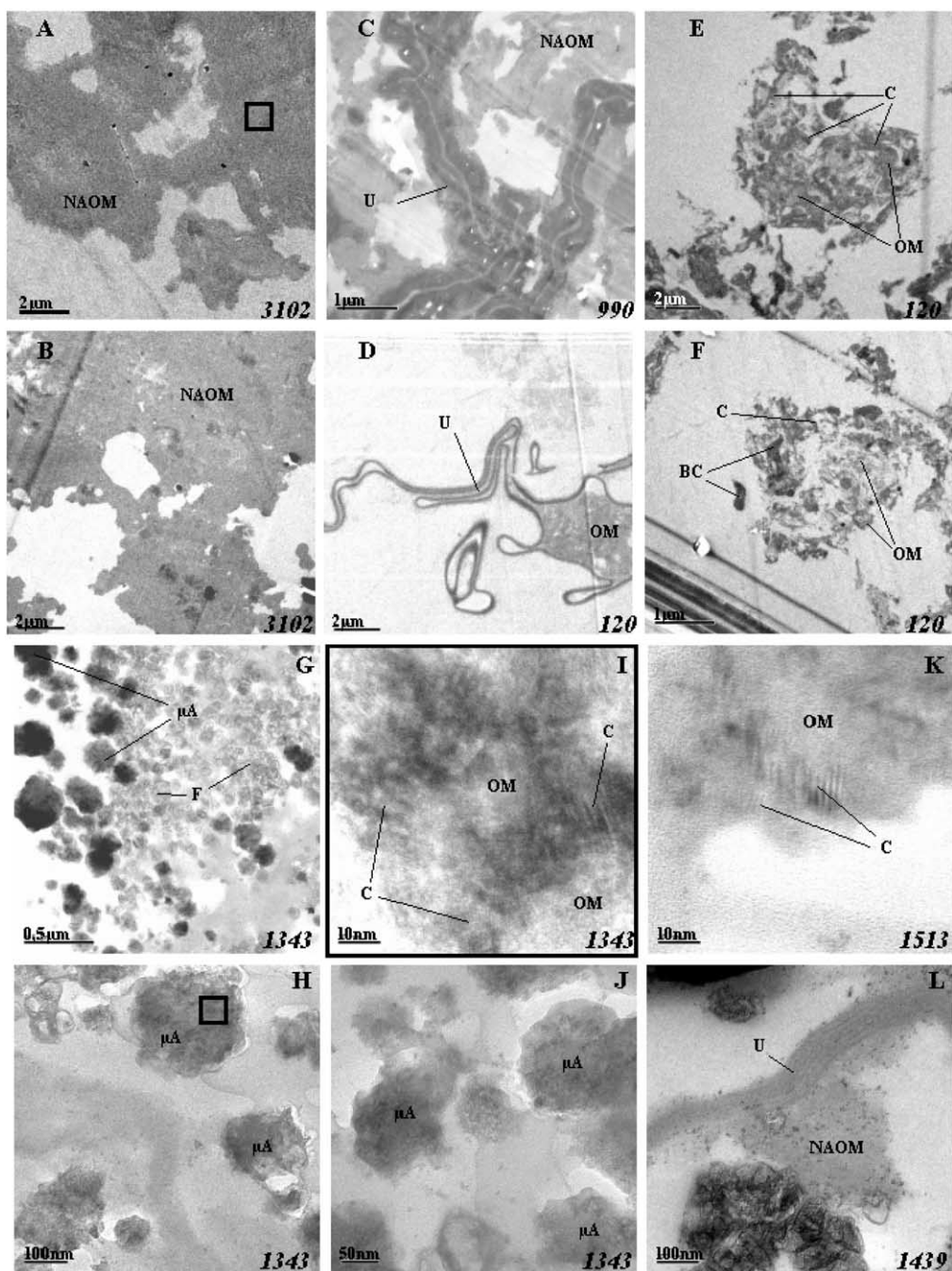


Fig. 5. TEM observations of isolated OM from the shallow core (A–F) and the deep core (G–L). Nanoscopically amorphous organic matter (NAOM) is the major constituent of samples 3102 and 990 (A, B and C). Typical upper slope aggregates involving organic matter (OM), clay (C) and bioclasts (BC) from sample 120 are shown on pictures E and F. Ultralaminar (U) are minor constituents of samples 990 (C) and 120 (D). On the lower slope, NAOM is scarce (L) whereas micro-aggregates (μ A) dominate in the three samples: 1343 (G–J), 1439 (L) and 1513 (K). Pictures G, H, J, I and K show the structure of the microaggregates at increasing magnifications. Microaggregates appear homogenous on pictures G, H and J. Higher magnification, however, reveals the ultrastructure of the aggregates: clay lattices are embedded in OM (I and K). (F) indicates 'pale flecks'. The black squares indicate the areas where EDS analyses were performed.

shown on Fig. 5L. Aggregates from both the upper and the lower Namibian slope result from organo-mineral associations. NAOM formation, on the other hand, is ascribed to the sulfurization mechanism. However, considering the nanoscopically amorphous texture of melanoidin compounds (Zegouagh et al., 1999), we cannot dismiss the possibility that the degradation–recondensation mechanism also contributed to NAOM formation.

5.4. Oxygenation index (*I_{ox}*) inferred from infrared spectroscopy

Infrared spectra show the distribution of major chemical bonds and their modes of vibration (Rouxhet et al., 1980). Subsequent to palynofacies description, 23 samples of isolated OM were analysed by FTIR. All exhibit essentially the same absorption bands, but the relative intensities differ, as shown in Fig. 7 and as described as follows:

OM from the upper slope core (15 samples) has a broad band around 3430 cm^{-1} , characteristic of OH and molecular water stretching vibrations. Although the highly hydrophilic pellets were dried in a desiccator in order to avoid the effect of moisture, water was not efficiently removed from the KBr. As a result, the intensity of the band at 3430 cm^{-1} does not reflect the OH group abundance in OM. At 2930 and 2860 cm^{-1} , a well defined double band is due to the asymmetric and symmetric stretching of alkyl groups (CH_2 , CH_3). Bending bands of CH_2 and CH_3 are seen around 1455 cm^{-1} and CH_3 bending at about 1380 cm^{-1} . Around 1710 cm^{-1} , a peak indicating the presence of $\text{C}=\text{O}$ bonds from carbonyl and/or carboxyl functions appears as a shoulder on the 1630 cm^{-1} band. This latter band is ascribed to $\text{C}=\text{C}$ stretching of aromatics and alkene double bonds. All the IR spectra of the upper slope OM are similar irrespective of the TOC content and the relative amount of NAOM/aggregates in the samples.

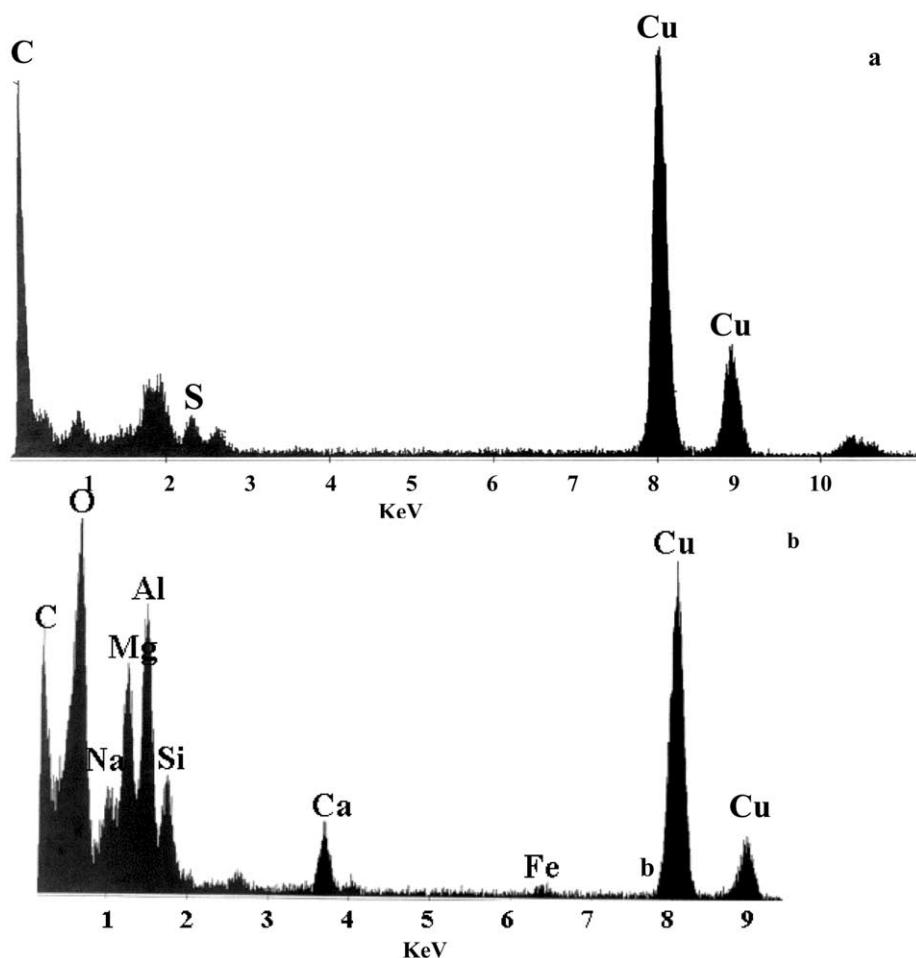


Fig. 6. Typical EDS pin point analyses showing major constituent elements of (a) NAOM and (b) aggregates. The peaks at 8 and 9 keV are due to the copper mount used for the ultrathin-sections.

Infrared spectra of the isolated OM from MD 962086 also show the above absorption bands but their relative intensity and shape differ from those of the shallow core spectra and vary according to TOC content and the petrographic composition of the samples. OM corresponding to organic-poor samples with low NAOM/aggregates ratios and slightly higher detrital OM contents yields weak alkyl bands and comparatively intense bands at 1630 cm^{-1} . Furthermore, an extra band around 1095 cm^{-1} is visible on all the spectra and corresponds to Si–O bonds typical of opal and clay crystals.

In order to constrain the differences between the IR absorptions and to assess the oxidation level of the OM, we calculated the I_{ox} parameter (modified from Benalioulhaj and Trichet, 1990) as follows:

$$I_{ox} = \frac{\text{maximum absorption of } 1710\text{--}1630\text{ cm}^{-1}\text{ band}}{\text{maximum absorption of } 2900\text{ cm}^{-1}\text{ double band}}$$

Clays and opal yield a band around 1600 cm^{-1} , which may result in an overestimation of the C=C, C=O stretching absorption intensity and hence affect I_{ox} significance. However, this peak is one order of magnitude less intense than the peak around 1095 cm^{-1} . Thus, we

assume that the overestimation of the C=C, C=O band at $1700\text{--}1630\text{ cm}^{-1}$ is low and does not invalidate I_{ox} significance.

Spectra from the shallow core are relatively invariant; consequently, I_{ox} is constant (Fig. 7, inset). This pattern is not surprising given the consistent petroleum quality observed in the core. In contrast, I_{ox} of the lower slope OM is higher than for the upper slope and generally increases as the TOC content decreases. In the light of the Rock-Eval results, we suggest that the OM is more oxidized when accumulated on the lower slope than on the upper slope.

6. Implications

Two main preservation processes have acted on the Luderitz slope with particular effectiveness and to a variable extent according to water depth and climate change.

6.1. Preservation processes: effects on OM quality

Organic matter from the shallow core appears mainly as NAOM, which is at least partly related to sulfuriza-

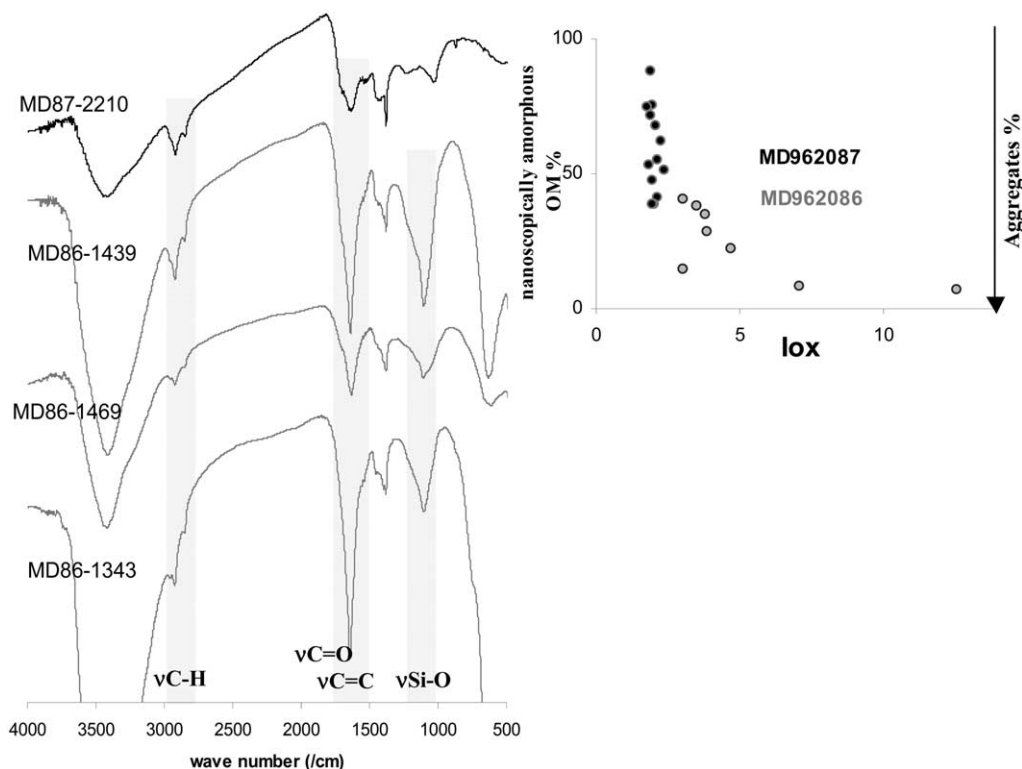


Fig. 7. FTIR spectra of isolated OM from MD962086 and MD962087. NAOM content of samples 2210, 1439, 1469 and 1343 are 51, 37.7, 28.5 and 8%, respectively, and TOC content before HF/HCl treatment were 6.7, 7.2, 2 and 1.6 wt.%. I_{ox} are expressed versus NAOM contents, as % of palynofacies. One sample does not follow the trend and shows a lower NAOM contribution (14%) than expected considering the TOC content (2.95 wt.%) of the bulk sediment.

tion. Adam et al. (2000) have reported the occurrence of sulfurization during early diagenesis off Walvis Bay. In addition, the 'degradation-recondensation' mechanism (Tissot and Welte, 1984) may have contributed to NAOM formation here. Organo-mineral associations and ultralaminae also exist on the upper slope, as shown by TEM observation, but they are minor constituents of the total OM. On the upper slope, the OM shows a consistently good petroleum quality (HI of 450 mg/g) and a low level of oxidation as evidenced by the low Iox and OI values. High contributions of sulfurized lipids on the upper slope can explain the good petroleum quality of the OM. Moreover, variations in the contribution of aggregates neither alter the petroleum quality nor enhance the oxidation level of the total OM. On the upper slope, both aggregation and sulfurization appear capable of preventing oxidation. Organic compounds deriving from degradation-recondensation processes have a low petroleum quality and presumably account for a minor fraction of the OM.

In the lower slope core, protection by aggregation is dominant. Sulfurization (and/or degradation-recondensation) does not play a major role, except for a few organic-rich levels from glacial isotopic stages 2–4 and 6, which have comparatively good petroleum quality and low extent of oxidation. Whether or not the good petroleum quality of these samples is related to the better efficiency of the sulfurization process compared to aggregation is debatable. Low sea level stands during glacial times may imply an offshore displacement of the upwelling cell and a faster export of OM to deep sites (Mollenhauer et al., 2002). Therefore, the duration of exposure to oxic respiration for OM reaching a given

depth was probably shorter during glacial periods than during high sea level stands. An alternative explanation would be related to the redox conditions at the sediment-water interface: enhanced melanoidin formation (by degradation-recondensation of saccharide and protein monomers) and decreased sulfurized lipid synthesis probably occurred during periods of low sulfate reduction, i.e. low OM flux to the sea floor. Variations in Iox and HI may be due to the predominance of melanoidin over organic sulfur compounds in NAOM rather than to an increased aggregates/NAOM ratio.

6.2. Relative contribution of different preservation processes: influence of organic and mineral fluxes

The percentage of organic carbon (OC) in the form of NAOM and aggregates (wt% bulk sediment) is shown on Figs. 8 and 9. The values were calculated by multiplying TOC content by the gel-like AOM contribution and the granular AOM (aggregates) contribution, respectively, determined using light microscopy. The percentage of OC protected by association with minerals is almost constant through time and between the two cores (0–4%), irrespective of TOC. NAOM contents vary, however, from almost 0 to >15% and are linearly correlated with TOC (Fig. 8). This suggests that factors controlling the occurrence of sulfurization reactions and the formation of aggregates are different.

At both sites, the percentage of NAOM is greater during glacial periods (Fig. 9), when export fluxes to the slope were enhanced due to high primary productivity and/or low sea level stand (Mollenhauer et al., 2002). This could indicate that the effectiveness of NAOM

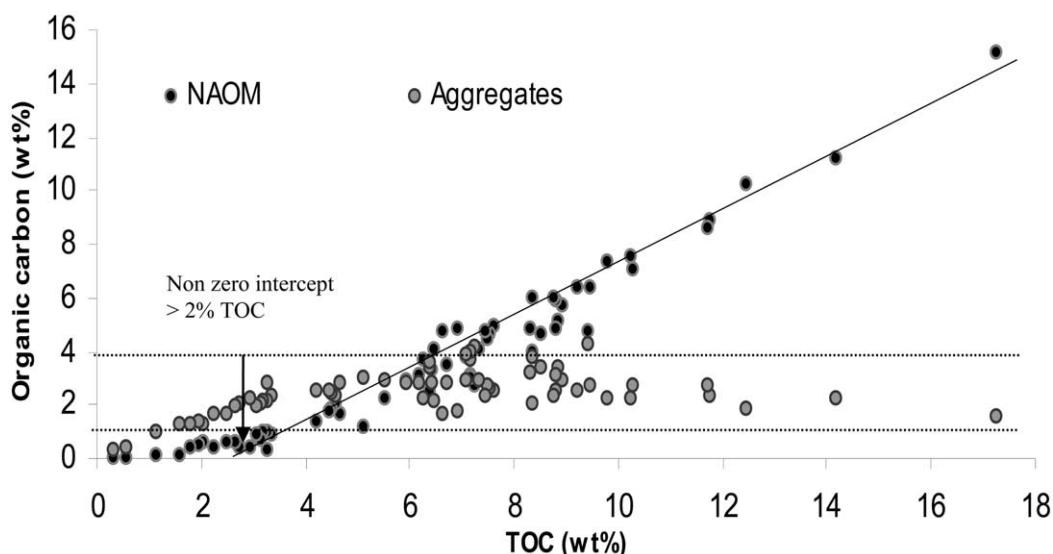


Fig. 8. Organic carbon (wt.% of bulk sediment) in the form of NAOM (black) and aggregates (grey) vs. TOC (wt.%); results from both cores are plotted together. NAOM is clearly correlated with TOC, while aggregates are invariant over the whole TOC range.

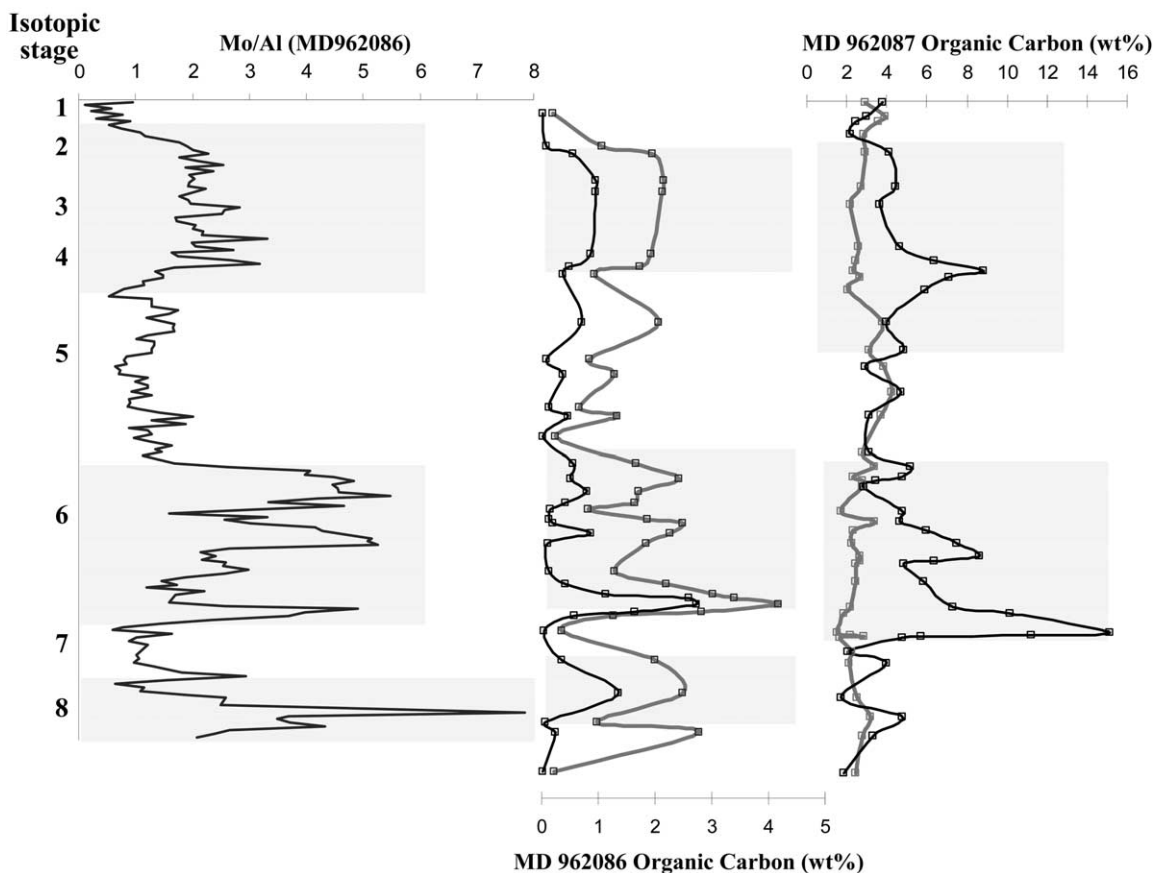


Fig. 9. Variation through time of TOC concentration (wt.% of bulk sediment) in the form of NAOM (black) and aggregates (grey) for MD 962087 and MD 962086. Also shown is the Mo:Al record of MD 962086, which can be interpreted as evidence of oxygen depletion in the surface sediments (Bertrand et al., 2002). Grey bands indicate glacial periods.

formation depends, here, on the flux of labile OM reaching the sea floor. High OM fluxes drive intense oxygen utilization, accelerating the establishment of sulfidic conditions and hence the activation of sulfurization. The Mo:Al record (Bertrand et al., 2002, Fig. 9) of MD962086 suggests that the first centimetres of the sediment were depleted in oxygen during glacial periods and particularly during stage 6 (Crusius et al., 1996). This indicates that labile OM fluxes were enhanced at this time and sufficient to enable sulfurization even on the lower slope. Considering that upwelling perennially occurred over the shelf and upper slope (Lutjeharms and Meeuwis, 1987; Dingle et al., 1996), we suggest that the redox conditions in the sediment were always favourable for sulfurization in the shallow-water core (Lückge et al., 1996). As a result, sulfurized lipids always dominate the NAOM in the upper slope. In addition, we consider that the degradation–recondensation process was also involved in NAOM formation, as previously emphasized. During periods of high fluxes of labile OM to the lower slope, the proportion of sulfur-

ized lipids in the NAOM increased in response to enhanced bacterial sulphate reduction. As a corollary, melanoidin contribution to NAOM formation probably increased during periods of moderate OM flux to the lower slope. This could explain the high I_{ox} recorded during interglacial periods. Moreover, a substantial export flux is required to enable accumulation of organic matter as NAOM rather than aggregates, as suggested by the non-zero intercept (TOC > 2%) shown in Fig. 8.

Aggregates occur in almost the same proportion at both water depths (between 0 and 4%). The abundance in the shallow-water core is quite constant over time and is clearly independent of climate-related changes in OM flux, in contrast to NAOM formation, which does apparently vary with OM flux. Like many authors (Mayer et al., 1988; Keil et al., 1994a,b; Ransom et al., 1997, 1998a), we propose that the proportion of OC associated with the mineral fraction depends on the abundance of siliciclastic minerals (such as clays) and diatom frustules at the sediment–water interface and in

the water column during deposition. Calculated percentages of OC involved in aggregates are correlated with biosilica + clay contents (Fig. 10) in the lower slope core; no correlation was found for the shallow core. The potential effect of carbonates in aggregation cannot be accurately estimated because of the intense diagenetic dissolution of this fraction. In addition, the collision frequency between particles and their stickiness related to the abundance of transparent exopolymer particles in sea water (Passow, 2002) may play an important role that is difficult to assess using sediment records.

6.3. Limitation of aggregation

In the study area, protection by minerals seems to be unable to protect more TOC than 4% of the bulk sediment, even when OM fluxes were high (Fig. 8). During stage 6.6, for example, OM is mainly preserved through sulfurization (and/or degradation-recondensation), whereas organo-mineral associations only account for a few percent of the TOC. In the literature, only rare examples show cases of OM–mineral associations which permit TOC accumulation higher than 5% (see Salmon et al., 2000 and Keil et al., 1994b for exceptions). This suggests that, in the absence of other preservation pathways, the potential for aggregation (itself limited by mineral particle abundance and collision) to enhance OM accumulation is limited under high rates of organic matter supply. Although recent studies show that thickening of OM particles tied to clay plates can enhance the preservation potential of minerals without increasing the surface occupied by OM (Bock and Mayer, 2000; Arnarson and Keil, 2001), our results suggest a plateau in the effect of aggregation on OM accumulation, in the case of high OM supply.

On the lower slope, the formation of aggregates is limited, first by OM supply in case of low organic fluxes (OC in form of aggregates increases with TOC increasing from 0 to 4 wt.%, Fig. 8) and second, by mineral availability when organic matter delivery exceeds the loading ability of minerals. At the upper slope, contrary to the lower one, organic fluxes are never limiting. This would explain the apparent climate-driven variation in aggregate content in the deep sediments and the absence of such changes in the shallow sediments (Fig. 9).

6.4. Aggregate formation

Aggregates begin to form during sinking in the water column, as discussed by Alldredge and Silver (1988). Traditionally, aggregation is defined as the process by which faecal matter, microorganisms and mineral particles clump together to form larger particles that settle rapidly (McCave, 1984; Alldredge and Silver, 1988). Hence, OM protection in mineral matrices probably begins in the surface layer. As a result, the percentage of OM preserved in the form of aggregates is almost equivalent at 1029 and 3606 m, and is independent of water depth and sinking time. Furthermore, in the case of low organic flux on the lower slope (during the Holocene and Eemian) only mineral–OM aggregates are seen in the sediments, while non-aggregated OM is almost completely absent. Non-ballasted OM has probably undergone drastic degradation in the water column due to the greater vulnerability and/or the slower sinking velocity of these particles. We propose that the aggregates observed on both the upper and lower slope originate from the pellets and marine snow that form in the water column, although disaggregation and re-aggregation phenomena in the benthic boundary layer

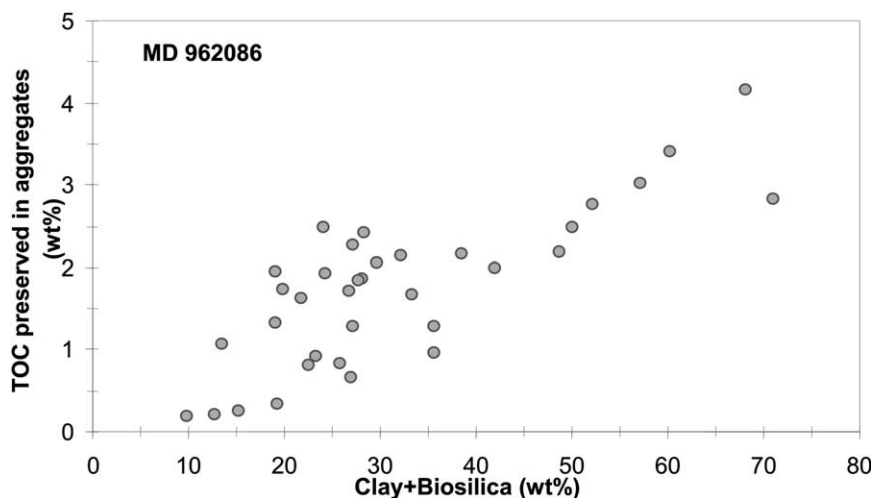


Fig. 10. TOC (wt.% of the bulk sediment) preserved by aggregation with minerals is weakly correlated with the Clay + Biosilica contents (wt.%) for the deep core. No correlation was found for the shallow core.

probably occurred before burial and modified the structure of the aggregates (Ransom et al., 1998b). Marine snow is known to be fragile and prone to break-up in the benthic boundary layer (Thomsen and McCave, 2000). However, in case of low shear velocity ($<1.6 \text{ cm s}^{-1}$) close to the sea floor, re-aggregation is promoted (Thomsen and McCave, 2000). Moreover, high sedimentation rates, such as those observed on the Namibian slope, enhance the burial efficiency of aggregates (Thomsen et al., 2002).

The size of water column aggregates depends on their 'age' (settling time) and on the concentration and types of discrete particles sinking in the surface, pelagic and nepheloid layers (Alldredge, 1998). According to Ransom et al. (1998b), a thick nepheloid layer facilitates aggregation, disaggregation and re-aggregation phenomena. Morphological differences between the upper and lower slope aggregates are clear: lower slope aggregates are smaller and denser (Fig. 5H) than those from the upper slope (Fig. 5E and F). This could be explained by the small size and sparseness of marine snow at the deep location and/or by the reduction of nepheloid layer thickness at greater depth (Giraudeau, personal communication). Both factors result from reduced productivity and OM flux off shore compared to near shore.

Also, the clay–OM association observed at 3606 m water depth and shown on the TEM micrographs, does not appear as patches or coating of organic compounds on clay particles: the clay crystals seem embedded in the amorphous OM. A so far undescribed pattern of aggregation between clay and OM may be displayed here, but further investigations are needed.

7. Conclusions

The application of different and complementary methods to a large number of samples and over extensive ranges of depth and time gives detailed information on the OM accumulated off Lüderitz and some insight into the factors and processes that mediate its preservation:

1. Biological structures, as cell walls and ultralaminae, related to the selective preservation mode, are observed at both sites but constitute a minor form of preserved OM on the slope.
2. Protection by aggregation with minerals occurs on both the lower and upper slopes but shows different features depending on depth. We suggest that this OM acquires resistance to degradation as aggregates formed during sinking. Aggregation appears to be an efficient preservation mode on the lower slope.
3. NAOM formation results from sulfurization and, presumably, degradation–recondensation reactions. NAOM accumulation depends on OM flux which controls the establishment of favourable suboxic conditions at the interface. This type of preserved OM dominates on the upper slope.

Lüderitz slope sediments are particularly rich in OM thanks to high surface productivity resulting from perennial upwelling, but also due to the occurrence of different OM preservation mechanisms operating in the sediment, at the sediment interface and presumably, during sinking. Two dominant preservation modes are recognized. Each yields particular forms of preserved OM which show a characteristic distribution on the slope. It is striking that preservation by organo-mineral association, although consistently operative through time at both depths, accounts for a relatively minor part of the OM accumulated on this organic-rich slope. It thus appears that, in the case of high organic fluxes, protection by aggregation has a limited effect on OM accumulation. Supplementary preservation mechanisms are required to permit TOC contents higher than $\sim 4\%$ in the sediment at this location.

Acknowledgements

This study was carried out within the framework of a collaboration between the Institut Français du Pétrole (IFP), the Museum National d'Histoire Naturelle de Paris, the Département de Géologie et Océanographie de Bordeaux and the Laboratoire de Géologie de la Matière Organique d'Orléans. Total Fina Elf provided the financial support. The cores were retrieved during NAUSICAA cruise (IMAGE II) with the R/V Marion Dufresne, which was made available by IPEV. The authors are grateful to D. Keravis for technical assistance in performing Rock-Eval analyses and to F. Frölich for help in interpretations of FTIR spectra. We also thank E. Galbraith for editing and improving the english version and Drs. S. Wakeham and Y. Furukawa for constructive comments.

Associate Editor—Claude Largeau

References

- Adam, P., Schneckenburger, P., Schaeffer, P., Albrecht, P., 2000. Clues to early diagenetic sulfurization processes from mild chemical cleavage of labile sulfur-rich geomacromolecules. *Geochimica et Cosmochimica Acta* 64, 3503–3585.
- Allredge, A.L., Silver, M.W., 1988. Characteristic, dynamics

- and significance of marine snow. *Progress in Oceanography* 20, 41–82.
- Allredge, A., 1998. The carbon, nitrogen and mass content of marine snow as a function of aggregate size. *Deep-Sea Research I* 45, 529–541.
- Armstrong, R.A., Lee, C., Hedges, J.I., Honjo, S., Wakeham, S.G., 2002. A new, mechanistic model for organic carbon fluxes in the ocean based on quantitative association of POC with ballast minerals. *Deep-Sea Research II* 49, 219–236.
- Arnarson, T.S., Keil, R.G., 2001. Organic-mineral interactions in marine sediments studied using density fractionation and X-ray photoelectron spectroscopy. *Organic Geochemistry* 32, 1401–1415.
- Barange, M., Pillar, S.C., 1992. Cross-Shelf circulation, zonation and maintenance mechanisms of *nyctiphanes-capensis* and *euphausia-hanseni* (euphausiacea) in the Northern Benguela upwelling system. *Continental Shelf Research* 12, 1027–1042.
- Behrenfeld, M.J., Falkowski, P.G., 1997. Photosynthetic rates derived from satellite-based chlorophyll concentration. *Limnology and Oceanography* 42, 1–20.
- Benaliouhaj, S., Trichet, J., 1990. Comparative study by infrared spectroscopy of the organic matter of phosphate-rich (Oulad Abdoun basin) and black shale (Timadhit basin) series (Morocco). *Organic Geochemistry* 16, 649–660.
- Bertrand, P., Giraudeau, J., Malaizé, B., Martinez, P., Gallinari, M., Pedersen, T.F., Pierre, C., Venec-Peyré, M.-T., 2002. Occurrence of an exceptional carbonate dissolution episode during early glacial isotope stage 6 in the Southern Atlantic. *Marine Geology* 180, 235–248.
- Bertrand, P., Pedersen, T.F., Schneider, R., Shimmiel, G., Lallier-Vergès, E., Disnar, J.-R., Massias, D., Villanueva, J., Tribouillard, N., Huc, A.Y., Giraud, X., Pierre, C., Venec-Peyré, M.-T., 2003. Organic-rich sediments in ventilated deep-sea environments: relationship to climate, sea level, and trophic changes. *Journal of Geophysical Research* 108, 1–11.
- Bock, M.J., Mayer, L.M., 2000. Mesodensity organo-clay associations in a near-shore sediment. *Marine Geology* 163, 65–75.
- Boussafir, M., Lallier-Vergès, E., Bertrand, P., Badaut-Trauth, D., 1994. Structure ultrafine de la matière organique des roches mères du Kimmeridgien du Yorkshire (UK). *Bulletin of the Geological Society France* 165, 355–363.
- Boussafir, M., Gelin, F., Lallier-Vergès, E., Derenne, S., Bertrand, P., Largeau, C., 1995. Electron microscopy and pyrolysis of kerogens from the Kimmeridge Clay Formation, UK: source organisms, preservation processes, and origin of microcycles. *Geochimica et Cosmochimica Acta* 59, 3731–3747.
- Boussafir, M., Lallier-Vergès, E., 1996. Accumulation of organic matter in the Kimmeridge Clay Formation (KCF): an update fossilisation model for marine petroleum source-rocks. *Marine and Petroleum Geology* 14, 75–83.
- Calvert, S.E., Pedersen, T.F., 1993. Geochemistry of Recent oxic and anoxic marine sediments: Implications for the geological record. *Marine Geology* 113, 67–88.
- Canfield, D.E., 1993. Organic matter oxidation in marine sediments. In: Wollast, R., Mackenzie, F.T., Chou, L. (Eds.), *Interactions of C, N, P and S Biogeochemical Cycles and Global Changes*. NATO Series. Springer, Berlin, pp. 1–61.
- Collins, M.J., Bishop, A.N., Farrimond, P., 1995. Sorption by mineral surfaces: rebirth of the classical condensation pathway for kerogen formation? *Geochimica et Cosmochimica Acta* 59, 2387–2391.
- Crusius, J., Calvert, S., Pedersen, T., Sage, D., 1996. Rhenium and molybdenum enrichments in sediments as indicators of oxic, suboxic and sulfidic conditions of deposition. *Earth and Planetary Science Letters* 145, 65–78.
- Derenne, S., Le Berre, F., Largeau, C., Hatcher, P., Connan, J., Raynaud, J.F., 1991. Formation of ultralaminae in marine kerogens via selective preservation of thin resistant outer walls of microalgae. *Organic Geochemistry* 19, 345–350.
- Derenne, S., Largeau, C., Hetényi, M., Brukner-Wein, A., Connan, J., Lugardon, B., 1997. Chemical structure of the organic matter in a Pliocene maar-type shale: Implicated *Botryococcus* race strains and formation pathways. *Geochimica et Cosmochimica Acta* 61, 1879–1889.
- Dingle, R.V., Bremner, J.M., Giraudeau, J., Buhmann, D., 1996. Modern and palaeo-oceanographic environments under Benguela upwelling cells off southern Namibia. *Palaeogeography Palaeoclimatology Palaeoecology* 123, 85–105.
- Durand, B., Nicaise, G., 1980. Procedures for kerogen isolation. In: Durand, B. (Ed.), *Kerogen*. Technip, Paris, pp. 33–53.
- Espitalié, J., Deroo, G., Marquis, F., 1985. La pyrolyse Rock-Eval et ses applications; première partie. *Revue de l'Institut Français du Pétrole* 40, 563–579.
- Furukawa, Y., 2000. Energy-filtering transmission electron microscopy (EFTEM) and electron energy loss spectroscopy (EELS) investigation of clay-organic matter aggregates in aquatic sediments. *Organic Geochemistry* 31, 735–744.
- Giraudeau, J., Bailey, G.W., 1995. Spatial dynamics of coccolithophore communities during an upwelling event in the Southern Benguela system. *Continental Shelf Research* 15, 1825–1852.
- Hagen, E., Feistel, R., Agenbag, J.J., Ohde, T., 2001. Seasonal and interannual changes in Intense Benguela Upwelling (1982–1999). *Oceanologica Acta* 24, 557–568.
- Hedges, J.I., Keil, R.G., 1999. Organic geochemical perspectives on estuarine processes: sorption reactions and consequences. *Marine Chemistry* 65, 55–65.
- Hedges, J.I., Baldock, J.A., Gelin, Y., Lee, C., Peterson, M., Wakeham, S.G., 2001. Evidence for non-selective preservation of organic matter in sinking marine particles. *Nature* 409, 801–804.
- Hedges, J.I., Hu, F.S., Devol, A.H., Hartnett, H.E., Tsamakis, E., Keil, R.G., 1999. Sedimentary organic matter preservation: a test for selective degradation under oxic conditions. *American Journal of Science* 299, 529–555.
- Imbrie, J., Hays, J.D., Martinson, D.G., McIntyre, A., Mix, A.C., Morley, J.J., Pisias, N.G., Prell, W.L., Shackleton, N.J., 1984. The orbital theory of Pleistocene climate support from a revised chronology of the marine $\delta^{18}\text{O}$ record. In: Berger, A.L., Imbrie, J., Hays, J., Kukla, G., Saltzman, B. (Eds.), *Milankovitch and Climate*. D. Reidel, Norwell, MA, pp. 269–305.
- Keil, R.G., Montluçon, D.B., Prahl, F.G., Hedges, J.I., 1994a. Sorptive preservation of labile organic matter in marine sediments. *Nature* 370, 549–552.
- Keil, R.G., Tsamakis, E., Fuh, C.B., Giddings, J.C., Hedges, J.I., 1994b. Mineralogical and textural controls on the organic composition of coastal marine sediments: hydro-

- dynamic separation using SPLITT-fractionation. *Geochimica et Cosmochimica Acta* 58, 879–893.
- Kirst, G.J., Schneider, R.R., Müller, P.J., von Storch, I., Wefer, G., 1999. Late quaternary temperature variability in the Benguela current system derived from alkenones. *Quaternary Research* 52, 92–103.
- Kok, M.D., Schouten, S., Sinninghe-Damsté, J.S., 2000. Formation of insoluble, non hydrolyzable, sulfur-rich macromolecules via incorporation of inorganic sulfur species into algal carbohydrates. *Geochimica et Cosmochimica Acta* 64, 2689–2699.
- Largeau, C., Casadevall, E., Kadouri, A., Metzger, P., 1984. Formation of Botryococcus Braunii kerogens. Comparative study of immature torbanite and the extant alga Botryococcus Braunii. In: Schenk, P.A., de Leeuw, J.W., Lijmbach, G.W.M. (Eds.), *Advances in Organic Geochemistry 1983 Organic Geochemistry 8*. Pergamon Press, Oxford, pp. 327–332.
- Largeau, C., Derenne, S., Casadevall, E., Kadouri, A., 1986. Pyrolysis of immature Torbanite and of the resistant biopolymer (PRB A) isolated from extant alga Botryococcus Braunii. Mechanism of formation and structure of Torbanite. In: Leythaeuser, D., Rullkötter, J. (Eds.), *Advances in Organic Geochemistry 1985, Organic Geochemistry 10*. Pergamon Press, Oxford, pp. 1023–1032.
- Largeau, C., Derenne, S., Casadevall, E., Berkaloff, C., Corolleur, M., Lugardon, B., Raynaud, J.F., Connan, J., 1989. Occurrence and origin of 'ultralaminar' structures in 'amorphous' kerogens of various source rocks and oil shales. *Organic Geochemistry* 16, 889–895.
- Lückge, A., Horsfield, B., Littke, R., Scheeder, G., 2002. Organic matter preservation and sulfur uptake in sediments from the continental margin of Pakistan. *Organic Geochemistry* 33, 477–488.
- Lückge, A., Boussafir, M., Lallier-Vergès, E., Littke, R., 1996. Comparative study of organic matter preservation in immature sediments along the continental margins of Peru and Oman. Part I: Results of petrographical and bulk geochemical data. *Organic Geochemistry* 24, 437–451.
- Lutjeharms, J.R.E., Meeuwis, J.M., 1987. The extent and variability of South-East Atlantic upwelling. *South African Journal of Marine Science* 5, 51–62.
- Mayer, L.M., Rahaim, P.T., Guerin, W., Macko, S.A., Waltling, L., Adersen, F.E., 1985. Biological and granulometric controls on sedimentary organic matter of an intertidal mudflat. *Estuarine and Coastal Shelf Science* 20, 491–504.
- Mayer, L.M., Macko, S.A., Cammen, L., 1988. Provenance, concentration and nature of sedimentary organic nitrogen in the Gulf of Maine. *Marine Chemistry* 25, 291–304.
- Mayer, L.M., 1993. Organic matter at the sediment-water interface. In: Engel, M.H., Macko, S.A. (Eds.), *Organic Geochemistry Principles and Applications*. Plenum Press, London, pp. 171–184.
- Mayer, L.M., 1994. Surface area control of organic carbon accumulation in continental shelf sediments. *Geochimica et Cosmochimica Acta* 58, 1271–1284.
- Mayer, L.M., 1999. Extent of coverage of mineral surfaces by organic matter in marine sediments. *Geochimica et Cosmochimica Acta* 63, 207–215.
- McCave, I.N., 1984. Size spectra and aggregation of suspended particles in the deep ocean. *Deep-Sea Research I* 31, 329–352.
- Mollenhauer, G., Schneider, R.R., Müller, P.J., Spiess, V., Wefer, G., 2002. Glacial/interglacial variability in the Benguela upwelling system: Spatial distribution and budgets of organic carbon accumulation. *Global Biogeochemical Cycles* 16, 1–5.
- Mongenot, T., Derenne, S., Largeau, C., Tribouillard, N.P., Lallier-Vergès, E., Dessort, D., Connan, J., 1999. Spectroscopic, kinetic and pyrolytic studies of kerogen from the dark parallel laminae facies of the sulfur-rich Orbagnoux deposit (Upper Kimmeridgian, Jura). *Organic Geochemistry* 30, 39–56.
- Oades, J.M., 1988. The retention of organic matter in soil. *Bio-Geochemistry* 5, 35–70.
- Passow, U., 2002. Transparent exopolymer particles (TEP) in aquatic environments. *Progress in Oceanography* 55, 287–333.
- Ramanampisoa, L., Disnar, J.R., 1994. Primary control of paleoproduction on organic matter preservation and accumulation in the Kimmeridge rocks of Yorkshire (UK). *Organic Geochemistry* 21, 1153–1167.
- Ransom, B., Bennett, R.H., Bearwald, R., Shea, K., 1997. TEM study of in situ organic matter on continental margins: occurrence and the 'monolayer' hypothesis. *Marine Geology* 138, 1–9.
- Ransom, B., Dongseon, K., Kastner, M., Wainwright, S., 1998a. Organic matter preservation on continental slopes: importance of mineralogy and surface area. *Geochimica et Cosmochimica Acta* 62, 1329–1345.
- Ransom, B., Shea, K.F., Burkett, P.J., Bennett, R.H., Baerwald, R., 1998b. Comparison of pelagic and nepheloid layer marine snow: implications for carbon cycling. *Marine Geology* 150, 39–50.
- Rouxhet, P.G., Robin, P.L., Nicaise, G., 1980. Characterisation of kerogens and their evolution by infrared spectroscopy. In: Durand, I.F.P. (Ed.), *Insoluble Organic Matter from Sedimentary Rocks*. TECHNIP, Paris, pp. 163–190.
- Saint-Germes, M., Baudin, F., Bazhenova, O., Derenne, S., Fadeeva, N., Largeau, C., 2002. Origin and preservation processes of amorphous organic matter in the Maykop Series (Oligocene-Lower Miocene) of Precaucasus and Azerbaijan. *Bulletin de La Société Géologique de France* 175, 423–436.
- Salmon, V., Derenne, S., Lallier-Vergès, E., Largeau, C., Beaudoin, B., 2000. Protection of organic matter by mineral matrix in a Cenomanian black shale. *Organic Geochemistry* 31, 463–474.
- Schouten, S., vanDriel, G.B., Sinninghe Damsté, J.S., de Leeuw, J.W., 1994. Natural sulfurisation of ketones and aldehydes: A key reaction in the formation of organic sulfur compounds. *Geochimica et Cosmochimica Acta* 57, 5111–5116.
- Schulz, H.D., Dahmke, A., Schinzel, U., Wallmann, K., Zabel, M., 1994. Early diagenetic processes, fluxes, and reaction rates in sediments of the South Atlantic. *Geochimica et Cosmochimica Acta* 58, 2041–2060.
- Shannon, L.V., Nelson, G., 1996. The Benguela: large scale features and processes and system variability. In: Wefer, G., Berger, W.H., Siedler, G., Webb, D. (Eds.), *The South Atlantic Ocean, Present and Past Circulation*. Springer, Berlin, pp. 163–210.
- Sinninghe-Damsté, J.S., Ripjstra, W.I.C., Kock-van Dalen, A.C., de Leeuw, J.W., Schenck, P.A., 1989. Quenching of labile functionalized lipids by inorganic sulfur species:

- Evidence for formation of sedimentary organic sulfur compounds at the early stage of diagenesis. *Geochimica et Cosmochimica Acta* 53, 1343–1355.
- Stuiver, M., Reimer, P.J., Bard, E., Beck, J.W., Burr, G.S., Hughen, K.A., Kromer, B., McCormick, G., van der Plicht, J., Spurk, M., 1998. INTCAL98 radiocarbon age calibration, 24,000-0 cal BP. *Radiocarbon* 40, 1041–1083.
- Suess, E., 1973. Interaction of organic compounds with calcium carbonates, II. Organo-carbonate associations in recent sediments. *Geochimica et Cosmochimica Acta* 37, 2435–2447.
- Tegelaar, E.W., de Leeuw, J.W., Derenne, S., Largeau, C., 1989. Reappraisal of kerogen formation. *Geochimica et Cosmochimica Acta* 53, 3103–3106.
- Thomsen, L., vanWeering, T., Gust, G., 2002. Processes in the benthic boundary layer at the Iberian continental margin and their implication for carbon mineralization. *Progress in Oceanography* 52, 315–329.
- Thomsen, L.A., McCave, I.N., 2000. Aggregation processes in the benthic boundary layer at the Celtic Sea continental margin. *Deep-Sea Research Part I-Oceanographic Research Papers* 47, 1389–1404.
- Tissot, B.P., Welte, D.H., 1984. *Petroleum, Formation and Occurrence*. Springer, Berlin.
- Wakeham, S., Sinninghe-Damsté, J.S., Kohnen, M.E.L., de Leeuw, J.W., 1995. Organic sulfur compounds formed during early diagenesis in the Black Sea. *Geochimica et Cosmochimica Acta* 59, 521–533.
- Wakeham, S.G., Lee, C., Hedges, J.I., Hernes, P.J., Peterson, M.L., 1997. Molecular indicators of diagenetic status in marine organic matter. *Geochimica et Cosmochimica Acta* 61, 5363–5369.
- Zegouagh, Y., Derenne, S., Largeau, C., Bertrand, P., Sicre, M.A., Saliot, A., Rousseau, B., 1999. Refractory organic matter in sediments from the North-West African upwelling system: abundance, chemical structure and origin. *Organic Geochemistry* 30, 101–117.



ELSEVIER

Available online at www.sciencedirect.com

SCIENCE @ DIRECT®

Palaeogeography, Palaeoclimatology, Palaeoecology 205 (2004) 183–197

PALAEO

www.elsevier.com/locate/palaeo

Research Papers

Major environmental changes recorded by lacustrine sedimentary organic matter since the last glacial maximum near the equator (Lagoa do Caçó, NE Brazil)

Jérémy Jacob^{a,*}, Jean-Robert Disnar^a, Mohammed Boussafir^a,
Abdelfettah Sifeddine^{b,c}, Bruno Turcq^c, Ana Luiza Spadano Albuquerque^b

^aLaboratoire de Géochimie Organique, Institut des Sciences de la Terre d'Orléans (ISTO)-UMR 6113 du CNRS, Bâtiment Géosciences, 45067 Orléans Cedex 2, France

^bDepartamento de Geoquímica, Universidade Federal Fluminense, Morro do Valonguinho s/n, 24020-007, Niteroi, RJ, Brazil

^cIRD/Bondy, 32 avenue Henry Varagnat, 93143 Bondy Cedex, France

Received 1 October 2002; received in revised form 2 December 2003; accepted 5 December 2003

Abstract

Sediment samples collected along a 6-m core, drilled in the deepest part of the Lagoa do Caçó (NE Brazil), have been investigated in order to determine source(s) and degradation conditions of the organic matter (OM) with special emphasis on paleoenvironmental implications. Bulk organic geochemistry (Rock-Eval pyrolysis, C/N determination, $\delta^{13}\text{C}$ and $\delta^{15}\text{N}$ measurement) and petrography combined with sedimentological evidence and radiocarbon dates allowed to identify four major intervals documenting major environmental changes that occurred during the last 20,000 years. The first interval, dating back to the end of the Last Glacial Maximum (LGM), contains well-preserved OM derived from higher plants. This material was most probably produced in an ephemeral palustrine system and rapidly buried by sands. This level is thought to have been deposited under relatively arid climate conditions associated with strong but episodic rainfalls. Between 19,240 and 17,250 Cal years BP, the climate appears to have been more humid and seasonality more pronounced as suggested by the presence of a permanent lake. After a drastic environmental change dating back to 17,250 Cal years BP, the sediment became truly lacustrine with restricted mineral input and highly degraded higher plant-derived organic matter. After that, a stepwise improvement in the preservation of OM occurred, as revealed by several pronounced shifts in the Rock-Eval TpS2 signal. These changes could document abrupt climatically driven changes during the Late Glacial. Finally, around 5610 Cal years BP, environmental conditions, approaching those prevailing today were established. Minor climatic changes during the Holocene were probably buffered by a high water table which might explain the lack of paleoenvironmental fluctuations.

© 2004 Elsevier B.V. All rights reserved.

Keywords: Brazil; Lacustrine organic matter; Paleoenvironments; Paleoclimate; Rock-Eval; Organic petrography

1. Introduction

Recent studies in tropical South America (Thompson et al., 1995; Sifeddine et al., 1998, 2001; Colinvaux et al., 1996; Behling et al., 2000; Ledru

* Corresponding author. Laboratoire des Sciences du Climat et de l'Environnement (LSCE), Bât 12, Domaine du CNRS, Avenue de la Terrasse, F-91198 Gif-sur-Yvette Cedex, France. Tel.: +33-1-69-82-35-12; fax:33-1-69-82-35-68.

E-mail address: jeremy.jacob@lsce.cnrs-gif.fr (J. Jacob).

et al., 2001, 2002) have improved our knowledge of past environmental changes and their driving mechanisms in this area. Nevertheless, major controversies still remain, for example, on the respective contribution of the InterTropical Convergence Zone (ITCZ) and polar advectons on regional climate variability (Ledru et al., 2002). These controversies emphasize the need to document better the climatic fluctuations that affected this area since the last glacial maximum (LGM). New analytical approaches applied on new records are needed in order to enhance our understanding of the nature, the extent and the origin of past paleoclimatic fluctuations. OM analyses have now proven their utility for paleoenvironmental reconstructions, in particular in lacustrine sedimentary records in temperate areas (Lallier-Vergès et al., 1993; Meyers and Lallier-Vergès, 1999; Manalt et al., 2001; Sifeddine et al., 1996), but rarely in tropical settings (Talbot and Livingstone, 1989; Street-Perrott et al., 1997; Sifeddine et al., 1998, 2001; Ficken et al., 1998; Huang et al., 1999). Sedimentary lacustrine series are attractive targets to document paleoenvironmental changes because they generally offer high temporal resolution due to high sedimentation rates. In addition and in contrast to high latitudinal settings which receive little or almost no organic input during glacial times, tropical settings might have benefited of a more favourable climate during such periods leading to a more continuous record of vegetation change in the drainage area. Located at the present southernmost limit of seasonal displacement of the ITCZ, near the Atlantic and on the border of the Amazon Basin, Lagoa do Caçó is in a key area to document paleoclimatic changes that affected the tropical South America. The lake record also lends itself especially well to record sedimentary OM. This study presents the results obtained from OM analyses carried out on a 6-m-long core covering nearly 20,000 years of sedimentation. Abundance, origin and quality of the OM are discussed and temporal fluctuations interpreted in terms of paleoenvironmental changes.

2. Study site

Lagoa do Caçó is located in northeastern Brazil (Maranhão State), about 80 km from the Atlantic coast

and close to the equator (2°58' S, 43°25' W and 120 m above sea level). The local present-day climate is tropical humid with pronounced seasonality. Precipitation, which annually reaches 1750 mm on average, mostly occurs during the rainy season, from November to May. The mean annual temperature is 26 °C. Located on the edge of the Amazon Basin, the vegetation in this region displays a strong zonation ranging from Restinga (grass steppe) near the coast, to Cerrado (shrub savanna) inland followed by Cerradao (woody savanna) in the more humid regions (Ledru et al., 2002). The lake (ca. 2.5 km² surface area) is enclosed in an SW–NE-oriented former river valley within a dune field dating back to Pleistocene times. The maximum water depth is 10 m during the wet season (austral summer) and 9 m during the dry season (austral winter). The opposite flow direction of the tributary river (from SW) and the trade winds (from N) results in a constant mixing of the water column. Today, the lake is oligotrophic to meso-oligotrophic. In fact, only few phytoplankton taxa live in the water column. Most of the organic production originates from semi-emerged plants (*Juncus* sp. highly dominant) growing around the lake at about 1–3 m water depth and from submerged plants. Attached to the rushes, some diatoms can be found as well as a unique species of sponge (*Metania spirata*; Volkmer-Ribeiro, personal communication). The rushes prevent almost all mineral transport from the sandy banks into the lake but export a part of their own production to the lake. A more than 2-m-thick floating meadow occupies the river inflow and filters most of mineral and organic influx from the small tributary. Thus, inorganic sedimentation is primarily derived from aeolian particles and authigenic minerals.

3. Sampling and methods

3.1. Sampling

Twin sedimentary cores 98-3 and 98-4 (6 m each) have been drilled with a vibracorer (Martin et al., 1995), less than 1 m apart, in the deepest part of the lake (Fig. 1). Samples were taken every 2 cm from 17 to 594 cm depth on core 98-3 and from 0 to 583 cm on core 98-4. The samples were dried at 40 °C in an oven and then crushed and stored.

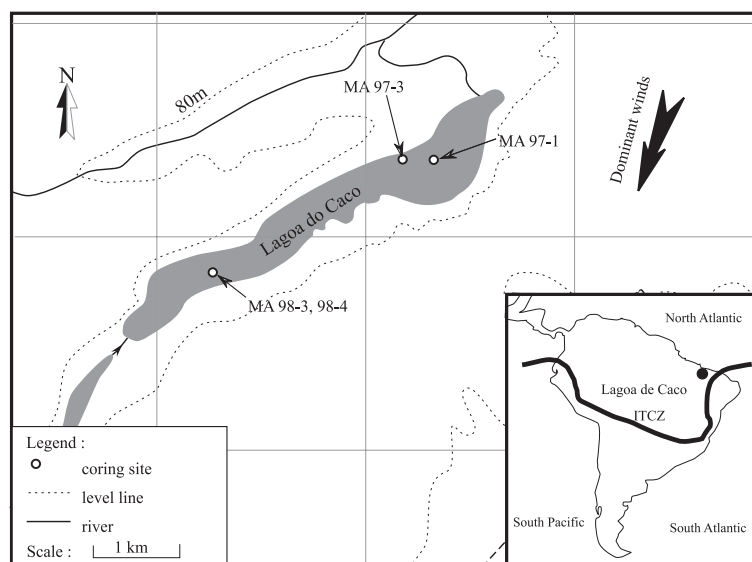


Fig. 1. Map of study area with location of coring sites.

3.2. Organic petrography

About 1 g of sediment was treated with HCl and HF to remove the mineral matrix. The resulting organic residues were then observed by natural transmitted light microscopy. Over 1000 surface units of particles were counted to estimate the relative proportions of each organic fraction. Distinction of hydrocarbon-rich fractions was achieved under UV excitation, and iron sulphides were recognized under natural reflected light.

3.3. Bulk organic geochemistry

3.3.1. Rock-Eval pyrolysis

Between 50 and 100 mg of dried sediments from core 98-3 were used for Rock-Eval6 (RE6) analysis, depending on the estimated OM content. The pyrolysis program starts with an isothermal stage of 2 min at 200 °C. Then, the pyrolysis oven temperature was raised at 30 °C/min to 650 °C, and held for 3 min at this temperature. The oxidation phase, performed in a second oven under an air stream, starts at an isothermal stage at 400 °C, followed by an increase to 850 °C at 30 °C/min and held at final temperature for 5 min.

Rock-Eval parameters have been described by Espitalié et al. (1977). Specific parameters provided

by the new RE6 device are presented by Lafargue et al. (1998). The Rock-Eval parameters we used for this study are the following ones: (i) mineral carbon (Minc) which represents the amount of inorganic carbon (from carbonates) released during pyrolysis and oxidation; (ii) total organic carbon (TOC, %) accounts for the quantity of organic matter (OM) present in the sediment; (iii) hydrogen index (HI, in mg HC/g TOC) is the amount of hydrocarbonaceous (HC) products released during pyrolysis (integrated from the S2 peak, in mg HC/g dry sediment) normalized to TOC; (iv) T_{max} is a well-known OM maturity indicator in ancient sediments (Espitalié et al., 1985b). It is the temperature of the pyrolysis oven recorded at the top of peak S2, which thus corresponds to the maximum release of hydrocarbonaceous products during pyrolysis, carried at 25 °C/min in previous Rock-Eval devices. However, this temperature is 30–40 °C lower than that effectively experienced by the sample (Espitalié et al., 1985a). As opposed to previous devices, RE6 measures the exact temperature experienced by the sample. The temperature determined at the top of the S2 peak is called TpS2. Because T_{max} has no significance in term of thermal maturity for recent OM (Manalt et al., 2001; Lüniger and Schwark, 2002; Disnar et al., 2003), we here used TpS2 values; (v) oxygen index OIR6 (in mg O₂/g

Table 1
Radiocarbon ages from Lagoa do Caçó sediments

Code	Sample	Measured ages ¹⁴ C years BP	¹³ C/ ¹² C (‰)	Conventional ages ¹⁴ C years BP	Calibrated ages years BP	Intercept years BP
Beta-162661	MA98/3/73–75	4930 ± 50	– 27.2	4890 ± 50	5720–5580	5610
Beta-162662	MA98/3/196–198	9850 ± 70	– 28.9	9790 ± 70	11,270–11,120	11,200
Beta-162663	MA98/3/286–288	14,450 ± 80	– 27.8	14,400 ± 80	17,680–16,830	17,250
Beta-162664	MA98/3/354–356	15,620 ± 80	– 19.9	15,700 ± 80	19,230–18,290	18,750
Beta-162665	MA98/3/426–428	16,100 ± 80	– 22.9	16,130 ± 80	19,740–18,770	19,240
Beta-162666	MA98/3/574–576	16,670 ± 100	– 24.3	16,670 ± 100	20,410–19,330	19,860

TOC), which gives the oxygen content of the OM. It is calculated from the amounts of CO (S3CO) and CO₂ (S3CO₂) released during pyrolysis, normalized to TOC.

3.3.2. C/N, $\delta^{13}C$ and $\delta^{15}N$

Total carbon and nitrogen as well as their stable isotopes ratios ($\delta^{13}C$ and $\delta^{15}N$) were measured on core 98-4 by combustion with a Shimadzu CHN analyser coupled to a Prism mass spectrometer. Because carbonates (siderite) were only found in a well-defined interval (Sifeddine et al., 2003), and because of the geological and hydrological context (sand dunes and ferralsols; acidic lake waters), these analyses were realized on bulk sediments, thus avoiding any artefact due to acid attacks. Accordingly, C/N ratios are expressed as total carbon over total nitrogen.

3.4. Dating

Six radiocarbon dates have been performed on bulk OM on core 98-3 by acceleration mass spectrometry (AMS) at the Beta-Analytic Laboratory (Florida, USA) (Table 1). Interpolated ages were calculated using the intercept of the mean conventional age interval with the calibration curve of ¹⁴C (CALIB version 4.3, Stuiver and Reimer, 1993; Stuiver et al., 1998).

4. Results

4.1. Lithology and mineralogy

The lowermost unit of the core (U1) consists of sands of the Pleistocene substratum that will not be further discussed. The remaining part of the core of

about 6 m length has been subdivided in two parts of equal length according to mineral content and granulometric criteria. The lower part, which mainly comprises detritic material, has been further divided into fine-grained sands (U2) and silts (U3). U2 contains between 60% and 80% of quartz, whereas unit U3 contains 50% of quartz and 50% of kaolinite. The upper half of the core consists of fine-grained OM-rich sediments. It has also been subdivided into two units related to their colour, i.e., brown-green silts (U4) and black silts (U5). Mineralogy of unit U4 strongly differs from the underlying sediments by its high content in goethite (0–26%), amorphous silica (4–20%) and, at specific levels, in siderite (35%). The inorganic assemblage of U5 is mainly composed of amorphous silica (sponge spicules and diatoms) (Fig. 2).

4.2. Organic petrography

In addition to pyrite, 11 classes of organic constituents have been distinguished according to morphological and textural criteria. The first of these criteria is the presence of recognizable biological structures. The structureless material is called “amorphous.” A description of the constituents is given in Table 2. The variations of the relative proportions of the different organic classes are plotted against depth in Fig. 2. Amorphous constituents are largely dominant (60–90%) along the core. The upper half-core contains primarily flaky amorphous OM (FIAOM), while the lower half is dominated by gelified amorphous OM (GelaOM). More or less well-preserved ligno-cellulosic debris (TLC, GelLC and AmLC) account for 20–40% of the organic constituents in U2 sands. These particles strongly decrease in the upper intervals, notably at the base of the greenish-

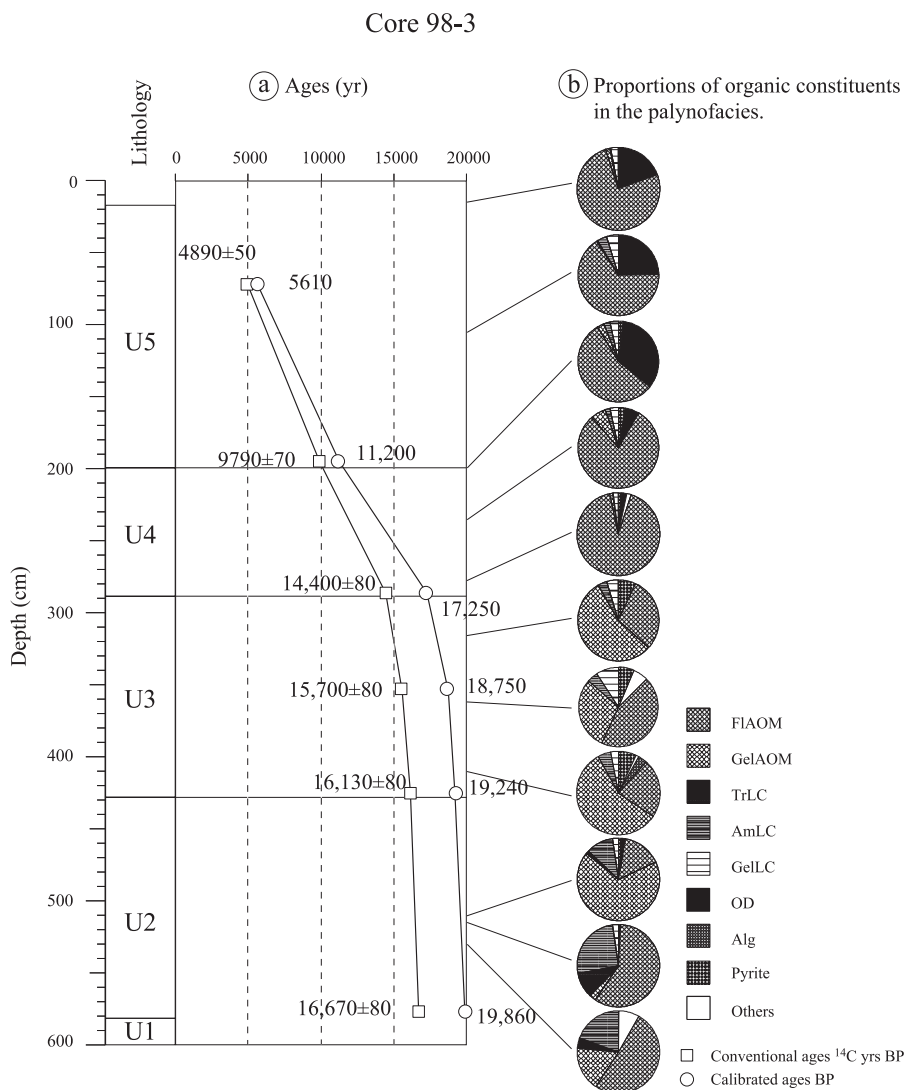


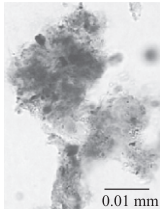
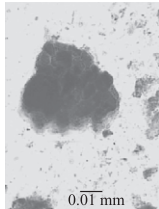
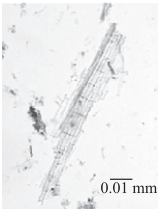
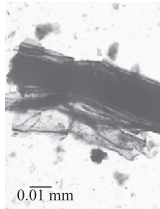
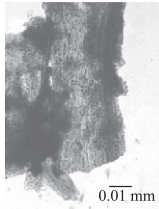
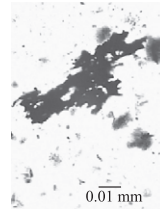
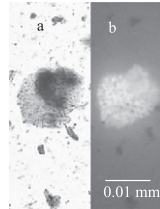
Fig. 2. Core 98-3 with radiocarbon chronology and results from organic petrography. (a) Chronology, showing ¹⁴C conventional and calibrated (Cal years BP) ages; (b) proportions of organic constituents in the palynofacies.

brown organic silts in U4. Opaque debris (OD), which are sparse or even absent in the lower half of the profile, increase slightly upcore in U4 to reach 10% at 3 m depth. In the upper unit U5, OD represent 20–30% of the organic constituents. Authentic phytoplanktonic OM constitutes only 5% of the total OM. Pyrite is recorded in U3 silts (7%) and, in lower proportions, in U4 greenish-brown organic silts. No trace of this mineral was identified in the lower and upper units U2 and U5.

4.3. $\delta^{15}N$, $\delta^{13}C$ and C/N

$\delta^{15}N$ is around 10‰ in U2 and U3 units and around 3–4‰ in U4 and U5 units after a strong decrease at the U3/U4 boundary. $\delta^{13}C$ values average -25 ‰ in U2, then increase to -20 ‰ in U3 and remain stable at ca. -27 ‰ in U4 and U5 except for the 2.6–2.3-m interval (-15 ‰) due to siderite concretions. C/N is high in U2 (ca. 40), and much lower in U3, U4 and U5. The siderite con-

Table 2
Description of the main organic classes identified in the palynofacies of Lagoa do Caçó sediments

Type of organic constituent	Flaky amorphous OM	Gelified amorphous OM	Translucent ligno-cellulosic debris	Amorphized ligno-cellulosic debris	Gelified ligno-cellulosic debris	Opaque debris	Algal OM
Abbreviation	FIAOM	GelAOM	TrLC	AmLC	GelLC	OD	Alg
Illustration							
Description - main features	Diffuse edge - heterogeneous texture	Sharp edges - homogeneous texture	Vascular structures still present - translucent texture	Progressive destruction of biological structures	Phytoclast morphology - homogeneous texture	Opaque up to edge - ± biostructures - devolatilisation features	(a) algal micro-colonies - (b) fluorescent under UV excitation
Possible origin	Submerged or emergent higher plants	Terrestrial higher plants	Higher plants	Higher plants	Higher plants	Higher plants	Phyto planktonic
Main depositional environment	Lacustrine	Palustrine	Paludal Increasing degradation	Paludal Increasing degradation	Paludal Increasing degradation	Allochthonous: - aerial degradation - fossil OM - charcoal	Essentially lacustrine

cretions are again responsible for high C/N in U4 (Fig. 3).

4.4. Rock-Eval pyrolysis

The main occurrence of mineral carbon (Minc), reaching 2–3%, is recorded at 2.3 m depth and can be ascribed to siderite concretions. TOC varies from ca. 1% in the Pleistocene sands of unit U1, to ca. 15% at the base of unit U5. TOC values increase slightly from the base of U2 to reach 6–7% at the top of this unit before decreasing to 5% at the U2/U3 limit, the boundary between sands and silts. Values then decrease from ca. 10% to 5% in U3 and increase again in

the upper part of the unit U3 to reach more than 15% at 2.2 m depth, before slightly decreasing again. From 1.4 m towards the top, TOC finally stabilizes at 10%. Two levels at 2.1 and 1.8 m depth have lower TOC values deviating from the general trend. In general, HI values range from 50 to 600 mg HC/g TOC. The lower half of the core exhibits relatively high HI values ranging from 200 to 755 mg HC/g TOC. After a strong decrease at 2.9 m, HI values remain between 50 and 250 mg HC/g TOC in the organic silts of units U4 and U5. The generally low Tps2 values, all in the 385–472 °C range (i.e., T_{\max} from ca. 345 to 432 °C), are typical for immature OM (i.e., $T_{\max} < 435$ °C, Espitalié et al., 1985a). Extremely low Tps2 values (< 400 °C)

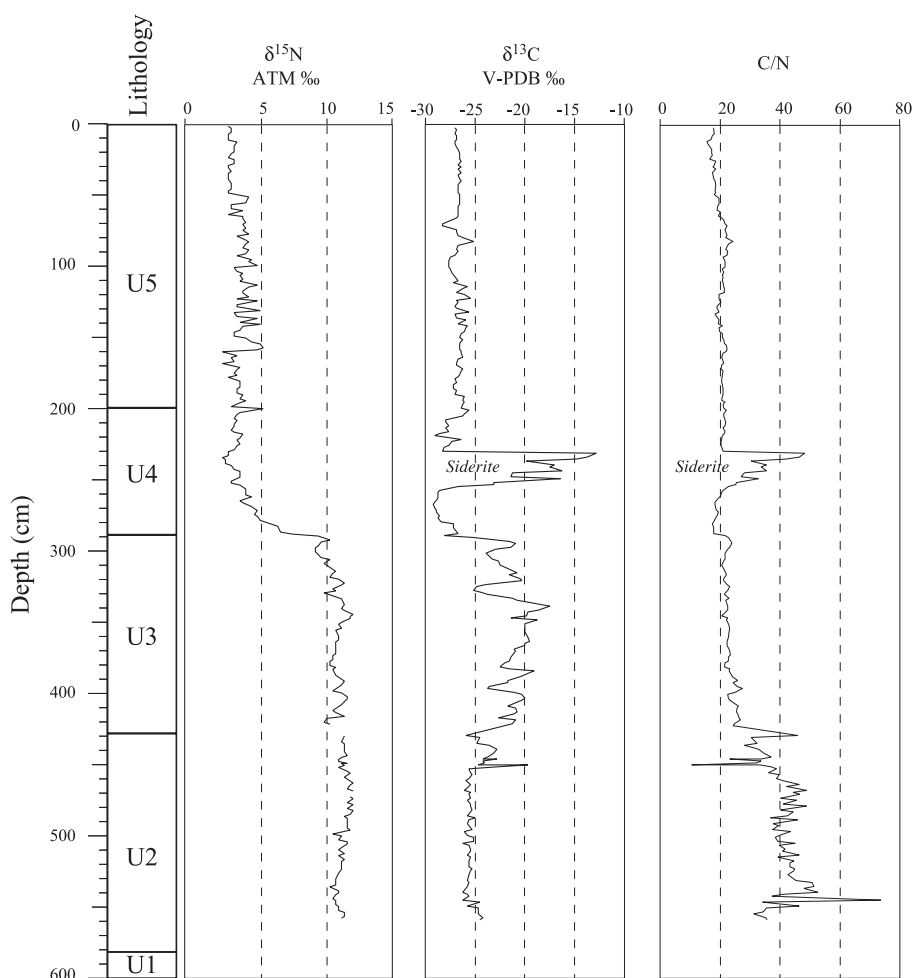


Fig. 3. Bulk organic geochemistry ($\delta^{15}\text{N}$, $\delta^{13}\text{C}$ and C/N) along core 98-4.

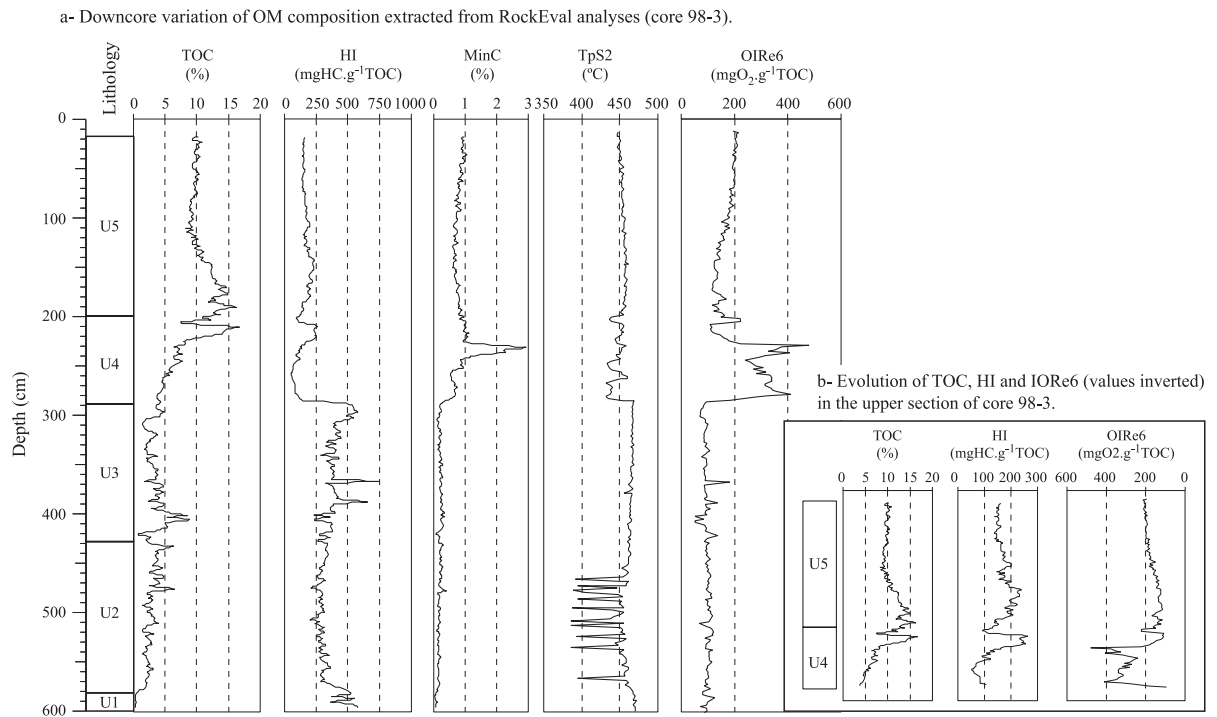


Fig. 4. (a) Downcore variations of OM abundance and composition deduced from Rock-Eval analyses (core 98-3); (b) evolution of TOC, HI and OIRe6 (values inverted) in the upper section of core 98-3.

have been determined in some levels in U2 sands. Above this unit, TpS2 remains relatively constant around 470 °C, before showing again marked variability in the 430–460 °C range in U4. TpS2 values then decrease slightly from 460 to ca. 450 °C towards the top of the core. OIRe6 values that average 100 mg O₂/g TOC in the lower part of the core increase strongly at 2.9 m to reach 400 mg O₂/g TOC. Subsequently, the values of this index decrease linearly up to 1.7 m depth, except for some levels around 2.3, 2.5 and 1.8 m depth. Finally, OIRe6 increases towards the top of the core to reach a value of about 200 mg O₂/g TOC (Fig. 4).

5. Discussion

5.1. Sediment fill

Sedimentological analyses supplemented by dating the boundaries of the different units of core 98-3 confirm that Lagoa do Caçó recorded an apparently

continuous sedimentation from 19,860 to 5610 Cal years BP and, by extrapolation, until present. If one excepts the lowermost core unit of Pleistocene age sands (U1), the sediment fill can be divided into two main units of comparable length. The lower segment, which consists mainly of detritic sediments, sands (U2) and silts (U3), was deposited rapidly (ca. 1.15 mm/year), at the end of the LGM. The upper section is fine grained, deposited under lower sedimentation rates (ca. 0.2 mm·year⁻¹), from Late Glacial times to present. These low sedimentation rates result from limited inorganic input, which preferentially consists of authigenic and bio-induced minerals (goethite, siderite and amorphous silica) with an important organic contribution.

5.2. Abundance and quality of OM

The lithological and dynamic contrast between the lower and the upper portions of the core reveals a major environmental change also recorded by sedimentary OM. TOC values are always lower than 5% in

U2 and U3 and much higher in U4 and U5. The distinction between the two major sections is even more pronounced when considering the $\delta^{15}\text{N}$ and the hydrogen index (HI). $\delta^{15}\text{N}$ values that first depend on the source of nitrogen used for biosynthesis (dissolved NO_3^- for phytoplankton and atmospheric N_2 for land plants) can also be affected by diagenesis through bond rupture (Macko et al., 1993). Thus, the very high $\delta^{15}\text{N}$ values ($>10\text{‰}$) found in units U2 and U3 can either be due to residual OM enriched in ^{14}N by deamination or hydrolysis reactions (Macko et al., 1993) or to the assimilation of nitrates previously enriched in ^{15}N by denitrification (as it might arrive for plants growing in swampy environments; Muzuka, 1999). In contrast, $\delta^{15}\text{N}$ values ranging from 3 to 5‰ in units U4 and U5 might indicate an assimilation of nitrates by plants, without any significant N-nitrate fractionation (Meyers and Lallier-Vergès, 1999). HI which represents the degree of OM hydrogenation depends first on the balance between phytoplanktonic (highly hydrogenated) and terrestrial contributions (e.g., Talbot and Livingstone, 1989; Noel, 2002) and second on the extent of biodegradation of the original material before burial (Espitalié et al., 1985a). HI values are greater than 250 mg HC/g TOC (and sometimes higher than 500 mg HC/g TOC) in sands and silts, but always smaller than this value in organic silts. This distinction between U2–U3 on one hand and U4–U5 on the other corroborates that already established by $\delta^{15}\text{N}$ values. Slightly lower C/N values in U4–U5 than in U2–U3 can be attributed to the preferential degradation of labile, higher plant, carbohydrates. The change in sedimentation is also recorded by OIRe6 which increases from values lower than 100 mg O_2/g TOC in U2 and U3 towards 400 mg O_2/g TOC at the U3/U4 limit. These shifts coincide with a significant lowering of TpS2 that is not accompanied by any notable TOC change.

The HI values of 250–350 mg HC/g TOC recorded in U2 are typical of well-preserved, higher plant OM, further supported by the presence of well-recognisable higher plant debris (sometimes more than 1 cm long). In the absence of carbonates, rather high C/N values of 30–40 are also indicative of a good preservation of nitrogen-depleted biopolymers, like polysaccharides and lignin. Low TpS2 values (ca. 380 °C) are also observed in several levels in this interval, typical of unaltered higher plant biopolymers

usually present in high proportions in upper soil horizons (Disnar et al., 2003). The sawtooth pattern of TpS2 values (between 380 and 460 °C) is attributed to the heterogeneity of the samples and depends on the amount of well-preserved higher plant debris in the sample.

In U3 silts, HI values of up to 500 mg HC/g TOC can be tentatively explained by a higher contribution of planktonic or microbial OM. This explanation is consistent with lower C/N and $\delta^{13}\text{C}$ values (-20‰) that effectively document a contribution of planktonic material, which is richer in hydrogen, nitrogen and heavy carbon isotope than C3 higher plants. A C4 higher plant contribution, shifting $\delta^{13}\text{C}$ to more positive numbers in U3, can also be evoked. U3 silts also contain pyrite that indicates deposition and/or early diagenesis under reducing conditions.

The OIRe6 values recorded in the lower half of the core are consistent with those of well-preserved modern lacustrine OM, but exceptionally high values in U4 (exceeding 300 mg O_2/g TOC) are uncommon in recent lacustrine sediments and point to a highly oxidized OM. This is corroborated by the low HI values found in this unit (<200 mg HC/g TOC). Covariant low HI and TOC values indicate extensive reworking during deposition and/or diagenesis. Furthermore, background values of about 1% of Minc recorded in the upper half-core appear to be an analytical artefact related to the presence of refractory OM which decomposes lately into CO and CO_2 during pyrolysis. The decrease of OIRe6 with increasing TOC towards the top of U4 could reflect better preservation. In U4 and U5 units, TOC and HI display similar trends, but opposite to OIRe6 (Fig. 4b). The presence of siderite at 2.2 m depth is responsible for high Minc (Fig. 4) and OIRe6 values as a result of early decomposition of this carbonate during pyrolysis (Espitalié et al., 1977). Three comparable siderite occurrences recorded in nearby cores (97-1 and 97-3) were interpreted as indicative of reducing conditions (Sifeddine et al., 2001). TpS2 values, fluctuating between 430 and 460 °C, coincide with high OIRe6 values and cannot be attributed to well-preserved higher plant OM as discussed above for U2 unit. In contrast, these fluctuations could be due to variable but extensive degradation of the OM in this unit. Because the S2 signals are of

low intensity in U4, slight variations in the shape of peak S2 leads to exaggerated shifts of TpS2. Consistently, TpS2 fluctuations decrease upcore with decreasing OM degradation.

Finally, high TOC and HI values observed immediately after the siderite interval in U4 could mark an improvement in OM quantity and quality under more reducing conditions. The last feature for unit U4 arise from petrographical investigations that indicate an increase of OD, probably resulting from an increase of forest fires.

In U5, OM appears homogeneous both from a quantitative and qualitative point of view. Only a slight decrease in TOC (15% to 10%) is recorded from the base of this unit to its top. HI values remain rather low (around 200 mg HC/g TOC), but OIRe6 increases slightly. These features are consistent with the accumulation of moderately preserved type III OM and limited dilution by mineral input as presently occurring. Larger amounts of OD in U5 (up to 25%) than in U4 point to a net intensification of forest fires.

To summarize these results, the Rock-Eval data from core 98-3 have been plotted in the diagrams shown in Fig. 5. In a classical pseudo-Van Krevelen HI–OI diagram (Fig. 5a), samples show a continuum between hydrogen-rich (represented by U2 and U3) and oxygen-rich end members (U4 and U5). This diagram distinguishes three main types of OM (Espitalié et al., 1977): (i) type I is attributed to a hydrogen-rich and oxygen-depleted lacustrine algal OM; (ii) type III is typical of an oxygen-rich and hydrogen-poor OM derived from lignin-rich parts of higher plants; (iii) intermediate type II corresponds to lacustrine or marine algal OM. In addition to these presumably pure materials, other (sub-) types arise from mixing of the abovementioned materials in various proportions and as a consequence of degradation upon sediment transport and/or deposition. For example, type IV OM corresponds to higher plant OM that suffered extensive oxidation, therefore exhibiting very low HI and high OI values. There are exceptions to these rules. Surficial soil horizons can have HI consistent with type II OM (Disnar et al., 2003). Hydrogen-rich epicuticular waxes of terrestrial plants can yield HI values similar to those of phytoplanktonic OM (Lüniger and Schwark, 2002). The distribution of core 98-3 samples, in a large part

of the HI–OI diagram, therefore indicates both changes in the contribution of biological sources (phytoplanktonic and terrestrial) but mostly drastic changes in depositional conditions and early diagenesis of this OM. The distinction between the lower detritic units (U2 and U3) and the upper organic silts (U4 and U5) becomes more obvious when plotted in a $S2=f(\text{TOC})$ diagram. While U2 and U3 data display a good correlation between S2 and TOC, U5 and especially U4 ones always show lower S2 values than expected from the preceding correlation. A similar pattern has been interpreted by Langford and Blanc-Valleron (1990) as the reflection of a mineral matrix effect. This effect is enhanced for OM-poor samples and results from the ability that some minerals, like clays (e.g., illite), have to retain hydrocarbons during pyrolysis (Espitalié et al., 1985b). This effect is negligible in our case because of the high TOC contents of the samples and the absence of active mineral species. Another notable difference between the upper and lower units is sensible in the $S3\text{CO}_2$ vs. TOC diagram (Fig. 5c). Similarly to the S2 vs. TOC diagram, a good correlation is observed between these two parameters for the U2 and U3 samples, whereas most of the U4 and U5 samples have unusually high $S3\text{CO}_2$ values with regard to TOC. The conclusion that can be drawn from these two diagrams is that in contrast to U2 and U3 units, which contain a rather well-preserved OM of predominant type III, the upper U4 and U5 units contain refractory OM, depleted in hydrogenated compounds and enriched in oxygenated constituents. The transition between the lower and upper parts of the core occurs in several successive stages, all recorded in U4. This transition apparently ends with the formation of siderite. The first drastic change is confined to no more than four samples (stage 1 in Fig. 5b and c) and corresponds to a rapid degradation of OM shown by a marked decrease of S2 (and TOC) and a $S3\text{CO}_2$ increase. The second stage is mainly characterized by a major increase of TOC reflecting increased organic input, with only a slight improvement in OM quality, as depicted by a slight increase of S2. If one excludes the peak of siderite recorded at 2.4 m, the simultaneous upcore decrease of IORe6 and increase of TOC recorded in U4 (Fig. 4) indicate increasing preservation of the original organic input to the sediment. This interpretation is

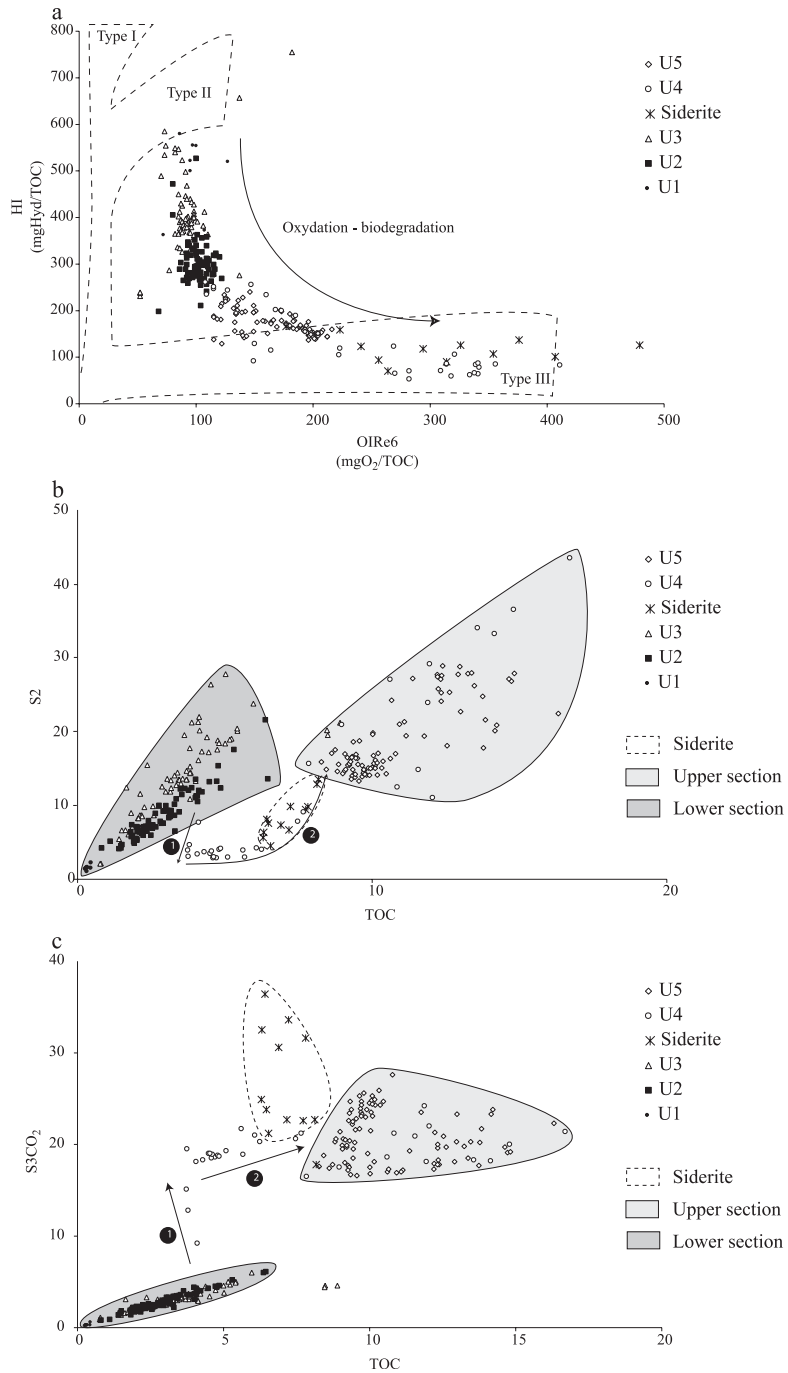


Fig. 5. Correlation of Rock-Eval parameters. (a) $IH=f(OIR6)$; Pseudo-Van Krevelen diagram; (b) $S_2=f(TOC)$; (c) $S_3CO_2=f(TOC)$.

strengthened by higher HI values in the top unit samples than in those from the base. Input of a different OM, richer in compounds producing CO₂ upon pyrolysis but also poorer in S2 may account for this difference. This OM is probably of higher plant origin and owe its refractory nature to the highly degrading conditions that existed during U4 deposition. The relative continuity of the TOC record at the U3/U4 transition is undoubtedly a coincidence, the dilution of the well-preserved OM by the mineral matrix in U3 being compensated by the considerable degradation of OM-rich input at the base of U4.

From a petrographical point of view and except for opaque debris, the distinction between the lower and upper sections is marked by the relative amounts of GeLAOM and FIAOM. An organic fraction similar to GeLAOM has been described in the Trittivakely (Madagascar) peaty marsh and was attributed to subaerial degradation of herbaceous plant remains (Bourdon et al., 2000). In addition, lacustrine sediment samples from the Siberia record (Bolivia) contain a similar reddish amorphous OM (Sifeddine et al., 1998) of pedogenic origin. In contrast, FIAOM appears as a degradation product of higher plants under a relatively constant water depth (Bourdon et al., 2000). Information from organic petrography can be summarized as follows: in the lower half core, organic constituents such as TLC, GeLC and GeLAOM document the degradation of higher plant remains in a palustrine context. In contrast, in the upper core interval, FIAOM documents subaquatic degradation of higher plant OM. An alternative explanation for such a distribution of plant remains could be different OM sources. For example, terrestrial higher plants with aerial vascular tissues could have led to the formation of GeLAOM associated with TLC and GeLC in the lower interval, while dominant FIAOM might derive from soft submerged or emergent aquatic macrophytes (e.g., *Juncus* sp.). Nevertheless, these two hypotheses on the respective origin of the amorphous fractions led to identical paleoenvironmental interpretations. With reference to the discussion on the interpretation of Rock-Eval parameters, the submerged/emergent origin and/or degradation of higher plants could be partly responsible for the high IORE6 and weak HI recorded in the upper interval (U4–U5).

5.3. Paleoenvironmental implications

5.3.1. Phase I (19,860 to 19,240 Cal years BP): unit U2

This phase is characterized by the rapid sedimentation of coarse-grained sediment with well-preserved and dispersed ligno-cellulosic OM. The relative abundance and good preservation of this material, which comprises numerous centimeter-size plant remains, imply short transport distances. The OM would thus originate from higher plants that grew within the basin or in its immediate vicinity. However, the local plant cover was sparse enough to allow mobilisation of sands. A semiarid environment is supposed to have prevailed at the end of the LGM in the study area (Ledru et al., 2001; 2002). River flow might have been temporarily fed by sporadic and heavy precipitation. The good preservation of the OM may thus result from rapid burial as well as the persistence of standing water in a swampy depression where fluvial sediments accumulated. During the same period, at the end of the LGM, several other South American sites also recorded comparable detritic intervals reflecting the erosion in the catchment areas (Turcq et al., 1997; 2002). The authors concluded that these deposits were formed under the influence of severe but scarce rainfall events while the vegetation had not yet stabilized soils.

5.3.2. Phase II (19,240 to 17,250 Cal years BP): unit U3

The deposition of silts (U3) may indicate the occurrence of erosive rainfall in a landscape with denser vegetation and soil development. A more humid climate and a more pronounced seasonality than during the previous period have probably favoured these environmental changes. The presence of notable proportions of kaolinite in unit U3 could point to an effective soil development, unless this mineral originates from the erosion/weathering of the Pleistocene substratum. The hypothesis of a more pronounced seasonality seems corroborated by sediment laminations, expressing depositional rhythmicity (Sifeddine et al., 2003). The top of unit U3 is also characterized by higher HI and $\delta^{13}\text{C}$ values and amorphous silica content. These features are consistent with a higher contribution of the phytoplanktonic biomass in a perennial lake resulting from regionally

wetter conditions than those that prevailed during the preceding phase.

These interpretations on phases I and II are in good agreement with palynological data showing sparse and residual vegetation at the end of the LGM (Ledru et al., 2002). Our results are also consistent with Stute et al. (1995), who hypothesized that the LGM was cooler but also more arid than presently, as demonstrated by the partial replacement of the Amazonian rainforest by savanna (van der Hammen and Absy, 1994; Colinvaux et al., 1996). Few records of sedimentary lacustrine deposits support our assumptions. As a matter of fact, during LGM, sedimentary records often display hiatuses due to dessication or intense subsequent erosion (Ledru et al., 1998). In contrast to other lacustrine records, Lagoa do Caçó appears to have recorded these erosive episodes, at least in core 98-3. Nevertheless, the remaining questions on the environmental setting during the deposition of U2 and most of U3 do not allow determining the true lacustrine nature of the basin.

5.3.3. Phase III (17,250 to 11,200 Cal years BP): unit U4

The major change in the detritic input and in the sedimentary regime that intervenes at mid-core points to a major modification of the local environmental conditions. These changes most likely became close to those that still prevail at present, i.e., an oligotrophic lake where the primary production is mostly confined to margins. The drastic lowering of the mineral input to the sediment suggests a stabilization of the surrounding soils, thus restricting aeolian erosion and river input transport. Apparently, the lateral and tributary-controlled mineral fluxes became very limited or even hindered by the *Juncus* sp. belt around the lake and by the floating meadow that developed upstream. If the mechanisms leading to the oxygen-rich organic matter that accumulated during much of this time interval remain unclear, the data indicate oxidising conditions due to the mixing of waters by the trade winds. As demonstrated by the presence of siderite at one level and by repeated Tps2 fluctuations, reducing conditions might have occurred from time to time, possibly caused by abrupt climatic changes. From this point of view, core 98-3 appears less responsive than core 97-1, drilled downstream in shallower waters, where siderite is recorded in three levels in unit U4 (Sifeddine et al., 2003). Palynological results on the

lake sediment filling (Ledru et al., 2001; 2002) reveal that a rapid reforestation occurred around 14,000 ¹⁴C years BP, at the level where the sedimentary change occurs. The development of the plant cover is suggested by the presence and expansion of gallery forest taxa, representative of cooler and more humid climates than at present. These observations are also consistent with marine data showing a phase that is considered the most humid phase in the area since LGM, between 15,500 and 11,800 ¹⁴C years BP (Behling et al., 2000). A subsequent important change that occurred between 11,000 and 10,000 ¹⁴C years BP led to the decline of humid forests, the expansion of savannas and the increase of fires (Ledru et al., 2001).

5.3.4. Phase IV (11,200 to 5610 Cal years BP): unit U5

Similar to the preceding unit, this latter phase is characterized by very low sedimentation rates that indicate efficient filtering of mineral input by the belt of rushes and by the floating meadow. In addition, the surrounding dense vegetation (Cerrado/Cerradao; i.e., shrub and woody savannas) prevents erosion. In this context, the sediment only consists of degraded and refractory OM with some biogenic minerals, namely, silica from sponge spicules and diatom valves. The decrease of OM contents and quality from 2 to 1 m depth is probably due to a lateral migration of the macrophyte belt in response to water level rise. This rise would result from an increase distance between the OM production and the deposition centre, with a subsequent increase of the residence time of the OM in oxygenated water column. In contrast, the slight increase in TOC recorded above 1 m could reflect progradation and aggradation of the *Juncus* sp. belt. The substantial increase of charcoal-like OD particles in this interval indicates an intensification of forest fires after 11,200 Cal years BP. In unit U5, the deposition of the sediments in the center of a permanent lake, under relatively deep water, could have substantially buffered the sensitivity to paleoenvironmental changes, under a relative climatic stability during the Holocene.

6. Conclusions

Our study of Lagoa do Caçó sediments allowed to complement earlier paleoenvironmental findings

(Ledru et al., 2001, 2002; Sifeddine et al., 2003) through a better understanding of depositional conditions and related environmental changes. From the sedimentary OM data, we could distinguish at least four major climatic phases since the end of the LGM: (i) phase I, arid or semiarid climate with strong but episodic rainfall. The precipitation allowed the development of ephemeral vegetation in the depression. Plant remains were rapidly buried and preserved under sands eroded from a poorly vegetated landscape; (ii) phase II, generally more humid conditions which favoured the development of a dense plant cover and soils and the formation of a permanent lake; (iii) phase III, after a drastic environmental and climatic change, lake sediments indicate abrupt climatic events evolving towards conditions approaching those prevailing today; (iv) phase IV, environmental and depositional conditions appear more stable and similar to present. In its deepest part, the lake did not record any notable change during the Holocene.

In addition to these paleoenvironmental conclusions, other aspects arise from the OM composition in this lacustrine setting. The detritic units (U2 and U3) contain scarce but well-preserved OM, unexpected in such deposits. This contrasts with strongly reworked OM deposited at the beginning of Late Glacial times (U4 and U5) after a longer residence time in a highly oxygenated water column. Lagoa do Caçó therefore exhibits a peculiar OM lacustrine record consisting exclusively of higher plant remains, where conventional geochemical parameters based on autochthonous versus terrestrial OM cannot be applied.

Acknowledgements

This research has been supported by an IRD (France)–CNPq (Brasil) convention and an ISTO (UMR 6113 du CNRS, France)–IRD cooperation. One of us (J.J.) receives financial support from the Conseil Régional du Centre. The authors wish to thank Dr. V. Markgraff (Boulder, CO, USA) and Dr. L. Schwark (University of Cologne, Germany) for their constructive remarks on the original manuscript and Marie-Alexandrine Sicre for improving the English writing.

References

- Behling, H., Arz, H.W., Pätzold, J., Wefer, G., 2000. Late quaternary vegetational and climate dynamics in northeastern Brazil, inferences from marine core GeoB 3104-1. *Quat. Sci. Rev.* 19, 981–994.
- Bourdon, S., Laggoun-Défarge, F., Disnar, J.R., Maman, O., Guillet, B., Derenne, S., Largeau, C., 2000. Organic matter sources and early diagenetic degradation in a tropical peaty marsh (Trivakely, Madagascar). Implications for environmental reconstruction during the sub-Atlantic. *Org. Geochem.* 31, 421–438.
- Colinvaux, P.A., de Oliveira, P.E., Moreno, J.E., Miller, M.C., Bush, M.C., 1996. A long pollen record from lowland Amazonia: forest cooling in glacial times. *Science* 274, 85–88.
- Disnar, J.R., Guillet, B., Kéravis, D., Di-Giovanni, C., Sebag, D., 2003. Soil organic matter (SOM) characterisation by Rock-Eval pyrolysis: scope and limitations. *Org. Geochem.* 34, 327–343.
- Espitalié, J., Laporte, J.L., Madec, M., Marquis, F., Leplat, P., Paulet, J., Boutefeu, A., 1977. Méthode rapide de caractérisation des roches mères, de leur potentiel pétrolier et de leur degré d'évolution. *Rev. Inst. Fr. Pét.* 32/1, 23–42.
- Espitalié, J., Deroo, G., Marquis, F., 1985a. La pyrolyse Rock-Eval et ses applications; première partie. *Rev. Inst. Fr. Pét.* 40, 563–579.
- Espitalié, J., Deroo, G., Marquis, F., 1985b. La pyrolyse Rock-Eval et ses applications; deuxième partie. *Rev. Inst. Fr. Pét.* 40, 755–784.
- Ficken, K.J., Street-Perrott, F.A., Perrott, R.A., Swain, D.L., Olago, D.O., Eglinton, G., 1998. Glacial/interglacial variations in carbon cycling revealed by molecular and isotope stratigraphy of Lake Nkunga, Mt. Kenya, East Africa. *Org. Geochem.* 29/5-7, 1701–1719.
- Huang, Y., Street-Perrott, F.A., Perrott, R.A., Metzger, P., Eglinton, G., 1999. Glacial-interglacial environmental changes inferred from molecular and compound-specific $\delta^{13}\text{C}$ analyses of sediments from Sacred Lake, Mt. Kenya—examples from Antarctic lakes. *Geochim. Cosmochim. Acta* 63/9, 1383–1400.
- Lafargue, E., Marquis, F., Pillot, D., 1998. Rock-Eval 6 applications in hydrocarbon exploration, production, and soil contamination studies. *Rev. Inst. Fr. Pét.* 53/4, 421–437.
- Lallier-Vergès, E., Sifeddine, A., de Beaulieu, J.L., Reille, M., Tribouillard, N., Bertrand, P., Mongenot, T., Thouveny, N., Disnar, J.R., Guillet, B., 1993. Sensibilité de la sédimentation organique aux variations climatiques du Tardi-Würm et de l'Holocène-Lac du Bouchet (Haute Loire, France). *Bull. Soc. Géol. Fr.* 164, 661–673.
- Langford, F.F., Blanc-Valleron, M.M., 1990. Interpreting Rock-Eval pyrolysis data using graphs of pyrolysable hydrocarbons vs. total organic carbon. *AAPG Bull.* 74, 799–804.
- Ledru, M.P., Bertaux, J., Sifeddine, A., Suguio, K., 1998. Absence of last glacial maximum record in lowland tropical forest. *Quat. Res.* 49, 233–237.
- Ledru, M.P., Cordeiro, R.C., Dominguez, J.M.L., Martin, L., Mourguiart, P., Sifeddine, A., Turcq, B., 2001. Late-glacial cooling in Amazonia as inferred from pollen at Lagoa do Caçó, northern Brazil. *Quat. Res.* 55, 47–56.

- Ledru, M.P., Mourguiart, P., Ceccantini, G., Turcq, B., Sifeddine, A., 2002. Tropical climates in the game of two hemispheres revealed by abrupt climatic change. *Geology* 30/3, 275–278.
- Lüniger, G., Schwark, L., 2002. Characterisation of sedimentary organic matter by bulk and molecular geochemical proxies: an example from an Oligocene maar-type Lake Enspel, Germany. *Sediment. Geol.* 148, 275–288.
- Macko, S.A., Engel, M.H., Parker, P.L., 1993. Early diagenesis of organic matter in sediments. Assessment of mechanisms and preservation by the use of isotopic molecular approaches. In: Engel, M.H., Macko, S.A. (Eds.), *Organic Geochemistry. Principles and Applications*. Plenum, New York, pp. 211–224.
- Muzuka, A.N.N., 1999. Isotopic compositions of tropical East African flora and their potential as source indicators of organic matter in coastal marine sediments. *J. Afr. Earth Sci.* 26, 757–766.
- Manalt, F., Beck, C., Disnar, J.R., Deconninck, J.-F., Recourt, P., 2001. Evolution of clay mineral assemblages and organic matter in the Late glacial–Holocene sedimentary infill of Lake Annecy (Northwestern Alps): paleoenvironmental implications. *J. Paleolimnol.* 25, 179–192.
- Martin, L., Flexor, J.M., Suguio, K., 1995. Vibrotestemunhador leve. Construção, utilização e potencialidades. *Rev. IG. Sao Paulo* 16, 59–66.
- Meyers, P.A., Lallier-Vergès, E., 1999. Lacustrine sedimentary organic matter records of late quaternary paleoclimates. *J. Paleolimnol.* 21, 345–372.
- Noël, H., 2002. Caractérisation et calibration des flux organiques sédimentaires dérivant du bassin versant et de la production aquatique (Annecy, le Petit Lac)—Rôles respectifs de l’Homme et du Climat sur l’évolution des flux organiques au cours des 6000 dernières années. PhD dissertation. University of Orléans, France. pp. 273. http://www.tel.ccsd.cnrs.fr/documents/archives0/00/00/16/35/index_fr.html.
- Sifeddine, A., Bertrand, Ph., Lallier-Vergès, E., Patience, A., 1996. The relationships between lacustrine organic sedimentation and palaeoclimatic variations. Lac du Bouchet, Massif Central, France. *Quat. Sci. Rev.* 15, 203–211.
- Sifeddine, A., Bertaux, J., Mourguiart, Ph., Disnar, J.R., Laggoun-Défarge, F., 1998. Etude de la sédimentation lacustre d’un site de forêt d’altitude des Andes centrales (Bolivie). Implications paléoclimatiques. *Bull. Soc. Géol. Fr.* 169, 395–402.
- Sifeddine, A., Martin, L., Turcq, B., Volkmer-Ribeiro, C., Soubiès, F., Campello Cordeiro, R., Suguio, K., 2001. Variations of the Amazonian rainforest environment: a sedimentological record covering 30,000 years. *Palaeogeogr., Palaeoclimatol., Palaeoecol.* 168, 221–235.
- Sifeddine, A., Albuquerque, A.L.S., Ledru, M.-P., Turcq, B., Knoppers, B., Martin, L., Zamboni de Mello, W., Passenau, H., Landim Dominguez, J.M., Campello Cordeiro, R., Abrao, J.J., Carlos da Silva Pinto Bittencourt, A.C., 2003. A 21000 cal years paleoclimatic record from Caçó Lake, northern Brazil: evidence from sedimentary and pollen analyses. *Palaeogeogr., Palaeoclimatol., Palaeoecol.* 189, 25–34.
- Street-Perrott, F.A., Huang, Y., Perrott, R.A., Eglinton, G., Barker, P., Ben Khelifa, L., Harkness, D.D., Olago, D.O., 1997. Impact of lower atmospheric carbon dioxide on tropical mountain ecosystems. *Science* 278, 1422–1426.
- Stuiver, M., Reimer, P.J., 1993. Extended ¹⁴C database and revised CALIB 3.0. ¹⁴C age calibration program. *Radiocarbon* 35, 215–230.
- Stuiver, M., Reimer, P.J., Braziunas, T.F., 1998. High-precision radiocarbon age calibration for terrestrial and marine samples. *Radiocarbon* 40, 1127–1151.
- Stute, M., Forster, M., Frischkorn, H., Serejo, A., Clark, J.F., Schlosser, P., Broecker, W.S., Bonani, G., 1995. Cooling of tropical Brazil (5 °C) during the last glacial maximum. *Science* 269, 379–383.
- Talbot, M.R., Livingstone, D.A., 1989. Hydrogen index and carbon isotopes of lacustrine organic matter as lake level indicators. *Palaeogeogr., Palaeoclimatol., Palaeoecol.* 70, 121–137.
- Thompson, L.G., Mosely-Thompson, E., Davis, M.E., Lin, P.-E., Henderson, K.A., Cole-Dai, B., Liu, K.B., 1995. Late glacial stage and Holocene tropical ice core records from Huascaren, Peru. *Science* 269, 46–50.
- Turcq, B., Pressinnoti, M.M.N., Martin, L., 1997. Paleohydrology and paleoclimate of the past 33,000 years at the Tamanduá River, Central Brazil. *Quat. Res.* 47, 284–294.
- Turcq, B., Cordeiro, R.C., Sifeddine, A., Simoes Filho, F.F., Abrao, J.J., Oliveira, F.B.O., Silva, A.O., Capitaneo, J.L., Lima, F.A.K., 2002. Carbon storage in Amazonia during the LGM: data and uncertainties. *Chemosphere* 49, 821–835.
- van der Hammen, T., Absy, M.L., 1994. Amazonia during the last glacial. *Palaeogeogr., Palaeoclimatol., Palaeoecol.* 109, 247–261.

Available online at www.sciencedirect.com

SCIENCE @ DIRECT®

Organic Geochemistry 35 (2004) 289–297

**Organic
Geochemistry**

www.elsevier.com/locate/orggeochem

Onocerane attests to dry climatic events during the Quaternary in the tropics

Jérémy Jacob^{a,*}, Jean-Robert Disnar^a, Mohammed Boussafir^a,
Marie-Pierre Ledru^b, Ana Luiza Spadano Albuquerque^c,
Abdelfettah Sifeddine^d, Bruno Turcq^e

^aLaboratoire de Géochimie Organique, Institut des Sciences de la Terre d'Orléans (ISTO)- UMR 6113 du CNRS,
Université d'Orléans, Bâtiment Géosciences, 45067 Orléans Cedex 2, France

^bIRD/CNPq, Universidade de Sao Paulo, Departamento Geologia Sedimentar e Ambiental, rua do Lago 562, 05508-900,
Sao Paulo, Sao Paulo, Brazil

^cDepartamento de Geoquímica, Universidade Federal Fluminense, Morro do Valonguinho s/no.24020-007 Niteroi,
Rio de Janeiro, Brazil

^dIRD/CNPq, Departamento de Geoquímica, Universidade Federal Fluminense, Morro do Valonguinho s/no. 24020-007 Niteroi,
Rio de Janeiro, Brazil

^eUR055, IRD, Centre d'Ile de France, Institut de Recherche pour le Développement, 32 av. Henri Varagnat, 93143,
Bondy Cedex, France

Received 6 January 2003; accepted 17 November 2003
(returned to author for revision 6 March 2003)

Abstract

An unusual molecular fossil (onocerane I) has been detected in Quaternary lacustrine sediments (Lagoa do Caçó, NE Brazil) for the first time. This component was initially thought to attest to the former presence of ferns or club mosses. From consideration of possible plant precursors of onocerane-related molecules recorded in the literature and comparison with palynological results and palaeoclimatic data, we here provide evidence that club mosses and ferns cannot account as sources of onocerane I in this setting. Onocerane I is abundant in the lipid extracts of sediments deposited during the two driest periods recorded in Northern Brazil (Last Glacial Maximum and Younger Dryas). This component is therefore suspected to be diagnostic of the development of plants adapted to dry or semi-arid conditions in this region.

© 2003 Elsevier Ltd. All rights reserved.

1. Introduction

Interpretation of terrestrial biomarker fingerprints in sediments is highly dependent on understanding present day plant–molecule relationships. Intensive research on

new molecules in living plants has greatly contributed to the taxonomical and ecological interpretation of the presence of fossil molecules. Nevertheless, despite the large amount of available data, uncertainties remain about the significance of the occurrence of some molecules. Therefore, there is a crucial need to more closely relate these molecules to their living precursors by calibration with recent sedimentary series.

The present work was carried out within the framework of a multidisciplinary research project conducted on Lagoa do Caçó (a small oligotrophic lake located in

* Corresponding author at current address: Laboratoire des Sciences du Climat et de l'Environnement (LSCE), Bât 12, Domaine du CNRS, Avenue de la Terrasse, F-91198 Gif-sur-Yvette Cedex, France.

E-mail address: jeremy.jacob@lsce.cnrs-gif.fr (J. Jacob).

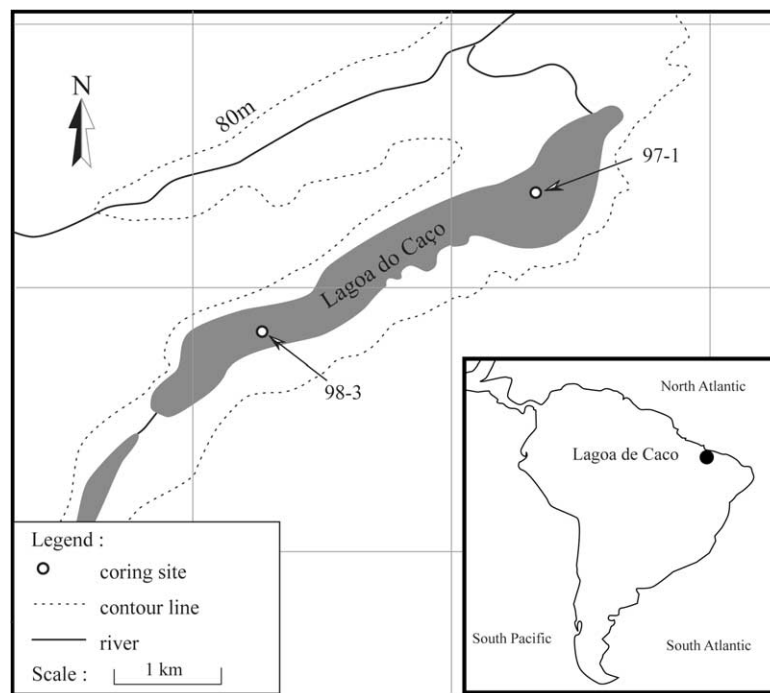


Fig. 1. Map of study area with indication of coring sites.

Northern Brazil, Fig. 1) and its surroundings, in order to detect palaeoenvironmental changes that affected the area during the Late Quaternary (Ledru et al., 2001, 2002; Sifeddine et al., 2003; Jacob et al., in press). This scientific context is highly relevant to terrestrial biomarker studies since the sedimentary organic matter consists mostly of higher plant remains (Jacob et al., in press). Indeed, several methyl ethers of pentacyclic triterpenes with oleanane, ursane, taraxerane, fernane and arborane structures have been identified in the sediments (Jacob et al., 2002). Here we compare the variation in onocerane I abundance along a 6 m core covering a 20,000 y record with independent results (especially palynology) and discuss the possible plant precursors of this compound as well as the palaeoenvironmental significance of its occurrence.

2. Experimental

2.1. Sample handling

Core 98-3 (6 m long) was collected with a vibra-corer (Martin et al., 1995) under 12 m of water, in the deepest part of the lake in the southernmost basin (Fig. 1). Core 97-1 (3 m long) was drilled using the same method in the northern sub-basin of the lake (Fig. 1) and has been the subject of previous publications (Ledru et al., 2001, 2002; Sifeddine et al., 2003).

2.2. Chronology

Six radiocarbon ages were measured within core 98-3 by acceleration mass spectrometry (AMS) at the Beta Analytic Laboratory and at the University of Arizona Tucson Laboratory, USA. Radiocarbon ages younger than 18,000 y B.P. were calibrated using the intercept of the mean of conventional ages with the calibration curve of ^{14}C (CALIB version 4.3; Stuiver et al., 1998). These data are summarized in Table 1.

2.3. Palynology

Pollen determinations in core 97-1 are according to Ledru (1993). The detailed methodology for pollen analysis is described in Ledru et al. (2001). Except for data on ferns and Lycophyta spores which were not previously published, pollen results have been published in Ledru et al. (2001, 2002) and Sifeddine et al. (2003). Detailed pollen counts are available on the Latin American Pollen Database website (www.ngdc.noaa.gov/paleo/lapd.html).

2.4. Extraction and separation of free lipids

Twenty two samples were selected from core 98-3 for detailed lipid analysis, following preliminary screening by Rock-Eval6 (RE6) of 300 regularly spaced samples (Jacob et al., in press). One gram of dried sediment was

Table 1
Radiocarbon and calendar ages of total organic matter (TOM) from core 98-3

Depth (cm)	Measured ages (^{14}C y BP)	$^{13}\text{C}/^{12}\text{C}$ (‰)	Conventional ages (^{14}C y BP)	Age range ^a (cal y BP)	Intercept (cal y BP)
Core					
73–75	4930 ± 50	–27.2	4890 ± 50	5720–5580	5610
196–198	9850 ± 60	–28.9	9790 ± 70	11,270–11,120	11200
286–288	14,450 ± 80	–27.8	14,400 ± 80	17,680–16,830	17250
354–356	15,620 ± 80	–19.9	15,700 ± 80	19,230–18,290	18750
426–428	16,100 ± 80	–22.9	16,130 ± 80	19,740–18,770	19240
574–576	16,670 ± 100	–24.3	16,670 ± 100	20,410–19,330	19850

^a Range at two standard deviations with error multiplier of 1.0.

ultrasonically extracted with acetone–pentane 1:1. The mixture was then separated according to the procedure described by Logan and Eglinton (1994). The neutral and acidic fractions were separated by Solid Phase Extraction (SPE) using AminoPropyl Bond Elute[®] cartridges with DCM–MeOH (1:1) for the elution of neutral components and acetic acid and ether for acidic compounds. The neutral fraction was then submitted to further fractionation on activated Florisil[®] to yield (i) aliphatic hydrocarbons (eluted with heptane), (ii) aromatic hydrocarbons and methyl ethers (DCM) and (iii) polar compounds (DCM–MeOH); 5 α -cholestane was added as an internal standard prior to analysis by gas chromatography/mass spectrometry.

2.5. Gas chromatography/mass spectrometry

Analyses were performed on a Thermofinnigan TRACE-GCQ gas chromatograph–mass spectrometer (GC–MS). The gas chromatograph was fitted with a Rtx[®]-5Sil MS capillary column (30 m × 0.32 mm i.d., 0.25 μm film) with 5 m of guard column. The injector was set at 280 °C and helium was the carrier gas. The temperature programme was 1 min isothermal at 40 °C, then 40–120 °C at 30 °C min^{–1}, 120–300 °C at 3 °C min^{–1} and finally 30 min hold at 300 °C. The mass spectrometer was operated in the electron ionisation (EI) mode over a m/z 50–650 amu range with a scan time of 0.55 s and an electron energy of 70 eV. Onocerane I was identified by comparison with published mass spectra and relative retention times. We further confirmed the identification of onocerane I by comparison with a sample of Nigerian oil shown previously to contain it (sample DA14, Pearson and Obaje, 1999; see Section 3.1.).

In order to avoid coelution, onocerane I relative abundance was determined by comparison of the peak area of onocerane I on the m/z 123 + 191 mass chromatogram with the peak area of 5 α -cholestane (internal standard) on the total ion current chromatogram (TIC).

3. Results

3.1. Assignment of onocerane I

On the m/z 191 mass chromatogram for sample 254 (520 cm), onocerane I elutes at 56.82 min under our chromatographic conditions, between the C₂₉ $\alpha\beta$ and C₂₉ $\beta\alpha$ hopanes (Fig. 2). This is in agreement with previous observations (Pearson and Obaje, 1999) on the elution position of onocerane I. The compound displays mass spectroscopic features that are also consistent with an onocerane I structure: (i) a molecular ion M⁺ 414; (ii) a base peak at m/z 123; (iii) another important fragment at m/z 191 (Fig. 3a). This fragmentation pattern is encountered in onoceranes (8,14-seco-gammaceranes) where breaking of the C(9)–C(11) or C(12)–C(13) bonds produces fragments of m/z 191, whereas the ion at m/z 123 results (Fig. 3b) from the rupture of bonds C(9)–C(10) and C(5)–C(6) or C(13)–C(18) and C(16)–C(17). Five-membered E-ring triterpenoids (hopanes, lupanes, fernanes, arboranes, adiananes) with the 8,14-seco structure can display similar fragmentation patterns (Schmitter et al., 1982). However, the lack of an ion at m/z 371 in the mass spectrum of the considered compound excludes the presence of an isopropyl group and hence any of the latter structures. Three onocerane isomers have been reported previously (Kimble et al., 1974). Structural changes between these compounds occur at positions C(8) and C(14). The compounds labelled onoceranes I, II and III have the configuration 8 β (H),14 α (H), 8 α (H),14 α (H) and 8 α (H),14 β (H), respectively. The relative abundances of ions m/z 191 and m/z 193 are diagnostic of this isomerism (Henderson et al., 1969; Kimble et al., 1974). In onocerane I, m/z 191 is far more abundant than m/z 193, in good agreement with the mass spectrum of the compound eluting at 56.82 min in our GC/MS analysis. Finally, comparison of the retention time of the compound with that of onocerane I previously found in a Nigerian oil sample (Fig. 2, sample DA14; Pearson and Obaje,

1999) and comparison of the mass spectra confirm this identification.

3.2. Sedimentology and organic matter composition

Five main sedimentary units, labelled U1 to U5 from bottom to top, have been described in core 98-3 (Jacob

et al., in press). Unit U1 corresponds to the Pleistocene sandy sub-stratum and is not discussed further. Units U2 and U3 (ca. 1.5 m thick each), which consist of fine sands and silts (quartz and kaolinite), respectively, were deposited rapidly at the end of the Last Glacial Maximum (LGM). The two uppermost units U4 and U5, made up of brownish and black organic silts,

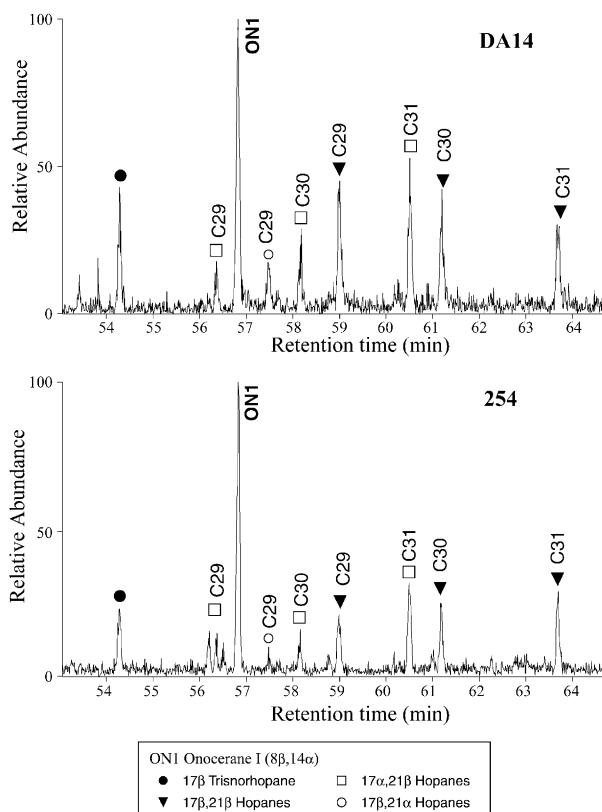


Fig. 2. m/z 191 chromatograms for a Nigerian crude oil extract (DA14; Pearson and Obaje, 1999) and for sample 254 collected from core 98-3 at 520 cm depth. Onocerane I is indicated as ON1. Other peaks are hopanoids as indicated in the key.

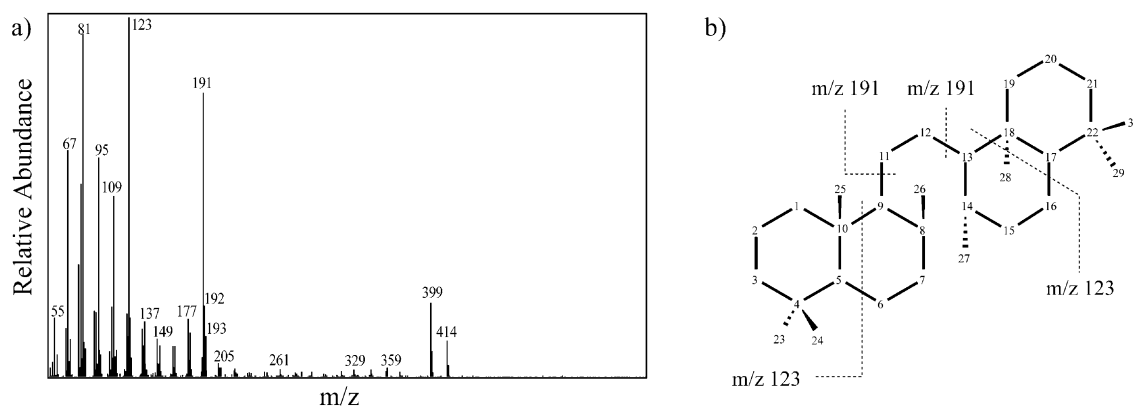


Fig. 3. (a) Mass spectrum of onocerane I identified in the sediments of Lagoa do Caçó; (b) structure of onocerane I, carbon numbering and major fragments.

respectively, exhibit lower sedimentation rates. This is consistent with a mineral input restricted to authigenic minerals (goethite and siderite) and biogenic silica in these two latter units. Combination of Rock-Eval pyrolysis, palynofacies, bulk and isotopic analyses (C/N,

$\delta^{13}\text{C}$ and ^{15}N) allowed us to attribute a highly predominant higher plant origin to the OM in the entire section of the core (Jacob et al., in press). Only unit U3 could contain small amounts of phytoplanktonic OM. Concerning the preservation of the OM, units U2 and U3 are composed of well preserved OM as a consequence of the rapid burial of higher plant remains. Conversely, units U4 and U5 contain degraded OM that suffered strong reworking in highly oxygenated waters.

The sedimentological, geochemical and palynological results obtained for core 97-1 have been published (Ledru et al., 2001, 2002; Sifeddine et al., 2003) and are not further discussed here. In this core, the marked transition from clastic material to organic silts is also recorded, around 14,000 ^{14}C y B.P.

3.3. Quantitation of onocerane I

The variation in the relative abundance of onocerane I in core 98-3 is shown in Fig. 4. The highest amounts of this compound are found between 580 and 430 cm in the bottom sandy unit (U2). Its abundance then decreases upcore before increasing again in the organic silts (U4), between 230 and 200 cm depth.

4. Discussion

4.1. Onocerane in sediments

Compared to other terrestrial biomarkers (oleanane, ursane, lupane), onoceranes are among the most uncommon in the sedimentary record. Since the first description of three onocerane isomers (I, II, III; Kimble et al., 1974) there have been only a few reports of their occurrence in the sedimentary record. Fig. 5 illustrates the preceding reports of onocerane-type molecules in the geological record. Onoceranes II and III have been reported back to the Carboniferous (Tieguan et al., 1988), in association with serratanoids. As demonstrated by Tsuda et al. (1964), onoceranes II and III can be produced by isomerisation of serratane-type compounds (serratandiols), these latter compounds being

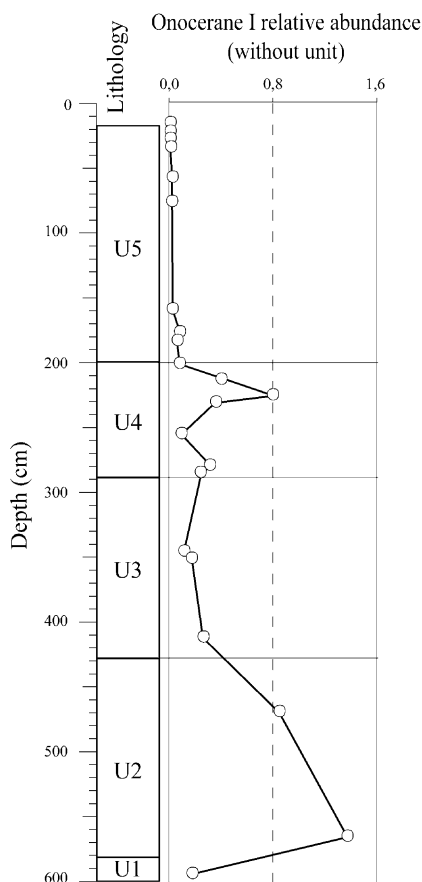


Fig. 4. Variations in onocerane I relative abundance in core 98-3. The values of onocerane abundance correspond to the ratio between the areas of the peak eluting at 56.82 min in the m/z 123 + 191 mass chromatogram normalized to the areas of the internal standard (5 α cholestane) in the TIC chromatogram.

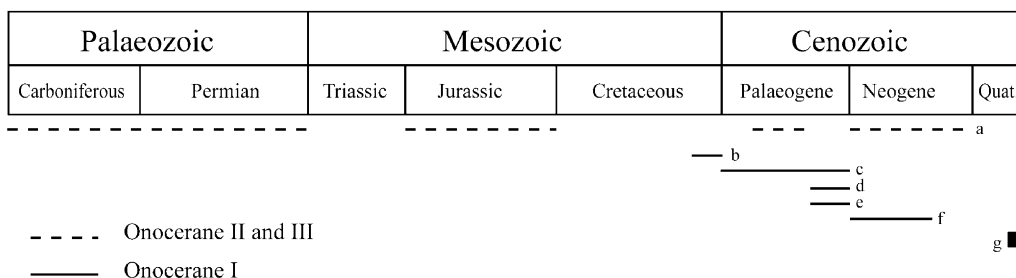


Fig. 5. Preceding records of onoceranoids in sediments and oils. References: a, f: Tieguan et al. (1988); b: Pearson and Obaje (1999); c: Fu et al. (1988); d: Curiale (1988); e: Giannasi and Niklas (1981); g: this study.

Table 2
Onocerane-related molecules and plant species containing them

Product	Plant precursor	Reference
Colysanoxide	<i>Colysis</i> sp. (Polypodiophyta, Polypodiaceae)	Ageta et al. (1982a)
Onoceradienes	<i>Lemmaphyllum microphyllum</i> (Polypodiophyta)	Ageta et al. (1982b)
Onoceranoxide		Masuda et al. (1989)
α -Onocerin	<i>Ononis</i> sp. (Fabaceae)	Barton and Overton (1955) Rowan and Dean (1972) Henderson et al. (1969)
Onocer-7-ene-3,21-diol	<i>Cissus quadrangularis</i> (Rhamnales, Vitaceae)	Bhutani et al. (1984)
Lansiosides	<i>Lansium domesticum</i> (Sapindales, Meliaceae)	Nishizawa et al. (1983)
Lansic acid		Habaguchi et al. (1968)
Onoceradienedione		
Onocerane II and III	<i>Pseudofagus</i> sp. (Fagaceae)	Giannasi and Niklas, (1985) Niklas and Giannasi, (1985)
α -Onocerin	<i>Lycopodium clavatum</i> , <i>L. obscurum</i> , <i>L. deuterodensum</i> (Lycopodiophyta)	Tsuda et al. (1964)

exclusively produced by ferns. Therefore, the occurrence of onocerane II and III in rocks and oils older than the Upper Cretaceous can be attributed to ferns via serrane-type molecules. In contrast, onocerane I has only been reported in Upper Cretaceous (Tieguan et al., 1988) and Tertiary sediments (Giannasi and Niklas, 1981; Curiale, 1988; Fu et al., 1988). This evidence claims an angiosperm origin for onocerane I, in contrast with the previous hypothesis (Pearson and Obaje, 1999). However, all previous studies point to the deposition of onoceranes in continental settings, including fluvial and lacustrine series in intramontane basins or in lagoonal-brackish contexts (Pearson and Obaje, 1999).

4.2. Onocerane-related compounds in living plants

The origin of onocerane in sediments is still debated because the possible plant sources (although not numerous) are distributed in very different taxa. Pteridophyta and Lycopodyta have been proposed as plant producers of the onoceranes recorded in Upper Cretaceous sediments (Pearson and Obaje, 1999) because possible precursors were isolated from these taxa (Tsuda et al., 1964; Ageta et al., 1982a,b; Masuda et al., 1989; Table 2). This interpretation is questionable since hop-22(29)-ene and neohop-13(18)-ene, also isolated from the same taxa, were absent from the studied sediments. The only undisputed source-product relationship in geological samples was ascertained by Giannasi and Niklas (1985) who isolated onocerane II and III from *Pseudofagus* sp. (Fagaceae) fossil leaves in the Clarkia deposit (Idaho, USA).

Onocerin, the alcohol derivative of onocerane, was first isolated from leaves and roots of *Ononis* sp. (Fabaceae; Barton and Overton, 1955; Henderson et al., 1969; Rowan and Dean, 1972) and from club mosses (Tsuda et al., 1964; Masuda et al., 1989). Other onocerane-related molecules have also been isolated from *Lansium*

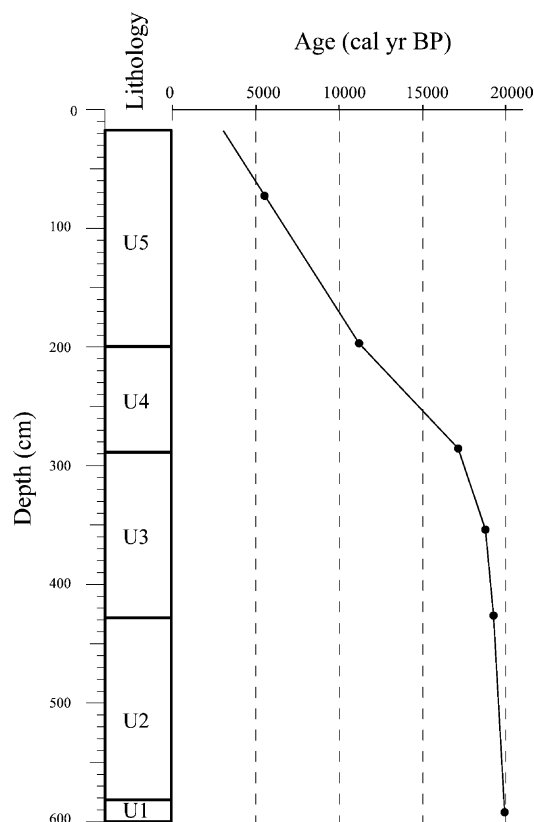


Fig. 6. Age model for core 98-3.

domesticum (Meliaceae; Habaguchi et al., 1968; Nishizawa et al., 1983) and *Cissus quadrangularis* (Vitaceae; Bhutani et al., 1984; Table 2). Contrary to most of the pentacyclic triterpenes that are biosynthesized from squalene monoepoxide (e.g. α - and β -amyrin), in *Ononis spinosa* α -onocerin synthesis involves both-ends cyclisa-

tion of a bis-epoxysqualene (Rowan et al., 1971). The term onoceroid has been proposed (Ageta et al., 1982b) for all the compounds produced by this pathway (i.e. serratane, ambreane and onocerane), which is uncommon in nature and might explain why onocerane-type molecules have been reported in such a limited number of species. However, the occurrence of such compounds in plant taxa as diverse as ferns, club mosses and angiosperms certainly denotes adaptative convergence.

The physiological role of onocerane-related molecules is uncertain but should strongly differ depending on the associated functional group(s). In the roots of *Ononis* sp., onocerin (onocera-8,14-dien-3 α ,21 β -diol) is thought to permit the colonization of water-deficient environments (Dean and Mayes, pers. com.). The role of onocerin in *Lycopodium clavatum* and of onoceradienes, onoceranoxide and other related molecules in ferns and club mosses must be very different since these taxa are well adapted to humid environments.

4.3. Comparison of onocerane abundance with palynology and other studies

For the purpose of comparison between cores 98-3 and 97-1, radiocarbon ages measured on samples from core 98-3 were converted into calendar ages, which were then interpolated by linear regression (Fig. 6). The age model for core 97-1 was previously established by Sifeddine et al. (2003).

The LGM (ca. 21,000 years ago) has proved to be difficult to describe in the Tropics because of the frequent hiatus observed in lowland tropical records (Ledru et al., 1998; Turcq et al., 2002). Lagoa do Caçó palaeoenvironmental history started at ca. 20,000 cal y BP, immediately after the peak of the glaciation, when a steppe-type environment is indicated, mainly by high frequencies of Poaceae, *Richardia* sp. (Rubiaceae), *Ceratosanthes* sp. (Cucurbitaceae) and various Amaranthaceae (Ledru et al., 2001) responsible for a low ratio

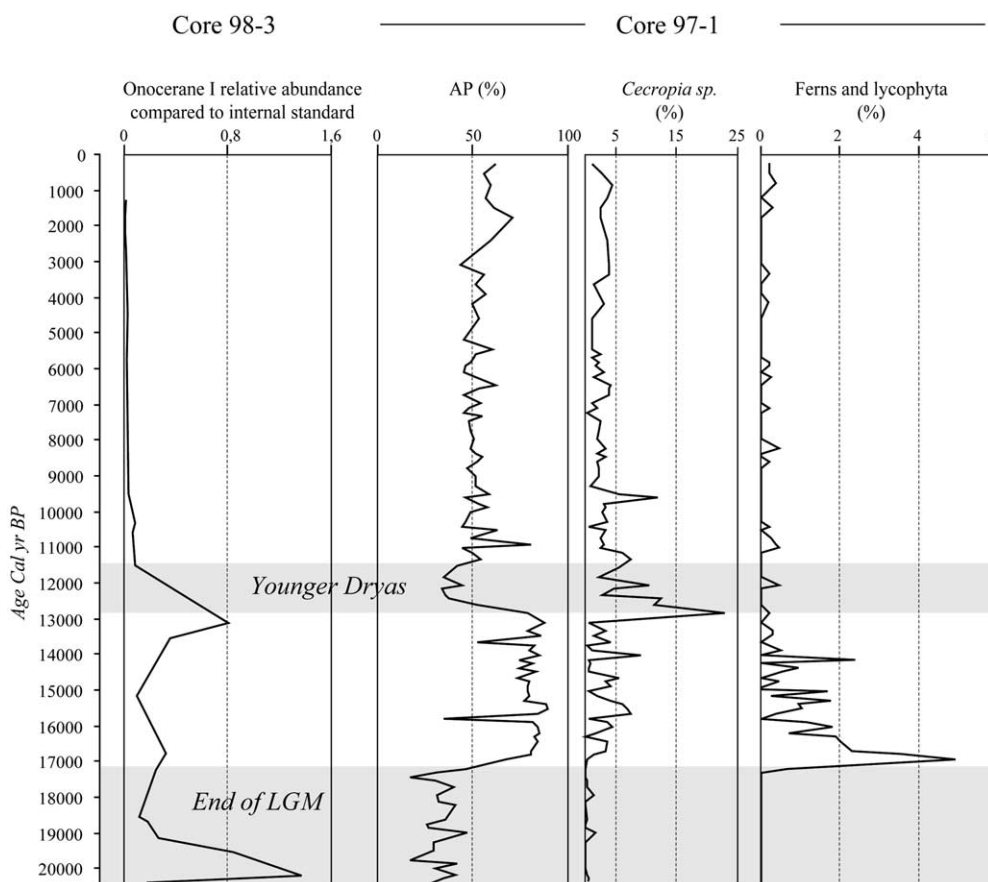


Fig. 7. Comparison of onocerane I relative abundance from core 98-3 with palynological results from core 97-1. AP represents the percentage of arboreal pollen compared to the total pollen. Ferns and Lycophyta spores comprise those of Adiantaceae, Polypodiaceae, Cyathea sp. and Lycophyta normalized to total pollen grains. Pollen results are from Ledru et al. (2001, 2002) and Sifeddine et al. (2003). Ferns and Lycophyta were not previously published but result from the same study.

between arboreal and non-arboreal pollen (AP/NAP, Fig. 7). Concordantly, a dry environment is also observed at the end of the LGM in marine sediments from Northern Brazil (Behling et al., 2000). These relatively dry climatic conditions are likely to have prevented the development of ferns or club moss taxa in the Lagoa do Caçó watershed, which is supported by the absence of their spores at that time from core 97-1. Therefore, these taxa cannot have been the sources of onocerane I between ca. 20,000 and 19,000 cal y BP.

The evidence for onocerane producers in the upper half of core 98-3 can also be deciphered by comparison with palynological data obtained from core 97-1 (Fig. 7). Spores from Adiantaceae, Polypodiaceae, *Cyathea* sp. and Lycophyta are abundant between 17,000 and 14,000 cal y BP. Ferns are generally related to rather humid environments. In the sediments deposited during the considered period, when such conditions prevailed as, attested also by high AP/NAP ratio and other palynological evidence (Ledru et al., 2001; Sifeddine et al., 2003), only low levels of onocerane I were detected (Fig. 7).

Higher levels of onocerane I are again recorded around ca. 13,000 cal y BP in core 98-3 (Fig. 7). As attested by palynological results from core 97-1, ferns and club mosses were not present around the lake at that time and thus cannot account for onocerane I production. At the same time, core 97-1 records lower AP/NAP values than before, denoting the regression of moist forest in favour of more open vegetation, and an increase in frequency of *Cecropia* sp., a pioneer species that colonizes areas left vacant after a reduction in humid forest. This drastic destruction of the forest is interpreted as a consequence of a dry and abrupt climatic change, correlated with the North Atlantic climatic reversal, specifically the Younger Dryas event (Ledru et al., 2002).

As the *Ononis* genus has not been described in NE Brazil, an unknown source of onocerane must certainly be considered here. From this evidence and in general agreement with the previous interpretation (Pearson and Obaje, 1999), onocerane I can be proposed as an indicator of dry to semi-arid conditions in post-Cretaceous sediments where fern remains are absent.

5. Conclusion

According to a literature review of possible plant precursors of onocerane-type molecules, from consideration of the physiological role of onocerin in some plants, and from comparison with palynological evidence, the onocerane I reported in sediments deposited in Lagoa do Caçó indicates the presence of a plant that lived in dry to semi-arid conditions, at the end of LGM and during the Younger Dryas, in NE Brazil. The specific plant precursor of this compound found in

Lagoa do Caçó sediments remains unknown but it could be closely related to the *Ononis* genus. Because pollen from Fabaceae is fragile and poorly specific, onocerane I could be the only recognizable remnant of its producer.

Acknowledgements

We are grateful to Dr. Peter Dean (Cambio, UK) and Dr. Sean Mayes (University of Canterbury, UK) for useful discussions on the role of onocerin in *Ononis* sp. We are fully indebted to Professor M.J. Pearson for providing the Nigerian crude oil sample and to Catherine Hanni (Brown University) for improving the English. We also thank Dr. H.P. Nytoft and Professor M.J. Pearson for their comments which significantly improved the quality of this manuscript. The research was supported by an IRD (France)-CNPq (Brasil) convention and an ISTO (UMR 6113 du CNRS, France)-IRD cooperation. One of us (J. J.) received financial support from the Conseil Régional du Centre.

Associate Editor—P. Farrimond

References

- Ageta, H., Masuda, K., Inoue, M., Ishida, T., 1982a. Fern constituent: colysanoxide, an onoceroid having a novel carbon skeleton, isolated from *Colysis species*. Tetrahedron Letters 23, 4349–4352.
- Ageta, H., Shiojima, K., Masuda, K., 1982b. Fern constituents: onoceroid, α -onoceradiene, serratene and onoceranoxide, isolated from *Lemmaphyllum microphyllum* varieties. Chemical and Pharmaceutical Bulletin 30, 2272–2274.
- Barton, D.H.R., Overton, K.H., 1955. Triterpenoids. Part XX. The constitution and stereochemistry of a novel tetracyclic triterpenoid. Journal of the Chemical Society 2639–2652.
- Behling, H., Arz, H.W., Pätzold, J., Wefer, G., 2000. Late Quaternary vegetational and climate dynamics in north-eastern Brazil, inferences from marine core GeoB 3104-1. Quaternary Science Reviews 19, 981–994.
- Bhutani, K.K., Kapoor, R., Atal, C.K., 1984. Two unsymmetric tetracyclic triterpenoids from *Cissus quadrangularis*. Phytochemistry 23, 407–410.
- Curiale, J.A., 1988. Molecular genetic markers and maturity indices in intermontane lacustrine facies: Kishenehn Formation, Montana. In: Matavelli, L., Novelli, L. (Eds.), Advances in Organic Geochemistry 1987. Organic Geochemistry 13, 633–638.
- Fu, J., Sheng, G., Liu, D., 1988. Organic geochemical characteristics of major types of terrestrial petroleum source rocks in China. In Fleet et al. (Eds.), Lacustrine Petroleum Source Rocks. Geological Society of London Special Publication 40, pp. 279–289.
- Giannasi, D.E., Niklas, K.L., 1981. Comparative palaeo-biochemistry of some fossil and extant Fagaceae. American Journal of Botany 68, 762–770.

- Giannasi, D.E., Niklas, K.L., 1985. The paleobiochemistry of fossil angiosperm floras. Part I. Chemosystematic aspects. In: Smiley, C.J. (Ed.), Late Cenozoic History of the Pacific Northwest. Proceedings of the American Association for the Advancement of Science Meeting, Pacific Division, San Francisco, 1985, pp. 175–183.
- Habaguchi, K., Watanabe, M., Nakadaira, Y., Nakanishi, K., Kiang, A.K., Lim, F.Y., 1968. The full structures of lansic acid and its minor congener, an unsymmetric onoceradienedione. Tetrahedron Letters 9, 3731–3734.
- Henderson, W., Wollrab, V., Eglinton, G., 1969. Identification of steranes and triterpanes from a geological source by capillary gas liquid chromatography and mass spectrometry. In: Schenck, P.A., Havenaar, I. (Eds.), Advances in Organic Geochemistry 1968. Pergamon, Oxford, pp. 181–207.
- Jacob, J., Disnar, J.-R., Boussafir, M., Sifeddine, A., 2002. Pentacyclic triterpene methyl ethers (PTME): a new class of biomarkers to trace Gramineae in tropical settings? Ancient Biomolecules 4 (3), 119.
- Jacob, J., Disnar, J.R., Boussafir, M., Sifeddine, A., Turcq, B. and Albuquerque, A.L.S. Major environmental changes recorded by lacustrine sedimentary organic matter since the Last Glacial Maximum near the Equator (Lagoa do Caçó, NE Brazil). Palaeogeography, Palaeoclimatology, Palaeoecology (in press).
- Kimble, B.J., Maxwell, J.R., Philp, R.P., Eglinton, G., 1974. Identification of steranes and triterpanes in geolipid extracts by high-resolution gas chromatography and mass spectrometry. Chemical Geology 14, 173–198.
- The Latin American Pollen Database website: www.ngdc.noaa.gov/paleo/lapd.html.
- Ledru, M.-P., 1993. Late Quaternary environmental and climatic changes in central Brazil. Quaternary Research 39, 90–98.
- Ledru, M.-P., Bertaux, J., Sifeddine, A., Suguio, K., 1998. Absence of Last Glacial Maximum records in lowland tropical forests. Quaternary Research 49, 233–237.
- Ledru, M.-P., Cordeiro, R.C., Dominguez, J.M.L., Martin, L., Mourguiart, P., Sifeddine, A., Turcq, B., 2001. Late-glacial cooling in Amazonia as inferred from pollen at Lagoa do Caçó, Northern Brazil. Quaternary Research 55, 47–56.
- Ledru, M.-P., Mourguiart, P., Ceccantini, G., Turcq, B., Sifeddine, A., 2002. Tropical climates in the game of two hemispheres revealed by abrupt climatic change. Geology 30, 275–278.
- Logan, G.A., Eglinton, G., 1994. Biogeochemistry of the Miocene lacustrine deposit, at Clarkia, northern Idaho, U.S.A. Organic Geochemistry 21, 857–870.
- Martin, L., Flexor, J.M., Suguio, K., 1995. Vibrostemunhador leve. Construção, utilização e potencialidades. Revista IG, São Paulo 16, 59–66.
- Masuda, K., Shiojima, K., Ageta, H., 1989. Fern constituents: four new onoceradienes isolated from *Lemmaphyllum microphyllum* Presl. Chemical and Pharmaceutical Bulletin 37, 263–265.
- Niklas, K.L., Giannasi, D.E., 1985. The paleobiochemistry of fossil angiosperm floras. Part II. Diagenesis of organic compounds with particular reference to steroids. In: Smiley, C.J. (Ed.), Late Cenozoic History of the Pacific Northwest. Proceedings of the American Association for the Advancement of Science Meeting, Pacific Division, San Francisco, 1985, pp. 175–183.
- Nishizawa, M., Nishide, H., Kosela, S., Hayashi, Y., 1983. Structure of lansiosides: biologically active new triterpene glycosides from *Lansium domesticum*. Journal of Organic Chemistry 48, 4462–4466.
- Pearson, M.J., Obaje, N.G., 1999. Onocerane and other triterpenoids in Late Cretaceous sediments from the Upper Benue Trough, Nigeria: tectonic and palaeoenvironmental implications. Organic Geochemistry 30, 583–592.
- Rowan, M.G., Dean, P.D.G., 1972. α -Onocerin and sterol content of twelve species of *Ononis*. Phytochemistry 11, 3263–3265.
- Rowan, M.G., Dean, P.D.G., Goodwin, T.W., 1971. The enzymic conversion of squalene, 2(3),22(23)-diepoxide to α -onocerin by a cell-free extract of *Ononis spinosa*. FEBS Letters 12, 229–232.
- Schmitter, J.M., Sucrow, W., Arpino, P.J., 1982. Occurrence of novel tetracyclic geochemical markers: 8,14-seco-hopanes in a Nigerian crude oil. Geochimica et Cosmochimica Acta 46, 2345–2350.
- Sifeddine, A., Albuquerque, A.L.S., Ledru, M.-P., Turcq, B., Knoppers, B., Martin, L., Zamboni de Mello, W., Passenau, H., Landim Dominguez, J.M., Campello Cordeiro, R., Abrão, J.J., Bittencourt, A.C.S.P., 2003. A 21,000 cal years paleoclimatic record from Caçó Lake, northern Brazil: evidence from sedimentary and pollen analyses. Palaeogeography, Palaeoclimatology, Palaeoecology 189, 25–34.
- Stuiver, M., Reimer, P.J., Brazianas, T.F., 1998. High-precision radiocarbon age calibration for terrestrial and marine samples. Radiocarbon 40, 1127–1151.
- Tieguan, W., Pu, F., Swain, F.M., 1988. Geochemical characteristics of crude oils and source beds in different continental facies of four oil-bearing basins, China. In: Fleet et al. (Eds.), Lacustrine Petroleum Source Rocks. Geological Society of London Special Publications 40, pp. 309–325.
- Tsuda, Y., Sano, T., Kawaguchi, K., Inubushi, Y., 1964. α -Onoceradiene-serratene isomerization and the configuration of serratenediol. Tetrahedron Letters 5, 1279–1284.
- Turcq, B., Cordeiro, R.C., Sifeddine, A., Simoes, Filho, F.F., Abrão, J.J., Oliveira, F.B.O., Silva, A.O., Capitaneo, J.L., Lima, F.A.K., 2002. Carbon storage in Amazonia during the LGM: data and uncertainties. Chemosphere 49, 821–835.

Anoxic sediments off Central Peru record interannual to multidecadal changes of climate and upwelling ecosystem during the last two centuries

D. Gutiérrez¹, A. Sifeddine², J. L. Reyss³, G. Vargas⁴, F. Velazco¹, R. Salvattecí¹, V. Ferreira⁵, L. Ortlieb², D. Field⁶, T. Baumgartner⁵, M. Boussafir⁷, H. Boucher², J. Valdés⁸, L. Marinovic⁷, P. Soler⁹, and P. Tapia¹⁰

¹Dirección de Investigaciones Oceanográficas, Instituto del Mar del Perú, P.O. Box 22, Callao, Peru

²UR Paléotropique, Institut de Recherche pour le Développement, IRD, Bondy, France

³Laboratoire du Sciences de Climat et le Environnement, CEA/CNRS, Gif-Sur-Yvette, France

⁴Departamento de Geología, Facultad de Ciencias Físicas y Matemáticas, Universidad de Chile, Chile

⁵Centro de Investigación Científica y de Educación Superior de Ensenada, Ensenada BC, Mexico

⁶Fisheries Resources Division, Southwest Fisheries Science Center, La Jolla, USA

⁷Institut des Sciences de la Terre (ISTO), Université de Orléans, Orléans, France

⁸Laboratorio de Sedimentología y Paleoambientes, Universidad de Antofagasta, Chile

⁹UR LOCEAN, Université Paris VI/IRD/CNRS/MNH, France

¹⁰Laboratorio de Palinología y Paleobotánica, Universidad Peruana Cayetano Heredia, Peru

Received: 20 July 2005 – Revised: 21 November 2005 – Accepted: 21 November 2005 – Published:

Abstract. High-resolution paleo-environmental and paleo-ecological archives in laminated sequences are present in selected areas from the upper continental Peruvian margin within the oxygen minimum zone. We present initial results of a multidisciplinary study (the PALEOPECES project) that aims to reconstruct environmental and ecosystem variability during the past 200 years from high-resolution records. We report chronology development, sediment structure, elemental, organic, and mineralogical compositions of a box core collected at 300 m depth off Pisco, central Peru. An average sedimentation rate of 2.2 mm y^{-1} was estimated from downcore excess ^{210}Pb activities for the last 100–150 years. Extending this rate further downcore indicates that a slump located at 52 cm depth from the top of the core can be correlated with a large tsunami that struck the coast of central Peru in 1746. X-ray analyses reveal laminated structures composed of couplets of light and dark laminae. Observations under polarized microscope show that light laminae are dominated by more dense, detrital and terrigenous material, while dark laminae are less dense with greater concentrations of amorphous biogenic silica. Downcore variations in dry bulk density and X-ray radioscopies of gray level show similar patterns, including a major shift at 34 cm depth (ca. mid-nineteenth century). A finely laminated sequence, which may include annual varves, is present between 34 cm depth and the slump layer. Sediment characteristics of the

sequence suggest increased seasonality of terrigenous versus biogenous sedimentation during the corresponding period. In addition to a mid-nineteenth century change and considerable multidecadal variability in TOC, there is a positive trend in the past 50 years. Mineralogical analyses from a Fourier Transformed Infrared Spectroscopy (FTIR) of the upper core covering the last 25 years, indicate higher concentrations of the mineral fraction (quartz, feldspar, kaolinite and illite) in layers including large El Niño events (1982–1983, 1986–1987 and 1997–1998), with the largest peak during the 1997–1998 episode. These results confirm that anoxic sediments off Pisco are suitable archives to investigate interannual and decadal changes in oceanographic conditions and climate of the northern Humboldt upwelling system.

1 Introduction

The Humboldt Current Ecosystem (HCE) off Peru undergoes large variations in productivity and ecosystem structure in association with the El Niño Southern Oscillation (ENSO), and decadal variability (Arntz and Fahrbach, 1996; Alheit and Ñiquen, 2004). Changes on decadal time scale are recognized as important sources of variability in atmospheric and oceanic structure (Miller, 1994; Field and Baumgartner, 2000). Decadal variability may also modulate the frequency, intensity and timing of the ENSO cycle (Wang and Picaut, 2004; Wang et al., 2004; Wang and Fiedler, 2005; Cobb et al.,

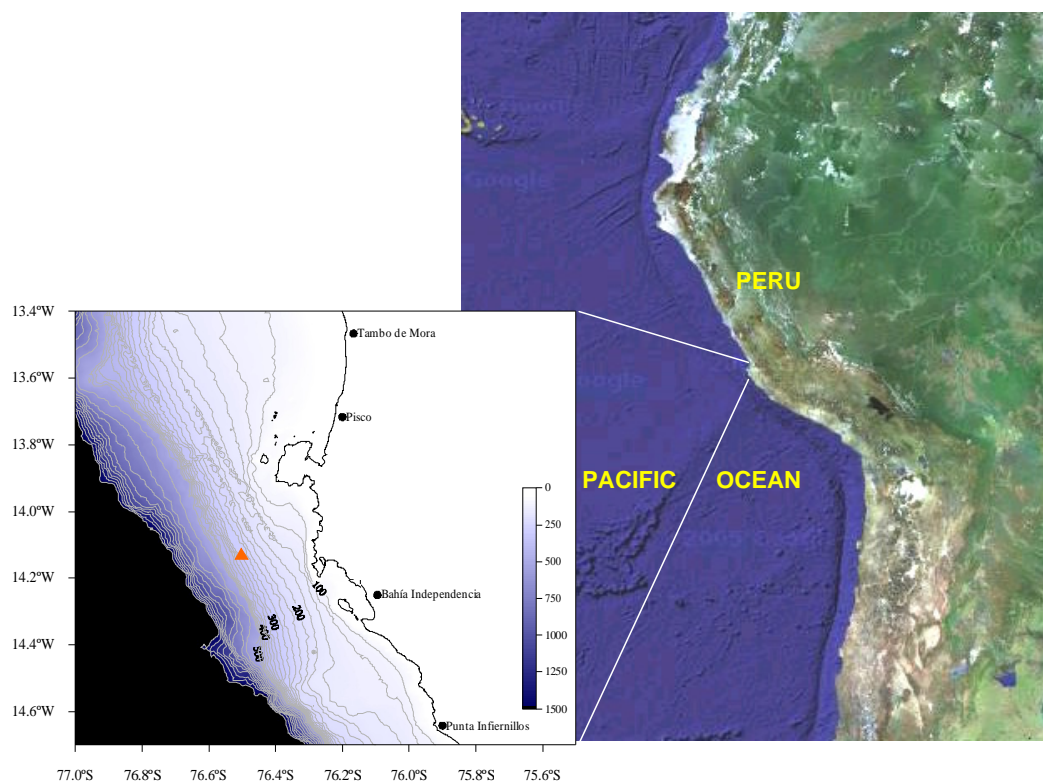


Fig. 1. Location of boxcore B0405-06 (red triangle, $14^{\circ}07.9' S$, $76^{\circ}30.1' W$, 299 m depth) off the central-south Peruvian coast. Bathymetric contour lines are in 25 m intervals from 100 m to 500 m, and in 100 m intervals from 500 m to 1500 m depth.

2004). These low frequency changes in the physical environment can result in large non-linear “regime shifts” in marine ecosystem structure in the Pacific Basin (Mantua and Hare, 2002; Schwartzlose et al., 1999; Hsieh et al., 2005). Within the HCE, two “anchovy regimes” (from the start of the fisheries until early 70s, and from early 90’s until present) separated by a “sardine regime” (from mid 70’s until early 90’s) have been proposed (Chávez et al., 2003; Alheit and Ñiquen, 2004). However, the extent to which decadal changes observed in the twentieth century are typical of regular decadal variability is not known.

The presence of an oxygen minimum zone inhibits bioturbation and facilitates the preservation of high-resolution records of past ecosystem changes in disoxic sediments in suitable topographic conditions (Krissek and Scheiddeger, 1983). Seasonal and/or interannual differences in particle composition and density may result in the formation of annual varves or laminae (Kemp et al., 1990; Valdés et al., 2003). However, sediments of the Peru slope are highly heterogeneous; authigenic precipitation of phosphorites, erosive processes and lateral transport are influential processes that can frequently supersede deposition and preservation of continuous laminae in disoxic environments (Levin et al., 2002; Reinhardt et al., 2003). Therefore, continuous high-resolution records in recent laminated sequences are present only in specific localities of the continental margin, particularly off the central Peruvian coast. Some studies in this

zone have described laminated sediments containing natural archives of climate and ecosystem change, such as diatoms, organic carbon and fish scales (e.g. Kemp et al., 1990; Schwartzlose et al., 1999). However, to our knowledge, the present study is the first multiproxy approach conducted at high-resolution in sediments containing laminated sequences that record different modes of variability during the recent past.

PALEOPECES is an international, multidisciplinary, research project that aims to reconstruct past variability in environmental (temperature and oxygen) and ecosystem (productivity, ecosystem structure and fish population dynamics) characteristics of the Peruvian upwelling ecosystem during the last 2000 years, with an emphasis on the last several hundred years. Our general objective here is to describe the nature of these laminated sedimentary records and assess their suitability to reconstruct environmental and biological signals at multiannual and decadal time-scales during the past several hundred years. In the first stage, we conducted exploratory surveys that enabled us to pinpoint continental margin localities where high-resolution records are preserved. The present work summarizes the initial analyses of a core spanning longer than the last 200 years from one of the most favorable regions found.

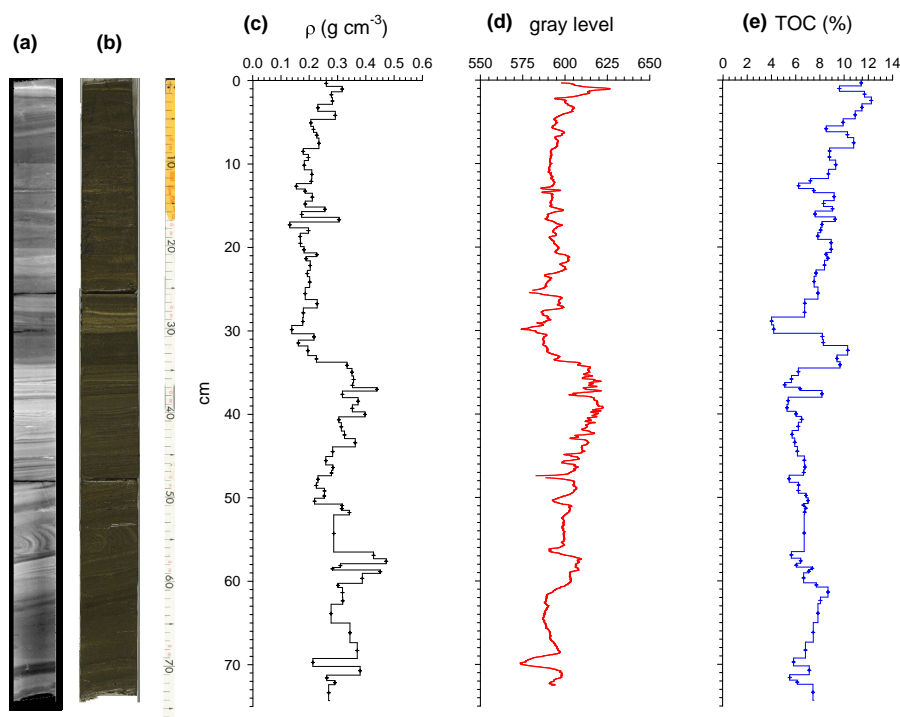


Fig. 2. Sedimentary characteristics of boxcore B0405-06. (a) Digital X-radiograph (SCOPIX), (b) digital photograph, (c) downcore distribution of dry bulk density (ρ), (d) X-ray gray level (arbitrary units), and (e) percent total organic carbon (TOC) from boxcore B0405-06.

2 Methodology

2.1 Environmental setting and sampling site

Based on previous studies (Suess et al., 1990; Reinhardt et al., 2002; IMARPE, unpublished data), exploratory coring was done on the upper slope off Callao ($11^{\circ}30' S$ – $12^{\circ}15' S$) and Pisco ($13^{\circ}15' S$ – $14^{\circ}00' S$), at depths varying between 100 and 400 m. This sampling involved a series of short Phleger gravity cores (6.3 cm internal diameter and 63 cm length) taken on the R/V Olaya (May 2003). These sediment cores showed different types of structures, including homogeneous, banded, or laminated layers, sometimes with nodules and unconformable laminations. The most continuously laminated cores were collected off Pisco between 200 and 300 m depth. This area is located downstream from the main upwelling center off Peru (San Juan, at $15^{\circ} S$) and within the core of the oxygen minimum zone (OMZ). The shelf-slope transition is smooth here and located around 350 m depth. A boxcore containing finely laminated sequences was retrieved using a Soutar Box Corer, off Pisco ($14^{\circ}07.9' S$, $76^{\circ}30.1' W$, 299 m depth) on a second cruise in May 2004 (Fig. 1).

2.2 Analytical methods

The relatively large area of the box core provided large sediment volume for small incremental downcore sub-sampling. The core was left to drain for several months before subsampling, which resulted in considerable core shrinkage. The core was then cut into four slabs of 2.5 cm thickness each for

bulk sedimentological and microfossil subsampling, and two slabs of 1 cm thickness each for X-radiography, chronology development, and geochemical analyses. Subsampling for chronology work and for bulk sedimentology was performed with centimeter to sub-centimeter resolution following the stratigraphy. Sediment dry bulk density (ρ) was estimated by mapping each sediment slice area and thickness.

Sedimentary structures were documented by analogic X-radiography and by high-resolution (sub-millimeter scale) digital X-radioscopy (SCOPIX, Migneon et al., 1999). Radioscopy outputs were expressed on a gray level scale that measures density-based differences in the transparency to X-rays, with higher gray levels indicating lower transparency due to greater density. The vertical distributions of excess ^{210}Pb and other radionuclides were determined by gamma spectrometry at the Laboratoire des Sciences du Climat et l'Environnement, at Gif-Sur-Yvette, France. Gamma spectrometry on sediment samples was done with one high-resolution, low background, “well-type” Ge detector at the Laboratoire Souterrain de Modane (Cochran, 1992; Reyss et al., 1995). In order to correct ^{210}Pb gamma countings by self-absorption, radiochemical assays were run for some sediment samples previously spiked with ^{208}Po , followed by alpha spectrometry. Sedimentation rates were obtained from a simple Constant Flux / Constant Supply Model (Appleby and Oldfield, 1978) using excess ^{210}Pb downcore profiles. Complete chronologies are in progress from these ^{210}Pb derived sedimentation rates and by radiocarbon ages corrected by local reservoir effects, as well as through comparisons of laminations, traces of slumps and biogenic structures.

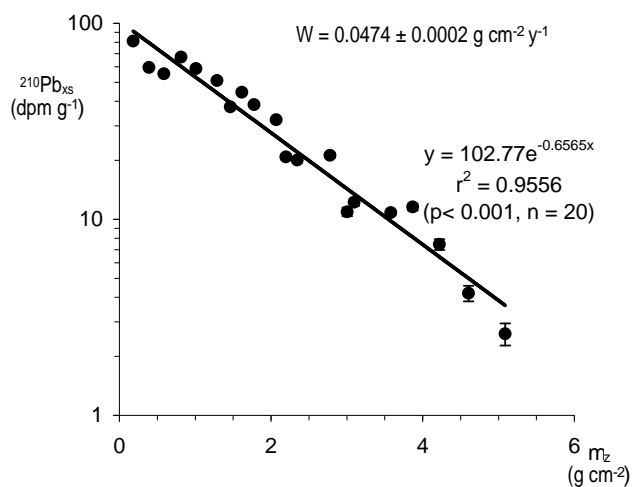


Fig. 3. Downcore distribution of excess ^{210}Pb versus depth-accumulated mass. Regression line corresponds to the least-squares fit of the Constant Flux – Constant Sedimentation model and yields a mass accumulation rate of $0.0424 \pm 0.0024 \text{ g cm}^{-2} \text{ y}^{-1}$.

Bulk elemental total organic carbon (TOC) was measured with a Thermo Electron CNS elemental analyzer (PALÉOTROPIQUE laboratory, Bondy). The mineralogical composition was assessed by Fourier Transformed Infrared Spectrometry (FTIR). Samples were prepared using a KBr disc, which ensures that Lambert-Beer's law is valid. A quantitative determination of the mineral content from various blends was performed by making a multicomponent analysis of the experimental spectrum using the spectra of each component in the mixture (Bertaux et al., 1998). Smear-slides of selected samples were microphotographed under a polarized microscope in order to observe, describe, and quantify the biogenic and detrital particles.

3 Results and discussion

Sedimentary characteristics, including X-radiographs, gray level, dry bulk density (ρ), and TOC values from the box-core are shown in Fig. 2. Gray level varies positively with ρ ($r^2=0.45$, $n=83$, $p<0.001$), indicating that sediment transparency to X-rays is at least partly explained by changes in dry bulk density. A major change in the sediment structure is observed at 34 cm depth below the core top. Above this 34 cm level, sediments are less dense on average with coarser laminations and higher and more variable TOC content. Below this level sediments are characterized by greater density, finer laminations, and a lower, less variable, TOC content. A finely laminated sequence of 20 cm is located immediately below this transition and extends down to a slump segment at 52–55 cm depth. Couplets of dark and light laminae range from 2–5 mm thickness within the finely laminated sequence. Above the 34 cm transition, the thickness of the coarse couplets are ~ 1 cm.

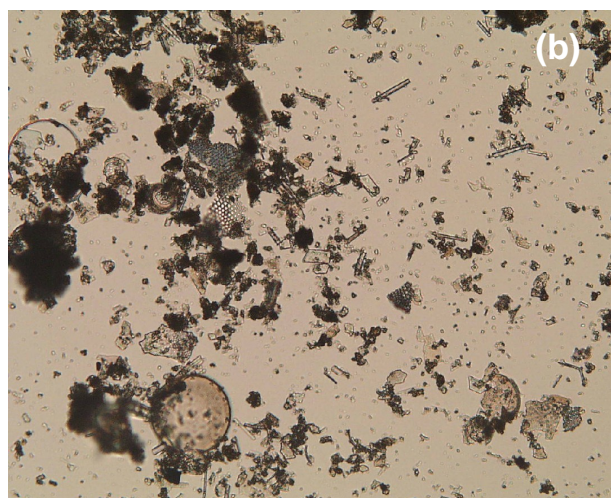
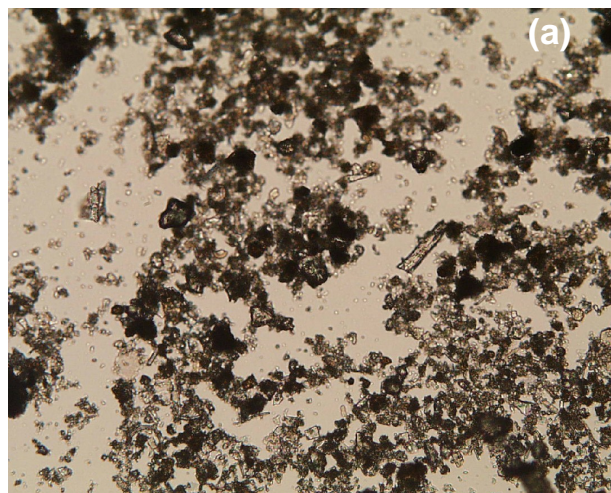


Fig. 4. Polarized microphotographs of a smear-slide of (a) a light-coloured lamina and (b) a dark-coloured lamina, showing higher abundances of mineral particles and diatom remains, respectively.

Excess ^{210}Pb is present down to 25 cm depth, showing a log-linear downcore decrease with accumulated mass (Fig. 3). Excess ^{210}Pb yields an average sediment accumulation rate of $0.047 \pm 0.002 \text{ g cm}^{-2} \text{ y}^{-1}$ ($r^2=0.96$). This rate roughly agrees with the downcore distribution of ^{241}Am and ^{137}Cs , which show peaks at ca. 7 cm depth (not shown). Excess ^{228}Th is present in the top layer, confirming the recovery of the sediment/water interface. The sediment accumulation rate was divided by the mean value of ρ in the upper 25 cm to yield an average sedimentation rate of 2.2 mm y^{-1} . Since the thickness of the finest couplets of dark and light laminae are from 2 to 5 mm, some laminae may represent annual layers of sedimentation. Applying the constant sediment accumulation rate for the whole sediment core suggests that the slump segment at ~ 54 cm depth corresponds to the mid-eighteenth century. We hypothesize that this slump coincides with a strong earthquake in 1746, which was followed by a tsunami

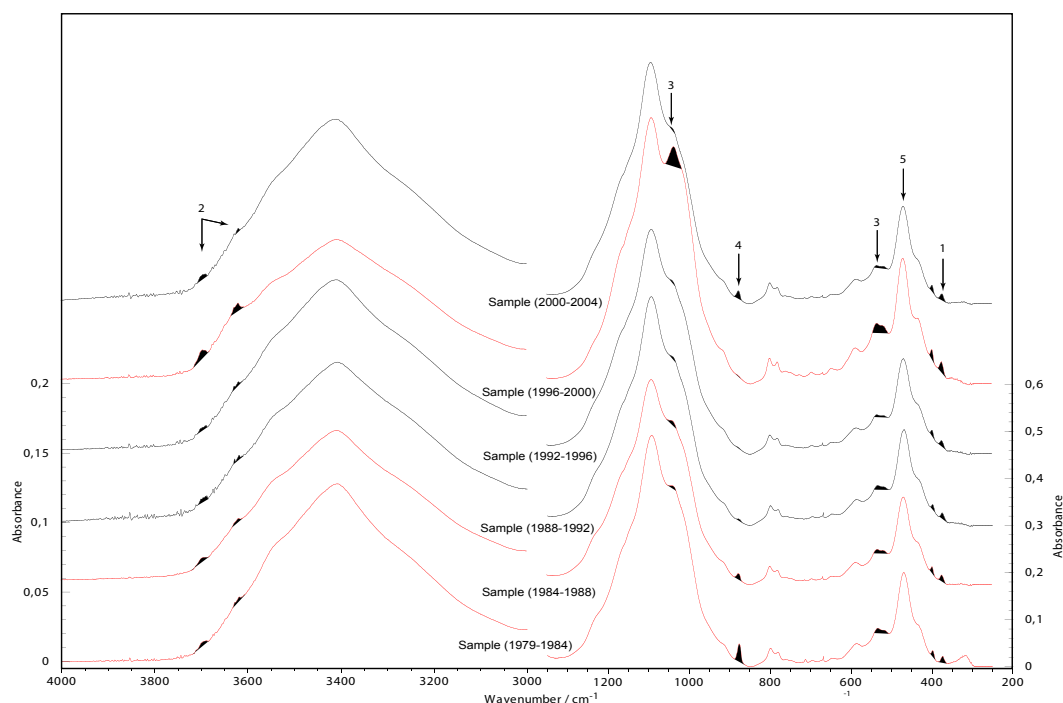


Fig. 5. FTIR spectra of the six upper sampling intervals (0–4.65 cm), showing the amplitude of absorbance vs wavenumber (cm^{-1}). The numbers indicate absorbance of 1) quartz, 2) kaolinite, 3) feldspar, 4) calcite (authigenic mineral), and 5) total silicates (terrigenous material). The variations of these absorbances show higher input of quartz, kaolinite and feldspar in intervals that include El Niño events (red lines) than in intervals with normal years (black lines). Black shading of some small peaks emphasizes the relative differences in absorbance between these sampling intervals.

that impacted the central Peruvian coast, completely destroying the port of Callao. Following this assumption, the 34 cm transition is dated at ca. 1850.

Combined evidence thus indicates that the mid-nineteenth century is a transitional period in terms of sediment density, total organic carbon content, and formation of laminae. The higher TOC values in the upper segment (the 12 uppermost sampling intervals corresponding to ~ 50 years) indicate a net TOC flux increase, although with significant multiannual variability superimposed. This 50 year period coincides with a trend of increasing upwelling favorable winds in instrumental records (Jahncke et al., 2004), suggesting that the augmentation of TOC flux results from higher primary production. An increase in TOC flux is also present at the same period in laminated sediments at Mejillones Bay (23°S) off northern Chile (Valdés et al., 2004; Vargas, 2002; Vargas et al., 2004), suggesting that these positive trends of inferred upwelling and primary production occur at a regional scale.

FTIR analyses show that the sediment is composed of quartz, feldspar, kaolinite, illite and amorphous silica. Polarized microphotographs of smear-slides show that concentrations of mineral particles are higher in light laminae and that amorphous silica, corresponding to diatom fragments (primarily *Thalassionema nitzschioides*, *Thalassionema bacillare* and resting spores of *Chaetoceros* spp.), is a primary constituent of dark laminae (Fig. 4). Note that lighter (darker) layers in the x-radiograph are also lighter (darker) in the pho-

tographic image. Light laminae and layers with thicker light laminae tend to present higher gray levels and higher ρ , respectively, and vice versa. Since the laminae couplets reflect an alternation in the sedimentation, with dark (biogenic) laminae deposited during more productive periods, the finely laminated sequence deposited before the mid-nineteenth century may be interpreted as an increase in seasonality of terrigenous and biogenous sedimentation.

Figure 5 shows the FTIR spectra of six different sampling intervals from the upper layers of the boxcore that span the last 25 years. Increases in the mineral fraction (quartz, feldspar, kaolinite and illite) were present in three sampling intervals that include El Niño events (1982–1983, 1986–1987 and 1997–1998), which can be interpreted as resulting from increased terrigenous input to the continental Peruvian margin. Higher deposition of terrigenous material in this area, where riverine sources are scarce, can result from a combination of increased fluvial discharges due to a greater regional rainfall (Bendix, 2000; Bendix et al., 2003) and enhanced poleward transport during the EN events (Strub et al., 1998 and references therein).

4 Conclusions

A boxcore collected off Pisco provides a continuous record of oceanographic and climatic changes during the last 100 to

250 years. Periods of mineral fractions increase, as those including the 1982–1983, 1986–1987 and 1997–1998 El Niño episodes, may be interpreted as resulting from a combination of increased regional fluvial discharges and enhanced poleward transport during the EN events. A change in sedimentological characteristics and variability of TOC is observed at ca. 1850, reflecting noteworthy changes in climate and ecosystem properties, (e.g. relatively higher seasonality in the fluxes of terrigenous components versus biogenous components prior to that stratigraphic level). Multidecadal variability of TOC is present over the past 150 years, including a positive trend in TOC for the past 50 years. Taking into account instrumental records of increasing alongshore wind stress off Peru and a similar pattern for the TOC flux off the northern Chilean coast during the last half century, we infer a regional intensification of the upwelling regime with enhanced primary productivity.

Acknowledgements. We deeply thank the Instituto del Mar del Perú (IMARPE) for full support of this research. We acknowledge the crew of the RV José Olaya Balandra and other scientific participants in the box-coring survey: E. Enríquez, J. Ledesma, R. Marquina, L. Quipúzcoa, J. Solís, and L. Vásquez, without their support this research could not have taken place. M. Gutiérrez and G. Herbozo kindly contributed the bathymetric map off Pisco shown in Fig. 1. M. Mandeng-Yogo, S. Caquineau and M. García from the IRD Research Unit Paléotropique contributed in several analytical tasks that were used for this research. We also acknowledge the Geology and Oceanography Department of the University of Bordeaux I, France, where the SCOPIX analyses were done. This research was financed by: IMARPE, the IAI Small Grant Program Round 2 project No. 03SGP211-222, IRD Research Unit Paléotropique, IRD DSF Scientific Short-term Exchange Fellowship for D.G., the IAI Collaborative Research Network EPCOR (Eastern Pacific Consortium for Oceanic Research), and the AIEA Coordinated Research Project “Nuclear and isotopic studies of El Niño Phenomenon in the Ocean”, research contract No. 12789. This study was also supported and conducted in the frame of the EU-project CENSOR (Climate variability and El Niño Southern Oscillation: Impacts for natural resources and management, contract 511071) and is CENSOR publication 0006.

Edited by: P. Fabian and J. L. Santos

Reviewed by: two anonymous referees

References

- Alheit, J. and Ñiquen, M.: Regime shifts in the Humboldt Current Ecosystem, *Prog. Oceanogr.*, 60, 201–222, 2004.
- Appleby, P. G. and Oldfield, F.: The calculation of lead-210 dates assuming a constant rate of supply of unsupported ^{210}Pb to the sediment, *Catena*, 5, 1–8, 1978.
- Arntz, W. and Fahrbach, E.: El Niño: experimento climático de la naturaleza. Causas físicas y efectos biológicos, Fondo de Cultura Económica, México, D.F, 309 p., 1996.
- Bendix, J.: A comparative analysis of the major El Niño events in Ecuador and Peru over the last two decades, *Zbl. Geol. & Paläontol., Teil I* 1999, H. 7/8, 1119–1131, 2000.
- Bendix, A., Bendix, J., Gämmerler, S., Reudenbach, Ch., and Weise, S.: The El Niño 1997/98 as seen from space – rainfall retrieval and investigation of rainfall dynamics with GOES-8 and TRMM data, *Proceedings 2002 Met. Sat. Users’ Conf.*, Dublin, 2–6 September 2002, EUMETSAT, 647–652, 2003.
- Bertaux, J., Frohlich, F., and Ildefonse, Ph.: A new application of FTIR spectroscopy for the quantification of amorphous and crystallized mineral phases, Example of organic rich sediments, *J. Sediment. Res.*, 68, 3, 440–447, 1998.
- Chávez, F., Ryan, J., Lluch-Cota, S., and Ñiquen, M.: Climate, fish, ocean productivity, and atmospheric carbon dioxide, *Science*, 299, 217–221, 2003.
- Cobb, K. M., Charles, C. D., Edwards, R. L., Cheng, H., and Kastner, M.: El Niño-Southern Oscillation and tropical Pacific climate during the last millennium, *Nature*, 424, 271–276, 2003.
- Cochran, K.: The oceanic chemistry of the U- and Th-series nuclides, in: *Uranium series disequilibrium: Applications to earth, marine and environmental sciences*, edited by: Ivanovich, M. and Harmon, R., Clarendon Press, Oxford, pp. 384–430, 1992.
- Field, D. B. and Baumgartner, T. R.: A 900 year stable isotope record of inter-decadal and centennial change from the California Current, *Paleoceanography*, 15, 695–708, 2000.
- Hsieh, C. H., Glaser, S. M., Lucas, A. J., and Sugihara, G.: Distinguishing random environmental fluctuations from ecological catastrophes for the North Pacific Ocean, *Nature*, 435, 336–340, doi:10.1038/nature02553, 2005.
- Jahncke, J., Checkley, D., and Hunt, G. L.: Trends in carbon flux to seabirds in the Peruvian upwelling system: effects of wind and fisheries on population regulation, *Fisheries Oceanography*, 13 (3), 208, doi:10.1111/j.1365-2419.2004.00283.x, 2004.
- Kemp, A. E.: Sedimentary fabrics and variation in lamination style in Peru continental upwelling sediments, in: *Proceedings of the Ocean Drilling Project, Scientific Results, ODP*, edited by: Suess, E., Von Huene, R., Emeis, K., Bourgeois, J., et al., College Station, Texas, 112, 45–58, 1990.
- Krissek, L. A. and Scheidegger, K. F.: Environmental controls on sediment texture and composition in low oxygen zones off Peru and Oregon, in: *Coastal upwelling; its sediment record, Part B: Sedimentary records of ancient coastal upwelling*, edited by: Suess, E. and Thiede, J., Plenum Press, New York, pp. 163–180, 1983.
- Levin, L. A., Gutiérrez, D., Rathburn, A., Neira, C., Sellanes, J., Muñoz, P., Gallardo, V. A., and Salamanca, M.: Benthic processes on the Peru Margin: A transect across the oxygen minimum zone during the 1997–98 El Niño, *Prog. Oceanogr.*, 53, 1–27, 2002.
- Mantua, N. J. and Hare, S. R.: The Pacific decadal oscillation, *J. Oceanogr.*, 58, 35–44, 2002.
- Migeon, S., Weber, O., Faugeres, J.-C., and Saint-Paul, J.: SCOPIX: a new X-ray imaging system for core analysis, *Geo-Marine Lett.*, 18, 251–225, 1999.
- Miller, A., Cayan, D. R., Barnett, T. P., Graham, N. E., Oberhuber, J.: Interdecadal variability of the Pacific Ocean: model response to observed heat flux and wind stress anomalies, *Clim. Dyn.*, 9, 287–302, 1994.
- Organization Panamericana de la salud (OPS): *Crónicas de desastres, Fenómeno El Niño – 1997–1998*, Washington, 2000.
- Reinhardt, L., Kudrass, H.-R., Lückge, A., Wiedicke, M., Wunderlich, J., and Wendt, G.: High-resolution sediment echosounding off Peru: Late Quaternary depositional sequences and sedimentary structures of a current-dominated shelf, *Mar. Geophys. Res.*, 23, 335–351, 2002.
- Reyss, J.-L., Schmidt, S., Legeleux, F., and Bonté P.: Large, low background well-type detectors for measurements of en-

- vironmental radioactivity, *Nuclear Instruments and Methods in Physics Research A*, 357, 391–397, 1995.
- Schwartzlose, R., Alheit, J., Bakun, A., Baumgartner, T., Cloete, R., Crawford, R., Fletcher, W., Green-ruiz, Y., Hagen, E., Kawasaki, T., Lluch-Belda, D., Lluch-cota, S., Maccall, A., Matsuura, Y., Nevarez-Martinez, M., Parrish, R., Roy, C., Serra, R., Shust, K., Ward, N., and Zuzunaga, J.: Worldwide large-scale fluctuations of sardine and anchovy populations, *S. Afr. J. Mar. Sci.*, 21, 289–347, 1999.
- Strub, P. T., Mesías, J. M., Montecino, V., and Rutllant, J.: Coastal ocean circulation off western South America, in: *The global coastal ocean*, edited by: Robinson, A. R. and Brink, K. H., *The Sea*, Vol. 11, Interscience, New York, p. 273–313, 1998.
- Suess, E., Von Huene, R., Emeis, K., Bourgois, J., et al.: *Proceedings of the Ocean Drilling Program, Scientific Results*, Vol. 112, 738 p., 1990.
- Valdés, J., Ortlieb, L., and Sifeddine, A.: Variaciones del sistema de surgencia de Punta Angamos (23°S) y la Zona de Mínimo de Oxígeno durante el pasado reciente: una aproximación desde el registro sedimentario de la Bahía Mejillones del Sur. *Rev. Chil. Hist. Nat.*, 76 (3): 347–362., 2003.
- Valdés, J., Sifeddine, A., Lallier-Verges, E., and Ortlieb, L.: Petrographic and geochemical study of organic matter in surficial laminated sediments from an upwelling system (mejillones del Sur Bay, northern Chile), *Org. Geochem.*, 35, 881–894, 2004.
- Vargas, G.: Interactions océan-atmosphère au cours des derniers siècles sur la côte du Désert d'Atacama: analyse multi-proxies des sédiments laminés de la baie de Mejillones (23° S), Ph.D. Thesis, Université Bordeaux I, 290 p., 2002.
- Vargas, G., Ortlieb, L., Pichon, J. J., Bertaux, J., and Pujos, M.: Sedimentary facies and high resolution primary production inferences from laminated diatomaceous sediments off northern Chile (23° S), *Mar. Geol.*, 211, 79–99, 2004.
- Wang, C. and Picaut, J.: Understanding ENSO physics – A review, in: *Earth's Climate: The Ocean-Atmosphere Interaction*, edited by: Wang, C., Xie, S.-P., and Carton, J. A., *AGU Geophysical Monograph Series*, 147, 21–48, 2004.
- Wang, C., Xie, S.-P., and Carton, J. A.: A global survey of ocean-atmosphere interaction and climate variability, in: *Earth's Climate: The Ocean-Atmosphere Interaction*, edited by: Wang, C., Xie, S.-P., and Carton, J. A., *AGU Geophysical Monograph Series*, 147, 1–19, 2004.
- Wang, C. and Fiedler, P. C.: ENSO variability and the eastern tropical Pacific: A review, *Prog. Oceanogr.*, in press, 2005.



Pentacyclic triterpene methyl ethers in recent lacustrine sediments (Lagoa do Caçó, Brazil)

Jérémy Jacob^{a,*}, Jean-Robert Disnar^a, Mohammed Boussafir^a,
Ana Luiza Spadano Albuquerque^b, Abdelfettah Sifeddine^c, Bruno Turcq^d

^a *Laboratoire de Sédimentation et Diagenèse de la Matière Organique, Institut des Sciences de la Terre d'Orléans (ISTO) – UMR 6113 du CNRS, Université d'Orléans, Bâtiment Géosciences, 45067 Orléans Cedex 2, France*

^b *Departamento de Geoquímica, Universidade Federal Fluminense, Morro do Valonguinho s/no. 24020-007 Niteroi, Rio de Janeiro, Brazil*
^c *IRD/CNPq, Departamento de Geoquímica, Universidade Federal Fluminense, Morro do Valonguinho s/no. 24020-007*

^d *UR055, IRD, Centre d'Ile de France, Institut de Recherche pour le Développement, 32 av. Henri Varagnat 93143, Bondy Cedex, France*

Received 8 August 2003; accepted 21 September 2004

(returned to author for revision 24 October 2003)

Available online 8 December 2004

Abstract

The lipid extracts of sediments collected from the Quaternary filling of a tropical lacustrine series (Lagoa do Caçó, Brazil) were investigated using gas chromatography–mass spectrometry (GC–MS). Various pentacyclic triterpene 3-methyl ethers (PTMEs) were present in the neutral fraction. Comparison of retention times and mass spectra with available standards allowed us to confirm the presence of olean-12-en-3 β -ol ME (β -amyrin ME), olean-18-en-3 β -ol ME (miliacin), taraxer-14-en-3 β -ol ME (crusgallin), fern-9(11)-en-3 β -ol ME (arundoin) and arbor-9(11)-en-3 β -ol ME (cylindrin). The following other compounds could also be tentatively identified from their GC–MS characteristics: urs-12-en-3 β -ol ME, bauer-7-en-3 β -ol ME and fern-8-en-3 β -ol ME. Other compounds such as possible 3 α isomers of the PTMEs as well as di- or tri-unsaturated counterparts might be PTME diagenetic derivatives. According to previous chemotaxonomic studies, all these compounds most probably originate from Gramineae that used to colonize the savanna of Northern Brazil at the time of deposition.

© 2004 Elsevier Ltd. All rights reserved.

1. Introduction and setting

Since the isolation of isoarborinol from the Messel Oil Shale (Albrecht and Ourisson, 1969), the literature has been continuously enriched with information on new pentacyclic triterpenes which have been used in

petroleum exploration or palaeoenvironmental studies (Cranwell, 1984). These compounds comprise higher plant triterpenes (e.g., oleanane, lupane and ursane derivatives) which occur widely in the plant kingdom in the free form or bound to glycosyl or phenolic moieties through a functional group (Pant and Rastogi, 1979; Das and Mahato, 1983; Mahato et al., 1988, 1992; Mahato and Sen, 1997). The complex molecular skeleton and the different functionality of the triterpenes make this family of compounds one of the most

* Corresponding author.

E-mail address: jeremy.jacob@univ-orleans.fr (J. Jacob).

diversified in Nature. Their chemotaxonomic potential, their ability to be degraded via specific diagenetic routes and their widespread occurrence in the sedimentary record can provide key information on floral changes and early diagenesis (e.g., Killups et al., 1995). As noted by van Aarssen et al. (2000), few studies have screened for these compounds or their diagenetic derivatives in order to reconstruct past environmental change and climatic fluctuation. Other relevant work was limited to assessing terrestrial input versus phytoplankton organic matter production (Peters and Moldovan, 1993).

Recent tropical lacustrine sedimentary records are usually poorly described with regard to their biomarker content. Nevertheless, they provide unique botanical and geological records which encourage the identification of new compounds. In addition, studies on biomarkers in these areas can reveal useful information for calibrating geochemical studies on older sediments deposited in similar settings.

Lagoa do Caçó is a small oligotrophic lake in north-east Brazil, close to the Equator (Fig. 1). The sedimentary filling has been studied using various approaches to better document palaeoclimatic development since the Last Glacial Maximum (LGM) in the Tropics (Ledru et al., 2001, 2002; Sifeddine et al., 2003; Jacob, 2003; Jacob et al., 2004a,b). Here, we report on the GC–MS characteristics of several series of pentacyclic triterpene methyl ethers (PTMEs) present in the lipid extracts of Quaternary sediments from this tropical setting and their significance as plant source indicators or diagenetic indicators.

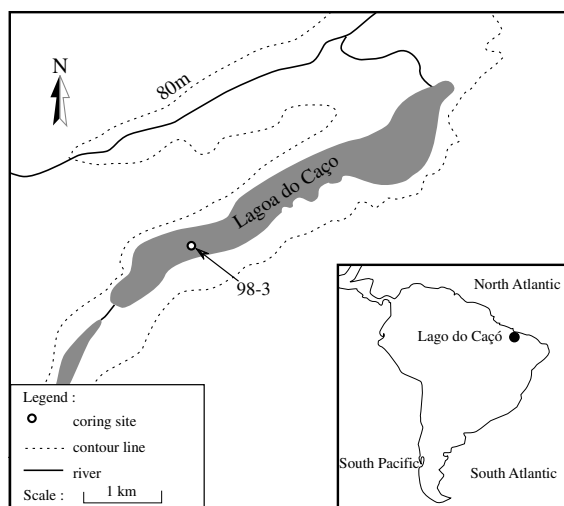


Fig. 1. Lagoa do Caçó position and location of the coring site.

2. Materials and methods

2.1. Sediment samples

The context and sample handling have been described (Jacob et al., 2004a). Briefly, a core (MA98-3; 6 m long) was divided into two main intervals. The lower (ca. 3 m long), which dates back to the end of the LGM, consists of fine-grained sands and silts. The upper half (ca. 3 m long), consisting of organic matter-rich silts, is divided into greenish-brown organic silts (Late Glacial) and black organic silts (Holocene). Two samples, which best illustrate the distribution of PTMEs, were selected following sedimentology and Rock-Eval 6 screening. Sample 170 (352 cm depth) belongs to a section dated back to the LGM, whereas sample 073 (150 cm depth) was deposited during the Holocene.

2.2. Extraction and separation of free lipids

The method for lipid extraction and separation was based on that of Logan and Eglinton (1994), with some modifications. One gram of dried sediment was ultrasonically extracted with acetone–pentane 1:1. The mixture was separated into a neutral and an acidic fraction by solid phase extraction using an AminoPropyl Bond Elute cartridge. Neutral compounds were eluted with DCM:CH₃OH (1:1) and acidic compounds with ether after acidification of the medium with ether:formic acid 9:1. The neutral fraction was submitted to further fractionation on activated Florisil[®] to give aliphatic hydrocarbons (eluted with heptane), aromatic hydrocarbons and ethers (DCM) and polar compounds (DCM:CH₃OH 1:1).

2.3. GC–MS

GC–MS was performed with a ThermoFinnigan TRACE–PolarisGCQ. The gas chromatograph was fitted with an Rtx[®]-5Sil MS capillary column (30 m × 0.32 mm i.d., 0.25 μm film thickness) with 5 m of guard column. The GC operating conditions were: temperature held at 40 °C for 1 min, then increased from 40 to 120 °C at 30 °C min⁻¹, 120 to 300 °C at 3 °C min⁻¹, with final isothermal hold at 300 °C over 30 min. The sample was injected splitless, with the injector temperature set at 280 °C. Helium was the carrier gas. The mass spectrometer was operated in the electron ionisation (EI) mode at 70 eV ionization energy and scanned from 50 to 650 Da. Where possible, the structures of individual compounds were assigned with authentic standards, isolated from extant plants, that were analysed with the same conditions. The remaining compounds were tentatively identified by comparison of mass spectra with literature data, relative retention times and interpretation of mass spectrometric fragmentation patterns.

3. Results

Total extract yields ranged between 0.5 and 4.2 mg g⁻¹ sediment. The neutral fraction afforded between 0.4 and 3.5 mg g⁻¹ sediment. The dominant compounds in this fraction were PTMEs and hopanoids. In total, at least sixteen compounds were distinguished using GC-MS. Two examples of the distribution of these compounds in Lagoa do Cacó sediments are shown in Fig. 2 together with a reconstructed total ion current (TIC) trace for reference compounds.

In total, 5 out of the 16 compounds were identified by comparison of the mass spectra and GC relative retention times with available standards, the identification of other compounds remaining tentative. The main characteristics of the compounds are summarized in Table 1. Thirteen of the sixteen have a molecular mass of 440 amu (Table 1). Compared to these compounds, two others with a molecular mass of 438 and another with 436, most probably have one and two additional double bonds, respectively. For most of the compounds having a molecular mass of 440 amu, the presence of fragments at *m/z* 408 [(M - 32)⁺] and *m/z* 393 [(M - 15)-32]⁺ points to the loss of a methoxy group as methanol during fragmentation (Bryce et al., 1967b). These characteristics, plus the fragmentation pattern typical for triterpene ethers as discussed below, led us to propose that the compounds with a molecular mass of 440 are unsaturated methoxy triterpenes having the formula C₃₁H₅₂O. At first sight, the compounds can be separated into two main groups, namely those whose

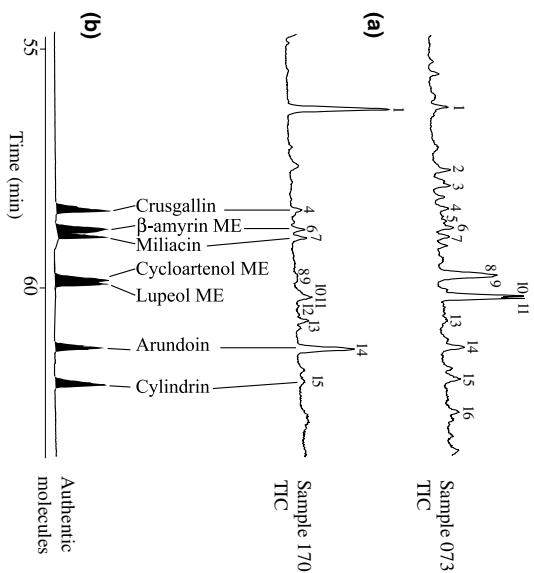


Fig. 2. (a) TIC chromatogram in the 55–65 min time range of the DCM fraction isolated from two sediment samples from Lagoa do Cacó. (b) Reconstructed TIC chromatogram of available reference compounds.

Table 1
Relation mass spectral data time for PTMEs

Retention time (min)	Peak No.	Structure	M ¹	Characteristic fragments (%)
56,3	1	<i>Lanostadien-3-ol ME</i>	440	425, 408, 393, 365, 355, 323, 287, 273, 261, 255, 241, 229, 215, 205, 191, 177, 163 (100)
57,59	2	<i>Taraxer-14-en-3α-ol ME</i>	440	425, 393, 355, 316, 301, 284, 269, 218 (100), 204, 190, 189, 175, 159
57,86	3	<i>Olean-12-en-3α-ol ME</i>	440	393, 325, 257, 218 (100), 203, 189, 175, 161
58,4	4	Taraxer-14-en-3β-ol	440	425, 408, 393, 355, 316, 301, 284, 269, 218, 204 (100), 189, 175, 159
58,68	5	<i>Urs-12-en-3β-ol ME</i>	440	425, 408, 393, 355, 255, 243, 229, 218 (100), 203, 189, 175, 161
58,84	6	Olean-12-en-3β-ol ME (b)^{a,b}	440	425, 408, 393, 323, 257, 243, 229, 218, 204, 189 (100), 177, 161
59,01	7	Olean-18-en-3β-ol ME (c)	440	425, 408, 393, 371, 339, 257, 243, 229, 218, 204, 189 (100), 177, 161
59,79	8	<i>Fern-9(11)-en-3α-ol ME</i>	440	425, 408, 393, 365, 323, 287, 273 (100), 261, 255, 241, 229, 215, 201, 189, 175, 159
59,87	9	<i>Arbor- or fern-7,9(11)-dien-3-ol ME</i>	438	423, 406, 391 (100), 363, 355, 323, 285, 267 (100), 253, 239, 227, 213, 199, 185, 171, 159
60,27	10	<i>Arbor-9(11)-en-3α-ol ME</i>	440	425, 408, 393, 365, 273 (100), 261, 255, 241, 229, 215, 201, 189, 175, 163
60,27	11	<i>Bauer-7-en-3β-ol ME</i>	440	425, 408, 393, 273, 261 (100), 255, 241, 229, 215, 201, 189, 175, 163
60,6	12	<i>Arbor or fern-7,9(11)-dien-3-ol ME</i>	438	423, 406, 391, 363, 321, 295 (?), 285 (100), 271, 253, 239, 225, 213, 197, 183, 171, 159
60,8	13	<i>Fern-8-en-3β-ol ME</i>	440	425, 408, 393, 365, 287, 273 (100), 261, 255, 241, 229, 213, 199, 187, 175, 159
61,3	14	Fern-9(11)-en-3β-ol ME (d)	440	425, 408, 393, 365, 355, 323, 287, 273 (100), 261, 255, 241, 229, 215, 201, 189, 175, 159
62,05	15	Arbor-9(11)-en-3β-ol ME (e)	440	425, 408, 393, 365, 355, 323, 287, 273 (100), 261, 255, 241, 229, 215, 201, 187, 173, 161
62,7	16	<i>Arbor- or Ferna-trien-3-ol ME</i>	436	421, 404, 389, 321, 283, 269, 257, 251 (100), 237, 225, 209, 195, 183, 169, 155

^a Trivial names in brackets: (a) sawamilletin or crusgallin; (b) isosawamilletin or β-amyryn ME; (c) miliacin or germanicol ME; (d) arundoin; (e) cylindrin.

^b Compounds in bold are those identified with authentic standards.

spectra are dominated by fragments at m/z 218, 203/204 and 189 (compounds 2–7) and those giving a base peak at m/z 273 and a major fragment at m/z 241 (compounds 8, 10, 13, 14 and 15). We discuss first the possible identity of the compounds belonging to these two different groups; then, we consider those having different general characteristics (compounds 1, 9, 11, 12 and 16).

3.1. Compounds 2–7

The intense fragments at m/z 218, 203/204 and 189 in the spectra of compounds 2–7 (Fig. 3) can arise from the D/E moiety of normal and D-friedo-triterpenes after C-ring breaking and possible retro-Diels Alder rearrangement (Budzikiewicz et al., 1962; Djerassi et al., 1962).

In addition to intense ions at m/z 218, 204 and 189, the spectra of compounds 2 and 4 (Fig. 4) show intense

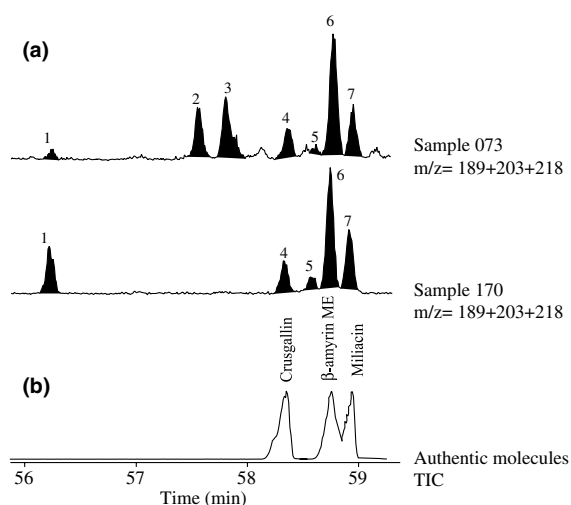
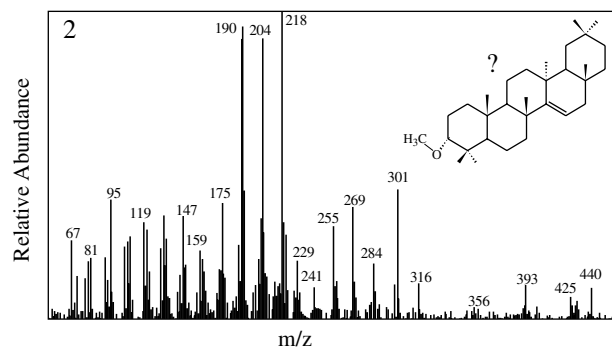


Fig. 3. (a) Specific ion mass chromatograms of DCM fraction isolated from sediments of Lagoa do Caçó. (b) Reconstructed TIC chromatogram from selected fragments of available reference compounds.



fragments at m/z 316, 301, 284 and 269 typical for taraxer-14-en-3 β -ol methyl ether (i.e., sawamilletin or crusgallin; Bryce et al., 1967a). As a matter of fact, comparison of retention time and mass spectrum with an authentic standard allowed us to identify compound 4 as taraxer-14-en-3 β -ol ME (Fig. 4). Compound 2 has a comparable mass spectrum to compound 4 except for the fragment at m/z 190, which could arise from hydrogen rearrangement involving the m/z 189 moiety or from a possible coeluting compound. Because only the mass spectrum of taraxer-14-en-3-ol ME is presently known to display fragments at m/z 316, 301, 284 and 269, it can be supposed that compound 2 could correspond to the taraxer-14-en-3-ol methyl ether isomer evidenced by Bryce et al. (1967a). The simplest change that taraxer-14-en-3 β -ol ME (compound 4) could undergo, without significantly affecting the fragmentation pattern, is epimerisation of the methyl ether group, at C-3. We therefore hypothesize that compound 2 is taraxer-14-en-3 α -ol ME.

Co-injection with an authentic standard (Fig. 3) allowed us to identify compound 6 as olean-12-en-3 β -ol ME (β -amyrin ME or isosawamilletin; Fig. 5). In a similar way as for compounds 2 and 4, the difference in retention time and spectral resemblance between compounds 3 and 6 (Fig. 5) led us to hypothesize that compound 3 could be the 3 α -epimer of compound 6, i.e., olean-12-en-3 α -ol ME.

In the absence of an available standard, but according to mass spectral resemblance (Bryce et al., 1967b), compound 5 is tentatively assigned as urs-12-en-3 β -ol ME (α -amyrin ME; Fig. 5). Identical retention time (Fig. 3) and mass spectrum to an authentic standard allowed us to identify compound 7 as olean-18-en-3 β -ol ME (miliacin or germanicol ME; Fig. 6).

3.2. Compounds 8, 10, 13, 14 and 15

Compounds 8, 10, 13, 14 and 15 (Fig. 7) display very similar spectral features, with significant fragments at

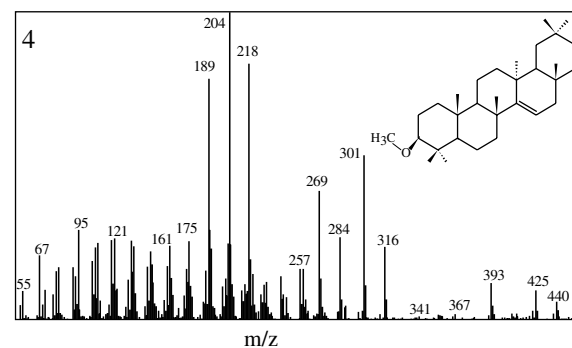


Fig. 4. Mass spectra of compounds 2 and 4 and proposed structures.

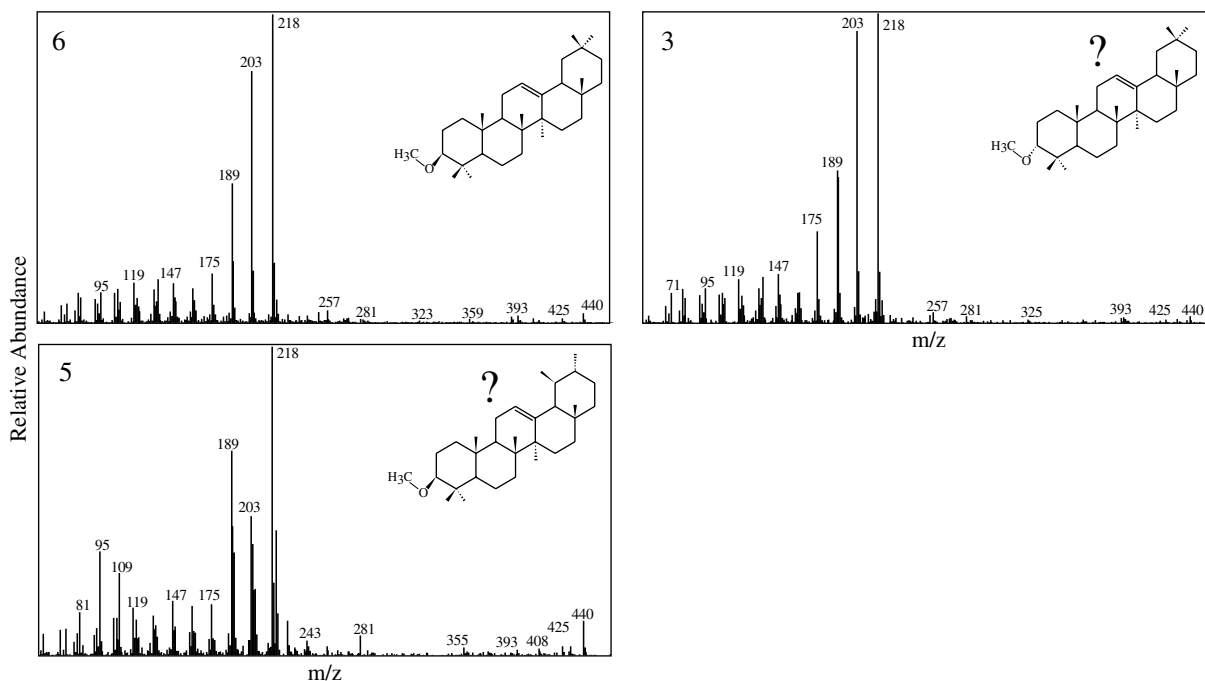


Fig. 5. Mass spectra of compounds 3, 5 and 6 and proposed structures.

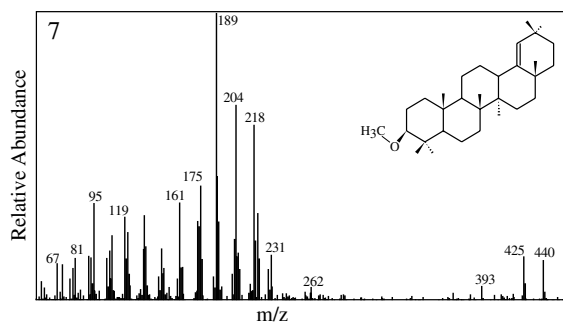


Fig. 6. Mass spectrum of compound 7 and proposed structure.

m/z 393, 287, 273, 255 and 241 in comparable proportions in the five spectra (Fig. 8). The dominant fragment at m/z 273 $[M - 167]^+$ is typical of D:C- or E:C-friedo triterpenes of the fernane, arborane, bauerane, or multiflorane type (Nishimoto et al., 1968; Shiojima et al., 1992). By loss of CH_3OH , this latter fragment produces the other important fragment at m/z 241. A small fragment at m/z 365 could be attributed to the loss of an isopropyl group from the m/z 408 $[(M - 32)^+]$ fragment. Therefore, compounds 8, 10, 13, 14 and 15 can be identified as D:C- or E:C-friedo triterpene methyl ethers with an isopropyl group on ring E and a double bond in the $\Delta^{9(11)}$ or Δ^8 positions (Nishimoto et al., 1968; Bryce et al., 1967a). By comparison of retention times (Fig. 7)

and mass spectra with authentic standards, compounds 14 and 15 can be assigned as fern-9(11)-en-3 β -ol ME (arundoin) and as arbor-9(11)-en-3 β -ol ME (cylindrin), respectively (Fig. 8).

Finally, there are few spectroscopic features to distinguish among the three remaining compounds (8, 10 and 13). In the same way as for taraxer-14-en-3 β -ol ME (compound 4) and its possible 3 α epimer (compound 2), comparable differences in retention time between compounds 8–14 and 10–15 (1.51 and 1.78 min, respectively) and mass spectral resemblances lead us to propose that compounds 8 and 10 could be the 3 α -epimers of fern-9(11)-en-3-ol ME and arbor-9(11)-en-3-ol ME, respectively. The remaining compound 13 could be the fern-8-en-3 β -ol ME, previously described by Nishimoto et al. (1968).

3.3. Compounds 11 and 1

Compound 11 coelutes with compound 10 under the GC temperature programme used routinely (Fig. 7). The mass spectra of 10 and 11 were obtained on samples containing greater proportions of one of these two compounds than of the other and by background subtraction. The spectrum of 11 is dominated by a strong doublet at m/z 261 and m/z 229 (Fig. 9). Small fragments at m/z 273 and m/z 241 may originate from the coeluting compound 10 (Fig. 7). No fragment indicative of the loss of an isopropyl group from the ion at m/z 408 was

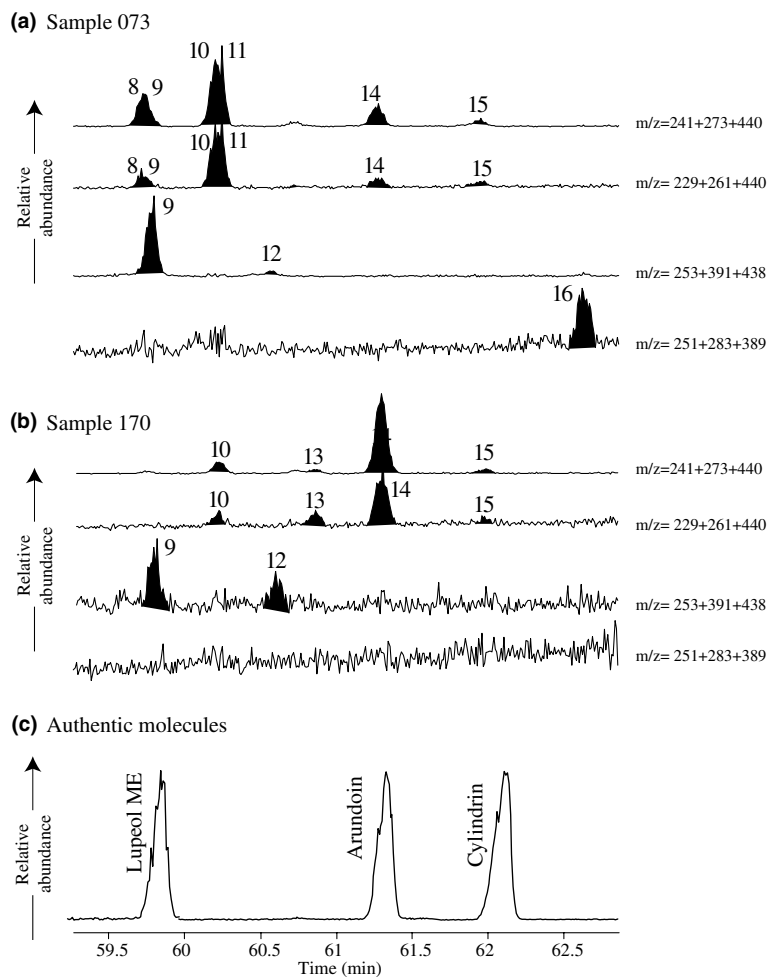


Fig. 7. Specific ion chromatograms illustrating the distribution of D:C- and E:C-friedo PTMEs in Lagoa do Caçó sediments ((a) sample 073 and (b) sample 170) and (c) reconstructed mass chromatogram of available authentic products.

detected. From this evidence and according to Nishimoto et al. (1968) and Bryce et al. (1967b), compound 11 is tentatively identified as bauer-7-en-3 β -ol ME.

Compound 1 (Fig. 3) shows a spectrum with a base peak at m/z 163 and intense ions at m/z 191 and m/z 205 (Fig. 10). Minor doublets at m/z 229 and 261, m/z 241 and 273, m/z 255 and 287 and m/z 323 and 355 suggest a D:C- or E:C-friedo structure with a methoxy group on ring A. Ions at m/z 365 and m/z 163 indicate the loss of an isopropyl group from fragments at m/z 408 and 206, respectively. The relatively short retention time could be indicative of a tetracyclic triterpene methyl ether. However, significant differences in retention times or fragmentation pattern exclude the possibility that it could be cycloartenol ME (Fig. 3) or parkeol ME (Russell et al., 1976), respectively. Because lanostene-type molecules have a similar fragmentation behaviour to that of arborenes/ferrenes (ascribed to the presence of

methyl groups located at the C/D-ring junction), compound 1 is tentatively assigned as a lanostadienol ME (Fig. 10; Uyeo et al., 1968).

3.4. Compounds 9, 12 and 16

The spectra of compounds 9 and 12 have comparable features: a molecular ion at m/z 438, fragments at m/z 423 [$M - 15$]⁺ and m/z 391 [$(M - 15) - 32$]⁺ (Fig. 11). Fragments at m/z 425 and 408 in the spectra of compound 9 arise from coeluting compound 8. The fragment at m/z 363 can be explained by loss of an isopropyl group from ion m/z 406, well expressed in the spectrum of 12. The spectra of both compounds exhibit doublets at m/z 285 and 253 and 271 and 239, indicative of an additional double bond on A, B or C-ring as compared with those of compounds 8, 10, 13, 14 and 15 (Fig. 8). Accordingly, 9 and 12 are thought to be di-unsaturated

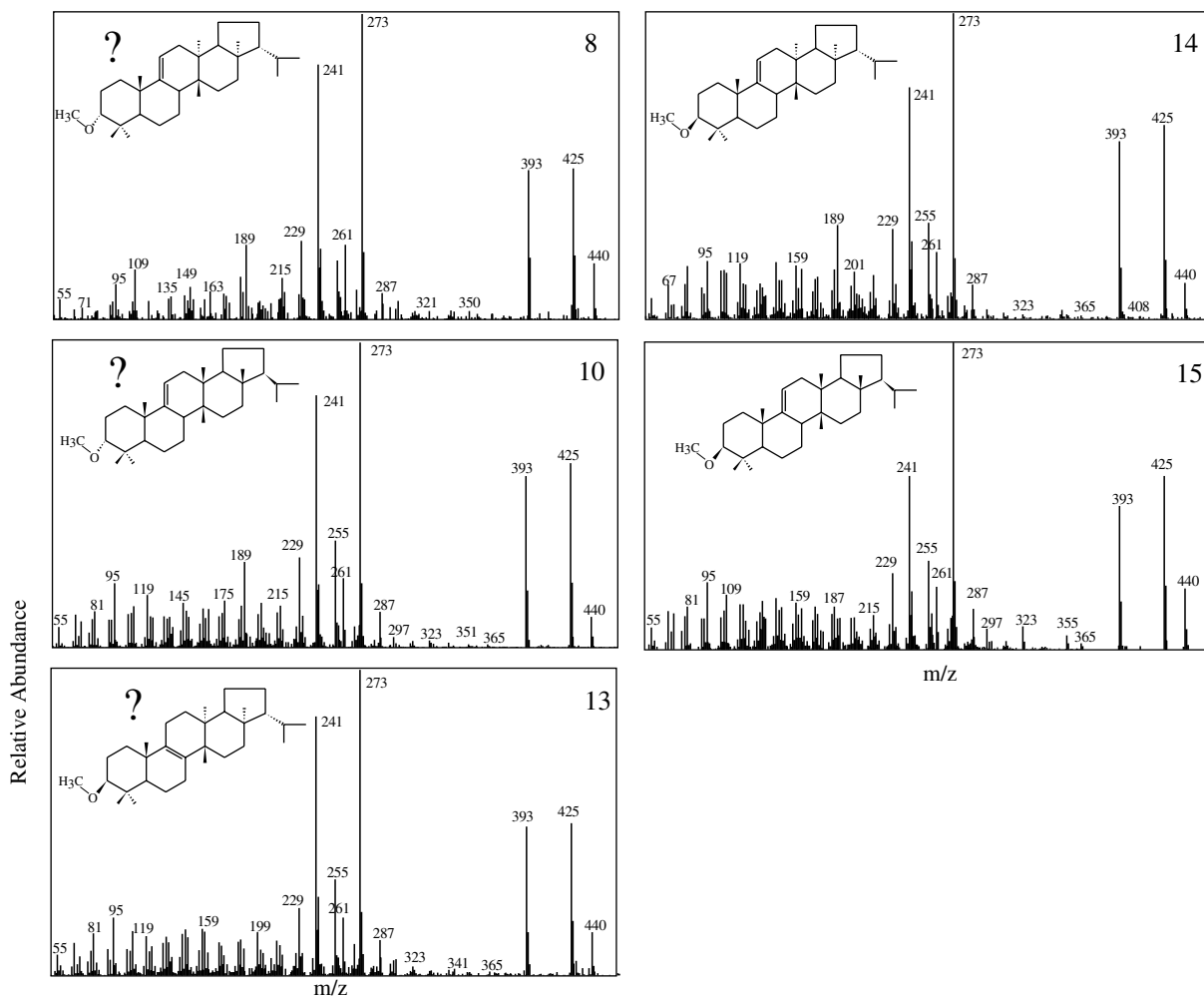


Fig. 8. Mass spectra of compounds 8, 14, 10, 15 and 13 and proposed structures.

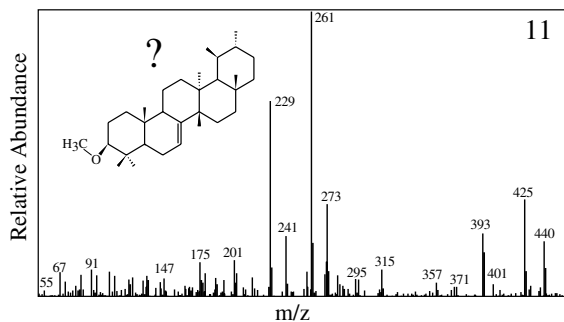


Fig. 9. Mass spectrum of compound 11 and proposed structure.

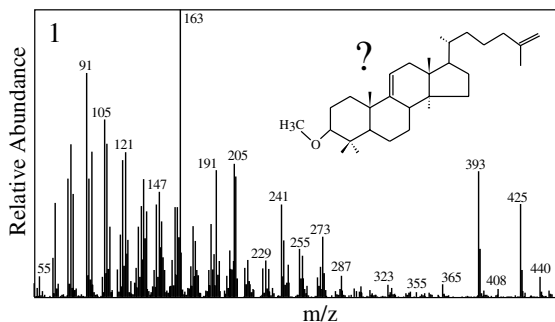


Fig. 10. Mass spectrum of compound 1 and proposed structure.

D:C- or E:C-friedo PTMEs with a fernane or arborane skeleton. Given the earlier elution of fernane-type compared to arborane-type compounds, we propose a ferna-7,9(11)-dien-ol ME structure for 9 and an arbora-7,9(11)-dien-ol ME structure for 12.

Compound 16 (Fig. 7) has a molecular ion at m/z 436, which is consistent with a structure of a PTME with three double bonds (Fig. 11). Its mass spectrum points to a D:C- or E:C-friedo structure. Comparison with

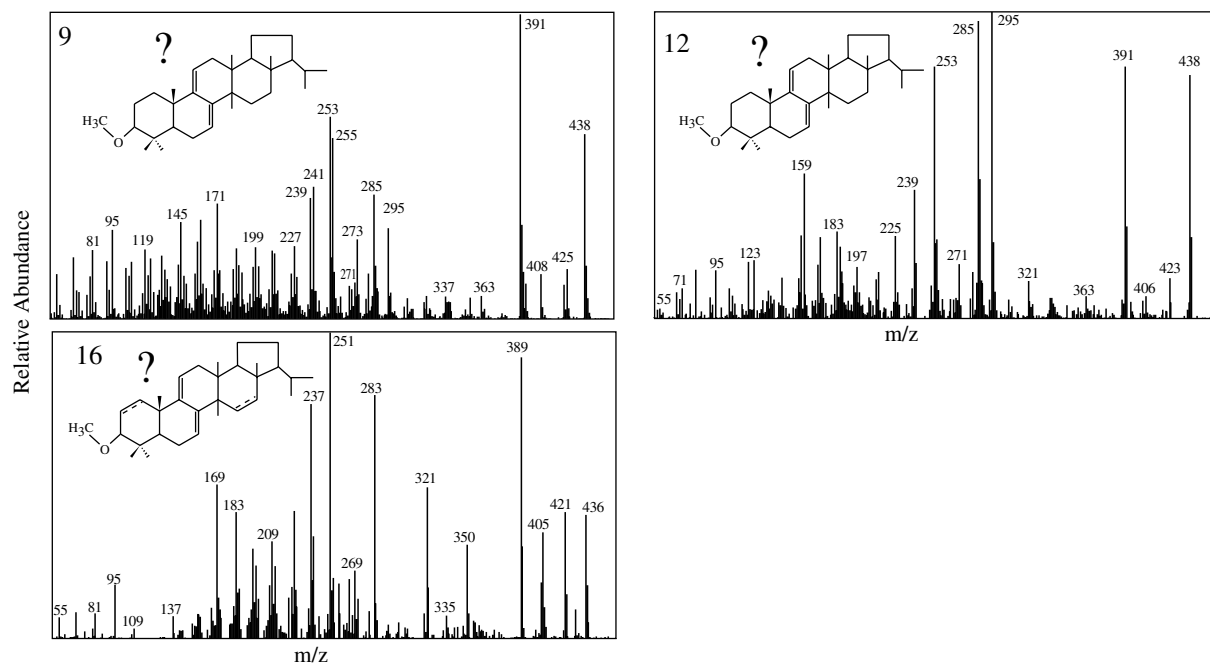


Fig. 11. Mass spectra of compound 9, 12 and 16 and proposed structures. Additional double bond (dashed line) in compound 16 can be located either in Δ^2 or Δ^{15} position.

the spectra of compounds 9 and 12 (Fig. 11) suggests that the additional double bond is located on ring A or B. From this evidence, an arboratriene or fernatriene ME structure is proposed for compound 16.

4. Discussion

To our knowledge, the only previous record of methoxy triterpenes in geological samples was made by Ries-Kautt (1986), who identified in soils one compound displaying a similar mass spectrum to that of fern-9(11)-en-3 β -ol ME and another unidentified one that could be related to taraxer-14-en-3 β -ol ME.

4.1. Biological sources of PTMEs

The following discussion is based mainly on available information on the occurrences of these compounds in living organisms and on a comparison with those detected from Lagoa do Caçó (Table 2). Pentacyclic triterpenes bearing an oxygenated group at position 3 are widely distributed in the plant kingdom (Pant and Rastogi, 1979; Das and Mahato, 1983; Mahato et al., 1988, 1992; Mahato and Sen, 1997). Nevertheless, methyl ethers are rather uncommon. Most of the PTME plant sources are monocots and belong to Gramineae (Poaceae). PTMEs from Gramineae have been largely studied during 1960s (review in Martin-Smith et al., 1967;

Ohmoto et al., 1970). Ohmoto et al. (1970) reported the occurrence of nine PTME structures from 31 species of Gramineae belonging to 14 tribes. Little chemotaxonomic evidence is available from these studies due to the few plants studied. More recently, arbor-9(11)-en-3 β -ol ME, lupanol ME and lupeol ME have been identified in palm trees (*Butia capitata* and *Orbignya* sp.; Garcia et al., 1995; *Elaeis guineensis*; Goh et al., 1988). Taraxer-14-en-3 β -ol ME, arbor-9(11)-en-3 α -ol ME and arbor-9(11)-en-3 β -ol ME have also been isolated from various dicots (*Diospyros ferrea*, *Bosistoa* sp. and *Mimusops littoralis*; Deshmane and Dev, 1971). Finally, Pinaceae (Rowe and Bower, 1965) and Burseraceae (Uyeo et al., 1968) have been cited as sources of PTMEs but, in the case of Pinaceae, the compounds were of the serratane-type. Injection of authentic lupeol ME (Bryce et al., 1967a) proves its absence from the samples (Fig. 2). In addition, none of the following compounds have been detected in our samples: hop-22(29)-en-3 β -ol ME (Rowan and Russell, 1992; Paupit et al., 1984), friedelenol ME (Oros and Simoneit, 2001) and serratenol ME (Rowe and Bower, 1965).

It is clear from the data in Table 2 that none of the species cited in the literature affords a range of PTMEs as wide as that encountered in our samples. Fern-9(11)-en-3 β -ol ME, arbor-9(11)-en-3 β -ol ME, taraxer-14-en-3 β -ol ME, olean-12-en-3 β -ol ME and olean-18-en-3 β -ol ME only co-occur in Poaceae species. The taxon displaying the distribution of PTMEs which is the more compa-

Table 2
Source inventory of PTMEs

		Compound structure	Taraxer-14-en-3 β -ol ME	Urs-12-en-3 β -ol ME	Olean-12-en-3 β -ol ME	Olean-18-en-3 β -ol ME	Fern-9(11)-en-3 α -ol ME	Arbor-9(11)-en-3 α -ol ME	Bauer-7-en-3 β -ol ME	Fern-8-en-3 β -ol ME	Fern-9(11)-en-3 β -ol ME	Arbor-9(11)-en-3 β -ol ME	Lup-20(29)-en-3 β -ol ME	Hop-22(29)-en-3 β -ol ME	Friedelane-type Mes	Serratane-type Mes	Cycloartenol ME	Parkeol ME			
Monocots	Arecaceae	<i>Butia capitata</i>																			
		<i>Elaeis guineensis</i>																			
	Poaceae	<i>Orbignya sp.</i>																			
		Danthonieae	<i>Cortaderia totoe*</i>		X																
			<i>Cortaderia fulvida</i>			X															
			<i>Cortaderia splendens</i>			X															
			<i>Cortaderia richardii</i>				X														
			<i>Chionocloa sp.</i>					X													
		Bambuseae	<i>Arundinaria chino</i>																		
		Oryzae	<i>Oryza sativa</i>						X												
		Centothecae	<i>Lophaterum gracile</i>																		
		Cynodontae	<i>Cynodon dactylon</i>												X						
		Eragrosteae	<i>Eragrostis curvula</i>		X																
			<i>Eragrostis ferruginea</i>			X															
		Zoysiaeae	<i>Zoysia japonica</i>							X											
			<i>Zoysia macrostachia</i>	X																	
			<i>Zoysia matrella</i>																		
			<i>Zoysia tenuifolia</i>						X												
		Andropogominae	<i>Arthraxon hispidus</i>																		
			<i>Imperata cylindrica</i>																		
			<i>Microstegium vimineum</i>					X													
			<i>Miscanthus floridulus</i>						X												
			<i>Miscanthus sacchariflorus</i>	X																	
			<i>Saccharum spontaneum</i>																		
			<i>Saccharum officinarum</i>	X																	
			<i>Saccharum robustum</i>	X																	
			<i>Saccharum edule</i>	X																	
			Rottboelliinae	<i>Hemarthria sibirica</i>																	
			<i>Phacelurus latifolius</i>	X																	
		Arundinelleae	<i>Arundinella hirta</i>																		
		Panicaceae	<i>Echionocloa crusgalli</i>	X																	
			<i>Oplismenus undulatifolius</i>																		
			<i>Panicum miliaceum</i>																		
			<i>Panicum dichotomiflorum</i>					X													
			<i>Paspalum dilatatum</i>												X						
			<i>Syntherisma sanguinalis</i>																		
			<i>Agrostis alba</i>																		
			Aveneae	<i>Alopercurus aequalis</i>																	
				<i>Phalaris arundinacea</i>																	
				<i>Calamagrostis epigeios</i>																	
		Meliceae	<i>Glyceria acutifolia</i>				X														
		Poeae	<i>Festuca arundinacea</i>																		
	<i>Poa pratensis</i>																				
	<i>Poa sphondylodes</i>																				
	Dicots	Rubiaceae	<i>Hedyotis acutangula</i>																		
			<i>Rubia oncotricha</i>																		
		Ebenaceae	<i>Diospyros ferrea</i>	X																	
		Fabaceae	<i>Humboldtia laurifolia</i>													X					
		Rutaceae	<i>Bosistoa sp.</i>	X																	
	Sapotaceae	<i>Glycosmis arborea</i>						X													
	Burseraceae	<i>Mimusops littoralis</i>	X																		
	Gymnosperms		<i>Picea jezoensis</i>																		
			<i>Tsuga mertensiana**</i>												X						
		Family	Genus	Species																	

Legend

X Compound described in taxa

* *Cortaderia Totoe* is the same species as *Arundo conspicua*

** Reported in burning aerosols

rable to that found in our samples is *Andropogonae*. As a matter of fact, plants belonging to this genus produce taraxer-14-en-3 β -ol ME, olean-18-en-3 β -ol ME, fern-9(11)-en-3 α -ol ME, bauer-7-en-3 β -ol ME, fern-9(11)-en-3 β -ol ME and arbor-9(11)-en-3 β -ol ME but not olean-12-en-3-ol ME. Therefore, although *Andropogonae* could appear as a likely source for the sedimentary PTMEs, at least one additional source must be envisaged. While screening chemotaxonomic relationships in the *Cortaderia* genus, Martin-Smith et al. (1967) noted that the South American strains (*C. selloana* and *C. atacamensis*) did not contain any PTMEs, in contrast to New Zealand species. It must thus be considered that the biological precursor(s) of the PTMEs identified in our samples could also originate from at least one of the twenty *Cortaderia* species that have not been analysed.

4.2. Diagenesis of PTMEs

PTMEs are minor components in living organisms and are defined as secondary metabolites (H.E. Connor, pers. comm.). They are found in leaf epicuticular waxes, where they play a crucial role in defending the organism against external agents (e.g., microbes, fungi, UV). In the upper section of Lagoa do Caçó sediments (i.e., since the Lateglacial), the OM is dominantly terrestrial in origin and is subjected to strong reworking in aerobic waters (Jacob, 2003; Jacob et al., 2004a). Therefore, the relatively high abundance of PTMEs in the core section, is probably due to their relative resistance to early degradation processes and hence a better preservation than many other biomarkers.

Despite this relative resistance, PTMEs could undergo alteration to their structure that might account for the enhanced diversity observed in the sediments of Lagoa do Caçó, as compared to their occurrence reported in the plant kingdom.

Pentacyclic triterpenes are known to undergo structural rearrangements (Courtney et al., 1958; Coates, 1967; Chatterjee et al., 1976; Ageta et al., 1987; Rullkötter et al., 1994). For example, ten Haven et al. (1992) showed that taraxerane-type structures are converted into thermodynamically more stable oleanane-type compounds. Similarly, Ageta et al. (1987) demonstrated that fern-9(11)-ene is converted into fern-8-ene when treated with BF₃. The presence of olean-12-en-3 β -ol ME, together with olean-18-en-3 β -ol ME in the sediments of Lagoa do Caçó could hence result from the diagenetic rearrangement of taraxer-14-en-3 β -ol ME. Similarly, the supposed fern-8-en-3 β -ol ME could be produced from fern-9(11)-en-3 β -ol ME.

Although the presence of 3 α - isomers in the sediments of Lagoa do Caçó remains speculative, it constitutes the simplest way to explain the diversity of PTMEs present in the sediments, especially with regard to their known occurrences in the plant kingdom. Few

3 α -PTMEs have been isolated from living sources (Table 2). Arborinol ME (arbor-9(11)-en-3 α -ol methyl ether) was isolated from thirteen plant species and fern-9(11)-en-3 α -ol methyl ether from two species; 3-friedelin methyl ether has been found in leaves of *Humboldtia laurifolia* (Samaraweera et al., 1983) and was suspected in aerosols from burning *Tsuga mertensiana* (Oros and Simoneit, 2001). If demonstrated, the presence of several 3 α - PTMEs in Lagoa do Caçó sediments would suggest a process of epimerisation during diagenesis. Such a possibility is supported by the observations of Bryce et al. (1967a) on the possible isomers of arundoin and sawamilletin. Acid catalysed epimerisation at position 3 of pentacyclic triterpenes is well known for alcohols (e.g., arborinol/isoarborinol: Pakrashi and Samanta, 1967; friedel-8-en-3 β -ol/friedel-8-en-3 α -ol: Chatterjee et al., 1976). Although there is no report of β to α isomerisation for PTMEs, this transformation could occur at the C-3 position, especially in an acidic medium (G. Eglinton, pers. comm.). It can be hypothesized that this process is promoted by microbial activity or mineral catalysis as in the case for alcohols (ten Haven et al., 1992). As a matter of fact, the decrease in the taraxer-14-en-3 β -ol/taraxer-14-en-3 α -ol ratio along the whole core suggests a precursor/byproduct relationship and the conversion from 3 β to 3 α configuration during early diagenesis (Jacob, 2003).

Bryce et al. (1967a) reported three synthetic diunsaturated PTMEs, namely multiflor-7,9(11)-dien-3 β -ol, bauer-7,9(11)-dien-3 β -ol ME and fern-7,9(11)-dien-3 β -ol ME. However, no natural di- or tri-unsaturated PTME has yet been reported, so compounds 9, 12 and 16 could then merely correspond to early diagenetic products deriving from mono-unsaturated PTMEs rather than be biological constituents.

4.3. Implications for palaeoenvironmental and phytochemical studies

Palaeoenvironmental reconstruction in tropical continental series often focusses mainly on the alternation of savannas and forests that document climate change from dry to humid and conversely. Contrary to pollen, which records vegetation from a rather large surrounding area, biomarkers can certify autochthonous production at the site of deposition or, at least, within the catchment area. Furthermore, the homogeneity in morphology of South American pollen from Gramineae (Salgado-Labouriau, 1997) prevents distinction between ecologically significant species, genus or families. Carbon isotopic ($\delta^{13}\text{C}$) and lignin analyses, which have been used to distinguish between savannas and forests (Guillet et al., 2000), were performed on bulk OM and thus did not offer the possibility of tracking ecologically significant species or genus as PTMEs might do. Some other key information could be gained from these bio-

markers. As noticed above, they seem to be resistant to degradation and may therefore be preserved, even under highly degrading conditions, as opposed to Gramineae pollen that is easily destroyed (M.-P. Ledru, personal communication).

Another field of investigation concerns the ecological role of PTMEs. Ohmoto et al. (1970) pointed out that the PTME content of Cortaderiae changes with season, probably as a consequence of a given physiological function of these compounds in plants. This assumption is also evidenced in Zoysiaeae, where arundoin dominates in inland species while sawamilletin dominates in plants growing on sandy seashores. Although the physiological role of PTMEs is not fully understood, their relative abundance in epicuticular waxes of a given species suggests that they could represent a response to environmental stress. As noticed by Martin-Smith et al. (1967), the co-occurrence of different PTME skeletons implies the existence of several types of oxido-squalene cyclases and methyl transferases in the parent plants. The involvement of these enzymes, and thus PTMEs synthesis, could be controlled by environmental stress. Finally, it is worthwhile noting that, while biochemical-phytochemical investigations are the main sources of information on plant-biomarker relationships in organic geochemistry, the detection of PTMEs in Lagoa do Caçó sediments might be a prelude to the discovery of yet unknown South American PTME plant producers.

4.4. Fernane and arborane type compounds in the sedimentary record

The origin of fernane and arborane derivatives in sedimentary series is still a matter of debate. Arborinone and isoarborinol have been identified together with des-A-arborenes in Lake Valencia sediments (Jaffé and Hausmann, 1995). Ourisson and Rohmer (1982) assumed a microbial origin for these compounds. This assumption was later supported by stable carbon isotopic data that were consistent with an algal origin (Hauke et al., 1992). Components of these molecular groups that have been recorded up to the Upper Carboniferous (Vliex et al., 1994) have been assigned a higher plant origin. This was consistent with the initial hypothesis of Albrecht and Ourisson (1969). Our findings provide further support to this interpretation and suggest that Gramineae might be an important source of fernane and arborane-type compounds in the sedimentary record.

5. Conclusions

The Quaternary filling of Lagoa do Caçó afforded a wide range of pentacyclic triterpene methyl ethers. These compounds dominate the neutral solvent-extractable

fraction. The identity of five has unambiguously been assigned with available reference compounds. Based on an inventory of plants from which PTMEs have been isolated, Gramineae that grew in the watershed at the time of sediment deposition appear as the most probable source. The presence of PTMEs in Lagoa do Caçó sediments attests to their peculiar resistance to degradation. Their structural diversity could result from: (a) a diversified set of plant producers; (b) the ability of an unknown species to produce several compounds; (c) early diagenetic transformation; (d) a combination of these three hypotheses. From a more general point of view, because of the existence of only few reports of PTMEs in plants (mostly in Gramineae but none from South America) and only two or three Gramineae species dominate savanna ecosystems in the tropics (D. Schwark, personal communication), it can be hypothesized that the PTMEs discussed in this study might have been produced by a single species of Gramineae. As a consequence, PTMEs might appear as a unique example of specific higher plant-derived biomarkers.

Acknowledgements

Professor R.M. Smith (Loughborough University, UK), Professor H.E. Connor (University of Canterbury, NZ) and Professor G. Eglinton (Bristol University, UK) are greatly acknowledged for providing reference compounds and valuable discussions about chemotaxonomy. The authors thank Professor G. Bouchoux (Ecole Polytechnique, France), Dr. P. Metzger (Ecole de Chimie de Paris, France) and Professor B. Simoneit (Oregon State University, US) for useful discussions on mass spectra interpretation. Dr. B. van Aarssen and two anonymous reviewers are also greatly acknowledged for improving the original version of this manuscript. The study has been supported by an IRD (France)-CNPq (Brazil) convention and a CNRS (France)-CNPq (Brazil) convention. One of us (J. Jacob) receives financial support from the Conseil Régional du Centre.

Associate Editor—P. Schaeffer

References

- van Aarssen, B.G.K., Alexander, R., Kagi, R.I., 2000. Higher plant biomarkers reflect palaeovegetation changes during Jurassic times. *Geochimica et Cosmochimica Acta* 64, 1417–1424.
- Ageta, H., Shiojima, K., Arai, Y., 1987. Acid-induced rearrangement of triterpenoid hydrocarbons belonging to the hopane and migrated hopane series. *Chemical and Pharmaceutical Bulletin* 35, 2705–2716.

- Albrecht, P., Ourisson, G., 1969. Triterpene alcohol isolation from oil shale. *Science* 163, 1192–1193.
- Bryce, T.A., Eglinton, G., Hamilton, R.J., Martin-Smith, M., Subramanian, G., 1967a. Triterpenoids from New Zealand plants – The triterpene methyl ethers of *Cortaderia toetoe* zotov. *Phytochemistry* 6, 727–733.
- Bryce, T.A., Martin-Smith, M., Osske, G., Schreiber, K., Subramanian, G., 1967b. Sterols and triterpenoids – isolation of arundoin and sawamilletin from Cuban sugar cane wax. *Tetrahedron* 23, 1283–1296.
- Budzikiewicz, H., Wilson, J.M., Djerassi, C., 1962. Mass spectrometry in structural and stereochemical problems. XXXII. Pentacyclic triterpenes. *Journal of the American Chemical Society* 85, 3688–3699.
- Chatterjee, A., Mukhopadhyay, S., Chattopadhyay, K., 1976. Lewis acid catalysed rearrangement of triterpenoids. *Tetrahedron* 32, 3051–3053.
- Coates, R.M., 1967. On the friedelane–oleanane rearrangement. *Tetrahedron Letters* 42, 4143–4146.
- Courtney, J.L., Gascoigne, R.M., Szmer, A.Z., 1958. Triterpenoids of the friedelane series. Part III. The course of friedelane–oleanane rearrangement. *Journal of the Chemical Society*, 881–886.
- Cranwell, P.A., 1984. Organic geochemistry of lacustrine sediments: triterpenoids of higher plant origin reflecting post-glacial vegetational succession. In: Haworth, E.Y., Lund, J.W.G. (Eds.), *Lakes Sediments and Environmental History*. University Press, Leicester, pp. 69–92.
- Das, M.C., Mahato, S.B., 1983. Triterpenoids. *Phytochemistry* 22, 1071–1095.
- Deshmane, S.S., Dev, S., 1971. Higher isoprenoids-II; Triterpenoids and steroids of *Saccharum officinarum* linn. *Tetrahedron* 27, 1109–1118.
- Djerassi, C., Budzikiewicz, H., Wilson, J.M., 1962. Mass spectrometry in structural and stereochemical problems. Unsaturated pentacyclic triterpenoids. *Tetrahedron Letters* 3, 263–270.
- Garcia, S., Heinzen, H., Hubbuch, C., Martinez, R., de Vries, P., Moyna, P., 1995. Triterpene methyl ethers from palmar epicuticular waxes. *Phytochemistry* 39, 1381–1382.
- Goh, S.H., Lai, F.L., Gee, P.T., 1988. Wax esters and triterpene methyl ethers from the exocarp of *Elaeis guineensis*. *Phytochemistry* 27, 877–880.
- Guillet, B., Maman, O., Achoundong, G., Mariotti, A., Girardin, C., Schwartz, D., Youta Happi, J., 2000. Evidences isotopiques et géochimiques de l'avancée de la forêt sur la savane au Cameroun. In: Servant, M., Servant-Vildary, S. (Eds.), *Dynamique à long terme des écosystèmes forestiers intertropicaux*. UNESCO and IRD Publication, Paris, pp. 169–174.
- Hauke, V., Graff, R., Wehrung, P., Trendel, J.M., Albrecht, P., Riva, A., Hopfgartner, G., Gülaçar, F.O., Buchs, A., Eakin, P.A., 1992. Novel triterpene-derived hydrocarbons of arborane/fernane series in sediments. Part II. *Geochimica et Cosmochimica Acta* 56, 3595–3602.
- ten Haven, H.L., Peakman, T.M., Rullkötter, J., 1992. Early diagenetic transformation of higher-plant triterpenoids in deep-sea sediments from Baffin Bay. *Geochimica et Cosmochimica Acta* 56, 2001–2024.
- Jacob, J., 2003. Enregistrement des variations paléoenvironnementales depuis 20000 ans dans le Nord Est du Brésil (Lac Caçó) par les triterpènes et autres marqueurs organiques. Ph.D. Thesis, Université d'Orléans, France. p. 296. Available from: <http://tel.ccsd.cnrs.fr/documents/archives0/00/00/29/42/index_fr.html>.
- Jacob, J., Disnar, J.R., Boussafir, M., Sifeddine, A., Albuquerque, A.L.S., Turcq, B., 2004a. Major environmental changes recorded by lacustrine sedimentary organic matter since the Last Glacial Maximum under the tropics (Lagoa do Caçó, NE Brazil). *Palaeogeography, Palaeoclimatology, Palaeoecology* 205, 183–197.
- Jacob, J., Disnar, J.R., Boussafir, M., Ledru, M.-P., Sifeddine, A.L.S., Albuquerque, A.L.S., Turcq, B., 2004b. Onocerane I attests to dry climatic events during the Quaternary in the Tropics. *Organic Geochemistry* 35, 289–297.
- Jaffé, R., Hausmann, K.B., 1995. Origin and early diagenesis of arborinone/isoarborinol in sediments of a highly productive freshwater lake. *Organic Geochemistry* 22, 231–235.
- Killops, S.D., Raine, J.I., Woolhouse, A.D., Weston, R.J., 1995. Chemostratigraphic evidence of higher plant evolution in the Taranaki Basin, New Zealand. *Organic Geochemistry* 23, 429–445.
- Ledru, M.P., Cordeiro, R.C., Dominguez, J.M.L., Martin, L., Mourguiart, P., Sifeddine, A., Turcq, B., 2001. Late-glacial cooling in Amazonia as inferred from pollen at Lagoa do Caçó, Northern Brazil. *Quaternary Research* 55, 47–56.
- Ledru, M.P., Mourguiart, P., Ceccantini, G., Turcq, B., Sifeddine, A., 2002. Tropical climates in the game of two hemispheres revealed by abrupt climatic change. *Geology* 30, 275–278.
- Logan, G.A., Eglinton, G., 1994. Biogeochemistry of the Miocene lacustrine deposit, at Clarkia, northern Idaho, USA. *Organic Geochemistry* 21, 857–870.
- Mahato, S.B., Sen, S., 1997. Advances in triterpenoid research 1990–1994. *Phytochemistry* 44, 1185–1236.
- Mahato, S.B., Sarkar, S.K., Poddar, S.G., 1988. Triterpenoid saponins. *Phytochemistry* 27, 3037–3067.
- Mahato, S.B., Nandy, A.K., Roy, G., 1992. Triterpenoids. *Phytochemistry* 9, 2199–2249.
- Martin-Smith, M., Subramanian, G., Connor, H.E., 1967. Surface wax components of five species of *Cortaderia* (Gramineae) – a chemotaxonomic comparison. *Phytochemistry* 6, 559.
- Nishimoto, K., Ito, M., Natori, S., Ohmoto, T., 1968. The structures of arundoin, cylindrin and fernenols. Triterpenoids of fernane and arborane groups of *Imperata cylindrical* var. *koenigii*. *Tetrahedron* 24, 735–752.
- Ohmoto, T., Ikuse, M., Natori, S., 1970. Triterpenoids of the Gramineae. *Phytochemistry* 6, 559.
- Oros, D.R., Simoneit, B., 2001. Identification and emission factors of molecular tracers in organic aerosols from biomass burning. Part 1. Temperate climate conifers. *Applied Geochemistry* 16, 1513–1544.
- Ourisson, G., Rohmer, M., 1982. Prokaryotic polyterpenes: phylogenetic precursors of sterols. *Current Topics in Membrane Transport* 17, 153–182.
- Pakrashi, S.C., Samanta, T.B., 1967. Acid induced epimerisation and rearrangements of Arborinol, the novel triterpene from *Glycosmis arborea*. *Tetrahedron Letters* 38, 3679–3684.
- Pant, P., Rastogi, R.P., 1979. The triterpenoids. *Phytochemistry* 18, 1095–1108.

- Paupit, R.A., Waters, J.M., Rowan, D.D., Russell, G.B., Connor, H.E., Purdie, A.W., 1984. The Structure of 19a H-Lupeol Methyl Ether from *Chionochloa bromoides*. *Australian Journal of Chemistry* 37, 1341–1347.
- Peters, K.E., Moldowan, J.M., 1993. *The Biomarker Guide*. Prentice-Hall, Englewood Cliffs, NJ.
- Ries-Kautt, M., 1986. Etude des lipides dans divers types de sols. Aspects Moléculaires. Ph.D. Thesis, Université Louis Pasteur de Strasbourg, p. 152.
- Rowan, D.D., Russell, G.B., 1992. 3 β -Methoxy-hop-22(29)-ene from *Chionochloa cheesmanii*. *Phytochemistry* 31, 702–703.
- Rowe, J.W., Bower, C.L., 1965. Triterpenes of Pine barks: naturally occurring derivatives of serratenediol. *Tetrahedron Letters* 32, 2745–2750.
- Rullkötter, J., Peakman, T.M., ten Haven, H.L., 1994. Early diagenesis of terrigenous triterpenoids and its implications for petroleum geochemistry. *Organic Geochemistry* 21, 215–233.
- Russell, G.B., Connor, H.E., Purdie, A.W., 1976. Triterpene methyl ethers of *Chionochloa* (Gramineae). *Phytochemistry* 15, 1933–1935.
- Salgado-Labouriau, M.L., 1997. Late Quaternary palaeoclimate in the savannas of South America. *Journal of Quaternary Science* 12, 371–379.
- Samaraweera, U., Subramaniam, S., Ubais, M., Sultanbawa, S., 1983. 3,5,7,3',5'-Pentahydroxyflavan and 3 α -methoxyfriedelan from *Humboldtia laurifolia*. *Phytochemistry* 22, 565–567.
- Shiojima, K., Arai, Y., Masuda, K., Takase, Y., Ageta, T., Ageta, H., 1992. Mass spectra of pentacyclic triterpenoids. *Chemical and Pharmaceutical Bulletin* 40, 1683–1690.
- Sifeddine, A., Albuquerque, A.L.S., Ledru, M.-P., Turcq, B., Knoppers, B., Martin, L., Zamboni de Mello, W., Passenau, J.M., Landim Dominguez, J.M., Campello Cordeiro, R., Abrao, J.J., Carlos da Silva Pinto Bittencourt, A.C., 2003. A 21000 cal years paleoclimatic record from Caçó Lake, northern Brazil: evidence from sedimentary and pollen analyses. *Palaeogeography, Palaeoclimatology, Palaeoecology* 189, 25–34.
- Uyeo, S., Okada, J., Matsunaga, S., Rowe, J.W., 1968. The structure and stereochemistry of abieslactone. *Tetrahedron* 24, 2859–2880.
- Vliex, M., Hagemann, H.W., Püttmann, W., 1994. Aromatized arborane/fernane hydrocarbons as molecular indicators of floral changes in Upper Carboniferous/Lower Permian strata of the Saar-Nahe Basin, southwest Germany. *Geochimica et Cosmochimica Acta* 58, 4689–4702.

Available online at www.sciencedirect.com

SCIENCE @ DIRECT®

Sedimentary Geology 177 (2005) 271–295

**Sedimentary
Geology**

www.elsevier.com/locate/sedgeo

Cenomanian–Turonian organic sedimentation in North-West Africa: A comparison between the Tarfaya (Morocco) and Senegal Basins

P. Nzoussi-Mbassani^a, N. Khamli^{b,1}, J.R. Disnar^{a,2},
F. Laggoun-Défarge^{a,*}, M. Boussafir^{a,2}

^a*Institut des Sciences de la Terre d'Orléans (ISTO), UMR 6113 CNRS-Université d'Orléans, Bâtiment de Géosciences, 45067 Orléans cedex 2, France*

^b*Université de Tétouan, Faculté des Sciences, Département de Géologie, B.P. 2121, Maroc, France*

Received 15 January 2004; accepted 18 March 2005

Abstract

The Cenomanian–Turonian Oceanic Anoxic Event was recognised in North Western Africa in various depositional settings from abyssal areas to continental shelves. To derive information on environmental conditions in these different settings and define a depositional model, a petrographical and geochemical study of the organic matter was performed on sediments from the Tarfaya (Morocco) and Senegal Basins. The results obtained for these two locations were compared to those of previous studies, namely from DSDP wells.

Petrographic and geochemical data allow the differentiation of two main organofacies: a shallow depositional facies (continental shelf) is characterised by low total organic carbon (TOC) contents (< 4%). As attested by low hydrogen index (HI) values (100 to 400 mg HC/g TOC), the organic matter (OM) is moderately preserved. Petrographically, this facies is composed of mixed OM with high proportions of reworked vitrinite indicating detrital material influence. The depositional environment is typical of dysoxic conditions ($S/C < 0.36$) exposed to high mineral inputs and oxygenated water currents.

The second organofacies deposited in the deep marine environment (slope and abyssal) shows a high TOC content (> 7%). The predominance of fluorescing amorphous OM combined with high HI values suggests good preservation conditions. The S/C ratio (> 0.36) and abundance of organic-sulphur compounds support this interpretation and indicate a development of anoxic conditions.

To explain the organic contrast between both environments a depositional model has been developed which is based on limited water exchange between both depositional settings. The main factor which has determined black shale sedimentation is the restricted water circulation related to the presence of isolated depositional environment during Atlantic Ocean opening.

* Corresponding author. Tel.: +33 238 49 46 63; fax: +33 238 41 73 08.

E-mail addresses: nzoussi@yahoo.fr (P. Nzoussi-Mbassani), n.khamli@fst.ac.ma (N. Khamli), Jean-Robert.Disnar@univ-orleans.fr (J.R. Disnar), Fatima.Laggoun-Defarge@univ-orleans.fr (F. Laggoun-Défarge), Mohammed.Boussafir@univ-orleans.fr (M. Boussafir).

¹ Fax: +33 212 39 99 45 00.

² Fax: +33 238 41 73 08.

Compared to present upwelling zones, the palaeoproductivity in the studied area was relatively moderate during Cenomanian–Turonian and seems not to be the only determining factor of organic matter accumulation.

© 2005 Elsevier B.V. All rights reserved.

Keywords: Tarfaya Basin; Senegal Basin; Organic matter; Primary productivity; Euxinic

1. Introduction

On the North African continental margin Cenomanian–Turonian (C–T) sediments have been recognised in present-day shelf and slope areas (Herbin et al., 1986; Leine, 1986; El Albani et al., 1999; Kolonic et al., 2002). These formations have also been penetrated by several ODP and DSDP wells (138, 367, 368 Sites) and petroleum exploration boreholes (CM7, CM10) in offshore Senegal. C–T sediments also occur at outcrops along the Moroccan Atlantic coast (Herbin et al., 1986) and in Bahloul Formation in Tunisia (El Albani et al., 1999). Since the introduction of the concept of Oceanic Anoxic Events (OAE) by Schlanger and Jenkyns (1976), aiming to explain the organic richness of these units, there are still active controversies on the origin and the extension of this event. Many authors have discussed the main factors which are responsible for high OM contents usually found in these sedimentary formations (Lancelot, 1980; Waples, 1983; Busson and Cornée, 1996; de Graciansky et al., 1984).

Euxinic conditions in a large part of the water column are presently considered one of the most susceptible mechanisms to explain black shale sedimentation in the North Atlantic area (Kuypers et al., 2002; Lüning et al., 2003). This assumption is essentially supported by the presence of molecular biomarkers (isorenieretane) derived from photosynthetic green sulphur bacteria (chlorobiaceae) found both in the Tarfaya Basin (Kolonic et al., 2002) and the Senegal offshore (DSDP 367) (Sinningh Damsté and Köster, 1998).

Based on recent work (Nzoussi-Mbassani et al., 2003) we assume that the supposed global anoxic conditions did not affect all depositional environments in the North Atlantic area and that organic matter sedimentation was also dependent on local paleogeographic and environmental factors. In addition, most of the work that has been done on C–T series lacked a comparison between shallow and deep environments that makes the establishment of a global depositional

model for these formations difficult. The similarity of the geological evolution between the sedimentary Basins of Morocco and Senegal gives us the opportunity to compare the C–T sediments in these two areas, along the Western coast of the Atlantic Ocean.

The present study includes petrographic and geochemical analyses from both the Senegal platform and the Tarfaya Basin (Morocco) in order to compare sediment characteristics, and especially organic matter contents. These data are compared to other C–T occurrences in the study area to propose a depositional model for the North African margin area.

2. Regional geological setting

The geological evolution of the North African domain was controlled by the Late Triassic–Jurassic break-up of the supercontinent Pangaea, resulting in the opening of oceanic Basins forming the Western NeoTethys and the central Atlantic (Baudin, 1995) (Fig. 1). During the Cenomano–Turonian, the Tethys and the Atlantic Ocean showed sluggish oceanic circulations due to limited connection to the neighbouring oceans (Handoh et al., 1999). These conditions contributed to the development of anoxic bottom waters (Philip et al., 1993, 2000). During the Late Cretaceous, a major oceanic reorganisation occurred when the direction of the deep water circulation reversed from Equator-wards to Polewards (Hay, 1982). Accordingly, the establishment of water exchange in response to the deepening and the widening of the Atlantic Ocean had an important impact on the resulting sedimentary facies due to the influence of oxic water currents (Herbin et al., 1986).

2.1. Senegal Basin

The Senegal Basin covers an area of 340,000 km² between 11 and 17°N latitudes (Fig. 2) occupying the



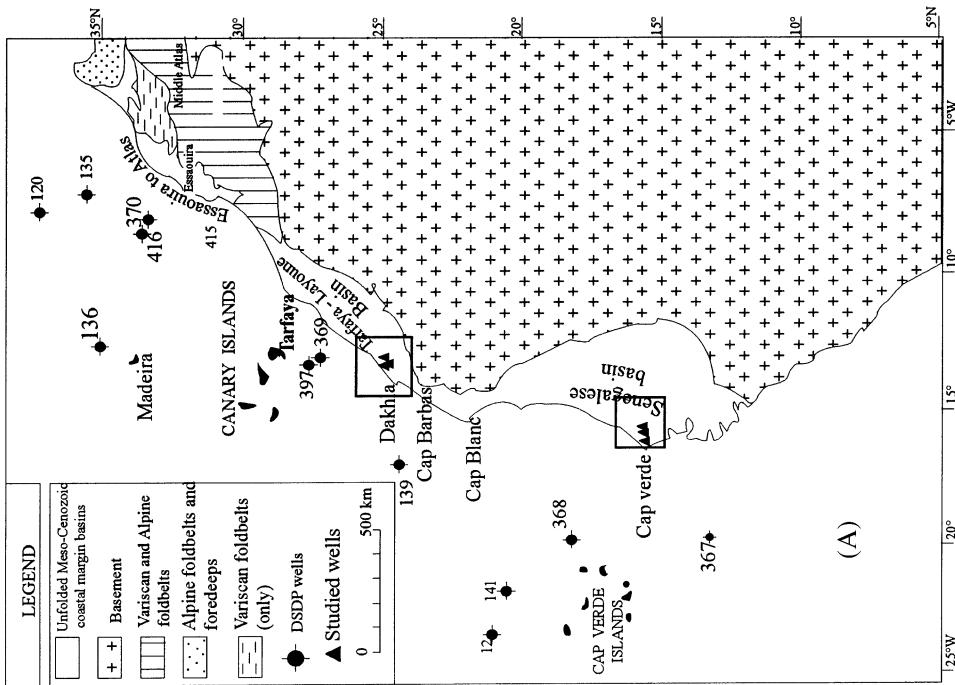
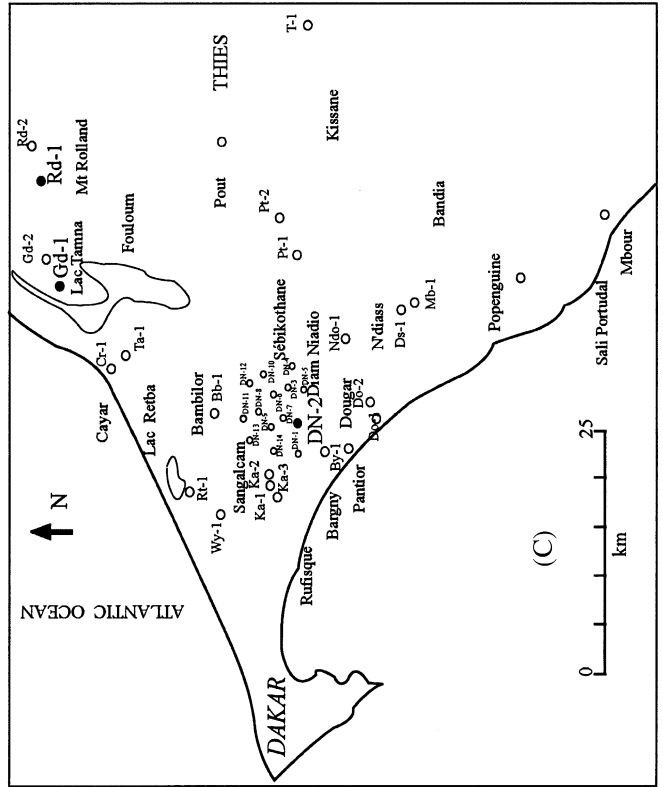
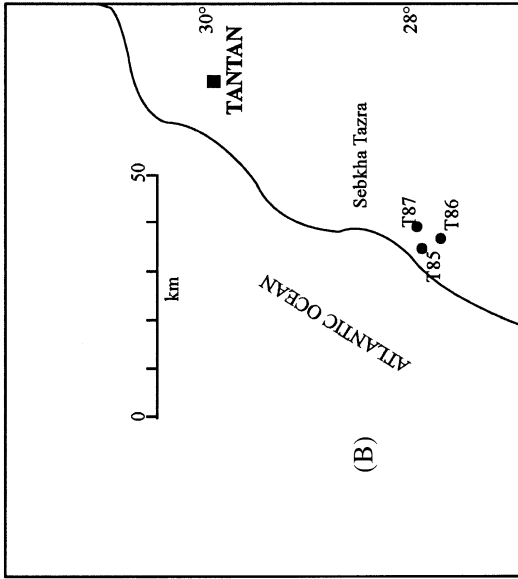
Fig. 1. Paleogeographic map during Cenomanian–Turonian period with DSDP sites according to Schlanger et al. (1987), Herbin et al. (1986) and Arthur et al. (1990).

central part of the large North-Western Africa Basin which extends along Senegal, Gambia, Guinea-Bissau, Mauritania and the Moroccan coastal areas. It opens westward to the Atlantic Ocean and is limited by the Panafrican to Hercynian Mauritanide chain to the east (Villeneuve and Da Rocha Araujo, 1984). This Basin contains more than 14 km thick Paleozoic to Tertiary sediments. Outcrops are rare and any known stratigraphy is based on deep wells. The thickness of the Meso-Cenozoic sediments partly exceeds 10,000 m in the western part of the Basin. It consists of transgressive and regressive series: (i) a Jurassic–Lower Cretaceous carbonate platform, (ii) a Cretaceous clastic wedge and (iii), a cap of Tertiary carbonates and shales (Michaud, 1984). Three facies characterise the lateral variations of the C–T sediments. The first consists of homogenous black shales deposited in the fully marine environment. This facies dominates the western part of the Thies-Diam Niadio area and reaches maximum thickness in Casamance. No well

has reached the base of this facies in the study area. However seismic profiles suggest a Basinward increase in thickness. The second facies is characterised by a succession of calcareous and shaly calcareous sediments typical of a transitional neritic environment. The third facies, typical of a sub-littoral to nearshore marine environment, is composed of shales with shaly siltstone intercalations. These sediments become increasingly rich in siltstone towards the shoreline.

2.2. Tarfaya Basin

The Tarfaya Basin (Fig. 2) is a tectonically stable Mesozoic Basin, which extends along the southern Moroccan coast between latitudes $27^{\circ}40'$ and $28^{\circ}40'$ N and covers an area of 10,000 km². It is bounded by the Anti-Atlas Mountains to the North, the Precambrian Reguibat Massif in the east and the Atlantic Ocean to the West. Studies based on correlations between deep onshore and offshore (DSDP 369, 397) wells allow to



make a synthesis of the stratigraphy and of tectonic evolution of the Basin (Wiedmann et al., 1982). During Triassic times, a synrift continental megasequence (1000 m) was deposited. The sediments include evaporite horizons followed by sills of dolerite basalts. The post rift phase started with the Jurassic marine transgression, which only affected the northern part of the Basin. Maximum transgression was reached in Late Cenomanian–Early Turonian times. The Cenomanian–Turonian sediments are composed of hemipelagic facies (Leine, 1986). The strata consist of dark brownish and greyish laminated kerogeneous chinks, alternating with non laminated lightly coloured, often nodular limestones having low kerogen content. The same strata were found far toward the east (Well 75) and the west of the basin (Kuhnt et al., 1990; Kolonic et al., 2002). Kerogen-rich chinks contain abundant fossils (foraminifera tests) and a carbonate matrix mainly composed of coccoliths and micrite (Leine, 1986; El Albani et al., 1999).

3. Material and methods

In the Tarfaya Basin, 94 core samples were obtained from three wells (T85, T86 and T87) (Fig. 2) drilled in the western part of the Sebkhia Tazra anticline (Fig. 2). Palaeontological investigations attribute them to Upper Cenomanian–Lower Turonian age (Leine, 1986) according to upper *Rotalipora cushmani* to lower *Whiteinella archaeocretacea* biozone (Kuhnt et al., 2001). Concerning the Senegal Basin, 115 samples of drill cuttings were collected from three wells (DN-2, Gd-1, Rd-1) (Fig. 2) which penetrated one of the main facies of the C–T succession in the area (Nzoussi-Mbassani et al., 2003). DN-2 corresponds to distal environment, while Rd-1 represents the proximal one.

3.1. Bulk geochemical analyses

Total Organic Carbon (TOC) contents (wt.%), Hydrogen Index (HI, mg HC g⁻¹ TOC), Oxygen Index

(OI, mg CO₂ g⁻¹ TOC), Tmax (°C) and Petroleum Potential (PI) were determined by Rock-Eval 6 pyrolysis (Espitalié et al., 1977; Lafargue et al., 1998). The analyses were carried out on 100 mg of crushed sample under standard conditions. The Tarfaya Basin samples were first analysed using Rock-Eval II. However, for a better comparison between both basins, some of these samples were re-analysed with the model 6 device. Elemental analyses have been performed on bulk material with a Leco CNS2000 analyser in order to determine Total C (TC), N and S contents.

3.2. Microscopic observations

OM petrographic studies were performed using a Leica DMR XP microscope under different illumination modes: identification and counting of organic constituents (palynofacies) were carried out under transmitted light on total organic matter (TOM) obtained after acid hydrolysis of carbonates and silicates. Specific characterisation (maceral analysis) of land-derived organic particles, i.e. mainly from vitrinite and inertinite groups, was performed on polished sections of OM densimetric concentrates under reflected light and fluorescence. Identifications were made following the nomenclatures of Stach et al. (1982) and the International Commission for Coal Petrology procedures (ICCP, 1971). Random vitrinite measurements (Rr expressed in %) were made on the same densimetric concentrates under reflected light using a × 50 oil immersion objective (ICCP, 1971).

The microtexture of selected samples showing geochemical and sedimentological contrasts was studied using a Scanning Electron Microscope (SEM, Hitachi S4200 apparatus) in backscattered electron (BSE) mode combined with energy dispersive X-ray spectrometry (EDS). The obtained imaging depends on atomic number (Z) contrasts between the different constituents of the sample, i.e. organic matter and mineral matrix. Investigations were carried out both on polished sections of bulk rocks and of palynofacies residues, previously coated with carbon, with an accelerating voltage of 15 kV.

Fig. 2. (A) Map showing generalised geological setting of West African margin and the location of the Senegalese and Tarfaya (Morocco) basins. (B) Location of studied boreholes (T85, T86, T87) within the Tarfaya basin. (C) Location of studied boreholes within the Senegal platform (full circles show the three studied wells, i.e. DN-2, Gd-1, Rd-1).

3.3. Flash pyrolysis–gas chromatography/mass spectrometry (Py–GC–MS)

The kerogens used for flash pyrolysis–gas chromatography/mass spectrometry analyses were isolated by HCl/HF treatment according to the Durand and Nicaise (1980) method. Py–GC–MS analyses were carried out on a Thermofinnigan GCQ TRACE gas chromatography–mass spectrometer equipped with Ficher GSG pyrolysis unit set at 300 °C.

The samples were applied to a ferromagnetic wire with a Curie temperature of 650 °C. Pyrolysis is a thermal degradation in an inert atmosphere which generates products with different weights depending on the temperature of pyrolysis and the type of molecular bounds within the macromolecular network. Only 10% of the pyrolysed products can be analysed by Py–GC–MS. However, NMR and other studies have shown that structural information which can be recovered is, in most cases, representative of bulk material subjected to pyrolysis (Gelin, 1996; Larter and Horsfield, 1993; Horsfield, 1989; Goth et al., 1988). Even if a precise chemical structure of the macromolecules involved cannot be elucidated by Py/GC/MS, the structural elements in the pyrolysis products can still provide information concerning the origin and the preservation state of sedimentary OM. In this study, pyrolysis products generated between 300 and 650 °C were analysed by Py–GC–MS according to the following oven temperature program: 40 °C during 2 min, then 40–100 °C at 30 °C/min, 100 °C–300 °C at 3 °C/min, and finally 30 min hold at 300 °C. Helium was used as a carrier gas. Separation was achieved using a fused silica capillary column (30 m × 2.5 mm) with 0.25 mm of stationary phase. The mass spectrometer operated at 70 eV in the electron ionisation mode with a mass range of m/z 50–650.

4. Results

4.1. Senegal Basin

4.1.1. Petrographic and bulk geochemical characteristics

C–T sediments are characterised by low to moderate TOC contents, which does not exceed

4% (Fig. 3D). HI values are generally low (< 300 mg HC g⁻¹ TOC) except in some samples originating from the distal part of the Basin. When plotted in a HI/OI diagram (Espitalié et al., 1977), the data points are mainly located in the type III OM field (Fig. 3B) thus suggesting an OM of predominant terrestrial origin (Tissot and Welte, 1984; Bordenave, 1993). Nevertheless, the high values observed toward the distal part of the Basin indicate marine OM influences. C/N ratios also depend on depositional area. In the proximal areas they are generally higher than 10 in contrast to the distal part where some intervals present C/N values lower than 10 (Fig. 3C). High C/N ratios could indicate terrestrial OM precursor, but should normally not be interpreted separately for OM source characterisation because of possible alteration impact. S/C ratio values are generally lower than 0.36 (Fig. 3D), thus suggesting that the deposition mostly occurred under medium oxic conditions (Raiswell and Berner, 1985; Morse and Berner, 1995).

As illustrated in a HI–Tmax diagram and by reflectance values, the studied C–T series have reached a degree of thermal evolution globally corresponding to the first part of the oil window, i.e. from its onset to its middle part. Such a moderate maturity suggests a limited thermal alteration of OM quality, e.g. depicted by Hydrogen Index values (Fig. 3A).

Two samples originating from the proximal (Rd-1) and distal area (DN-2) (Fig. 2), respectively, were selected for Scanning Electron Microscopic (SEM) observations. No major distinction in OM distribution has been made between these two samples. In both cases, the OM shows two main morphological features. Firstly, it occurs as thin laminated bands interbedded within the mineral matrix. In the second case, the OM occurs as rounded to subrounded structures/particles finely dispersed/disseminated in the mineral matrix.

EDS microanalysis (Fig. 4) shows that, unlike the particulate OM (Fig. 4B), the laminated OM systematically presents sulphur enrichment (Fig. 4A). Such results suggest that (i) sulphurisation reaction does not affect all of OM particles and/or (ii) particulate and laminated OM do not have the same origin.

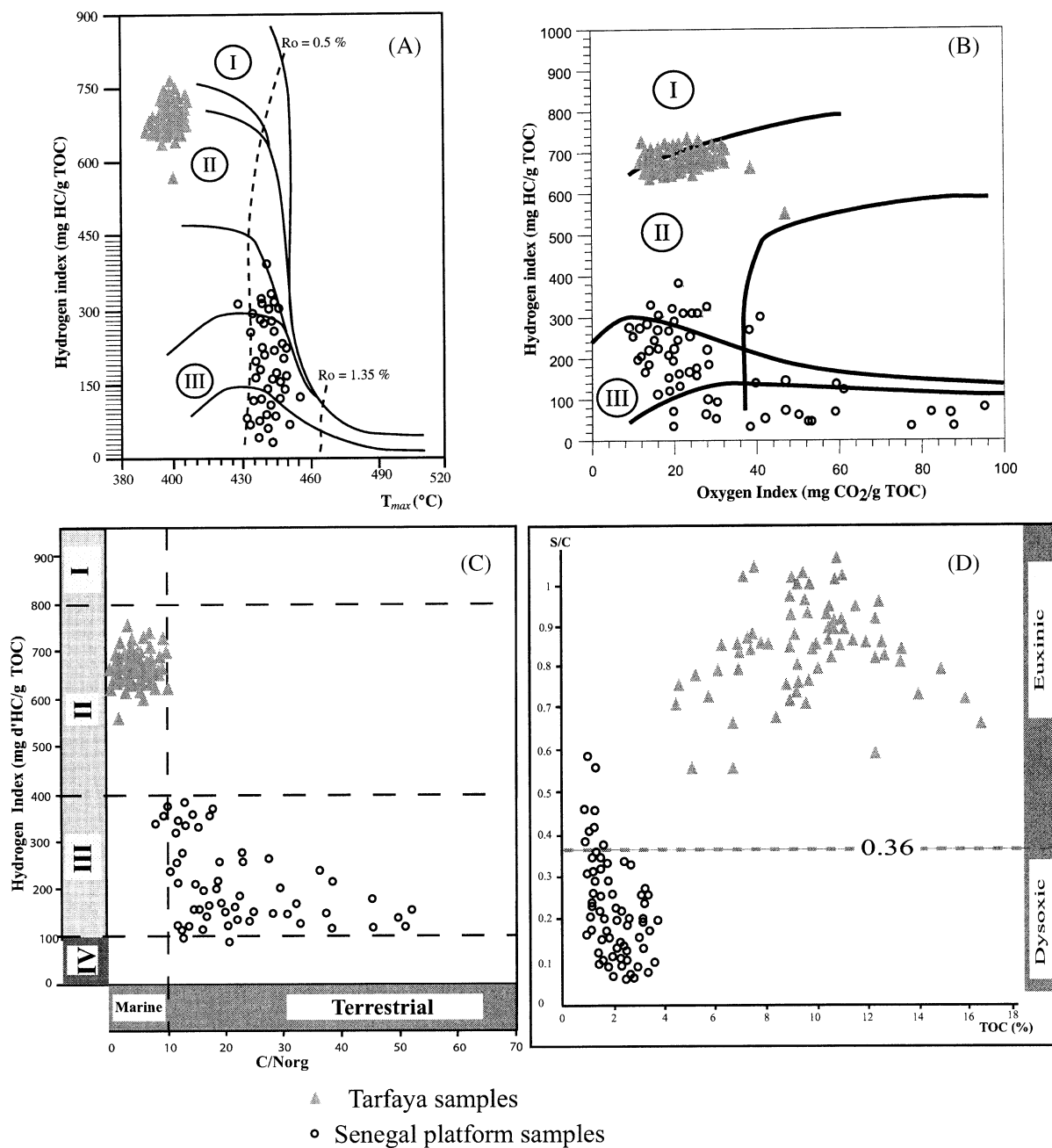


Fig. 3. Bulk geochemical characteristics of studied samples. HI-Tmax diagram (A); HI vs. OI diagram (B); total organic carbon (TOC) and nitrogen ratio vs. HI (C); sulphur and carbon ratio vs. TOC (D).

The mineral matrix is dominated by Al, Fe, K, Si while Ca is rare (Fig. 5A). The notable presence of Titanium indicates terrigenous influences (Latimer and Filippelli, 2002). Element chemical mapping that

have been performed in order to gain a more comprehensive view of elemental distribution, mostly confirms the association of sulphur either with OM or iron in pyrite (Fig. 5B).

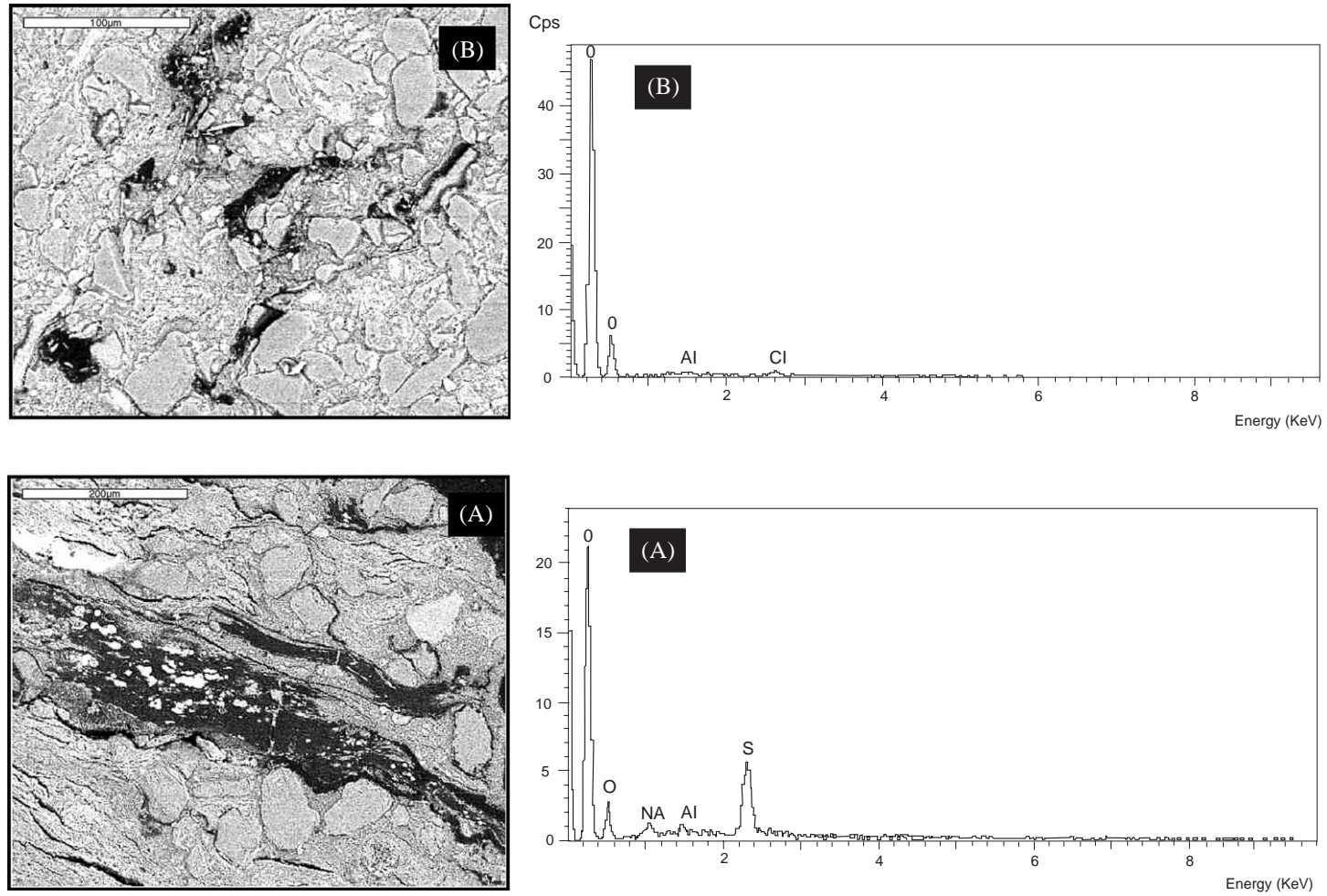


Fig. 4. SEM images of Senegal samples showing two OM morphological features with corresponding EDS analyses: (A) thin laminated bands with sulphur enrichment; (B) dispersed OM without sulphur presence.

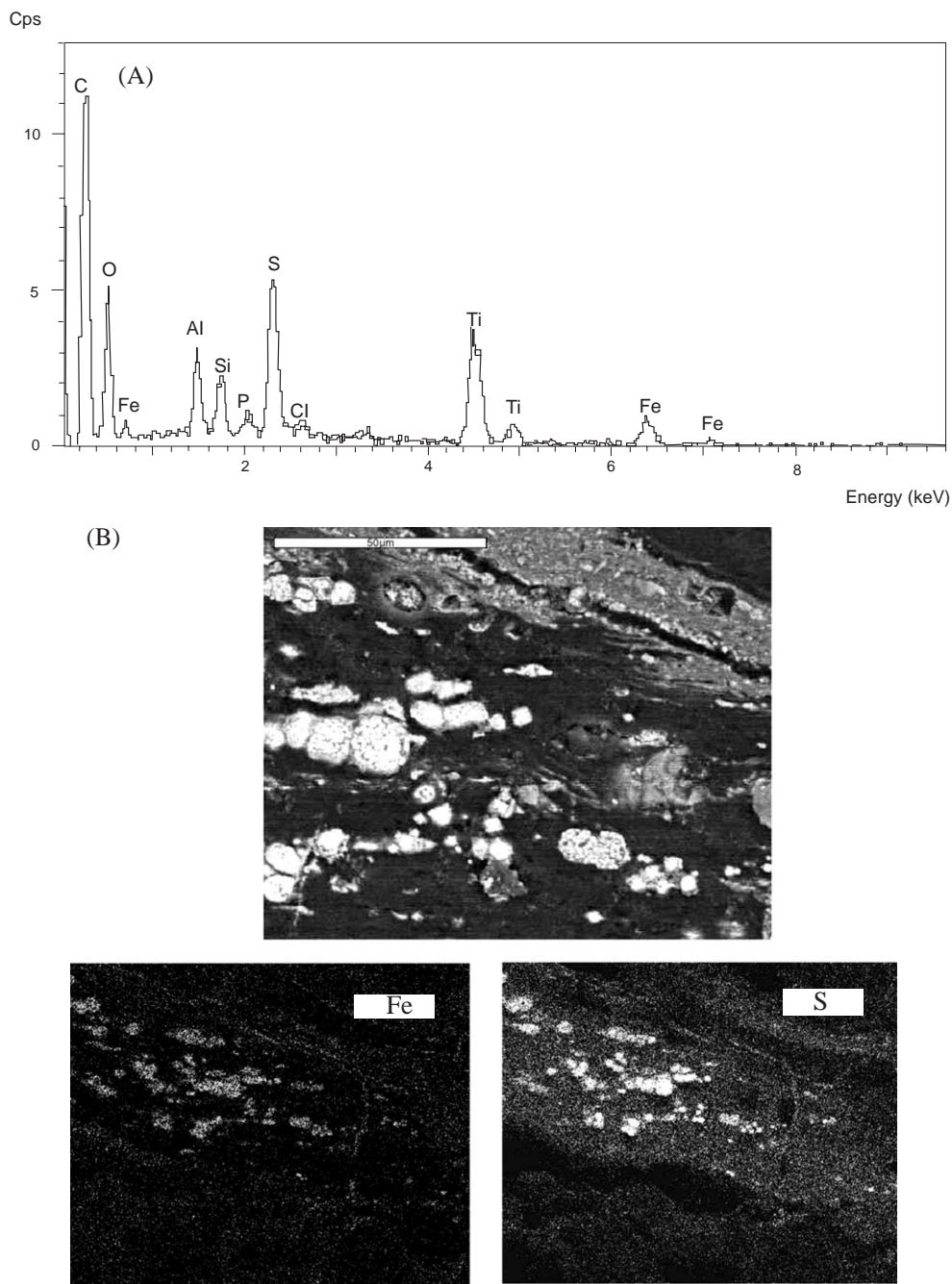


Fig. 5. (A) EDS analysis spectra showing mineral composition of Senegal sediments; (B) an example of elemental (Fe, S) fingerprints of Senegal samples.

4.1.2. Molecular organic geochemical data

The distributions of the major classes of compounds found in the pyrolyzates can be appreciated

in the chromatograms displayed in Fig. 6. These latter ones comprise alkylbenzenes, *n*-alkanes and alkylnaphthalenes (Tables 1 and 2). There is a slight

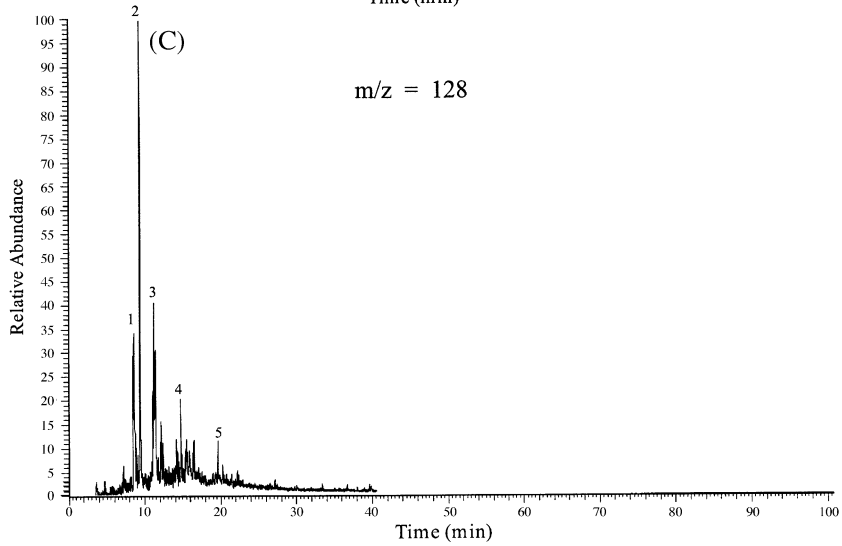
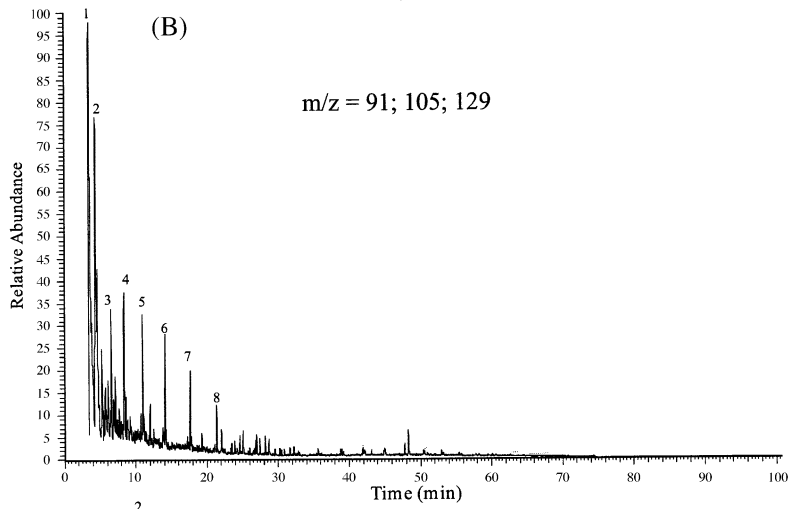
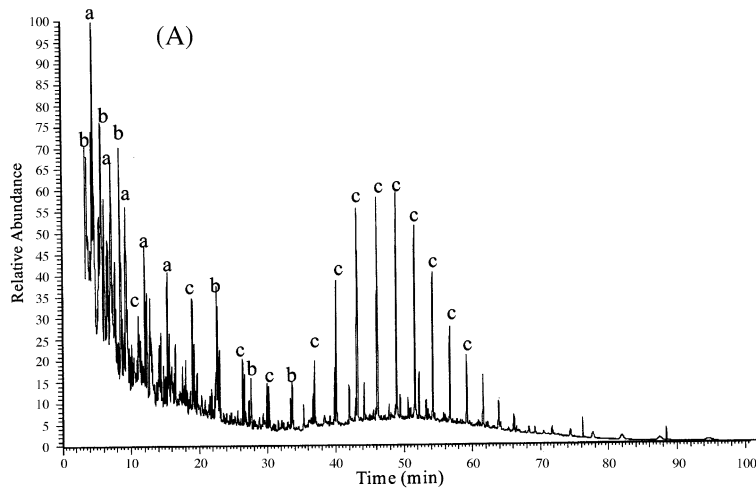


Table 1
Alkylbenzenes identified in Senegal samples

Peak	Compounds
1	Methyl benzene
2	1,2 Dimethylbenzene
3	Ethylbenzene
4	1-Ethyl-3 methylbenzene
5	1,3 Dimethylbenzene
6	1-Methyl -3 ethylbenzene
7	1-Ethyl -2 methylbenzene
8	Propylbenzene

predominance of alkylbenzene compounds, which show similar distribution in the proximal and the distal Senegal areas. Ethylbenzene is the dominant alkylbenzene compound. The occurrence of these compounds in the pyrolysates could result from the cyclisation and further aromatisation of primary linear functionalised lipid precursors such as fatty acids and fatty alcohols (Largeau et al., 1986; Derenne et al., 1990).

The *n*-alkane distributions (Fig. 7) differ between the distal to the proximal sites. The chromatogram from the proximal environment shows a bimodal distribution with a major mode centred on nC_{13} , and the second one on nC_{23} , with no obvious odd–over–even predominance in the C_{23} – C_{29} range. The classical *n*-alkane bimodal distribution in sample pyrolysates indicates a mixed terrestrial and marine-derived OM.

In contrast, the chromatogram from the distal environment is characterised by a unimodal *n*-alkane distribution pattern centred on compounds in C_{13} – C_{17} , fully representative of a marine-derived OM.

In addition to alkylbenzene compounds, aromatic fractions also comprise alkyl-naphthalenes (Fig. 6) and minor alkylphenanthrenes. These compounds, which are particularly well represented in the sample from the proximal environment, confirm the importance of terrestrial OM inputs in this area. Minor amounts of hopanoids (C_{27} – C_{31}), which were identified in the distal area sample (Fig. 8) witness the development of anaerobic bacteria in the

Table 2
Naphthalene identified in Senegal samples

Peak number	Compounds
1	Naphthalene
2	Methylnaphthalene
3	Dimethylnaphthalene
4	Trimethylnaphthalene
5	Ethyl-naphthalene

deposition environment (Peters and Moldowan, 1993).

4.2. Tarfaya Basin

4.2.1. Petrographic and bulk geochemical characteristics

Tarfaya sediments show much higher TOC contents than lateral equivalent samples from the Senegal (Fig. 3). As a matter of fact, despite some organic-poor levels (ca. 1.5% TOC), the mean TOC contents of these sediments is about 7.5% and can reach up to 16% in some samples (Fig. 3D). HI values vary from 500 to 850 mg HC g⁻¹ TOC with an average around 600 mg HC g⁻¹ TOC. According to HI vs. OI as well as HI vs. Tmax diagrams, OM fall close to the maturation pathways typical for type I and type II kerogens (Fig. 3A,B). Such high TOC and HI contents suggest high primary phytoplanktonic productivity and/or favourable OM preservation conditions (Tissot and Welte, 1984).

In this general context, C/N ratios lower than 10 (Fig. 3C) could be indicative of a notable contribution of nitrogen-rich OM of marine origin and/or OM alteration. S/C ratios (Fig. 3D) greater than 0.36 suggest euxinic conditions in the depositional environment (Raiswell and Berner, 1985; Morse and Berner, 1995).

Organic particles observed under photonic microscope (Fig. 9) consist mainly of liptinite (90–95%). The prevailing liptinite groups are alginite and bituminite, while liptodetrinite is seldom observed. Alginite occurs as small (usually less than 20 μm

Fig. 6. (A) Gas chromatogram showing relative abundance of major compounds in Senegal samples. (a) Alkylbenzene; (b) naphthalene; (c) alkane. (B) Gas chromatogram showing distribution of the alkylbenzene series (see Table 1 for identification). (C) Gas chromatogram showing the distribution of the naphthalene series (see Table 2 for identification).

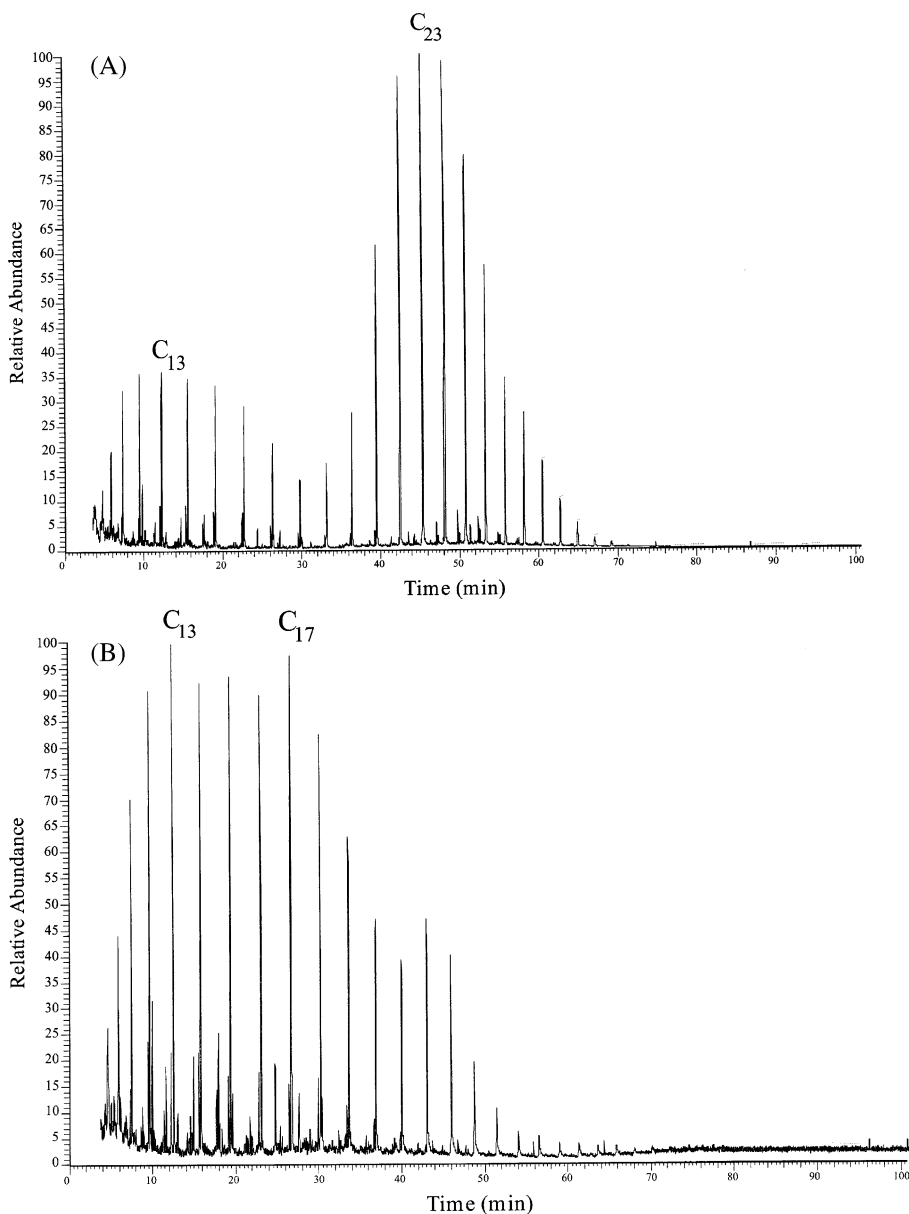


Fig. 7. Gas chromatograms showing *n*-alkane distributions in Senegal samples. (A) Proximal area with bimodal distribution; (B) distal showing unimodal distribution.

long) elongated particles (lamalginite). In marine sediments, alginite and liptodetrinite, respectively, represent the morphologically well and little preserved remains of marine plankton. Bituminite is commonly regarded as a microbial degradation product of more labile OM that can only be (partly) preserved under exceptional conditions such as anoxic bottom waters

(Teichmüller, 1982; Tyson, 1995). Thus, in addition to other indicators such as the abundance of organic carbon and high S/C ratios, high proportions of bituminite witness the establishment of anoxic bottom waters during deposition. A subordinate proportion of particles of inertinite or vitrinite of terrigenous origin was also observed. The scarcity of such terrigenous

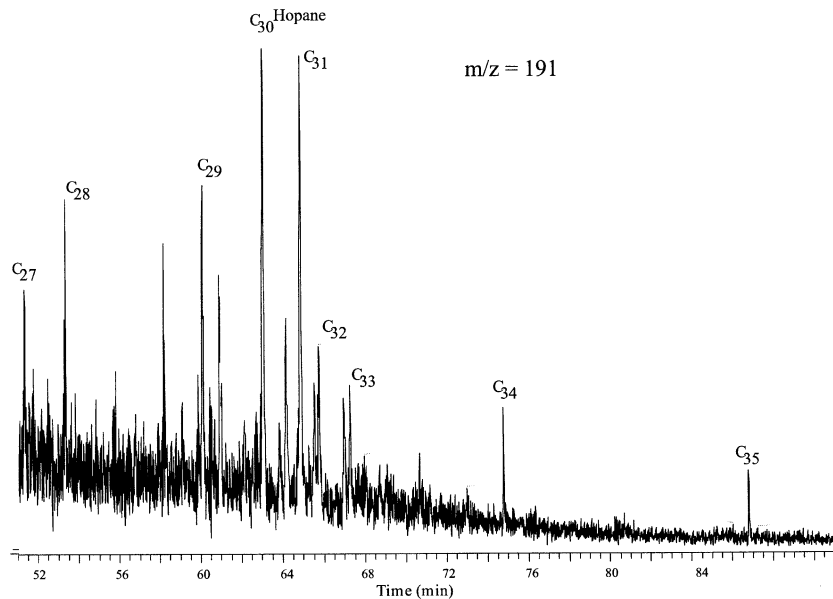


Fig. 8. Gas chromatogram showing the hopane series in distal part of Senegal platform.

particles indicates low inputs of eroded material in the Basin.

Under transmitted light (Fig. 9), OM particles isolated by destruction of the mineral matrix (paly-nofaciès extracts), appear highly dominated by homogenous reddish-brown gelified AOM flakes with frequent inclusions of pyrite flamboids. AOM flakes present variable morphologic appearance and often fluoresces under blue incident light. This fluorescence suggests an oil-prone composition and favourable OM depositional conditions (Lewan, 1986). Rare opaque debris can be identified as inertinite and vitrinite particles. The palynomorphs also contain algal remains and dinocysts and acritarchs. The absence of contrasted OM composition suggests the existence of a single OM source (i.e. marine).

Vitrinite reflectance values determined from the very few particles observed usually vary between 0.3% and 0.45%. These values are in general agreement with Tmax data which range between 419 °C and 422 °C and thus indicate that the OM is still immature (Fig. 3A).

SEM investigations show that the microtexture of Tarfaya sediments is similar to that of the Senegal

samples, except for the predominance of thick OM laminations in organic-rich sediments. The main difference between the two series concerns sulphur distribution, since EDS microanalyses reveal that the whole OM here is enriched in this element (Fig. 10). This observation points out the role of sulphurisation processes in OM preservation in Tarfaya. The analyses of the mineral fraction (Fig. 11) and elemental X-ray mapping show the predominance of Ca, and in a lesser extent, the presence of carbonate formations.

5. Molecular organic geochemical proxies

The gas chromatogram obtained from samples of the Tarfaya formations are shown in Fig. 12 (Tables 3 and 4 for identification). The major compounds comprise a long series of alkylthiophenes dominated by 2-ethyl 5-butyl thiophene. A high alkylthiophene content is characteristic of type II-S kerogens (Sinningh e Damst e et al., 1989). According to various authors (e.g. Boussafir et al., 1995; Boussafir and Lallier-Verg es, 1997; Riboulleau et al., 2000

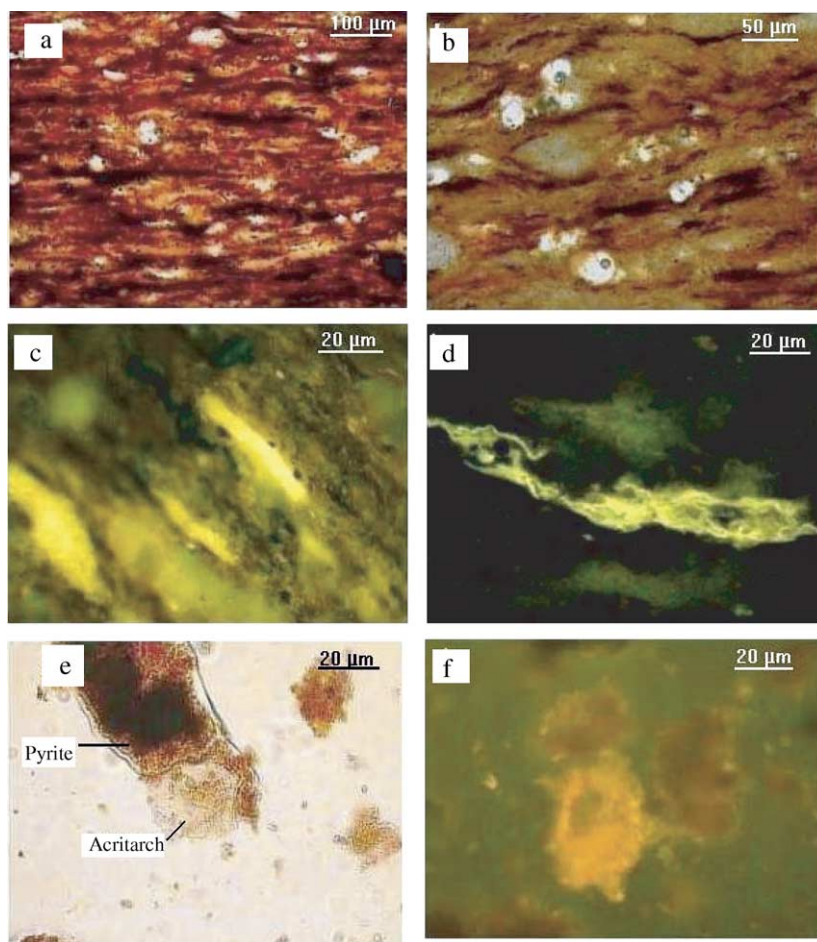


Fig. 9. Photomicrographs illustrating the typical maceral composition of Tarfaya samples. (a) Organic-rich sample showing high OM bands. (b) Organic poor sample with dense mineral. (c) and (d) Strong fluorescing alginite. (e) Reddish brown amorphous organic matter (AOM) and (f) fluorescing AOM.

and references therein), the abundance of sulphur-containing compounds results from the sulphurisation of planktonic lipids and carbohydrates during early diagenesis. Rare benzothiophenes are also observed.

The *n*-alkane series (Fig. 13) shows short chain predominance with a maximum abundance at C₁₃. This distribution indicates a predominance of marine OM. Pentacyclic triterpane biomarkers are low abundant or even absent. Hopanoids mainly occur as trisnorhopane (Fig. 13), higher homologues in C₂₈–C₃₂ are not well developed. Steranes, usually rare in flash pyrolysis products, are not present in high level enough to be identified.

6. Discussion

Comparison between Senegal and Tarfaya Basins (Table 5) shows large contrast in OM abundance and characteristics. Senegal sediments exhibit mixed OM composition from terrestrial and marine origin. This feature is corroborated by bimodal *n*-alkane distributions, generally high C/N ratio values and medium to low HI values. Unlike Senegal, Tarfaya sediments show nearly homogenous OM composition highly dominated by marine-derived amorphous organic matter (AOM). High HI values, rather low C/N ratio values and *n*-alkane distributions dominated by short-chain compounds, all

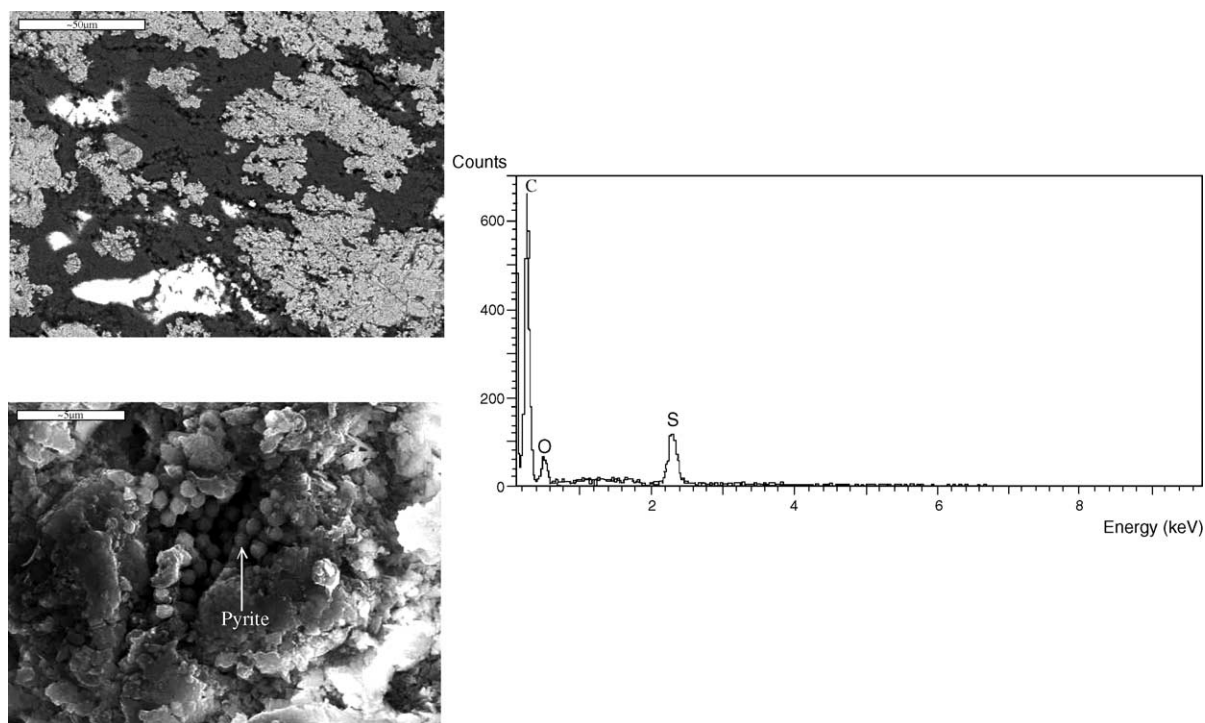


Fig. 10. SEM images of Tarfaya samples showing both OM and mineral matrix relationship and pyrite distribution in mineral matrix. The EDS spectra show the presence of sulphur in OM.

support the predominance of phytoplanktonic-derived OM.

Senegal and Tarfaya Basins also differ on another fundamental factor that is OM preservation conditions. The low S/C values and the lack of organo-sulphur compounds observed on the Senegal platform suggest that C–T sediments were deposited in suboxic medium conditions little favourable to OM preservation. These unfavourable conditions were most probably at least partly counterbalanced by a relatively rapid burial due to a high sedimentation rate (> 10 cm/ky; Nzoussi-Mbassani, 2003) (Table 5). Nevertheless, the latter factor also entailed a notable dilution of the organic inputs. Finally, a poor preservation conditions and high inorganic inputs globally result in the observed low TOC contents. Such features are not observed in Tarfaya where high S/C ratio values and the abundance of molecular organo-sulphur compounds typify anoxic depositional conditions whereas a low sedimentation rate (ca. 0.1 cm/ky; de Graciansky et al., 1982;

Herbin et al., 1986; Müller et al., 1983) excludes a dilution of the organic inputs by the mineral matter. In addition, it is worth underlying that the high sulphur content of Tarfaya sediments is mostly due to S-bearing organic compounds. This is clearly indicative of high reduced sulphur production and incorporation in the OM, during early diagenesis, and thus necessarily of pronounced anoxic medium conditions.

In order to determine a more coherent depositional model for NW Africa margin, the results obtained on Tarfaya and the Senegal Basins are compared to other C–T occurrences in the study area (Table 5). The first of these sites is the DSDP 367 well drilled offshore Senegal (Fig. 1) which penetrated a C–T series consisting of alternating black and green claystones deposited in pelagic environment (Lancelot and Seibold, 1977). At this site the sediments show the highest TOC contents (about 40%) recorded on the NW African margin, with HI values comprised between 300 to 900 mg HC g⁻¹ TOC (Herbin et al.,

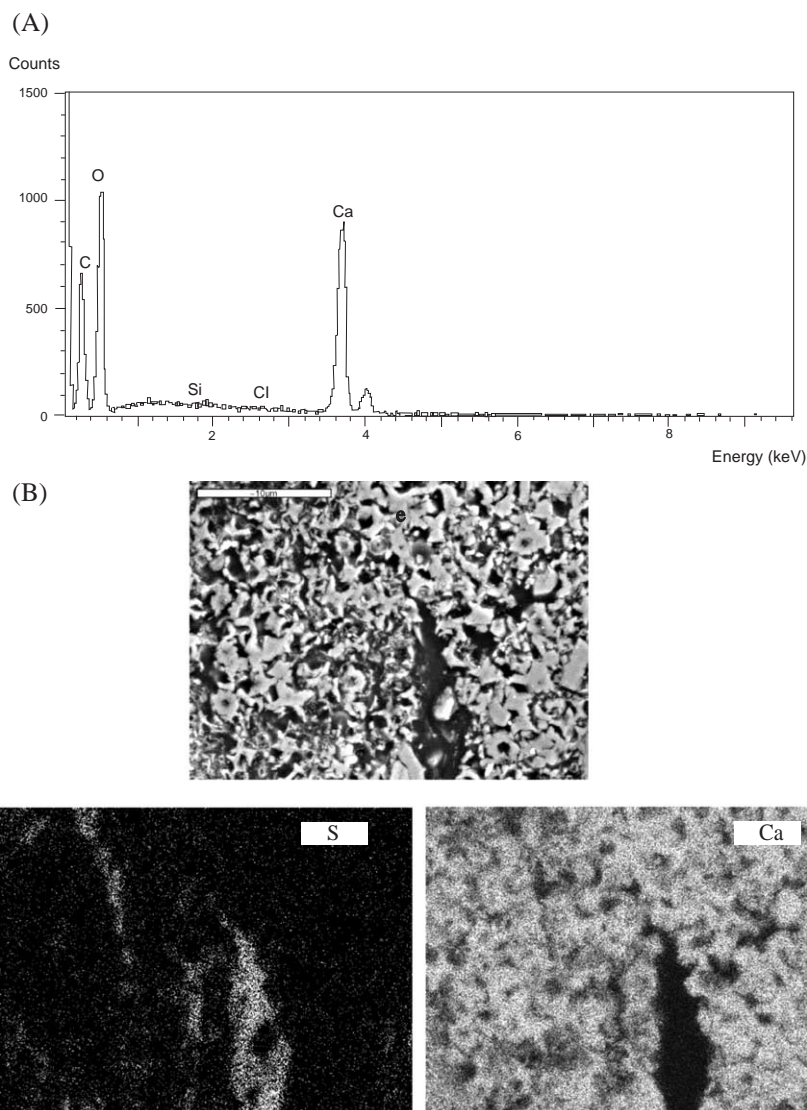


Fig. 11. (A) EDS analysis spectra showing the mineral composition of Tarfaya sediments; (B) an example of elemental (S, Ca) fingerprints of Tarfaya samples.

1986). The second site, the CM7 exploration well in the Senegal Basin is also situated offshore Senegal, in southern Casamance. It is representative of a slope or a hemipelagic environment, and thus could be compared to the Tarfaya Basin. The sediments from this site exhibit moderate TOC values (1% to 8%, Table 5) (Lancelot, 1980).

The comparison of OM data from these two sites with those of Tarfaya and Senegal onshore area (Table 5) suggests a northward increase in OM productivity

and/or preservation from the shelf (Senegal platform), to the transitional slope (Tarfaya and South Casamance) and the abyssal area (DSDP 367). Such evolution contrasts with the distribution of organic carbon contents observed in major recent and present depositional marine settings (Suess, 1980; Tissot and Welte, 1984; Bordenave, 1993). Indeed, the OM export flux from the euphotic zone decreases exponentially with depth throughout the water column (Suess, 1980), even in the case of high primary

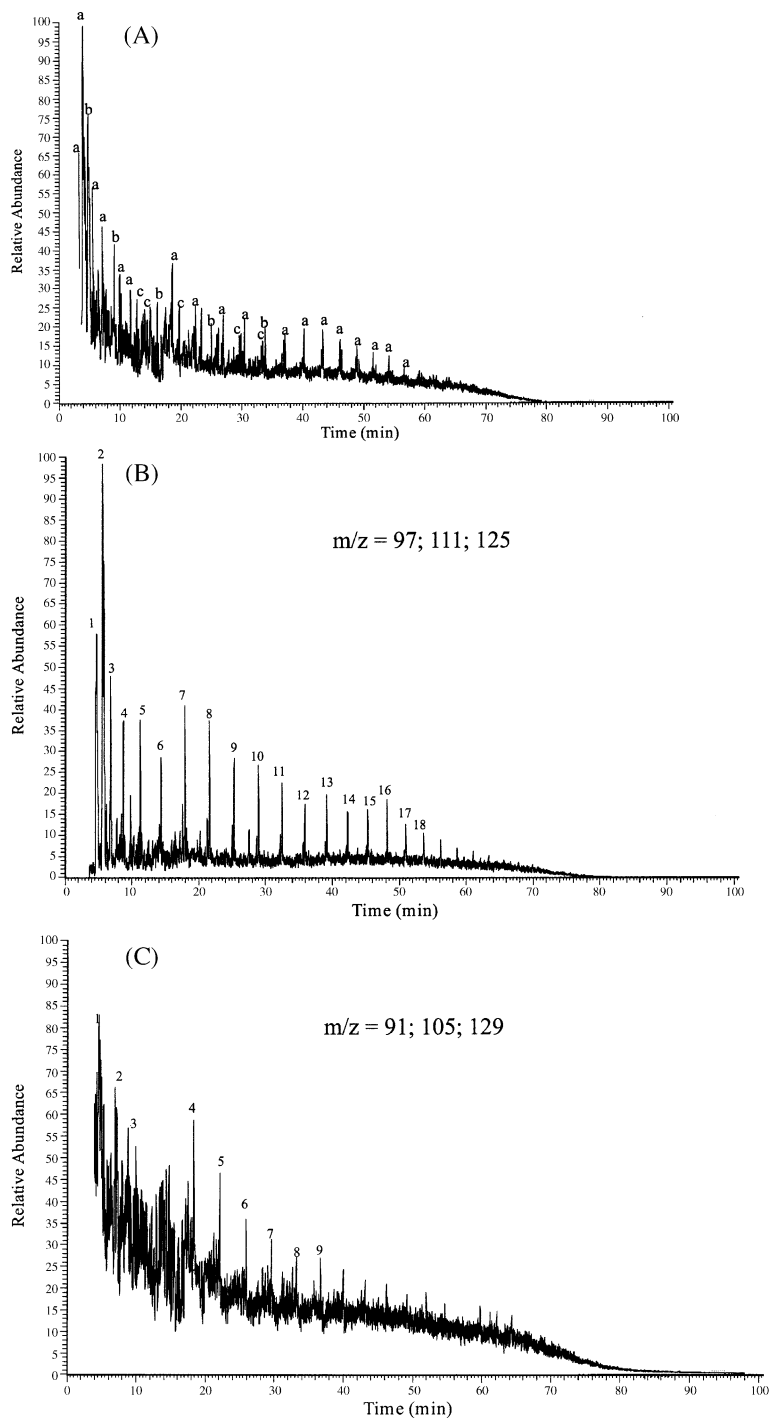


Fig. 12. (A) Gas chromatogram showing relative abundance of major compounds in Tarfaya samples. (a) Alkylthiophene; (b) alkylbenzene; (c) alkane. (B) Gas chromatogram showing distribution of the alkylthiophene series (see Table 3 for identification). (C) Gas chromatogram showing the distribution of the alkylbenzene series (see Table 4 for identification).

productivity such as in upwelling areas (Bertrand et al., 2003). This process necessarily results in the deposition of OM depleted sediments in deep water settings (abyssal area) compared to shelf areas. The processes that might have influenced OM accumulation in the NW African margin during the C–T period are discussed below, and conflict with those observed by many authors in modern high OM sedimentation environments.

6.1. C–T primary productivity on the NW African margin: comparison with present-day upwelling areas

The reconstruction of primary palaeoproductivity in general poses a number of problems. One of the main enigmas concerns the source of nutrients that must have supported high OM production. Generally, an abundant supply of nutrients to the surface photic layer can originate from terrestrial environments with riverine transport to the sea and/or directly from the sea, by upwelling currents.

The importance of terrestrial material inputs can be assessed by the rate of sediment accumulation (Waples, 1983). The average rate of sediment accumulation (Table 5) during C–T black shale deposition is estimated to ca. 0.1 cm/ky for deep areas (DSDP 367; de Graciansky et al., 1982; Herbin et al., 1986, consistently with datations provided by Müller et al.,

Table 3
Alkylthiophene identified in Tarfaya samples

Peak	Compounds
1	2-Hexyl thiophene
2	2-Ethyl 5-butyl thiophene
3	2-Ethyl 5-methyl thiophene
4	2-Butyl 5-ethyl thiophene
5	2,5 Diethyl thiophene
6	2-Pentyl thiophene
7	2-Isopropyl thiophene
8	2-Butyl thiophene
9	Benzothiophene
10	3-Methyl 2-butyl thiophene
11	Benzothiophene
12	3-Pentyl 3 methyl thiophene
13	2-Hexyl 3-ethyl thiophene
14	3-Methyl 2-butyl thiophene
15	Benzothiophene
16	Propylthiophene
17	2,3,5 Trimethylthiophene
18	2-Propyl 3-methyl thiophene

Table 4
Alkylbenzenes identified in Tarfaya samples

Peak	Compounds
1	2-Butyl benzene
2	Ethylbenzene
3	1,4 Dimethylbenzene
4	1,2,3,4 Tetramethylbenzene
5	1-Methyl 4-methylbenzene
6	Propylbenzene
7	Hexylbenzene
8	3-Methyl 2-ethylbenzene
9	1,2,4-Trimethylbenzene

1983) and to ca. 1.1 to 1.7 cm/ky at Tarfaya, and around 10 to 22 cm/ky for continental shelves (Nzoussi-Mbassani, 2003). In comparison, sediment accumulation in modern high productivity areas such as the Peruvian margin is about 19 cm/ky (Oberhänsli et al., 1990; Wefer et al., 1990) and about 30 to 120 cm/ky for the Namibian continental margin (Calvert and Price, 1983). However, the relatively low terrestrial inputs observed in hemipelagic and abyssal areas cannot explain the high OM productivity of these latter sites.

The other possible mechanism for nutrient supply and therefore high bioproductivity in marine area is the upwelling process. The assumption concerning the existence of a palaeo-upwelling regime along the NW African coast during C–T was initially mainly based on the existence of high OM contents in the sediments (Herbin et al., 1986). A key to the identification of this process in ancient series requires the identification of some characteristic markers within the sediments. In this respect, recent studies emphasise the distinction between nutrient markers (e.g. nitrates, phosphates, silicates. . .) and those related to OM production (e.g. diatomaceous ooze, microfossils. . .) (Romero and Hebbeln, 2003). For example, particular benthic foraminifera assemblages support the existence of palaeoecological conditions specific to upwelling regime in slope to shelf margin environments in NW Africa (Kuhnt and Wiedmann, 1995). Thus, the abundance of *Gabonita* (typical benthic foraminifera of high productivity areas) in Tarfaya sediments is considered as a proxy of considerable paleoproductivity due to upwelling system (Kuhnt and Wiedmann, 1995).

Other arguments can also be found in modern, supposedly comparable depositional settings. Two

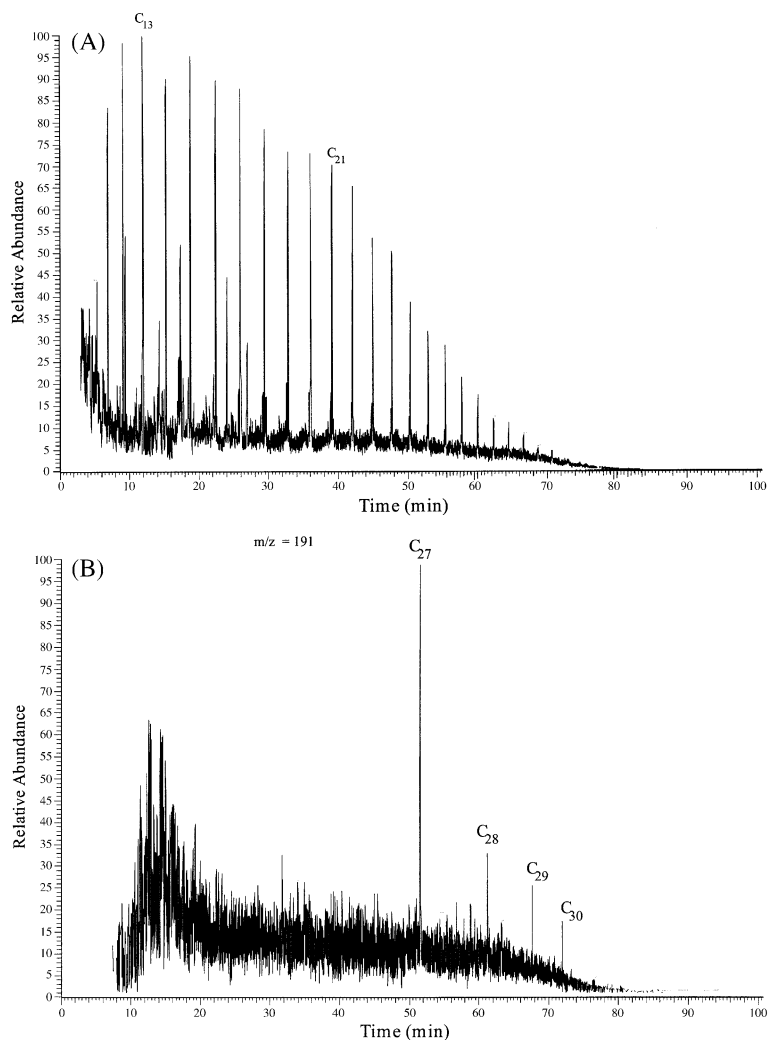


Fig. 13. Gas chromatograms showing *n*-alkane unimodal distribution (A) and hopane distribution (B).

areas presently well known to be the site for efficient coastal upwelling responsible of high primary productivity are here considered: the Peruvian margin and the Namibian shelf. Both occur under vigorous coastal upwelling system responsible of high primary productivity in the photic zone (Devries and Percy, 1982; Calvert and Price, 1983; Dingle, 1995). On the Peruvian margin, OM-rich sediments are accumulating on the continental shelf (depth lower than 300 m) along the eastern Pacific Ocean coast. The sedimentation rate of about 19 cm/ky contributes to a maximum sediment organic carbon content of about 12% (Dingle, 1995). Such values strongly contrast

with the low TOC content of the Senegal platform deposits despite a roughly similar sediment accumulation rate. On the Namibian shelf, recent studies have evidenced the presence of OM-rich sediments deposited in hemipelagic and pelagic environment with an average TOC content of 3.5% (Bertrand et al., 2003). On the platform (i.e. below 150 m depth) TOC contents reach 9% in an average, but they locally reach 25% (Calvert and Price, 1971). Some authors proposed that the abyssal OM-rich sediments might be composed of material redeposited from slope, after having been transported to depth by turbidity currents (Huc et al., 2001; Stow et al., 2001). This assumption

Table 5
Synthesised petrographic and geochemical data of Cenomanian–Turonian sediments North-Western Atlantic margin area

Samples	Senegal onshore (shelf environment) ^a	Tarfaya (hemipelagic) ^a	Senegal offshore (CM7) (hemipelagic) ^b	DSDP 367 (pelagic) ^c
Thickness (m)	500–2050	100–150	300	150
Sedimentation rate (cm/1000 year)	10–22	1.1–1.7	3.3	Ca. 0.1
TOC (%)	< 4%	1.5–16%	1.27–8.72	10–40%
HI (mg HC/g TOC)	< 400	500–850	152–660	300–900
Kerogen type	II and III	II	II rarely III	II
C/N	> 10	< 10		
S/C	< 0.36	> 0.36		
Liptinite	Very low	90–95% (alginite; bituminite)		
AOM	> 60%	Highly predominant		Highly predominant
Vitrinite I	Notable	Very low		rare
Vitrinite II	Notable	Very low		rare
Inertinite	Notable	Very low		rare
Molecular predominance	Alkyl benzene	Alkylthiophenes		Benzothiophene
Tmax (°C)	435–445	419–422	434–438	396–431
R ₀	0.3–0.9	0.3–0.4	0.57–0.64	0.24

^a This study and Nzoussi-Mbassani (2003).

^b Lancelot (1980).

^c de Graciansky et al. (1982), Herbin et al. (1986) and Müller et al. (1983).

is supported by absence of features characteristic of anoxic environment such as laminations and benthic foraminifers (Giraudeau et al., 2002).

There are some similarities in term of high OM content in deep sea sediments between present sedimentation from Namibia and NW African C–T series. However, in contrast to Namibian sediments, the abyssal black shales investigated in NW Africa exhibit fine laminations and no evidence of bioturbation (Herbin et al., 1986; Lancelot and Seibold, 1977). Such features are typical for anoxic depositional conditions. In addition, the absence of carbonates indicates that these black shales were deposited below the carbonate compensation zone (CCD), in pelagic environment (Lancelot and Seibold, 1977).

Assuming a preservation factor of 2%, Bralower and Thierstein (1984) estimated the primary productivity to ca. 50 g C m⁻²/year corresponding to the middle Cretaceous North Atlantic black shale. Such a value is markedly lower to that measured in present-day upwelling systems and which amounts to 200–360 g C m⁻²/year (Pedersen and Calvert, 1990).

In light of the above discussion which throws some doubts on the role of upwelling systems in the formation of OM-rich sediments we suggest that this process probably did not control the deposition of C–T sediments on NW African coastal area.

6.2. Euxinic depositional conditions: role of isorenieratane

The discovery of isorenieratane in sediments from Cenomanian–Turonian in North Atlantic Ocean (Sinningh  Damst  and K ster, 1998), the Pliocene from Mediterranean Sea (Bosch et al., 1998; Passier et al., 1999) and recently, in the Tarfaya Basin (Kolonic et al., 2002) shed some new light on the conditions of black shale deposition. This molecule derives from the reduction of isorenieratene, a carotenoid uniquely biosynthesized by the brown-colored strains of photosynthetic green sulphur bacteria (*chlorobiaceae*). In modern environments like the Black Sea the *chlorobiaceae* proliferate only in sulphate and sulphide-rich waters below the oxic/anoxic boundary (Repeta, 1993; Sinningh  Damst  et al., 1993). Their presence in sediments thus strongly suggests that water-column euxinia extended into the photic zone at the time of their deposition (Sinningh  Damst  et al., 1993).

The absence of such a marker in the Senegal platform series suggests the inexistence of Photic Zone Euxinia and corroborates previous studies suggesting global suboxic depositional conditions in this Basin (Nzoussi-Mbassani, 2003). In contrast to Kolonic et al. (2002), we did not directly identify any isorenieratene derivative in the pyrolysates of our Tarfaya samples.

However, the 1,2,3,4 tetramethylbenzene (TMB) molecule found in the alkylbenzene series could be related to the presence of isorenieratene in these sediments (Hartgers et al., 1994). Indeed, the 1,2,3,4 tetramethylbenzene (TMB) could be considered as originating from the β cleavage of aromatic carotenoid moieties such as isorenieratene during pyrolysis (Hartgers et al., 1994). Various studies such as in the Western Canada sedimentary Basin (Fowler et al., 1993), in the Bakken Formation (Muscio et al., 1994) and more recently in Holocene series (Aycard et al., 2003) established the possible link of this compound and isorenieratene presence. However, its real diagnostic value depends on alkylbenzene distribution (Hartgers et al., 1994; Hoefs et al., 1995). More explicitly, Hartgers et al. (1994) considered the abundance of TMB as an indicator of isorenieratene incorporation during early diagenesis, when coupled to the co-occurrence of 1-ethyl-2,3,6-trimethylbenzene. The abundance of TMB in our samples coupled to high content in alkylbenzene compounds may strongly link to isorenieratene (Hoefs et al., 1995). The development of an anoxic column can then be regarded as a global

phenomenon that affected only deep waters as suggested by similar evidences of anoxic deposition medium found in Tarfaya and Senegal offshore sediments. In this context, the presence of benthic fossil suggested by Kuhnt and Wiedmann (1995) could indicate temporary or periodic development of dysoxic and oxic bottom waters (Kening et al., 2004).

6.3. Depositional model

The appraisal of Cenomanian–Turonian depositional conditions also requires taking into account the whole Basin evolution since the rifting period. The development of a rifting system such as that initiated by Gondwana break up during Early Cretaceous times, usually results in the development of normal faults bounding downthrown and upthrown sides (Anders and Schlische, 1994). As the faults increase in length and displacement, the system attains a typical half-graben geometry, which results in the formation of many isolated Basins delimited by high accommodation zone (Anders and Schlische, 1994; Gawthorpe, 1999). The existence of a half-graben

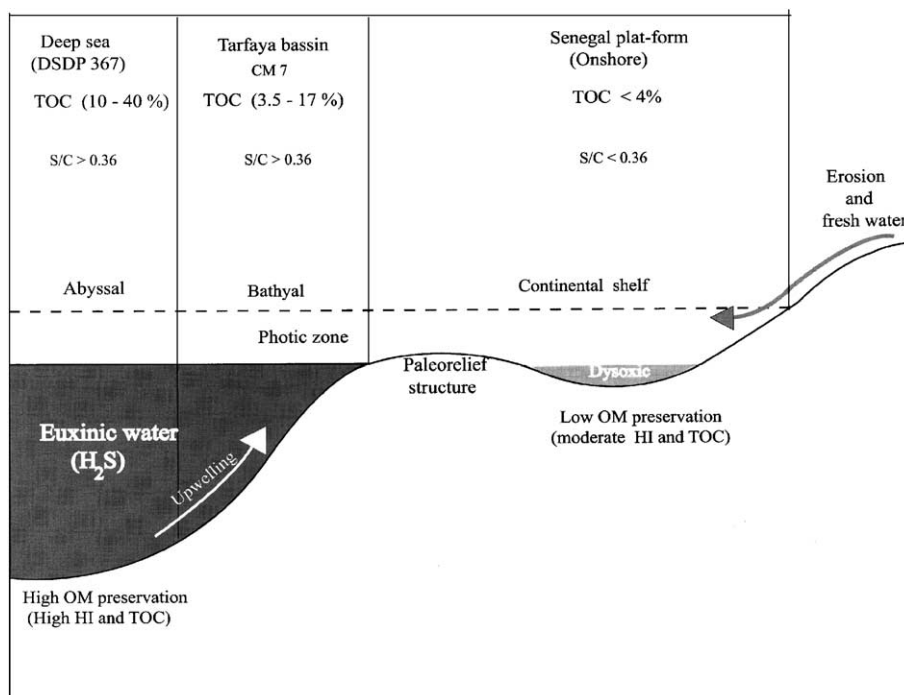


Fig. 14. Paleooceanography and depositional setting during Cenomanian–Turonian time. Note the presence of paleorelief structure between the continental shelf and the bathyal and abyssal environment. This structure restricted water exchange between both depositional settings.

system responsible of isolated and rift related Basins has been recognised by numerous authors at the North African margin (Orgeval, 1994). The implication of such a tectonic system for further sediment filling and OM accumulation is investigated here after according to the depositional model summarised in Fig. 14.

In the general framework of the geological evolution of the whole study area, the different expressions of the so-called C–T anoxic events in the various sites examined led us to suggest that positive palaeorelief features might have isolated deep and anoxic areas from the platform and related suboxic environments. This palaeorelief could have been the relict of the upthrown side/compartiment formed during rifting. This structural element might have played a key role in limiting exchanges between water bodies and especially in isolating the deep environment (Tarfaya, CM7, DSDP 367) and open shallow marine settings (Senegal shelf). This latter area was characterised by full water circulation and high terrigenous inputs from hinterlands (siliciclastics, plant material). This detrital material mostly originated from Mauritanides chain to the East and the Reguibat structure to the North.

The described model agrees with some previous observations concerning C–T sediment distribution (Orgeval, 1994; Latil-Brun and Lucazeau, 1988; Braun and Beaumont, 1989; Arthur et al., 1987). Those authors observed that C–T strata in West and North Africa was restricted to a marine facies deposited under minimum water depth and with a distribution that followed palaeoreliefs that existed at that time. This feature appears susceptible to explain the East–West increase in organic carbon content observed from platform to hemipelagic and pelagic environment.

7. Conclusion

Organic-rich strata of two North Western African Atlantic Basins were compared through organic petrography and bulk and molecular geochemistry approaches. Each setting revealed specific features of these strata related to depositional environment conditions during Cenomanian–Turonian period. At the scale of North Africa margin those differences may be attributable to paleogeographic configuration and

particular geodynamic evolution. The OM-rich sediments were most probably preferentially deposited in isolated and stagnant basins, with oxygen depleted bottom waters. The main factor, which has determined and further increased OM preservation conditions, was certainly the limited communication between southern oxygenated water (opened platform) and northern confined ones (mini-basins). Water stratification, salinity increase, H₂S production related to sulphuration processes have certainly contributed to preservation conditions increase. Confined environments are rift related basins originating from horst and graben structures resulting from Atlantic Ocean formation.

One implication of our results is that the occurrence of black shale is a consequence of interaction between particular Middle Cretaceous climate and *local factors* (paleogeographic conditions). Consequently, behind apparently homogenous facies of black shale sediment, there are many disparities in terms of organic matter composition, depositional environment and preservation conditions. Additionally, primary productivity was certainly not the key factor of C–T black shale deposition. This productivity mainly appeared moderate, especially when compared to present-day upwelling areas.

Finally, according to this study, the conditions that prevailed along the NW African margin during Cenomanian–Turonian times probably differed from those found in the environment of modern upwelling cells.

Acknowledgements

The authors would like to thank A.O. Wane and J. Medou from the Senegal Petroleum Corporation for allowing us to access the data and collect the samples. They are grateful to M. Hatton and D. Kéravis for technical assistance and are indebted to P.A. Meyers and an anonymous referee for constructive comments on the manuscript.

References

- Anders, M.H., Schlische, R.W., 1994. Overlapping faults, intrabasin highs, and the growth of normal faults. *J. Geol.* 102, 165–180.

- Arthur, M.A., Schlanger, S.O., Jenkyns, H.C., 1987. The Cenomanian–Turonian oceanic anoxia event: II. Paleooceanographic controls on organic matter production and preservation. In: Brooks, J., Fleet, A.J. (Eds.), *Marine and Petroleum Source Rocks*. Spec. Publ.-Geol. Soc. Lond., vol. 26, pp. 401–420.
- Arthur, M.A., Jenkyns, H.C., Brumsack, H.J., Schlanger, S.O., 1990. Stratigraphy, geochemistry and paleoceanography of organic carbon rich cretaceous sequences. In: Ginsburg, R.N., Beaudoin, B. (Eds.), *Cretaceous Resources, Events and Rhythms*. Kluwer Academic Publisher, pp. 75–119.
- Aycard, M., Derenne, S., Largeau, C., Mongenot, T., Tribouillard, N., Baudin, F., 2003. Formation pathways of proto-kerogens in Holocene sediments of the upwelling influenced Cariaco Trench, Venezuela. *Org. Geochem.* 34, 701–718.
- Baudin, F., 1995. Depositional controls on Mesozoic source rocks in the Tethys. In: Huc, A.-Y. (Ed.), *Paleogeography, Paleoclimate and Source Rocks*, Am. Assoc. Pet. Geol. Stud. Geol., vol. 40, pp. 191–211.
- Bertrand, P., Pedersen, T.F., Schneider, R., Shimmiel, G., Lallier-Vergès, E., Disnar, J.R., Massias, J., Tribouillard, N., Huc, A.Y., Giraud, X., Pierre, C., Vénec-Peyré, M.T., 2003. Organic-rich sediments in ventilated deep-sea environments: relationship to climate, sea level, and tectonic changes. *J. Geophys. Res.* 108, 1–11.
- Bordenave, M.L., 1993. The sedimentation of organic matter. In: Bordenave, M.L. (Ed.), *Applied Petroleum Geochemistry*. Technip, Paris, pp. 16–73.
- Bosch, H.-J., Sinningh Damsté, J.S., de Leeuw, J.W., 1998. Molecular palaeontology of Eastern Mediterranean sapropels: evidence for photic zone euxinia. In: Robertson, A.H.F., Emeis, K.C., Richter, C., Camerlenghi, A. (Eds.), *Proceedings of the Ocean Drilling Program. Scientific Results*, vol. 160, pp. 725–735.
- Boussafir, M., Lallier-Vergès, E., 1997. Accumulation of organic matter in the Kimmeridge Clay Formation (KCF): an update fossilisation model for petroleum source-rocks. *Mar. Pet. Geol.* 14, 75–83.
- Boussafir, M., Gelin, F., Lallier-Vergès, E., Derenne, S., Bertrand, P., Largeau, C., 1995. Electron microscopy and pyrolysis of kerogens from the Kimmeridge Clay Formation, UK: source organisms, preservation process and origin of microcycles. *Geochim. Cosmochim. Acta* 59, 3731–3747.
- Bralower, T.J., Thierstein, H.R., 1984. Low productivity and slow deep circulation in mid-Cretaceous oceans. *Geology* 12, 614–618.
- Braun, J., Beaumont, C., 1989. A physical explanation of the relation between flank uplifts and the breakup unconformity at rifted continental margins. *Geology* 17, 760–764.
- Busson, G., Comée, J., 1996. L'évènement océanique anoxique du Cénomaniens supérieur-terminal. *Publ.-Soc. Géol. Nord* 23 (143 pp.).
- Calvert, S.E., Price, N.B., 1971. Recent sediments of the South West African shelf. In: Delaby, F.M. (Ed.), *Geology of the East Atlantic Continental Margin*. Her Majesty's Stationery Office, London, pp. 175–185.
- Calvert, S.E., Price, N.B., 1983. Geochemistry of Namibian Shelf sediments. In: Thiede, J., Duess, E. (Eds.), *Coastal Upwelling: Its Sediment Record: Part B. Sedimentary Records of Ancient Coastal Upwelling*. Plenum Press, New York, pp. 337–375.
- Derenne, S., Largeau, C., Casadevall, E., Sinningh Damsté, J.S., Tegelaar, E.W., de Leeuw, J.W., 1990. Characterisation of Estonian kukersite by spectroscopy and pyrolysis: evidence for abundant alkyl phenolic moieties in an Ordovician, marine type II/I kerogen. In: Durand, B., Behar, F. (Eds.), *Advances in Organic Geochemistry*. Pergamon Press, Oxford, pp. 873–888.
- Devries, T.J., Pearcey, W.G., 1982. Fish debris in sediments of the upwelling zone off central Peru: a late quaternary record. *Deep-Sea Res.* 28, 87–109.
- Dingle, R.V., 1995. Continental shelf upwelling and benthic Ostracoda in the Benguela System (south-eastern Atlantic Ocean). *Mar. Geol.* 122, 207–225.
- Durand, B., Nicaise, G., 1980. Procedures for kerogen isolations. In: Durand, B. (Ed.), *Kerogen*. Technip, Paris, pp. 35–53.
- El Albani, A., Kuhnt, W., Luderer, F., Herbin, J.P., Caron, M., 1999. Palaeoenvironmental evolution of the Late Cretaceous sequence in the Tarfaya Basin (southwest of Morocco). In: Cameron, N.R., Bâte, R.H., Dure, V.S. (Eds.), *The Oil and Gas Habitats of South Atlantic*. Spec. Publ.-Geol. Soc. Lond., vol. 153, pp. 223–240.
- Espalià, J., Laporte, J.L., Madec, M., Marquis, F., Leplat, P., Paulet, J., Boutefeu, A., 1977. Méthode rapide de caractérisation des roches mères, de leur potentiel pétrolier et de leur degré d'évolution. *Rev. Inst. Fr. Pet.* 32, 23–42.
- Fowler, M.G., Stasiuk, L.D., Brooks, P.W., 1993. Middle Devonian oils and source rocks from western Canada sedimentary Basin. Abstract of presentation given at 1993 GAC-MAC Joint Meeting, Edmonton.
- de Graciansky, P.C., Brosse, E., Deroo, G., Herbin, J.P., Montadert, L., Müller, C., Sigal, J., Schaaf, A., 1982. Les formations d'âge crétacé de l'Atlantique Nord et leur matière organique: paléogéographie et milieux de dépôt. *Rev. Inst. Fr. Pet.* 37, 275–336.
- de Graciansky, P.C., Deroo, G., Herbin, J.P., Montadert, L., Müller, C., Schaaf, A., Sigal, J., 1984. Ocean-wide stagnation episode in the late Cretaceous. *Nature* 308, 346–349.
- Gawthorpe, R.L., 1999. Role of fault interactions controlling synrift sediment dispersal patterns: Miocene, Abu Alaqa group, Suez rift, Sinai, Egypt. *Basin Res.* 11, 167–189.
- Gelin, F., 1996. Isolation and chemical characterisation of resistant macromolecular constituents in microalgae and marine sediments. PhD thesis, Univ. Utrecht. 139 (147 pp.).
- Girardeau, J., Meyers, P.A., Christensen, B.A., 2002. Accumulation of organic and inorganic carbon in Pliocene–Pleistocene sediments along the SW African margin. *Mar. Geol.* 180, 49–69.
- Goth, K., de Leeuw, J.W., Püttman, W., Tegelaar, E.W., 1988. Origin of Messel Oil Shale kerogen. *Nature* 336, 759–761.
- Handoh, I.C., Bigg, G.R., Jones, E.J.W., Inoue, M., 1999. An ocean modeling study of the Cenomanian Atlantic: equatorial paleo-upwelling, organic-rich sediments and the consequences for a connection between the proto-North and South Atlantic. *Geophys. Res. Lett.* 26, 223–226.
- Hartgers, W.A., Sinningh Damsté, J.S., Requejo, A.G., Allan, J., Hayes, J.M., Ling, Y., Xie, T.M., Primack, J., de Leeuw, J.W., 1994. A molecular and carbon isotopic study towards the origin

- and diagenetic fate of diaromatic carotenoids. *Org. Geochem.* 22, 703–725.
- Hay, W.W., 1982. Mesozoic paleo-oceanography of Atlantic and Western Interior Seaway. *Am. Assoc. Pet. Geol. Bull.* 66, 568–579.
- Herbin, J.P., Montadert, L., Müller, C., Gomez, R., Thurow, J., Wiedmann, J., 1986. Organic-rich sedimentation at the Cenomanian–Turonian boundary in oceanic and coastal Basins in the North Atlantic and Tethys. *Spec. Publ.-Geol. Soc. Lond.* 21, 389–422.
- Hoefs, M.J.L., Van Heemst, J.D., Gelin, F., Schouten, S., de Leeuw, J.W., Sinningh  Damst , J.S., 1995. Alternative biological sources of 1,2,3,4 tetramethylbenzene in flash pyrolysate of kerogen. *Org. Geochem.* 23, 975–979.
- Horsfield, B., 1989. Practical criteria for classifying kerogens: some observations from pyrolysis–gas chromatography. *Geochim. Cosmochim. Acta* 53, 891–901.
- Huc, A.Y., Bertrand, P., Stow, D.A.V., Gayet, J., Vandembroucke, M., 2001. Organic sedimentation in deep offshore settings: the Quaternary sediments approach. *Mar. Pet. Geol.* 18, 513–517.
- International Committee of Coal Petrology, 1971. *International Handbook of Coal Petrography*, 2nd ed. CNRS, Paris.
- Kening, F., Hudson, J.D., Sinningh  Damst , J.S., Popp, B.N., 2004. Intermittent euxinia: reconciliation of Jurassic black shale with its biofacies. *Geology* 32, 421–424.
- Kolonic, S., Sinningh  Damst , J.S., B ttcher, M.E., Kuypers, M.M.M., Kuhnt, W., Beckmann, B., Scheeder, G., Wagner, T., 2002. Geochemical characterization of Cenomanian/Turonian Black shales from the Tarfaya Basin (SW Morocco). Relationships between palaeoenvironmental conditions and early sulphurization of sedimentary organic matter. *J. Pet. Geol.* 25, 325–350.
- Kuhnt, W., Wiedmann, J., 1995. Cenomanian–Turonian source rocks: paleobiogeographic and paleoenvironmental aspects. In: Huc, A.Y. (Ed.), *Paleogeography, Paleoclimate, and Source Rocks*. *Am. Assoc. Pet. Geol. Stud. Geol.*, vol. 40, pp. 213–231.
- Kuhnt, W., Herbin, J.P., Thorow, T., Wiedmann, J., 1990. Distribution of Cenomanian–Turonian organic facies in the western Mediterranean and along the adjacent Atlantic margin. In: Huc, A.Y. (Ed.), *Depositional of Organic Facies*. *Am. Assoc. Pet. Geol. Stud. Geol.*, vol. 30, pp. 133–160.
- Kuhnt, W., El Chellai, H., Holhoum, A., Luderer, F., Thurow, J., Wagner, I., El Albani, A., Beckmann, B., Herbin, J.P., Kawamura, H., Kolonic, S., Nederbragt, S., Street, C., Ravillious, K., 2001. Morocco Basin's sedimentary record may provide correlations for Cretaceous paleoceanographic events worldwide. *EOS* 82, 361–364.
- Kuypers, M.M.M., Pancost, R.D., Nijenhuis, I.A., Sinningh  Damst , J.S., 2002. Enhanced productivity led to increased organic carbon burial in the euxinic North Atlantic Basin during the late Cenomanian oceanic anoxic event. *Paleoceanography*.
- Lafargue, E., Marquis, F., Pillot, D., 1998. Rock-Eval 6 applications in hydrocarbon exploration, production, and soil contamination studies. *Rev. Inst. Fr. Pet.* 5, 421–437.
- Lancelot, Y., 1980. Birth and evolution of the "Atlantic Tethys". *Mem. Bur. Rech. G ol. Min.* 115, 215–223.
- Lancelot, Y., Seibold, E., 1977. Initial reports of Deep Sea Drilling Project, vol. 41. U.S. Govt. Printing Office, Washington (1259 pp.).
- Largeau, C., Derenne, S., Casadevall, E., Kadouri, A., Sellier, N., 1986. Pyrolysis of immature Torbanite and of the assistant biopolymer (PBR A) isolated from extant alga *Botryococcus braunii*. Mechanism of formation and structure of Torbanite. In: Leythaeuser, D., Rullk ter, J. (Eds.), *Advances in Organic Geochemistry 1985*. Pergamon Press, Oxford, pp. 1023–1032.
- Larter, S., Horsfield, B., 1993. Determination of structural components of kerogens by the use of analytical pyrolysis methods. In: Engel, M.H., Macko, S.A. (Eds.), *Org. Geochem. Principle and Applications*. Plenum Press, pp. 271–287.
- Latil-Brun, M.V., Lucazeau, F., 1988. Subsidence, extension and thermal history of the West African margin in Senegal. *Earth Planet. Sci. Lett.* 90, 204–220.
- Latimer, J.C., Filippelli, G.M., 2002. Eocene to Miocene terrigenous inputs and export production: geochemical evidence from ODP Leg 177, Site 1090. *Palaeogeogr. Palaeoclimatol. Palaeoecol.* 182, 151–164.
- Leine, L., 1986. Geology of the Tarfaya oil shale deposit, Morocco. *Geology* 65, 57–74.
- Lewan, M.D., 1986. Stable carbon isotopes of amorphous kerogens from Phanerozoic sedimentary rocks. *Geochim. Cosmochim. Acta* 50, 1581–1591.
- L ning, S., Kolonic, S., Belhadj, E.M., Belhadj, Z., Cota, L., Baric, G., Wagner, T., 2003. Integrated depositional model of Cenomanian–Turonian organic rich strata in North Africa. *Earth. Sci. Rev.* 64, 51–117.
- Michaud, L., 1984. Les milieux s dimentaires cr tac s du S n gal et leur  volution diag n tique (Etude de subsurface). PhD thesis, Univ. Marseille, France.
- Morse, W.J., Berner, A.R., 1995. What determines sedimentary C/S ratio. *Geochim. Cosmochim. Acta* 59, 1073–1077.
- M ller, C., Schaaf, A., Sigal, J., 1983. Biochronostratigraphie des formations d' ge cr tac  dans les forages du DSDP dans l'oc an Atlantique Nord. *Rev. Inst. Fr. Pet.* 38, 683–707.
- Muscio, G.P.A., Horsfield, B., Welte, D.H., 1994. Occurrence of thermogenic gas in the immature zone—implications from the Bakken in source reservoir system. *Org. Geochem.* 22, 461–476.
- Nzoussi-Mbassani, P., 2003. Le C nomano–Turonien de l'Atlantique Nord (Bassin du S n gal): environnement de d p t et  volution diag n tique. Implications p troli res. PhD thesis, Univ. Orl ans, France.
- Nzoussi-Mbassani, P., Disnar, J.-R., Laggoun-D farge, F., 2003. Organic matter characteristics of Cenomanian–Turonian source rocks: implications for petroleum and gas exploration onshore Senegal. *Mar. Pet. Geol.* 20, 411–427.
- Oberh nsli, H., Heinze, P., Diester-Haass, L., Wefer, G., 1990. Upwelling of Peru during the last 430,000 yrs and its relationship to the bottom-water environments, as deduced from coarse grain-size distributions and analyses of benthic foraminifers at holes 679D, 680B, and 681B, leg 112. ODP 112, 369–382.
- Orgeval, J.J., 1994. Peridiapiric m tal concentration: example of the Bougrine deposit (Tunisian Atlas). In: Fontbote, B. (Ed.),

- Sediment-hosted Zn–Pb ores. *Spec. Publ.-Soc. Geol.*, vol. 10. Springer, Berlin, pp. 354–389.
- Passier, H.F., Bosch, H.J., Nijenhuis, I.A., Lourens, L.J., Böttcher, M.E., Leendres, A., Sinningh  Damst , J.S., de Lange, G.J., de Leeuw, J.W., 1999. Sulphidic Mediterranean surface waters during Pliocene sapropel formation. *Nature* 397, 146–149.
- Pedersen, T.F., Calvert, S.E., 1990. Anoxia vs. productivity: what controls the formation of organic-carbon-rich sediments and sedimentary rocks? *Am. Assoc. Pet. Geol. Bull.* 74, 454–466.
- Peters, E.K., Moldowan, J.M., 1993. *The Biomarker Guide: Interpreting Molecular Fossils in Petroleum and Ancient Sediment*. Prentice Hall, Englewood Cliffs, NJ.
- Philip, J., Babinot, J.F., Tronchetti, G., Fourcade, E., Ricou, L.E., Guiraud, R., Bellion, Y., Herbin, J.P., Combes, P.J., Corn e, J.J., Decourt, J., 1993. Late Cenomanian (94 to 92 Ma). In: Dercourt, J., Ricou, L.E., Vrielynck, B. (Eds.), *Atlas Tethys Palaeo-environment Maps*. Gauthier–Villars, Paris, pp. 153–178.
- Philip, J., Babinot, J.F., Tronchetti, G., Fourcade, E., Ricou, L.E., Guiraud, R., Bellion, Y., Herbin, J.P., Combes, P.J., Corn e, J.J., Decourt, J., 2000. Late Cenomanian. In: Dercourt, J., Ricou, L.E., Vrielynck, B. (Eds.), *Atlas Peri-Tethys, Palaeogeographical Maps*. Paris, map 14.
- Raiswell, R., Berner, R.A., 1985. Pyrite formation in euxinic and semi-euxinic sediments. *Am. J. Sci.* 285, 710–724.
- Repeta, D.J., 1993. A high resolution historical record of Holocene anoxygenic primary production in the Black Sea. *Geochim. Cosmochim. Acta* 57, 4337–4342.
- Riboulleau, A., Derenne, S., Sarret, G., Largeau, C., Baudin, F., Connan, J., 2000. Origin of organic sulphur compounds and sulphur-containing high molecular weight substances in sediments and immature crude oils. *Org. Geochem.* 13, 593–606.
- Romero, O., Hebbeln, D., 2003. Biogenic silica and diatom thanatocoenosis in surface sediments below the Peru–Chile Current: controlling mechanisms and relationship with productivity of surface waters. *Mar. Micropaleontol.* 48, 71–90.
- Schlanger, S.O., Jenkyns, H.C., 1976. Cretaceous oceanic anoxic events: causes and consequences. *Geology* 55, 179–184.
- Schlanger, S.O., Arthur, M.A., Jenkyns, H.C., Scholle, P.A., 1987. The Cenomanian–Turonian oceanic anoxic event: I. Stratigraphy and distribution of organic carbon-rich beds and the marine $\delta^{13}\text{C}$ excursion. In: Brooks, J., Fleet, A.J. (Eds.), *Marine Petroleum Source Rocks*. Special Publication–Geological Society of London, vol. 26, pp. 371–399 (London).
- Sinningh  Damst , J.S., K ster, J., 1998. A euxinic southern North Atlantic Ocean during the Cenomanian/Turonian oceanic anoxic event. *Earth Planet. Sci. Lett.* 158, 165–173.
- Sinningh  Damst , J.S., Englinton, T.I., de Leeuw, J.W., Schenck, P.A., 1989. Organic sulphur in macromolecular sedimentary organic matter: structure and origin of sulphur-containing moieties in kerogen, asphaltenes and coal as revealed by flash pyrolysis. *Geochim. Cosmochim. Acta* 53, 873–889.
- Sinningh  Damst , J.S., Wakeham, S.G., Kohnel, M.E.L., Hayes, J.M., Leeuw, J.W., 1993. A 6,000 year sedimentary molecular record of chemocline excursions in the black sea. *Nature* 362, 827–829.
- Stach, E., Mackowsky, M.T., Teichm ller, M., Taylor, G.H., Chandra, D., Teichm ller, R., 1982. *Stach’s Textbook of Coal Petrology*. Gebr der Borntraeger, Berlin (535 pp.).
- Stow, D.A.V., Huc, A.Y., Bertrand, P., 2001. Depositional processes of black shales in deep water. *Mar. Pet. Geol.* 18, 491–498.
- Suess, E., 1980. Particulate organic carbon flux in the ocean. *Nature* 288, 260–263.
- Teichm ller, M., 1982. Origin of organic constituents of coal. In: Stach, M. (Ed.), *Textbook of Coal Petrology*. Gebr der Borntraeger, Berlin, pp. 219–294.
- Tissot, B.P., Welte, D.H., 1984. *Petroleum Formation and Occurrence*. Springer-Verlag, Berlin (699 pp.).
- Tyson, R.V., 1995. *Sedimentary Organic Matter. Organic Facies and Palynofaci s*. Chapman and Hall, London (615 pp.).
- Villeneuve, M., Da Rocha Araujo, P.R., 1984. La stratigraphie du bassin pal ozoique de Guin e (Afrique de l’Ouest). *Bull. Soc. G ol. Fr.* 32, 29–40.
- Waples, D.W., 1983. Reappraisal of anoxia and organic richness, with emphasis on cretaceous of North Atlantic. *Am. Assoc. Pet. Geol. Bull.* 67, 963–978.
- Wefer, G., Heinze, P., Suess, E., 1990. Stratigraphy and sedimentation rates from oxygen isotope composition, organic carbon content, and grain-size distribution at the Peru upwelling region: holes 680B and 686B. *ODP* 112, 355–362.
- Wiedmann, J., Butt, A., Einsele, G., 1982. Cretaceous stratigraphy, environment, and subsidence history at Moroccan continental margin. In: Von Rad, U., Hinz, K., Sarntheim, M., Seibold, E. (Eds.), *Geology of the North West African Continental Margin*. Springer, Berlin, pp. 366–395.



Contrasted distributions of triterpene derivatives in the sediments of Lake Caçó reflect paleoenvironmental changes during the last 20,000 yrs in NE Brazil

Jérémy Jacob ^{a,*}, Jean-Robert Disnar ^a, Mohammed Boussafir ^a, Ana Luiza Spadano Albuquerque ^b, Abdelfettah Sifeddine ^c, Bruno Turcq ^c

^a *Institut des Sciences de la Terre d'Orléans (ISTO), UMR6113 CNRS/Université d'Orléans, Bâtiment Géosciences, Rue de Saint Amand, BP 6759, 45067 Orléans Cedex 2, France*

^b *IRD/CNPq, Universidade Federal Fluminense, Morro do Valonguinho s/no. 24020-007 Niteroi, Brazil*

^c *UR055, IRD, Institut de Recherche pour le Développement, 32 av. Henri Varagnat, 93143, Bondy, France*

Received 9 November 2005; received in revised form 24 October 2006; accepted 27 October 2006

Available online 3 January 2007

Abstract

Lipid fractions extracted from sediment layers deposited in a small Brazilian lake during the last 20,000 yrs were investigated by gas chromatography–mass spectrometry. Considerable differences in the distribution and the amount of triterpene derivatives in the aliphatic as well as in the aromatic fractions were observed all along the series. Although no precise identification of these compounds was undertaken, our interpretation of mass spectral data allowed us to discriminate between des-A-triterpenes, mono- and triaromatic derivatives of pentacyclic triterpenes and a series of compounds tentatively identified as diaromatic derivatives of tetracyclic triterpenes. The largest compound diversity was found in the lowest levels of the series dated back to the end of the Last Glacial Maximum when good preservation of terrestrial plant debris was ensured by rapid burial in a semi-arid climate. Then, except for a period corresponding to the Younger Dryas, only des-A-lupane was detected in significant amounts. The high predominance of des-A-lupane is interpreted to result from the development of a belt of *Eleocharis* sp. (spike-rush) that filtered most of organic inputs from the catchment and was the site of des-A-lupane production and exportation towards the lake centre. During the Younger Dryas, a strong influx of des-A-lupane is attributed to the destruction of the spike-rush belt consecutive to the lowering of the lake level under drier conditions. The temporary destruction of this barrier allowed other triterpene derivatives to reach the lake. The distinct dynamics of des-A and aromatic triterpene derivatives under variable medium conditions led us to hypothesis that these two families of compounds derive from distinct pools that contributed differently to the sediment depending on environmental and climatic conditions. Des-A-lupane was most probably produced in sub-aquatic conditions within the belt of spike-rush. Conversely, aromatic derivatives of triterpenes could have resulted from the degradation of their biological precursors within reducing micro-environments in the catchment.

© 2006 Elsevier Ltd. All rights reserved.

* Corresponding author.

E-mail address: jeremy.jacob@univ-orleans.fr (J. Jacob).

1. Introduction

Pentacyclic triterpenes constitute a highly diversified family of molecules that are mostly produced by higher plants (Pant and Rastogi, 1979; Das and Mahato, 1983; Mahato et al., 1988, 1992; Mahato and Sen, 1997). Their extensive study for medicinal and pharmaceutical purposes provided abundant information that can be used for taxonomic purposes. Despite the high potential they thus offer for reconstructing past depositional environments, neither these compounds nor their diagenetic transformation products are frequently used for such a purpose, especially in recent sedimentary records (Cranwell, 1984; Hauke, 1994; Jaffé and Hausmann, 1995; Prartono and Wolff, 1998). The degradation products of triterpenes also can put some constraints on medium conditions during sediment deposition and early diagenesis. Indeed, the negative consequences that diagenesis can have by reducing structural specificities (Rullkötter et al., 1994; van Aarssen et al., 2000), can be counterbalanced by allowing the determination of the physico-chemical conditions that prevailed when molecular transformations occurred. Numerous studies were carried out on the diagenesis of triterpenes (Spyckerelle, 1975; Corbet, 1980; Lohmann, 1988; ten Haven and Rullkötter, 1988; Trendel et al., 1989; ten Haven et al., 1991; Hauke, 1994; Rullkötter et al., 1994) but the compound transformation routes are still incomplete. Furthermore, few compounds benefited from complete identification that would allow the establishment of precise product-precursor relationships. In addition, previous studies were carried out on organic-rich sediments, especially lignites and brown coals that were deposited under oxygen deficient conditions.

This study intends to contribute to our understanding of terrestrial triterpene diagenesis by comparing the distributions of triterpene derivatives in samples deposited under different environmental conditions. The studied samples were collected in the sedimentary infill of a small oligotrophic lake located in northern Brazil (Fig. 1). The major paleo-environmental changes that have affected the area since the end of the Last Glacial Maximum (LGM) have been assessed from the detailed study of a sedimentary core (Jacob, 2003; Jacob et al., 2004a). The almost exclusive contribution of higher plant material to the sediment and contrasting conditions of degradation offer an outstanding context to monitor the diagenetic fate of higher plant triter-

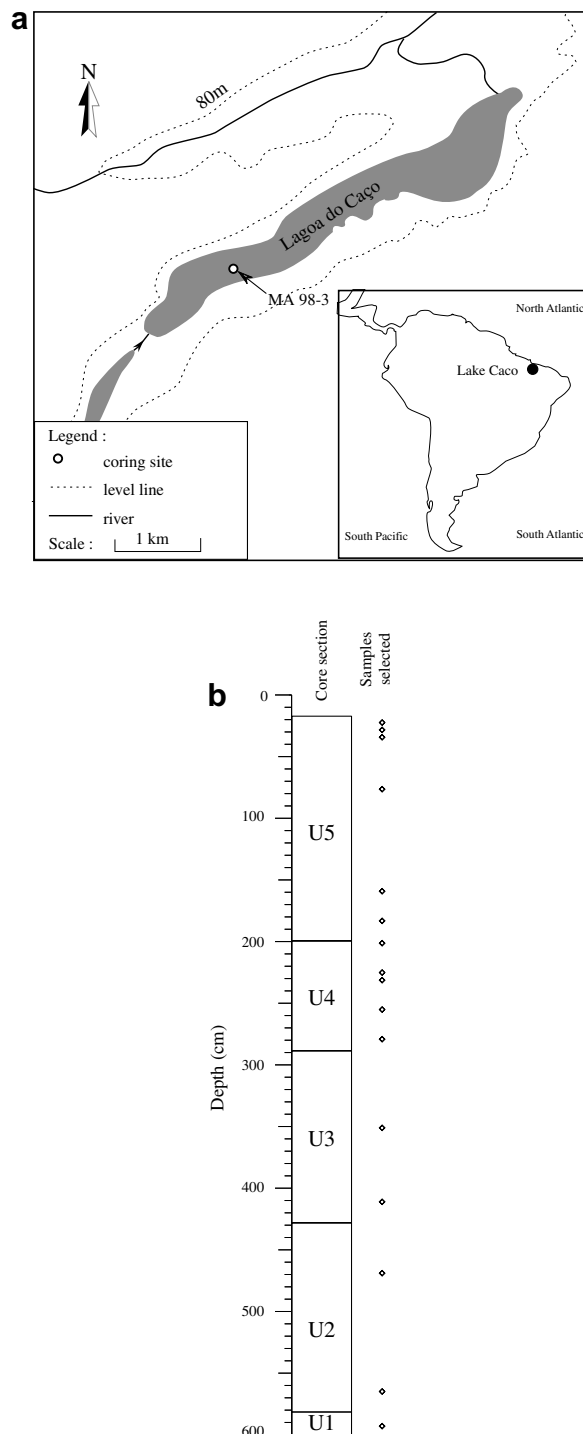


Fig. 1. (a) Map of study area with location of the coring site and (b) location of samples selected for this study on core MA 98-3.

penes and other biomolecules. In previous reports on the biomarker content of these sediments, we discussed the presence and the significance of

onocerane I and of a series of pentacyclic triterpene methyl ethers (Jacob et al., 2004b, 2005). The numerous types of molecular skeletons that have so far been detected in these sediments (namely oleanane, ursane, taraxerane, bauerane, fernane, arborane and onocerane) strengthen the interest of biomarker studies to apprehend the different degradation pathways followed by triterpenes depending on (paleo)environmental conditions.

2. Materials and methods

2.1. Sample selection

Sixteen samples were selected from a 6 m core drilled in the sediments of Lake Caçó, in north eastern Brazil (Fig. 1). These samples are representative of the five main sedimentary units defined by sedimentology, organic petrography and bulk geochemistry (Jacob et al., 2004a, see paragraph 4.1).

2.2. Extraction and separation of free lipids

The method for lipid extraction and separation was described elsewhere (Jacob et al., 2005). Briefly: one gram of dried sediment was ultrasonically extracted with acetone-pentane (50:50 v/v). The mixture was then separated into a neutral and an acidic fraction by solid phase extraction using AminoPropyl Bond Elute[®] cartridges. Neutral compounds were eluted with CH₂Cl₂-CH₃OH (50:50 v/v) and acidic compounds with ether after acidification of the medium with ether-formic acid (90:10 v/v). The neutral fraction was submitted to further fractionation on activated Florisil[®] to give aliphatic hydrocarbons (eluted with heptane), aromatic hydrocarbons and ethers (with CH₂Cl₂) and polar compounds (with CH₂Cl₂-CH₃OH 50:50 v/v). 5 α -Cholestane was added as internal standard prior to injection.

2.3. GC-MS analysis

GC-MS analyses were performed on a Thermo-Finnigan TRACE-PolarisGCQ gas chromatograph-mass spectrometer. The gas chromatograph was fitted with an Rtx[®]-5Sil MS capillary column (30 m \times 0.32 mm i.d., 0.25 μ m film thickness) with 5 m of guard column. The GC operating conditions were as follows: temperature hold at 40 °C for 1 min, then increase from 40 to 120 °C at 30 °C/min, 120 to 300 °C at 3 °C/min with final isothermal

hold at 300 °C for 30 min. The samples were injected splitless, with the injector temperature set at 280 °C. Helium was the carrier gas. The mass spectrometer was operated in the electron ionisation (EI) mode at 70 eV ionization energy and scanned from 50 to 650 Daltons. Compounds were tentatively identified by comparison with published mass spectra and relative retention times. The mass spectra of several compounds discussed in the text are given in Appendix 1 and 2 together with the proposed structures. Because of frequent coelutions, quantitations were performed on ion specific chromatograms drawn with the three major ions of the analysed compounds (see Table 1). Then, the obtained peak areas were normalized to the intensity of the peak of 5 α -Cholestane, measured on the TIC record. In the ignorance of individual response factors, this procedure precludes the determination of the real concentration of individual compounds but allows us to assess the variations of abundance along the core, which is the scope of this paper.

3. Results

3.1. Aliphatic hydrocarbons

Seven compounds eluting between *n*-C₂₃ and *n*-C₂₅ alkanes (Fig. 2) in the GC-trace of the aliphatic hydrocarbon fraction of sample 229 (470 cm depth) are interpreted as des-A-triterpenes (numbered 1–7 after their elution order). Their mass spectral characteristics are summarized in Table 1. Compounds 1 to 4 plus 6 that have a molecular mass of 328 amu (C₂₄H₄₀) were identified as unsaturated des-A-triterpenes. Compounds 5 and 7 exhibit a molecular ion at *m/z* 330 (C₂₄H₄₂) and are most certainly saturated counterparts. Compounds 1 to 4, the mass spectra of which do not display any fragment characteristic of the loss of an isopropyl group [M-43]⁺, are thus identified as des-A-triterpenes having a six-membered ring E. Abundant fragments at *m/z* 189, 203, 204 and 218 are typical for C-ring cleavage in oleanene and ursene structures, followed by retro-Diels Alder rearrangement (Djerassi et al., 1962; Budzikiewicz et al., 1962). According to relative retention times of oleanane and ursane-type triterpenes and mass spectral resemblance with already proposed structures (Corbet, 1980; Logan and Eglinton, 1994), we tentatively identify compound 1 as des-A-olean-13(18)-ene, compound 2 as des-A-olean-12-ene, compound 3 as des-A-urs-13(18)-ene and compound 4 as des-

Table 1

List of compounds discussed in the text with retention times, mass spectral data, tentative identification and references

Peak no.	Ret. time	Molecular mass	Most significant ions (by decreasing relative abundance order)	Formula	Tentative identification	References
<i>Des-A-triterpenes</i>						
1	37.83	328	189,204,313,161,328,161,218	C ₂₄ H ₄₀	Des-A-olean-13(18)-ene	A, B
2	37.99	328	203,218,189,231,313,161,175,328,243	C ₂₄ H ₄₀	Des-A-olean-12-ene	A, B
3	38.28	328	313,189,161,175,204,328,218	C ₂₄ H ₄₀	Des-A-urs-13(18)-ene	A, B
4	39.07	328	218,313,189,231,203,243,328	C ₂₄ H ₄₀	Des-A-urs-12-ene	A, B
5	39.83	330	163,149,191,177,206,287,217,315,330	C ₂₄ H ₄₂	Des-A-lupane	B, C (235), D, E
6	41.92	328	161,313,175,149,191,328,231,257,243	C ₂₄ H ₄₀	Des-A-arbor-9(11)-ene	F
7	42.07	330	191,177,206,315,330,219,233	C ₂₄ H ₄₂	Des-A-oleanane/ursane	E
<i>Aromatics</i>						
8	50.82	336	145,157,172,336,285,217	C ₂₅ H ₃₆	Pentanor-lupa-1,3,5(10)-triene	
9	52.02	380	145,351,173,380,213	C ₂₈ H ₄₄	Unknown	
10	53.13	380	172,145,157,380	C ₂₈ H ₄₄	Unknown	
11	54.16	376	145,172,156,189,204,361,376	C ₂₈ H ₄₀	Dinor-oleana(<i>ursa</i>)-1,3,5(10),12-tetraene	G (27, 28 or 31), H (38,34,35,31), I (7c), J (18)
12	54.43	376	170,155,145,209,285,225,361,376	C ₂₈ H ₄₀	Dinor-oleana(<i>ursa</i>)-1,3,5(10),13(18)-tetraene	G (29)
13	55.3	376	158,145,143,204,361,376	C ₂₈ H ₄₀	Dinor-oleana(<i>ursa</i>)-1,3,5(10),12-tetraene	G (31), H(38,34,35,31), I (7b), J(20)
14	55.44	376	195,207,361,376,249,181,221,235	C ₂₈ H ₄₀	Lanosta(<i>eupha</i>)pentaene	
15	55.55	378	145,157,172,378	C ₂₈ H ₄₂	Dinor-oleana(<i>ursa</i>)-1,3,5(10)-triene	G (32), H(43), N (F)
16	55.84	340	255,188,325,340	C ₂₆ H ₂₈	Tetranor-oleana(<i>ursa</i>)-1,3,5(10),6,8,11,13-octaene	G (46)
17	56.05	360	207,181,345,360,221,195	C ₂₇ H ₃₆	Nor-lanosta(<i>eupha</i>)hexaene	
18	56.3	376	195,361,207,181,376,249,235,221	C ₂₈ H ₄₀	Lanosta(<i>eupha</i>)pentaene	
19	56.42	340	255,340,270,239,325,283	C ₂₆ H ₃₀	Tetranor-oleana(<i>ursa</i>)-1,3,5(10),6,8,11,13-octaene	G (46), K (D')
20	57.56	342	342,218,231,243,257,327,271,285	C ₂₆ H ₃₀	Tetranor-oleana(<i>ursa</i>)-1,3,5(10),6,8,11,13-heptaene	G (39), H (39), J (22), K(F',H'), L(XI, XII), M(19)
21	57.77	374	195,207,374,359,221	C ₂₈ H ₃₈	Lanosta(<i>eupha</i>)hexaene	
22	57.84	378	145,157,172	C ₂₈ H ₄₂	Dinor-lupa-1,3,5(10)-triene	I (7a), J(21), N(F)
23	57.88	342	257,342,242,228	C ₂₆ H ₃₀	Tetranor-oleana(<i>ursa</i>)-1,3,5(10),6,8,11,13-heptaene	G (42), H(40), M(20), J(23)
24	58.12	342	257,342,243,299	C ₂₆ H ₃₀	Tetranor-lupa-1,3,5(10),6,8,11,13-heptaene	G (43), H (47), L(XII), M(21)
25	58.54	374	195,207,374,221	C ₂₈ H ₃₈	Lanosta(<i>eupha</i>)hexaene	H (42)
26	58.63	374	145,157,172,325	C ₂₈ H ₃₈	Dinor-oleana(<i>ursa</i>)-1,3,5(10),12,14-pentaene	G (38)
27	58.69	374	195,374,207,221,359,281	C ₂₈ H ₃₈	Lanosta(<i>eupha</i>)hexaene	G (41), H(42)

References: A: Logan and Eglinton (1994); B: Corbet (1980); C: Philp (1985); D: Trendel et al. (1989); E: Woolhouse et al. (1992); F: Jaffé and Hausmann (1995); G: Stout (1992); H: Hazai et al. (1986); I: Wolff et al. (1989); J: ten Haven et al. (1992); K: Chaffee et al. (1984); L: Chaffee and Fookes (1988); M: Wakeham et al. (1980); N: Loureiro and Cardoso (1990). The designation of related compounds found in the reference are indicated between brackets.

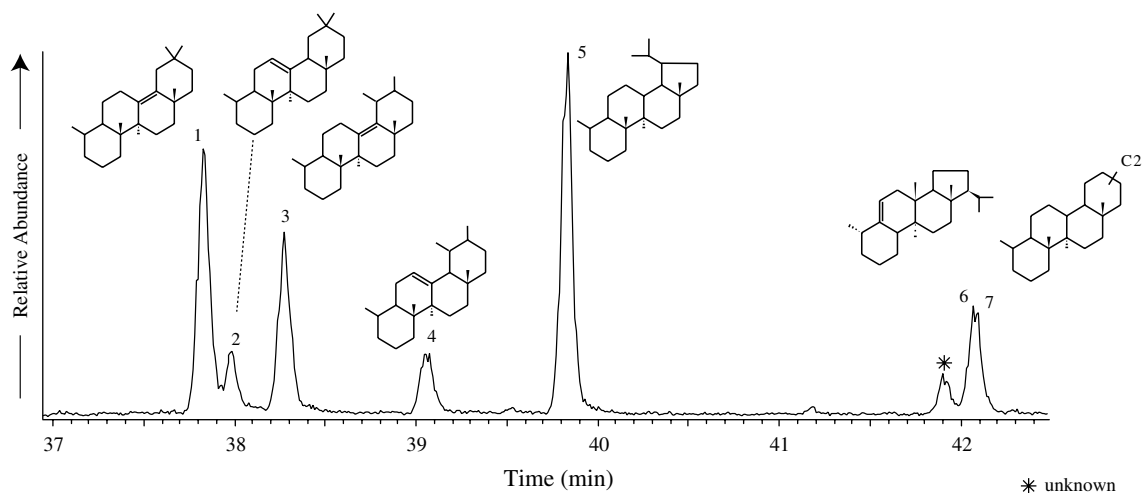


Fig. 2. Distribution of des-A-triterpenes in the partial selected ion chromatogram (m/z 163 + 177 + 189 + 203 + 218) of the aliphatic hydrocarbon fraction extracted from sample 229. The mass spectral data, retention times and proposed identity of compounds 1 to 7 are given in Table 1.

A-urs-12-ene. Compound 5 was identified as 10 β -des-A-lupane by comparison with published mass spectra (Corbet, 1980; Philp, 1985; Trendel et al., 1989; Woolhouse et al., 1992). The mass spectrum of compound 6 displays intense fragments at m/z 175, 161 and 149 that are common in D:C or E:C-friedo triterpenes (Shiojima et al., 1992). According to Jaffé and Hausmann (1995), compound 6 might be 10 β -des-A-arbor-9(11)-ene. The mass spectrum of compound 7 displays a molecular ion at 330 amu, consistent with a des-A-triterpane structure (C₂₄H₄₂). It is tentatively identified as des-A-oleanane/ursane by comparison with a published spectrum (Woolhouse et al., 1992).

3.2. Aromatic hydrocarbons

In the aromatic fractions, 20 compounds are tentatively identified as aromatic derivatives of triterpenes. They are divided into three main groups with regard to their mass spectra, the most significant fragments of which are listed in Table 1. The mass spectra of compounds from the first group exhibit prominent fragments at m/z 145, 158, 172. The mass spectra of those from the second group show abundant ions at m/z 195, 207 and 221. The compounds of the third group are characterized by spectra displaying molecular ions at m/z 340 or 342. The chromatographic distributions of these compounds on ion-specific chromatograms are displayed in Fig. 3 and their mass spectra are displayed in Appendix 1 and 2.

3.2.1. Ring A monoaromatic pentacyclic triterpenes

The mass spectra of these compounds exhibit molecular ions at m/z 336 (compound 8), m/z 380 (compounds 9 and 10), m/z 378 (compounds 15 and 22), m/z 376 (compounds 11, 12 and 13) and m/z 374 (compound 26). The mass spectra of compounds 8 to 13, 15, 22 and 26 show intense ions at m/z 145, 157, 158, 170 and 172 that is consistent with A-ring monoaromatic triterpenes with oleanane, ursane or lupane skeletons (LaFlamme and Hites, 1978; Wakeham et al., 1980; Chaffee et al., 1984; Hazai et al., 1986; Chaffee and Fookes, 1988; Loureiro and Cardoso, 1990; Stout, 1992). The relative intensities of ions m/z 145, 157, 158, 170 and 172 depend on whether additional unsaturations are located on rings B, C, D or E. As demonstrated by several authors (Lohmann, 1988; Loureiro and Cardoso, 1990), the double bond position in natural product precursors is often preserved in diagenetic derivatives. For example, Δ^{12} oleanenes are transformed into aromatic oleanoids in which the Δ^{12} double bond is preserved as long as aromatisation does not affect ring C.

The mass spectra of compounds 15 and 22 display an intense ion at m/z 145 and minor ions at m/z 157 and 172. Their molecular weight of 378 amu is consistent with a C₂₈H₄₂ formula. Comparable spectra have been described in Hazai et al. (1986), Wolff et al. (1989), ten Haven et al. (1992) and Stout (1992) where they were attributed to ring A monoaromatic triterpenes with oleanane, ursane or lupane structures. Accordingly, we propose the

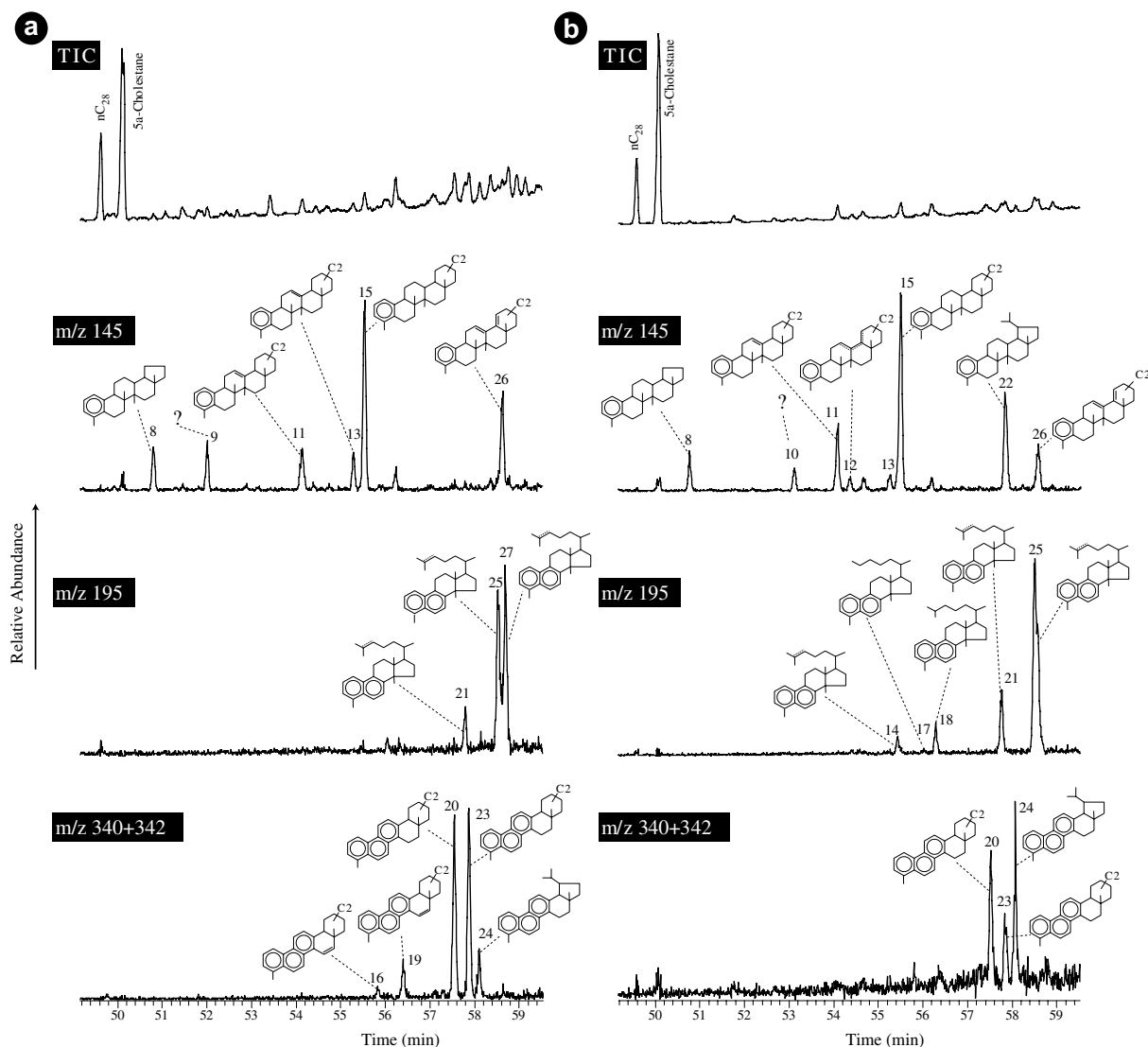


Fig. 3. Distribution of aromatic triterpenes depicted on the total ion chromatogram, m/z 145, m/z 195 and m/z 340 + 342 mass chromatograms of samples 073 (a) and 229 (b). The mass spectral data, retention times and proposed identity of compounds 8 to 27 are given in Table 1.

structures of oleana(*ursa*)-1,3,5(10)-triene and dinor-lupa-1,3,5(10)-triene for compounds 15 and 22, respectively.

The mass spectra of compounds 11, 12 and 13 display a molecular ion at m/z 376 that denotes ring A monoaromatic structures with one double bond ($C_{28}H_{40}$). Compounds displaying resembling mass spectra have been reported in sub-bituminous coals (Hazai et al., 1986), in Tertiary angiospermous lignite (Stout, 1992) and were identified with synthetic standards (Wolff et al., 1989). According to spectral data and relative retention times, compounds 11, 12

and 13 could be dinor-oleana(*ursa*)-1,3,5(10),13(18)-tetraene isomers.

The molecular ion of compound 26 (374 amu) is consistent with a $C_{28}H_{40}$ formula, i.e. a monoaromatic compound with two additional double bonds. Abundant fragments at m/z 145, 157 and 172 attest to an A-ring monoaromatic structure. No isopropyl loss is expressed by any $[M-43]^+$ ion. As suggested by the preservation of the already mentioned ions at m/z 145, 157 and 172, the two additional double bonds cannot be both located on rings B or C since this latter configuration would lead to dominant

m/z 221 fragment (Stout, 1992). Therefore we propose a ring A-aromatic pentacyclic structure derived from oleanane or ursane and bearing two additional double bonds at Δ^{12} and Δ^{18} positions for compound 26. The molecular ion at m/z 336 of compound 8 differs from 42 amu from that of compound 22. This difference could be taken as evidence that compound 8 is the 22,29,30-trisnor-derivative of compound 22. Therefore, the structure of pentanor-lupa-1,3,5(10)-triene is proposed for compound 8.

The mass spectra of both compounds 9 and 10 show fragmentation patterns similar to those discussed above (prominent fragments at m/z 145, 157, 159, 172 and 173 in the mass spectra) but a molecular weight of 380 amu ($C_{28}H_{44}$). Such a molecular weight supposes the addition of two hydrogen atoms on the already discussed compounds that exhibit a molecular weight of 378 amu, but without affecting the double bonds that participate in aromatisation. Therefore, compounds 9 and 10 could be ring A-monoaromatic derivatives of seco-triterpenes or of tetracyclic triterpenes possessing a lateral side chain. This latter assumption is corroborated by the presence of an abundant fragment at m/z 351 in the mass spectra of compound 9 that attests to the loss of an ethyl moiety.

3.2.2. Triaromatics

The mass spectra of compounds 20, 23 and 24 all exhibit a molecular ion at m/z 342 and a strong fragment at m/z 257 that characterise ring A, B, C triaromatic triterpenes (Wakeham et al., 1980; Chaffee and Fookes, 1988; Stout, 1992). Comparison of mass spectral data allowed us to identify compounds 20 and 23 as tetranor-oleana(*ursa*)-1,3,5(10),6,8,11,13-heptaene isomers and compound 24 as tetranor-lupa-1,3,5(10),6,8,11,13-heptaene, respectively, with undefined stereochemistry at the D/E ring junction (Chaffee and Fookes, 1988). The mass spectra of two other compounds (16 and 19) resemble the previous ones, but with a molecular ion at m/z 340 and a prominent ion at m/z 255. Compounds 16 and 19 are therefore interpreted as ring A, B, C triaromatic triterpenes with an additional double bond, probably with oleanane and ursane structures, respectively.

3.2.3. Ring A, B diaromatic tetracyclic triterpenes

The mass spectra of compounds from the third group (compounds 14, 17, 18, 21, 25 and 27) often exhibit prominent fragments at m/z 181, 195, 207

and 221 and a molecular mass of 360, 374 and 376 amu. To our knowledge, few reports of such mass spectra have been published (Hazai et al., 1986; Stout, 1992; Hauke, 1994; Killops et al., 1995). According to Hauke (1994), ions at m/z 195, 207 and 221 with a molecular ion at m/z 374 correspond to the A,B-diaromatic 24,25-dinor-arbora-1,3,5,7,9-pentaene. In contrast, in the mass spectrum of 24,25-dinor-arbora-1,3,5(10),9(11)-tetraene (molecular ion at m/z 376), major fragments are recorded at m/z 209, 219 and 187. Therefore, one can hypothesize that the m/z 181, 195, 207 and 221 fragments characterise ring A, B diaromatic structures with methyl groups located at the C, D ring junction. This assumption cannot account for compounds 14 and 18. The mass spectra of these compounds both have a base peak at m/z 195 but a molecular ion at m/z 376 ($C_{28}H_{40}$), thus requiring two additional hydrogen atoms as compared with the compound with a molecular ion at m/z 374. This is incompatible with a structure of diaromatic pentacyclic triterpene. According to these observations, the considered compounds could be ring A, B diaromatic derivatives of tetracyclic triterpenes with methyl groups located at C(13) and C(14) positions (e.g. lanostane, tirucallane or euphane structures) for which a proposed fragmentation mechanism is reported in Fig. 4. Because the fragmentation pattern is rather similar for compounds with a molecular ion at m/z 376 and those with a molecular ion at m/z 374, the additional double bond in these latter cannot occur in the vicinity of rings C and D but is most probably located on the side chain. According to these observations, compounds 14 and 18 are tentatively identified as ring A, B diaromatic derivatives of lanostane, euphane or tirucallane type compounds. Differences in the spectral signature of these molecules could arise from different configurations at C(13) and C(14) positions. Compounds 21, 25 and 27 appear as possible derivatives of compounds 14 and 18 with one additional double bond. In addition to the isomerism at C(13) and C(14) positions, the position of the double bond on the lateral side chain could participate in the diversity of fragmentation patterns. Finally, compound 17, which has a molecular mass of 360, is assumed to have a similar structure with a shorter side chain.

3.3. Oxygenated triterpenes

The polar fraction that contains oxygenated triterpenes has been investigated but, as for most

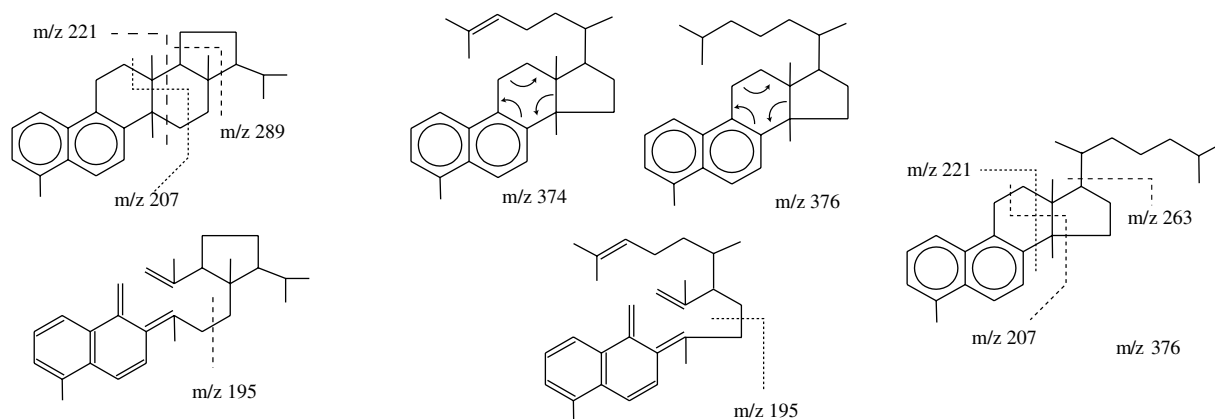


Fig. 4. Fragmentation mechanism for 24,25-dinor-arbora-1,3,5,7,9-pentaene (adapted from Hauke, 1994) and proposed fragmentation mechanism for ring A–B diaromatic derivatives of tetracyclic triterpenes with euphane or lanostane structure. Note that the structures shown are tentative.

recent lake sediment samples, the large diversity of unknown compounds excludes the possibility to relate the triterpene derivatives to their possible biochemical precursors. Only triterpene methyl ethers were identified (Jacob et al., 2005).

3.4. Evolution through the core

In order to interpret the changes in evolution of triterpene derivatives along the studied sedimentary record, we compare it with the evolution of Rock-Eval parameters and δD values of triacontanic (n -C₃₀) acid that are interpreted in terms of variations of humidity.

3.4.1. Rock-Eval

Rock-Eval results are displayed in Fig. 6. A detailed description of Rock-Eval results was published in Jacob et al. (2004a). Total Organic Carbon (TOC) values are lower than 5% between 6 m and ca. 3 m depth before increasing up to ca. 15% at 2 m, then decreasing and remaining around 10% in the first meter. HI values range between 200 and 500 mg HC/g TOC in the lower half of the core and around 150 mg HC/g TOC in the upper half. Mineral inorganic carbon values (MinC) are very low in the lower half of the core. They are around 1% upcore except for a single interval where values reaching 3% attest to the presence of siderite. TpS2 is the temperature of maximum release of hydrocarbonaceous compounds during pyrolysis, as opposed to the Tmax, the well-known maturity indicator, which is 30–40 °C lower than TpS2. TpS2 values are higher than 450 °C in the lower half of the core

except for single intervals characterized by values lower than 400 °C. In the upper half of the core TpS2 values vary between 450 °C and 430 °C in the 2.9–2 m interval before remaining stable around 450 °C upcore.

3.4.2. δD values of triacontanic acid

The results concerning hydrogen isotope measurements on individual fatty acids have been published elsewhere (Jacob, 2004). δD values of triacontanic acid average -120‰ in the lower half of the core and decrease abruptly at 2.9 m down to values averaging -160‰ . A single event between 2.4 and 1.9 m is characterized by slightly higher values (i.e. up to -140‰).

3.4.3. Triterpene derivatives

The distribution of des-A-lupane does not appear to be related to that of the other des-A-triterpenes (Fig. 5). In order to depict the distinct evolution of these compounds, we report the evolution of the des-A-lupane over des-A-triterpenes ratio in Fig. 6.

The abundance of des-A-triterpenes is moderate in the lower half of the core. It increases sharply from 2.4 m, to reach a maximum around 2.2 m. Then it decreases down to 2 m and before remaining at very low levels. The des-A-lupane over des-A-triterpenes ratio does not show much change except in the lower quarter of the core where it exhibits much lower values. Aromatic derivatives show intermediate relative abundance from 6 to 4.2 m. Then, and up to 2.3 m, these compounds are negligible in the sediment. Their abundance increases suddenly to

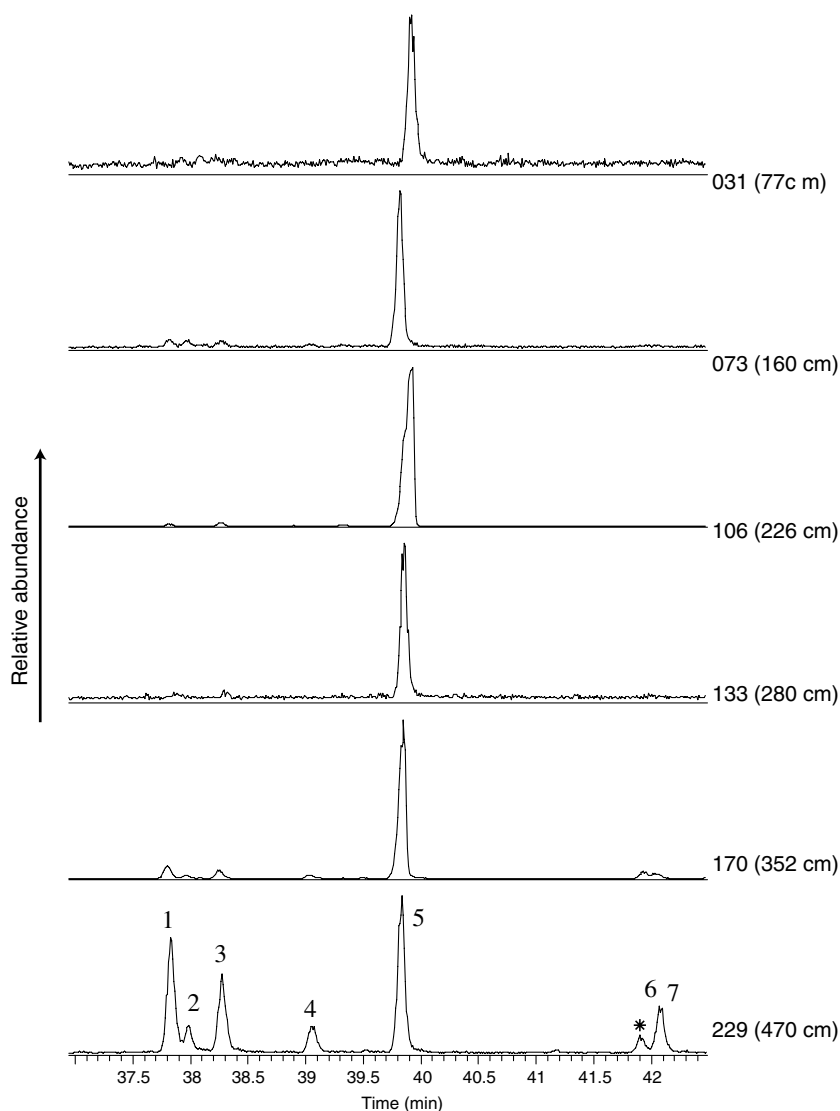


Fig. 5. Evolution of the distribution of des-A-triterpenes illustrated on the m/z 163 + 177 + 189 + 203 + 218 mass chromatograms in selected samples from core MA-98-3.

reach a maximum value at 2 m before decreasing towards the top of the core.

4. Discussion

4.1. Organic sedimentation and paleoclimatic changes

The Pleistocene sand dunes and the laterites that are the only outcropping geological formations in the region exclude any possibility of contamination of Lake Caçó sediments by fossil organic matter (OM). The lacustrine sedimentary infill has been

divided into 5 units according to lithofacies, organic petrography and Rock-Eval parameters (Fig. 6; Jacob et al., 2004a). The lowest unit (U1) consists of fine grained sands of the Pleistocene substratum that will not be discussed further. Unit 2 presents rather low contents of OM (TOC < 5%) but consisting of exceptionally well preserved higher plant debris. The high preservation of this material is in particular depicted by low TpS2 values attributable to the presence of fresh biopolymers in the samples (Disnar et al., 2003). This remarkable OM preservation is thought to result

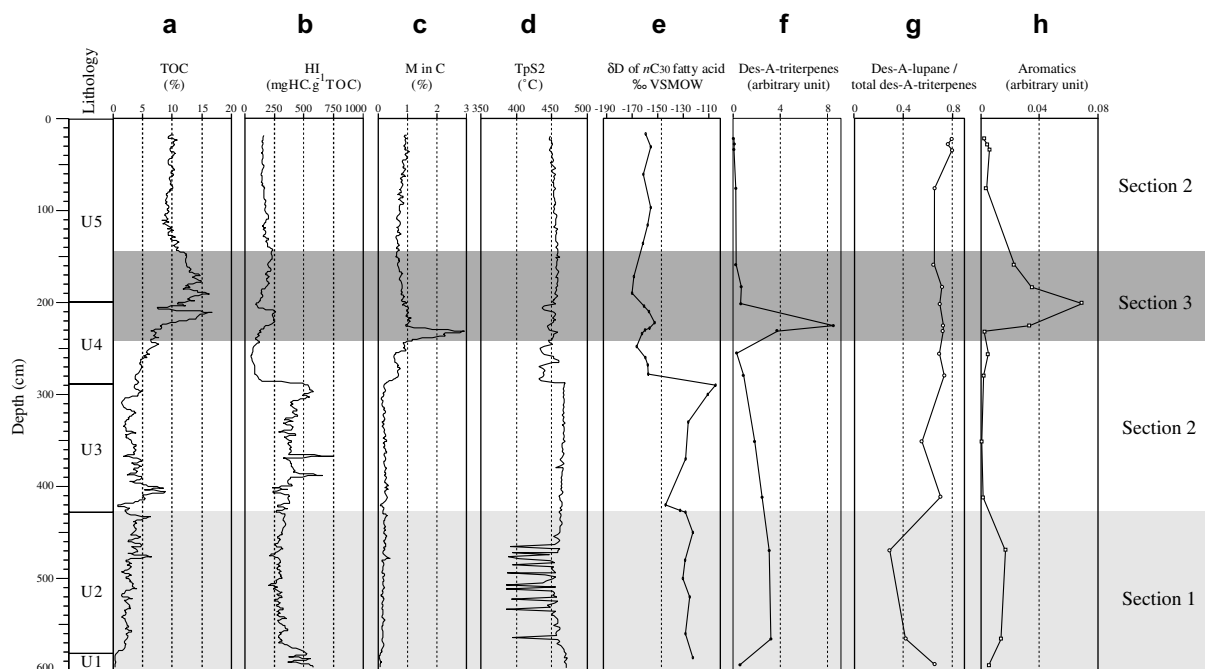


Fig. 6. Evolution of the abundance of des-A-triterpenes and aromatic derivatives of triterpenes as compared to Rock-Eval parameters along core MA-98-3: (a) total organic carbon (TOC; %), (b) hydrogen index (HI; mgHC/g TOC), (c) mineral inorganic carbon (MINC; %), (d) true temperature of maximum release of hydrocarbonaceous compounds during pyrolysis (TpS2; °C), (e) evolution of the δD values of the triacontanic acid through the core (Jacob, 2004), (f) relative abundance of des-A-triterpenes (arbitrary units), (g) relative abundance of des-A-lupane as compared to other des-A-triterpenes (arbitrary units) and (h) Relative abundance of aromatic derivatives of triterpenes (arbitrary units).

from the rapid burial of higher plant detritus by episodic but strong mineral inputs in an ephemeral lake (Jacob et al., 2004a). At this time, soils developing on the sand dunes were poorly vegetated due to a harsh climate with a long dry season as depicted by the high δD values of the triacontanic acid (Fig. 6e; Jacob, 2004). Sparse vegetation developed in wet hollows. During the short rainy season, sand that was mobilized by heavy showers allowed the burial of OM in these hollows. During unit U3 deposition the climate was slightly more humid than during the previous period. There were still erosive rainfalls but soils were more developed and there was a denser plant cover. The U3–U4 transition marks a drastic change in environmental conditions as depicted by a sudden decrease in HI values, a change in lithology from silts to clays and a sharp decrease in δD values of the triacontanic acid (Fig. 6). These changes are attributed to an increase in the precipitation regime especially with a longer rainy season (Jacob, 2004). These rather humid conditions allowed forest develop-

ment around the lake (Ledru et al., 2001) that became perennial with a notable water level. Nevertheless, the lake waters were well oxygenated as a result of a strong mixing by the westerlies. A belt of *Eleocharis* sp. (spike-rush) that developed on the lake border hindered any mineral and organic input from the watershed. The sedimentary OM, which was still mainly derived from higher plants, was highly degraded as a result of a rather long stay in oxygenated waters and a very slow burial consequential to low inorganic input (Jacob et al., 2004a). Despite these conditions unfavourable to OM preservation, but thanks to very low allochthonous (watershed) and autochthonous (e.g. diatom frustules) inorganic inputs, samples from U4 and U5 present high TOC values, reaching up to 15%. At ca. 2.2 m depth, the presence of siderite attests to the development of more reducing conditions during diagenesis. It is followed by a dry episode coincident with the Younger Dryas as attested by slightly higher values for the δD values of the triacontanic acid between 2.4 and 1.8 m.

The OM preserved in the sediments is hence essentially derived from terrestrial plants that suffered distinct environmental and diagenetic histories along the record. These highly contrasted conditions during sedimentation and early diagenesis are also depicted by triterpene derivative distributions.

4.2. Diagenesis of higher-plant triterpenes

Transformation processes initiating the early diagenesis of higher plant pentacyclic triterpenes are thought to begin during leaf senescence (Corbet, 1980; Trendel, 1985; Lohmann, 1988, and references therein), possibly thanks to microbial and/or photochemical mediation (Corbet, 1980). The main degradation routes have already been summarized by various authors (Carruthers and Watkins, 1964; Jarolim et al., 1965; Chaffee and Fookes, 1988; Trendel et al., 1989; Wolff et al., 1989; Stout, 1992; Rullkötter et al., 1994). Basically, the first step in higher plant pentacyclic triterpene degradation is the loss of the oxygenated function at C(3) position from unsaturated compounds such as α and β -amyrins. This leads to the corresponding di-unsaturated counterparts such as ursadiene and oleanadiene (ten Haven et al., 1992). After this primary transformation, various pathways lead to (i) the formation of Δ^2 triterpenes, $\Delta^{2,x}$ triterpadienes or ring A contracted triterpenes (Elgamal et al., 1969; Ekweozor et al., 1979; ten Haven et al., 1992); (ii) the progressive aromatisation of the skeleton from ring A to finally produce fully aromatised pentacyclic moieties (LaFlamme and Hites, 1978; Wakeham et al., 1980; Wolff et al., 1989); (iii) the loss of ring A (des-A-compounds), followed by the progressive aromatisation towards ring E (Corbet, 1980; Trendel et al., 1989). The loss of ring A is initiated by its opening leading to the formation of A-seco-intermediates, a phenomenon that readily occurs in plant leaves under photochemical/photomimetic control (Corbet, 1980).

4.3. Triterpene fingerprint

The various triterpene derivatives detected in the sediments of Lake Caçó are listed in Table 1 together with their main mass spectral data. Their variety highlights the large contribution of higher plant OM to the sediments. This is fully consistent the wide diversity of triterpenes already reported in previous studies (onocerane: Jacob et al., 2004b;

“PTME”: Jacob et al., 2005). If one excludes onocerane and some hopanoids, the only triterpenes found in the non-aromatic fractions of Lake Caçó sediments are des-A derivatives. Nor saturated tetra- or pentacyclic triterpane, neither Δ^2 triterpenes or $\Delta^{2,x}$ triterpadienes were found in the sample extracts. In contrast to unsaturated and fully saturated compounds which require several reaction steps to be formed from a parent triterpenoid, the corresponding triterpadiene only requires the loss of the alcohol functional group. Thus, the absence of such compounds is explained by the fact that these olefinic compounds only acted as transitory intermediates in the degradation of original triterpenes into aromatics and/or des-A-triterpenes, depending on medium conditions. For triterpenes, another reaction pathway would be the direct elimination of the oxygenated function of natural triterpenes together with their double bond. Such reactions would require much more reducing conditions than those which developed in Lake Caçó sediments. Finally, the absence of triterpenes and of their mono- and di-unsaturated counterparts is consistent with the conclusions from Spyckerelle (1975) who proposed that, in contrast to hopanoids, the early diagenetic transformation of higher plant triterpenes preferentially leads to aromatics or des-A-triterpenes rather than to unsaturated or saturated pentacyclic compounds.

Surprisingly, the fingerprints of aromatic derivatives in samples taken at 1.6 and 4.7 m depth globally resemble those described by Stout (1992) and Hazai et al. (1986) for a lignite and a sub-bituminous coal, respectively. They comprise a series of monoaromatic pentacyclic compounds with various structures and degrees of unsaturation, a series of pentacyclic triaromatics and a series interpreted as diaromatic derivatives of tetracyclic triterpenes. Concerning these latter ones, Stout (1992) and Hazai et al. (1986) also detected compounds the mass spectra of which displayed a m/z 195 ion as dominant peak. We here propose a first tentative identification of this series of compounds as diaromatic tetracyclic triterpenes of the lanostane/euphane series. This tentative identification is substantiated by the presence, in the considered samples, firstly of a methyl ether having such a structure (Jacob et al., 2005), and secondly, by the presence of a ketone and an alcohol derivative in more polar fractions (unpublished results). No ring A, B diaromatic triterpene derivative, fully aromatised triterpene or aromatic derivative of

des-A-triterpene was detected in the studied aromatic fractions. The absence of ring A, B diaromatic derivatives could be explained by the pre-existence of one or two double bonds on the rings C or D of molecular precursors (β - and α -amyrin). As suggested by Lohmann (1988), little additional energy is necessary to aromatise ring C following rings A and B when one or two double bonds already exist in ring C. This explains the sole occurrence of mono- and triaromatic derivatives of pentacyclic triterpenes. Such an absence of A-B diaromatic derivatives of pentacyclic triterpenes was also noted by Stout (1992) who also did not detect any aromatic derivative of des-A-triterpene in the Brandon lignite. The co-occurrence of des-A-triterpenes and mono- and triaromatic derivatives of triterpenes in our samples, without any des-A-triterpene aromatic derivative, indicates that the aromatisation of des-A-triterpenes was hindered or that adventitious aromatic des-A-triterpenes were rapidly degraded once formed. The aromatisation of triterpene biomolecules is unlikely to occur in oxygenated waters (Jaffé et al., 1995). Therefore, this phenomenon most probably occurred before functionalized triterpenes entered the water column and the sediment. Finally, no fully aromatised triterpene was found in the selected samples. This highlights that more drastic diagenetic conditions or longer times (Jaffé and Hausmann, 1995) are required to further aromatise the precursor compounds. In summary, the coexistence of des-A-triterpenes and triterpene derivatives with various degrees of unsaturation/aromatization substantiates the possibility that there were distinct pools of triterpene precursors and/or that there are different diagenetic pathways in the studied system (i.e. lake surroundings plus water column and sediment) throughout the lake history.

4.4. Evolution of triterpene derivatives fingerprint along the sedimentary record

As shown in Fig. 6, the distribution of triterpene derivatives (des-A-triterpenes on one hand and aromatic derivatives on the other hand) in the sedimentary record allows us to distinguish three sections differing in the abundance and/or the nature of such compounds. Section 1 coincides with unit U2. Section 2 corresponds to U3, the base of U4 and the uppermost recent part of the series that belong to U5. Section 3 extends from ca. 2.4 m up to 0.6 m depth.

4.4.1. Section 1

The samples from this section reveal a great diversity of triterpene derivatives: monounsaturated and saturated des-A-triterpenes (des-A-lupane and compound 7), mono and triaromatic derivatives of pentacyclic triterpenes and diaromatic derivatives of tetracyclic triterpenes. Such compound distributions are very comparable to those described in previous studies, especially on brown coals and lignite (Hazai et al., 1986; Stout, 1992) and are also consistent with the conditions of OM deposition and diagenesis of the considered section, at the end of the Last Glacial Maximum (ca. 18,000 yrs cal BP). Fresh higher plant debris was rapidly buried by sands mobilized from the denuded substratum during rare but abundant tropical rainfalls (Jacob et al., 2004a). These distributions are also fully consistent with the well-accepted ideas on triterpenes diagenesis: (i) a very early transformation of original triterpenes that can steadily occur in senescent leaves and thus does not require extensive diagenesis; and (ii) two main diagenetic pathways that prevail under dysoxic conditions and lead either to des-A-triterpenes or to mono- and triaromatic derivatives of triterpenes.

The alternation of a long dry season and a short rainy season during which the ephemeral lake developed (Jacob, 2004) could straightforwardly result in two distinct degradation modes of triterpene biomolecules: (i) firstly, the formation of aromatic derivatives during the dry season, in aerial conditions; and (ii) secondly, the production of des-A-triterpenes from their triterpene precursors in sub-aquatic conditions during the rainy season. This latter conclusion is in agreement with the assumptions of Trendel (1985) who remarked that the formation of des-A-triterpenes is favoured in soils or sediments that are at least temporarily submerged.

4.4.2. Section 2

In contrast to Section 4.4.1, des-A-lupane is by far the dominant triterpene derivative in Section 4.4.2 (Fig. 5). There, des-A-lupane can represent up to 80% of the total amount of des-A-triterpenes (Fig. 6g). Other des-A-triterpenes with oleanane, ursane or arborane structures were only found in low amounts around 2 m depth (see paragraph 5.4.1.). In addition, there are very few or even no aromatic derivatives in this Section 4.4.2 (Fig. 6h). Such a low molecular diversity and the high predominance of des-A-lupane can be interpreted as resulting from (i) a higher sensitivity of

other des-A-triterpenes than des-A-lupane and aromatic derivatives to degradation into the lake water column and sediment; (ii) environmental changes leading to changing sources (vegetation) and transportation modalities. The near uniqueness of des-A-lupane in the specified samples can result from its preferential formation or peculiar resistance to diagenetic transformations. In contrast to the most common higher plant pentacyclic triterpenes (α - and β -amyrins for example), biomolecules with a lupane structure often own an external double bond on the isopropyl group. Under favourable conditions the external location of this double bond would favour its reduction rather than the initiation of aromatisation that is facilitated in the presence of an internal double bond (in Δ^{12} position for example in α - and β -amyrins). In addition, des-A-lupane is relatively stable to diagenesis. Therefore, the exclusiveness of des-A-lupane in Section 4.4.2 could indicate harsh diagenesis whereas its co-occurrence with other des-A-triterpenes in Section 4.4.1 and at ca. 2 m depth (Fig. 5) would result from better preservation conditions. However, this hypothesis is somewhat weakened by a closer study of Section 4.4.2. The sharp decrease in HI values recorded at ca. 2.9 m (i.e. U3/U4 transition) attests to a marked change in OM preservation conditions that is not recorded by triterpene fingerprints. Therefore, diagenetic conditions cannot solely be invoked for the distributions of triterpene derivatives in the considered section. Alternatively, the upcore strong predominance of des-A-lupane could be related to specific environmental conditions. Presently, the belt of *Eleocharis* sp. (from 1 to 3 m depth; Fig. 7a) practically prevents any organic input from the watershed. In addition, the relatively high productivity in the protected medium that constitutes this belt, leads to more reducing conditions than in the open basin (under oligotrophic conditions). We did not determine the triterpenes of *Eleocharis* sp. However, previous investigations showed that the pentacyclic triterpenes synthesized by this species are of the lupane type, namely betulinic acid, betulin and lup-20(29)-en-3 β ,16 β -diol, with minor contributions from neohop-13(18)-en-3 α -ol and fern-9(11)-en-3 α -ol (Miles et al., 1994; Amaral et al., 2004). Similarly, geochemical investigations of surficial sediments from a marsh covered with *Eleocharis* sp. and developing within a mangrove system did not show any pentacyclic triterpene but lupeol (Koch et al., 2003). Accordingly, it can be hypoth-

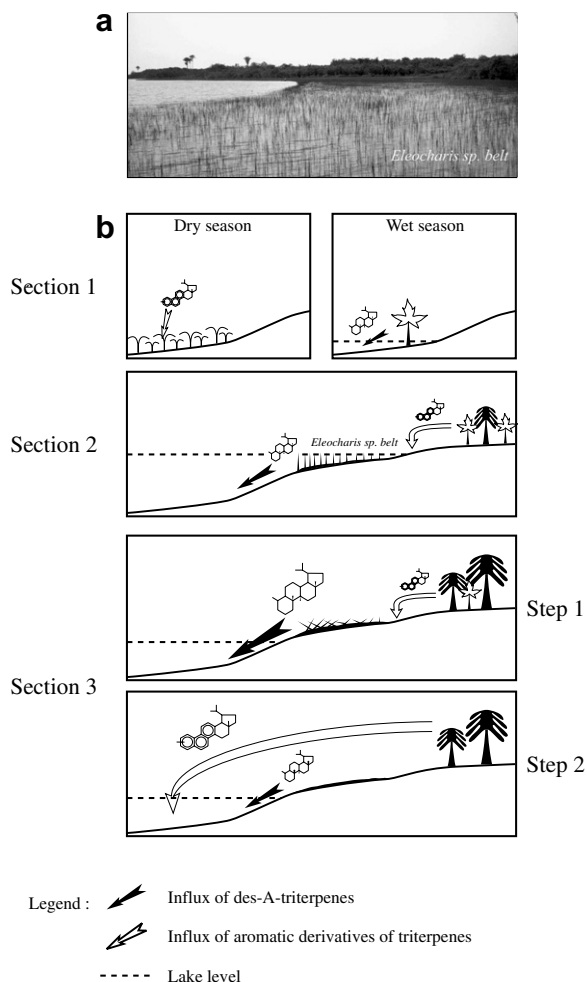


Fig. 7. (a) Picture of the lake margins illustrating the development of a belt of *Eleocharis* sp. (spike-rush) around the lake, between 1 and 3 m depth; (b) schematic scenario of the paleoenvironmental changes that occurred around Lake Caçó during the last 20,000 yrs explaining the evolution of triterpene derivative fingerprint in the sediments.

esized that des-A-lupane could originate from lupane-type precursors synthesized by *Eleocharis* sp., whereas other triterpenes are subordinates. The sub-aerial and reducing conditions that prevailed within the *Eleocharis* sp. belt could favour the transformation of lupane-type precursors into des-A-lupane, again in agreement with the observations of Trendel (1985). Then, des-A-lupane would be exported to the open basin to be buried with no or only limited degradation. As previously assumed in paragraph 4.4.2., aromatisation processes do not occur in the water column or even in the sediment. Therefore, aromatic derivatives must have been

produced in the watershed, before reaching the lake. For sediments belonging to Section 4.4.2, such compounds were most probably filtered by the *Eleocharis* sp. belt as were non lupane-type des-A-triterpenes. Altogether, the predominance of des-A-lupane over other triterpene derivatives in Section 4.4.2 could attest to the settling of the *Eleocharis* sp. belt around the lake, first during the deposition of the sediments that are presently found at ca. 4.5 m depth, and, secondly, in recent times.

4.4.3. Section 3

The short episode depicted by high amounts of des-A-lupane between 2.3 and 3 m (Fig. 6f) is interpreted as resulting from the destruction of the *Eleocharis* sp. belt, entailing a strong influx of *Eleocharis* sp.-derived material (and especially des-A-lupane) to the sediment. Subsequently, the disappearance of this barrier also allowed the strong discharge of aromatic derivatives to the sediment (Fig. 6g). The destruction of the *Eleocharis* sp. belt was probably favoured by a lowering of the lake level as a consequence of dry conditions illustrated by rather high δD values of the triacontanic acid, during this episode.

4.5. Palaeoenvironmental scenario

The scenario leading to the distinct triterpene derivative fingerprints detected in the sedimentary record is summarized in Fig. 7. In Section 1, the degradation of triterpene biomolecules occurred under reducing conditions due to rapid burial. During the short wet season, the development of an ephemeral lake with a low water level, allowed the (sub-) aquatic degradation of triterpene biomolecules into des-A derivatives. More seasonal precipitation during the deposition of Section 2 sediments was responsible for the development of lacustrine conditions and of a belt of *Eleocharis* sp. This belt was the site of production of the precursor(s) of the des-A-lupane that was exported to the sediment. The *Eleocharis* sp. belt also hindered the input of organic products from the catchment. During the deposition of Section 3, more arid conditions (due to longer dry seasons) provoked a lowering of the lake level. Then, the destabilization of the *Eleocharis* sp. belt allowed the exportation towards the centre of the lake of the OM that had accumulated within the belt, with a notable contribution of des-A-lupane (Step 1). The OM that had accumulated

in more or less reducing micro-environments within the watershed, and/or that could not have reached the lake because of the presence of the *Eleocharis* sp. belt, was also partly leached and transported to the sediment (Step 2). When the *Eleocharis* sp. belt built up again under more stable climatic conditions (Section 2 in upper most levels of the core), detrital material from the watershed with associated aromatic derivatives could not anymore reach the basin. Then, only the OM produced within the *Eleocharis* sp. and the associated des-A-lupane could contribute to the sediment.

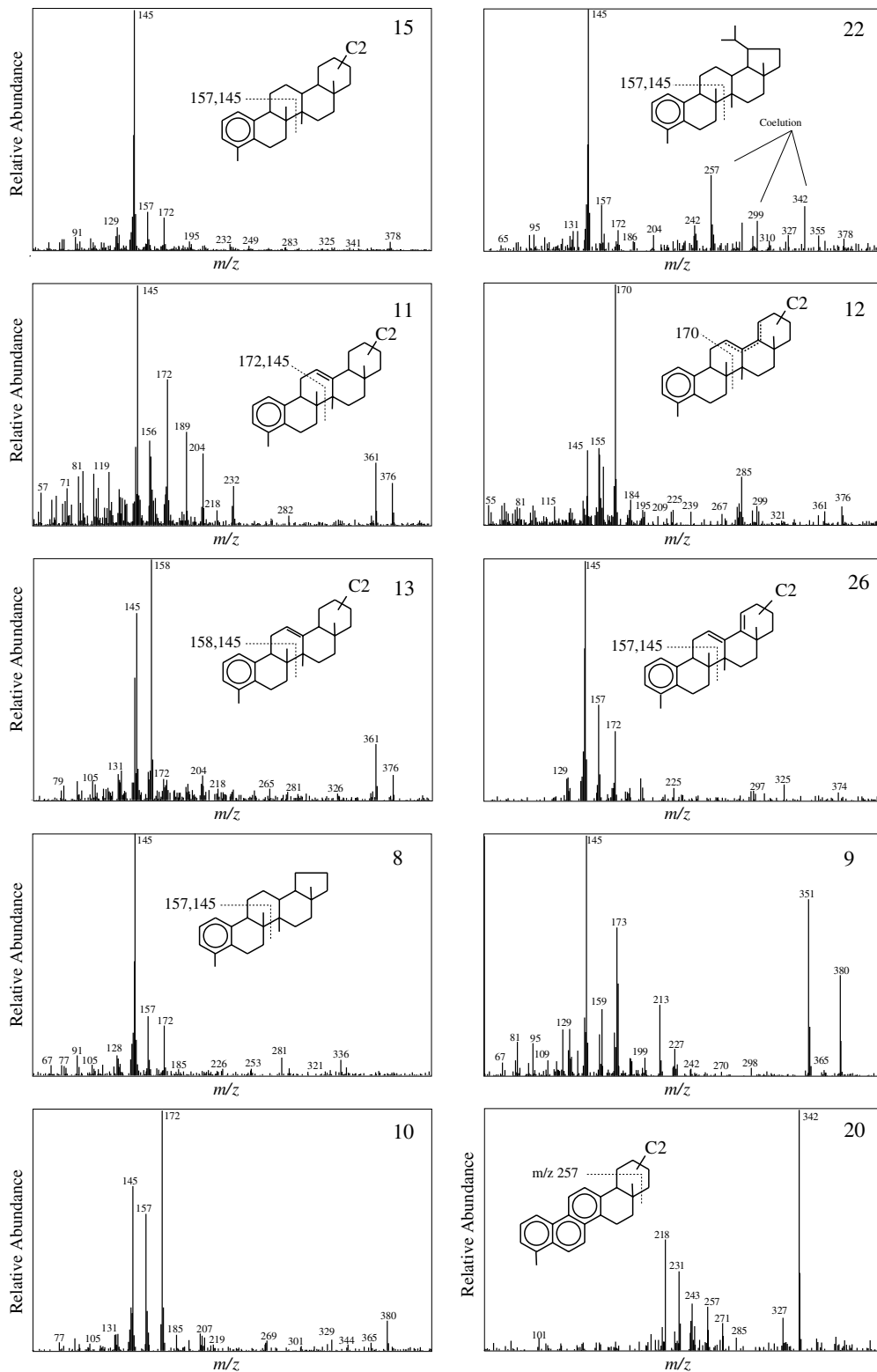
5. Conclusions

The detection of various by-products of biological triterpenes (des-A-triterpenes and aromatic derivatives of triterpenes) and their screening in the hydrocarbon extracts of sediments pertaining to a 6 m long core, allowed us to gain insight into the origin and the dynamics of these compounds depending on environmental conditions. Presumably, des-A-triterpenes and aromatic derivatives of triterpenes were both produced in anoxic or at least dysaerobic environments. Nevertheless, the respective dynamics of these two groups of compounds depends on distinct early diagenetic transformation pathways that probably occurred within distinct (micro-) environments. Although this hypothesis would require further investigations, the relative abundance of des-A-triterpenes and aromatic derivatives of pentacyclic triterpenes could provide an index of the degree of hydromorphism of the ecosystems where the sedimentary OM was produced, within the watershed of lacustrine systems. We also tentatively identified a new class of compounds that would result from the aromatisation of higher plant tetracyclic triterpenes with euphane/lanostane basic structures.

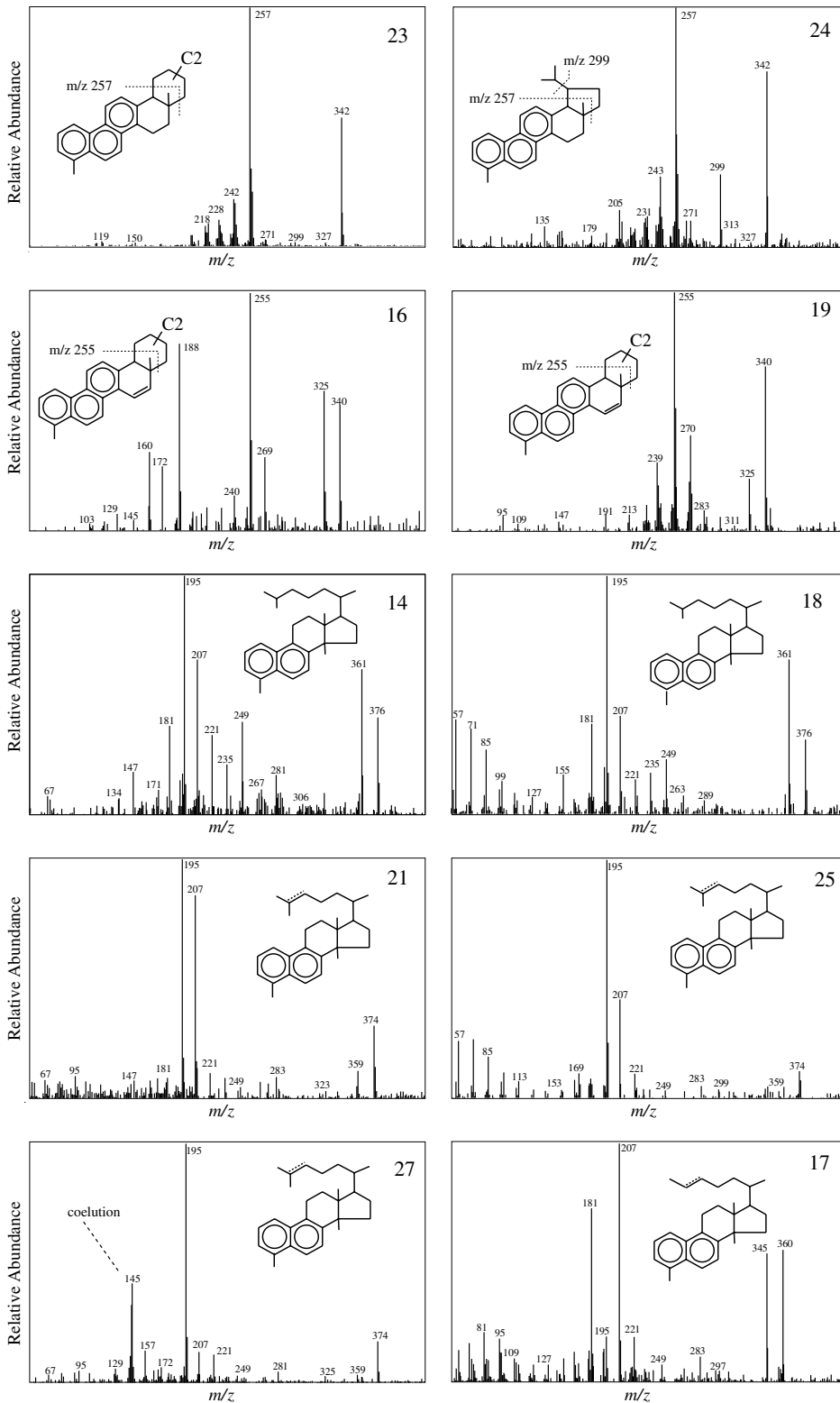
Acknowledgements

This research has been supported by an IRD (France)-CNPq (Brasil) convention and an ISTO (UMR 6113 du CNRS, France)-IRD cooperation. One of us (J.J.) received financial support from the Conseil Régional du Centre. The authors wish to thank Pr. J.K. de Leeuw, Pr. J. Rullkötter, Dr. P. Schaeffer and two anonymous reviewers for their constructive remarks on a previous version of the manuscript.

Appendix 1



Appendix 2



Associate Editor—Philippe Schaeffer

References

- van Aarssen, B.G.K., Alexander, R., Kagi, R.I., 2000. Higher plant biomarkers reflect palaeovegetation changes during Jurassic times. *Geochimica et Cosmochimica Acta* 64, 1417–1424.
- Amaral, M.C.E., Faria, A.D., Magalhães, A.F., Magalhães, E.G., Ruiz, A.L.T.G., 2004. Steroids and triterpenes from *Eleocharis acutangula* and *E. sellowiana* (Cyperaceae). *Phytochemical Analysis* 15, 125–129.
- Budzikiewicz, H., Wilson, J.M., Djerassi, C., 1962. Mass spectrometry in structural and stereochemical problems. XXXII. Pentacyclic triterpenes. *Journal of the American Chemical Society* 85, 3688–3699.
- Carruthers, W., Watkins, D.A.M., 1964. The constituents of high-boiling petroleum distillates. VIII. Identification of 1,2,3,4-tetrahydro-2,2,9-trimethylpicene in an American crude oil. *Journal of the Chemical Society of London* 1964, 724–729.
- Chaffee, A.L., Fookes, C.J.R., 1988. Polycyclic aromatic hydrocarbons in Australian coals – III. Structural elucidation by proton nuclear magnetic resonance spectroscopy. *Organic Geochemistry* 12, 261–271.
- Chaffee, A.L., Strachan, M.G., Johns, R.B., 1984. Polycyclic aromatic hydrocarbons in Australian coals: novel tetracyclic components from Victorian brown coal. *Geochimica et Cosmochimica Acta* 48, 2037–2043.
- Corbet, B., 1980. Origine et transformation des triterpènes dans les sédiments récents. Ph.D. thesis, Université Louis Pasteur, Strasbourg, France, 106 p.
- Cranwell, P.A., 1984. Organic geochemistry of lacustrine sediments: triterpenoids of higher plant origin reflecting post-glacial vegetational succession. In: Haworth, E.Y., Lund, J.W.G. (Eds.), *Lake Sediments and Environmental History*. University Press, Leicester, pp. 69–92.
- Das, M.C., Mahato, S.B., 1983. Triterpenoids. *Phytochemistry* 22, 1071–1095.
- Disnar, J.R., Guillet, B., Kéravis, D., Di-Giovanni, C., Sebag, D., 2003. Soil organic matter (SOM) characterisation by Rock-Eval pyrolysis: scope and limitations. *Organic Geochemistry* 34, 327–343.
- Djerassi, C., Budzikiewicz, H., Wilson, J.M., 1962. Mass spectrometry in structural and stereochemical problems. Unsaturated pentacyclic triterpenoids. *Tetrahedron Letters*, 263–270.
- Ekweozor, C.M., Okogun, J.I., Ekong, D.E.U., Maxwell, J.R., 1979. Preliminary organic geochemical studies of samples from the Niger Delta (Nigeria). II. Analyses of shale for triterpenoid derivatives. *Chemical Geology* 27, 29–37.
- Elgamal, M.H.A., Fayez, M.B.E., Kemp, T.R., 1969. The mass spectra of some triterpenoid dehydration products. *Organic Mass Spectrometry* 2, 175–194.
- Hauke, V., 1994. Reconstruction de paléoenvironnements de dépôts en séries sédimentaires: étude au moyen de marqueurs biologiques. Ph.D. thesis, Université Louis Pasteur, Strasbourg, France, 252 p.
- ten Haven, H.L., Rullkötter, J., 1988. The diagenetic fate of taraxer-14-ene and oleanene isomers. *Geochimica et Cosmochimica Acta* 52, 2543–2548.
- ten Haven, H.L., Peakman, T.M., Rullkötter, J., 1991. Δ^2 -triterpenes: early intermediates in the diagenesis of terrigenous triterpenoids. *Geochimica et Cosmochimica Acta* 56, 1993–2000.
- ten Haven, H.L., Rullkötter, J., Stein, R., 1992. Preliminary analysis of extractable lipids in sediments from the eastern North Atlantic (Leg 108): Comparison of a coastal upwelling area (Site 658) with a non upwelling area (Site 659). *Proceedings of the Ocean Drilling Project Scientific Results* 108, 351–360.
- Hazai, I., Alexander, G., Szekely, T., Essing, B., Radek, D., 1986. Investigations of hydrocarbons constituents of a young sub-bituminous coal by gas chromatography–mass spectrometry. *Journal of Chromatography* 367, 117–133.
- Jacob, J., 2003. Enregistrement des variations paléoenvironnementales depuis 20000 ans dans le Nord Est du Brésil (Lac Caçó) par les triterpènes et autres marqueurs organiques. Ph.D. thesis, Université d'Orléans, France, 296 p.
- Jacob, J., 2004. Water balance over the last 20,000 yrs in Northeastern Brazil. Insights from the δD variations of fatty acids from a lacustrine series (Lagoa do Caçó). *EAOG Newsletter* 18, 6–10.
- Jacob, J., Disnar, J.R., Boussafir, M., Sifeddine, A., Albuquerque, A.L.S., Turcq, B., 2004a. Major environmental changes recorded by lacustrine sedimentary organic matter since the Last Glacial Maximum under the tropics (Lake Caçó, NE Brazil). *Palaeogeography, Palaeoclimatology, Palaeoecology* 205, 183–197.
- Jacob, J., Disnar, J.R., Boussafir, M., Ledru, M.-P., Sifeddine, A., Albuquerque, A.L.S., Turcq, B., 2004b. Onocerane attests to dry climatic events during the Quaternary in the Tropics. *Organic Geochemistry* 35, 289–297.
- Jacob, J., Disnar, J.R., Boussafir, M., Sifeddine, A., Albuquerque, A.L.S., Turcq, B., 2005. Pentacyclic triterpene methyl ethers in recent lacustrine sediments (Lake Caçó, Brazil). *Organic Geochemistry* 36, 449–461.
- Jaffé, R., Hausmann, K.B., 1995. Origin and early diagenesis of arborinone/isoarborinol in sediments of a highly productive freshwater lake. *Organic Geochemistry* 22, 231–235.
- Jaffé, R., Wolf, G.A., Cabrera, A.C., Carvajal-Chitty, H.I., 1995. The biogeochemistry of lipids in rivers of the Orinoco Basin. *Geochimica et Cosmochimica Acta* 59, 4507–4522.
- Jarolim, V., Hejno, K., Hemmert, F., Sorm, F., 1965. Über die Zusammensetzung der Braunkohle, IX. Über einige aromatische Kohlenwasserstoffe des Harzanteils des Montanwachses. *Collection of Czechoslovak Chemical Communications* 30, 873–879.
- Killips, S.D., Raine, J.I., Woolhouse, A.D., Weston, R.J., 1995. Chemostratigraphic evidence of higher-plant evolution in the Taranaki Basin, New-Zealand. *Organic Geochemistry* 23, 429–445.
- Koch, B.P., Rullkötter, J., Lara, R.J., 2003. Evaluation of triterpenoids and sterols as organic matter biomarkers in a mangrove ecosystem in northern Brazil. *Wetlands Ecology and Management* 11, 257–263.
- LaFlamme, R.E., Hites, R.A., 1978. The global distribution of polycyclic aromatic hydrocarbons in recent sediments. *Geochimica et Cosmochimica Acta* 42, 289–303.
- Ledru, M.P., Cordeiro, R.C., Dominguez, J.M.L., Martin, L., Mourguiart, P., Sifeddine, A., Turcq, B., 2001. Late-glacial cooling in Amazonia as inferred from pollen at Lagoa do Caçó, northern Brazil. *Quaternary Research* 55, 47–56.
- Logan, G.A., Eglinton, G., 1994. Biogeochemistry of the Miocene lacustrine deposit, at Clarkia, northern Idaho, USA. *Organic Geochemistry* 21, 857–870.

- Lohmann, F., 1988. Aromatisations microbiennes de triterpènes végétaux. Ph.D. thesis, Université Louis Pasteur, Strasbourg, France.
- Loureiro, M.R.B., Cardoso, J.N., 1990. Aromatic hydrocarbons in the Paraíba Valley oil shale. *Organic Geochemistry* 15, 351–359.
- Mahato, S.B., Sen, S., 1997. Advances in triterpenoid research 1990–1994. *Phytochemistry* 44, 1185–1236.
- Mahato, S.B., Nandy, A.K., Roy, G., 1992. Triterpenoids. *Phytochemistry* 9, 2199–2249.
- Mahato, S.B., Sarkar, S.K., Poddar, S.G., 1988. Triterpenoid saponins. *Phytochemistry* 27, 3037–3067.
- Miles, D.H., Tunswan, K., Chittawong, V., Hedin, P.A., Kokpol, U., 1994. Boll weevil antifeedants from *Eleocharis dulcis* Trin. *Journal of Agricultural and Food Chemistry* 42, 1561–1562.
- Pant, P., Rastogi, R.P., 1979. The triterpenoids. *Phytochemistry* 18, 1095–1108.
- Philp, R.P., 1985. *Fossil Fuel Biomarkers. Applications and Spectra*. Elsevier, Amsterdam.
- Prartono, T., Wolff, G.A., 1998. Organic geochemistry of lacustrine sediments: a record of the changing trophic status of Rostherne Mere, UK. *Organic Geochemistry* 28, 729–747.
- Rullkötter, J., Peakman, T.M., ten Haven, H.L., 1994. Early diagenesis of terrigenous triterpenoids and its implications for petroleum geochemistry. *Organic Geochemistry* 21, 215–233.
- Shiojima, K., Arai, Y., Masuda, K., Takase, Y., Ageta, T., Ageta, H., 1992. Mass spectra of pentacyclic triterpenoids. *Chemical Pharmacology Bulletin* 40, 1683–1690.
- Spyckerelle, C., 1975. Constituants aromatiques de sédiments. Ph.D. thesis, Université Louis Pasteur, Strasbourg, France, 134 p.
- Stout, S., 1992. Aliphatic and aromatic triterpenoid hydrocarbons in a Tertiary angiospermous lignite. *Organic Geochemistry* 18, 51–66.
- Trendel, J., 1985. Dégénération des triterpènes dans les sédiments. Aspects photochimiques et microbiologiques. Ph.D. thesis, Université Louis Pasteur, Strasbourg, France, 126 p.
- Trendel, J.M., Lohmann, F., Kintzinger, J.P., Albrecht, P., Chiaroni, A., Riche, C., Cesario, M., Guilhem, J., Pascard, C., 1989. Identification of des-A-triterpenoid hydrocarbons occurring in surface sediments. *Tetrahedron* 45, 4457–4470.
- Wakeham, S.G., Schaffner, C., Giger, W., 1980. Polycyclic aromatic hydrocarbons in recent lake sediments – II. Compounds derived from biogenic precursors during early diagenesis. *Geochimica et Cosmochimica Acta* 44, 415–429.
- Wolff, G.A., Trendel, J.M., Albrecht, P., 1989. Novel monoaromatic triterpenoid hydrocarbons occurring in sediments. *Tetrahedron* 45, 6721–6728.
- Woolhouse, A.D., Oung, J.-N., Philp, R.P., Weston, R.J., 1992. Triterpanes and ring-A triterpanes as biomarkers characteristic of tertiary oils derived from predominantly higher plant sources. *Organic Geochemistry* 18, 23–31.



Paleohydrological changes during the last deglaciation in Northern Brazil

Jérémy Jacob^{a,b,*}, Yongsong Huang^a, Jean-Robert Disnar^b, Abdelfettah Sifeddine^c, Mohammed Boussafir^b, Ana Luiza Spadano Albuquerque^d, Bruno Turcq^{c,d}

^aDepartment of Geological Sciences, Brown University, Providence, RI 02912, USA

^bInstitut des Sciences de la Terre d'Orléans - UMR 6113 du CNRS - Université d'Orléans, Bâtiment Géosciences, 45067 Orléans Cedex 2, France

^cIRD/Bondy, 32 Avenue Henry Varagnat, 93143 Bondy Cedex, France

^dDepartamento de Geoquímica, Universidade Federal Fluminense, Morro do Valonguinho s/n, 24020-007 Niterói, RJ, Brazil

Received 13 April 2006; received in revised form 19 September 2006; accepted 5 December 2006

Abstract

We here report a reconstruction of hydrological balance variations in Northern Brazil for the last 20 ka deduced from the δD values of aquatic and land plant molecules extracted from the sediment infill of Lake Caçó. Our reconstructed precipitation, lake water isotope ratio and evaporation–evapotranspiration isotope effect allows us to obtain an estimate of moisture balance, and, to a lesser extent, precipitation amount and seasonality changes. During the end of the Last Glacial Maximum (LGM, between ca 20 and 17.3 ka), high δD values and smaller fractionation of leaf waxes indicate an arid to semi-arid climate with a long lasting dry season. An abrupt change towards much wetter conditions occurred within ca 500 years from 17.3 to 16.8 ka, as shown by a 50% decrease in D/H ratios and a marked increase in H isotopic fractionation of leaf waxes. This abrupt isotopic change coincides with a major transformation from savanna-dominated vegetation to humid rain forest around the lake, based on pollen data. Comparisons with other paleo-precipitation records from South American sites indicate that Lateglacial humid conditions were controlled by intensification of the ITCZ and/or a southward shift of its mean position across our study site. Our isotope data show only a small rise in aridity during Younger Dryas event (13–11.5 ka). Although the Holocene was not screened in details, D/H ratios of terrestrial and aquatic compounds show near constant offsets, suggesting stable and relatively humid climate conditions during this period.

© 2007 Elsevier Ltd. All rights reserved.

1. Introduction

The tropics are key areas for past and present climate dynamics because this region is the main heat engine and water vapour source of the Earth. Recent studies indicate that past variations in the water vapour cycle over tropical South America are closely related to oceanic and atmospheric circulation patterns at global scale (Peterson et al., 2000; Wang et al., 2004; Cruz et al., 2005). Nonetheless, there is not yet a clear consensus on the role of the tropics in driving global climate variability and on the possible

extratropical feedbacks (Stoecker et al., 2003). An important atmospheric system that controls the tropical climate variations is the InterTropical Convergence Zone (ITCZ). Previous studies have indicated that the mean positioning of the ITCZ has shifted significantly on seasonal, decadal and longer timescales (Martin et al., 1997; Ronchail et al., 2002; Wang et al., 2004). In order to track past ITCZ shifts and changes in intensity, we have explored the sedimentary infill of Lake Caçó. This lake is located in Northern Brazil, on the eastern edge of Amazon rain forest, where the ITCZ shifts from its winter to summer position (Fig. 1). It is therefore highly sensitive to mean positioning of the ITCZ.

There are major controversies remaining on the occurrence of wet/dry episodes in South America and their impacts on continental ecosystems, biological diversity and biogeochemical cycling (CH_4 , CO_2 and H_2O). For example,

*Corresponding author. Institut des Sciences de la Terre d'Orléans, UMR 6113 du CNRS - Université d'Orléans, Bâtiment Géosciences, 45067 Orléans Cedex 2, France.

E-mail addresses: jeremy.jacob@univ-orleans.fr (J. Jacob), jeremy.jacob@univ-orleans.fr (J.-R. Disnar).

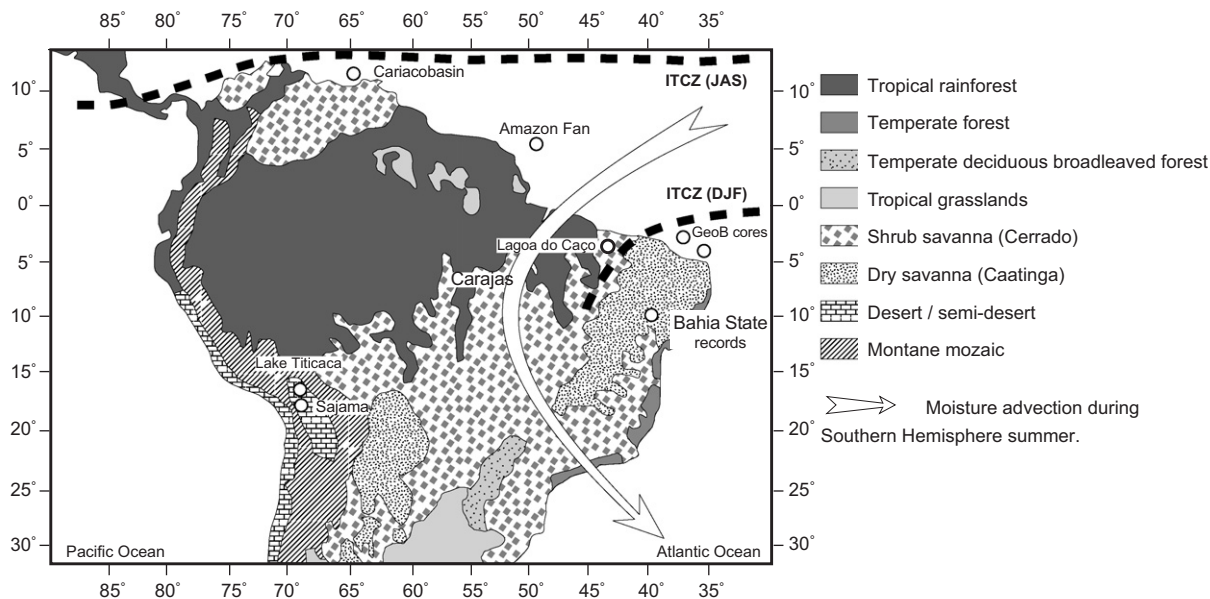


Fig. 1. Location of Lake Caçó site within the context of present day potential vegetation types encountered in Northern Brazil. Open circles indicate the sites discussed in the text. The Lake Caçó lies in a shrub savanna (cerrado) corridor inserted between the dry savanna (caatinga) to the east and the humid rainforest to the west. The Present day positions of the InterTropical Convergence Zone (ITCZ) during the austral summer (DJF) and austral winter (JAS) are depicted with a dotted black line. The trajectory of moisture advection during austral summer is illustrated with a white arrow.

a globally drier climate is suspected for the LGM. The extent to which this supposedly dry episode impacted the Amazon rainforest surface is strongly debated (Colinvaux et al., 2000; Turcq et al., 2002). Similar to the LGM, the tropical extension and influence of the Younger Dryas (YD) cold reversal, as defined in the Northern Hemisphere, is not fully elucidated in the South American tropics.

Most of these controversies arise from the lack of pertinent parameters allowing the quantitative estimate of humidity changes. For instance, broadly defined pollen classes include several taxa that can colonize various habitats. Furthermore, pollen data are interpreted as changes in vegetation distribution that are affected by atmospheric $p\text{CO}_2$, temperature, humidity and soil properties, thus avoiding any quantitative reconstruction. Similarly, marine sedimentary cores record regional conditions inland and buffer spatial discrepancies.

In order to address the question of humidity variations in Southern America since the last deglaciation, we apply for the first time in the South American tropics the combination of hydrogen isotopic composition (δD)¹ of aquatic and land plant molecules preserved in lake sediments. As it has recently been shown, the δD values of sedimentary palmitic ($n\text{C}_{16}$) and behenic ($n\text{C}_{22}$) acids as well as short chain n -alkanes capture the δD of meteoric waters (Huang et al., 2002, 2004; Sachse et al., 2004; Hou et al., 2006), that is related to precipitation amount in the tropics (Dansgaard, 1964). The δD of leaf wax lipids produced by land plants, such as triacontanic acid ($n\text{C}_{30}$) and other long chain fatty acids (Eglinton and Hamilton,

1967), although dependent on the δD of meteoric waters (Sachse et al., 2006), is also affected by evaporation and transpiration processes (Sauer et al., 2001; Liu and Huang, 2005). As a matter of fact, the δD of leaf wax lipids has been recently used to track humidity changes in tropical Africa from marine sediments (Schefuß et al., 2005). In a first approximation, the fractionation factor between the δD values of lipids from land plants and the calculated δD values of water allows us to estimate evapotranspiration. Here, we present the first hydrogen isotopic record from Lake Caçó sediments in North-eastern Brazil covering the last 20,000 cal. yr, which brings new insights into the interconnecting mechanisms between ocean-atmosphere-continent in the tropics.

2. Settings

The study site (Lake Caçó, Maranhão State, Brazil) is located about 80 km from the Atlantic coast and close to the Equator (Fig. 1, and $2^{\circ}58'S$, $43^{\circ}25'W$ and 120 m above sea-level). The local present-day climate is tropical humid with pronounced seasonality. Average rainfall annually reaches 1500 mm and mostly occurs during the rainy season, from November to May (Ledru et al., 2006). Rainfall distribution and river discharge in this region are impacted by the seasonal migration of the InterTropical Convergence Zone (ITCZ; Fig. 1; Hastenrath, 1990). Modern δD of precipitation in Sao Luiz (the closest IAEA/WMO² station), range from -10‰ (during austral

¹ $\delta\text{D} = [\text{D}/\text{H}_{\text{sample}} / \text{D}/\text{H}_{\text{standard}} - 1] \times 1000$. VSMOW is the standard for δD , expressed as permil (‰).

²IAEA/WMO International Atomic Energy Agency/World Meteorological Organization (2004). Global Network of Isotopes in Precipitation. The GNIP Database. Accessible at: <http://isohis.iaea.org>

summer) to 0‰ (during austral winter). The mean annual temperature is 26 °C. The lake (surface: ca 2.5 km²; volume: 8.6 × 10⁶ m³) occupies a former river valley within a dune field and collects waters from a watershed of ca 15 km². The maximum water depth recorded is 12 m during the wet season and ca 11 m during the dry season. The lake is river charged during the rainy season and both river and groundwater charged during the dry season. The outflow rate being on average 0.4 m³ s⁻¹, the calculated turnover time of waters is ca 0.65 year. Modern vegetation that is governed by dune dynamics and topography ranges from littoral steppe vegetation “*restinga*” to sandy savanna “*cerrado*” with “*restinga*” species admixed (Ledru et al., 2001). Most of the primary production from terrestrial and aquatic plants occurs during the rainy season.

3. Sample collection and lipid analyses

Core MA-98-3 (6 m long) was collected in 1998 in the middle of the lake (10 m depth) with a vibracorer (Martin et al., 1995) and kept under 5 °C until analysis. We have observed some compaction in the first meter of sediment but the water–sediment interface has been preserved. Thirty-one 2 cm thick samples were selected for this study. The samples were oven-dried at 50 °C for 12 h before crushing.

The method for lipid preparation is the same as described in Huang et al. (2002) and Hou et al. (2006). Two grams of powdered sediment were used for free lipid extraction using an accelerated solvent extractor (ASE 200, Dionex) with CH₂Cl₂:CH₃OH (1:1). The carboxylic acids were separated from the total extract using solid phase extraction on Aminopropyl Bond Elute[®] cartridges according to Huang et al. (1999). Then, they were converted into fatty acid methyl esters using anhydrous 2% HCl in CH₃OH. Hydroxyl acids were removed using silica gel column chromatography with CH₂Cl₂ in order to further purify the fatty acid methyl esters and avoid chromatographic coelution.

The δD and δ¹³C measurements of individual fatty acid methyl esters were performed by GC-C-IRMS according to Huang et al. (2002) and Hou et al. (2006). A Hewlett Packard 6890 GC interfaced to a Finnigan Delta + XL stable isotope spectrometer through high-temperature pyrolysis and combustion reactors were used for hydrogen and carbon isotopic analysis. Ultra high purity hydrogen and carbon dioxide gas with known δD and δ¹³C values were pulsed three times at the beginning and end of each analysis. The H₃ factor was determined daily.

The accuracy of hydrogen isotope measurements was evaluated using a mixture of four *n*-alkane standards (*n*C₁₆, *n*C₁₈, *n*C₂₀, and *n*C₃₀) with offline measured δD values (acquired from Arndt Schimmelmann, Indiana University). This mixture was analysed every 6 injections and the standard deviation for these isotopic standards was on average less than ±4.5 ‰ during the course of this study.

Because these results were satisfactory, we did not proceed to a normalization of δD results.

The reported δD and δ¹³C values for fatty acids methyl esters were corrected by mathematically removing the isotopic contribution of carbon and hydrogen atoms added during methylation. The δD (−123‰) and δ¹³C (−35.62‰) values of the added methyl group were determined by acidifying and then methylating the disodium salt of succinic acid with a predetermined δD and δ¹³C values (using TC/EA-IRMS). Triplicate (for deuterium) and duplicate (for ¹³C) analyses of the samples resulted in an overall precision better than ±3‰ (δD) and ±0.35‰ (δ¹³C) for *n*C₁₆, *n*C₂₂ and *n*C₃₀ fatty acid methyl esters.

4. Results

4.1. Age model

The age model (Fig. 2) is constrained by six radiocarbon ages (Table 1) that have been performed on bulk organic matter by acceleration mass spectrometry (AMS) at the Beta Analytic Laboratory (Florida, USA). Due to the poor soil cover presently found in the region, and the globally dry climate experienced in the region during the last 20 ka, we consider that few or even no aged organic carbon contributed to the sediment. In addition, the substratum is exclusively made of inorganic sand dunes (quartz and kaolinite) and, locally, laterites, in the region. This excludes a contribution from fossil organic matter. Interpolated ages were calculated using the intercept of the mean conventional age interval with the calibration curve of ¹⁴C (CALIB version 4.3, Stuiver and Reimer, 1993; Stuiver et al., 1998). In combination with radiocarbon dates obtained on other cores drilled in the lake centre (Sifeddine et al., 2003; Ledru et al., 2006) we assume the sedimentation continuous over the record with mean sedimentation rates from 0.15 to 0.24 cm/yr in the lower half of the core and from 0.01 to 0.05 cm/yr in the upper half of the core.

4.2. Downcore variations

The δD variations for palmitic (δD_{PA}), behenic (δD_{BA}) and triacontanic (δD_{TA}) fatty acids as well as their δ¹³C values are plotted against time in Fig. 3. For convenience, the δD values (‰ VSMOW) and δ¹³C values (‰ VPDB) are given as ‰ (per mil) in the text.

The δ¹³C values for *n*C₁₆ fatty acid start at ca −24‰ in the oldest samples and then decrease down to −32‰ around 12 ka before increasing up to −29‰ at 8 ka and then remaining stable. The general trend depicted by behenic acid δ¹³C values is comparable to that of palmitic acid. However, a mean isotopic enrichment of ca 6‰ for behenic acid as compared to palmitic acid is recorded in samples younger than 17 ka. δ¹³C values for triacontanic acid average −31‰ in the 20–19 ka interval, reaches up to −29‰ between 19 and 17 ka and then remains around −32‰ until present.

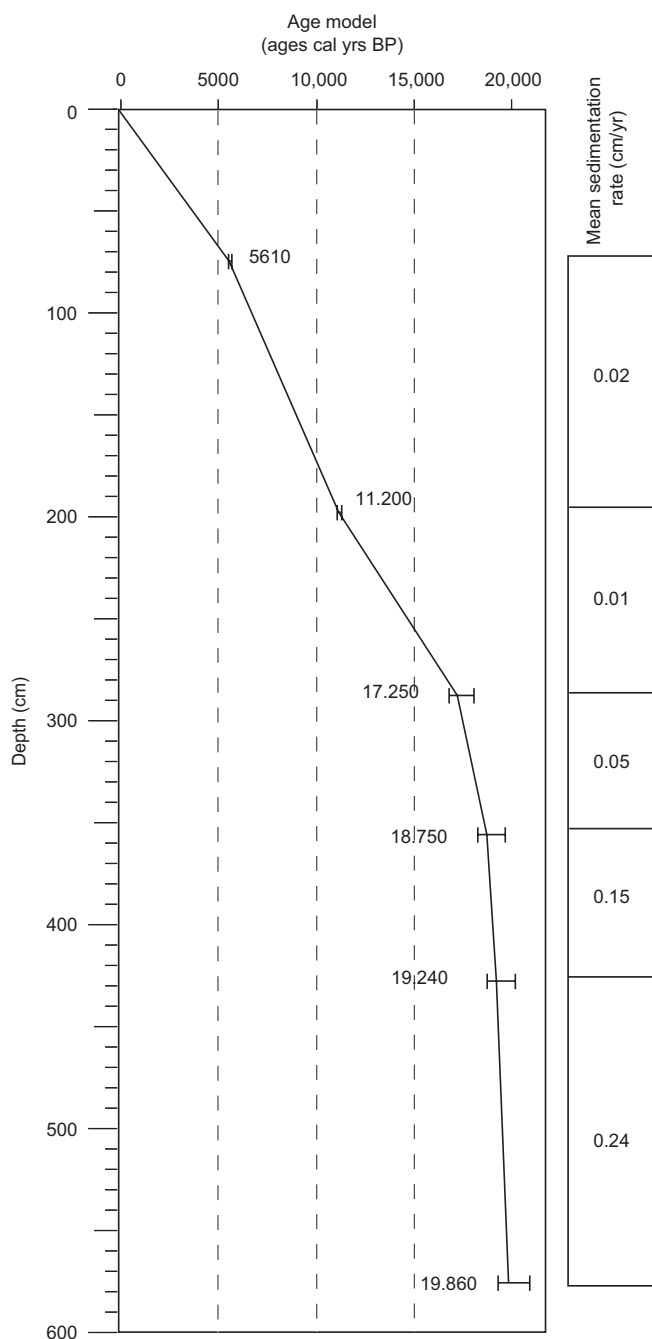


Fig. 2. Age model for core MA-98-3 and sedimentation rates. The error bars represent the range of calibrated ages.

δD_{PA} values range from -240 to -160‰ . The 20–19 ka interval shows strong variations in δD_{PA} between -240 and -190‰ . Then, δD_{PA} values remain around ca -190‰ between 19 and 17 ka and around -180‰ from 17 to 13.5 ka. δD_{PA} values become lower between 13.5 and 11.8 ka (-190 – -200‰) before slightly increasing up to -180‰ at ca 11.5 ka. For more recent samples, the values progressively decrease from -180‰ down to -200‰ . δD_{BA} shows a comparable trend as δD_{PA} with a mean enrichment of ca 40‰ . The detailed differences between the two records will be discussed in paragraph 5.3. The δD_{TA} values are higher during the 20–17 ka time interval as compared to younger samples (average -128‰ compared to -157‰ , respectively), the highest values being recorded around 17 ka. A slight increase in δD_{TA} values up to -150‰ occurs around 12–13 ka and offsets the YD. This increase is followed by a minima of δD_{TA} (-170‰) at 11 ka. From 10 ka to the present, both δD_{TA} and δD_{PA} slightly increase up to ca -160 and -190‰ , respectively.

5. Discussion

5.1. Origin of palmitic, behenic, and triacontanic acids

Previous results acquired from bulk and molecular geochemistry attest to a large contribution of higher plant organic matter to the sediment (Jacob, 2003; Jacob et al., 2004; Jacob et al., 2005). However, the use of molecular markers allows for distinguishing between different source organisms within a complex organic matter.

Triacontanic acid, as other long chain *n*-alkyl lipids, originates from leaf epicuticular waxes (Eglinton and Hamilton, 1967). High $\delta^{13}C$ values (ca -30‰) recorded from 20 to 17 ka for this compound attests to a great contribution of C4 plants and/or lower stomatal conductance of C3 plants due to dryer conditions (Farquhar et al., 1989). After 17 ka, the vegetation mainly consists of C3 plants as attested by rather low $\delta^{13}C$ values for triacontanic acid.

Behenic acid, as well as other mid-length chain *n*-alkyl lipids, is mainly derived from aquatic macrophytes (Ficken et al., 2000). In the case of Lake Caçó, emergent aquatic macrophytes are abundant and mainly consist of *Eleocharis* sp. (spike-rush), a Cyperaceae that develops around the lake between 1 and 3 m depth (Jacob, 2003).

Table 1
Radiocarbon ages of total organic matter from core MA-98-3

Code	Sample depth (cm)	Measured ages ^{14}C yr BP	$\delta^{13}C$	Conventional ages ^{14}C BP	Calibrated ages yr BP	Intercept yr BP
Beta-162661	73–75	4930 ± 50	-27.2‰	890 ± 50	5720–5580	5610
Beta-162662	196–198	9850 ± 70	-28.9‰	9790 ± 70	11270–11120	11200
Beta-162663	286–288	14450 ± 80	-27.8‰	14400 ± 80	17680–16830	17250
Beta-162664	354–356	15620 ± 80	-19.9‰	15700 ± 80	19230–18290	18750
Beta-162665	426–428	16100 ± 80	-22.9‰	16130 ± 80	19740–18770	19240
Beta-162666	574–576	16670 ± 100	24.3‰	16670 ± 100	20410–19330	19860

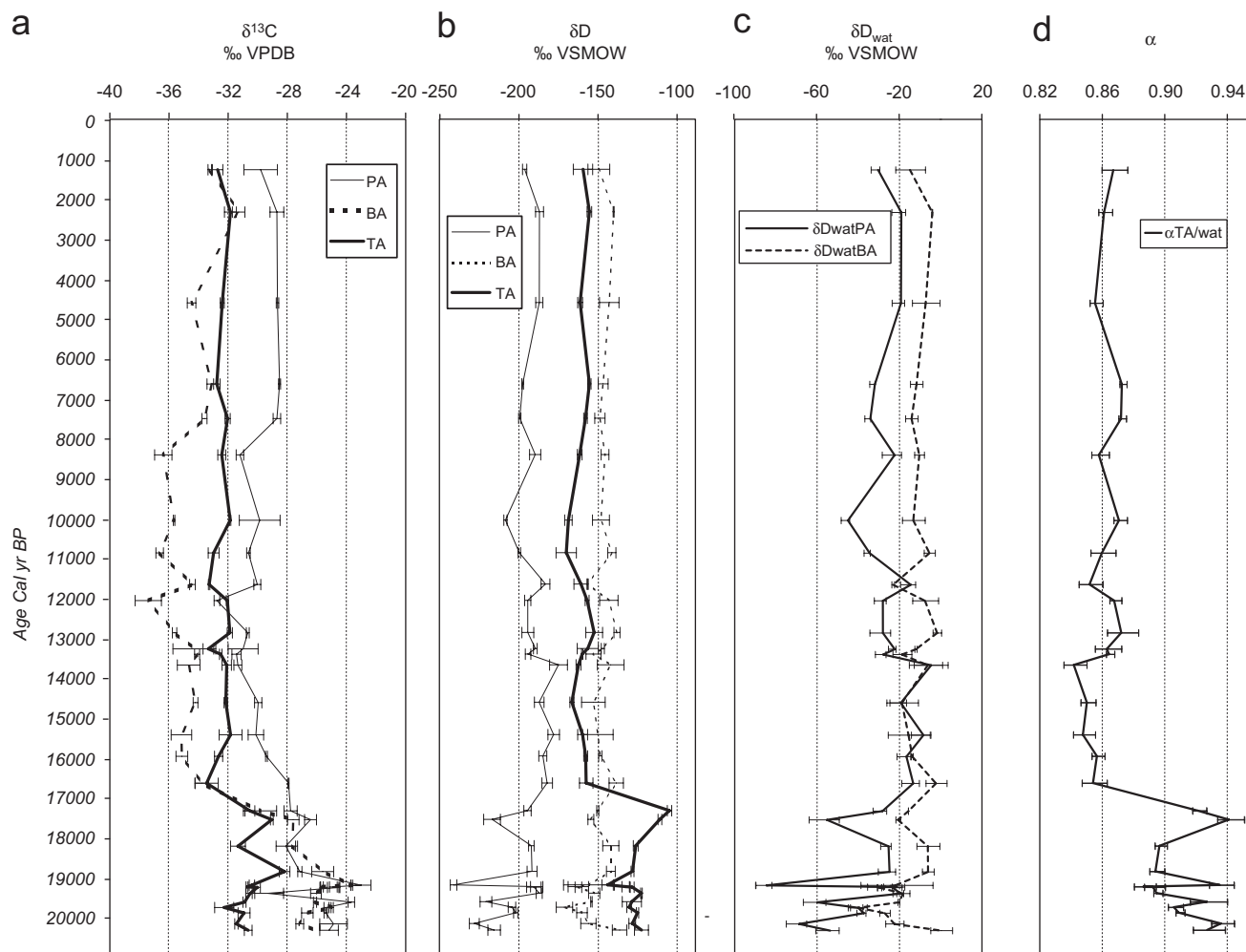


Fig. 3. Variations of $\delta^{13}\text{C}$ (a) and δD values (b) for palmitic ($\delta\text{D}_{\text{PA}}$), behenic ($\delta\text{D}_{\text{BA}}$) and triacontanic ($\delta\text{D}_{\text{TA}}$) acids along the 20 ka sedimentary record of Lake Caçó. The error bars correspond to the standard deviation for duplicate ($\delta^{13}\text{C}$) and triplicate (δD) analyses. (c) Reconstructed hydrogen isotopic composition of the lake waters from $\delta\text{D}_{\text{PA}}$ ($\delta\text{D}_{\text{watPA}}$) and $\delta\text{D}_{\text{BA}}$ ($\delta\text{D}_{\text{watBA}}$) as calculated in paragraph 5.2. Lower values are interpreted as higher precipitation and reverse. (d) Evolution of the fractionation factor between lake waters ($\delta\text{D}_{\text{watPA}}$, calculated from $\delta\text{D}_{\text{PA}}$) and triacontanic acid ($\alpha_{\text{TA/wat}}$). Higher values indicate stronger evapotranspiration. VSMOW is Vienna Standard Mean Ocean Water. VPDB is Vienna Pee Dee Belemnite. PA is palmitic ($n\text{C}_{16}$) acid; BA is behenic ($n\text{C}_{22}$) acid and TA is triacontanic ($n\text{C}_{30}$) acid.

Palmitic acid is produced by most organisms. Nevertheless, it has been shown that this compound is rapidly degraded in leaves or litters when produced by higher plants (Marseille et al., 1999; Bourdon et al., 2000; Disnar et al., 2005). Therefore, higher plant-derived palmitic acid is unlikely to reach the sediment. A dominantly aquatic origin for palmitic acid in lake sediments is further supported by the fact that δD values of this compound found in lake surface sediments track lake water δD values in 33 lakes in the Eastern North America (Huang et al., 2002). Furthermore, the evolution of δD and $\delta^{13}\text{C}$ values for palmitic and behenic acids show comparable trends, distinct from those of triacontanic acid, hence indicating a common reservoir different from those of higher plants both for hydrogen and carbon.

The difference in carbon isotopic discrimination recorded between the end of the LGM and more recent

samples by both palmitic (ca $-25/30\text{‰}$) and behenic acids (ca $-24/-36\text{‰}$) is coherent with a similar shift displayed by the $\delta^{13}\text{C}$ of phytoplanktonic lipids in an African tropical lake (Sacred Lake, Kenya; Huang et al., 1999). Increased $\delta^{13}\text{C}$ values for palmitic and behenic acids at the end of the LGM are attributed to lower atmospheric pCO_2 and higher pH leading to inorganic carbon limitation (low dissolved CO_2) in the lake waters. Lower lake level and smaller volume may have also induced nutrient concentration and higher productivity, causing further draw down of dissolved and CO_2 and higher $\delta^{13}\text{C}$ values of algal biomass. During the Lateglacial and after, higher $[\text{CO}_2]_{\text{aq}}$ due to higher dissolved CO_2 favoured the isotopic discrimination by aquatic organisms, leading to lower $\delta^{13}\text{C}$ values. This isotopic effect was enhanced by a stronger carbon input from C3 plants to the lake that entailed a lowering of the $\delta^{13}\text{C}$ values of DIC in the lake waters, via remineralization of organic carbon.

5.2. Uncertainties in linking δD of lipids with environmental parameters

The complex way allowing an isotopic signal depending on a given set of climatic parameters to be preserved in sedimentary lipids is summarized in Fig. 4. Although non-exhaustive, this diagram allows understanding the different factors that influence the final isotopic signal in sedimentary archives, and therefore, the sources of uncertainty. These can be divided into environmental, biological and geological factors.

5.2.1. Environmental factors

Environmental factors controlling the hydrogen isotopic composition of water used by organisms for lipid biosynthesis are the same as those affecting the $\delta^{18}O$ composition of water used for carbonate precipitation. These factors have been reviewed recently in Leng and Marshall (2004). The δD of rainfall for a given

region is dependent on the δD of the source water (the ocean), isotopic effects due to temperature and latitude, continentality and altitude but also the amount of rainfall and the seasonality of precipitation. Since Lake Caçó is located in the tropics, close to the Atlantic Ocean and at a low altitude, the δD of precipitation is mostly dependent on the amount and seasonality of rainfall. Then, meteoric waters suffer runoff, infiltration and recharge of aquifers. The isotopic composition of soil water is affected by evaporation and transpiration processes that are influenced by wind speed, insolation and vegetation cover. If the δD of lake waters is considered, the limnology of the lake must be taken into account (von Grafenstein, 2002; Leng and Marshall, 2004). Wherever the lake waters are in steady state (i.e. reflect the isotopic composition of rainfall) depends on the ratio between the watershed and the lake surfaces, the turnover time of water in the lake and evaporation processes.

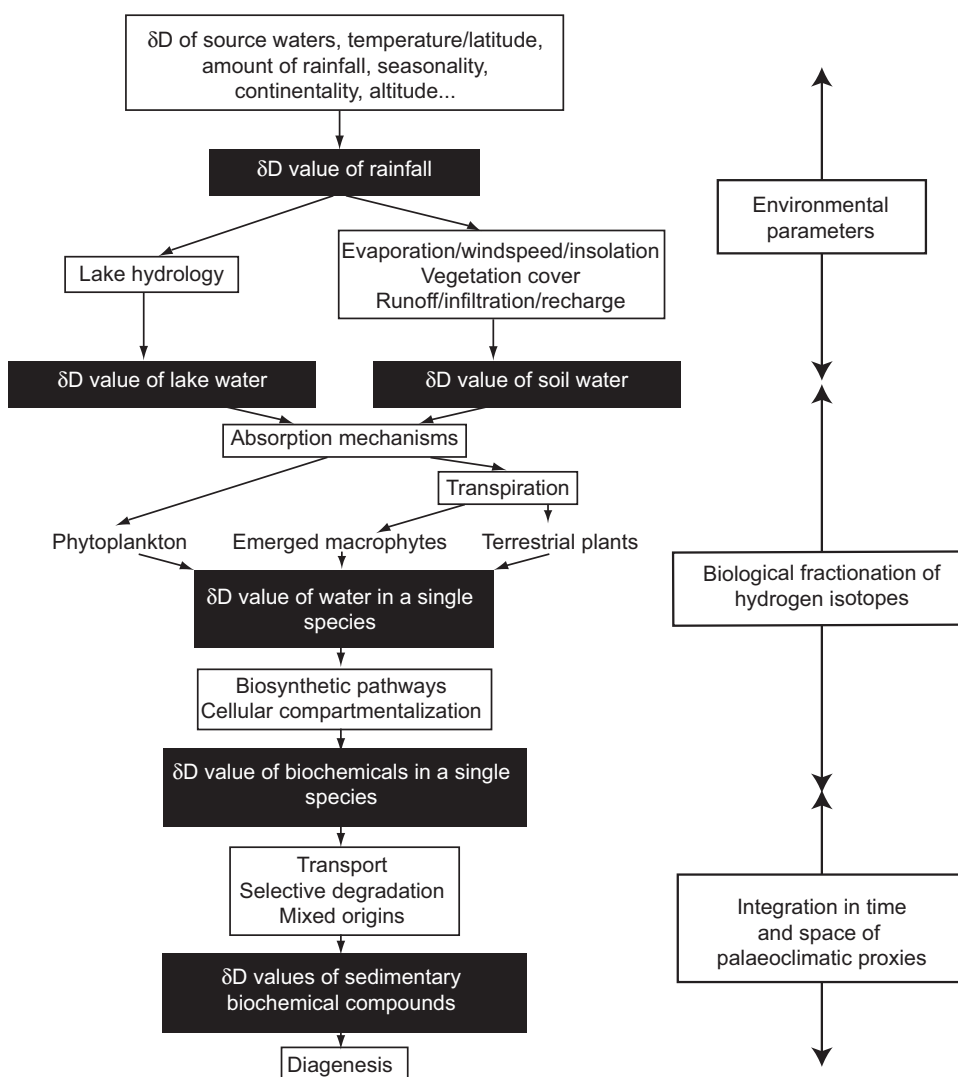


Fig. 4. Sketch diagram illustrating the sources of uncertainty when attempting to relate an isotopic signal measured on organic molecules retrieved from sedimentary archives with paleoclimatic parameters.

5.2.2. Biological factors

The soil or lake water is then used by organisms for their biosynthesis. The isotopic fractionation between plant water and environmental water depends on physiological factors affecting water uptake, transport and evapotranspiration, considering aerial plants for this latter (Sessions, 2006; Smith and Freeman, 2006). The main isotopic fractionation occurs during lipid biosynthesis, depending on biosynthetic pathways (*n*-alkyl lipids versus isoprenoids for example) and compartmentalization of water use. This leads to net a biological fractionation of more than 150 ‰ between environmental waters and lipids (Sessions, 2006 and references therein).

5.2.3. Geological factors

Organic matter produced from different sources within the watershed is then transported towards the lake and suffers differential degradation. It is mixed with autochthonous organic matter within the water column before entering the sediment. Considering these phenomena, it is worthwhile accounting for the residence time of organic matter within each compartment, inducing a delayed record of the sedimentary archive to climatic variations. In conclusion, the sediment integrates organic-derived paleoclimatic information in both time and space.

Despite these numerous pitfalls, one can assume that original isotopic signals are preserved within sedimentary organic matter, i.e. that the correlation between the δD values of sedimentary lipids and the δD values of past environmental waters is dependent on few variables that can be constrained by using lipids of distinct origins. The challenge remains to deconvolute these different effects and to reconstitute past climate variability. It is what we tried in the following discussion.

5.3. Paleoenvironmental interpretation of compound-specific isotopic trends

Interpretation of our isotopic records from Lake Caçó is based on a number of established relationships and/or assumptions:

(i) Consistent with surface sediment calibration from eastern North American lakes, δD values of palmitic (δD_{PA}) and behenic (δD_{BA}) acids record the lake water isotope ratios (Huang et al., 2002, 2004; Hou et al., 2006). The constant D/H fractionation factor is 0.829 ± 0.014 between palmitic acid and lake waters (Huang et al., 2002) and 0.8681 between behenic acid and lake waters (Hou et al., 2006). For this later an error of ± 0.0414 is assumed. This value corresponds to the maximum discrepancy for the behenic acid/lake water fractionation factor between the slope and the intercept of the calibration curve described by Hou et al. (2006). The hydrogen isotopic composition of the lake waters is calculated from δD_{PA} as follows:

$$\delta D_{\text{watPA}} = (\delta D_{PA} + 170)/0.829$$

and from δD_{BA} as follows :

$$\delta D_{\text{watBA}} = (\delta D_{BA} + 136.4)/0.8681.$$

The reconstructed hydrogen isotopic evolutions of the lake waters are reported in Fig. 3. Considering for each value the analytical error ($\Delta \delta D_{PA}$ and $\Delta \delta D_{BA}$) and the error affecting the isotopic fractionation factor (0.014 for palmitic acid and 0.0414 for behenic acid), the resulting errors are calculated as follow:

$$\Delta \delta D_{\text{watPA}} = (\Delta \delta D_{PA} \times 0.829 + 0.014 \times \delta D_{PA})/0.829^2$$

and

$$\Delta \delta D_{\text{watBA}} = (\Delta \delta D_{BA} \times 0.8681 + 0.0414 \times \delta D_{BA})/0.8681^2,$$

δD_{watPA} values between 20 and 17 ka are highly variable within a $-85/20\text{‰}$ range. Then, and up to ca 13.5 ka, δD_{watPA} values are relatively constant above -20‰ . After the 13.5–11.8 interval characterized by values lower than -20‰ , δD_{watPA} values raise at ca -15‰ in a single sample before decreasing down to -45‰ and then increasing towards -20‰ . The variations of δD_{watBA} values are less marked except in the 20–17 ka interval.

Although δD_{watPA} and δD_{watBA} records are in general agreement, again indicating that palmitic and behenic acids both record the isotopic composition of the lake waters, the best fit between the two curves occurs for samples belonging to the 17–13 ka interval, that corresponds to the most humid conditions recorded in the region for the last 20 ka (see Section 5.3.2). Higher values of δD_{watBA} relative to δD_{watPA} recorded in the other intervals are not well understood although they could result from an enrichment in deuterium due to evapotranspiration affecting emerged plants (the supposed producers of behenic acid), when lake level lowers. Therefore, we use the δD_{wat} derived from δD_{PA} (δD_{watPA}) as an estimate of the δD values of the lake waters. In the tropics, the main parameter that controls the δD of meteoric waters is the amount of precipitation (“amount effect”; Dansgaard, 1964). This parameter is therefore used as an estimate of precipitation, with high δD_{watPA} values indicating reduced precipitation and reversely.

(ii) We assume that lake water (\approx mean annual precipitation) represents the water used by land plants, since there is currently no alternative to reconstruct groundwater used by land plants. The variations in $\alpha_{TA/\text{wat}}$, the fractionation factor between δD_{TA} and δD_{watPA} ($\alpha_{TA/\text{wat}} = [\delta D_{TA} + 1000]/[\delta D_{\text{watPA}} + 1000]$), result from the enrichment of leaf waters in deuterium as compared to meteoric waters. Higher $\alpha_{TA/\text{wat}}$ values result from higher soil evaporation and leaf transpiration (Huang et al., 2004; Sachse et al., 2004, 2006; Hou et al., 2006). Error bars displayed on the $\alpha_{TA/\text{wat}}$ curve in Fig. 3 are calculated by combining the analytical error on δD_{TA} and

the calculated error on δD_{watPA} as follows:

$$\Delta\alpha_{\text{TA/wat}} = (\Delta\delta D_{\text{watPA}} \times (\delta D_{\text{TA}} + 1000) + (\delta D_{\text{watPA}} + 1000) \times \Delta\delta D_{\text{TA}}) / (\delta D_{\text{watPA}} + 1000)^2,$$

$\alpha_{\text{TA/wat}}$ values are high (between 0.9 and 0.94) during the 20–17 ka period. After a sudden decrease down to 0.86, $\alpha_{\text{TA/wat}}$ values remain stable around 0.85 up to 13.5 ka. The 13.5–11.8 ka interval is characterized by slightly higher coefficient (ca 0.867) that remain around this figure in more recent samples, except for single points.

(iii) The δD_{TA} parameter is affected both by δD_{wat} and by soil evaporation and leaf transpiration that cause a deuterium enrichment of plant leaf water: hence the value is higher under low relative humidity conditions and reversely (Yapp and Epstein, 1982). In order to decipher relative changes in relative humidity, we converted differences in δD_{TA} into differences in relative humidity, using the equation of Yapp and Epstein (1982): $\delta D_{\text{TAa}} - \delta D_{\text{TA b}} = 124 (h_a - h_b)$. δD_{TAa} and $\delta D_{\text{TA b}}$ are the δD_{TA} values during periods *a* and *b* and h_a and h_b are the relative humidity that prevailed during times *a* and *b*. If this relationship, which was established for a single species at a given time, can be directly applied to a whole ecosystem (without taking account differences in evapo-transpiration due to forest/savanna successions for example) and remains valid over longer periods, it allows us obtaining an order of magnitude for humidity changes. Since this approach raises a large number of uncertainties, we did not report any uncertainty estimate.

5.4. Evolution of climatic conditions in the region

5.4.1. The end of Last Glacial Maximum

High δD_{TA} values (mean = -129%) during the 20–19 ka interval (Fig. 5a) result from a reduced hydrological balance (i.e. less precipitation and more evaporation leading to dry conditions). Using the equation of Yapp and Epstein (1982), the relative humidity is reduced by ca 30% at this time, when referring to the Lateglacial interval (e.g., 15 ka), taken as a reference (100%). The rather high $\delta^{13}\text{C}$ for palmitic acid at this time most probably results from carbon limitation in the lake waters due to dry/arid conditions in the surrounding area. The highly variable δD_{watPA} (~from -84.87 to -19.49% ; Fig. 5b) and $\alpha_{\text{TA/wat}}$ values (~from 0.89 to 0.94) during this interval indicate that these conditions result from a combination of high evaporation and severe rainfalls (Fig. 5b and c). In fact, we interpret the low δD_{watPA} values during the 20–19 ka phase as resulting from episodic rainfalls. Sporadic but strong showers during a short rainy season allowed the existence of ephemeral lakes within sand dunes (Jacob et al., 2004). Within these ephemeral lakes, opportunistic phytoplanktonic communities developed during the short rainy season and captured an isotopic signal attesting to high precipitation. This short rainy season was followed by a long dry

season with strong evaporation rates, as indicated by the high figures of $\alpha_{\text{TA/wat}}$.

The 19–17.3 ka period is characterized by lower precipitation than previously (δD_{watPA} increases up to $\sim -34\%$) accompanied by still high evapotranspiration (mean $\alpha_{\text{TA/wat}} \sim 0.91$). This suggests slightly drier conditions than before with a maximum around 17.3 ka ($\delta D_{\text{TA}} \sim 104\%$). The calculated average relative humidity over this time period is reduced by 40% with respect to the Lateglacial period. We interpret these results as a decrease of the rainy season length and still high evapotranspiration rates.

Our results are in agreement with previous work on cores collected in the same lake (Fig. 5d and e). The very low AP/NAP ratios (arboreal against herbaceous pollens) during the considered time span indicate sparse vegetation dominated by grasses, typical of semi-arid climate (Ledru et al., 2001, 2002). This is also depicted by low $\delta^{13}\text{C}$ values for triacontanic acid that attest to a strong contribution of C4 plants and/or lower stomatal conductance of C3 plants (Fig. 3). Increased quartz fluxes into the sediment at these times result from the intensification of eolian dune transport, a phenomenon that only occurs when the dry season lasts more than four months (Sifeddine et al., 2003). The presence of sandy sub-horizontal to oblique parallel laminations confirms the occurrences of flash floods during events of heavy rainfalls.

5.4.2. The abrupt climate change at Lateglacial

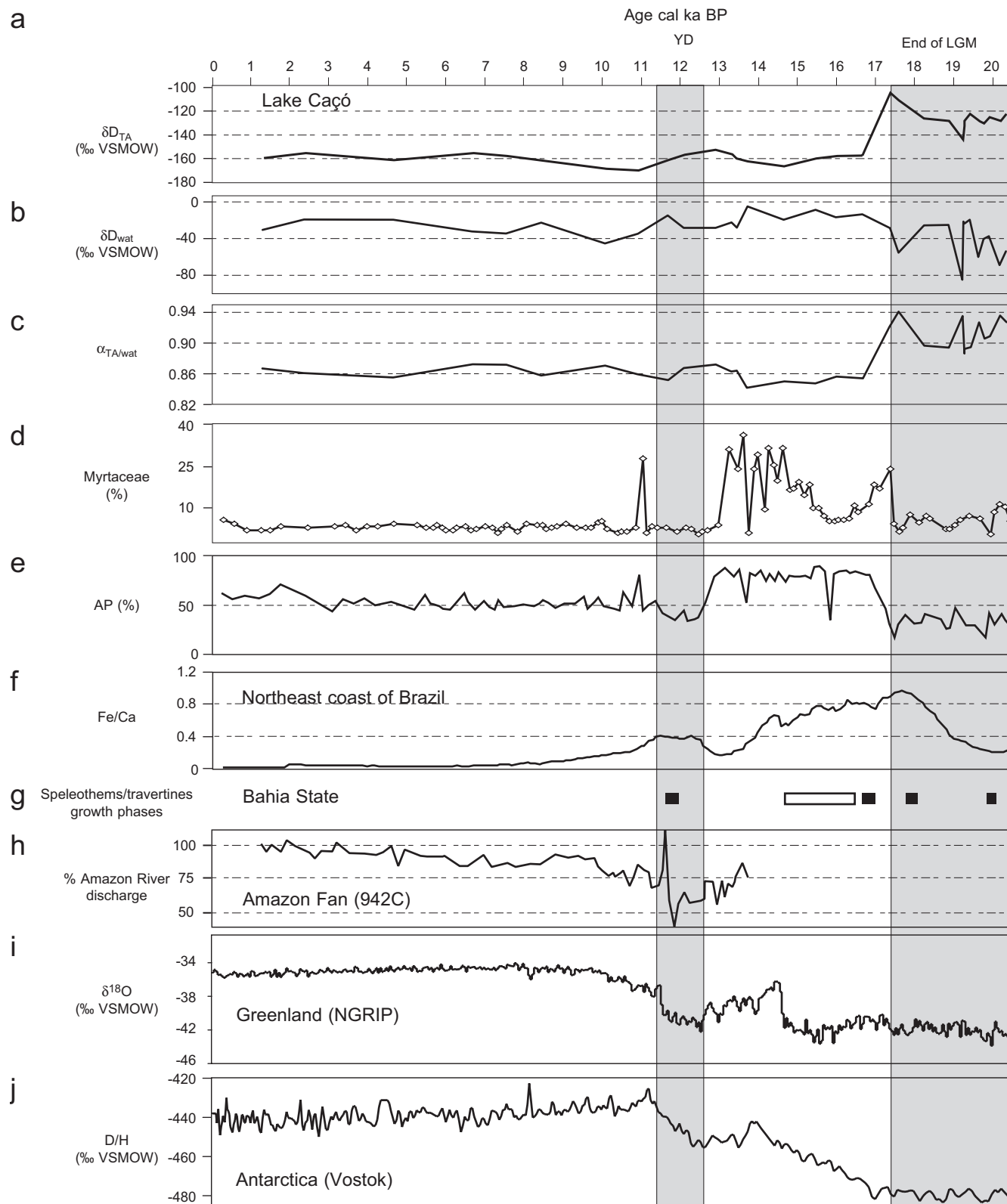
Between 17.3 and 16.8 ka, a rapid transition from arid/semi-arid conditions to humid conditions is reflected in the large decrease in δD_{TA} values. Then, during the Lateglacial period (from 16.8 to 13.5 ka), the enhanced precipitation ($\delta D_{\text{watPA}} \sim -15\%$) and lower soil evaporation and leaf transpiration ($\alpha_{\text{TA/wat}} \sim 0.85$) enables the establishment of humid conditions ($\delta D_{\text{TA}} \sim -160\%$). During this period, pollen results show an increase of forest percentages dominated by Myrtaceae (Fig. 5d and 5e), providing evidence for the development of a humid forest, in agreement with lower figures of triacontanic acid $\delta^{13}\text{C}$ values that reflect a stronger contribution of C3 plants.

5.4.3. The Younger Dryas and the Holocene

Climatic conditions appear slightly drier during the 13.5–11.8 ka time period, with δD_{TA} values reaching -158% indicating relative moisture reduced by 7% as compared to the Lateglacial. The δD_{watPA} values exhibit a shift toward -21% coupled to a shift of the $\alpha_{\text{TA/wat}}$ values (maximum 0.87). These figures are interpreted as sporadic showers during a shorter rain season coupled with enhanced evaporation, as during the 20–19 ka interval, but to a lesser extent. In the meantime lower AP/NAP ratios indicate the replacement of the humid forest by open vegetation. It is worthwhile noting that triacontanic acid $\delta^{13}\text{C}$ does not exhibit a stronger contribution of C4 plants at this time, as opposed to the end of LGM. A sedimentary hiatus in a marginal core is noted and corresponds to the

lowering of the lake level (Sifeddine et al., 2003). This episode is also characterized by higher quartz fluxes, probably of eolian origin, that point to a longer dry season (Sifeddine et al., 2003). During the period dated between 11.8 and 10 ka (Preboreal), δD_{TA} , δD_{watPA} and $\alpha_{TA/wat}$

values reach similar figures as during the Lateglacial, indicating similar hydrological conditions, accompanied by a discrete increase in arboreal pollen percentages. Then, the δD_{TA} values slightly increase through the early Holocene up to -161‰, illustrating a drying trend.



5.5. Regional integration within South American records

The changes in humidity evidenced in the sedimentological sequence of Lake Caçó provide the first continuous continental record in Northern South America for the last 20 ka. It allows improved chronostratigraphic correlation of other paleoenvironmental time-series (e.g., vegetation changes) with our well-dated record of reconstructed paleohumidity.

Our results suggest that drier conditions prevailed at the end of the LGM in the region and attest to a probable reduction of the eastern border of the rainforest. They are consistent with the pattern of vegetation distribution proposed for the LGM (Adams and Faure, 1998). The drier mean climate probably originates from a weakening of the ITCZ and of the global hydrological cycle during the LGM. Moreover, the stronger seasonality would indicate a northward shift of the ITCZ due to a stronger pole-equator temperature gradient in the North hemisphere. The heavy rainfalls at the end of the LGM would be related to interannual climate variability during episodes when ITCZ, which was on average at a northernmost position, occasionally reached its present-day southern position.

The Lateglacial humid period, which is marked by an abrupt increase of precipitation and humidity at ca 17 ka around Lake Caçó, is also recorded in the north-eastern region by travertine and speleothem active phases (Auler and Smart, 2001; Wang et al., 2004; Fig. 5(g)). It is also synchronous with the increase in the Fe/Ca ratio in a sediment core from the north-eastern Brazilian continental margin, which corresponds to increased terrigenous inputs related to more humid conditions in the hinterland (Fig. 5f; Arz et al., 1998, 1999). This paleoclimate change is interpreted as a warmer sea-surface temperature episode that began with Heinrich event 1 (Arz et al., 1998). This global climatic event provoked changes in Atlantic Ocean circulation resulting in the intensification of the ITCZ and an increased moisture transport to the north-eastern South America hinterlands.

The reinforcement of these humid conditions from 15 to 13.5 ka (e.g. the Bølling-Allerød period), marked by the stability of moisture, corresponds to the beginning of lacustrine sedimentation in Lake Carajas (Sifeddine et al., 2001) and in several Brazilian records (Sifeddine et al.,

1998; Auler and Smart, 2001). It is explained by a southward shift of the ITCZ which could be related to a cold reversal in the Northern Hemisphere while Antarctic temperature remained stable (Fig. 5i and j).

The YD is marked by a weak decrease of precipitation and relative humidity that can be attributed to more intense evapotranspiration. Drier conditions are also reported in the Bolivian cordillera (van't Veer et al., 2000) A reduction of 60% of the Amazon discharge, as compared to the modern flow, is noticed from the Amazon fan sediments (Fig. 5h, Maslin and Burns, 2000) and reduced precipitations in Northern Amazonia (Peterson et al., 2000) accompanied by the development of a dry savanna are inferred from the Cariaco Trench (Haug et al., 2001; Hughen et al., 2004). Oppositely, the YD has been interpreted as more humid from marine cores from Northern Brazil (Fig. 5f, Arz et al., 1999; Behling et al., 2000). These results indicate a southern position of ITCZ which probably reached higher Southern Hemisphere latitudes during the summer of this hemisphere than its present-day shift. Based on δD data, we interpret this period as resulting from a shorter humid season, which agrees with a southern position of ITCZ in Southern Hemisphere summer.

The Preboreal period is characterized by reduced precipitation and even more reduced evaporation leading to more humid conditions in Lake Caçó region. This episode coincides with active phases of speleothems and travertines growth in the State of Bahia (Fig. 5g, Wang et al., 2004) that attest to a rapid return of humid conditions in the north-eastern tip of Brazil.

6. Conclusion

Our results provide an estimate of the humidity variations in a South American tropical lake since the last deglaciation. By combining hydrogen isotope measurements on aquatic and terrestrial lipids, we show the potential of this approach to deconvolute the effects of precipitation (amount and seasonality) and evapotranspiration on the humidity. In addition, this approach would allow in certain cases the estimation of changes in seasonality of precipitation, a parameter that remains hard to discriminate in paleorecords. Despite the numerous

Fig. 5. Comparison of the variations of paleohumidity in Lake Caçó with other proxy records for the last 20 ka. (a) The δD_{TA} is the δD value for triacontanoic acid, synthesised by terrestrial higher plants. It is interpreted as a proxy of relative humidity. Higher values correspond to drier conditions and reverse. (b) The δD_{watPA} (δD of meteoric waters) is calculated from the δD of the palmitic acid (δD_{PA}) using a constant fractionation factor of 0.829 (see text and Huang et al., 2002). Low figures of δD_{watPA} correspond to abundant precipitation. (c), $\alpha_{TA/wat}$ is the coefficient of isotopic fractionation of hydrogen between leaf wax lipids and meteoric waters. High values of $\alpha_{TA/wat}$ correspond to intense evapotranspiration and reverse. (d) Percentages of Myrtaceae pollen measured on another core from the same lake (MA-97-1). High percentages of Myrtaceae pollen indicate the development of a humid and warm forest. (e) The AP/NAP ratio reflects the relative abundance of arboreal pollens (AP) and non-arboreal pollen (NAP) in the sample (Ledru et al., 2001; Sifeddine et al., 2003). Low AP values reflect the development of a savana whereas high values attest to the presence of a humid forest. (f) Variations of the normalized Fe/Ca ratios obtained on several marine cores from north-eastern Brazil (Arz et al. 1998; Arz et al., 1999). Increased Fe/Ca ratios are interpreted as enhanced moisture supply over the north east of Brazil. (g) Speleothems (white bars) and travertines (blackbars) growth phases in north-eastern Brazil, reflecting humid periods (Wang et al., 2004). (h) Variations of the Amazon River outflow calculated from the oxygen isotopic composition ($\delta^{18}O$) of planktonic foraminifera in the sediments of the Amazon fan (Maslin and Burns, 2000). (i) $\delta^{18}O$ in GRIP ice core (North Greenland Ice Core Project members, 2004). (j) Deuterium in Vostok ice core (Petit et al., 1999). The location of the sites from which (f–h) records were obtained is indicated in Fig. 1. YD is Younger Dryas and LGM is Last Glacial Maximum.

approximations involved in our study (integration in time and space of hydrological processes, few controls on intimate physical, chemical and biological mechanisms), the outstanding correlation of our hydrogen isotope records with independent data shows the potential of this approach to track past hydrological changes in the tropics. Our ability to track more sensible hydrological changes will depend on future work on calibration that are now required in the tropics.

The comparison with other proxy records for the same period underlines the role of ITCZ position in climate changes. ITCZ position is controlled by interhemispheric gradients of temperature, insolation and ocean dynamics. Our data suggest that abrupt changes in regional climate in the tropics can be due to shifts in the ITCZ position. The sharp increase in humidity at ca 17ka is thought to coincide with Heinrich event 1. High humidity levels are maintained up to ca 13.5 ka and may be related to a cooling of the Northern Hemisphere while Antarctic temperature remained quite stable. Such conditions should push ITCZ southward. The still high Southern Hemisphere summer insolation at that time also contributed directly to this humid climate phase.

Acknowledgements

This research was sponsored by a Travel Scholarship attributed by the European Association of Organic Geochemists (EAOG) to J.J. The study of Lake Caçó sediments results from a programme PALEOTROPICA supported by an IRD (France)-CNPq (Brazil) convention and an ISTO (UMR 6113 du CNRS, France)-UR055 (PALEOTROPIQUE-IRD) cooperation. The research at Brown University is supported by funds from the Earth System History Program at the National Science Foundation to Y.H. (NSF0081478, 0318050, 0318123, 0402383). The authors wish to thank A. Schimmelmann, A. Sessions, F. Palhol and A. Mangini for their constructive comments on a previous version of the manuscript.

References

- Adams, J.M., Faure, H., 1998. A new estimate of changing carbon storage on land since the Last Glacial Maximum based on global land ecosystem reconstruction. *Global and Planetary Change* 16–17, 3–24.
- Arz, H.W., Pätzold, J., Wefer, G., 1998. Correlated millennial-scale changes in surface hydrography and terrigenous sediment yield inferred from Last-Glacial marine deposits off Northeastern Brazil. *Quaternary Research* 50, 157–166.
- Arz, H.W., Pätzold, J., Wefer, G., 1999. Climatic changes during the last deglaciation recorded in sediment cores from the northeastern Brazilian Continental Margin. *Geo-Marine Letters* 19, 209–218.
- Auler, A.S., Smart, P.L., 2001. Late Quaternary paleoclimate in semiarid northeastern Brazil from U-series dating of travertine and water-table Speleothems. *Quaternary Research* 55, 159–167.
- Behling, H., Arz, H.W., Pätzold, J., Wefer, G., 2000. Late Quaternary vegetational and climate dynamics in northeastern Brazil, inferences from marine core GeoB 3104-1. *Quaternary Science Reviews* 19, 981–994.
- Bourdon, S., Laggoun-Déferge, F., Maman, O., Disnar, J.-R., Guillet, B., Derenne, S., Largeau, C., 2000. Organic matter sources and early diagenetic degradation in a tropical peaty marsh (Tririvakely, Madagascar). Implications for environmental reconstruction during the Sub-Atlantic. *Organic Geochemistry* 31, 421–438.
- Colinvaux, P.A., De Oliveira, P.E., Bush, M.B., 2000. Amazonian and neotropical plant communities on glacial time-scales: the failure of the aridity and refuge hypotheses. *Quaternary Science Reviews* 19, 141–169.
- Cruz Jr., F.W., Burns, S.J., Karmann, I., Sharp, W.D., Vuille, M., Cardoso, A.O., Ferrari, J.A., Silva Dias, P.L., Viana Jr, O., 2005. Insolation-driven changes in atmospheric circulation over the past 116,000 years in subtropical Brazil. *Nature* 434, 63–66.
- Dansgaard, W., 1964. Stable isotopes in precipitation. *Tellus* 16, 436–468.
- Disnar, J.R., Stefanova, M., Bourdon, S., Laggoun-Déferge, F., 2005. Sequential fatty acid analysis of a peat core covering the last two millennia (Tririvakely lake, Madagascar): diagenesis appraisal and consequences for palaeoenvironmental reconstruction. *Organic Geochemistry* 36, 1391–1404.
- Eglinton, G., Hamilton, R.J., 1967. Leaf epicuticular waxes. *Science* 156, 1322–1335.
- Farquhar, G.D., Ehleringer, J.R., Hubick, K.T., 1989. Carbon isotope discrimination and photosynthesis. *Annual Review of Plant Physiology and Plant Molecular Biology* 40, 503–537.
- Ficken, K.J., Li, B., Swain, D.L., Eglinton, G., 2000. An n-alkane proxy for the sedimentary input of submerged/floating freshwater aquatic macrophytes. *Organic Geochemistry* 31, 745–749.
- Grafenstein, U. von., 2002. Oxygen-isotope studies of Ostracods from deep lakes. *The Ostracoda: Applications in Quaternary Research. Geophysical Research Monograph* 131, 249–266.
- Hastenrath, S., 1990. Decadal-scale changes of the circulation in the tropical Atlantic sector associated with Sahel drought. *International Journal of Climatology* 10, 459–472.
- Haug, G.H., Hughen, K.A., Sigman, D.M., Peterson, L.C., Röhl, U., 2001. Southward migration of the Intertropical Convergence Zone through the Holocene. *Science* 293, 1304–1308.
- Hou, J., Huang, Y., Wang, Y., Shuman, B., Oswald, W. W., Faison, E., Foster, D. R., 2006. Postglacial climate reconstruction based on compound-specific D/H ratios of fatty acids from Blood Pond, New England. *Geochemistry Geophysics Geosystems* 7, Q03008, doi:10.1029/2005GC001076.
- Huang, Y., Street-Perrott, F.A., Perrott, F.A., Metzger, P., Eglinton, G., 1999. Glacial-interglacial environmental changes inferred from the molecular and compound-specific $\delta^{13}\text{C}$ analyses of sediments from Sacred Lake, Mt. Kenya. *Geochimica et Cosmochimica Acta* 63, 1383–1404.
- Huang, Y., Shuman, B., Wang, Y., Webb III, T., 2002. Hydrogen isotope ratios of palmitic acid in lacustrine sediments record late Quaternary climate variations. *Geology* 30, 1103–1106.
- Huang, Y., Shuman, B., Wang, Y., Webb III, T., 2004. Hydrogen isotope ratios of individual lipids in lake sediments as novel tracers of climatic and environmental change: a surface sediment test. *Journal of Paleolimnology* 31, 363–375.
- Hughen, K.A., Eglinton, T.I., Xu, ., Makou, M., 2004. Abrupt tropical vegetation response to rapid climate changes. *Science* 304, 1955–1959.
- Jacob, J., 2003. Enregistrement des variations paléoenvironnementales depuis 20000 ans dans le Nord Est du Brésil (Lac Caçó) par les triterpènes et autres marqueurs organiques. Ph.D. Thesis, Université d'Orléans, 296pp. <http://tel.ccsd.cnrs.fr/documents/archives0/00/00/29/42/index_fr.html>.
- Jacob, J., Disnar, J.R., Boussafir, M., Sifeddine, A., Albuquerque, A.L.S., Turcq, B., 2004. Major environmental changes recorded by lacustrine sedimentary organic matter since the Last Glacial Maximum under the tropics (Lagoa do Caçó, NE Brazil). *Palaeogeography, Palaeoclimatology, Palaeoecology* 205, 183–197.
- Jacob, J., Disnar, J.R., Boussafir, M., Sifeddine, A., Albuquerque, A.L.S., Turcq, B., 2005. Pentacyclic triterpene methyl ethers in recent

- lacustrine sediments (Lagoa do Caçó, Brazil). *Organic Geochemistry* 36, 449–461.
- Ledru, M.P., Cordeiro, R.C., Dominguez, J.M.L., Martin, L., Mourguiart, P., Sifeddine, A., Turcq, B., 2001. Late-glacial cooling in Amazonia as inferred from pollen at Lagoa do Caçó, Northern Brazil. *Quaternary Research* 55, 47–56.
- Ledru, M.P., Mourguiart, P., Ceccantini, G., Turcq, B., Sifeddine, A., 2002. Tropical climates in the game of two hemispheres revealed by abrupt climatic change. *Geology* 30, 275–278.
- Ledru, M.P., Ceccantini, G., Gouveia, S.E.M., López-Sáez, J.A., Pessenda, L.C.R., Ribeiro, A.S., 2006. Millennial-scale climatic and vegetation changes in a northern Cerrado (Northeast, Brazil) since the Last Glacial Maximum. *Quaternary Science Reviews* 25, 1110–1126.
- Leng, M.J., Marshall, J.D., 2004. Palaeoclimate interpretation of stable isotope data from lake sediment archives. *Quaternary Science Reviews* 23, 811–831.
- Liu, W., Huang, Y., 2005. Compound specific D/H ratios and molecular distributions of higher plant leaf waxes as novel paleoenvironmental indicators in the Chinese Loess Plateau. *Organic Geochemistry* 36, 851–860.
- Martin, L., Flexor, J.M., Suguio, K., 1995. Vibrotestemunhador leve. Construção, utilização e potencialidades. *Rev. IG. Sao Paulo* 16, 59–66.
- Martin, L., Mourguiart, P., Sifeddine, A., Soubiès, F., Wirmann, D., Suguio, K., Turcq, B., 1997. Astronomical forcing of contrasting rainfall changes in tropical South America between 12,400 and 8800 cal yr BP. *Quaternary Research* 47, 117–122.
- Marseille, F., Disnar, J.R., Guillet, B., Noack, Y., 1999. *n*-Alkanes and free fatty acids in humus and A1 horizons of soils under beech, spruce and grass in the Massif Central (Mont-Lozère) France. *European Journal of Soil Science* 50, 433–441.
- Maslin, M.A., Burns, S.J., 2000. Reconstruction of the Amazon basin effective moisture availability over the past 14,000 Years. *Science* 290, 228–2287.
- North Greenland Ice Core Project members, 2004. High-resolution record of Northern Hemisphere climate extending into the Last Interglacial period. *Nature* 431, 147–151.
- Peterson, L.C., Haug, G.H., Hughen, K.A., Röhl, U., 2000. Rapid changes in the hydrologic cycle of the Tropical Atlantic during the Last Glacial. *Science* 290, 1947–1951.
- Petit, J.R., Jouzel, J., Raynaud, D., Barkov, N.I., Barnola, J.M., Basile, I., Bender, M., Chappellaz, J., Davis, J., Delaygue, G., Delmotte, M., Kotlyakov, V.M., Legrand, M., Lipenkov, V., Lorius, C., Pépin, L., Ritz, C., Saltzman, E., Stievenard, M., 1999. Climate and Atmospheric History of the Past 420,000 years from the Vostok Ice Core, Antarctica. *Nature* 399, 429–436.
- Ronchail, J., Cochonneau, G., Molinier, M., Guyot, J.L., Goretto de Miranda Chaves, A., Guimarães, V., de Oliveira, E., 2002. Rainfall variability in the Amazon Basin and SSTs in the tropical Pacific and Atlantic oceans. *International Journal of Climatology* 22, 1663–1686.
- Sachse, D., Radke, J., Gleixner, G., 2004. Hydrogen isotope ratios of recent lacustrine *n*-alkanes record modern climate variability. *Geochimica et Cosmochimica Acta* 68, 4877–4889.
- Sachse, D., Radke, J., Gleixner, G., 2006. δ D values of individual *n*-alkanes from terrestrial plants along a climatic gradient—implications for the sedimentary biomarker record. *Organic Geochemistry* 37, 469–483.
- Sauer, P., Eglinton, T.I., Hayes, J.M., Schimmelmann, A., Sessions, A., 2001. Compound-specific D/H ratios of lipid biomarkers from sediments as a proxy for environmental and climatic conditions. *Geochimica et Cosmochimica Acta* 65, 213–222.
- Schefuß, E., Schouten, S., Schneider, R.R., 2005. Climatic controls on central African hydrology during the past 20,000 years. *Nature* 437, 1003–1006.
- Sessions, A.L., 2006. Seasonal changes in D/H fractionation accompanying lipid biosynthesis in *Spartina alterniflora*. *Geochimica et Cosmochimica Acta* 70, 2153–2162.
- Sifeddine, A., Bertaux, J., Mourguiart, Ph., Disnar, J.R., Laggoun-Défarge, F., 1998. Etude de la sédimentation lacustre d'un site de forêt d'altitude des Andes centrales (Bolivie). Implications Paléoclimatiques. *Bulletin de la Societe Geologique de France* 169, 395–402.
- Sifeddine, A., Martin, L., Turcq, B., Volkmer-Ribeiro, C., Soubiès, F., Campello Cordeiro, R., Suguio, K., 2001. Variations of the Amazonian rainforest environment: a sedimentological record covering 30,000 years. *Palaeogeography, Palaeoclimatology, Palaeoecology* 168, 221–235.
- Sifeddine, A., Albuquerque, A.L.S., Ledru, M-P., Turcq, B., Knoppers, B., Martin, L., Zamboni de Mello, W., Passenau, H., Landim Dominguez, J.M., Campello Cordeiro, R., Abrao, J.J., Bittencourt, A.C., 2003. A 21000 cal years paleoclimatic record from Caçó Lake, Northern Brazil: evidence from sedimentary and pollen analyses. *Palaeogeography, Palaeoclimatology, Palaeoecology* 189, 25–34.
- Smith, F.A., Freeman, K.A., 2006. Influence of physiology and climate on δ D of leaf wax *n*-alkanes from C3 and C4 grasses. *Geochimica et Cosmochimica Acta* 70, 1172–1187.
- Stoecker, T.F., 2003. South dials north. *Nature* 424, 496–499.
- Stuiver, M., Reimer, P.J., 1993. Extended 14 C database and revised CALIB 3.0. 14 C age calibration program. *Radiocarbon* 35, 215–230.
- Stuiver, M., Reimer, P.J., Braziunas, T.F., 1998. High-precision radiocarbon age calibration for terrestrial and marine samples. *Radiocarbon* 40, 1127–1151.
- Turcq, B., Cordeiro, R.C., Sifeddine, A., Simoes Filho, F.F., Abrao, J.J., Oliveira, F.B.O., Silva, A.O., Capitaneo, J.L., Lima, F.A.K., 2002. Carbon storage in Amazonia during the LGM: data and uncertainties. *Chemosphere* 49, 821–835.
- van't Veer, R., Islebe, G.A., Hooghiemstra, H., 2000. Climatic change during the Younger Dryas chron in northern South America: a test of the evidence. *Quaternary Science Reviews* 19, 1821–1835.
- Wang, X., Auler, A.S., Edwards, R.L., Cheng, H., Cristalli, P., Smart, P.L., Richards, D.A., Shen, C.-C., 2004. Wet periods in northeastern Brazil over the past 210 kyr linked to distant climate anomalies. *Nature* 432, 740–743.
- Yapp, C.J., Epstein, S., 1982. Climatic significance of the hydrogen isotope ratios in tree cellulose. *Nature* 297, 636–639.

Laminated sediments off the Central Peruvian Coast record changes in terrestrial runoff, water mass oxygenation and upwelling productivity over recent centuries.

Sifeddine, A.¹, Gutierrez, D.², Ortlieb, L.¹, Boucher, H.¹, Velazco, F.², Field, D.³, Vargas, G.⁴, Boussafir, M.⁵, Salvatelli, R.², Ferreira, V.⁶, García, M.¹, Valdes⁷, J., Caquineau, S.¹, Mandeng Yogo, M.¹, Cetin, F.¹, Solis, J.², Soler, P.⁸, Baumgartner, T.⁶

1. UR 055. PALEOTROPIQUE. IRD. 32, Avenue Varagnat 93 143 Bondy. France.
2. IMARPE, Esquina Gamarra y General Valle s/n, Callao, 22000 Peru.
3. Monterey Bay Aquarium Research Institute, 7700 Sandholdt Road, Moss Landing, CA 95039, USA.
4. Departamento de Geología, Facultad de Ciencias Físicas y Matemáticas, Universidad de Chile.
5. Institut des Sciences de la Terre (ISTO), Université de Orléans, Orléans, France.
6. CICESE, Km. 107 Carretera Tijuana - Ensenada, Ensenada, 22860 Mexico.
7. Facultad de Recursos del Mar, Universidad de Antofagasta, Casilla 170, Antofagasta, Chile
8. UMR-LOCEAN. 5, Place Jussieu, Paris, 75005 France.

Key words: Humboldt Current System, laminated sediments, centennial variability, recent Holocene, paleoceanography.

Abstract:

Sedimentological studies including X-Ray digital analyses, mineralogy, inorganic contents, and organic geochemistry on laminated sediments accumulated in the Oxygen Minimum Zone (OMZ) of the Central Peruvian margin reveal variable oceanographic and climate conditions during the last 500 years. Coherent downcore variations in sedimentological and geochemical markers in box cores taken off Pisco and Callao indicate that the studied proxies have a regional significance. Most noteworthy is a large shift in proxies at ~1815 AD, as determined by ²¹⁰Pb and ¹⁴C radiometric dating. This shift is characterized by an abrupt increase in the enrichment factor for Mo, indicating a regional intensification of the oxygen minimum zone, in parallel with an increase in Total Organic Carbon (TOC) and inferred productivity. In addition, there is a lower terrestrial input of quartz, feldspar and clays to the margin. Based on these results, we interpret that during several centuries prior to 1815 (AD), which corresponds to the Little Ice Age (LIA), the northern Humboldt Current region was marked by lower productivity, a weaker Oxygen Minimum Zone (OMZ), and higher terrestrial input related with more humid conditions in the continent and/or an intensified poleward subsurface circulation. We interpret this shift as being caused by a southward displacement of the InterTropical Convergence Zone during the LIA. Since 1870, a simultaneous increase in Total Organic Carbon (TOC) and mineral terrigenous fluxes suggest an increase of wind-driven upwelling resulting in higher productivity. These conditions were intensified during the 20th century, which is supported by instrumental records of wind forcing.

1. Introduction.

The Humboldt Current System is characterized by coastal upwelling and is considered one of the most productive marine ecosystems in the world. Due to its large latitudinal extension, the system exhibits varying intensity and persistency of upwelling along the year (Thomas et al., 1994). Off the Peruvian coast, the perennial upwelling and high rates of primary production support the largest portion of the Humboldt's fish production and one of the world's largest fisheries. At the interannual time scale, oceanic circulation and upwelling processes are modulated periodically by the El Niño-Southern Oscillation (ENSO) cycle, manifested as changes in the surface biological production, subsurface oxygenation, and terrestrial runoff to the continental margin. Variability on decadal timescales is observed in instrumental records (Chavez et al., 2003), but understanding the nature of long-term variability is hindered by long records.

Paleoceanographic and paleoclimatic changes can be recovered from marine sediments at different temporal resolutions, depending on preservation conditions of the proxies during sedimentation and post deposition. Preservations of paleo records are enhanced along portions of the Peruvian margin by an intense Oxygen Minimum Zone (OMZ) in the water column (Helly & Levin, 2004). In the Southern Hemisphere, this layer extends from the Southeastern to the Equatorial Pacific, and its formation and maintenance is supported by basin-scale circulation processes (Lukas, 1986). The high surface-water productivity and resulting high organic carbon fluxes contribute to amplify the oxygen consumption in the subsurface waters near the coast.

Most paleoceanographic studies in the western margin off South America have focused at glacial and interglacial time scales, by reconstructing changes in temperature, salinity, and paleoproductivity (Suess et al., 1990; Fink et al., 2006; Rein et al., 2007) while only a few studies have examined paleoenvironmental changes during the last millennium (McCaffrey et al., 1990, Rein et al., 2005, Gutierrez et al., 2006). Several sedimentary accumulation zones along the Central Peruvian continental margin have optimum conditions (disoxia, high sedimentation rates, topography among others factors) to preserve past environmental events with high temporal resolution (Suess et al., 1988; Reinhardt et al., 2002; Gutierrez et al., 2006). Sedimentological observations by Gutierrez et al., 2006 indicate that laminated sediments from the central Peruvian margin can lead to detailed reconstructions of paleoceanographic evolution during the last few centuries. Like in other favourable regions, the combination of high productivity and near-anoxic conditions over the Peruvian margin result in the preservation of interannual to decadal-scale variations in upwelling and climate by organic and inorganic geochemical processes (Krissek & Scheidegger, 1983; Suess et al., 1990, Böning et al., 2004; MacManus et al., 2006).

The objective of this study is to investigate changes in terrestrial input, water mass oxygenation and upwelling productivity during the last 500 years for the Central Peruvian margin. To achieve our goal, we analyzed the mineral content, as well as organic and inorganic geochemical proxies from two sediment boxcores collected off Central Peru. To identify long-term variations in productivity and oxygen content, we examined the TOC content, which indicates the abundance of organic matter and inferred productivity, and an Oxygen Index (OI) that accounts to the degree of oxygenation of the organic matter. Additionally, we studied the downcore mineralogical composition to infer the terrigenous input from the continent, as related to wind-driven transport and runoff (Vargas et al., 2004; Rein et al., 2007). Past changes of oxygenation were inferred from the downcore distribution of the redox-sensitive metal Molybdenum. Redox-sensitive metals tend to switch from dissolved to particulate phases upon changes in their oxidation state. This particular behavior has permitted their use as proxies of the oxidation state of both the water column and the sedimentary environment that prevailed when the sediment was deposited. In particular, Molybdenum has been considered a sensitive proxy for the intensity and displacement of OMZ (MacManus et al., 2006; Böning, 2004).

2. Oceanographic Setting

Coastal upwelling occurs along the eastern margins of major oceanic basins when predominantly along-shore winds and Coriolis force drive surface waters offshore and these are replaced by deeper, cooler and nutrient-rich waters. The enhanced biological productivity observed close to these upwelling cells induces an increased flux of organic material to the coastal ocean floor, resulting in characteristic biogeochemical properties of the water column and sediments. The oxygen deficiency in the water column and relatively shallow shelf limit organic matter degradation processes favor the preservation of biogenic remains. Thus the organic carbon content of sediments beneath upwelling environments may reach 10% (Libes, 1992; Hedges and Keil, 1995) while mean oceanic values vary between 0.2% and 0.4% (Muller and Suess, 1979; Duan, 2000).

Upwelling favorable alongshore winds are present along the Peruvian coast all year long. Coastal upwelling reaches its maximum intensity near 14°S-16°S, and weakens towards the north, near Punta Falsa (6°S) (Echevin et al., 2004). Upwelling events last from a few days to a week and are stronger and more frequent in winter due to increases in winds offshore associated with a strengthened subtropical high pressure cell. The wind-driven surface circulation consists in a shallow, equatorward, coastal jet (Strub et al., 1998), with maximum intensity in winter, known as the Peruvian Coastal Current (PCC). This current can be identified by the shoaling of isopycnals in the surface layers nearshore. Offshore, the circulation is dominated by poleward flows, identified as the Peru Chile Counter Current (PCCC), which advect warm and saline waters from tropical origin (Lukas, 1986). Below the surface coastal current, the subsurface, coastally trapped, Peru-Chile Undercurrent (PCUC) advects saline (35.0-35.1 PSU) tropical waters poleward. Its signature is characterized by the deepening of isopycnals towards the coast at 50-200 m depth (Echevin et al., 2004).

Off the Central Peruvian coast (09 – 15°S), the upper margin sediments are typically organic-rich, becoming disoxic in the continental shelf. Excess ^{210}Pb - derived sedimentation rates vary from 0.04 to 0.15 cm yr^{-1} (Reimers & Suess, 1983, Levin et al., 2003). Based on previous sedimentological and geochemical information from exploratory surveys and literature, the Callao (~12°S) and Pisco (~14°S) areas were selected to perform box coring on board the R/V Olaya (IMARPE) in May 2004. Two Soutar-box cores were collected: one from the shelf off Callao (B0405-13, 12°00'S, 72°42'S, 184 m)

and the other one from the upper slope off Pisco (B0405-06, 14°07'S, 76°30'S, 299 m) (Gutierrez et al., 2006) (Figure 1).

3. Analytical Procedures

Sedimentary structures were documented by X-radiography (SCOPIX, Migneon et al., 1999). Chronological models for the last 130 years were developed by using the downcore distributions of natural excess ^{210}Pb and ^{228}Th and of the bomb-derived ^{241}Am . The chronology beyond the last 130 years was inferred from radiocarbon ages, properly calibrated from local reservoir effects (Gutiérrez et al., 2006b).

The qualitative and quantitative mineralogical composition was obtained by X-Ray Diffraction (XRD) and by Fourier Transformed Infrared Spectrometry (FTIR) respectively. For FTIR analyses, samples were placed in a KBr disc, which ensures that Lambert-Beer's law is valid. A quantitative determination of the mineral content from various blends was performed by making a multi-component analysis of the experimental spectrum using the spectra of each component in the mixture (Bertaux et al., 1998).

Organic matter characterization and quantification were done using Rock-Eval 6 programmed pyrolysis, from which the following parameters were obtained: Total Organic carbon (TOC %) reflects the quantity of organic matter (OM) present in the sediment, the hydrogen Index (HI, in mg HC/g TOC) is the amount of hydrocarbonaceous (HC) products released during pyrolysis, and the Oxygen Index (OI, OIRe6 in mg O₂/g TOC) gives the oxygen content of the OM. OI is calculated from the amounts of CO and CO₂ released during pyrolysis. The two indexes are normalized to TOC (Lafargue et al., 1998). Analyses of Molybdenum (Mo) and Aluminum (Al) concentrations was carried out by (ICP-MS, Ultramass Varian) and (ICP-AES) respectively after hot plate acid digestion (combination of acid HF, HNO₃, HClO₄), which was used to eliminate organic matter and to remove silicates (Zwolsman et al., 1996; Cho et al., 1999).

Here, we show the Molybdenum (Mo) concentrations, which are used in this study to reconstruct the variations of anoxic conditions. Our choice is based on McManus et al., (2006) work, which showed how Mo scavenging is principally controlled by anoxic conditions. Under disoxic to anoxic conditions, soluble Mo is converted to particle reactive thiomolybdates, which are removed from solution via sulfidized organic material or via sequestration by Fe–S phases. A normalization procedure using Al for the metal concentrations permitted the variation to be compensated-for in both textural and composition characteristics. Moreover, according to Valdes et al. (2005), this method is a powerful tool for regional comparison and evaluating the terrestrial input of trace metals in the sediments; the method is also applied to determine Enrichment Factors (EFs) according the equation described by Tribouillard et al. (2006): $EF = (\text{Mo}/\text{Al})_{\text{sample}}/(\text{Mo}/\text{Al})_{\text{average shale}}$. The Average Shale values correspond to Turekian and Wedepohl (1961). EFs close to one indicate a crustal origin of the metal, whereas EFs over 10 denote non-crustal sources.

The particulate fluxes for each constituent are calculated by multiplying the concentration of each constituent by the sediment accumulation rate. In general terms, this relation can be expressed as: sediment flux ($\text{mg}\cdot\text{cm}^{-2}\cdot\text{yr}^{-1}$) = element concentration ($\text{mg}\cdot\text{g}^{-1}$) x sediment accumulation rate ($\text{g}\cdot\text{cm}^{-2}\cdot\text{yr}^{-1}$). This approach has the advantage of providing information on the inputs of different constituents independent of their relative dilution in the matrix. The fluxes estimation for each element thus provides information on the inputs of different constituents independent of their relative dilution in the matrix.

Thin sections were prepared constructed every 10 cm from resin-impregnated samples of the core B0405-13. The water in the sediments is replaced by acetone prior to impregnation with resin following Bénard, (1996), Zaragosi, et al. (2006). The marine sediment section is exposed to the vapour of aqueous acetone of increasing concentration up to 100 percent acetone. After impregnation with resin, high quality thin sections were obtained. The structure of the laminations was analysed using a polarised light microscope, with a magnification of 20.

In order to estimate the shared variability of the environmental proxies and their relationships with one another, we applied a Principal Component Analysis (PCA).

4. Results

4.1. Lithology and chronology

Core X-ray images reveal the existence of band and laminations (< 5 mm thickness), formed by the succession of light (dense) and dark (low) layers, which were probably deposited with negligible bioturbation under nearly anoxic conditions (Figure 1). Three stratigraphic units can be distinguished

within the Pisco core. The basal unit (74-62 cm) is formed by the succession of several primarily banded sediments. The second unit, which starts at 62 and extends to 34 cm presents a slump at the base (55-52 cm). This unit, which is characterized by a greater density, showing up as light in the x-radiograph (Figure. 1), corresponds to a sequence of couplets of dark and light laminae, which range from 2-5 mm in thickness. The upper unit (34-0cm), with average lower density, is marked by the successions of primarily thick band couplets (ca. 1 cm thick). In the core of Callao, the x-ray image reveals also the existence of three units that are similar to the Pisco core in density and depth. The first one (84-66 cm) is also characterized by the existence of banded structures. The second unit (66-34cm) is more dense, as it is in the Pisco core, but is formed by thick bands couplets of ~1 cm (rather than fine laminations observed in Pisco) and is interrupted by several slumps in the middle of the unit. The last unit (34-0cm), is characterized by a low density and is formed by both the succession of altogether millimetric laminae and broader bands.

Average sedimentation rates for the period after 1870 are 2.2 mm yr⁻¹ and 2.1 mm yr⁻¹ for the Pisco core and Callao cores respectively. For the centuries prior to 1870 respective average sedimentation rates of 1 mm yr⁻¹ and 0.6 mm yr⁻¹ have been estimated (Gutiérrez et al., 2006b). As chronological models do not resolve interannual and decadal-scale variability of sedimentation rates, especially prior to 1870, the results are presented both in terms of concentrations (%) and fluxes.

4.2. Characterization of the mineral fraction

X ray diffraction analyses (XRD) performed on samples from both cores (B6 and B13) show that the mineral terrigenous fraction is composed of quartz, feldspar, kaolinite, illite and vermiculite. The variations in downcore contents of those fractions show similar patterns at both sites (Figure 2) and broadly fall into three units, which confirm the lithological description.

Unit I (before 1400) is characterized by low quartz, feldspar and clays content, corresponding to mean abundances of 6, 10 and 10% respectively. Unit II (~1400-1815) begins with an increase of quartz (5 to 15%), feldspar (10 to 20%) and clays (10 to 28%) and concentrations remain relatively stable until the top of the unit. Unit III (1815-2002) starts with a decrease in concentrations of quartz, feldspar and clays which reach minimum values and then show a progressive increase to the top of this unit reaching values around 10, 15 and 20% respectively.

The variations in downcore fluxes of those fractions, show similar patterns than, the variations in percent composition at both sites (Figure 3) and broadly correspond to the three different stratigraphic units. The time period dated before 1400 (Unit I) is marked by low fluxes of quartz, feldspar and clays with mean values varying around 2, 2 and 4 mg.cm⁻².yr⁻¹ respectively. The time period spanning Unit II (1400-1815) is characterized by high fluxes of quartz, feldspar and clays with mean values varying around 4, 3 and 6 mg.cm⁻².yr⁻¹, respectively. The time period spanning the early period of Unit III (1815 to 1870) begins with an abrupt decrease in fluxes of quartz (4 to 0.5 mg.cm⁻².yr⁻¹), feldspar (3 to 1 mg.cm⁻².yr⁻¹) and clays (6 to 1 mg.cm⁻².yr⁻¹). Finally the latter period within stratigraphic Unit III (1870-2002) is characterized by a trend towards increasing fluxes of quartz, feldspar and clays, beginning around 1870, and intensifying around 1950 with values around 6, 7 and 8 mg.cm⁻².yr⁻¹ respectively in the surficial sediments.

4.3. Characterization of inorganic fraction

Downcore variations in Aluminium (Al) concentrations are similar to the variability in clays described above (Figure 2). Al values are moderately low (3%) during the first Unit and then increase, reaching highest concentrations during stratigraphic Unit II, from 1400 to 1815 (5%). During the last stratigraphic unit (1815-2002), the Al content initially decreases, reaching minimum values around 1870 (1%), and then shows a progressive trend towards the top (6%).

In contrast, the downcore variations in Mo content (mg.kg⁻¹) show a similar trend than variable mineral fraction only into the last unit, i.e from 1815 to 2002 (Figure 2). The Mo content varies around 75 (mg.Kg⁻¹) before 1400 (Unit I), decreases and stays stable varying around low values (25 mg.Kg⁻¹) throughout stratigraphic Unit II (1400-2002). For the last unit (1815 to 2002), the Mo content increases progressively reaching maximum values (75 mg.kg⁻¹)

The enrichment Factor (EF) measured for Mo in both cores is greater than the crustal average which suggests another origin than continental input of this metal. The downcore variation in EF for Mo mimics the variability of mineral fractions only during the last period described above (Figure 3). The period before 1400 (Unit I) is marked by an EF around 120. From 1400 to 1815 (unit II), the EF shows a decrease with minimum values around 50. There are increases in EF ratios in both cores beginning around 1815 (Unit III), although Callao has a much higher maximum (500) than Pisco (300). With

respect to the aforementioned periods, EF values fluctuate around relatively moderate values in Callao from 1870 to 2002. Whereas EF values in the Pisco core fluctuate around similar levels from 1815 to 2002.

4.4. Characterization of the organic fraction

Variability in total organic carbon (TOC) shows some correspondence and differences with the sedimentological and mineralogical variability observed in cores B6 and B13 respectively (Figure 2). Stratigraphic Units I and II are characterized by low TOC content (5%) accompanied by high values of Oxygen Index (OI) around 120 and 80 respectively at Pisco and Callao. There is a large increase in TOC content during the last Unit, with higher values in the Callao core (16%) than at Pisco (12 %). This trend in TOC is accompanied by a progressive decrease of OI reaching values around 80 at Callao and 100 at Pisco.

TOC fluxes downcore show some correspondence and differences with the sedimentological and mineralogical variability observed in cores B6 and B13 respectively (Figure 3). Units I and II are characterized by low TOC fluxes (around $1 \text{ mg.cm}^{-2}.\text{yr}^{-1}$). There is a large increase in percent TOC content around 1815, which is associated with decreases in quartz and other minerals. However, estimated TOC fluxes do not increase until 1870 in both records.

4.5. Principal Component Analysis.

The PCA was applied to a matrix including mineral contents (quartz, feldspar, and sum of clays), metal contents (Al and Mo), TOC content and Oxygen Index for each core. Concentrations were used rather than fluxes since uncertainties in chronology can modify estimated flux rates. In particular, if the change in sedimentation rates reported at 1870 is associated with changes in % TOC, then the period from 1815-1850 may also have higher sedimentation rates and consequently, higher fluxes of TOC and other constituents. At each site more than 74% of variance is explained by two factors (Figure 4). The first principal component factor indicates a negative correlation between the contents of the terrigenous fraction (quartz, feldspar, clays and Aluminum) on one hand and primarily Molybdenum, and secondarily TOC, on the other hand. The second factor has a strong loading on the organic fraction, which marks a negative correlation between the TOC content and the oxygenation OI of the sedimentary organic matter (Figure 4).

5. Discussion:

The parallel downcore variations of PC1 (Figure 5) in the Pisco and Callao sites indicate that the developed proxies have a regional significance, of which a clear shift at ~1815 AD in both stratigraphic observations and the sedimentological constituents is most noteworthy. In contrast, the change in sedimentological units at the base of the cores (between Units I and II) does not show an associated change in sedimentological constituents. Although density and color vary little within the upper stratigraphic unit (Unit III) relative to differences between stratigraphic units, there are noteworthy fluctuations in the sedimentological constituents within Unit III that arise from variations in fluxes of TOC and other constituents. Based on these results, we interpret that a large reorganization of climatic conditions occurred at ~1815, which was of greater magnitude than other climate fluctuations of the last several centuries.

The Climatic Shift around 1815

High mineral fluxes characterize the period from 1400 to 1815 (AD), which corresponds to the Little Ice Age (LIA or rather its South-American equivalent). The simultaneous decrease of terrigenous fluxes marks probably a change from humid to drier conditions in the hinterland. Examination of thin sections of samples deposited at Callao, during this period, shows that most terrigenous particles (quartz and feldspar), which have sizes of 50 to 80 μm , present angular to sub-angular aspects, , thus suggesting rather a fluvial than aeolian source (Photo 1), rather than aeolian. Based on the particle shapes, we interpret the higher terrigenous fluxes in Pisco in the same period as reflecting an increase of river discharge along the Peruvian coast. Since there are more riverine mouths near Callao than at Pisco, the similar patterns of flux at both sites suggest that some common cause may involve alluvial input, near-shore mixing, and southward transport of the particles toward Pisco by poleward subsurface circulation.

The negative values of PC1 (Figure 5), during the period that corresponds to the LIA reflect both the high mineral content and low Mo content (Figure 3). Deposition of Mo requires an intense oxygen deficiency to scavenge it from solution (Boning et al., 2004; Valdes et al., 2005, MacManus et al., 2006). Low values of EF for Mo from 1400 to 1815 can be explained by higher contents of dissolved

oxygen in the water column due to a weaker Oxygen Minimum Zone (OMZ). A more oxygenated water column is associated with lower productivity and greater oxidation of organic matter, but it is difficult to discriminate the relative influences of each phenomena.

Based on these results, we interpret that the period dated from 1400 to 1815 (AD), which corresponds to the LIA period was marked by a lower productivity, a weaker Oxygen Minimum Zone (OMZ), a deeper thermocline and higher terrestrial input related with more humid conditions on the continent. Paleotemperature reconstructions from a short sediment core retrieved from the coastal upwelling center at 15°S off southern Peru (McCaffrey et al., 1990) show, during the same period, higher SSTs associated with lower total organic carbon fluxes also suggest a deeper thermocline.

Deciphering possible mechanisms, which forced the climate shift of ~1815 may benefit from comparisons with other paleo records (Figure 6). In the Cariaco basin (Haug et al., 2001; Peterson and Haug, 2006) drier conditions are indicated for the LIA by generally decreased Ti contents linked to decreased detrital delivery to Cariaco basin from local rivers during the same period. This has been interpreted by Peterson and Haug (2006) as a southward shift in the mean latitudinal position of the InterTropical Convergence Zone (ITCZ). That shift of the ITCZ should cause increased humid conditions in the regions to the south of the current ITCZ, such as the Peruvian hinterland, favoring detrital delivery to the Peruvian margin.

The increase of Ti content around 1815 in the Cariaco basin (Figure 6) is linked to an increase of detrital delivery from local rivers to this basin, suggesting a northward shift in the ITCZ. Note that the increase in the EF for Mo is inconsistent with an increase in Mo attributed to terrestrial fluxes. Rather, these simultaneous changes in redox sensitive metal and terrigenous contents in Pisco and Callao are consistent with changes in oceanographic conditions. This regional response is likely a result of the establishment of new ocean-atmosphere connections that control the position of the ITCZ.

At seasonal and interannual time-scales, an ITCZ southward shift is associated with the southward projection of surface Equatorial and Tropical water masses. During El Niño events, there is also a deepening of the thermocline and nutriclines off the Peruvian coast due to changes in Walker circulation across the tropical Pacific (Zuta & Guillén, 1970; Arntz & Fahrbcch, 1996). Hence, a prolonged southward shift of the mean ITCZ latitudinal position over the eastern Pacific and South American continent may explain both a different water mass structure (warmer, more oxygenated and nutrient-poorer) and higher terrestrial influx before ca. 1815 AD. However, an additional consequence of a southward shift in the ITCZ would be a reduced strength of the subtropical high pressure cell that drive the upwelling favorable winds. Reduced wind forcing may also result in lower productivity and hence lower export production, accounting for less oxygen consumption through the water column. Thus we interpret the period of higher oxygenation as a consequence of both basin-scale forcing and reduced regional upwelling and export production.

Variations since the climatic shift

Within stratigraphic Unit III, there is an overall tendency towards increasing TOC associated with two different periods. From 1815 onwards, the increase of PC1 values in the two sites, related to higher values of EF for Mo is due to high Mo removal rates from solution, increasing its accumulation in bottom sediments under anoxic conditions and indicating a regional enhancement of the oxygen deficiency (Figure 5). This result is also marked by the negative shift of PC2 values that reflect an increase in the TOC flux and reduced oxygenation of the sedimentary organic matter, which is consistent with an enhancement of the productivity and consequently oxygen deficiency in the water column.

The increase in PC2 between 1850 and 1870 reflects a reduced TOC flux and an increase in oxygenation of the organic matter. The hydrographic link to an abrupt increase of OI marks an oxygenation event of the water column and a decrease in TOC favoring both the oxidation of organic matter. Following the excursion in PC2 from 1850-1870, we note a negative shift of PC2 values that reflect, an increase in TOC fluxes and reduced oxygenation of the sedimentary organic matter. This trend coincides with an increase of the dominance of anoxia tolerant taxa in the benthic foraminiferal assemblage at Pisco (Morales et al., 2006). An increase in TOC flux is also recorded at the same period by laminated sediments at 15°S off the Peruvian margin (McCaffrey et al., 1990) and at Mejillones Bay (23°S) off northern Chile (Valdés et al., 2004; Vargas et al., 2004, Vargas et al., in

press), suggesting a regional response of primary production. These conditions are probably the result of a progressive intensification of the upwelling regime, following the major shift of the water mass structure several decades before.

Finally, the intensification of PC2 in Pisco during the 20th century reflects a further increase in TOC flux, simultaneously with an additional OI decrease. Records of instrumental data show an enhanced intensity of alongshore winds during the same period (Jahncke et al., 2004) (Figure 6). Thus these results indicate an enhancement of anoxic conditions generated by the intensification of productivity due to enhanced wind forcing. This interpretation is supported by the negative trend of PC1, that is also present in other records of the Peruvian margin (Rein, 2007), reflecting mostly a higher terrigenous input, but explained by stronger winds rather than by runoff.

6. Conclusion.

Laminated sediments off the Central Peruvian margin which are accumulated under specific oceanographic conditions (intense upwelling, disoxia, high sedimentation rates) preserve and record different oceanographic and climatic changes during the last half millennium. The use of different organic, mineral and inorganic proxies result in different temporal and spatial signals linked to productivity, structure of the OMZ, and terrigenous input. Changes in the terrigenous input prior to the twentieth century likely correspond to changes in continental humidity, which affects fluvial transport and is consequently homogenized by oceanic mixing. A comparison with Cariaco basin downcore records of regional precipitation and runoff supports our interpretation that before 1815, a more southerly position of the InterTropical Convergence Zone (ITCZ), resulted in prevailing more humid conditions in the hinterland. In addition, a southerly position of the ITCZ is associated to a shift in water mass circulation, reduced subtropical high pressure that results in weaker alongshore winds, lower primary productivity, and a weaker OMZ due to reduced organic matter flux and a deepening of the water column structure off the Peruvian coast.

The enhancement of the oxygen deficiency (OMZ intensification) during the last century is simultaneous with a positive trend in TOC and inferred productivity as results from increased upwelling. An increase in upwelling favorable winds is supported by the increase of terrigenous wind-driven transport as well as by instrumental records.

Acknowledgements:

This study was supported by the IRD PALEOTROPIQUE research unit (UR 055, IRD) and the IMARPE PALEOMAP research program, as well as by the PALEOPECES project (IMARPE-IRD), the IAI small grant project SGP 211-222 (PI: D. Gutiérrez), the Humboldt Current System program (ATI-IRD) and finally the PCCC project (French national research agency ANR, P.I. B. Dewitte). We thank the Instituto del Mar del Peru (IMARPE) for full support of this research and acknowledge the crew of the RV José Olaya Balandra and other scientific participants in the box-coring survey.

References.

- Arntz, W. and Fahrbach, E. (1996). El Niño: experimento climático de la naturaleza. Causas físicas y efectos biológicos, Fondo de Cultura Económica, México, D.F, 309 p.
- Bénard, Y. (1996). Les techniques de fabrication des lames minces de sol. Cahiers Techniques INRA, v.37, 29-42.
- Bertaux, J., Frohlich, F., Ildelfonse, Ph. (1998). Multicomponent analysis of FTIR spectra: quantification of amorphous silica and crystallized mineral phases in synthetic and natural sediments. *J. Sediment. Res.* 68 (3), 440–447.
- Böning, Ph., Brumsack, H.J., Böttcher, M.E., Schnetger, B., Kriete, C., Kallmeyer, J., Borchert, S.L. (2004). Geochemistry of Peruvian near-surface sediments. *Geochimica et Cosmochimica Acta*, 68, 4429–4451.
- Chavez, F.P., Ryan, J., Lluch-Cota, S. E., Ñiquen, M.C. (2003). From anchovies to sardines and back: Multidecadal change in the Pacific Ocean. *Science* 299, 217-221
- Cho, Y., Lee, C., Choi, M., (1999). Geochemistry of surface sediments off the southern and western coast of Korea. *Marine Geology* 159, 111–129.
- Didyk, B., Simoneit, B., Brassell, S., Eglinton, G., (1978). Organic geochemical indicators of paleoenvironmental conditions of sedimentation. *Nature* 272 (5660): 216-222.
- Duan, Y. (2000). Organic geochemistry of recent marine sediments from the Nansha Sea, China. *Organic Geochemistry* 31, 159–167.

- Echevin, V., Puillat, I., Grados, C., Dewitte, B., (2004). Seasonal and mesoscale variability in the Peru upwelling system from in situ data during the years 2000 to 2004. *Gayana*, 68 (2), supl., p.167-173. ISSN 0717-6538.
- Gutierrez, D., Sifeddine, A., Reyss, J.L., Vargas, G., Salvattecchi, R., Ferreira, V., Ortlieb, L., Field, D., Baumgartner, T., Boussafir, M., Boucher, H., Valdes, J., Marinovic, L., Soler, P., Tapia, P. (2006a). Anoxic sediments off central Peru record interannual to multidecadal changes of climate and upwelling ecosystem during the last two centuries. *Advances in Geosciences*, 6, 119-125.
- Gutierrez, D., Vargas, G., Ortlieb, L., Reyss J.L., Sifeddine, A. (2006b). Precise age models from recent laminated sediments of the Central Peruvian margin. XIII Congreso Peruano de Geología. Resúmenes Extendidos Sociedad Geológica del Perú, p. 541 – 542.
- Hedges, J., Keil, R. (1995). Sedimentary organic matter preservation, an assessment and speculative synthesis. *Marine Chemistry* 49, 81–115.
- Helly, J., Levin, L. (2004). Global distribution of naturally occurring marine hypoxia on continental margins. *Deep-Sea Research I* 51, 1159-1168.
- Haug, G.H., Hughen, K.A., Sigman, D.M., Peterson, L.C., Röhl, U. (2001). Southward migration of the Intertropical Convergence Zone through the Holocene. *Science* 293, 1304– 1308.
- Jahncke, J., Checkley, D., Hunt, G. L. (2004). Trends in carbon flux to seabirds in the Peruvian upwelling system: effects of wind and fisheries on population regulation, *Fisheries Oceanography*, 13 (3), 208.
- Krissek, L.A., Scheidegger, K.F. (1983). Environmental controls on sediment texture and composition in low oxygen zones off Peru and Oregon. In: Suess, E. & J. Thiede (eds.). *Coastal upwelling; its sediment record. Part B: Sedimentary records of ancient coastal upwelling*. Plenum Press, New York, pp. 163-180.
- Lafargue, E., Marquis, F., Pillot, D. (1998). Rock-Eval 6 applications in hydrocarbon exploration, production, and soil contamination studies. *Revue de L'Institut Francais du Pétrole* 53 (4), 421–437.
- Levin, L.A., Rathburn, A.E.R., Gutiérrez, D., Muñoz, P., Shankle, A. (2003). Bioturbation by symbiont-bearing annelids in near-anoxic sediments: Implications for biofacies models and paleo-oxygen assessments. *Palaeogeography, Palaeoclimatology, Palaeoecology*. 199, 120-140.
- Libes, S. (1992). *An Introduction to Marine Biogeochemistry*. John Wiley & Sons, Inc., New York. 289 pp
- Lukas, R., (1986). The termination of the equatorial undercurrent in the eastern Pacific, *Prog. Oceanogr.*, 16, 5, 63-90.
- McManus, J., Berelson, W.M., Severmann, S., Poulson, R.L., Hammond, D.E., Klinkhammer, G.P., Holm, Ch. (2006). Molybdenum and uranium geochemistry in continental margin sediments: Paleoproxy potential. *Geochimica et Cosmochimica Acta* 70 (2006) 4643–4662
- Morales, M.C., Field, D., Pastor, S.M., Gutierrez, D., Sifeddine, A., Ortlieb, L., Ferreira, V., Salvattecchi, R., Velasco, F. (2006). Variations in foraminifera over the last 460 years from laminated sediments off the coast of Peru. *Bol. Soc Perú* 101. 5-18.
- Muller, P., Suess, E. (1979). Productivity, sedimentation rate, and sedimentary organic matter in the ocean – I. Organic carbon preservation. *Deep-Sea Research* 26A, 1347– 1362.
- Peterson, L.C. and Haug, G.H. (2006). Variability in the mean latitude of the Atlantic Intertropical Convergence Zone as recorded by riverine input of sediments to the Cariaco Basin (Venezuela). *Palaeogeography, Paeoclimatology, Palaeoecology*, 243, 97-113.
- Reimers, C. E., Suess, E. (1983). Spatial and temporal patterns of organic matter accumulation on the Peru continental margin. In J. Thiede, & E. Suess (Eds.), *Coastal Upwelling: Its sediment record. Part B: Sedimentary records of ancient coastal upwelling* (pp. 311–346). New York: Plenum.
- Rein, B. (2007). How do the 1982/83 and 1997/98 El Niños rank in a geological record from Peru. *Quaternary International*. 161, 56-66.
- Rein, B. Lückge, A., Reinhardt, L., Sirocko, F., Wolf, A., Dullo, W.C. (2005). El Niño variability off Peru during the last 20,000 years. *Paleoceanography*, 20, PA4003, doi:10.1029/2004PA001099.
- Reinhardt, L., Kudrass, H.-R., Lückge, A., Wiedicke, M., Wunderlich, J., and Wendt, G. (2002). High-resolution sediment echosounding off Peru: Late Quaternary depositional sequences and sedimentary structures of a current-dominated shelf, *Mar. Geophys. Res.*, 23, 335–351.
- Strub, P.T., Mesías, J. M., Montecino, V., Rutilant, J. (1998). Coastal ocean circulation off western South America, in: *The global coastal ocean*, edited by: Robinson, A. R. and Brink, K. H., The Sea, Vol. 11, Interscience, New York, p. 273–313.
- Suess, E., R. Von Huene et al. (1990). *Proceedings of the Ocean Drilling Program, Scientific Results*, Vol. 112, 738 p.
- Suess, E., von Huene, R., et al., (1988). *Proc. ODP., Sci. Results*, 112: College Station, TX (Ocean Drilling Program).

- Thomas, A.C., Huang, F., Strub, P.T., James, C. (1994). Comparison of the seasonal and interannual variability of phytoplankton pigment concentrations in the Peru and California Current systems. *J. Geophys. Res.*, 99 (C4), doi: 10.1029/93JC02146.
- Tribouillard, N., Algeo, Th., Lyons, T., Riboulleau, A. (2006). Trace metals as paleoredox and paleoproductivity proxies: An update. *Chem. Geol.*, 232,12-32.
- Turekian, K., Wedepohl, K. (1961). Distribution of the elements in some major units of the earth's crust. *Geol. Soc. Amer. Bull.* 72, 175-192.
- Valdés, J., Sifeddine, A., Lallier-Verges, E., Ortlieb, L. (2004). Petrographic and geochemical study of organic matter in surficial laminated sediments from an upwelling system (mejillones del Sur Bay, northern Chile), *Org. Geochem.*, 35, 881-894.
- Valdés, J., Vargas, G., Sifeddine, A., Ortlieb, L., Guíñez, M. (2005). Distribution and enrichment evaluation of heavy metals in Mejillones Bay (23°S), Northern Chile: Geochemical and statistical approach. *Marine Pollution Bulletin.* 50, 1558–1568.
- Vargas, G., Ortlieb, L., Pichon, J. J., Bertaux, J., Pujos, M. (2004). Sedimentary facies and high resolution primary production inferences from laminated diatomaceous sediments off northern Chile (23° S), *Mar. Geol.*, 211, 79–99.
- Vargas, G., Pantoja, S., Rutllant, J.A., Lange, C.B., Ortlieb, L. Enhancement of coastal upwelling and interdecadal ENSO-like variability in the Peru-Chile Current since late 19th century. *Geophysical Research Letters.* In press.
- Zuta, S., Guillén, O. (1970). Oceanografía de las Aguas Costera del Perú, Dpto de Oceanografía. *Boletín IMARPE*, Vol. 2 N° 5, Callao, Perú, 193-196

Figure captions

Figure 1. Location and X-Ray images of B0405-06 (14°07.90 S, 76°30.10W, 299m depth) and B0405-13 (B0405-13, 12°00'S, 72°42'S, 184 m) off the central-south Peruvian coast. Light laminae (dense), dark laminae (lower). Photo 1. Thin section of Callao core observed with polarized light. Q: quartz. F: feldspar, OCM: organic clay matrix.

Figure 2. Downcore variations of TOC content (%), Oxygen Index, Minerals (quartz, Felspar) content, clays content, Aluminium (%) and Mo content of Callao (black circle) and Pisco (clear circle).

Figure 3. Downcore variations of TOC fluxes, Mineral (Quartz, Feldspar, Clays) fluxes, and EF for Mo, for the Callao (black circle) and Pisco (clear circle) box cores. Slumps are considered instantaneous deposits and not considered in chronological development or flux calculations.

Figure 4. Projection of the proxy variables on the factor-plane PC1 (quartz, feldspar and clays vs Mo) vs. PC2 (TOC vs Oxygen Index) at Callao (black circle) and Pisco (clear circle) cores.

Figure 5. Downcore variations of PC1, sum of the different terrigenous fractions, Mo content, PC2, TOC and the Oxygen Index.

Figure 6. Comparison between a. PC1 downcore variation of Callao (black line) and Pisco (grey line) and PC2 downcore variation of Callao (black line) and Pisco (grey line). b. Ti content of sediments from ODP Hole 1002C, record from Peterson et al., 2006. c. PC2 downcore variation of Callao (black line) and Pisco (grey line). d. Instrumentals wind stress data from 1925 to 1995 by Jahncke et al., 2004. TR: Transport, OMZ: Oxygen Minimum Zone. TR = terrestrial input, P = export production, OMZ = Oxygen minimum zone.

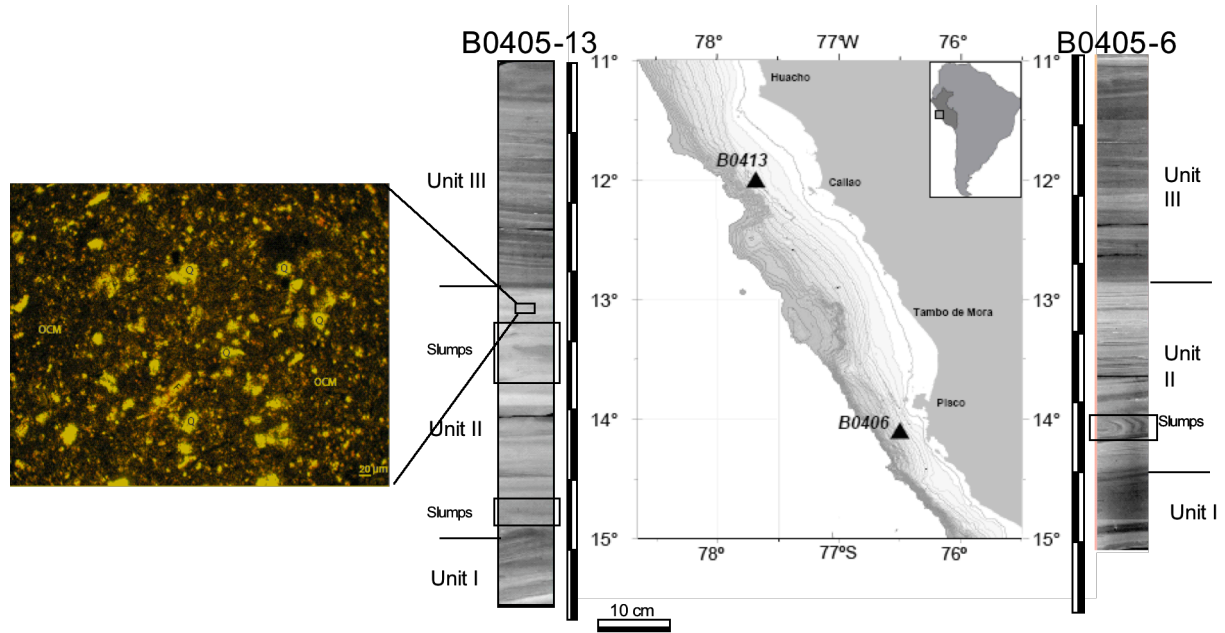


Figure 1.

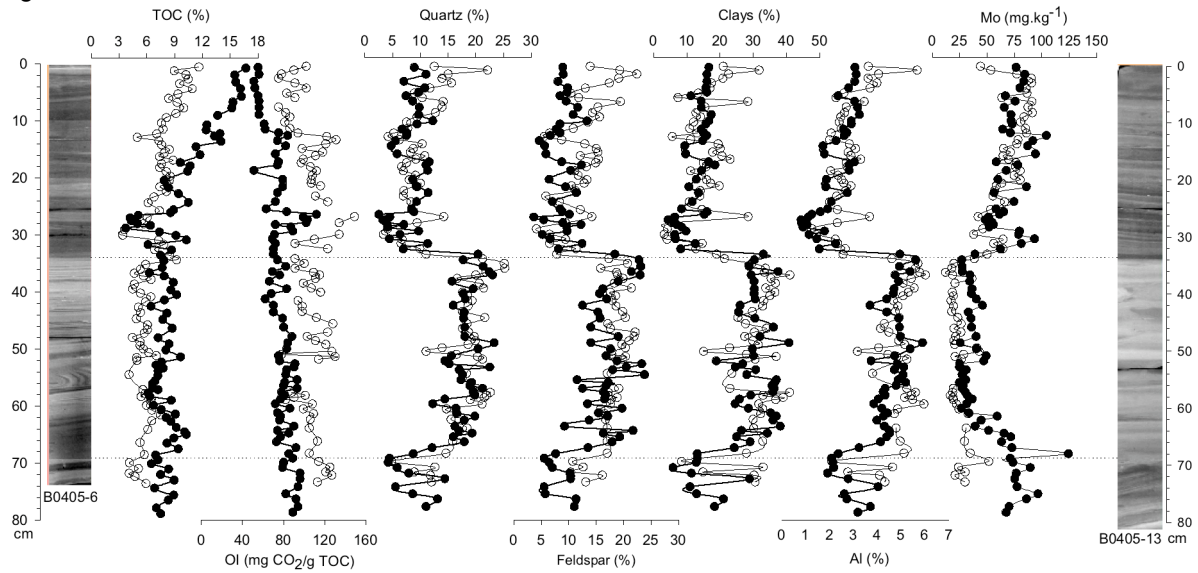


Figure 2.

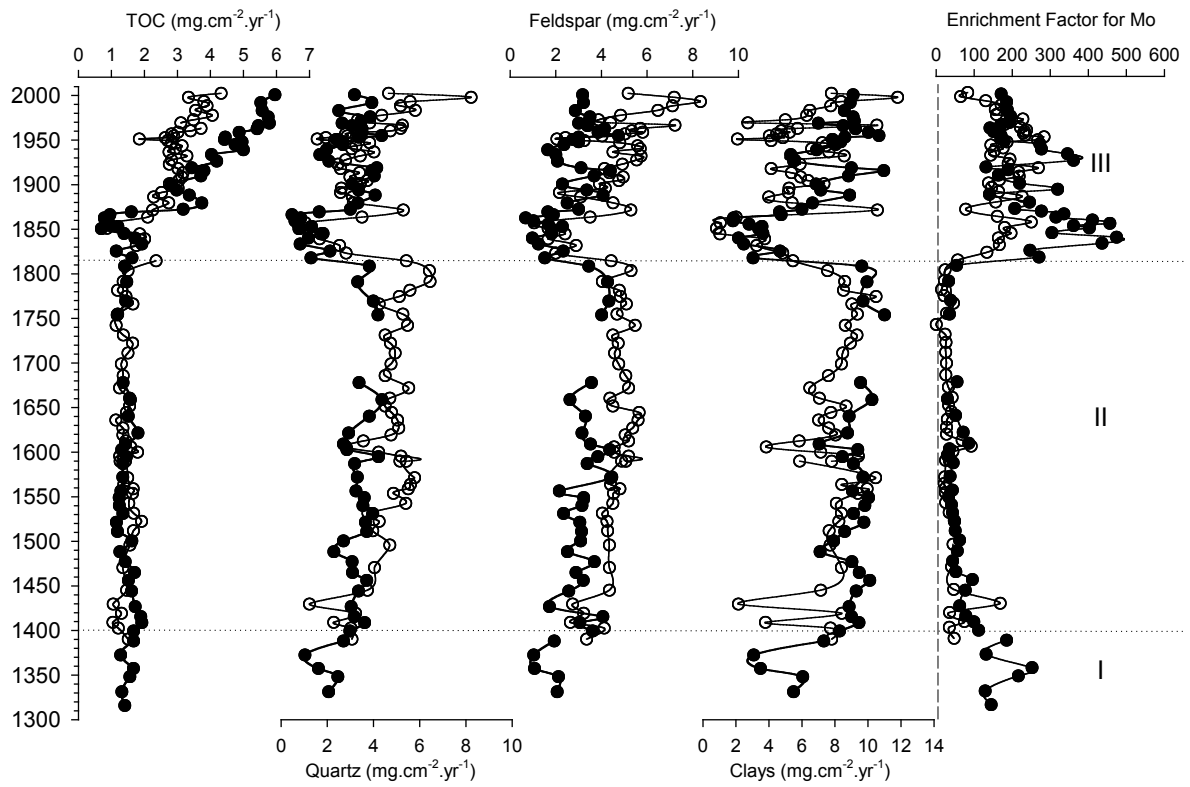


Figure 3.

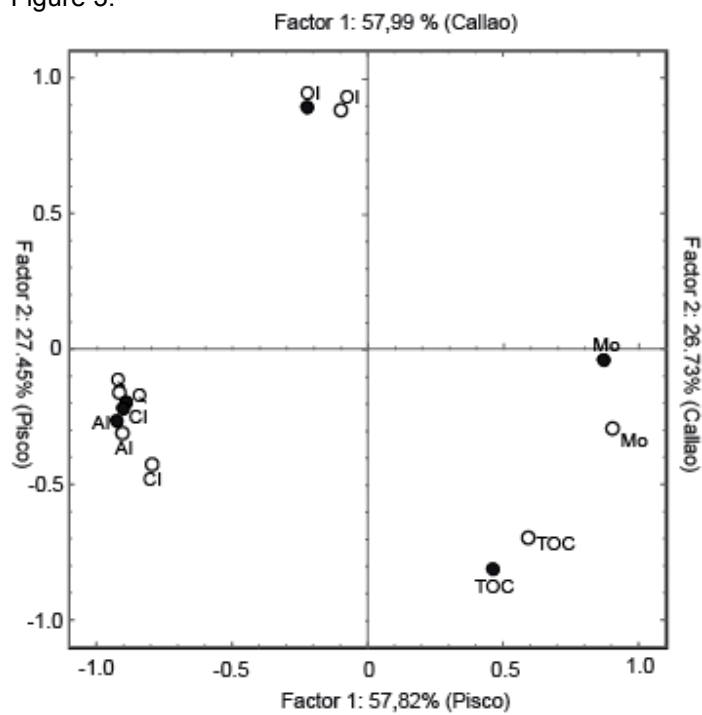


Figure 4.

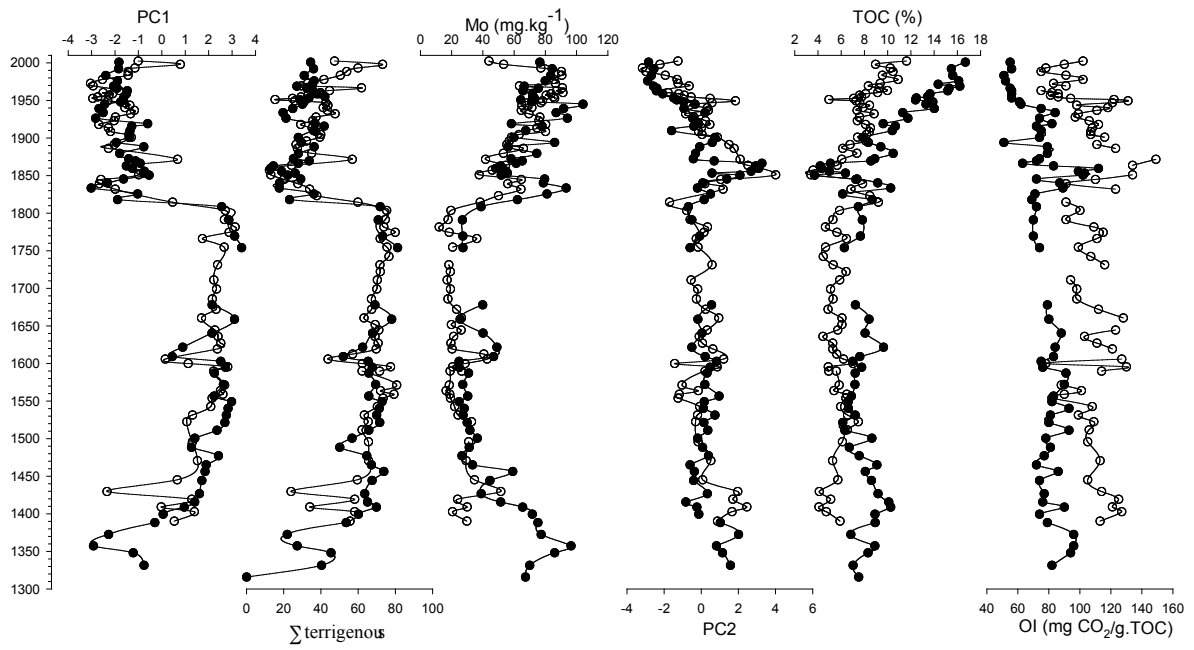


Figure 5.

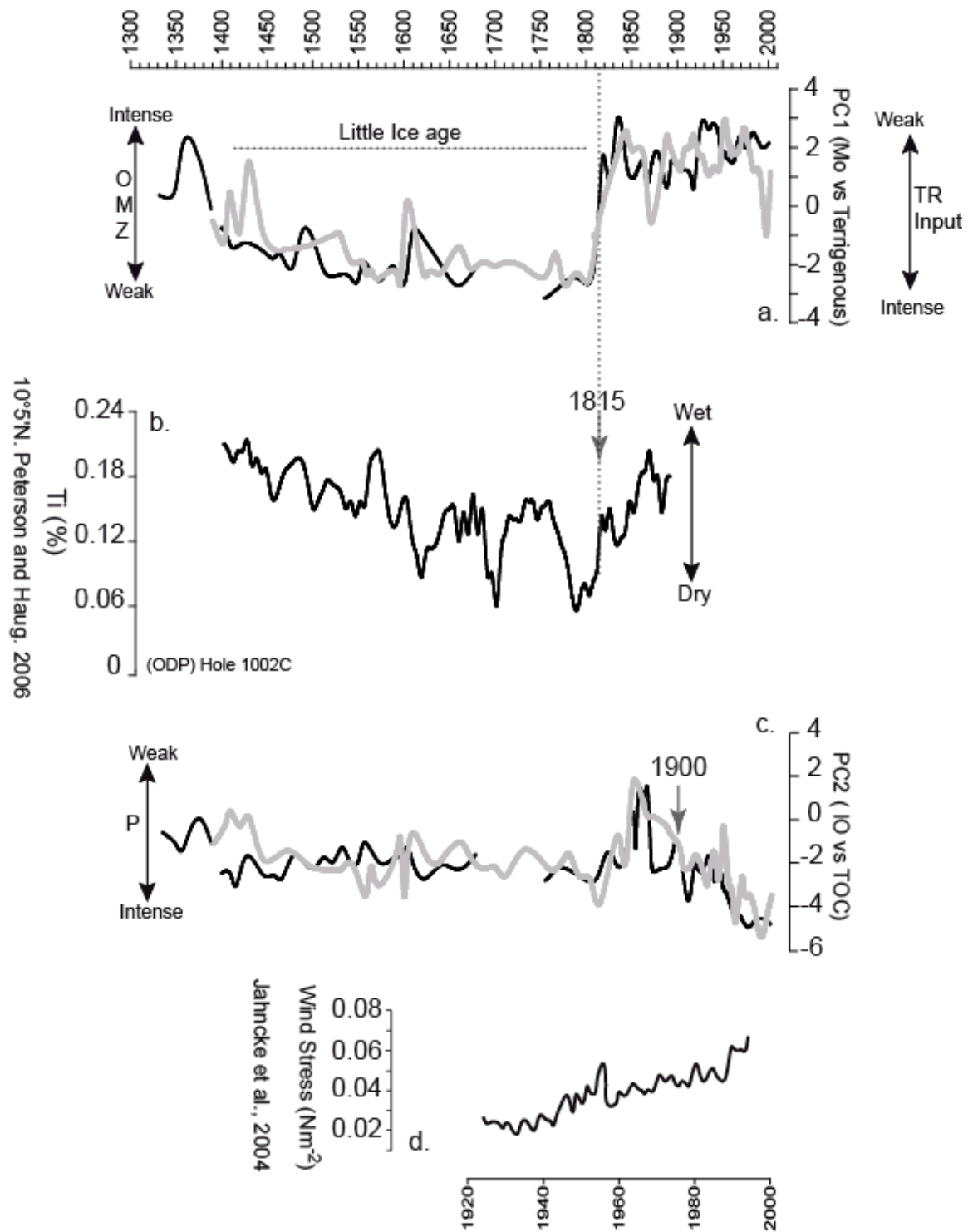


Figure 6.